



This document was produced
by scanning the original publication.

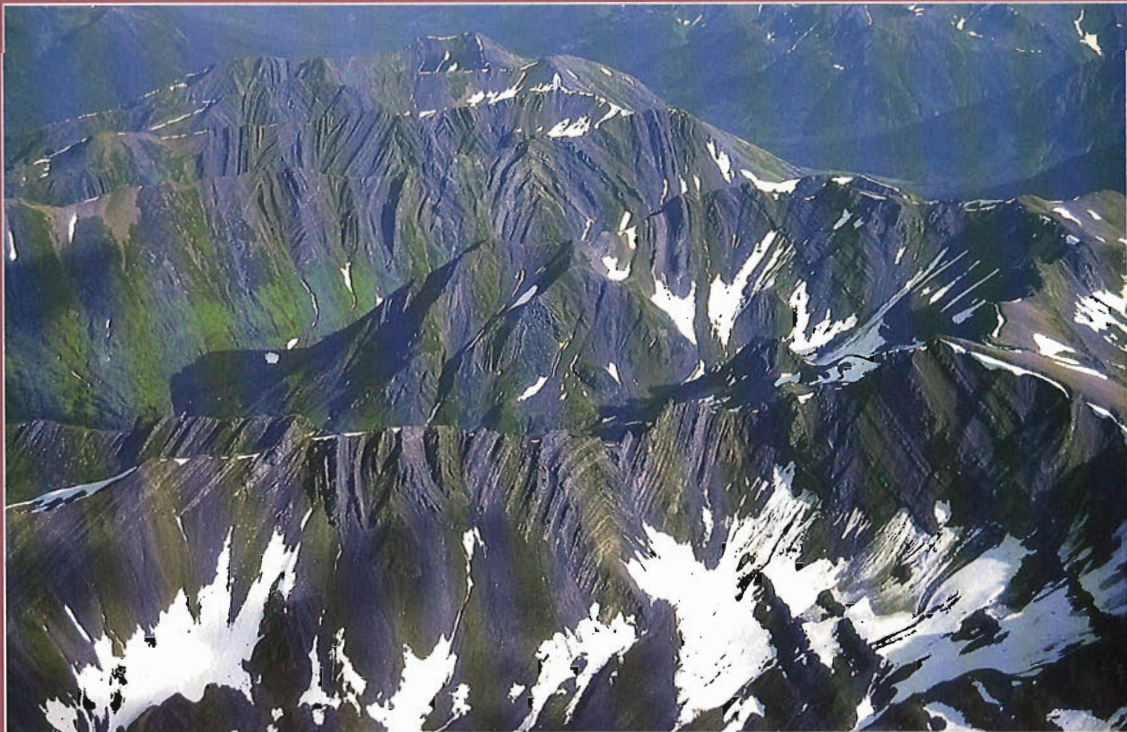
Ce document est le produit d'une
numérisation par balayage
de la publication originale.

GEOLOGICAL SURVEY OF CANADA
COMMISSION GÉOLOGIQUE DU CANADA

PAPER/ÉTUDE
93-1A

CURRENT RESEARCH, PART A
CORDILLERA AND PACIFIC MARGIN

RECHERCHES EN COURS, PARTIE A
CORDILLÈRE ET MARGE DU PACIFIQUE



Energy, Mines and
Resources Canada

Énergie, Mines et
Ressources Canada

Canada

THE ENERGY OF OUR RESOURCES - THE POWER OF OUR IDEAS

L'ÉNERGIE DE NOS RESSOURCES - NOTRE FORCE CRÉATRICE

NOTICE TO LIBRARIANS AND INDEXERS

The Geological Survey's Current Research series contains many reports comparable in scope and subject matter to those appearing in scientific journals and other serials. Most contributions to Current Research include an abstract and bibliographic citation. It is hoped that these will assist you in cataloguing and indexing these reports and that this will result in a still wider dissemination of the results of the Geological Survey's research activities.

AVIS AUX BIBLIOTHÉCAIRES ET PRÉPARATEURS D'INDEX

La série Recherches en cours de la Commission géologique contient plusieurs rapports dont la portée et la nature sont comparables à ceux qui paraissent dans les revues scientifiques et autres périodiques. La plupart des articles publiés dans Recherches en cours sont accompagnés d'un résumé et d'une bibliographie, ce qui vous permettra, on l'espère, de cataloguer et d'indexer ces rapports, d'où une meilleure diffusion des résultats de recherche de la Commission géologique.

**GEOLOGICAL SURVEY OF CANADA
COMMISSION GÉOLOGIQUE DU CANADA**

**PAPER / ÉTUDE
93-1A**

**CURRENT RESEARCH, PART A
CORDILLERA AND PACIFIC MARGIN**

**RECHERCHES EN COURS, PARTIE A
CORDILLÈRE ET MARGE DU PACIFIQUE**

1993

© Minister of Supply and Services Canada 1993

Available in Canada through authorized
bookstore agents and other bookstores

or by mail from

Canada Communication Group — Publishing
Ottawa, Canada K1A 0S9

and from

Geological Survey of Canada offices:

601 Booth Street
Ottawa, Canada K1A 0E8

3303-33rd Street N.W.,
Calgary, Alberta T2L 2A7

100 West Pender Street
Vancouver, B.C. V6B 1R8

A deposit copy of this publication is also available for
reference in public libraries across Canada

Cat. No. M44-93/1A
ISBN 0-660-57948-0

Price subject to change without notice

Cover description

View southeast to chevron and disharmonic folds of the Skeena Fold Belt in shallow marine strata of the Bowser Basin (northern Bowser Lake (104A) map area) (photographed by C.A. Evenchick, 1992).

Description de la photo couverture

Perspective vers le sud-est de plis disharmoniques et en chevron de la zone de plissement de Skeena située dans des strates marines du bassin de Bowser mises en place en eau peu profonde (secteur cartographique de Bowser Lake [104A]). Photo prise par C.A. Evenchick en 1992.

**GEOLOGICAL SURVEY OF CANADA
SECTOR
ASSISTANT DEPUTY MINISTER
SOUS-MINISTRE ADJOINT
SECTEUR DE LA
COMMISSION GÉOLOGIQUE du CANADA**

Office of the
Chief Scientist
Bureau du
Scientifique principal

**Minerals and Continental
Geoscience Branch
Direction des ressources minérales
et de la géologie du continent**

**Geophysics, Sedimentary and
Marine Geoscience Branch
Direction de la géophysique,
et de la géologie
sédimentaire et marine**

**Mineral
Resources
Division
Division des
ressources
minérales**

**Continental
Geoscience
Division
Division de la
géologie du
continent**

**Quebec
Geoscience
Centre
Centre
géoscientifique
de Québec**

**Pacific
Geoscience
Centre
Centre
géoscientifique
du Pacifique**

**Atlantic
Geoscience
Centre
Centre
géoscientifique
de l'Atlantique**

**Geophysics
Division
Division de la
géophysique**

**Cordilleran
Division
Division de la
Cordillère**

**Terrain
Sciences
Division
Division de la
sciences des
Terrains**

**Institute of
Sedimentary
and Petroleum
Geology
Institut de
géologie
sédimentaire et
pétrolière**

**Coordination and Planning
Division
Division de la coordination
et de la planification**

**Geoscience
Information and
Communications
Division
Division de
l'information
géoscientifique
et des
communications**

**Polar
Continental
Shelf Project
Étude du
plateau
continental
polaire**

Separates

A limited number of separates of the papers that appear in this volume are available by direct request to the individual authors. The addresses of the Geological Survey of Canada offices follow:

601 Booth Street
OTTAWA, Ontario
K1A 0E8
(FAX: 613-996-9990)

Institute of Sedimentary and Petroleum Geology
3303-33rd Street N.W.
CALGARY, Alberta
T2L 2A7
(FAX: 403-292-5377)

Cordilleran Division
100 West Pender Street
VANCOUVER, B.C.
V6B 1R8
(FAX: 604-666-1124)

Pacific Geoscience Centre
P.O. Box 6000
9860 Saanich Road
SIDNEY, B.C.
V8L 4B2
(Fax: 604-363-6565)

Atlantic Geoscience Centre
Bedford Institute of Oceanography
P.O. Box 1006
DARTMOUTH, N.S.
B2Y 4A2
(FAX: 902-426-2256)

Québec Geoscience Centre
2700, rue Einstein
C.P. 7500
Ste-Foy (Québec)
G1V 4C7
(FAX: 418-654-2615)

When no location accompanies an author's name in the title of a paper, the Ottawa address should be used.

Tirés à part

On peut obtenir un nombre limité de «tirés à part» des articles qui paraissent dans cette publication en s'adressant directement à chaque auteur. Les adresses des différents bureaux de la Commission géologique du Canada sont les suivantes:

601, rue Booth
OTTAWA, Ontario
K1A 0E8
(facsimilé : 613-996-9990)

Institut de géologie sédimentaire et pétrolière
3303-33rd St. N.W.,
CALGARY, Alberta
T2L 2A7
(facsimilé : 403-292-5377)

Division de la Cordillère
100 West Pender Street
VANCOUVER, British Columbia
V6B 1R8
(facsimilé : 604-666-1124)

Centre géoscientifique du Pacifique
P.O. Box 6000
9860 Saanich Road
SIDNEY, British Columbia
V8L 4B2
(facsimilé : 604-363-6565)

Centre géoscientifique de l'Atlantique
Institut océanographique Bedford
B.P. 1006
DARTMOUTH, Nova Scotia
B2Y 4A2
(facsimilé : 902-426-2256)

Centre géoscientifique de Québec
2700, rue Einstein
C.P. 7500
Ste-Foy (Québec)
G1V 4C7
(facsimilé : 418-654-2615)

Lorsque l'adresse de l'auteur ne figure pas sous le titre d'un document, on doit alors utiliser l'adresse d'Ottawa.

CONTENTS

- 1 L.E. JACKSON, Jr.
Origin and stratigraphy of Pleistocene gravels in Dawson Range and suggestions for future exploration of gold placers, southwestern Carmacks map area, Yukon Territory
- 11 R.A. STEVENS and P. ERDMER
Geology and structure of the Teslin suture zone and related rocks in parts of Laberge, Quiet Lake, and Teslin map areas, Yukon Territory
- 21 C.F. ROOTS and L.D. CURRIE
Geodetic and geological observations from the 1992 Mount Logan expedition, Yukon Territory
- 27 M.H. GUNNING
Character of upper Paleozoic strata and plutons, lower Forrest Kerr Creek area, northwestern British Columbia
- 37 G.G. JOHANNSON
Preliminary report on the stratigraphy, sedimentology, and biochronology of the Inklin Formation in the Atlin Lake area, northern British Columbia
- 43 G. JAKOBS
Jurassic stratigraphy of the Diagonal Mountain area, McConnell Creek map area, north-central British Columbia
- 47 C.A. EVENCHICK and J.S. PORTER
Geology of west McConnell Creek map area, British Columbia
- 57 J.G. SOUTHER and I. WEILAND
Crow Lagoon tephra – new evidence of Recent volcanism in west-central British Columbia
- 63 C.J. HICKSON and S. HIGMAN
Geology of the northwest quadrant, Taseko Lakes map area, west-central British Columbia
- 69 B.D. RICKETTS and R. CROSSLEY
Aquifer mapping in the Prince George region, British Columbia: a pilot project
- 75 P.D. LEWIS, J.F.H. THOMPSON, G. NADARAJU, R.G. ANDERSON,
and G.G. JOHANNSON
Lower and Middle Jurassic stratigraphy in the Treaty Glacier area and geological setting of the Treaty Glacier alteration system, northwestern British Columbia
- 87 K.V. ROSS, K.M. DAWSON, C.I. GODWIN, and L. BOND
Major lithologies and alteration of the Ajax East orebody, a sub-alkalic copper-gold porphyry deposit, Kamloops, south-central British Columbia
- 97 D.R. SHAW, C.J. HODGSON, C.H.B. LEITCH, and R.J.W. TURNER
Geochemistry of tourmalinite, muscovite, and chlorite-garnet-biotite alteration, Sullivan Zn-Pb deposit, British Columbia
- 109 D.R. SHAW, C.J. HODGSON, C.H.B. LEITCH, and R.J.W. TURNER
Geochemistry of albite-chlorite-pyrite and chlorite-pyrrhotite alteration, Sullivan Zn-Pb deposit, British Columbia
- 119 H.W. JOSEPHANS, J.V. BARRIE, K.W. CONWAY, R.T. PATTERSON, R.W. MATHEWES, and
G.J. WOODSWORTH
Surficial geology of the Queen Charlotte Basin: evidence of submerged proglacial lakes at 170 m on the continental shelf of western Canada
- 129 J.G. SOUTHER
Tertiary volcanic and subvolcanic rocks of central Moresby and Talunkwan islands, Queen Charlotte Islands, British Columbia

- 139 C.A. GAMBA
Stratigraphy and sedimentology of the Upper Jurassic to Lower Cretaceous Longarm Formation, Queen Charlotte Islands, British Columbia
- 149 J.W.H. MONGER
Georgia Basin Project – geology of Vancouver map area, British Columbia
- 159 P.B. READ
Geology of northeast Taseko Lakes map area, southwestern British Columbia
- 167 D.H. HUNTLEY and B.E. BROSTER
Glacier flow patterns of the Cordilleran Ice Sheet during the Fraser Glaciation, Taseko Lakes map area, British Columbia
- 173 J.B. MAHONEY
Facies reconstructions in the Lower to Middle Jurassic Ladner Group, southern British Columbia
- 183 W.H. FRITZ and G.J. SIMANDL
New Middle Cambrian fossil and geological data from the Brussilof magnesite mine area, southeastern British Columbia
- 191 M. COLPRON and R.A. PRICE
Geology of the Illecillewaet synclinorium in the Durrand/Dismal glaciers area, western Selkirk Mountains, British Columbia
- 199 S.E. GRASBY and R.L. BROWN
New correlations of the Hadrynian Windermere Supergroup in the northern Selkirk Mountains, British Columbia
- 207 A.D. LECLAIR, R.R. PARRISH, and D.A. ARCHIBALD
Evidence for Cretaceous deformation in the Kootenay Arc based on U-Pb and $^{40}\text{Ar}/^{39}\text{Ar}$ dating, southeastern British Columbia
- 221 J.M. JOURNEY
Tectonic assemblages of the Eastern Coast Belt, southwestern British Columbia: implications for the history and mechanisms of terrane accretion
- 235 J.B. MAHONEY and J.M. JOURNEY
The Cayoosh Assemblage, southwestern British Columbia: last vestige of the Bridge River Ocean
- 245 R.T. PATTERSON and J.L. LUTERNAUER
Holocene foraminiferal faunas from cores collected on the Fraser River delta, British Columbia: a paleoecological interpretation
- 255 T.F. MOSLOW, R.W. EVOY, and J.L. LUTERNAUER
Implications of ^{137}Cs sediment profiles for sediment accumulation rates on the Fraser River delta foreslope, British Columbia
- 263 P.A. MONAHAN, J.L. LUTERNAUER, and J.V. BARRIE
A delta topset sheet sand and modern sedimentary processes in the Fraser River delta, British Columbia
- 273 R.W. EVOY, T.F. MOSLOW, and J.L. LUTERNAUER
Sedimentology and lithofacies associations of the Fraser River delta foreslope, British Columbia
- 281 J.A. RODDICK
Implications of viscosity on pluton emplacement
- 287 Author Index

Origin and stratigraphy of Pleistocene gravels in Dawson Range and suggestions for future exploration of gold placers, southwestern Carmacks map area, Yukon Territory

Lionel E. Jackson, Jr.

Terrain Sciences Division, Vancouver

Jackson, L.E. Jr., 1993: Origin and stratigraphy of Pleistocene gravels in Dawson Range and suggestions for future exploration of gold placers, southwestern Carmacks map area, Yukon Territory; in Current Research, Part A; Geological Survey of Canada, Paper 93-1A, p. 1-10.

Abstract: The Nansen-Big Creek placer district has been a centre of placer mining and prospecting in Dawson Range since the turn-of-the century. Placers occur in this region due to a lack of glaciation for more than 1 Ma and the presence of late Cretaceous granites and the subvolcanic Mount Nansen Group which are gold sources or induced mineralization in country rocks. Placers were created during stream degradation following the pre-Reid glaciations. Significant aggradation occurred along streams in the Dawson Range as a result of the Reid Glaciation. The subsequent McConnell Glaciation had a minimal affect on them by comparison. All streams that cross or drain late Cretaceous granites and the Mount Nansen Group and are beyond the limits of Reid Glaciation are prospective for gold placers.

Résumé : Le district alluvionnaire de Nansen-Big Creek est un centre d'exploitation minière et de prospection de des gisements alluviaux (placers) dans le chaînon Dawson depuis le début du siècle. Il existe de tels gisements dans cette région en raison de l'absence de glaciations pendant plus de 1 Ma ainsi que de la présence de roches granitiques formées à la fin du Crétacé et du Groupe de Mount Nansen, de caractère subvolcanique, tous deux des sources de minéraux aurifères ou responsables de la minéralisation en or de la roche encaissante. Les gisements alluviaux se sont formés au cours de l'abaissement du profil des cours d'eau, phénomène antérieur aux glaciations ayant précédées la glaciation de Reid. Cette dernière est à l'origine d'un important relèvement du profil des cours d'eau dans le chaînon Dawson. La glaciation de McConnell ultérieure a eu, comparativement, peu d'effet sur les cours d'eau. Tous les cours d'eau qui traversent les roches granitiques formées à la fin du Crétacé et les roches du Groupe de Mount Nansen, et qui se situent en dehors des limites de la glaciation de Reid, conviennent à la prospection des gisements alluviaux.

INTRODUCTION

Placer gold prospecting and mining have been carried out in Dawson Range, central Yukon (Fig. 1) since 1898 (Bostock, 1936). Prospecting and mining activity have centred in the areas of Victoria Creek and the main fork of Nansen Creek and Big Creek and its tributaries above Stoddart Creek (Fig. 1). This area will henceforth be referred to as the Nansen-Big Creek placer district. Regional surficial geology mapping and Quaternary stratigraphic investigations of the Carmacks map area (115I) were carried out from 1988 to 1992 as a part of Geological Survey of Canada Project 800001 "Quaternary geology and terrain inventory, east-central Yukon". This report presents observations on the origin of major gravel units within these placer districts and stratigraphic and paleoenvironmental information which sheds some light on the Quaternary history of them. Suggestions are made for the applications of these findings to the search for new placers within this region.

SETTING

Bedrock geology

The Carmacks map area (115I) includes the Yukon Cataclastic and the Yukon Crystalline terranes and the Whitehorse Trough (Tempelman-Kluit, 1978; Fig. 2). The terranes are composed of Paleozoic to Jurassic sedimentary and volcanic rocks and their cataclastic equivalents which have been intruded by plutons of Triassic and Jurassic age. The Whitehorse Trough is a former fore-arc basin which received volcanolithic and arkosic clastics from late Triassic through mid-Jurassic times. These terranes were sutured during episodes of continental accretion during the Middle Jurassic to Late Cretaceous. Suturing was accompanied by the intrusion of biotite leucogranite, biotite hornblende granodiorite, and hornblende syenite plutons. The Late Cretaceous Mount Nansen Group consists of andesite, dacite, and rhyolite that were erupted in the southwestern quarter of the map area during or shortly after suturing. The extensive basalt flows and related volcanoclastic sediments of the Carmacks Group were erupted contemporaneously with the Mount Nansen Group over an eroded surface with local relief of up to 700 m (Tempelman-Kluit, 1974, 1980).

Physiography

The Nansen-Big Creek placer district lies entirely within the Yukon Plateaus (Mathews, 1986), a rolling upland with broad and generally accordant summits and ridges that typically lie below 1500 m. Relief is generally in the range of 750 to 900 m (Fig. 1), although isolated peaks in the Dawson Range such as Tritop Peak, Victoria Mountain, and Klaza Mountain rise to more than 1820 m. Within the Carmacks map area (115I), Yukon Plateaus show no evidence of recent glaciation although scattered incised cirque-like valleys do occur near the summits of some of the highest peaks such as Prospector Mountain and Mt. Nansen. The rolling morphology of the contemporary Yukon Plateaus with higher mountain groups

rising above the generally accordant summits is inherited from a period when the region was eroded to a relative relief of less than about 550 m. Previous estimates of the age of this surface have ranged from Miocene to Eocene (Bostock, 1936; Tempelman-Kluit, 1980). Drainage patterns in Dawson Range, beyond the limit of the penultimate Reid Glaciation, are generally dendritic, trellis where major faults control stream courses, or recurved trellis where trunk streams follow the curvilinear boundaries of plutonic bodies or other nonlinear discontinuities in the bedrock. Drainage is disrupted in areas of thick bog, drift and sands of inactive dunes.

The contemporary westerly flow of the Klaza River drainage network into Nisling River (Fig. 1, 3) was preceded by flow to the south through the broad swampy valley presently occupied by Lonely Creek (Bostock, 1936, 1966; Hughes, 1990). It was diverted to its present course through glacially induced stream diversion and capture in the early Pleistocene (Bostock, 1966).

QUATERNARY CONTEXT

A chronology of four glaciations of Carmacks map area and adjacent areas of central and southern Yukon was constructed by Bostock (1966) based upon morphostratigraphic, stratigraphic, and geomorphic evidence. These were named Nansen (oldest), Klaza, Reid, and McConnell (youngest). Although till, outwash gravels, and erratics and ice marginal features up to 1250 m elevation associated with the two oldest glaciations were recognized by the present author and previous workers (Cairnes, 1914; Bostock, 1936) within the Nansen-Victoria and Big Creek placer districts, deposits of these glaciations have been largely removed by erosion or buried by colluvium. Consequently, discrimination between them is not usually possible. The informal name "pre-Reid glaciations" is used here in reference to these glaciations.

Deposits of these two glaciations can be discriminated in the area of Fort Selkirk 80 km to the north of the Nansen-Big Creek placer districts. Basalts there erupted during the younger pre-Reid glaciation (Jackson et al., 1990). Two K-Ar ages have been determined on these basalts: 1.08 ± 0.05 Ma (Naeser et al., 1982) and 1.28 ± 0.03 Ma (GSC K-Ar 4168). These basalts are magnetically reversed (Jackson et al., 1990) which corroborates that they were erupted prior to 0.78 Ma BP and are consistent with the time spans of reversed geomagnetism established in the geomagnetic polarity time scale (Mankinen and Dalrymple, 1979; Shackleton et al., 1990). The penultimate Reid Glaciation is thought to have occurred between about 80 and 130 ka BP (Jackson et al., 1991). During this event, the Cordilleran Ice Sheet pressed against the western and southern margins of the Dawson Range. Meltwater spilled into the Big Creek and Nisling River basins across divides as high as 1000 m on the west margin and south flowing streams were dammed at elevations up to 1000 m along the south.

The McConnell Glaciation occurred between ca. 25 and 12 ka BP (Jackson et al., 1990). The Cordilleran Ice Sheet also pressed against the Dawson Range but its upper limit was

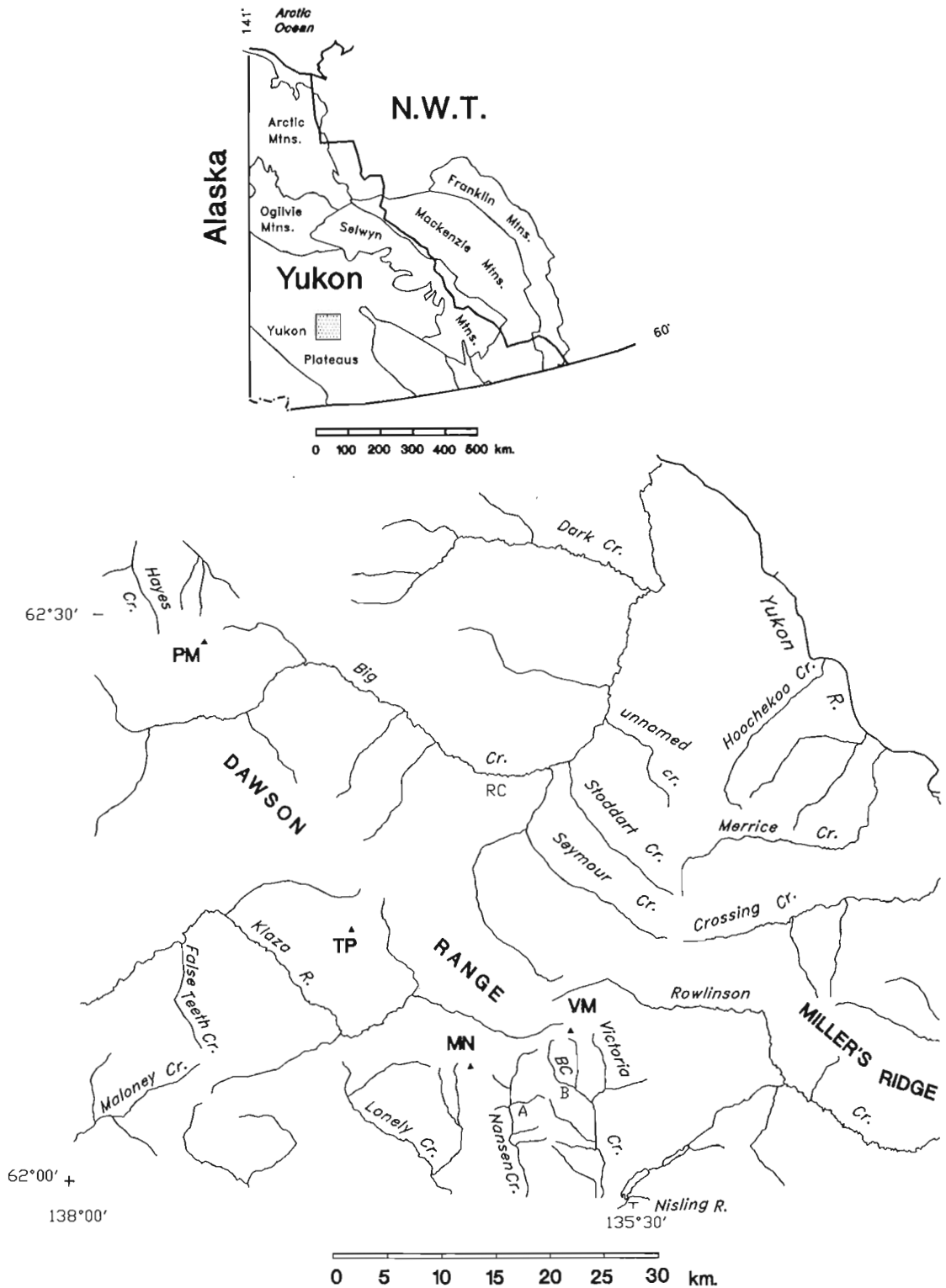


Figure 1. Location of the Nansen-Big Creek placer district. Large bold type: PM – Prospecter Mountain, TP – Tritop Peak, MN – Mount Nansen, VM – Victoria Mountain. Smaller type: RC – Revenue Creek, BC – Back Creek, A – location of pre-Reid outwash and Wounded Moose soil, B – core 88 DDH 115 and pre-Reid meltwater channel.

about 300 m below that of the Reid-age glacier. Meltwaters crossed the Dawson Range only between Crossing Creek and Nisling River (Fig. 1).

Late Tertiary and Quaternary weathering history of unglaciated areas of Yukon

Analysis of fossil soils and fossil pollen from associated sediments indicates that the Yukon enjoyed a much milder climate until the onset of periodic glaciation in the Early Pleistocene (Tarnocai and Valentine, 1989; Tarnocai and Schweger, 1991). The vegetation and soils existed in the Old Crow area (contemporary mean annual temperature and precipitation -10.1°C and 214 mm, respectively) at that time which are presently found no farther north than central British Columbia (contemporary mean annual temperature and

precipitation 4°C and 550 mm, respectively; Drumke, 1964; Atmospheric Environment Service, 1982a,b; Tarnocai and Schweger, 1991). The climate existing in the area of Dawson Range 6° of latitude farther south likely contrasted as dramatically with the present climate. Such a climate persisting over hundreds of thousands or millions of years almost certainly resulted in a deeply weathered mantle over the Dawson Range. The well known White Channel Gravel in the Klondike District (McConnell, 1905) was deposited during this period; the quartzose composition of this unit, from which its colour and name derive, reflects a climate warm and wet enough for chemical weathering to eliminate less chemically resistant lithologies (Boyle, 1979, p. 356).

Following the pre-Reid glaciations, the climate returned to warmer and wetter conditions at least once. The Wounded Moose paleosol is commonly found developed in pre-Reid

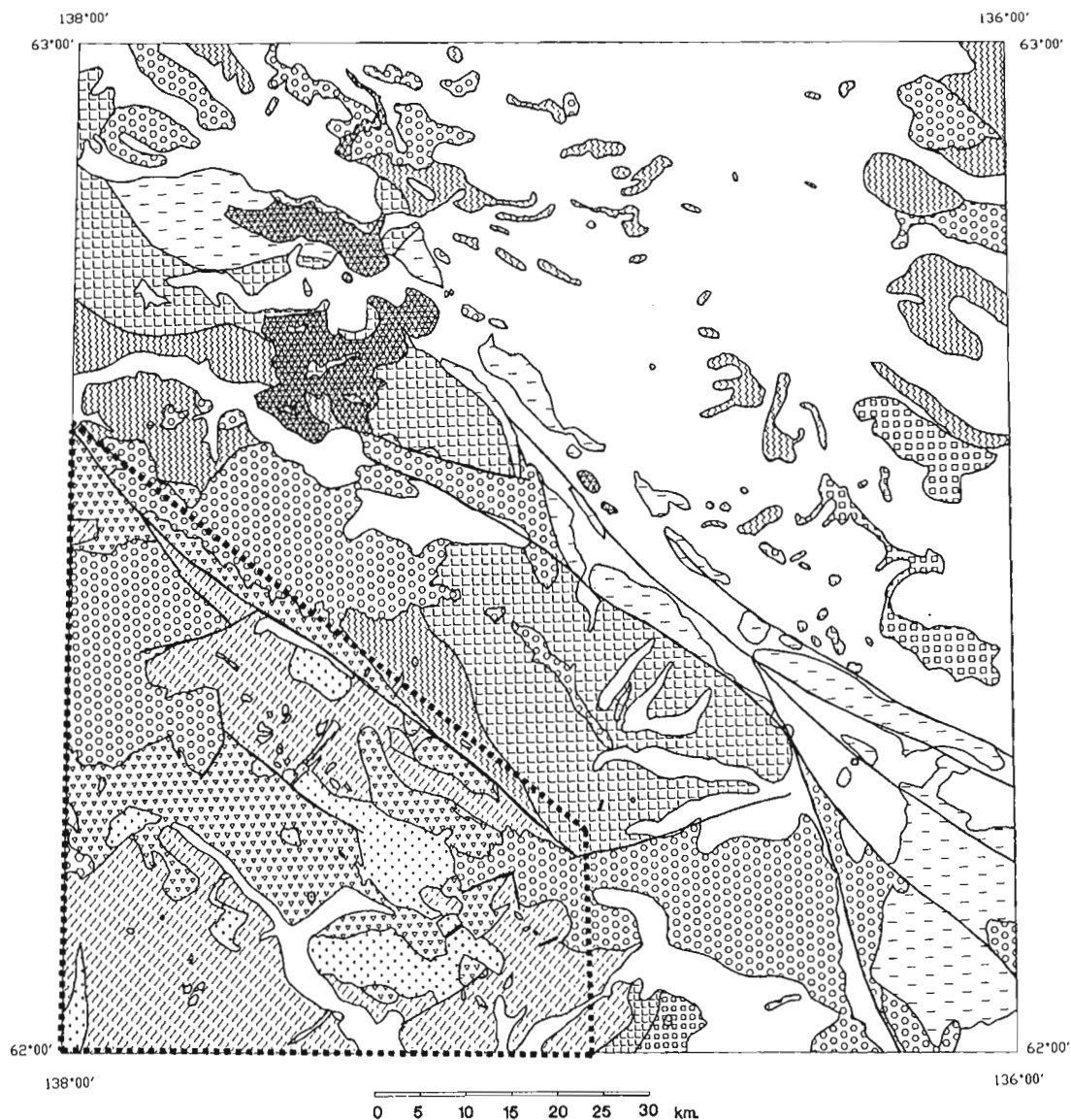


Figure 2. Bedrock geology generalized and modified from Tempelman-Kluit (1979) using the chronologic information of Grond et al. (1984). The dashed line outlines the Nansen-Big Creek placer district.

outwash in central Yukon (Smith et al., 1986; Tarnocai and Schweger, 1991). It formed under a climate with a mean annual temperature of 7°C or greater and mean annual precipitation of more than 500 mm. A Wounded Moose paleosol, developed in pre-Reid gravels overlying till, was exposed beneath colluvial overburden along the valley side above Discovery Creek during exploratory trenching in 1989 (UTM 386000 6884000; A in Fig. 1) and has been observed elsewhere within the Nansen Creek basin (Lebarge, pers. comm., 1992).

The temperate period during which the thick (>1 m) and deep red Wounded Moose Paleosol developed was of an unknown duration. Between that time and the onset of the Reid Glaciation (<ca. 1.2 Ma BP and ca. 80-130 ka BP), the climate likely alternated between glacial climates and one similar to the contemporary interglacial climate. Climatic

conditions during at least some of these glaciations were as severe as any contemporary climates. Wounded Moose soil and the pre-Reid outwash gravels are commonly cut by sand wedges, periglacial features presently forming in unglacierized areas of Antarctica (Péwé, 1959).

The exposure of Wounded Moose soil examined in the Discovery Creek basin is cut by well formed sand wedges. Evidence for climatic conditions during at least one interglacial period comes from core 88 DDH 115 recovered by Archer-Cathro and Associates (1981) Ltd. above Pony Creek in the Victoria Creek basin in 1988 (UTM 382300 6956000; B in Fig. 1). It intersected a pre-Reid meltwater channel filled with 21 m of sediment. Three zones indicative of soil forming activity were noted in lower 15 m of fill recovered in the core. Based on the intensity of weathering, the lowest soil was equivalent to the Wounded Moose soil.

LEGEND TO FIGURE 2

QUATERNARY



undivided glacial deposits, alluvium and bog.



Selkirk volcanics: basalt, hyaloclastites and minor glacial deposits.

UPPER CRETACEOUS



Carmacks Group: basalt, andesitic basalt, volcanic sandstone and conglomerate.



Mount Nansen Group: andesite, dacite and rhyolite.



Casino Granodiorite (plutonic phase of Mount Nansen Group).

JURASSIC AND/OR CRETACEOUS



Whitehorse Trough: feldspathic sandstone, granite pebble conglomerate, andesitic basalt and breccia.

JURASSIC



Tatchun Batholith: foliated biotite hornblende granodiorite.

TRIASSIC



Minto Pluton: foliated biotite hornblende granodiorite.

PALEOZOIC



Yukon Crystalline Terrane: granite to granodiorite gneiss and quartz mica schist.



Yukon Cataclastic Terrane: amphibolite, greenstone, dunite, mylonite, blastomylonite, muscovite quartz schist, gneiss.

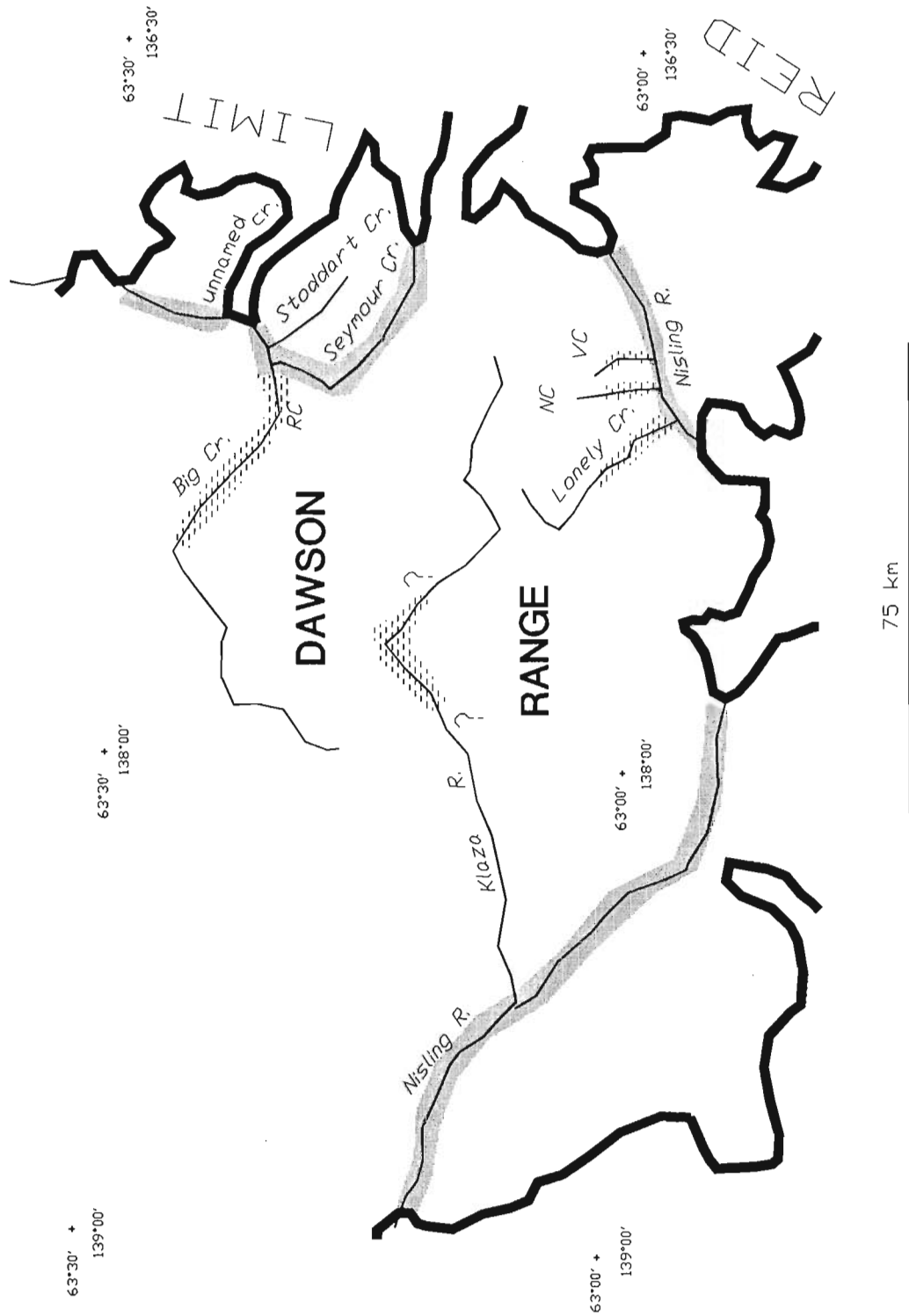


Figure 3. Limits of the Cordilleran Ice Sheet during the Reid glaciation in the area of Dawson Range generalized from Hughes et al. (1969) and Hughes (1990). The stipple patterns indicate areas where stream aggradation occurred during Reid Glaciation as a result of deposition of outwash. The dash pattern indicates aggradation along streams draining unglacierized basins.

Pollen recovered from fine sediment associated with less well developed soils were indicative of climates similar or more severe than today's. These pedologic layers are separated by coarse and angular stony diamictons likely colluvium deposited through gelifluction when the margins of the meltwater channel were devoid of vegetation and edaphically unstable.

MAJOR GRAVEL UNITS OF THE NANSEN-BIG CREEKS PLACER DISTRICTS

Pre-Reid glaciation outwash

The oldest gravels in the Nansen-Victoria and Big Creek placer Districts are outwash deposited during the waning stages of the last pre-Reid glaciation. One exposure of this gravel, previously mentioned in conjunction with the discussion on the Wounded Moose soil, has been noted on the valley side approximately 45 m above the floor of Discovery Creek (A in Fig. 1) and elsewhere in the Nansen Creek basin (Lebarge, pers. comm., 1992). Gravels are discontinuously present along the north side of the Big Creek valley up to the divide with Bow Creek where former pre-Reid meltwater channels are apparent at approximately 1100 m elevation. With few exceptions, these gravels and pre-Reid tills noted in the upper Nansen Creek and Klaza River basins only contain lithologies known to occur in Dawson Range and thus indicate that the glacial ice present in the upper parts of the Nansen Creek, Big Creek, and Klaza River basins originated from ice centres within Dawson Range.

Reid outwash and Reid-age gravels graded to glacial impoundment

During the Reid Glaciation, the Cordilleran ice sheet advanced into the glacier-ice-free Dawson Range from the west and south. This affected fluvial sedimentation in Dawson Range through climatic change, input of outwash, and base level changes.

Climatic Change

The glacial climate resulted in the uplands largely denuded of vegetation. Treeline was depressed more than 850 m in the central Yukon during McConnell Glaciation and the mean July temperature is estimated to have been $\leq 5^{\circ}\text{C}$ colder than the present (Matthews et al., 1990). The Reid Glaciation was more severe than the McConnell so the effects of glaciation on the vegetative cover were even more pronounced. The resulting denudation made the weathered overburden, formerly stabilized by vegetation, available for erosion and transport, as well as sediment created by the intense physical weathering environment active during glaciation. This likely increased erosion rates and delivery of sediment to adjacent lowlands.

Outwash input

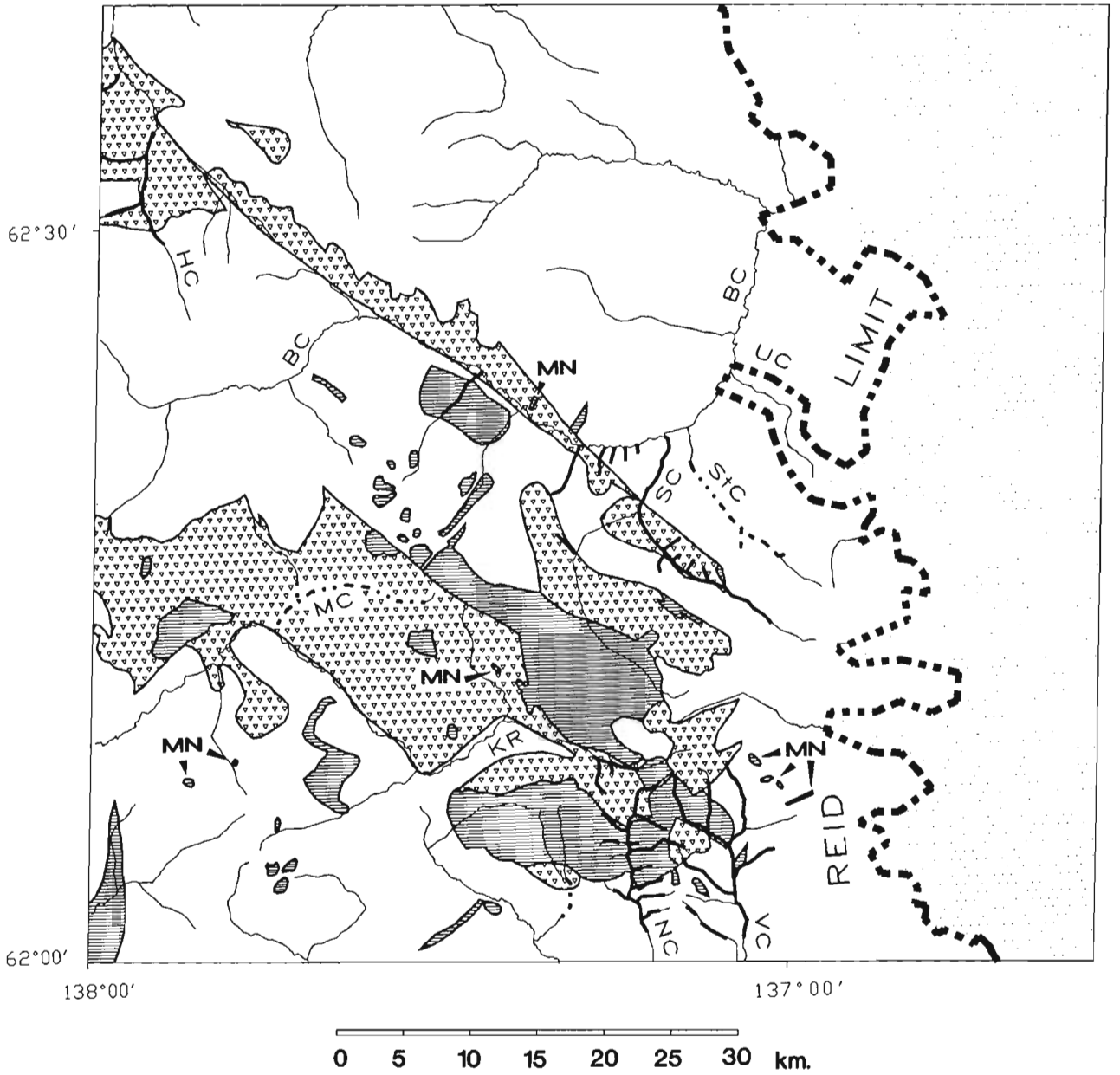
Meltwaters from the ice sheet spilled across passes between Crossing Creek and Seymour Creek and down the unnamed creek which shares its divide with Merris and Hoochekoo creeks (Bostock, 1936) in the Big Creek basin and between Rowlinson Creek and upper reaches of Nisling River (Fig. 3) farther south. These meltwaters carried outwash gravels down Seymour and Big creeks and Nisling River.

Base level changes

Ice sheet encroachment into Dawson Range raised base levels of streams flowing out of the Dawson Range by impoundment and diversion of these streams along ice margins. Aggradation of as much as 20 m occurred along streams draining unglaciated basins such as Nansen Creek, Victoria Creek, Lonely Creek, and Klaza River. Basins that were dammed and also received outwash locally accumulated exceptionally thick deposits of gravel. A tongue of the Cordilleran Ice Sheet pressed up Big Creek to no more than 15 km below the confluence of Big Creek and Seymour Creek and no less than 610 m elevation raising the base level approximately 150 m. Glacial ice apparently crossed the low (945 m) divide between Merrice and Hoochekoo creeks and the unnamed creek that joins Big Creek 5 km below Stoddart Creek (unnamed creek in Fig. 1 and 3). This glacial tongue or outwash sediment from it blocked Big Creek. These events caused up to 183 m of gravel to be deposited in the area of confluences of Seymour and Stoddart creeks with Big Creek. Terraces underlain by unweathered gravels at approximately 823 m on the ridge separating Seymour and Stoddart Creeks near their confluences with Big Creek mark the top of this fill (area of UTM 382300 6913400).

Tributaries to Big Creek above the Seymour Creek confluence would have had to aggrade in response to this significant aggradation downstream. The approximately 12 m of gravel and muck overlying a highly productive gold placer at Revenue Creek may have been deposited at this time. Nonfinite radiocarbon ages of >40 000 years BP (GSC 4935) and >38 000 years BP (GSC 4963) have been determined on wood from the top of the fill. Although these ages do not demonstrate clear linkage to aggradation during Reid Glaciation, they at least demonstrate that it predated McConnell Glaciation.

Lithology and physical appearance allow easy discrimination between Reid outwash gravels and gravels deposited by streams that drained glacier-ice-free basins during Reid Glaciation. Outwash contains a significant content of lithologies external to the basin whereas nonglacial gravels have lithologies only occurring upstream. However, the most striking difference is in the physical appearance of the two. Outwash gravel typically is coarse, subangular to subrounded which maintains a similar planar stratified to massive facies for many kilometres beyond the glacial margin. The non-outwash gravels are angular to subangular and contain ventifacted clasts, commonly wind sculpted on several sides. Ice wedge pseudomorphs are also common in



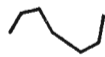
LEGEND



Mount Nansen Group: andesite, rhyolite and dacite dykes and plugs



granodiorite, granite and hornblende diorite. (plutonic equivalent of Mt. Nansen Group.)



presently or formerly mined placer station



placer stream: no or limited mining

NC

Stream name (explained in text)

MN small occurrence of Mt. Nansen Group

these sediments. The non-outwash sediments display marked textural changes vertically between angular gravel and coarse sand and laterally with texture fining markedly downstream.

The difference in physical appearance relates to depositional history. The alternation of coarse frost-shattered and ventifacted gravels and coarse sand in non-outwash appears to reflect episodic fluvial events during which coarse sediments were washed out of uplands into fans and braided streams environments. The periglacial climate and catabatic winds frost shattered and ventifacted clasts before they were buried by shifting channels or another flood event. In contrast, deposition and aggradation of outwash plains was rapid and periglacial modification of clasts relatively rare.

McConnell Glaciation gravels

Meltwaters from the Cordilleran Ice Sheet had minimal effect on the placer bearing basins of southwestern Carmacks sheet during the McConnell Glaciation. Meltwaters only crossed Dawson Range between Rowlinson and Nisling River and this served to truncate and incise gravels at the confluences of Victoria and Nansen creeks with Nisling River. Glacial ice did not extend far enough down Yukon River to block the mouth of Big Creek. Consequently, base level was not affected significantly in that basin.

Probably the most significant effect of McConnell Glaciation was simply denudation of Dawson Range by the onslaught of a glacial climate. This likely resulted in enhanced rates of erosion and sedimentation. In addition, loess and sand driven by catabatic winds were deposited in fens and bogs forming muck deposits in valley and gulch bottoms.

OBSERVATIONS ON ORIGIN OF GOLD PLACERS

Bostock (1936) noted a close association between placer and lode gold and felsic intrusives in the Nansen Creek and Mt. Freegold areas. Subsequent investigations have corroborated his original observations. In Figure 4, existing placer operations are overlain upon bedrock geology generalized from Tempelman-Kluit (1978). All existing placer operations either overlie or are topographically downslope from Cretaceous age granites and granodiorites or their volcanic or subvolcanic equivalents, the Mount Nansen Group (Fig. 4). Placer gold in these districts either originated within these rocks or in mineralized zones where these rocks contact country rock. All of the placers in these districts have formed between the end of the pre-Reid glaciations and the Reid

Glaciation. If Tertiary weathering produced placers similar to the White Channel Gravel, they would have been incorporated in to pre-Reid glacial deposits.

Placers in the Nansen-Big Creek districts are usually found resting on deeply weathered bedrock (e.g., Revenue Creek) or on cohesive bouldery clay-rich diamicton (e.g., W.D.P. Placers in upper Klaza River basin). The bouldery clay-rich diamictons are interpreted to be till or reworked till because of the presence of bullet- and flatiron-shaped striated boulders indicative of glacial action. It may be concluded, based on the position of the placers, that following the pre-Reid glaciations, streams in Dawson Range degraded their beds to bedrock or to clay-rich erosionally resistant glaciogenic diamicton. It was during this period of fluvial degradation that the placers were formed. Erosion through unknown but significant thicknesses of glacial sediments likely concentrated their gold contents as well as gold contributed by direct erosion of bedrock or erosion of the colluvial mantle.

Placers along second and third order streams were eventually buried by Reid-age outwash and related aggradation. "Gulch" placers on higher and steeper first order streams were buried by angular, poorly sorted gravels (commonly with ventifacted clasts) delivered to the channel by creep of the colluvial mantle and progradation of small steep alluvial fans. This aggradation cannot be linked to any specific glaciation or interglaciation at present. Placers along Back Creek on the west side of the Victoria Creek basin (Fig. 1) are capped by such coarse angular gravels.

SUGGESTIONS FOR FUTURE PROSPECTING

Five recommendations may be made with respect to future placer prospecting in Dawson Range:

1. The factors that led to the deposition of known gold placers in the Nansen-Big Creek placer district should also have been coincident elsewhere in the Dawson Range. Areas suggested for particular attention include drainage basins within or partly within the outcrop area of the Late Cretaceous granites and Mount Nansen Group (Fig. 4).
2. Placers that may exist on some of the larger streams such as Big Creek and Lonely Creek may be buried under a considerable depth of valley fill due to extensive aggradation during the Reid Glaciation. Smaller steep first order tributaries in the upper parts of basins have the least overburden and are likely the most economically viable prospects.
3. Exploration should be concentrated beyond the limit of the Reid Glaciation because glacial ice would have likely removed preexisting placers.
4. Existing geological maps and the outcrop pattern shown in Figure 4 should only be regarded as guides because outcrops are sparse and colluvial mantles are thick in Dawson Range. Clasts of granitics or Mount Nansen Group lithologies present in stream gravels or in

Figure 4. Superposition of present and past placer mines and distribution of Late Cretaceous granitics and Mount Nansen Group from Tempelman-Kluit (1979). HC – Hayes Creek, BC – Big Creek, SC – Seymour Creek, StC – Stoddart Creek, KR – Klaza River, MC – Magpie Creek, NC – Nansen Creek, VC – Victoria Creek, UN – unnamed creek.

colluvium (exclusive of areas that received Reid outwash) indicate that these potential gold source rocks are present within the basin whether or not they have been mapped and should be regarded as indicators of gold potential.

5. Pre-Reid outwash may locally constitute low grade placers. Glacial erosion acted upon a weathered bedrock mantle relict from Tertiary climates. This mantle was likely locally enriched in gold which may have been further concentrated by glaciofluvial sorting.

ACKNOWLEDGMENTS

The author thanks the many placer miners of the Nansen-Big Creek placer district for access to their claims and for their hospitality. Particular thanks go to Wayne and Pat Perry, Jack Coglein, Frank Cochran, Aurchem Exploration, John Gow and Torfin Djuckenstein. The author benefitted from joint fieldwork and discussions with Steve Morison and Bill Leberge of the Department of Indian and Northern Affairs and Charles Tarnocai of Agriculture Canada. Paleoeological information was supplied by Bob Mott of the Paleoeology Section of Terrain Sciences Division, Geological Survey of Canada. This report benefitted from a constructive review by Brent Ward and his comments are gratefully acknowledged.

REFERENCES

- Atmosphere Environment Service**
 1982a: Canadian climate normals, temperature and precipitation: the North--British Columbia; Atmospheric Environment Service, UDC:551.582(711), 268 p.
 1982b: Canadian climate normals, temperature and precipitation: the North - Yukon Territory and Northwest Territories; Atmospheric Environment Service, UDC:551.582(712), 268 p.
- Bostock, H.S.**
 1936: Carmacks district, Yukon; Geological Survey of Canada, Memoir 189, 58 p.
 1966: Notes on glaciation in central Yukon Territory; Geological Survey of Canada, Paper 65-56, 18 p.
- Boyle, R.W.**
 1979: The geochemistry of gold and its deposits; Geological Survey of Canada, Bulletin 280, 584 p.
- Cairnes, D.D.**
 1914: Southwestern Yukon; Geological Survey of Canada, Summary Report 1914, p. 10-33.
- Drumke, J.S.**
 1964: A systematic survey of *Corylus* in North America; Ph.D. thesis, University of Tennessee, 142 p.
- Grond, H.C., Churchill, S.J., Armstrong, R.L., Harakal, J.E., and Nixon, G.T.**
 1984: Late Cretaceous age of the Hutshi, Mt. Nansen, and Carmacks groups, southwestern Yukon; Canadian Journal of Earth Sciences, v. 21, p. 554-558.
- Hughes, O.L.**
 1990: Surficial geology and geomorphology, Aishihik Lake, Yukon Territory; Geological Survey of Canada, Paper 87-29, 23 p.
- Hughes, O.L., Campbell, R.B., Muller, J.E., and Wheeler, J.O.**
 1969: Glacial limits and flow patterns, Yukon Territory south of 65 degrees north latitude; Geological Survey of Canada, Paper 68-34, 9 p.
- Jackson, L.E., Jr., Ward, B., Duk-Rodkin, A., and Hughes, O.L.**
 1990: The last Cordilleran Ice Sheet in Yukon Territory; in *The Cordilleran Ice Sheet*, (ed.) Jackson, L.E., Jr. and Clague, J.J.; Géographie physique et Quaternaire, v. 45, p. 341-354.
 1991: The last Cordilleran ice sheet in southern Yukon Territory; Géographie physique et Quaternaire, v. 45, p. 341-354.
- Mankinen, E.A. and Dalrymple, G.B.**
 1978: Revised geopolarity time scale for the interval 0-5 m.y.; Journal of Geophysical Research, v. 84, p. 615-626.
- Mathews, W.H.**
 1986: Physiographic map of the Canadian Cordillera; Geological Survey of Canada, Map 1701A, scale 1:5 M.
- Matthews, J.V., Schweger, C.E., and Hughes, O.L.**
 1990: Plant and insect fossils from the Mayo Indian Village section (central Yukon): new data on middle Wisconsinan environments; Géographie physique et Quaternaire, v. 44 p. 15-26.
- McConnell, R.G.**
 1905: Report on the Klondike gold fields; Geological Survey of Canada, Annual Report, v. 14, 1901, Part B, p. 1B-71B.
- Naeser, N.D., Westgate, J.A., Hughes, O.L., and Péwé, T.L.**
 1982: Fission-track ages of late Cenozoic distal tephra beds in the Yukon Territory and Alaska; Canadian Journal of Earth Sciences, v. 19, p. 2167-2178.
- Péwé, T.L.**
 1959: Sand wedge polygons (Tessellations) in the McMurdo Sound region, Antarctica. A progress report; American Journal of Science, v. 257, p. 545-552.
- Shackleton, N.J., Berges, A., and Peltier, W.R.**
 1990: An alternate astronomical calculation of the lower Pleistocene time-scale based on ODP site 677; Transactions of the Royal Society of Edinburgh: Earth Sciences, v. 81, p. 251-261.
- Smith, C.A.S., Tarnocai, C., and Hughes, O.L.**
 1986: Pedological investigations of Pleistocene and glacial drift surfaces in the central Yukon; Géographie physique et Quaternaire v. 40, p. 29-37.
- Tarnocai, C. and Schweger, C.E.**
 1991: Late Tertiary and early Pleistocene paleosols in northwestern Canada; Arctic, v. 44, p.1-11.
- Tarnocai, C. and Valentine, K.W.G.**
 1989: Relict soil properties of the Arctic and subarctic regions of Canada; in *Paleopedology*, (ed.) Broger, A. and Catt, J.A.; Catena Supplement 16, p. 9-39, Cremlingen-Desteldt, Germany.
- Tempelman-Kluit, D.K.**
 1974: Reconnaissance geology of Aishihik, Snag, and part of Stewart River map areas, west-central Yukon; Geological Survey of Canada, Paper 73-41, 97 p.
 1978: Geology of the Laberge (105E) and Carmacks (115I) Yukon Territory; Geological Survey of Canada, Open File 1101.
 1979: Transported cataclastite, ophiolite and granodiorite in Yukon: evidence of arc-continent collision; Geological Survey of Canada, Paper 79-14, 27 p.
 1980: Evolution of the physiography and drainage of southern Yukon; Canadian Journal of Earth Sciences, v. 17, p. 1189-1203.

Geological Survey of Canada Project 800001

Geology and structure of the Teslin suture zone and related rocks in parts of Laberge, Quiet Lake, and Teslin map areas, Yukon Territory

R.A. Stevens¹ and P. Erdmer¹

Cordilleran Division

Stevens, R.A. and Erdmer, P., 1993: Geology and structure of the Teslin suture zone and related rocks in parts of Laberge, Quiet Lake, and Teslin map areas, Yukon Territory; in Current Research, Part A; Geological Survey of Canada, Paper 93-1A, p. 11-20.

Abstract: This report outlines the geology of four areas mapped in 1992 and describes in detail the structure along one transect across the Teslin suture zone. Several units are recognized and include: hornblende±augite diorite or gabbro (**Mhdg**), conglomeratic grit of the Boswell Formation (**PBs**), felsic to mafic schist and gneiss, quartzite, metaplutonic rock, and pegmatite (**PMv**), meta-hornblende diorite or gabbro (**PMhdg**), biotite±sillimanite±muscovite schist and gneiss (**Pn+?**), and autochthonous North American rocks (**NA?**). Along the transect seven structural domains are recognized. Each is characterized by distinct foliation and mineral lineation orientations. Structures along this transect record two deformation phases: an early penetrative ductile deformation, and late folding. Mapping along the margin of the suture zone shows that faults and undeformed volcanic rocks mark the western contact.

Résumé : Dans le présent rapport, on esquisse la géologie de quatre secteurs cartographiés en 1992, et l'on décrit en détail la structure le long d'un transect suivi de part et d'autre de la zone de suture de Teslin. Parmi les nombreuses unités reconnues, on remarque : une diorite ou un gabbro à hornblende augite (**Mhdg**), un grès grossier conglomératique de la Formation de Boswell (**PBs**), un schiste et un gneiss felsiques à mafiques, un quartzite, des roches métaplutoniques et une pegmatite (**PMv**), une métadiorite ou un métagabbro à hornblende (**PMhdg**), un schiste et un gneiss à biotite±sillimanite±muscovite (**Pn+?**) et des roches autochtones, nord-américaines (**NA?**). Le long du transect, ont été identifiés sept domaines structuraux. Chacun est caractérisé par des orientations distinctes de la foliation et de la linéation minérale. Les structures observées le long de ce transect témoignent de deux phases de déformation: une déformation ductile initiale, de type pénétratif, et un plissement tardif. La cartographie de la marge de la zone de suture montre que la présence de failles et de roches volcaniques non déformées caractérise le contact occidental.

¹ Department of Geology, University of Alberta, #1-26 Earth Sciences Building, Edmonton, Alberta T6G 2E3

INTRODUCTION

The Teslin suture zone, a part of the Yukon-Tanana composite terrane (Kootenay terrane of Wheeler et al., 1991) of southern Yukon and east-central Alaska, marks the fundamental boundary between deformed autochthonous North American rocks of the Omineca Belt to the east and accreted terranes of the Intermontane Belt to the west. It includes a variety of S-, L-S, and L-tectonites derived from sedimentary, volcanic, and plutonic rocks metamorphosed under greenschist to amphibolite facies conditions (Stevens, 1991, 1992). Current models of formation of the suture zone hypothesize that its

rocks were the product of deformation within the deep-seated portion of a west-dipping Permo-Triassic subduction complex west of ancient North America. The rocks were subsequently thrust eastward onto North American strata in the Early Jurassic, and the Teslin suture zone is interpreted to represent the root zone to these obducted rocks (Hansen, 1991, 1992; Tempelman-Kluit, 1979).

Exposures of Teslin suture zone rocks studied for this project underlie parts of Laberge (NTS 105E), Quiet Lake (NTS 105F), and Teslin (NTS 105C) map areas. The geology of part of all three map areas was described by Lees (1936). The Quiet Lake and Laberge map areas were mapped by

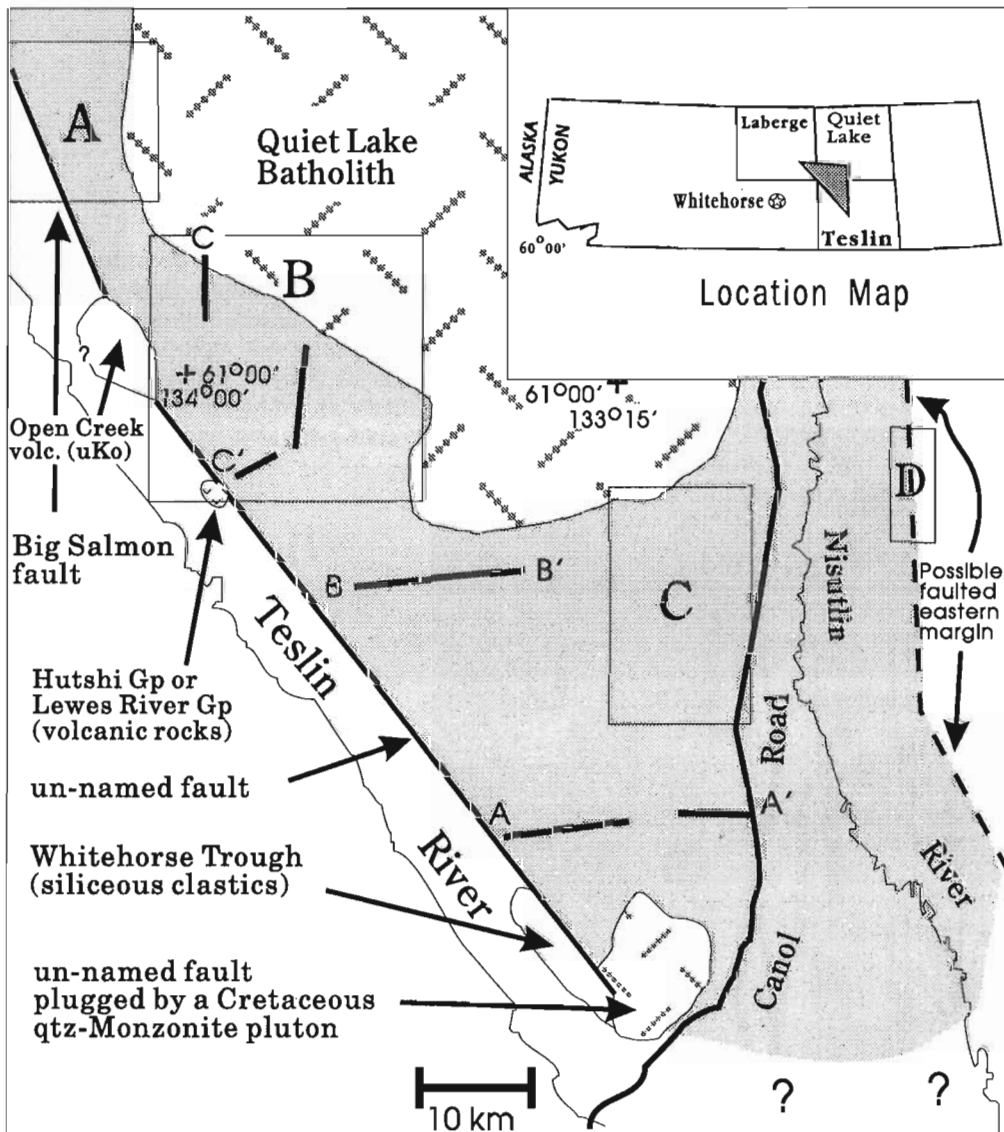


Figure 1. Location map, showing the part of the Teslin suture zone considered in this study (grey shading), the type of contacts that define the margins of the Teslin suture zone, the location of three structural transects described in Stevens (1992) (AA' and BB') or in this report (CC') and the location of four map areas (A-D) described in this report.

Tempelman-Kluit (1977, 1984) and the geology of the Teslin map area was described by Mulligan (1963). The Teslin map area is being remapped at 1:50 000 and 1:250 000 scales by the Geological Survey of Canada (Gordey, 1991, 1992). Teslin suture zone-related rocks in the southern half of the Teslin map area are the focus of a continuing study by Gareau (1992).

This report outlines the geology of four areas (A-D) mapped in 1992 (see Fig. 2-6), and describes the structure along one transect (CC' on Fig. 1 and 4). Many of the units recognized in areas A-D were described by Stevens (1991, 1992) (units **PMs**, **PMm**, **PMgp**, **PMga**, **Kqm**, **KRM**, and **Mtqd**) in adjacent areas and are not described in detail here. Unit **OD_N** (see Stevens, 1992) is equivalent to unit **PMgp** in this report (see discussion).

MAP AREA A

Many of the units mapped in area A (Fig. 3) can be correlated with rocks to the south described by Stevens (1991, 1992) (units **PMs**, **PMm** and **Kqm**) or in this report (**PMgr**), and only brief descriptions of these are given below. Two new units (**Mhdg**, **PBs**) and one sub-unit (**PMsm**) are described in detail.

Unit **PMs** rocks are muscovite- and quartz-rich schist with minor muscovite-bearing quartzite, calcareous schist, and marble. Garnetiferous schist occurs in the northern part of the area. Unit **PMs** rocks east of the Loon Lakes locally contain biotite and chlorite. Marble (**PMm**) outcrops in the northern part of the area. Quartz-monzonite of the Quiet Lake Batholith (Tempelman-Kluit, 1977) (**Kqm**) outcrops along the western edge of the map area. Margin parallel foliation is developed within 200-300 m of the contact. Unit **PMgr** is medium to dark green chlorite-actinolite greenstone and compositionally banded chlorite-actinolite-epidote schist.

Schist (**PMsm**)

Brown to green weathering fine- to medium-grained chlorite-muscovite-actinolite-biotite quartzofeldspathic schist occurs in the central part of the area. Locally, medium grained phases suggest derivation from an intermediate plutonic rock. These rocks are grouped in subunit **PMsm**, because they are consistently more mafic (containing more chlorite+actinolite+biotite than muscovite) and less schistose than other **PMs** rock.

Hornblende-augite diorite or gabbro (**Mhdg**)

East of Loon Lakes occurs a 1 km² body of grey-green to slightly red weathering, massive, medium grained hornblende diorite to gabbro. Locally, the pluton is porphyritic, with up to 30% phenocrysts of medium- to coarse-grained hornblende and augite. The main mass of rock and the matrix in porphyritic phases consist of approximately 40-60% hornblende, 40-60% altered feldspar, and minor quartz. Hints of an igneous flow fabric are seen locally. The body includes screens of country rock (mostly quartzite and schist). The

intrusive relationship to metamorphic rock of unit **PMs**, the massive texture, local hints of flow banding and the abundance of hornblende are similar to unit **Mtqd** mapped in the Sawtooth Range (Stevens, 1992) (Fig. 4). **Mhdg** may thus be part of an intrusive suite that includes unit **Mtqd**.

Boswell Formation (**PBs**)

The Boswell Formation (**PBs**) (Tempelman-Kluit, 1984) west of Loon Lakes consists of black-weathering fine- to medium-grained, unmetamorphosed, conglomeratic grit with clasts of chert, black fine grained rock, and possible hornblende or augite grains.

Regional faults

Previous maps of the area show two large faults, the d'Abbadie fault (Hansen, 1989, 1991) and the Big Salmon fault (Tempelman-Kluit, 1984). The d'Abbadie fault was interpreted to trend north and separate the Teslin suture zone proper in the west from orthogneiss to the east that is structurally similar to rock of the Teslin suture zone proper but which has undergone a different cooling history (Hansen, 1989). The Big Salmon fault was shown to trend northwest, 3-4 km east of Loon Lakes (Fig. 3) and to separate Teslin suture zone rock in the east from unmetamorphosed allochthonous rocks of the Semenof Hills Block (including the Boswell Formation) to the west.

Our mapping did not locate either of the faults in the proposed locations. In both cases the contacts are interpreted as fabric-parallel contacts within the Teslin suture zone (Fig. 3). We conclude that the d'Abbadie fault does not extend into the area as proposed by Hansen (1989, 1991), and that it terminates to the north or west. We also conclude that the Big Salmon fault is located farther west than interpreted by Tempelman-Kluit (1984), likely in the valley of the Loon Lakes separating unit **PMs** in the east from the Boswell Formation in the west.

MAP AREA B

Most of the units in map area B (Fig. 4) (**PMs**, **PMgp**, **PMm**, **PMga**, **Kqm**, **KRM**, **Mtqd**) were described by Stevens (1991, 1992). A new description of unit **PMgr** (Stevens, 1992) is presented that encompasses the results of the new mapping, and two new units are defined (**PMv** and **PMhdg**).

Mafic schist and greenstone (**PMgr**)

The most common rock types of this unit are: medium to dark green foliated and locally lineated actinolite-chlorite-epidote±biotite±hornblende schist and greenstone; light to dark green, sheared, compositionally banded chlorite-epidote-actinolite±biotite quartzofeldspathic schist; medium to dark green, massive, locally porphyritic hornblende-actinolite-chlorite-epidote greenstone; and sheared amphibolite. Massive hornblende-bearing greenstone is confined to

Teslin suture zone units

- PMs Quartz-muscovite±chlorite±epidote±biotite±amphibole±garnet schist to impure quartzite and quartzite
- PMsm Chlorite-muscovite-actinolite-biotite quartzofeldspathic schist
- PMm Marble
- PMgr Actinolite-chlorite-epidote±biotite±hornblende schist and greenstone
- PMga Metagabbro
- PMgp Graphitic phyllite
- PMv Felsic to mafic schist and gneiss, quartzite, meta-plutonic rock and pegmatite
- PMhdg Meta-hornblende diorite or gabbro
- TSZ? Rock correlated with the Teslin suture zone (map area D)

Autochthonous North American units?

- Pn+? Biotite±sillimanite±muscovite schist, gneiss and quartzite with sills and dykes of pegmatite and granitic rock
- NA? Autochthonous North American strata? (map area D)

Other units

- PBs Conglomeratic grit (Boswell Formation)
 - Mhdg Hornblende±augite diorite or gabbro
 - Mtqd Hornblende tonalite to quartz diorite
 - Kqm Biotite quartz monzonite (QLB - Quiet Lake Batholith)
 - K_{RM} Dacite(?), quartz monzonite porphyry (Red Mountain)
 - uKo Open Creek Volcanics
- Limit of outcrop or mapping
- Contacts (defined, approx.)

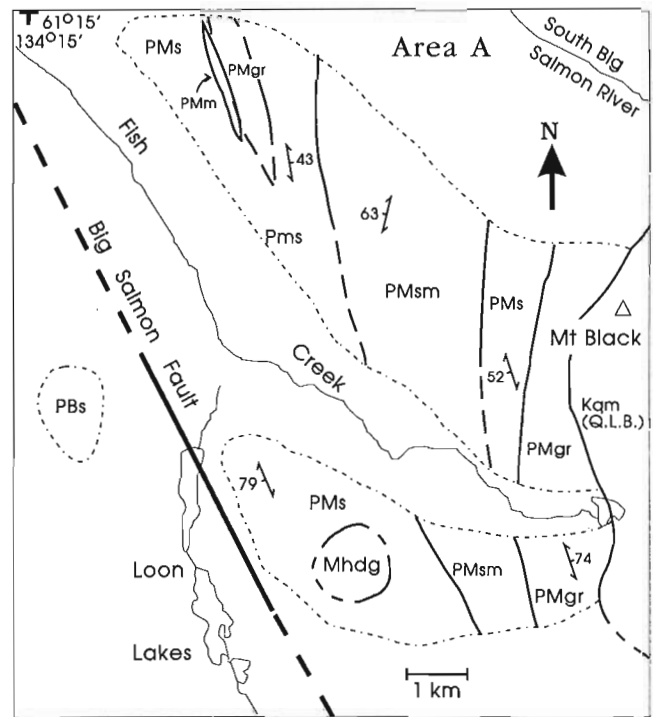


Figure 3. Simplified geology of area A.

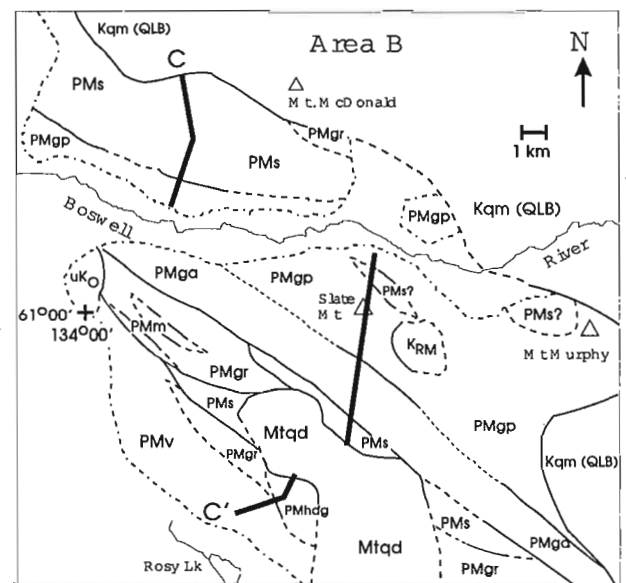


Figure 4. Simplified geology of area B.

Figure 2. Legend for map areas A-D (Fig. 3-6). Teslin suture zone units consist of rock that shows the development of penetrative ductile deformation fabrics. Autochthonous North American units consist of rock tentatively correlated as deformed autochthonous North American strata. Other units consist of rock that lacks a foliation.

the area southeast of unit **Mtqd** (Fig. 4). Bands and pods of marble tens of metres across are common within the unit and several of these are shown on Figure 4.

The rocks of this unit are likely derived from basaltic to andesitic flows and tuffs deposited in or near a shallow water environment where small carbonate reefs or banks formed. In addition, rocks of this unit are interleaved, with gabbro of unit **PMga**, along their contact and within unit **PMga**. This suggests that the two units are genetically related, especially since **PMga** gabbro is not interlayered with other units.

Felsic to mafic schist and gneiss, quartzite, meta-plutonic rock and pegmatite (PMv)

A range of rock types, interlayered at a scale of 10 cm to several hundred metres, comprise unit **PMv**. The most common members are: sheared quartzite and muscovite quartzite, quartz-muscovite schist, biotite-muscovite-quartz-amphibole-garnet schist and gneiss, biotite-amphibole-chlorite-epidote schist and gneiss, amphibolite, massive to sheared hornblende-bearing tonalite, quartz-diorite and diorite, and massive felsic pegmatite. Pegmatite occurs as thin apparently sheared wisps and bands and as massive dykes a few metres wide.

The variety of rock types and their interlayering suggest that, prior to deformation and metamorphism, the assemblage consisted of sedimentary and possibly volcanic rocks intruded by dykes and small plugs of intermediate composition.

Meta-hornblende diorite or gabbro (PMhdg)

South of unit **Mtqd** (Fig. 4), is an area of moderately deformed to ultramylonitic S-, L-S, and L-tectonites of dark green and white hornblende diorite or gabbro and amphibolite. Cutting these rocks are massive, felsic to mafic dykes including a feldspar porphyritic phase, hornblende and hornblende diorite. Most of the mafic intrusions are likely related to unit **Mtqd** exposed to the north. Foliation surfaces generally strike northeast and dip southeast, an orientation uncommon elsewhere in the suture zone.

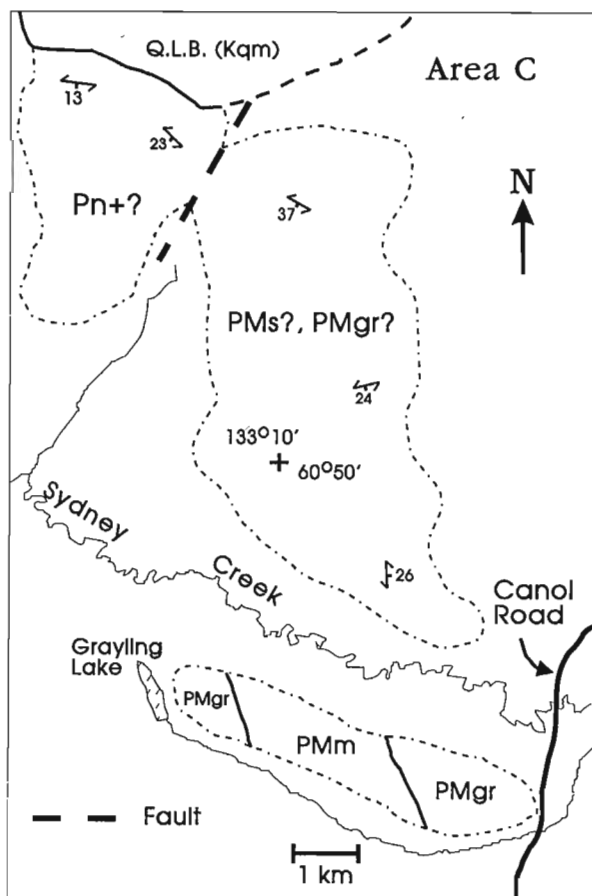


Figure 5. Simplified geology of area C.

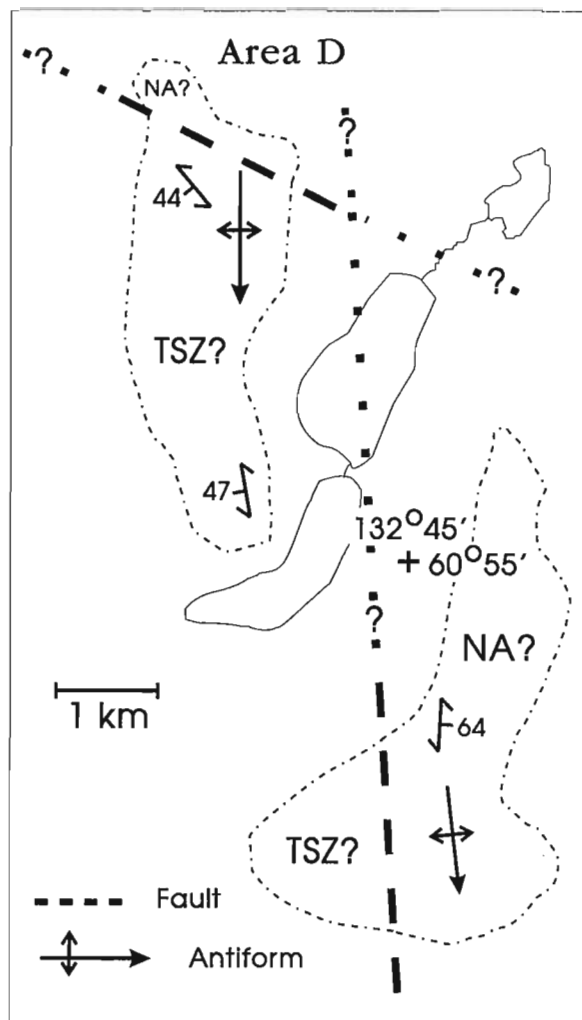


Figure 6. Simplified geology of area D.

MAP AREA C

Units **PMgr** and **PMm** outcrop south of Sydney Creek and east of Grayling Lake (see Stevens, 1992 and this report) (Fig. 5).

Biotite±sillimanite±muscovite schist, gneiss and quartzite with sills and dykes of pegmatite and granitic rock (Pn+?)

North of Sydney Creek and south of the Quiet Lake Batholith (Fig. 5) occur brownish grey to red, medium grained biotite±sillimanite±muscovite quartzofeldspathic schist to gneiss and red-weathering to strongly gossaned biotite-pyrite quartzite to quartz-schist. These are cut by and include generally massive sills and dykes of biotite-bearing quartz-monzonite and felsic pegmatite. Schist and gneiss are strongly

sheared L-S tectonites with mineral lineations defined by quartz rodding and by alignment of biotite and sillimanite. The strike of foliation surfaces varies and dips average between 10° to 20°.

This unit is distinguished from other units by the presence of abundant sillimanite, local gneissic character, the abundant dykes and sills, and the subhorizontal foliation. Similar rocks in the Quiet Lake map area are included in unit **Pn+**, and are interpreted to be metamorphosed autochthonous rocks of the Omineca Belt (Tempelman-Kluit, 1977).

Heterogenous meta-sedimentary, meta-tuffaceous and meta-volcanic rocks (PMs, PMgr)

North of Sydney Creek and west of the unit described above is a unit of considerable lithological variability (Fig. 5). The main rock types are: quartzite, marble, quartz-chlorite±

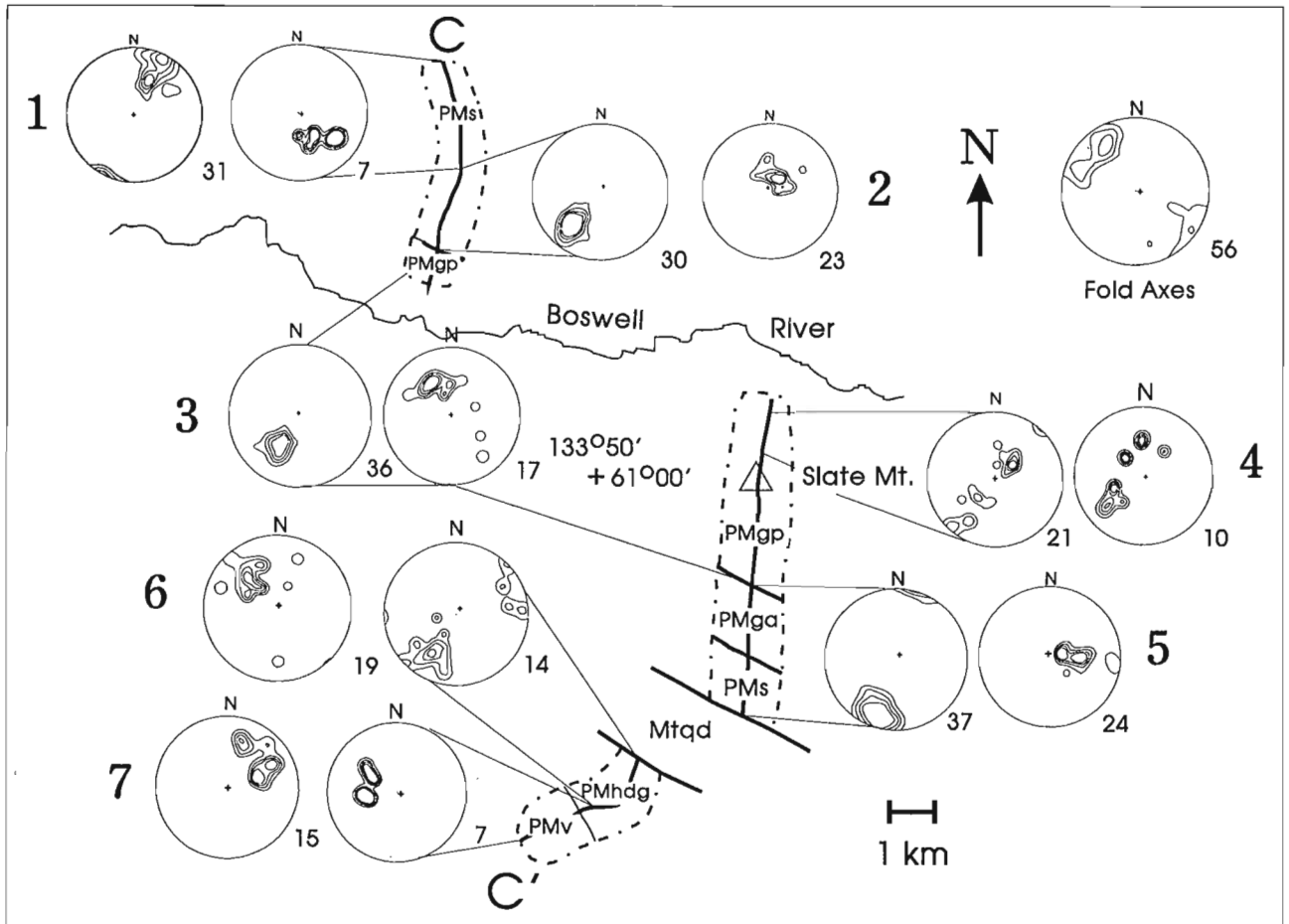


Figure 7. Strip map for transect CC' showing rock types along the transect. Stereographic projection plot are for the seven structural domains recognized in this transect. The bold number represents the domain, the left stereonet shows poles to foliation and the right stereonet, mineral/stretching lineation orientations. Contours are densities expressed as multiples of a uniform density with contours at densities of 3, 6, 9, and 12.

muscovite±actinolite schist, light to medium green, compositionally banded chlorite-epidote±actinolite-quartz schist, and actinolite-chlorite±hornblende greenstone. Green compositionally banded schist likely has tuffaceous parentage and greenstone volcanic parentage. Foliation surfaces have variable strikes, and dips between 20° and 35°. These rocks are interpreted as part of unit **PMs** possibly intercalated with unit **PMgr**.

MAP AREA D

North American rocks? (NA?)

The northern and eastern parts of area D (Fig. 6) include carbonate (locally crinoidal), impure muscovite- and chlorite-bearing metasandstone to meta-arkose, minor interlayered graphitic phyllite, and biotite-chlorite±actinolite greenstone. Most areas show weak to moderate tectonic foliation, with local development of mylonitic fabric. Quartz microstructures show evidence of recrystallization and fracturing. At least one open antiform is present (see Fig. 6). Metamorphism locally reached biotite grade, but most rocks are not strongly metamorphosed or recrystallized. Rocks similar in composition, degree of metamorphism and state of deformation outcrop in the Thirtymile Range, to the southeast (S.P. Gordey, pers. comm., 1992). Recent mapping led Gordey (1992) to suggest that strata in the Thirtymile Range are of autochthonous North American affinity.

Teslin suture zone rock? (TSZ?)

To the south and west on Figure 6 occur red-brown to green weathering, locally compositionally banded biotite-epidote±actinolite greenstone or schist. In places, they are interbanded with quartz-muscovite±biotite schist to impure quartzite and in one place with quartz-muscovite graphitic schist. The rocks are mostly L-S tectonites with foliation surfaces that strike south to southeast and dip moderately southwest or northeast. One map-scale antiform is present (Fig. 6). Rock similar in composition, metamorphic grade and state of deformation outcrop west of the Nisutlin River and are interpreted to be part of the Teslin suture zone (Stevens, 1992). These rocks are tentatively correlated with the Teslin suture zone, (units **PMgr** and/or **PMs**).

Strata in area D are folded and show widespread crenulations, cleavage, and at least two regional antiforms. Fold axes trend south and plunge 5-10°. Steep faults separate units **NA?** and **TSZ?**. One fault trends north across the centre of the area and the second trends west-northwest along the top of the map area. Rock of unit **NA?** north of the second fault may have been uplifted and may represent in part, the type of strata that unit **TSZ?** to the south of the fault are resting on.

STRUCTURAL TRANSECT

One detailed structural transect was completed during the summer of 1992 (CC' on Fig. 1). This transect complements two previous transects (Stevens, 1992) (AA' and BB' on Fig. 1). The CC' transect comprises three segments totalling 15 km. Measurement stations located 150-250 m apart, resulted in 70 stations across the transect. Oriented samples were collected at each station.

Seven structural domains are recognized. Some are rock type independent, meaning that the boundaries of the domain are not controlled by a change in rock type. In other cases, a domain is confined to, and likely controlled by, a single rock type. Figure 7 is a strip map of the transect, with contoured stereoplots of fabric orientation for each domain. Fold axis measurements along this transect are summarized in a separate stereoplot (see Fig. 7).

Domain 1

Moderately to strongly deformed S and L-S tectonites with steeply southwest-dipping foliation and crenulation hinge lineations characterize this domain. A few mineral lineations occur near the southern edge of the domain. A spaced (5-30 cm) crenulation cleavage has developed locally, which strikes roughly southeast and dips moderately southwest. These are late cleavage surfaces that cut earlier fabrics. Shear sense from the crenulation asymmetry between cleavage surfaces is hanging wall-up, or southwest face thrust to the northeast during folding (Bell and Johnson, 1992) (Fig. 8).

The northern boundary of the domain is placed at the edge of the Quiet Lake Batholith. The southern boundary is a 200-300 m wide zone where foliation surfaces switch from southwest to northeast dipping.

Domain 2

Strongly deformed to mylonitic L-S tectonites with steeply northeast dipping foliation and lineations defined by stretched and preferentially oriented minerals such as quartz, muscovite, and chlorite characterize this domain. Crenulation and mesoscopic folds are developed together with a spaced (5-30 cm) cleavage that strikes west-northwest and dips moderately northeast. Crenulation asymmetry between cleavage surfaces indicates that the hanging wall moved down to the northeast.

The southern boundary of the domain is marked by a change from muscovite- and quartz-rich schist to graphitic phyllite.



Figure 8. Shear sense from the crenulation asymmetry between cleavage surfaces is hanging wall-up, which for this figure means the southwest face was thrust to the northeast.

Domain 3

Moderately to strongly deformed S and L-S tectonites of graphitic phyllite with moderately to steeply northeast dipping foliation and crenulation hinge lineations characterize this domain. Mineral lineations are best developed north of Slate Mountain in siliceous and/or schistose graphitic phyllite. A crenulation cleavage is developed locally, with crenulation asymmetry indicating that the hanging wall moved down the northeast.

The northern and southern boundaries of this domain are defined by the contacts of the graphitic phyllite unit.

Domain 4

Domain 4 is characterized by closed to tight folds with rounded to chevron hinges, wavelengths of 10-30 m and amplitudes of approximately 10-40 m. The folds occur in an area dominated by strong L-S tectonites of quartz-chlorite±muscovite schist within the graphitic phyllite unit of domain 3. Poles to foliation surfaces approximate a great

circle (Fig. 7) whose pole, oriented at 309/2, is the fold axis for the domain. This orientation is similar to the average orientation (311/9) for all fold axis measurements from the transect. Mineral/stretching lineation orientations are variable, possibly due to folding of the tectonites.

Domain 5

Domain 5 includes two rock types. Gabbro of unit **PMga** occurs to the north. The gabbro is massive to weakly deformed, with local discrete zones of high strain. L-S tectonites are developed in these zones and rarely elsewhere in the unit. Lineations are defined by aggregates of feldspar, pyroxene, and amphibole. The southern half of the domain includes a variety of interleaved schistose rocks of unit **PMs**. These are strongly deformed to mylonitic L-S tectonites. Lineations are defined by quartz rodding and alignment of elongate muscovite, biotite, amphibole, and quartz. Folding has not developed in this domain.

The northern boundary coincides with the edge of unit **PMgp** and the southern boundary is the intrusive contact with unit **Mtqd**.

Domain 6

Moderately deformed to ultramylonitic S-, L-S, and L-tectonites of unit **PMhdg**, with foliation surfaces that strike northeast and dip moderately to steeply southeast characterize domain 6. Mineral lineations, defined by elongate trains of feldspar or by grains of amphibole, show a fair degree of scatter. Outcrop-scale folds are present locally and may be responsible for the scatter in lineation orientations.

The northern boundary of the domain is an intrusive contact with unit **Mtqd**, and the southern boundary is placed at an inferred fault, where the northeast-striking foliation surfaces change to west-northwest striking foliation surfaces.

Domain 7

Variably deformed rock of units **PMhdg** and **PMv** with northwest-striking and southwest-dipping foliation surfaces marks this domain. L-S tectonites and late folds are developed locally.

The southern boundary of the domain is unconstrained.

DISCUSSION

Two deformation events or phases of a single event are recorded in the Teslin suture zone (Fig. 1). The first was a penetrative ductile deformation event that produced mylonite and S-, L-S, and L-tectonites under greenschist to lower amphibolite facies metamorphic conditions. The second was a folding event, under similar metamorphic conditions that produced widespread crenulation of earlier fabrics and development of a cleavage.

The orientation of fabrics along CC' is characteristic of much of the Teslin suture zone considered in this study. For example early schistosity and mylonitic foliation generally strike northwest-southeast, and dip either northeast or southwest, and mineral lineations which form local orientation clusters (Fig. 7) show a wide range of orientation between the clusters. In addition, second phase folding does not appear responsible for these variations, because attempts at rotating structures about common fold axes from the map area were unsuccessful in bringing structures from adjacent or similar domains into a common orientation. We believe that most of the variations in fabric orientations developed during the early ductile deformation.

Strain partitioning throughout the map area is primarily controlled by rock type. Relatively incompetent rocks such as mica schist and graphitic phyllite are most highly deformed, followed by mafic and quartzofeldspathic schist and finally by metaplutonic rocks. The fabrics that develop are also controlled by rock type. For example, graphitic phyllite shows strong crenulation lineations but few mineral lineations, whereas schist, especially quartz rich varieties, shows strong development of mineral and fold lineations; metaplutonic rocks show little of either.

A previously defined graphitic phyllite unit (OD_N) (Stevens, 1991, 1992) is equivalent to unit **PMgp** in this report. This graphitic phyllite was correlated with the autochthonous Nasina Formation by Stevens (1991). Assignment of the graphitic phyllite to the Nasina facies (Stevens, 1991) is considered inappropriate because present mapping shows that it may be part of a single depositional sequence that includes rocks of unit **PMs**. Unit **PMs** is correlated with the Nisutlin Allochthon (Stevens, 1991). In the contact zone between **PMs** and **PMgp**, graphite first appears in unit **PMs** 400 to 600 m from the contact, and within 100-200 m one of the main rock types is quartz-muscovite-graphite schist. South of the contact, muscovite-graphite schist is interlayered with graphitic phyllite over 100-200 m. This suggests that the contact was originally depositional and that the two units may result from different depositional environments or sources within a continuous sedimentary sequence.

REGIONAL EXTENT OF THE TESLIN SUTURE ZONE

North of the study area (Fig. 1) the Teslin suture zone trends across the Laberge map area to the southern part of the Glenlyon map area (Tempelman-Kluit, 1979; Hansen 1989). Results presented by Stevens (1991, 1992) and in this report show that the suture zone continues southward from Laberge map area to the Canol Road in central Teslin map area. South of the Canol Road, the distribution of Teslin suture zone rock is unclear (see Gareau, 1992). The western margin of the suture zone in Figure 1 is marked by faults or undeformed volcanic rocks. The Big Salmon fault marks the western contact in the northern part of

the map area. It is masked to the south by volcanic rocks of unit **UKO** which overlie Teslin suture zone rocks. From the northwest corner of the Teslin map area ($61^{\circ}00'N$, $134^{\circ}00'W$) to the Canol Road, the contact is a second fault (unnamed) (see Gordey, 1991). Volcanic rocks equivalent to the Hutshi or Lewes River groups in the Whitehorse map area (Wheeler, 1961) and siliceous clastic rock of the Whitehorse trough (unit 9 of Mulligan, 1963) were mapped west of this unnamed fault (Fig. 1). North of the Canol Road, a massive biotite quartz-monzonite pluton cuts the fault. The location of the eastern margin of the suture zone is unclear. It may pass through map area D (Fig. 1 and Fig. 6) or, if Teslin suture zone rocks in that map area are parts of klippen, the contact may lie farther west, possibly in the Nisutlin River valley.

ACKNOWLEDGMENTS

Field work was supported by a joint EMR/NSERC research agreement to P. Erdmer and a Northern Scientific Training Program grant from the Department of Indian Affairs and Northern Development, a grant from the Canadian Circumpolar Institute of the University of Alberta and an NSERC Post Graduate Scholarship awarded to R.A. Stevens. Logistical support provided by the Department of Indian Affairs and Northern Development and the Geological Survey of Canada is greatly appreciated. S.P. Gordey is thanked for a visit in the field and for reviewing an early version of this report. D.J. Tempelman-Kluit is thanked for reviewing the manuscript. Gord Stretch provided excellent assistance in the field.

REFERENCES

- Bell, T.H. and Johnson, S.E.**
1992: Shear sense: a new approach that resolves conflicts between criteria in metamorphic rocks; *Journal of Metamorphic Geology*, v. 10, p. 99-124.
- Gareau, S.A.**
1992: Report on fieldwork in the southern Big Salmon metamorphic complex, Teslin map area, Yukon Territory; in *Current Research, Part A*; Geological Survey of Canada, Paper 92-1A, p. 267-277.
- Gordey, S.P.**
1991: Teslin map area, a new geological mapping project in Southern Yukon; in *Current Research, Part A*; Geological Survey of Canada, Paper 91-1A, p. 171-178.
1992: Geological fieldwork in Teslin map area, southern Yukon Territory; in *Current Research, Part A*; Geological Survey of Canada, Paper 92-1A, p. 279-286.
- Hansen, V.L.**
1989: Structural and kinematic evolution of the Teslin suture zone, Yukon: record of an ancient transpressional margin; *Journal of Structural Geology*, v. 11, no. 6, p. 717-733.
1991: Mesozoic thermal evolution of the Yukon-Tanana composite terrane: new evidence from $^{40}Ar/^{39}Ar$ data; *Tectonics*, v. 10, no. 1, p. 51-76.
1992: Backflow and margin-parallel shear within an ancient subduction complex; *Geology*, v. 20, no. 1, p. 71-74.

- Lees, E.J.**
1936: Geology of the Teslin-Quiet Lake area Yukon Territory; Geological Survey of Canada, Memoir 203.
- Mulligan, R.**
1963: Geology of the Teslin map area, Yukon Territory (105C); Geological Survey of Canada, Memoir 326.
- Stevens, R.A.**
1991: The Teslin suture zone in northwest Teslin map area, Yukon; in Current Research, Part A; Geological Survey of Canada, Paper 91-1A, p. 271-277.
1992: Regional geology, fabric, and structure of the Teslin suture zone in northwest Teslin map area, Yukon Territory; in Current Research, Part A; Geological Survey of Canada, Paper 92-1A, p. 287-295.
- Tempelman-Kluit, D.J.**
1977: Quiet Lake (105F) and Finlayson Lake (105G) map areas, Yukon; Geological Survey of Canada, Open File 486.
- Tempelman-Kluit, D.J. (cont.)**
1979: Transported cataclasite, ophiolite and granodiorite in Yukon: evidence of arc-continent collision; Geological Survey of Canada, Paper 79-14.
1984: Geology, Laberge (105E) and Carmacks (1151), Yukon Territory; Geological Survey of Canada, Open File 1101.
- Wheeler, J.O.**
1961: Whitehorse map-area, Yukon Territory (105 D); Geological Survey of Canada, Memoir 312.
- Wheeler, J.O., Brookfield, A.J., Gabrielse, H., Monger, J.W.H., Tipper, H.W., and Woodsworth, G.J.**
1991: Terrane map of the Canadian Cordillera; Geological Survey of Canada, Map 1713A, scale 1:2 000 000.

Geodetic and geological observations from the 1992 Mount Logan expedition, Yukon Territory

Charlie F. Roots¹ and Lisel D. Currie²

Cordilleran Division

Roots, C.F. and Currie, L.D., 1993: Geodetic and geological observations from the 1992 Mount Logan expedition, Yukon Territory; in Current Research, Part A; Geological Survey of Canada, Paper 93-1A, p. 21-26.

Abstract: Mount Logan, the highest point in Canada, was climbed in 1992 and Global Positioning System (GPS) receivers were set up on the summit and at three monumented bedrock sites. GPS data were collected during two 4-hour observations and used to calculate the summit elevation of 5959 m. The GPS surveying equipment performed successfully in cold, high altitude conditions.

The St. Elias Mountains have been rising for at least 25 Ma. The 3 km topographic relief at Mount Logan could allow derivation of cooling curves from which paleo-uplift rates might be inferred. Toward this end variably deformed granite to tonalite and undeformed tonalite were examined on the west side of the mountain. Most samples collected during the climb lack K-feldspar, precluding use of ⁴⁰Ar-³⁹Ar geochronometry on K-feldspar to determine the local cooling history.

Resumé : L'ascension du mont Logan, point culminant du Canada, a été effectuée en 1992. Des récepteurs de «Système de positionnement global» (GPS) ont été installés au sommet et sur trois emplacements rocheux repérés. Les données GPS ont été recueillies pendant deux levés de quatre heures, et utilisées pour calculer l'altitude du sommet, soit 5959 m. Le matériel GPS a fonctionné efficacement malgré les basses températures et la haute altitude.

La chaîne des monts St. Elias n'a cessé de se soulever depuis au moins 25 Ma. La dénivellation de 3 km du mont Logan pourrait entraîner une dérive des courbes de refroidissement à partir desquelles les vitesses de paléo-soulèvement sont déduites. On a examiné à ces fins du granite et de la tonalite plus ou moins déformés ainsi que de la tonalite non déformée de la face ouest du massif. La plupart des échantillons ne contiennent pas de feldspaths potassiques, excluant ainsi l'utilisation de la méthode de datation radiométrique ⁴⁰Ar-³⁹Ar sur feldspath potassique pour déterminer l'histoire locale du refroidissement.

¹ Canada-Yukon Geoscience Office, P.O. Box 2073 (F3), 2099 - 2nd Avenue, Whitehorse, Yukon Y1A 2C6

² Department of Earth Sciences, Carleton University and Ottawa-Carleton Geoscience Centre, Ottawa, Ontario K1S 5B6

INTRODUCTION

Mount Logan lies in the heart of the St. Elias Mountains of southwestern Yukon. These mountains lie on a convergent continental margin at the transition from a dominantly transcurrent structural margin in southeast Alaska to the south, to one characterized by thrust faults and back-thrusts in southern Alaska to the west. The area has Neogene uplift and frequent seismicity (e.g., Eisbacher and Hopkins, 1977; Horner, 1983). A fundamental tool for monitoring active movement is precision surveying, but conventional land-based methods are hampered in the St. Elias region by difficult access, extremely rugged and unstable terrain, high altitude and frequent poor weather.

One goal of the Logan '92 expedition was to test the feasibility of using the Global Positioning satellite System (GPS) for making precision measurements in the St. Elias Mountains by determining the elevation of the summit of Mount Logan. A second objective was to install survey monuments in secure bedrock from which re-measurement, years or decades hence, might reveal changes in elevation or position, depending on the rate of crustal deformation. In addition, plutonic rock samples were collected for studies of cooling and uplift at known elevations up the mountain.

This climb, part of the commemoration of the 150th anniversary of the founding of the GSC as well as Canada's 125th birthday, was sponsored by the Royal Canadian Geographic Society in partnership with the Geological Survey of Canada, the Geodetic Survey Division of Surveys, Mapping and Remote Sensing Sector, and the Canadian Parks Service.

REGIONAL TECTONIC SETTING

On the basis of reconnaissance mapping (Wheeler, 1963; MacKevett, 1978; Campbell and Dodds, 1982) and K-Ar dates for large plutonic bodies (Dodds and Campbell, 1988) the St. Elias Mountains are known to be northwest-trending slivers of Alexander, Chugach and Yakutat terranes (Fig. 1) as well as three elements of Wrangellia. These terranes have been juxtaposed along major, throughgoing fault systems and were accreted to the Coast Belt and rest of North America during late Mesozoic and Cenozoic eras (Dodds and Campbell, 1988).

The Border Ranges Fault is a major terrane boundary exposed on the south side of Mount Logan. South of the fault are variably metamorphosed and deformed late Mesozoic, deep marine and flyschoid and basic volcanic rocks of the Chugach terrane. North of, and truncated by the Border Ranges Fault is a Late Jurassic hornblende-biotite quartz diorite, the Mount Logan batholith (ca. 153 Ma; Dodds and Campbell, 1988) of Wrangellia Terrane. The Eocene King Peak pluton (ca. 50 Ma; Dodds and Campbell, 1988) intrudes the Mount Logan batholith, the Chugach metasedimentary rocks and the Border Ranges Fault, thus limiting the age of

motion on the Border Ranges Fault to between 153 and 50 Ma ago. In southern Alaska motion on the Border Ranges Fault occurred between about 135 and 120 Ma ago (Pavlis, 1982).

The Border Ranges Fault trends east-southeast and is interpreted to join with the dominantly transcurrent Fairweather Fault in southeast Alaska. Dextral motion on the Fairweather Fault results from northwestward motion of the Pacific plate (5.8 cm annually; Lahr and Plafker, 1980). Because the faults curve westward in the St. Elias Mountains, oblique convergence results, and the Pacific plate is subducted beneath the Gulf of Alaska. Thrust faults near Mount St. Elias, 30 km south of Mount Logan, have north-side-up displacement (Campbell and Dodds, 1978).

The pattern of uplift in the St. Elias Mountains is not understood. The area along the Fairweather Fault has risen perhaps 14 km in about the last Ma (Brew, 1990) and the shore of Yakutat Bay bears evidence of continued emergence. Parrish (1981) analyzed fission tracks in apatite collected at various elevations from the southeast side of Mount Logan and determined an uplift rate of 0.35 mm annually from 16-13 Ma ago. The uplift may be a consequence of strain buildup along the transform boundary (Horner, 1990), plate convergence, or thermal expansion of the upper mantle. Whether the mountain belt is arching, tilting landward, rising on discrete thrust faults or deforming internally is unclear at present.

The region has high seismicity, including four $M > 7.0$ earthquakes since 1899 (Horner, 1983). In this area a seismic monitoring network would help understand the strain rate variations associated with large earthquakes (R.B. Horner,

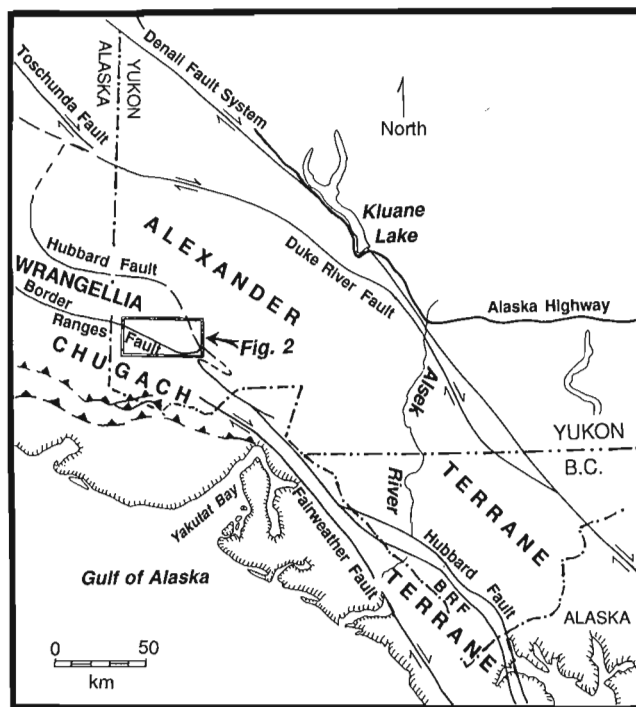


Figure 1. Terranes comprising the St. Elias Mountains (from Dodds and Campbell, 1988), showing location of Figure 2.

pers. comm., 1991). A greater understanding of these data could come from time-averaged paleo-uplift rates inferred from cooling curves, analysis of micro-structures in rocks, or the study of structural patterns during regional mapping.

EXPEDITION CHRONOLOGY

Mount Logan is located 180 km southwest of Kluane Lake, Yukon. Access for mountaineers is provided by single-engine ski-equipped airplane from Kluane Lake. Although this plane has landed on snowfields as high as 5200 m, most climbing expeditions begin at about 3000 m elevation to allow gradual acclimatization by ascending slowly to the 5000 m plateau.

The activities of the Royal Canadian Geographic Society expedition are reported by Schmidt (1992). Briefly, the 13-person team left a base camp on the Quintino Sella Glacier (Fig. 2) on May 14, skied eastward up King Trench, then northward on snow slopes to the Logan Plateau (about 5500 m), following the route of the 1925 first ascent. On June 6th simultaneous GPS observations were made at four points: on Mount Logan's summit, at a monumented bedrock site near Prospector Peak, and at two geodetic survey control

points along the Alaska Highway. The two GPS receivers on the Mount Logan massif were then exchanged and the GPS survey was repeated on June 8. Weather remained stable while the expedition was above 5000 m, with winds 5-25 km/hr, air temperature reaching -5°C in late afternoon and dipping to -38°C overnight. Upon return to base camp, GPS bedrock monuments were installed on Quintino Sella Glacier ($60^{\circ}37.0'N$, $139^{\circ}49.5'W$; 2800 m) and on Mount Upton ($60^{\circ}46'N$, $139^{\circ}17'W$) and all climbers flown back to Kluane Lake by June 17.

GEOLOGICAL OBSERVATIONS

Mount Logan is a massive snow- and ice-covered plateau: the area above 5000 m is over 18 km long and 5 km wide. With the exception of King Peak to the southwest, surrounding ridges are lower than 4000 m, and the precipitous sides of Mount Logan drop to valley glaciers at least 2 km below. The King Trench route provides the most gradual ascent of Mount Logan but affords only limited opportunities to examine rocks. Some exposed rocks are separated from glacier ice by a bergschrund and others cannot be approached

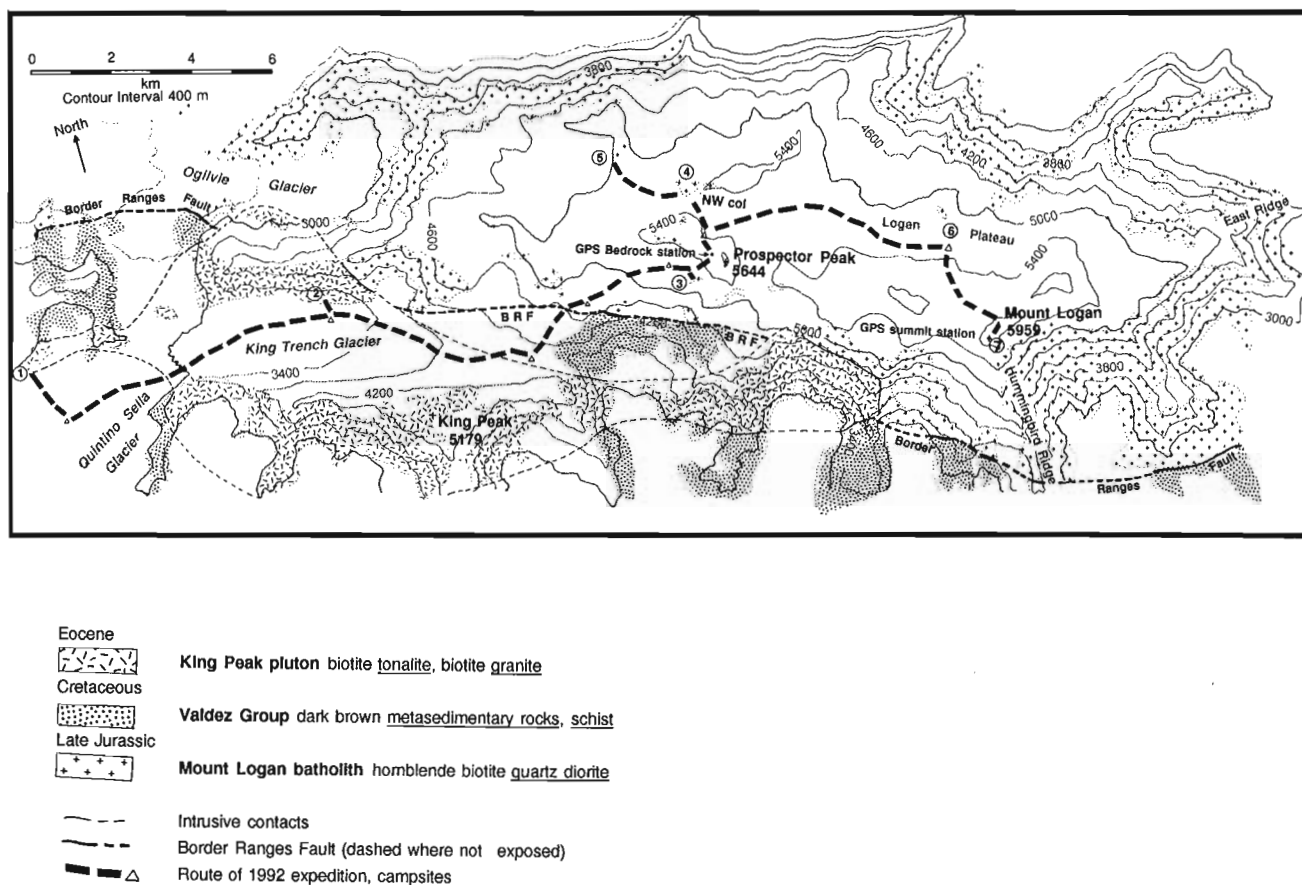


Figure 2. Topography of Mount Logan showing climbing route (heavy dashes) and geological localities (numbered). Topography from Surveys and Mapping Branch, EMR, 115 C/9 and C/10, 1987; geology modified from Campbell and Dodds (1982).

due to avalanche hazard. The seven localities we examined (Fig. 2) are described below because they are only rarely visited by geologists.

1. Quintino Sella Glacier: A ridge spur 1 km west of Base Camp (60°37.5'N 140°41.0'W; 2850 m). A medium grained granite, mapped by Campbell and Dodds (1982) as King Peak pluton, (15% biotite, 35% quartz, 30% plagioclase and 20% K-feldspar) is locally sheared on discrete planes that are 0.5-1 cm apart. Quartz and feldspar grains between the shear planes have undergone dynamic recrystallization and together with the biotite grains define a well-developed stretching lineation.

The granite is intruded by foliated biotite feldspar porphyry dykes containing medium-grained feldspar (20%) and biotite (20%) in a fine grained mesocratic quartz-feldspathic matrix. Foliation is defined by the preferred orientation of biotite and pressure shadows that have formed around some of the feldspar porphyroclasts. The well-developed fabric of the dykes indicate that shearing was concentrated in the dykes before they had completely cooled.

The granite is also intruded by a medium grained garnet-biotite tonalite (2% garnet, 10% biotite, 25% quartz, 70% plagioclase) that is undeformed to very weakly foliated (possibly an igneous fabric). This rock is interpreted as an apophysis of the King Peak pluton.

2. North side of King Trench (60°37'N 140°41'W; 3350 m). These cliffs consist of medium grained hornblende-biotite quartz diorite (10% hornblende, 15% biotite, 10% quartz, 65% feldspar) with a weak foliation. Dykes, including a vertical slab-like intrusion about 250 m long and some 20 m thick visible high in the cliffs 4 km northwest of King Peak, are beige-weathering, unfoliated tonalite. These rocks are interpreted as phases of King Peak pluton that were not widely separated in time. The intrusive contact between these rocks exhibits flow-folds and 1 cm chill margins (Fig. 3).

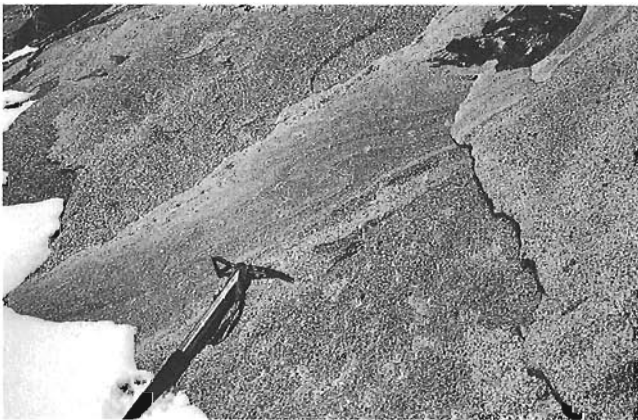


Figure 3. Flow folds in chill margin of quartz diorite where intruded by tonalite of the King Peak pluton (locality 2).

3. Cliff-top facing southeast over Seward Glacier (60°36'N 140°32'W; 5240 m). This outcrop is 500 m north of the Border Ranges Fault. It consists of unfoliated, medium grained biotite quartz diorite with 20% biotite ± chlorite, 10% quartz, 70% zoned plagioclase and no K-feldspar.

4. Prospector Peak and northwest col, including the bedrock GPS site at 60°36'N 140°31'W; 5520 m; Fig. 4). Most of discontinuous outcrop in the col west of Prospector Peak is medium grained, slightly foliated hornblende quartz diorite. It contains slightly foliated chloritized biotite (15%) as well as 65% white and pink plagioclase and 20% quartz, typical of the Mount Logan batholith. Thin sections of this rock reveal intensely fractured quartz and dusky altered plagioclase.

A low ridge extending west on the north side of the col 1.5 km northwest of Prospector Peak exposes a dark-brown weathering pendant and crosscutting intrusive relationships (Fig. 5). The pendant and adjacent inclusions in the Mount Logan batholith are melanocratic gneiss composed of medium grained hornblende and fine grained quartz and feldspar. Some of the inclusions are folded; the feldspathic layers within them are bent parallel to margins of the inclusion. Enclosing granitic rock are not folded, indicating that the country rock was deformed before the pluton solidified. The banded inclusions may have had a sedimentary protolith. An area of schist, amphibolite and argillite of Paleozoic or Mesozoic age mapped by Campbell and Dodds (1982) about 8 km northwest of Prospector Peak may be equivalent to this pendant.

White-weathering biotite tonalite dykes cut the hornblende quartz diorite. The tonalite is medium- to coarse-grained, with 15% biotite ± chlorite, 35% plagioclase, 50% quartz. These dykes are likely apophyses of King Peak pluton. Both the quartz diorite and tonalite are extensively fractured by: 1) north-trending micro-shears with a few centimetres offset, 2) epidote/quartz/muscovite pegmatite veins, and 3) quartzofeldspathic, flexion-textured veinlets.



Figure 4. View of Prospector Peak (right) and GPS bedrock site (knoll above left-hand figure), looking north from about 5200 m, during the approach by the climbing team.

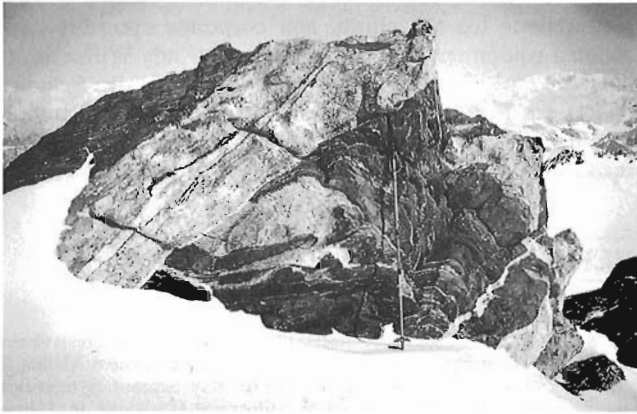


Figure 5. Sequence of intrusions at northwest col (locality 4). A biotite tonalite dyke (probably from the Eocene King Peak pluton) truncates hornblende-biotite quartz diorite (lower right) of Mount Logan batholith. Note the feldspathic chilled margin (bottom centre) and a younger quartz vein in the tonalite dyke. The dark host rock is a mafic gneiss pendant.

5. Nunatak 2 km west of northwest col ($60^{\circ}37.5'N$, $140^{\circ}34'W$, 5050 m). This 200 m wide knob consists of medium grained hornblende quartz monzonite typical of the Mount Logan batholith. At the north end of the outcrop is a 10 m wide zone of shattered and altered monzonite with brown-weathering calcareous metasiltstone. Hornblende clusters in the fault zone have a moderately dipping, southwestern orientation.

6. Nunatak ridge 2 km north of Mount Logan summit ($60^{\circ}35'N$ $140^{\circ}25'W$; 5320 m). Light orange weathering, medium grained, unfoliated, porphyritic quartz diorite contains 15% translucent quartz grains (2 x 3 mm), 70% white plagioclase to 1 mm; 5% pink subrounded phenocrysts of K-feldspar(?) to 2 cm; 10% chloritized biotite to 1 mm and lesser hornblende. In this rock the quartz is not fractured but intergrowths along rims of grains are visible in thin section.

7. South side of Mount Logan summit ($60^{\circ}34.4'N$ $140^{\circ}24.5'W$; 5940 m). The highest exposed rock in Canada is a medium grained biotite tonalite (15% biotite, 30% quartz and 55% zoned plagioclase) with a weak igneous(?) foliation defined by aligned biotite. It is exposed 20 m below the ice-covered summit, at the top of the Hummingbird Ridge.

DISCUSSION

Plutonic rocks and paleo-uplift rates

The granite at locality 1 displays evidence of ductile deformation (shear bands and dynamic recrystallization of quartz and feldspar). Granitic intrusions are noted in the map legend of Campbell and Dodds (1982; their unit **KVm**) with Cretaceous and(?) older metasedimentary rocks, but the age of this granite is unknown. Brittle-ductile deformation of these rocks may be related to movement on the Border Ranges Fault (see below).

Rocks of the Mount Logan batholith were found at localities 3-7. They have undergone extensive brittle deformation only in the northwest col area. All these rocks contained chloritized biotite unsuitable for K-Ar dating, but fresh hornblende is present at locality 6.

Undeformed tonalite correlated with King Peak pluton is exposed at localities 1 and 2, as well as dykes at locality 4. The age of the quartz diorite at locality 2 is unknown if it is not a phase of King Peak pluton earlier than the tonalite.

The lack of K-feldspar in most samples prohibits use of ^{40}Ar - ^{39}Ar geochronometry on K-feldspar to determine a cooling history and therefore an uplift history for this area. The East Ridge of Mount Logan is an alternate climbing route that has granitic rock exposed over significant topographic relief. If samples from that area contain K-feldspar, it may be possible to use ^{40}Ar - ^{39}Ar on K-feldspar to augment the apatite fission track study by Parrish (1981).

Border Ranges Fault

The Border Ranges Fault was early recognized as a major terrane boundary (MacKevett and Plafker, 1974) but has recently received increased attention as the fundamental break between a late Mesozoic subduction complex (which includes Chugach Terrane) and older crystalline rocks (Pavlis, 1982). The nature of this fault in Yukon needs further study. Unlike most faults in the western Elias Mountains which lie beneath broad valley glaciers, the Border Ranges Fault is easily traced. It is spectacularly exposed on the south face of Mount Logan (see cover of Current Research, GSC Paper 92-1A), although it was inaccessible where crossed by our expedition. It is possible that the sheer south face of Mount Logan was formed from juxtaposition of resistant Mount Logan plutonic rock against the crumbling, recessive metasedimentary rocks along the Border Ranges Fault.

It is unclear whether the Border Ranges Fault was a transcurrent fault that was later deformed, a north-dipping thrust, or a combination of several movements. Fifteen kilometres east of Mount Logan summit, black shale and Cretaceous conglomerate outcrops (R.B. Campbell, pers. comm., 1992) are mapped as a northward re-entrant on the Border Ranges Fault (Campbell and Dodds, 1982). Alternatively these rocks could lie atop Wrangellia terrane or be shoved northward on a splay of the Border Ranges or Hubbard faults.

The alignment of the elongate, lobate King Peak pluton with the Border Ranges Fault suggests that it intruded a weakened zone. About 350 km west of Mount Logan, tonalite-trondhjemite complexes along the Border Ranges Fault are interpreted as crustal melt injections during ductile thrusting (Pavlis et al., 1988). Although no folded dykes or boudins were observed in the King Trench area, the presence of protomylonitic granite indicates that some plutonism may have been synchronous with fault movement. Coexisting brittle- and ductile-deformed phases may be present in other Eocene Seward Plutonic Suite (Dodds and Campbell, 1988) intrusions adjacent to the Border Ranges Fault in north-western British Columbia.

Using GPS for geoscience studies in the St. Elias Mountains

This expedition demonstrated the capability of GPS for providing precise positions of remote places. The data collected on Mount Logan and at the two survey control points, combined with data from permanent GPS tracker sites, were processed at Surveys, Mapping and Remote Sensing Sector (EMR) in Ottawa and the elevation of the summit above mean sea-level was computed at 5959 ± 3 m at the 95% confidence level (Y. Mireault, pers. comm., 1992). Although the vertical precision of the GPS technique is better than 3 m, the geoid-ellipsoidal separation for this region was modelled with an accuracy of about 3 m (M. Verroneaut, pers. comm., 1992). The accuracy of the elevation will be improved once additional gravity values are obtained in the St. Elias Mountains. The generally accepted elevation (5956 m on map 115C/9, McArthur Pk., Edition 1, 1987, Surveys and Mapping Branch, EMR) is within the error range of the GPS value.

The monitoring of crustal deformation does not require computation of mean sea-level, thereby eliminating the need to determine the geoid. For this work the results of surveys using GPS-derived co-ordinates can be directly compared.

GPS is a highly portable (the receiver, antenna and battery units used by the expedition weighed about 15 kg), all-weather survey system that can make regional crustal deformation studies cost-efficient. Furthermore, because GPS does not rely upon line-of-sight survey points, there is much greater flexibility in designing arrays for strain monitoring. As the full GPS satellite constellation becomes operational, the limitations on times of observation experienced in 1992 will be minimized, if not eliminated (M. Schmidt, pers. comm., 1992). With care during initial planning almost any area with a clear overhead view can be surveyed using GPS when the system is fully deployed.

A considerable problem for any precision survey in the St. Elias Mountains, including GPS, is the paucity of stable rock sites that are both accessible and not covered by snow and ice during most of the short summer. The extent of frost heave on flat outcrops, and the likelihood of creep and other mass movements in areas of high relief poses a significant risk to the stability of long-term survey sites. We observed that most bedrock surfaces along our route, even intact surfaces 8 m by 10 m across, had been frost-heaved. Because changes in azimuth and vertical angle are critical to crustal deformation studies, a GPS station in such terrain might necessarily consist of clusters of surveyed markers. If one or more markers shifted before the subsequent re-survey, a change in the local array would allow them to be recognized.

ACKNOWLEDGMENTS

This work would not have been possible without the generous co-operation of the Logan '92 team members, in particular leader Mike Schmidt and project manager, George Hobson. The Alpine Club of Canada and Arctic Institute of North America Research Station provided accommodation during

preparations for the climb, and corporate sponsors contributed equipment and food. We thank Andy Williams for his thoroughly competent flying service, and Ulrike Schmidt and Helen Butler for maintaining prompt radio communication with the climbing team. Glenn Woodsworth's critical read and Bev Vanlier's re-typing greatly improved the paper.

REFERENCES

- Brew, D.A.**
1990: Plate tectonic setting of Glacier Bay National Park and Preserve and of Admiralty Island National Monument, southeastern Alaska; in Proceedings of the Second Glacier Bay Science Symposium (Sept. 19-22, 1988), (ed.) A.M. Milner and J.D. Wood, Jr.; United States Department of the Interior, National Park Service, Alaska Regional Office, Anchorage, p. 1-5.
- Campbell, R.B. and Dodds, C.J.**
1978: Operation Saint Elias, Yukon Territory; in Current Research, Part A; Geological Survey of Canada, Paper 78-1A, p. 35-41.
1982: Geology of Mount St. Elias map area, Yukon Territory (115 B and C, east half); Geological Survey of Canada, Open File 830.
- Dodds, C.J. and Campbell, R.B.**
1988: Potassium-argon ages of mainly intrusive rocks in the St. Elias Mountains, Yukon and British Columbia; Geological Survey of Canada, Paper 87-16.
- Eisbacher, G.H. and Hopkins, S.L.**
1977: Mid-Cenozoic paleogeomorphology and tectonic setting of the St. Elias Mountains, Yukon Territory; in Report of Activities, Part B; Geological Survey of Canada, Paper 77-1B, p. 319-335.
- Horner, R.B.**
1983: Seismicity in the St. Elias region of northwestern Canada and southeastern Alaska; Bulletin of the Seismological Society of America, v. 73, p. 1117-1137.
1990: Seismicity in the Glacier Bay region of southeast Alaska and adjacent areas of British Columbia; in Proceedings of the Second Glacier Bay Science Symposium (Sept. 19-22, 1988), (ed.) A.M. Milner and J.D. Wood, Jr.; United States Department of the Interior, National Park Service, Alaska Regional Office, Anchorage, p. 6-11.
- Lahr, J.C. and Plafker, G.**
1980: Holocene Pacific-North American plate interaction in southern Alaska: implications for the Yakataga seismic gap; Geology, v. 8, p. 483-486.
- MacKevett, E.M., Jr.**
1978: Geologic map of McCarthy quadrangle, Alaska; United States Geological Survey, Map I-1032.
- MacKevett, E.M., Jr. and Plafker, G.**
1974: The Border Ranges Fault in south-central Alaska; United States Geological Survey, Journal of Research, v. 2, p. 322-329.
- Parrish, R.R.**
1981: Uplift rates of Mount Logan and British Columbia's central Coast Mountains using fission track dating methods; EOS, v. 62, p. 60.
- Pavlis, T.L.**
1982: Origin and age of the Border Ranges Fault of southern Alaska and its bearing on the late Mesozoic tectonic evolution of Alaska; Tectonics, v. 1, p. 343-368.
- Pavlis, T.L., Monteverde, D.H., Bowman, J.R., Rubenstone, J.L., and Reason, M.D.**
1988: Early Cretaceous near-trench plutonism in southern Alaska: a tonalite-trondhjemite intrusive complex injected during ductile thrusting along the Border Ranges Fault system; Tectonics, v. 7, p. 1179-1199.
- Schmidt, M.**
1992: To the top: (Royal Canadian Geographical) Society team measures the height of Mount Logan, our highest peak; Canadian Geographic, September/October, 1992, p. 22-35.
- Wheeler, J.O.**
1963: Kaskawulsh (Mt. St. Elias, east half); Geological Survey of Canada, Map 1134A.

Character of upper Paleozoic strata and plutons, lower Forrest Kerr Creek area, northwestern British Columbia

M.H. Gunning¹

Cordilleran Division

Gunning, M.H., 1993: Character of upper Paleozoic strata and plutons, lower Forrest Kerr Creek area, northwestern British Columbia; in Current Research, Part A; Geological Survey of Canada, Paper 93-1A, p. 27-36.

Abstract: Upper Paleozoic strata and late Paleozoic plutons are in the lower Forrest Kerr Creek region of the Iskut River map area. Black chert, siliceous shale and thin-bedded ash tuff occur with recrystallized limestone of Early to Middle Devonian age. Foliated basalt sheet flow, flow breccia, and minor grey lapilli tuff, ash tuff, and phyllite east of the Devonian rocks are no younger than Permian. A heterogeneous, Mississippian or older pluton of granite, quartz monzodiorite, and hornblende diorite intrudes Devonian and younger strata. Triassic strata are faulted against the upper Paleozoic rocks to the east.

Strata and plutonic apophyses are folded and faulted. Prominent north-trending structural grain is from bedding, mineral foliation, and minor folds with subvertical axial planes. North-trending structures are deformed by north-vergent minor folds that plunge moderately east, and larger scale antiforms with subvertical northeast-trending axial traces. North-trending, subvertical faults are post-Late Triassic.

Résumé : Des strates du Paléozoïque supérieur et des plutons datés de la fin du Paléozoïque apparaissent dans la partie inférieure de la région de Forrest Kerr Creek, située dans le secteur cartographique d'Iskut River. Un chert noir, un shale siliceux et une cinérite finement litée accompagnent un calcaire recristallisé daté du Dévonien précoce à moyen. Des coulées de basaltes en nappes, d'aspect feuilleté, des brèches de coulée de lave, et de petites quantités de conglomérat volcanique gris à lapilli, de cinérites et de phyllites à l'est des roches dévoniennes sont d'âge antérieur au Permien, ou même plus anciennes. Un pluton hétérogène, d'âge mississippien ou plus vieux, composé de granite, de monzodiorite quartzique et de diorite à hornblende, pénètre des strates dévoniennes et plus jeunes. Les strates triasiques sont faillées au contact des roches de la partie supérieure du Paléozoïque à l'est.

Les strates et les apophyses plutoniques sont plissées et faillées. Des structures bien visibles de direction générale nord correspondent à la stratification, à une foliation minérale, et à des plis subverticaux mineurs. Les structures de direction générale nord sont déformées par des plis mineurs de vergence nord qui plongent modérément vers l'est, et par des antiformes de plus grande envergure caractérisées par des traces axiales subverticales de direction générale nord-est. Des failles subverticales de direction générale nord se sont formées à une époque postérieure au Trias tardif.

¹ Department of Geology, University of Western Ontario, London, Ontario N6A 5B7

INTRODUCTION

The oldest dated rocks and plutons in Stikinia are northwest of the junction of Forrest Kerr Creek and the Iskut River near the east margin of the Coast Belt (Fig. 1). The aim of this report is to define time-stratigraphic successions by rock type, age and structural style, to characterize phases and contacts of a heterogeneous Mississippian or older pluton (Logan et al., 1990a), and to provide lithological correlation to well-dated middle Paleozoic rocks elsewhere in the region. A thin but laterally extensive limestone unit assigned Early to Middle Devonian age (Read et al., 1989; Anderson, 1989; Logan et al., 1990a,b; Brown et al., 1991) is in the middle of the study area. Description of rocks and structures is in context with map units and structures in Figures 2 and 3 respectively. This work forms part of a PhD thesis on the character and evolution of the Stikine assemblage in the Iskut River region, and builds on previous work by Read et al. (1989) and Logan et al. (1990b).

STRATIFIED ROCKS

General statement

Paleozoic strata in the "Henry Lake" area are disrupted by folds, faults, and plutonic rocks. Planar lamination, layering of dark and light grey spar and rare fracture cleavage in well-dated Devonian limestone strikes north to northwest and are generally inclined steeply to the west. Foliated metavolcanic rocks and thin-bedded chert and shale are generally concordant with limestone, but there is no representative stratigraphic section because strata are tightly folded throughout the area.

There are few dated rocks in the area. Isolated lenses of sparry limestone within metavolcanic rocks east of, and structurally below, Devonian limestone contain Early

Permian conodonts (Read et al., 1989; Fig. 2). Thin-bedded sedimentary rocks and foliated metavolcanic rocks of units a to g could be a stratigraphically continuous succession of Devonian to Permian age because: 1. There is no evidence for a thrust fault at the base of the Devonian limestone because chert and tuff are tightly folded with limestone at the east and west margin of the limestone throughout the study area; 2. Metavolcanic strata in gradational contact with Devonian sedimentary rocks are similar to metavolcanic strata that contain lenses of Permian limestone; and 3. There is no sedimentological or biostratigraphic evidence of an unconformity within the deformed succession of foliated metavolcanic and metasedimentary strata.

Units a to c

A belt of folded and recrystallized limestone (unit a), and lesser interbedded chert and siltstone (unit b) occur in four separate areas in a north-trending belt about 4.5 km long and up to 500 m wide north of "Henry Lake". Structural thickness of thin-bedded metasedimentary rocks is about 50 m in the south part of the belt and about 400 m in the north part. Thin-bedded sericitic ash tuff and lesser varicoloured chert structurally underlie limestone everywhere. The west margin of the belt is defined by granite and diorite and is characterized by infolded black chert, limestone, and aplitic apophyses.

Dark grey to black limy mudstone with local planar lamination, even-textured light grey and pale brown to orange sparry limestone, and layered white and light grey recrystallized limestone are unit a. Dark grey limestone is generally fissile and argillaceous. Near pluton margins there are disharmonically folded bands of milky white calcite in pale grey spar. Fracture cleavage is rare, and there are irregular blebs, bands, and mesh of pale brown silica in scattered vertically restricted intervals. Small silicified colonial corals and ductilely deformed echinoderm ossicles are in restricted intervals away from pluton margins.

Thin-bedded shale, chert, siltstone, and ash tuff is intercalated with, and structurally above and below the limestone. Varicoloured chert and siliceous and graphitic shale of unit b is in coherent 2-5 cm thick ribbons separated by a warped fracture parting. Symmetric minor folds with rounded hinges are abundant. Pale green, white, and dull to dark green ash tuff of unit c is generally in internally massive, laterally continuous 2-5 cm thick tabular and warped beds separated by a sericitic fracture parting. Some outcrops are thick non-bedded successions with pervasive but diffuse, lenticular compositional laminae and sericite foliation. Tuff is dense, siliceous and aphanitic. Vertically restricted disseminations of euhedra of pyrite 3-7 mm in size are in some outcrops.

Age

Coral and microfossil collections are mainly near "Henry Lake" (Fig. 2, 4, Table 1). Conodonts in unit a are assigned Early and Middle Devonian age and there are no demonstrable time-transgressive trends.

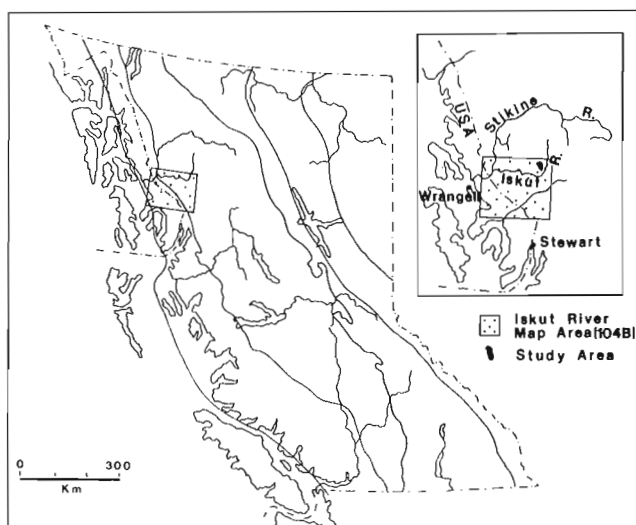


Figure 1. Location of study area.

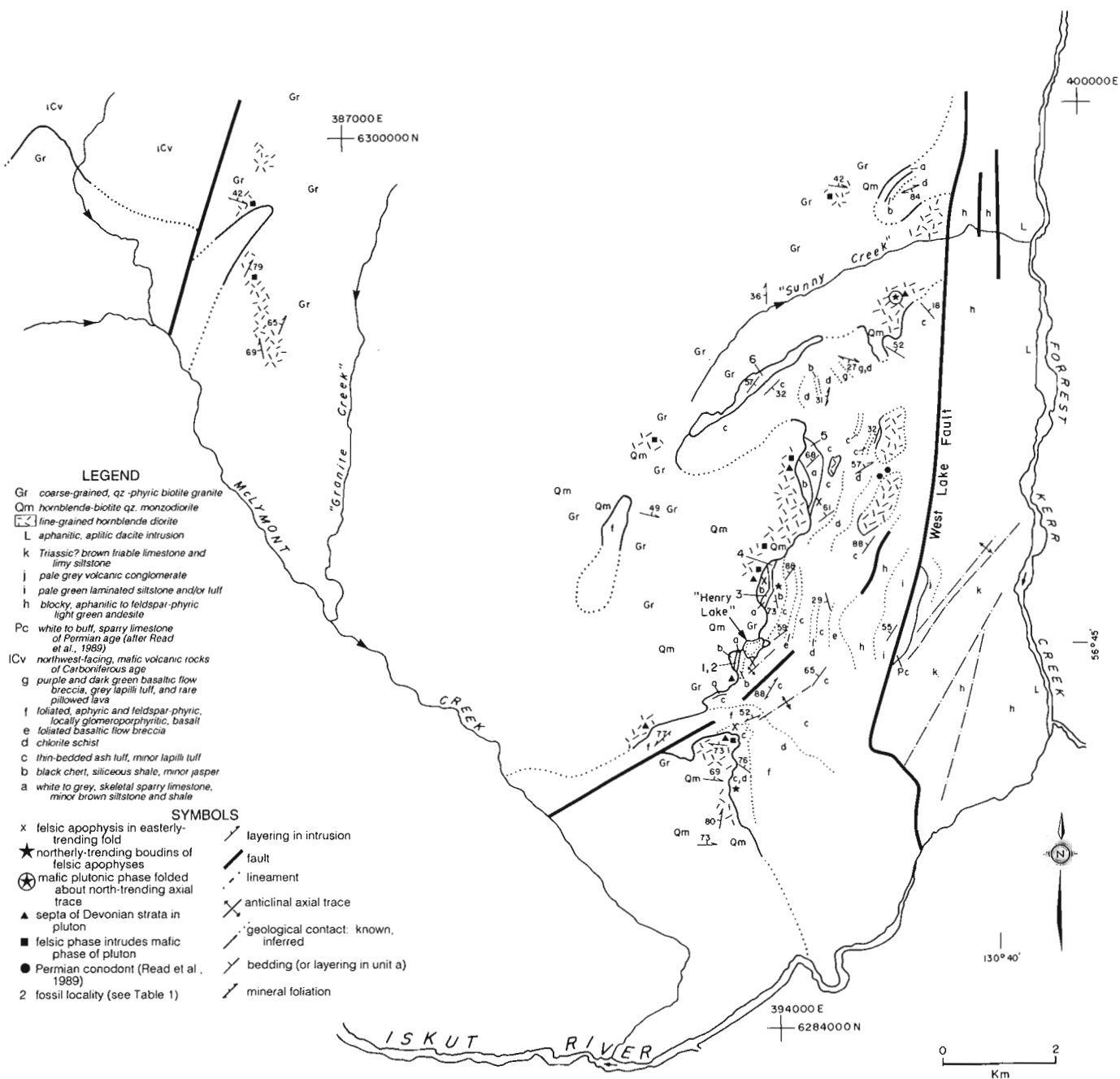


Figure 2. Geological sketch map of the "Henry Lake" area.

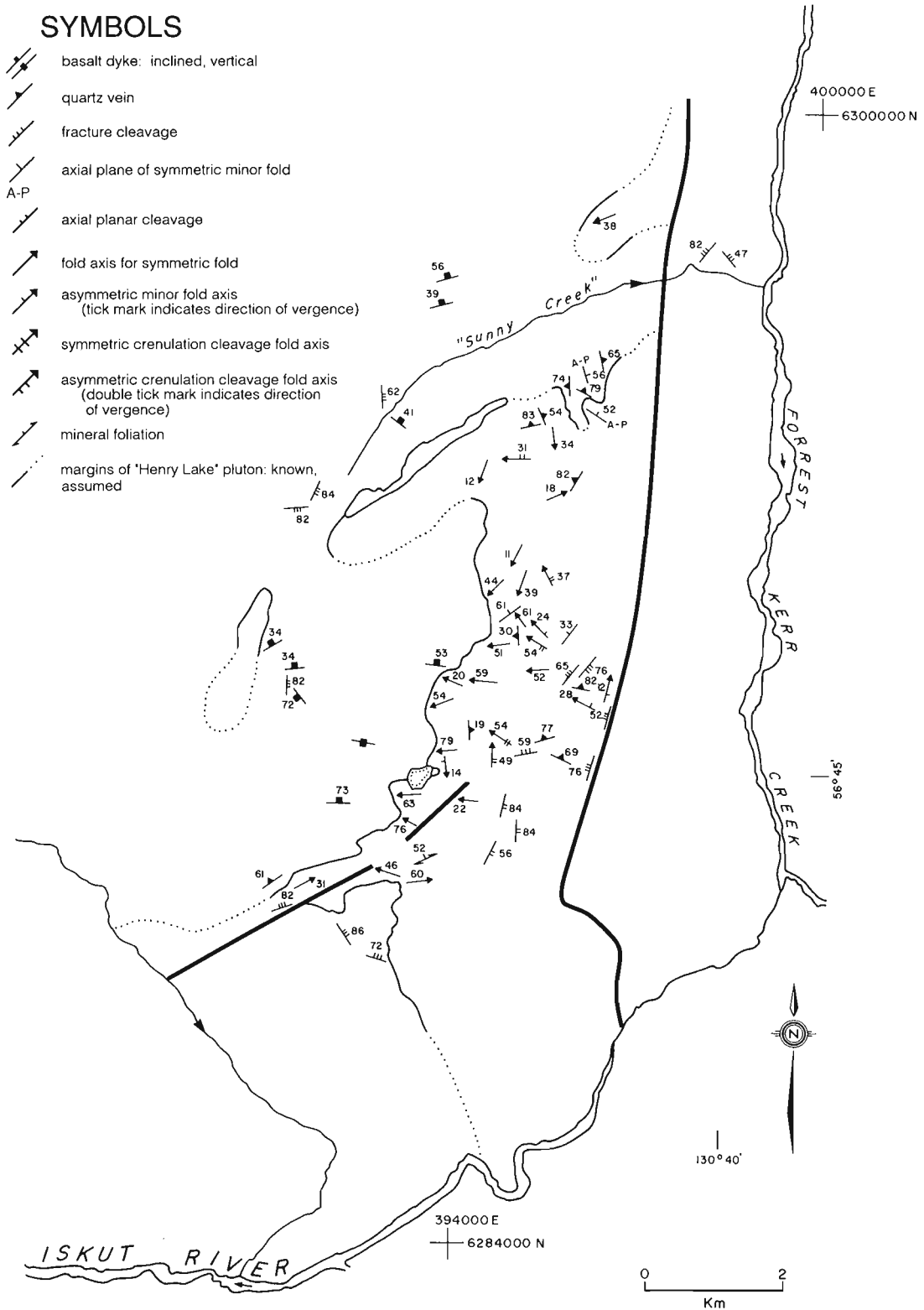


Figure 3. Structural style in the "Henry Lake" area. Margins of "Henry Lake" pluton, shown by solid and dotted lines, are from Figure 2.

Units d to g

Ash tuff, foliated basalt and chlorite schist are intercalated at the contact between units c and d. Units d to g are a heterogeneous mafic metavolcanic succession with characteristic thin but laterally continuous intervals of pale green ash tuff, siliceous phyllite and lesser pale grey lapilli tuff. Unit f is massive and foliated, aphanitic, feldspar-porphyrific and feldspar glomerocrystic basalt and lesser amygdaloidal basalt; basalt sheet flows are the most abundant rock type in the area. Beige feldspar phenocrysts are generally less than 3 mm in size and glomerocrysts are globular and radiating clusters of 2 to 4 crystals (Fig. 5a). Boundaries of individual cooling units are generally overprinted by chlorite mineral foliation. Dark green chlorite lines fracture in foliated basalt and defines a penetrative mineral foliation in chlorite schist in unit d.



Figure 4. View north at the east margin of the "Henry Lake" pluton that is outlined by a solid white line. Numbers refer to fossil localities in Figure 2 and Table 1.

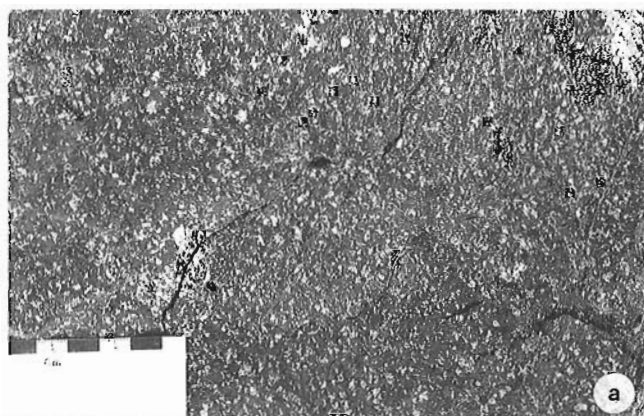


Figure 5. (a) Feldspar glomerocrystic basalt sheet flows of unit f, and (b) agglutinate texture characteristic of monomictic basalt flow breccia of unit e. Basaltic flows are the most abundant rock type in metavolcanic strata east and south of Devonian limestone in the "Henry Lake" area.

Table 1. Ages of fossils from limestone in unit a

NUMBER	GSC #	FAUNA	AGE	REFERENCE
1	C-087673	Conodont	Pragian	1
2	C-116608	Conodont	possibly Emsian - probable Eifelian	2
3	C-116616	Conodont	Early Devonian (?)	2
4	C-087672	Conodont	Pragian	3
5	C-101189	Conodont	Lochkovian	2
6	C-168163	Coral	Silurian or Devonian	4

Number refers to location in Figure 2. References are: 1. GSC Internal Fossil Report, OF-1992-2; 2. M.J. Orchard, unpub. data; 3. Read et al., 1989; 4. Logan et al., 1990a.

Massive and foliated dark green and purple flow breccia of units e and g have a characteristic pitted weathered surface and irregular-shaped varitextured basalt and scoria fragments generally less than 10 cm across have sharp and assimilated margins and define agglutinate and autobreccia textures (Fig. 5b). Monomictic breccia is aphanitic to faintly feldspar-porphyrific and commonly occurs with foliated pillow basalt. Unsorted white and light grey felsic accidental lithic fragments are distinctive in outcrops of pale grey and dull green lapilli tuff of unit g. There is a faint to moderate chlorite foliation in tuff, and most lapilli and blocks are flattened in the plane of foliation.

Feldspar glomerocrystic basalt sheet flows and basalt flow breccia are abundant stratigraphically below well-dated Lower Carboniferous limestone in the Forrest Kerr Glacier and Newmont Lake areas about 25 km and 10 km to the northwest respectively, of the "Henry Lake" (Logan et al., 1990a; Gunning, 1992). They are similar to basalt in the study area and are the basis for a correlation between Early Carboniferous or older, and Devonian and younger mafic volcanic successions; similarity of rock types and flow textures may reflect extrusion within the same volcanic regime.

Units h to l

Aphanitic and faintly feldspar-porphyrific light green andesite and aphanitic dacite are predominant in units h to l that are mainly east of the West Lake Fault (cf. Read et al., 1989). Brittle deformation is a characteristic of most outcrops and there are numerous swarms of subvertical east-trending quartz veins in unit h east and northeast of "Henry Lake". Massive cliffs of nondescript pale green and grey siliceous rock along the west bank of Forrest Kerr Creek are interpreted to be a large high level felsic intrusion.

Northeast of "Henry Lake" there is an abrupt change from chlorite schist to blocky light green andesite across a curvilinear fault west of, and broadly parallel with the West Lake Fault (Fig. 2). Thin-bedded ash tuff and laminated light green siltstone between the two faults is commonly tightly folded and similar to tuff in unit c, but is interpreted to be Upper Triassic because of fault juxtaposition with chlorite schist to the west, and spatial association with andesite that is similar to well-dated Upper Triassic andesite and dacite east of the West Lake Fault (Read et al., 1989). A post-Late Triassic age for compressional deformational events that produced folds with north-plunging and west-plunging fold axes is implicit in this interpretation.

INTRUSIVE ROCKS

Distribution

The compositionally and texturally heterogeneous "Henry Lake" pluton west of "Henry Lake" is granite, quartz monzodiorite, and diorite. The pluton extends north into the southern part of the Telegraph Creek map area (Logan et al., 1992b), it intrudes upper Paleozoic strata in the "Henry lake" area and

is in fault contact with Lower Carboniferous volcanic strata southeast of Newmont Lake (Fig. 2). Intermediate and felsic phases of the pluton are the most extensive and diorite is generally in small irregular areas along the periphery of the pluton. In one area south of "Henry Lake" tan to pale orange aplite at the pluton margin grades inward into quartz-phyric granite over about 50 m. Apophyses that extend into surrounding bedded rock are generally tan aplite, white-weathered fine grained biotite granite, and light grey hornblende-biotite quartz monzodiorite. Complex zones of mixed mafic and felsic phases, and zones of intrusive breccia that comprise diorite and amphibolite blocks in a matrix of aplite and biotite granite, are characteristic of the northern part of the pluton in the Telegraph Creek map area (Logan et al., 1992a).

Composition

Dark grey equigranular hornblende diorite is a fine grained subpoikilitic mesh of subhedral hornblende and subordinate feathery and lath-shaped feldspar. At contacts with bedded rocks, diorite is commonly fractured, friable and chloritic. Near the head of McLymont Creek there are metre-thick tabular intrusive layers of equigranular hornblende diorite, plagioclase-phyric diorite and pistachio green epidote-rich layers in the mafic phase of the pluton. South of "Henry Lake" discontinuous centimetre-thick milky and cloudy grey quartz segregations are throughout diorite and may be from post-emplacement deformation.

This phase is fine- to medium-grained, generally equigranular and light grey weathered. Mafic minerals are interstitial to cloudy grey and chalky white subhedral plagioclase. Hornblende is generally 1-4 mm long acicular grains or scattered green poikilitic subhedral clots that are generally less than 15% of the rock. Evenly disseminated green and black biotite is in fine grained plates and books less than 5 mm in size. Equant beige potassium feldspar megacrysts up to 2 cm in size are scattered throughout some outcrops. In some areas there are concentrations of subparallel, irregular spaced, 2-5 cm wide aplitic intrusive layers with diffuse margins.

Fine- to coarse-grained quartz-phyric biotite granite is the most extensive phase and is in tan, light grey to white and pale orange outcrops. Centimetre- to rarely decimetre-thick aplitic layers are similar to those in quartz monzodiorite. Granite is texturally heterogeneous but compositionally homogeneous. Euhedral single grains and rare books of brown and black biotite are evenly disseminated and generally less than 5% of granite. Conspicuous cloudy grey subhedral "eyes" of quartz are up to 10 mm in size and 40% of some outcrops. Chalky white and dull grey plagioclase is generally finer-grained than submegacrystic grains of potassium feldspar. Hematite is along fractures and is a faint to pervasive alteration of feldspar. Wispy mafic schlieren and centimetre- to decimetre-scale rounded xenoliths of fine-grained diorite and plagioclase-phyric diorite are locally abundant. A northeast-trending swarm of crosscutting and subparallel dykes of fine grained diorite and aphanitic basalt is in quartz monzodiorite

and granite north of "Sunny creek". Similar swarms of mafic dykes and irregular intrusive bodies are throughout the northern part of the pluton (Logan et al., 1990a).

Tabular mafic dykes that are subvertical or inclined steeply to the north are throughout the "Henry Lake" pluton (Fig. 3). Swarms of 2-5 dark green and brown dykes are generally over a 20-50 m interval. Centimetre-scale granite xenoliths, wispy small-scale basalt apophyses and sharp coherent dyke margins are characteristic. Dykes are aphanitic basalt and/or andesite and feldspar and feldspar-pyroxene porphyritic basalt. Coplanar basalt dykes are throughout upper Paleozoic strata elsewhere in the Iskut River map area (Anderson, 1989).

Age

The pluton is younger than Early to Middle Devonian meta-sedimentary rocks because: 1. Diorite, quartz monzodiorite and granite truncate strata on both an outcrop and regional scale; 2. Beds of limestone are chaotically rotated at the pluton margin north of "Sunny creek"; 3. Small- and large-scale xenoliths of limestone, chert, and chlorite and sericite schist are within diorite and granite near the pluton margin; and 4. A pyritic hornfels is in ash tuff peripheral to aplite at one locality. The mafic phase is interpreted to be the oldest because xenoliths of fine grained diorite and plagioclase-phryic diorite in granite near contacts with the mafic phase have concentric centimetre-thick reaction rims, and granite, aplite, and quartz monzodiorite dykes and apophyses intrude diorite throughout the pluton. Mafic, intermediate, and felsic plutonic rocks are interpreted to be broadly coeval phases of a heterogeneous pluton because diorite, quartz monzodiorite and granite crosscut Paleozoic strata, have cospatial distribution and have similar structural style. The intermediate phase

of the pluton is at least as old as middle Early Carboniferous (Harland et al., 1990) (346 ± 10 Ma, K-Ar, biotite; Logan et al., 1992a).

STRUCTURAL STYLE

Folds in stratified rocks

Paleozoic strata are foliated and metamorphosed to greenschist facies, tightly folded, and juxtaposed against Upper Triassic rocks to the east along a north-trending fault. Regional strike of beds and mineral foliation planes is north to northeast, but structural style varies with the competency of units. There are three distinct fold geometries in upper Paleozoic strata (Fig. 3), but relative age of fold events is obscured by disharmonic folding, rootless fold structures, chaotic axial traces, and contradictory crosscutting relationships in some outcrops of thin-bedded ash tuff.

The first, or oldest episode of contractional deformation produced open, closed and rarely tight minor folds with rounded hinges in thin-bedded sedimentary rocks, and asymmetric decimetre- to rarely metre-spaced crenulation in foliated basalt. Fold wavelengths are generally decimetre-scale and most fold axes plunge moderately south. Axial planes are north-trending and subvertical or steep west-dipping. Crenulation cleavage in foliated basalt generally dips west and is east-vergent (Fig. 6a).

The second fold geometry is minor folds that plunge moderately west and transpose bedding, foliation planes, and north-trending fold structures (Fig. 6b). Closed and tight minor folds with decimetre-scale wavelengths and upright axial planes are exclusively in thin-bedded ash tuff and rarely have an associated axial planar cleavage. Asymmetric recumbent minor folds in tuff and regular-spaced crenulation

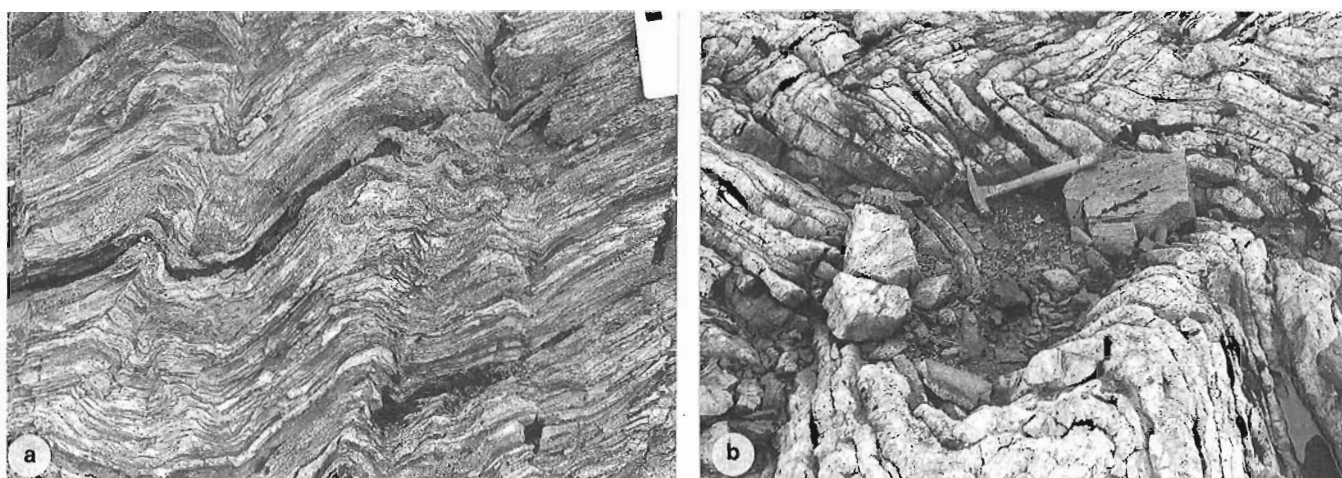


Figure 6. (a) Regular-spaced crenulation is common in foliated basalt and chlorite schist of units d and f. View to the north, along trend, shows east-vergent structural style typical of folds of this phase of deformation. Dark square on scale bar in top right is 1 cm long. (b) Minor folds with rounded, closed hinges are characteristic of thin-bedded ash tuff of unit c, and the view to the south shows truncation of north-trending folds by folds that trend east.

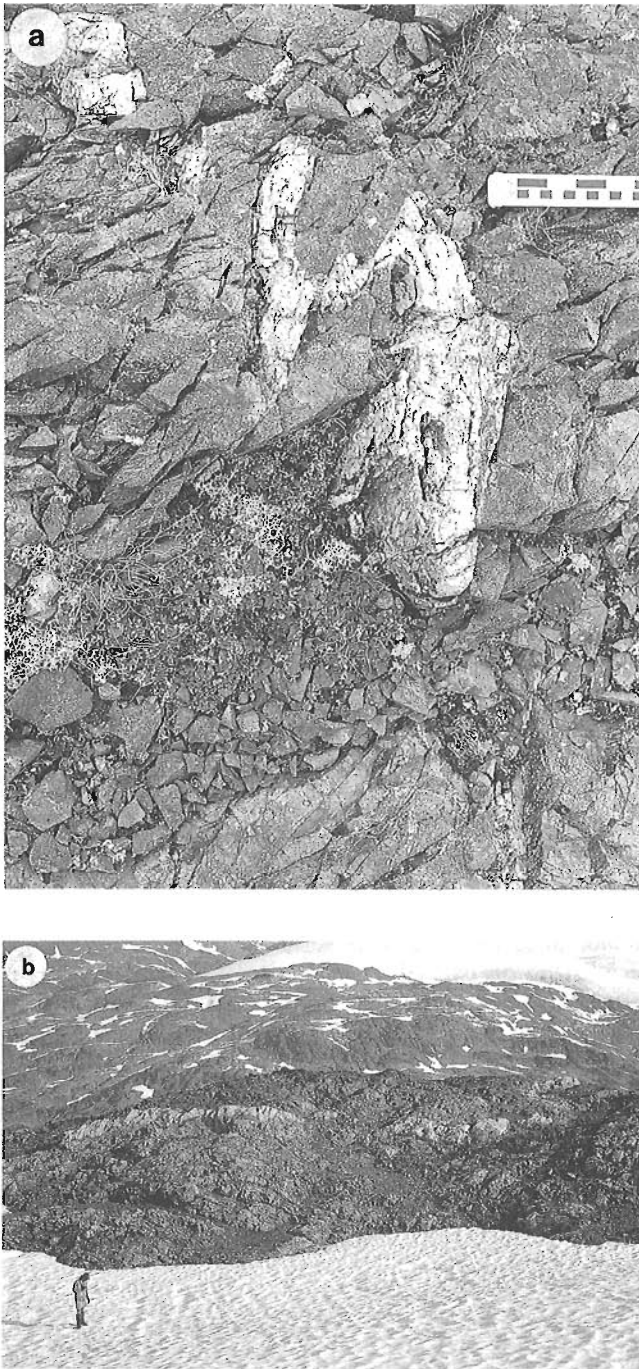


Figure 7. The two oldest sets of fold geometries in Paleozoic strata are in marginal diorite bodies and felsic apophyses of the "Henry Lake" pluton. View in (a) is to the north along strike of axial plane of north-plunging fold that deforms a quartz vein in fine grained diorite south of "Sunny creek". View to the northwest in (b) is of light grey weathering quartz monzodiorite dyke (in centre foreground of photo) in layered ash tuff. Dyke is folded about a west-trending axial plane (right centre part of photograph).

in foliated basalt are generally north-vergent and have axial planes that dip south. Northwest-plunging minor folds could either be transposed folds from the first phase of deformation, or syntectonic with the second folding event that was north-vergent and produced west-plunging minor folds.

The third, or youngest fold geometry is open northeast-trending antiforms in the south part of the study area with wavelengths of hundreds of metres or kilometres. There are no parasitic minor folds but there are coplanar faults that juxtapose diorite and foliated basalt southwest of "Henry Lake". Read et al. (1989) suggest this fold geometry is folded by, but overall coeval with, compression that produced west-plunging folds.

There is a north-trending cleavage discordant to bedding and sericite foliation in ash tuff of unit c south of "Henry Lake" (Fig. 3). The cleavage is not interpreted to be axial planar to first phase minor folds because it dips steeply east, and first phase folds generally lack an axial planar cleavage. The cleavage may be axial planar to a fourth phase of compression that produced regional scale folds with subvertical north-trending axial planes.

Folds in plutonic rocks

Tabular dykes and irregular apophyses of aplite, granite, and quartz monzodiorite intrude Paleozoic strata throughout the area and are generally nearly concordant with bedded and foliated rocks. Diorite bodies and felsic apophyses are affected by the first three contractional events that folded stratified rocks. Aplite and granite dykes and apophyses in strata south of "Henry Lake" are boudinaged along a north-trending subvertical plane and folded about subvertical north-trending axial planes. Quartz veins in diorite south of "Sunny creek" are folded about steeply north-plunging axes (Fig. 7a). Aplite and quartz monzodiorite dykes in thin-bedded ash tuff south of "Henry Lake" are in west-plunging open folds with rounded hinges and east-trending subvertical axial traces (Fig. 7b). Irregular orientation of quartz segregation in pseudo-gneissic diorite south of "Henry Lake" may be from the compression that folded surrounding metavolcanic strata about a subvertical, northeast-trending axial plane.

Age of folds

Structural style of diorite bodies and felsic apophyses compared with structures in stratified rocks suggest the first three phases of compression postdate Early Carboniferous pluton emplacement. If Paleozoic strata are in one time-stratigraphic succession of Devonian to Permian age there were three, and possibly four episodes of post-Paleozoic contractional deformation. If folded tuff and siltstone in units h and i west of the West Lake Fault are Upper Triassic then these events must be post-Late Triassic. Read et al. (1989)

suggested the first phase of folds are post-Permian but pre-Late Triassic, and the second and third phases are post-Middle to Late Jurassic.

Faults

Devonian to Permian metavolcanic and metasedimentary strata, Lower Carboniferous volcanic rocks, Early Mississippian or older plutons, Permian limestone, and Upper Triassic volcano-sedimentary successions were affected by subvertical to west- and northwest-dipping, north- and northeast-trending faults. There are isolated decimetre-thick zones of pervasive fracture cleavage in granite that are juxtaposed against brecciated and ankeritic Permian limestone along a regionally extensive north-trending fault east of the head of McLymont Creek. The east to northeast-trending West Lake Fault (cf. Read et al., 1989) juxtaposes upper Paleozoic and Upper Triassic strata east of "Henry Lake". Pervasive fracture cleavage and a chloritic mineral foliation are in rusty friable outcrops of Upper Triassic andesite at the fault. The fault locally truncates west-dipping beds and foliation planes in Paleozoic strata in the west block, and there is a decimetre- to metre-spaced fracture parting subparallel to the fault in a discontinuous interval of Permian limestone in the east block. Read et al. (1989) suggested that there is at least 4 km of oblique right-lateral offset along a coplanar fault south of the Iskut River.

Upper Triassic and Paleozoic strata west of Forrest Kerr Creek are juxtaposed against Lower Jurassic volcanic rocks east of the creek along the subvertical, north-trending Forrest Kerr Creek Fault (cf. Read et al., 1989). Regional north-trending faults that bound major tectono-stratigraphic successions in the area have been active from Early Jurassic to late Tertiary time (Souther, 1972; Souther and Symons, 1974; Read et al., 1989), and Read et al. (1989) suggested there has been more than 2.5 km of east-block-down displacement along the Forrest Kerr Creek Fault.

South of "Sunny creek" there are two north-trending quartz vein swarms in metavolcanic strata that are continuous for over 3 km. Veins are locally in isoclinal minor folds that plunge north, and everywhere cut less abundant subvertical east-trending quartz vein sets. Crosscutting relationships indicate both episodes of extension and fracture filling predate the first phase of compression that folded strata and plutons. The veins are not related to regional transpressive deformation because sinistral offset along some north-trending vein/fracture systems is opposite to sense of movement on major faults.

SUMMARY

Fossil ages, structural style, and rock distribution suggest that metavolcanic and metasedimentary rocks in the lower Forrest Kerr Creek area could be in a single time-stratigraphic succession of Devonian to Permian age. Rock types and flow textures in a heterogeneous mafic metavolcanic succession associated with well-dated Devonian sedimentary rocks are

similar to volcanic strata below Lower Carboniferous limestone elsewhere in the region. If the mafic rocks are correlative, they represent a widespread volcanic regime.

Upper Paleozoic strata are disrupted by the composite "Henry Lake" pluton. Coarse grained quartz-phyric biotite granite and acicular hornblende quartz monzodiorite dominate over scattered bodies of fine grained diorite at the pluton margin. Structural style and contact relations with upper Paleozoic strata suggest rocks are broadly coeval phases of a heterogeneous pluton of Mississippian or older age.

There are at least three, and perhaps four contractional deformational events that fold upper Paleozoic strata and apophyses of the "Henry Lake" pluton. East-vergent north-plunging minor folds are most abundant and are deformed by folds that plunge moderately west. Large-scale antiforms with subvertical northeast-trending axial planes and north-trending axial planar cleavage are youngest. If strata are a single Devonian to Permian succession, all folding events are post-Paleozoic; the two youngest events, and probably the two older events are post-Late Triassic. Distribution of upper Paleozoic, Upper Triassic, and Lower Jurassic volcano-sedimentary successions in the region is controlled by regional north-trending faults that have been active from Jurassic to Tertiary time (Souther and Symons, 1974; Read et al., 1989).

ACKNOWLEDGMENTS

Fieldwork for the project is supported by R.G. Anderson of the Cordilleran Division of the Geological Survey of Canada (Project 840046) and direction and encouragement from him and other officers is appreciated. Darwin Green and Kevin Hodder assisted during geological mapping and made valuable contributions to this study. Joint funding from Energy, Mines, and Resources Canada (Grant No. 190492) and NSERC (Grant No. CRD 117589) through the Research Agreements Program has been instrumental to completing fieldwork. Cost of laboratory work that complements geological mapping is generously supported by R.W. Hodder, thesis supervisor, and the University of Western Ontario. This article has been improved by comments from R.G. Anderson and G.J. Woodsworth. Tonia Oliveric meticulously drafted the geology and structure maps. Steve Irwin and Mike Orchard are thanked for their scrutiny and verification of data in Table 1.

REFERENCES

- Anderson, R.G.**
1989: A stratigraphic, plutonic, and structural framework for the Iskut River map area, northwestern British Columbia; in *Current Research, Part E*; Geological Survey of Canada, Paper 89-1E, p. 145-154.
- Brown, D.A., Logan, J.M., Gunning, M.H., Orchard, M.J., and Bamber, W.E.**
1991: Stratigraphic evolution of the Paleozoic Stikine assemblage in the Stikine and Iskut rivers area, northwestern British Columbia (NTS 104G and 104B); *Canadian Journal of Earth Sciences*, v. 28, p. 958-972.

Gunning, M.H.

1992: Carboniferous limestone, Iskut River region, northwest British Columbia; in *Current Research, Part A*; Geological Survey of Canada, Paper 92-1A, p. 315-322.

Harland, W.B., Armstrong, R.L., Cox, A.V., Craig, L.E., Smith, A.G., and Smith, P.G.

1990: *A geologic time scale 1989*; Cambridge University Press, Cambridge, 263 p.

Logan, J.M., Koyanagi, V.M., and Drobe, J.R.

1990a: Geology of the Forrest Kerr Creek area, northwestern British Columbia (104G/15); in *Geological Fieldwork 1989*; British Columbia Ministry of Energy, Mines and Petroleum Resources, Paper 1990-1, p. 127-140.

1990b: Geology and mineral occurrences of the Forrest Kerr-Iskut River area, northwestern British Columbia (104G/15); British Columbia Ministry of Energy, Mines and Petroleum Resources, Open File 1990-2.

Logan, J.M., Drobe, J.R., and Elsby, D.C.

1992a: Geology of the More Creek area, northwestern British Columbia; in *Geological Fieldwork 1991*; British Columbia Ministry of Energy, Mines and Petroleum Resources, Paper 1992-1, p. 161-178.

Logan, J.M., Drobe, J.R., and Elsby, D.C. (cont.)

1992b: Geology, geochemistry, and mineral occurrences of the More Creek area, northwest British Columbia; British Columbia Ministry of Energy, Mines and Petroleum Resources, Open File 1992-5, 2 sheets.

Read, P.B., Brown, R.L., Psutka, J.F., Moore, J.M., Journeay, M., Lane, L.S., and Orchard, M.J.

1989: Geology of parts of Snippaker Creek (104B/10), Forrest Kerr Creek (104B/15), Bob Quinn Lake (104B/16), Iskut River (104G/1) and Moore Creek (104G/2); Geological Survey of Canada, Open File 2094.

Souther, J.G.

1972: Telegraph Creek map area, British Columbia; Geological Survey of Canada, Paper 71-44, 68 p.

Souther, J.G. and Symons, D.T.A.

1974: Stratigraphy and paleomagnetism of Mount Edziza Volcanic Complex, northwestern British Columbia; Geological Survey of Canada, Paper 73-32, 25 p.

Geological Survey of Canada Project 840046

Preliminary report on the stratigraphy, sedimentology, and biochronology of the Inklin Formation in the Atlin Lake area, northern British Columbia

Gary G. Johannson¹
Cordilleran Division, Vancouver

Johannson, G.G., 1993: Preliminary report on the stratigraphy, sedimentology, and biochronology of the Inklin Formation in the Atlin Lake area, northern British Columbia; in Current Research, Part A; Geological Survey of Canada, Paper 93-1A, p. 37-42.

Abstract: The Lower Jurassic Inklin Formation of the Laberge Group ranges in age from Early Sinemurian to Late Pliensbachian and possibly Early Toarcian in the Atlin Lake area. Sinemurian strata are dominated by thin-bedded muddy turbidites that indicate northeasterly paleoflow. Paleocurrent patterns in the Pliensbachian indicate a major shift in regional sedimentation. Northeast-derived clastics become a significant component of basin-fill during the Early Pliensbachian and persist until at least Late Pliensbachian (Kunae Zone) time. Upper and mid-fan greywacke of the northern facies contain a significant component of pyroclastic and volcanoclastic equivalents that display a marked lithological similarity to the Nordenskiöld dacite. An ammonite fauna of strong Boreal affinity was identified in Upper Pliensbachian (Kunae Zone) strata derived from the northeast that has not been previously recognized in the Inklin Formation.

Résumé : La Formation d'Inklin (Jurassique inférieur) du Groupe de Laberge couvre l'intervalle du Sinémurien précoce au Pliensbachien tardif et peut-être au Toarcien précoce dans la région d'Atlin Lake. Les strates du Sinémurien contiennent principalement des turbidites boueuses finement litées qui témoignent d'un paléocoulement vers le nord-est. La configuration des paléocourants datés du Pliensbachien indiquent une importante modification des modèles de sédimentation régionale. Des roches clastiques en provenance du nord-est deviennent une importante composante du remplissage sédimentaire de bassin au cours du Pliensbachien précoce et persistent au moins jusqu'au Pliensbachien tardif (zone de Kunae). Les grauwackes des parties supérieure et intermédiaire de cône alluvial, dans le faciès nord, contiennent une composante significative de roches pyroclastiques et d'équivalents volcanoclastiques affichant une ressemblance lithologique marquée avec la dacite de Nordenskiöld. Une faune à ammonites, présentant de nettes affinités boréales, a été identifiée dans des strates du Pliensbachien supérieur (zone de Kunae), dont les matériaux proviennent du nord-est; cette faune n'avait pas jusque-là été reconnue dans la Formation d'Inklin.

¹ Department of Geological Sciences, University of British Columbia, 6339 Stores Road, Vancouver, B.C. V6T 1Z4

INTRODUCTION

An understanding of the age, sedimentology and stratigraphy of the Inklin Formation is essential in deciphering Cache Creek, Stikine and Quesnel (?) terrane interactions in the northern Cordillera. Although the formation has been previously described during regional mapping projects (Souther, 1971; Mihalyuk et al., 1989) and in a thesis (Bultman, 1979), little detailed work has been done.

Field research in 1992 focused on the sedimentology and biochronology of ten measured stratigraphic sections ranging from 200 to 700 m thick that include Lower Sinemurian through Upper Pliensbachian strata. This was complemented by detailed examination of extensive outcrop exposures along the shores and islands of southern Atlin Lake. Over 60 ammonite collections provide age control. Systematic microfossil sampling, mainly for radiolarians, was also conducted. Collections of clasts were made from conglomerates of various ages for provenance studies. Granitoid clasts from Upper Sinemurian and Upper Pliensbachian conglomerates were also collected for radiometric age determinations. Data on thermal maturation will be gathered through analysis of samples from carbon-rich horizons.

REGIONAL SETTING

The study area lies within the Intermontane Belt in the Atlin Lake region of northern British Columbia (Fig. 1). Mesozoic clastic strata of the Whitehorse Trough form a northwest-trending linear belt that extends through the study area, where sediments of the Laberge Group overlie the major tectonic boundary between the Stikine and Cache Creek (Atlin) terranes. Laberge Group sediments of the Whitehorse Trough have been subdivided in northern British Columbia into two partly coeval formations: the Inklin and the Takwahoni (Souther, 1971). The Lower Jurassic Inklin Formation is a largely deep-marine facies of submarine fan origin that is extensively underlain by Cache Creek basement (Monger et al., 1991). The Upper Pliensbachian to Lower Bajocian 'proximal' Takwahoni Formation unconformably overlies Stikinian (Stuhini Group) basement along much of the southwest margin of the trough in British Columbia (Wheeler et al., 1988). In the mid-Jurassic the two facies were juxtaposed across the southwesterly directed King Salmon Fault. The Takwahoni-Inklin formations form a Lower to Middle Jurassic overlap sequence that links the Stikine and Cache Creek terranes along much of the length of the Whitehorse Trough (Wheeler et al., 1988). Its marginal boundaries are defined by major faults – Nahlin Fault to the northeast and King Salmon (and Llewellyn) Fault to the southwest. Inklin strata have undergone at least one major phase of deformation (Bultman, 1979), so that stratigraphic continuity is disrupted by folds, faults, and bed parallel shear. The Takwahoni Formation is not exposed in the study area.

STRATIGRAPHY

Sinemurian

The oldest dated rocks of the Inklin Formation in the study area are Lower Sinemurian strata containing the ammonite genus *Arnioceras*. Upper Sinemurian strata containing *Paltechioceras* display similar sedimentological characteristics to Lower Sinemurian strata. Overall lithology of the succession is dominated by muddy turbidites. The modal (Bouma) sequence T_{c-e} is characteristic and represented by fine sand/silt-mud couplets, thick to thin silt-mud laminae, and graded, stratified muddy silt to silty mud deposited from low-concentration turbidity currents. These deposits are typical of lower fan, fan-fringe and basin-plain settings but also occur throughout fans in interchannel environments, particularly in overbank settings (Pickering et al., 1986). Mud-silt ratios exhibit considerable variability both between and within particular sub-facies. Intercalations of tabular medium bedded fine greywacke ($T_a, T_{b(c)}$) occur throughout the muddy turbidite succession but are minor constituents except in the uppermost Sinemurian. Ripple cross-stratification foresets were measured in a number of localities in Sinemurian strata and consistently indicate a northeasterly paleoflow. The predominance of muddy turbidites and lack of proximal facies suggest lower-fan to basin plain settings for much of the succession.

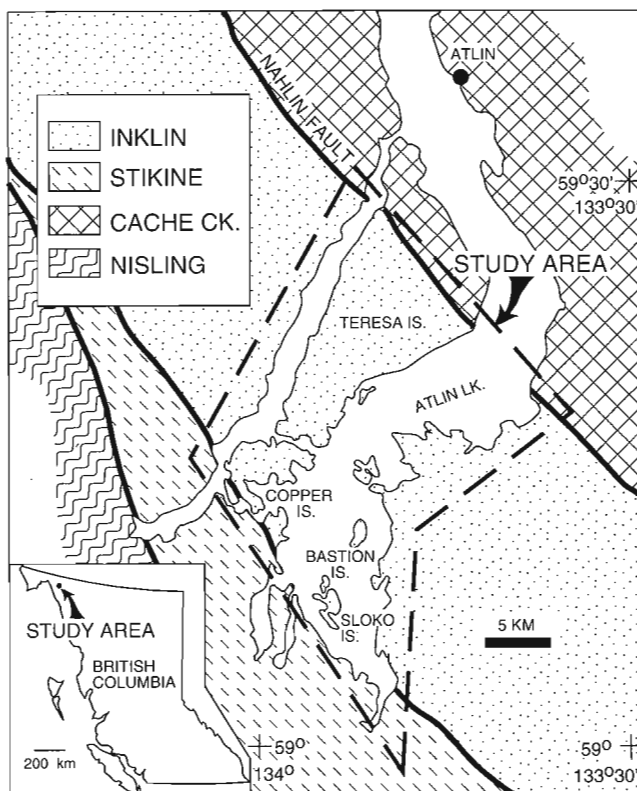


Figure 1. Map showing location of the study area and regional setting of the Whitehorse Trough (Inklin Formation) in the Atlin Lake area (modified after Wheeler et al., 1988).

Within Sinemurian strata rare slumped intervals and debris flow deposits are commonly associated. Slump deposits are generally in the range of a few metres thick (rarely more than 10 m) and are represented by coherent/semi-coherent contorted and folded strata, to dislocated and balled strata in a silty mud matrix. In most cases these slide deposits are found in close stratigraphic proximity to heterolithic pebbly mudstone and muddy pebble-cobble conglomerate of cohesive debris flow origin. The conglomerates are generally thin (<8 m) and usually have lensoid (channel) geometry, though thinner tabular varieties also occur. They are usually matrix-supported, poorly sorted to unsorted, and of pebble to cobble grade. Clasts include volcanics, intrusives, carbonates, sedimentary intraclasts and rare chert. Carbonate clasts are common and resemble limestones of the Upper Triassic 'Sinwa' Formation exposed on the west side of Atlin Lake (Bultman, 1979). The absence of any appreciable proximal facies, restricted thickness of slumped intervals, and predominance of fine facies (muddy turbidites) favour lower-fan channel and interchannel overbank environments for these slumped deposits.

A number of sedimentological features distinguish the Sinemurian from other parts of the succession that contain similar lithofacies. The most diagnostic criterion is the common occurrence of intensely bioturbated horizons within the thinly-bedded muddy turbidites. The bioturbation consists of worm trails and shallow burrows of variable size and generally occurs within the graded stratified muddy silts and less pervasively in the silt-mud couplets (Fig. 2). Another diagnostic feature is the occurrence of thin (10-30 cm) interbeds of buff weathering muddy lime siltstone and lime mudstone containing abundant worm burrows. These distinctive beds are commonly normally graded with silty convolute or wispy laminae at their base. Typical Sinemurian strata display flaggy weathering of a crumbly dark grey/black to rusty aspect with resistant rusty brown to buff interbeds. In addition the silts and fine sands of the couplets generally weather rusty shades of brown and red, helping distinguish them from Pliensbachian sediments of similar lithological aspect, which tend to weather shades of white and light grey.



Figure 2. Sinemurian graded stratified muddy siltstone with typical bioturbation.

The upper part of the section coarsens upward and is dominated by thin to medium bedded fine sands containing abundant plant material. The sandstone is moderately to well indurated fine greywacke ($T_a, T_{ab(c)}$) that commonly weathers shades of tan and red. This coarsening upward shift in sedimentation suggests a change to a mid-fan setting that is marked near the top of the section by widespread pebble-cobble and cobble-boulder conglomerates that are commonly associated with underlying submarine slumps (Fig. 3). The coarsening-upward trend occurs in Upper Sinemurian strata across the study area and is apparently near the Sinemurian-Pliensbachian transition.

The contact between the Upper Triassic Stuhini Group and Lower Jurassic Inklin Formation is exposed at two localities on the southwest shore of Atlin Lake. The structural nature of the contact is evident on the southwest shore of Torres Channel where highly sheared and interleaved fault slices of Inklin strata and Sinwa Formation equivalents are well exposed. Sinemurian strata are rare in the southern part of the study area and absent along the southwest boundary where Lower Pliensbachian strata are found in fault contact with Sinwa-equivalent carbonates.

Lower Pliensbachian

The overall lithology of Lower Pliensbachian strata exhibit two distinct lithofacies of different provenance. In the northern part of the study area the Lower Pliensbachian is dominated by proximal facies of upper and mid-fan affinity which contain a significant volcanoclastic component. In the southwest (Sloko Island) a thick sequence (>150 m) dominated by thin rhythmically bedded argillite composed of fine sand/silt-mud couplets forms the upper 'half' of a Lower Pliensbachian positive (fining/bed-thinning upward) mega-sequence (*sensu* Heward, 1978). The basal section (>200 m: base not seen) comprises deposits dominated by medium- and thick-bedded, well-indurated tabular greywacke ($T_a, T_{ab(c)}$) with minor fine pebble-granule conglomerate and gritty sand near the base. The greywacke (typical of mid-fan settings) lacks a significant tuffaceous component. Ammonites are relatively common and locally abundant throughout the upper



Figure 3. Upper Sinemurian conglomerate overlying slumped muddy turbidites.

half of the megasequence and allow tight age constraints for this section. The lowest fauna encountered in the 'muddy' facies is dominated by *Dubariceras*, followed closely upsection by the appearance of abundant *Metaderoceras* with subordinate *Dubariceras*. These genera range from the basal Whiteavesi through Freboldi (ammonite) Zones of the Lower Pliensbachian (Smith et al., 1988). Species identifications are expected to refine the biochronology for this sequence. This upper lithofacies persists well into the Upper Pliensbachian in the southwest, forming a continuous section spanning most of the Pliensbachian stage.

Rocks of this upper lithofacies are distinctive, comprising related finer subfacies of mid-fan and lower fan settings. They are commonly thin to very thin-bedded, planar to rippled fine sand/silt-mud couplets, and thick to thin silt-mud laminae (Fig. 4). The sand-silt fraction commonly weathers shades of white and light grey and the muds dark grey to black, producing a distinctive rhythmically banded appearance. The 'coarse' fraction contains numerous small scale current-generated structures in the form of planar to wispy laminations, ripple cross-lamination, and rippled beds which consistently indicate a northeasterly paleoflow. The fine fraction is locally finely laminated and can also be bioturbated but the bioturbation is generally finer and far less abundant than that found in Sinemurian beds. Thin to medium interbeds of brown to buff weathering fine (T_{ab} , T_b) greywacke and buff weathering lime mudstone and muddy limestones are scattered throughout this section.

The second lithofacies is widespread in the north and east regions of the study area and forms the thickest member of the Inklin Formation (800+ m). There is a paucity of paleocurrent indicators in this coarse northern facies but foresets at a few localities indicate a southwest paleoflow. This sequence is characterized by medium to very thick bedded massive to graded (T_a , $T_{ab(c)}$) greywacke that is typically fine- to medium-grained but includes pebbly and conglomeratic sandstone. The greywacke is well indurated and weathers grey-green to dark grey and tan. Thin intercalations of dark brown siltstone and mudstone separate beds and thick units of stacked sandstone. Spherical brown sand concretions and shale rip-up clasts are common. The

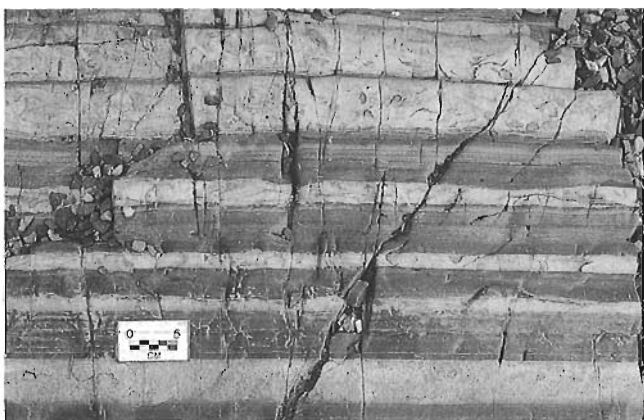


Figure 4. Lower Pliensbachian rhythmically bedded cross-stratified fine sand-mud couplets (Sloko Island).

dominance of these coarse facies is indicative of upper and mid-fan settings. A primary association in this Lower Pliensbachian section is the presence of distinctive pyroclastic and related volcanoclastic deposits that exhibit a marked lithological similarity to the Nordenskiöld dacite (Cairnes, 1910) and correlative volcanics in the Atlin area. In the study area the volcanoclastic deposits are generally found as reworked fine lapilli tuffs and are relatively uncommon as primary pyroclastic deposits (Fig. 5). They probably originated as crystal-lithic lapilli tuffs of intermediate (dacitic) composition and are characterized by abundant feldspar, quartz, hornblende, and biotite. These rocks weather a distinctive light grey that is commonly mottled and display a salt-and-pepper texture on fresh surfaces. The volcanoclastics are fine- to medium-grained and commonly sorted to well sorted. Coarser variants do occur, including pebbly to conglomeratic litharenite, but are minor. These deposits are widespread in this coarse northern facies where they can form well-bedded units in excess of 150 m. They grade into and are associated with tuffaceous greywacke. Although the common occurrence of these deposits is confined to the Lower Pliensbachian of the north and northeast part of the study area, a late episode of similar volcanism was identified in Upper Pliensbachian strata.

Upper Pliensbachian

The Upper Pliensbachian section also exhibits different lithological characteristics that are due, in part, to provenance rather than lateral facies changes. The lithofacies are more closely related in depositional setting and exhibit greater variability in gross lithology than is the case in Lower Pliensbachian strata of dual provenance. Ammonites are relatively common in finer grained ('muddy') facies and are dominated by Hildoceratids (notably *Protogrammoceras*) with subordinate Dactyloceratids (*Aveyroniceras*) in lower sections.

In the southwest (Sloko Island section) Upper Pliensbachian strata form an unbroken section with Lower Pliensbachian rocks of similar lithofacies. These muddy turbidites of lower-fan affinity are indistinguishable from similar Lower

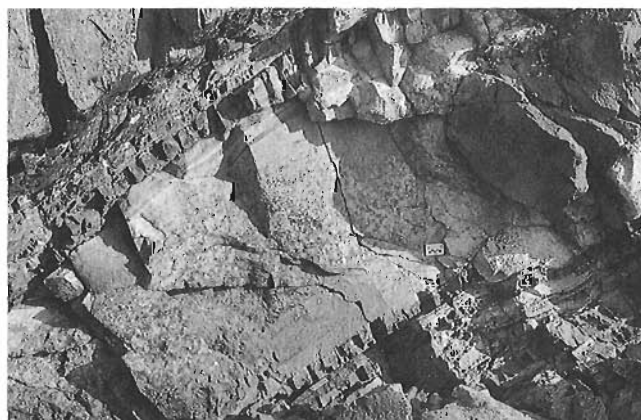


Figure 5. Lower Pliensbachian volcanoclastic litharenite: note mottled appearance (scale right centre).

Pliensbachian strata, being also dominated by T_{c-e} fine sand/silt-mud couplets (Fig. 6). Similar small-scale current-generated structures are common as well and also clearly indicate northeasterly paleoflow. The lower section of the Upper Pliensbachian extends well into the Kunae Zone in the south and central regions of the study area and forms the top of the positive megasequence initiated in the Lower Pliensbachian. During Kunae Zone time the sudden influx of coarse clastics marks a change in sedimentation that affects much of the study area in the south. It begins with the appearance of a distinctive cobble-boulder conglomerate overlain by coarse to medium greywacke and subordinate litharenite. This unit differs markedly from earlier conglomerates through the presence of abundant granitoid clasts (Fig. 7), which are minor constituents in Sinemurian and Lower Pliensbachian conglomerates. This channelized conglomerate grades laterally into and is overlain by, coarser greywacke that is less feldspathic and more quartzose than similar Lower Pliensbachian greywacke. This unit is separated from a second, coarse fining-up sequence by a thinner succession of muddy turbidites similar to those beneath the granitoid conglomerate which also contain ammonites of Kunae Zone age. The fining-upward sequence begins with a similar (though finer) basal conglomerate that grades into coarse and fine sands. Correlatives of these two coarse Upper Pliensbachian units also occur farther north on Bastion Island.

Probable Upper Pliensbachian strata are relatively poorly constrained in the north and east regions of the study area with the exception of Copper Island where fossils are more common. There, strata have a complex structural history that involves overturned folding and major faulting. Paleocurrent indicators are relatively common in Upper Pliensbachian strata on Copper Island and indicate paleoflow to the southwest. The section is well constrained biochronologically with the base of the Upper Pliensbachian marked by the co-occurrence of *Aveyronicerias* and *Protogrammoceras*. The base marks the beginning of a thick negative (coarsening/bed-thickening upward) megasequence (500+ m) which spans much of the Kunae Zone on Copper Island and forms a continuous section with an underlying Lower Pliensbachian



Figure 6. Upper Pliensbachian thin-bedded coarse silt-mud couplets and laminae (Sloko Island).



Figure 7. Upper Pliensbachian granitoid cobble-boulder conglomerate (Sloko Island).

positive megasequence (300+ m). Strata coarsen upward from a thin section of muddy turbidites and are dominated by coarser sub-facies of mid-fan affinity deposited mainly from high-concentration turbidity currents. The bulk of the negative megasequence comprises medium- to thick-bedded massive graded (T_{a}, T_{ab}) to parallel stratified sands with intercalations of thin (1-5 m) fine sand/silt-mud couplets that contain ammonites of Kunae zone age. Thin-bedded muddy turbidites have a higher siliciclastic content in both the fine and coarse fraction than similar lithofacies derived from the southwest. Near the top of the negative megasequence a thick unit (>50 m) of mixed pyroclastics and associated volcanoclastics was found. This unit exhibits the same distinctive lithological characteristics of volcanoclastic/pyroclastic deposits previously found only in Lower Pliensbachian strata derived from the northeast. Tight biochronological brackets constrain this unit to the Kunae Zone of the Upper Pliensbachian.

One other feature of note in this section concerns ammonite faunas. The Copper Island section contains a markedly different ammonite fauna from other Upper Pliensbachian strata. The fauna is strongly dominated by Amaltheids which have been found at no other locality. The

essentially monogeneric occurrence of Amaltheid horizons strongly argues for a distinct Boreal affinity, as opposed to the mixed Tethyan/Boreal faunas found everywhere else in the study area.

Paleocurrent data

An important aim of the study was to determine paleocurrent patterns and establish the existence and chronology of regional shifts in provenance. Data collected for paleocurrent analysis consist mainly of ripple cross-stratification foresets but also include flute cast directions and groove cast orientations. A total of approximately 140 such measurements were made.

Paleocurrent data indicate a westerly to southwesterly Stikinian source for Sinemurian strata. No evidence of a northerly source was found for the Sinemurian section in the study area. Paleocurrent patterns for the Pliensbachian exhibit greater variability and indicate the initiation of a bimodal input to the trough. In the southwest region of Atlin Lake (Sloko Island section) Lower Pliensbachian through Upper Pliensbachian strata clearly indicate a source to the west and southwest, but strata of equivalent age in the north appear to have a source to the northeast. The Early Pliensbachian appears to mark a significant shift in regional sedimentation patterns with the onset of major clastic input from the northeast. Lower Pliensbachian sediments derived from this source are dominated by coarse proximal facies and include a significant pyroclastic/volcaniclastic component, forming the thickest member of the Inklin Formation in the study area. This sedimentation regime continued through the Upper Pliensbachian. The areal distribution of coeval Upper Pliensbachian strata of dual provenance is more restricted and less clearly defined than in the Lower Pliensbachian and may indicate a waning clastic input from the northeast.

SUMMARY

Ammonite biochronology constrains Inklin strata in the study area to an age of Early Sinemurian to Late Pliensbachian. No unequivocal Toarcian faunas were collected but pending species identifications of *Protogrammoceras* may confirm the presence of Lower Toarcian strata. The presence of Amaltheid dominated horizons in Upper Pliensbachian strata derived from the northeast indicates a previously unknown Boreal influence in this region of the Whitehorse Trough.

Paleocurrent patterns confirm the existence of a dual provenance for the Inklin Formation. Sediments derived from Stikinia to the west and southwest comprise a submarine fan succession of diverse lithofacies that spans Lower Sinemurian through Upper Pliensbachian strata. Northeast-derived clastics become a significant component of basin-fill no later than Early Pliensbachian and comprise coarser facies of upper- and mid-fan affinity. Distinctive pyroclastic and volcaniclastic equivalents are likely correlatives of the Nordenskiöld dacite and appear to be confined to the succession derived from the northeast.

ACKNOWLEDGMENTS

The field research reported herein forms the basis of the author's M.Sc. thesis at the University of British Columbia, supervised by Paul Smith and funded through a Natural Science and Engineering Research Council grant, with additional support from Energy, Mines, and Resources, Canada. Special thanks to Steve Gordey of the Geological Survey of Canada for logistical support and valuable advice during discussions in the field. Invaluable guidance provided by Howard Tipper during enlightening discussions and on a visit to the field is greatly appreciated. Insightful comments from Paul Smith in the field are also appreciated. Able field assistance was provided by Brendan Wilson. A critical review by Steve Gordey substantially improved sections of this paper.

REFERENCES

- Bultman, T.R.**
1979: Geology and tectonic history of the Whitehorse Trough west of Atlin, British Columbia; Ph.D. thesis, Yale University, New Haven, Connecticut, 284 p.
- Cairnes, D.D.**
1910: Preliminary memoir on the Lewes and Nordenskiöld Rivers coal district; Geological Survey of Canada, Memoir 5, 70 p.
- Heward, A.P.**
1978: Alluvial fan sequence and megasequence models: with examples from Westphalian D – Stephanian B coalfields, northern Spain; in *Fluvial Sedimentology*, (ed.) A.D. Miall; Canadian Society of Petroleum Geologists, Memoir 5, p. 669-702.
- Mihalynuk, M.G., Currie, L.D., and Arksey, R.L.**
1989: The geology of the Tagish Lake area (Fantail Lake and Warm Creek) (104M/9W and 10E); in *Geological Fieldwork 1989*; British Columbia Ministry of Energy, Mines and Petroleum Resources, Paper 1989-1, p. 293-310.
- Monger, J.W.H., Wheeler, J.O., Tipper, H.W., Gabrielse, H., Harms, T., Struik, L.C., Campbell, R.B., Dodds, C.J., Gehrels, G.E., and O'Brien, J.**
1991: Part B. Cordilleran terranes; in *Upper Devonian to Middle Jurassic assemblages*, Chapter 8 of *Geology of the Cordilleran Orogen in Canada*, (ed.) H. Gabrielse and C.J. Yorath; Geological Survey of Canada, *Geology of Canada*, no. 4, p. 281-327.
- Pickering, K., Stow, D.A.V., Watson, M., and Hiscott, R.**
1986: Deep-water facies, processes and models: a review and classification scheme for modern and ancient sediments; *Earth Science Review*, v. 23, p. 75-174.
- Smith, P.L., Tipper, H.W., Taylor, D.G., and Guex, J.**
1988: An ammonite zonation for the Lower Jurassic of Canada and the United States: the Pliensbachian; *Canadian Journal of Earth Sciences*, v. 25, p. 1503-1523.
- Souther, J.G.**
1971: Geology and mineral deposits of the Tulsequah map-area, British Columbia; Geological Survey of Canada, Memoir 362, 84 p.
- Wheeler, J.O., Brookfield, A.J., Gabrielse, H., Monger, J.W.H., Tipper, H.W., and Woodsworth, G.J.**
1988: Terrane map of the Canadian Cordillera; Geological Survey of Canada, Open File 1894, 9 pages and 1:2 000 000 map.

Jurassic stratigraphy of the Diagonal Mountain area, McConnell Creek map area, north-central British Columbia

Giselle Jakobs

Cordilleran Division, Vancouver

Jakobs, G., 1993: Jurassic stratigraphy of the Diagonal Mountain area, McConnell Creek map area, north-central British Columbia; in Current Research, Part A; Geological Survey of Canada, Paper 93-1A, p. 43-46.

Abstract: Field work along the eastern margin of the Bowser Basin confirms the presence of a relatively complete stratigraphic sequence from the Diagonal Mountain area (McConnell Creek map area (94D west half)). This section encompasses the Hazelton Group "pyjama beds" and the Bowser Lake Group Ashman Formation. Ammonites collected from the measured sections range from the Toarcian through to the Callovian, but the previously recorded occurrence of Pliensbachian and Oxfordian fossils was not confirmed. Pre-Bowser Lake Group strata outcrop in a northwest-southeast band extending from Diagonal Mountain (94D/11) northwest to Melanistic Peak (94D/13).

Résumé : Les travaux de terrain effectués sur la marge est du bassin de Bowser confirment la présence d'une séquence stratigraphique relativement complète à partir de la région de Diagonal Mountain (région cartographique de McConnell Creek, 94D, moitié ouest). Ce profil stratigraphique englobe les couches rayées («pyjama beds») du Groupe de Hazelton et la Formation d'Ashman du Groupe de Bowser Lake. Les ammonites recueillies dans les profils mesurés datent de la période s'étendant du Toarcien à la fin du Callovien, mais la présence auparavant notée de fossiles datant du Pliensbachien et de l'Oxfordien n'a pas été confirmée. Des strates antérieures au Groupe de Bowser Lake affleurent suivant une bande nord-ouest sud-est allant du mont Diagonal (94D/11) vers le nord-ouest au pic Melanistic (94D/13).

INTRODUCTION

Strata of the Bowser Basin are critical to understanding the geological history of the Stikine and Cache Creek terranes. Bowser Lake Group strata cover much of the basin, and pre-Bowser Lake Group rocks of the Hazelton Group are generally restricted to the margins of the basin. Clastic sediments of the Hazelton Group and coeval strata of the Spatsizi Group occur in the Iskut, Telegraph Creek, Spatsizi, McConnell Creek, Hazelton, and Smithers map areas. Complete stratigraphic sections are rare along the eastern margin of the basin. Preliminary work (Jeletzky, 1976; Tipper, 1976; Tipper and Richards, 1976) indicated that the stratigraphic sequence at Diagonal Mountain is the most complete section along the eastern margin of the basin, ranging in age from Pliensbachian to Oxfordian. This central area is of critical importance in linking the northern and southern margins of the basin. The extent of pre-Bowser Lake Group rocks in the Diagonal Mountain area was not known prior to this study, and the mapping of such strata to the northwest and southeast was undertaken. In addition, selected areas underlain by Bowser Lake Group and Sustut Group were mapped.

STRATIGRAPHY

In the Diagonal Mountain area, distinctive "pyjama beds" assigned to the Hazelton Group by Tipper and Richards (1976) grade up through a transitional zone into rocks of the Ashman Formation of the Bowser Lake Group. These are overlain in turn by the Tango Creek Formation of the Sustut Group.

Hazelton Group

In the study area (Fig. 1), pre-Bowser Lake Group rocks are represented by "pyjama beds", distinctive laminated siliceous siltstones with a banded appearance. They are widespread and occur in the Iskut, Telegraph Creek, and Spatsizi map areas (Anderson and Thorkelson, 1990; Evenchick, 1988, 1991, 1992). Tipper and Richards (1976) assigned them to the Yuen Member of the Smithers Formation (Hazelton Group) in the southern Bowser Basin. Thomson et al. (1986), working in the Spatsizi area, assigned them to the Quock Formation of the Spatsizi Group.

The "pyjama beds" are extremely hard, siliceous rocks and are well bedded, usually 10 to 15 cm thick but some beds may be 1 to 30 cm thick. The beds are commonly interbedded with fine- to medium-grained tuff layers (1-3 cm thick) which are in many places greenish to white and weather rusty to black. The siltstone usually weathers rusty but some black manganese oxidation may also be present. Some siltstone beds are finely layered and may have convoluted bedding or slump structures. Buff- to rusty-weathering calcareous concretions are present and may exceed 1 m in diameter. Several intervals within the "pyjama bed" sequence contain pink weathering tuff layers in a black siltstone which may weather light grey. The "pyjama beds" are highly variable with some parts showing distinctive black/white banding with some pinkish weathering layers as well. Other parts are primarily black siltstone with thin (0.5 to 1 cm) white bands and rusty weathering, light coloured ash layers. The well banded sequence seems to repeat at least three times, once near the base of the section, once near the middle, and once at the top. Based on ammonites collected in 1992, this unit is

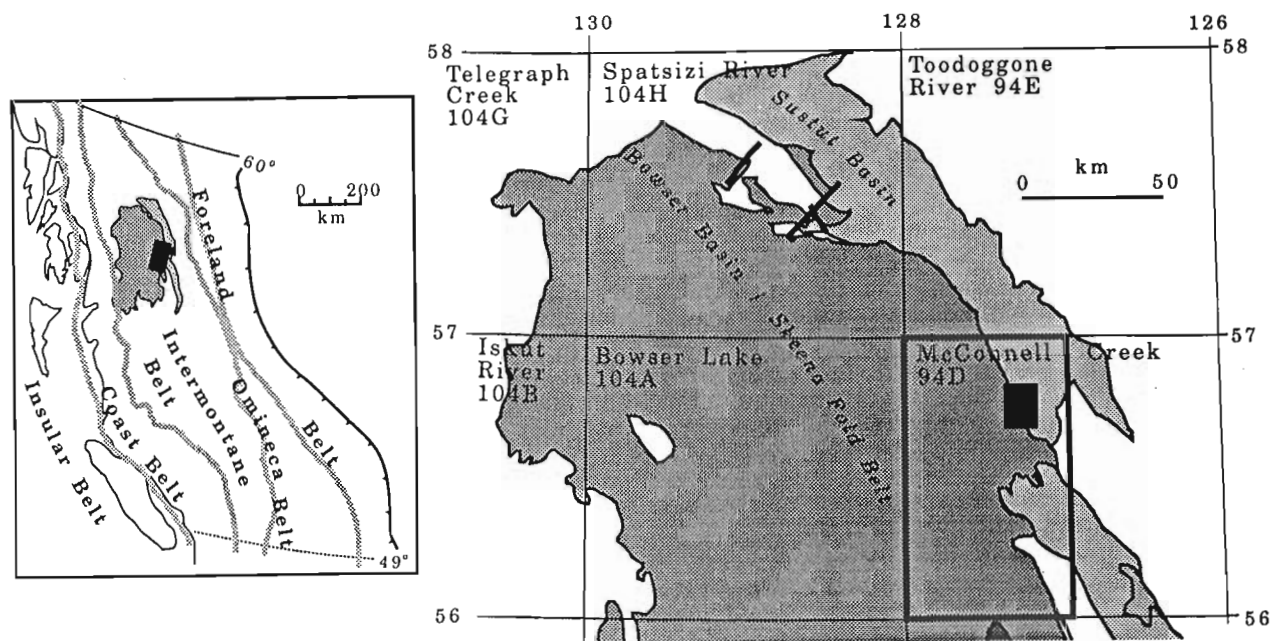


Figure 1. Location of the Bowser and Sustut basins with respect to morphogeological belts in the Canadian Cordillera (left), and location of the study area in McConnell Creek map area with respect to the Bowser and Sustut basins (morphogeological belts after Gabrielse and Yorath, 1989). Solid rectangle is location of Figure 2.

Toarcian to Bajocian in age. Tipper and Richards (1976) mentioned the occurrence of Pliensbachian strata but this was not confirmed. Fossils in the "pyjama beds" are more common than in the overlying Ashman Formation, which is intensely cleaved. Belemnites, bivalves, and ammonites are common.

The basal contact of the "pyjama beds" is not exposed in the study area. The contact with the overlying Ashman Formation of the Bowser Lake Group is transitional. The frequency and thickness of the tuff bands and ash layers decreases upsection and the rocks become intensely cleaved. This interval is similar to some of the less tuffaceous "pyjama beds", and it is probably better at this time to include the transitional rocks in the "pyjama beds" rather than the Ashman Formation.

Ashman Formation of the Bowser Lake Group

Two facies can be recognized in the study area, a fine- to medium-grained siltstone/sandstone unit with minor chert granule/pebble conglomerate overlain by a medium-grained sandstone unit with thick (up to 10 m) chert-pebble conglomerate beds.

The basal siltstone/sandstone unit coarsens upwards with siltstone predominating at the base of the unit and sandstone and conglomerate predominating at the top of the unit. The siltstone commonly weathers a rusty colour, although lower in the unit a more medium- to dark-grey weathering is also seen. Buff- to grey-weathering calcareous concretions are present and may contain pyrite. The siltstone is generally intensely cleaved and faulted and fossils are poorly preserved, although limestone concretions yielded several well preserved ammonite collections.

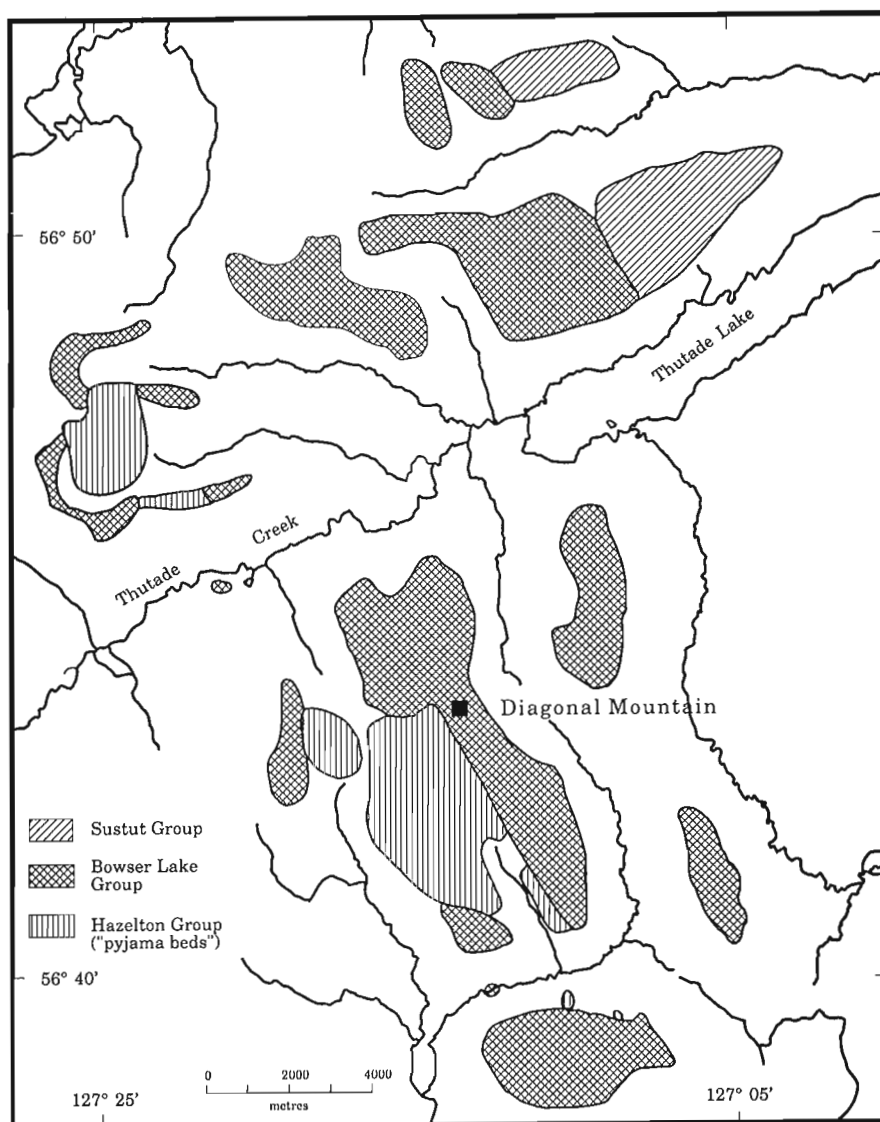


Figure 2. General geological map of the Diagonal Mountain area in northeast McConnell Creek map area.

The siltstone is overlain by interbedded siltstone, sandstone, and conglomerate. The lowermost sandstone bed (approximately 10-20 m thick) contains a basal chert-granule layer just above the siltstone. Above this unit is a sequence of interbedded siltstones and sandstones. The siltstones are black with rusty weathering and intensely cleaved. Some sandstone units contain chert granule/pebble conglomerate layers. The medium grained, grey sandstone may contain whitish weathering, black siltstone clasts and often contains graded bedding, crossbedding, and ball and pillow structures. Ammonites are rare and generally poorly preserved due to the pervasive cleavage. The upper contact is not exposed in the study area.

The overlying medium grained sandstone/conglomerate unit is exposed north of Thutade Lake. Interbedded fine grained, medium grey sandstone and black siltstone occur in beds 10 to 20 m thick. These are interbedded with thick (10-20 m) beds of rusty weathering chert-pebble conglomerate. Ripple marks, bioturbation marks, and crossbedding occur in the sandstone. Several coquina layers containing abundant ammonites, belemnites, bivalves, and plant fragments were encountered. This unit is Oxfordian in age. The lower contact of the unit is not exposed in the study area.

Tango Creek Formation of the Sustut Group

Rocks of the nonmarine Tango Creek Formation were encountered north of Thutade Lake. They are composed primarily of buff weathering, coarse- to medium-grained sandstone. Plant fragments and black siltstone clasts are common. The sandstone is interbedded with siltstone and conglomerate. The siltstone is generally black, recessive, and weathers a brownish green. In the western part of the outcrop area, purple and green siltstones and fine sandstones are more common and are key marker units. Several conglomerate units are present: a siltstone-pebble conglomerate, a chert-pebble conglomerate, and a quartz pebble/cobble conglomerate. The upper contact of the Tango Creek Formation was not encountered in the study area. The disconformable basal contact with the Bowser Lake Group is well exposed at several areas. On the ridge to the north of Thutade Lake, the contact as drawn by Eisbacher (1974) should be positioned 1 km to the east.

DISCUSSION

Work completed during the field season indicates that the clastic strata of the Hazelton Group extend in a roughly northwest-southeast band from Diagonal Mountain (Fig. 2). Evenchick and Porter (1993) also reported the occurrence of Hazelton Group rocks at Melanistic Peak (94D/13), some 15 km to the northwest of the study area, on trend with the strata at Diagonal Mountain.

A series of biostratigraphic sections measured at Diagonal Mountain yielded a succession ranging in age from Toarcian to Callovian. Sedimentological and organic maturation samples collected from the sequence will aid in unravelling the geological history of this part of the Bowser Basin.

ACKNOWLEDGMENTS

This study is part of a Post-doctoral Fellowship under the supervision of C.A. Evenchick, whose support and advice is greatly appreciated. Jim Reed (Pacific Western Helicopters) provided friendly and professional service. The people at Suskeena Lodge deserve special thanks for their warm hospitality, the excellent cooking, and all the little extras which made us feel right at home. Field assistance was ably provided by M. Marchuk (U.B.C.). G. Woodsworth made several helpful comments in reviewing the manuscript.

REFERENCES

- Anderson, R.G. and Thorkelson, D.J.**
1990: Mesozoic stratigraphy and setting for some mineral deposits in Iskut River map area, northwestern British Columbia; in Current Research, Part E; Geological Survey of Canada, Paper 90-1E, p. 131-139.
- Eisbacher, G.H.**
1974: Sedimentary history and tectonic evolution of the Sustut and Sifton basins, north-central British Columbia; Geological Survey of Canada, Paper 73-31.
- Evenchick, C.A.**
1988: Structural style and stratigraphy in northeast Bowser and Sustut basins, north-central British Columbia; in Current Research, Part E; Geological Survey of Canada, Paper 88-1E, p. 91-95.
1991: Jurassic stratigraphy of east Telegraph Creek and west Spatsizi map areas, British Columbia; in Current Research, Part A; Geological Survey of Canada, Paper 91-1A, p. 155-162.
1992: Bowser Basin facies and map units in southwest Toadoggonne map area, British Columbia; in Current Research, Part A; Geological Survey of Canada, Paper 92-1A, p. 77-84.
- Evenchick, C.A. and Porter, S.**
1993: Geology of the McConnell Creek map-area, British Columbia; in Current Research, Part A; Geological Survey of Canada, Paper 93-1A.
- Gabrielse, H. and Yorath, C.J.**
1989: Decade of North American Geology, Volume #4. The Cordilleran Orogen in Canada; Geoscience Canada, v. 16, p. 67-83.
- Jeletzky, O.L.**
1976: Preliminary report on stratigraphy and depositional history of Middle to Upper Jurassic strata in McConnell Creek map-area (94D west half), British Columbia; in Report of Activities, Part A; Geological Survey of Canada, Paper 76-1A, p. 63-67.
- Thomson, R.C., Smith, P.L., and Tipper, H.W.**
1986: Lower to Middle Jurassic (Pliensbachian to Bajocian) stratigraphy of the northern Spatsizi area, north-central British Columbia; Canadian Journal of Earth Sciences, v. 23, p. 1963-1973.
- Tipper, H.W.**
1976: Biostratigraphic study of Mesozoic rocks in Intermontane and Insular belts of the Canadian Cordillera, British Columbia; in Report of Activities, Part A; Geological Survey of Canada, Paper 76-1A, p. 57-61.
- Tipper, H.W. and Richards, T.A.**
1976: Jurassic stratigraphy and history of north-central British Columbia; Geological Survey of Canada, Bulletin 270.

Geology of west McConnell Creek map area, British Columbia

C.A. Evenchick and J.S. Porter¹
Cordilleran Division, Vancouver

C.A. Evenchick and Porter, J.S., 1993: Geology of west McConnell Creek map area, British Columbia; in Current Research, Part A; Geological Survey of Canada, Paper 93-1A, p. 47-55.

Abstract: West McConnell Creek map area (94D) is underlain mainly by Middle Jurassic to Upper Jurassic Bowser Lake Group. Other bedrock map units, in order of abundance, are the Lower to Upper Cretaceous Sustut Group, Late Cretaceous plutonic rocks, and Lower Jurassic Hazelton Group volcanic and clastic rock, including clastic rocks stratigraphically equivalent to the Troy Ridge facies of the Salmon River Formation in Iskut area, and Yuen member of the Smithers Formation in the Hazelton area. Strata of the Bowser Lake Group are divided into 5 lithofacies assemblages, representing depositional environments ranging from deep marine, to open shallow marine, deltaic, and nonmarine.

Cretaceous and older stratified rocks are intensely folded and faulted, and are considered part of the Skeena Fold Belt. Northeast verging structures are ubiquitous.

Résumé : Le sous-sol du secteur cartographique de West McConnell Creek (94D) contient principalement des roches du Groupe de Bowser Lake du Jurassique moyen à supérieur. Les autres unités cartographiques du substratum rocheux, selon leur ordre d'abondance, sont le Groupe de Sustut du Crétacé inférieur à moyen, des roches plutoniques datées du Crétacé tardif, et des roches volcaniques et clastiques du Groupe de Hazelton situé dans le Jurassique inférieur, notamment des roches clastiques qui sont les équivalents stratigraphiques du faciès de Troy Ridge dans la formation de Salmon River, située dans la région d'Iskut, et du membre de Yuen dans la Formation de Smithers située dans la région de Hazelton. On peut subdiviser les strates du Groupe de Bowser Lake en cinq assemblages de lithofaciès, qui représentent des milieux sédimentaires variés, du type milieu marin profond passant à un milieu épicontinental ouvert, puis à un milieu deltaïque, et enfin à un milieu non marin.

Les roches crétacées et d'autres roches stratifiées plus anciennes sont intensément plissées et faillées, et on considère qu'elles font partie de la zone de plissement de Skeena. Des structures de vergence nord-est se retrouvent partout.

¹ Department of Geology and Geophysics, University of Calgary, 2500 University Drive N.W., Calgary, Alberta T2N 1N4

INTRODUCTION

Regional mapping of west McConnell Creek map area (94D; Fig. 1) was undertaken in June and July 1992 as part of a 3-month reconnaissance of the central Bowser Basin (see Evenchick et al., 1993¹) intended to complement the more detailed mapping to the north (Evenchick, 1987, 1988, 1989, 1991a,b, 1992; Evenchick and Green, 1990) and south (Tipper and Richards, 1976; Richards, 1990). Study of the northern Bowser Basin was initiated in 1985 to gain an understanding of the depositional, thermal, and structural histories of the northern basin. West McConnell Creek map area was a crucial gap of mapping on the east side of the basin.

The study area is underlain primarily by Middle to Upper Jurassic strata of the Bowser Lake Group (Fig. 2). The northeast and east-central areas are underlain by the Cretaceous Sustut Group, mapped by Eisbacher (1974). Small areas of Lower to Middle Jurassic Hazelton Group occur along the east side of the map, and late Cretaceous(?) plutons (Bulkley intrusions) occur in the southeast. Although east McConnell Creek area has been mapped at a regional scale (Richards, 1976a,b), the only published data on west McConnell area are a stratigraphic study of the Bowser Lake Group by Jeletzky (1976), and a regional study of the Sustut Basin by Eisbacher (1974). Eisbacher's map outlining the Sustut Basin and surrounding strata is the only available map of the area. Tipper and Richards (1976) referred to some sections in the area in a treatment of Mesozoic stratigraphy of north-central British Columbia. Ubiquitous folds in Cretaceous and older strata are part of the Skeena Fold Belt,

encompassing the entire Bowser Basin, southwest Sustut Basin, and involving underlying Hazelton Group and lower strata (Evenchick, 1991b). This preliminary report of reconnaissance mapping in McConnell Creek map area focuses on the Bowser Lake Group.

HAZELTON GROUP

The Lower to Middle Jurassic Hazelton Group is widespread in east McConnell Creek map area, but underlies less than 10 km² of the west side of the map area (Fig. 2). In the east, it is typical in that it is mainly volcanic and volcanoclastic, with a clastic upper part below the Bowser Lake Group. The upper strata include distinctive thinly bedded siliceous siltstone, shale and tuff(?), informally called "pyjama beds" throughout the region, but with local names of Quock Formation (of Spatsizi Group) in Spatsizi map area, Troy Ridge facies of the Salmon River Formation in Iskut area, and Yuen member of the Smithers Formation in Smithers and Hazelton map areas (Tipper and Richards, 1976; Thomson et al., 1986; Anderson and Thorkelson, 1990).

Most of the volcanic rock in west McConnell Creek map area is exposed along a ridge northwest of Mount Patcha. There, amygdaloidal basalt and andesite flows are interbedded with breccia and grey and maroon weathering tuff. Metavolcanics also occur east of Motase Peak where they are overlain by slate and phyllite. East of Bird Hill are coarse-bladed feldspar porphyry, maroon weathering volcanoclastics, and massive rhyolite or dacite, continuous

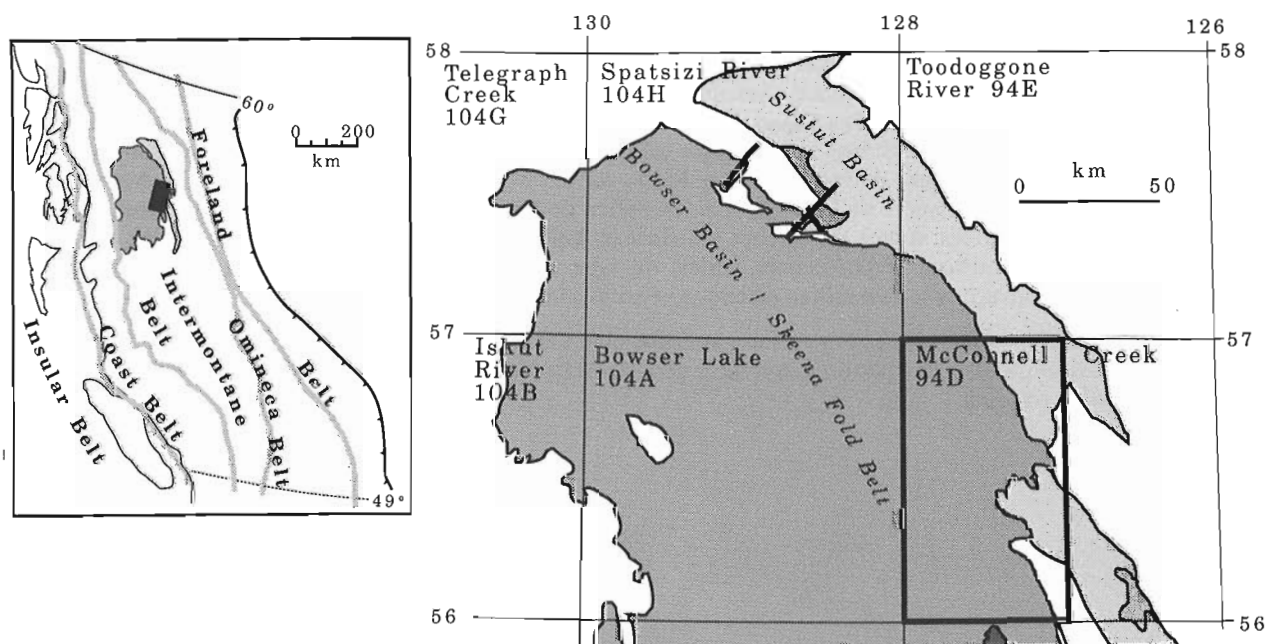


Figure 1. Location of the Bowser Basin in the Canadian Cordillera, McConnell Creek (west half) map area, and NTS map areas referred to in text.

¹ This preliminary report on the geology of the Bowser Lake map area (NTS 104 A) will be released as GSC Open File 2582 in January 1993.

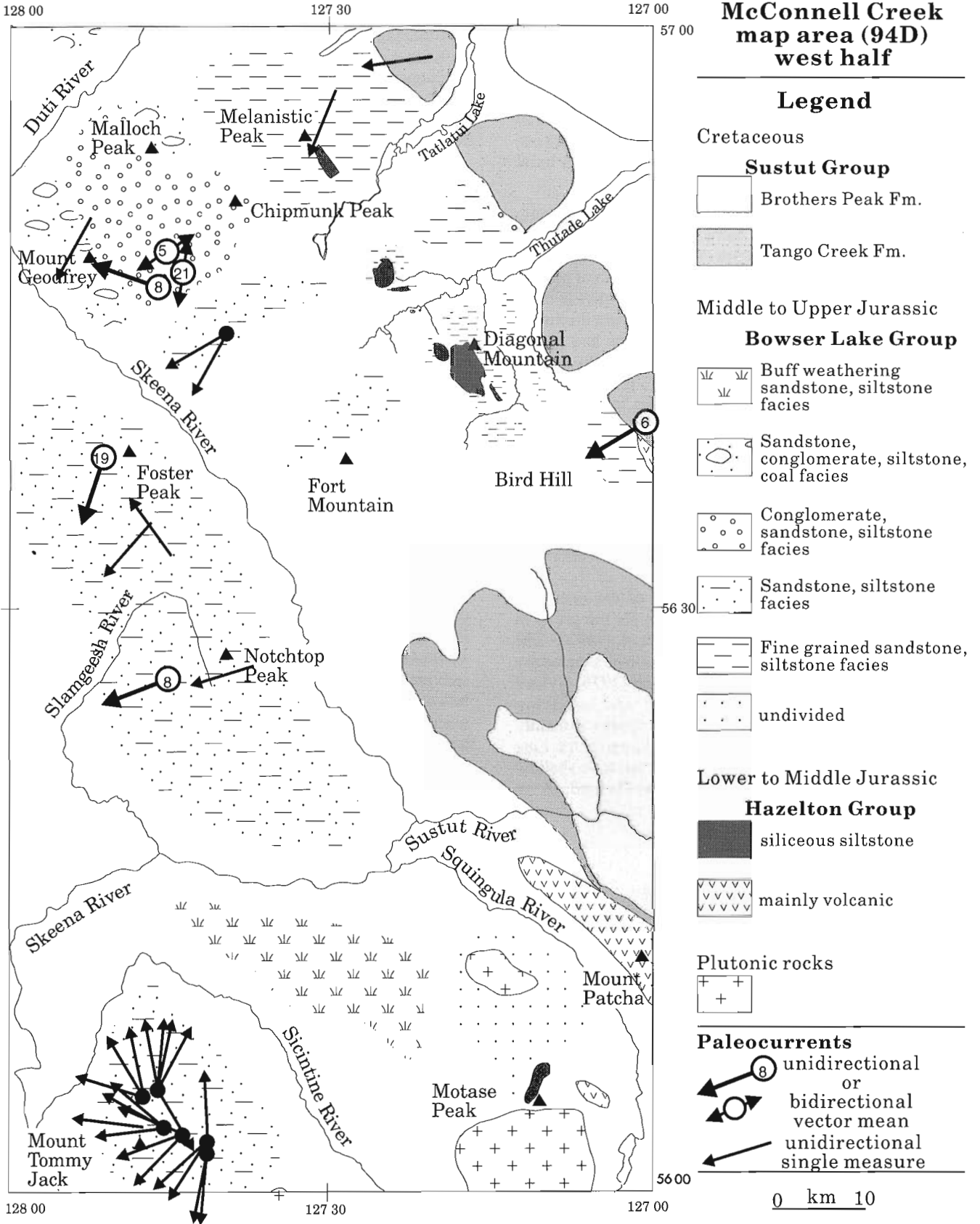


Figure 2. Geology of west McConnell Creek map area (94D west half). Paleocurrents are shown as vector mean arrows from sites where statistically significant trends were measured (number of measurements shown in circle placed over or near site of measurements). All paleocurrents are corrected for bed tilt.

with volcanic rocks in east McConnell Creek area considered to be Lower Jurassic Hazelton Group (Telkwa Formation) by Richards (1976b). Primary relationships here are poorly exposed, but it seems that the volcanic rocks are overlain by typical "pyjama beds"; found only in talus. The presence of Bowser Lake Group to the southwest limits the thickness of these strata to less than 100 m. All strata are overlain by basal Sustut Group.

"Pyjama beds" are also spatially associated with volcanic rocks east of Motase Peak, but more detailed work is required to determine the extent and nature of Hazelton Group clastic rock. Clastic rock west of Mount Patcha and north of Motase Peak may also include Hazelton Group. A relatively large area underlain mainly by "pyjama beds" occurs in a northwest belt through Diagonal Mountain. Descriptions and age of these strata are given by Jeletzky (1976) and Jakobs (1993). At Melanistic Peak about 100 m of rusty, grey and white weathering siliceous siltstone including rare "pyjama beds" and lenses of grey limestone occur in the core of an overturned anticline, and are gradationally overlain by dark weathering fine grained sandstone and medium grained chert arenite of the Bowser Lake Group.

BOWSER LAKE GROUP

The Bowser Lake Group underlies 80% of the map area (Fig. 2). A summary of the nomenclature for the group in surrounding areas is given by Evenchick et al. (1993). The first descriptions of the Bowser Lake Group in this region are those of Jeletzky (1976). Tipper and Richards (1976) divided the group into the Ashman Formation and overlying undivided Bowser Lake Group. The former applies to mainly marine shale, sandstone and minor conglomerate of Late Bajocian to Early Oxfordian age, and the latter to shallow marine to nonmarine facies of Late Oxfordian to

Kimmeridgian age. Included in the upper, undivided, Bowser Lake Group are the Netalzul volcanics, minor components of the group not present in the northern basin. Bowser Lake Group in McConnell Creek west half is tentatively divided into 5 lithofacies assemblages inferred to represent general environments of deposition.

Fine grained sandstone and siltstone facies

Sections composed mainly of fine grained sandstone, siltstone, and mudstone occur in the northeast corner of the map (Fig. 2). Strata between the two areas described below are the subject of research begun in 1992 by Jakobs (1993).

Melanistic Peak

Northwest and southeast of Melanistic Peak is a section at least 1000 m thick, composed of more than 90% black siltstone and fine grained sandstone. Sedimentary structures are parallel lamination, graded bedding, fine bioturbation, slump folds, and rare flame structures. Less than 10% of the section is composed of 10-20 m thick sheets of medium grained chert arenite, and lenses of chert pebble conglomerate. The thickest accumulation of medium grained arenite is in the basal 200 m of the Bowser Lake Group, where about 50% is composed of massive or parallel laminated thin to thick sandstone beds in 3 to 10 m intervals. Conglomerate occurs only as thin beds near the base of some sandstone intervals, and as discrete lenses up to 40 m thick higher in the section (west of Melanistic Peak, Fig. 3). These strata are interpreted to have been deposited as distal, or low density turbidites. Sandy submarine fans are rare, with the largest accumulation at the base of the group. The thick, repetitive sandy turbidite fans common in west Bowser Lake area (Evenchick et al., 1993) are absent. Higher in the section lenses of chert-pebble conglomerate may represent submarine channels cut through the shelf or slope. These



Figure 3. View west to lens of chert-pebble conglomerate in fine grained sandstone and siltstone facies.

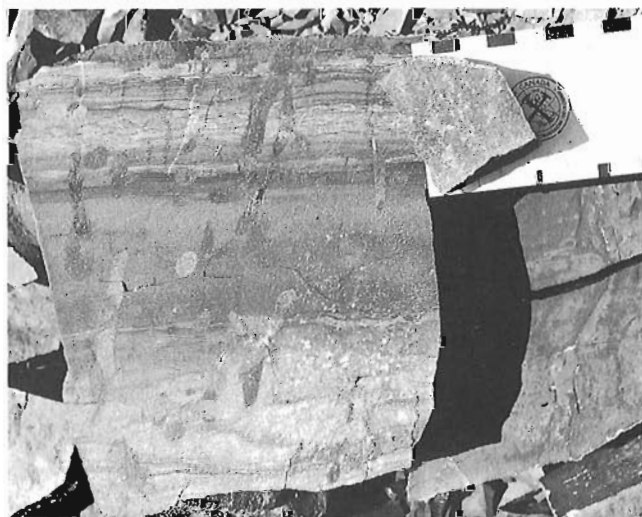


Figure 4. Rippled and bioturbated siltstone and fine grained sandstone near Mount Tommy Jack.

strata are lithologically similar to, and continuous with, the fine grained sandstone/siltstone facies in Toodoggone map area to the north (Evenchick, 1992).

East of Bird Hill

East of Bird Hill is at least 1000 m of moderately rusty weathering mainly fine grained clastics. Resistant siliceous fine grained sandstone beds 5-100 cm thick are interbedded with 1-100 cm thick crumbly to fissile dark very fine grained sandstone and siltstone. The upper part of this succession includes white weathering, moderately siliceous, thin to thick bedded fine and medium grained sandstone, in places rippled, 1 to 2 m of volcanic breccia (probably Netalzul volcanics) and rare thin grey weathering limestone. Ammonites in the upper part are Oxfordian in age (G. Jakobs, pers. comm., 1992). The repetitive interbedded sheets of fine and medium grained sandstone are interpreted to be distal turbidites.

Sandstone, siltstone facies

Mount Tommy Jack and east

From Mount Tommy Jack east, and north to the Sicintine River is a thinly layered succession of grey and green weathering siltstone, fine grained sandstone, medium grained sandstone, coquina, and rare conglomerate. One to three metres of thinly interbedded to laminated fine grained sandstone and siltstone are intercalated with 1-20 m of massive litharenite (including calcareous bivalve rich sands and coquina marker beds), and with thick intervals dominated by siltstone. Sedimentary structures in the finer grained strata are parallel lamination, ripple marks, flaser bedding, bioturbation (including vertical burrows), and escape structures (Fig. 4). Plant debris is common on bedding planes. In general, the section is about 50% medium grained sandstone, and 50% finer grained rocks, although the proportion varies considerably through the section. Sedimentary structures are indicative of very shallow marine environment. Paleocurrents show a wide range from southwest to north-northeast, similar to those reported by Jeletzky (1976) for the lower part of the section. These strata have many similarities to those south of Poison Mountain in Bowser Lake area (Evenchick et al., 1993). According to Jeletzky, they are Late Oxfordian in age.

Notchttop Peak and Foster Peak region

Ranges from south of Notchttop Peak to Foster Peak are underlain by at least 800 m of distinctively dark and resistant weathering strata. Most of the section is more than 70% medium grained sandstone, which occurs in 3-8 m intervals separated by <1-4 m of black laminated fine grained sandstone and siltstone (Fig. 5). The medium grained sandstone intervals are massive to vaguely parallel laminated, and commonly include random siltstone rip up clasts. In places thin bedded to laminated black fine grained sandstone is also included, and sandstone may be capped by thin bedded

rippled sandstone. In the east, (lower in section ?) the bases of sandstones may include pebble conglomerate. Near the top of the section west of Notchttop Peak, up to 200 m is composed almost entirely of dark weathering laminated, thin bedded, and massive siltstone and fine grained sandstone. The dominantly sandstone intervals may represent storm deposits with ripples formed during post-storm reworking. They may also have been deposited on the delta front, but the section does not coarsen up. Jeletzky (1976) grouped these strata with those at Mount Tommy Jack, but these have consistently more medium grained sandstone and lack the assemblage of very shallow marine sedimentary structures present at Mount Tommy Jack.

North of Fort Mountain

Immediately northwest of Fort Mountain (Fig. 2) strata comprise 1-15 m massive medium grained sandstone separated by similar thicknesses of black to grey fine grained sandstone and siltstone. Medium grained sandstone is thin to thick bedded, with parallel to irregular bedding, and rounded large siltstone rip up clasts. Finer grained clastics are massive to laminated, have common bioturbation and rare crossbedding. Conglomerate is rare, comprising less than 5% of the section. These strata have many similarities with those between Foster Peak and Notchttop Peak, particularly the nature of medium grained sandstone intervals, but this area has a smaller proportion of medium grained sandstone, and although rare, conglomerate is present.

Farther northwest, strata are mainly sandstone (and pebbly sandstone) and siltstone, with minor massive clast supported chert-pebble conglomerate units to 10+ m. Crossbedding and hummocky cross-stratification occur, as well as bivalves, belemnites, and plant fossils. The presence of hummocky cross-stratification is an indication of a shallow



Figure 5. View southwest of 150 m of resistant sandstone beds in sandstone, siltstone facies.

marine environment. Areas northwest of Fort Mountain appear to represent a transition between strata of the Foster - Notchtop area, and the Geodfrey - Malloch - Chipmunk area, with the proportion of conglomerate increasing northwards from Fort Mountain.



Figure 6. View northwest to folded conglomerate in the conglomerate, sandstone, siltstone facies northeast of Mount Geodfrey.

Conglomerate, sandstone, siltstone facies

Mount Geodfrey, Malloch Peak and Chipmunk Peak

Between Mount Geodfrey, and Chipmunk and Malloch peaks is at least 1000 m of section with up to 30% chert-pebble conglomerate. Siltstone and fine and medium grained sandstone are generally thinly interbedded between the conglomerate sheets, although in places up to 30 m or more is dominated by either medium grained sandstone or siltstone and fine grained sandstone. Siltstone and fine grained sandstone is parallel laminated to massive. Some siltstone and mudstone is carbonaceous and densely packed with plants. Medium grained sandstone is massive to crossbedded and rippled, and some is clean chert arenite. Conglomerate is clast supported, often appears massive or crudely bedded, with rare crossbedding, and generally occurs as sheets, but lateral pinching out is apparent in many places. Conglomerates range from 5 to 50 m thick (Fig. 6), in places as part of coarsening up cycles, but also as channels cut into siltstone and fine grained sandstone. Bioturbation, marine and nonmarine fossils, including delicate plants and silicified tree parts are common. These strata were probably deposited in a shallow marine / deltaic environment. They are on trend with similar facies to the northwest in Toadogone map area (Evenchick, 1992).

Sandstone, conglomerate, siltstone and coal facies

East of Malloch Peak and around Mount Geodfrey are strata with many characteristics described above, but including coal. The section at Mount Geodfrey is different in that conglomerate is rare in the upper part. About 300 m of section is composed of 0.5 to 1 m of sandstone interbedded

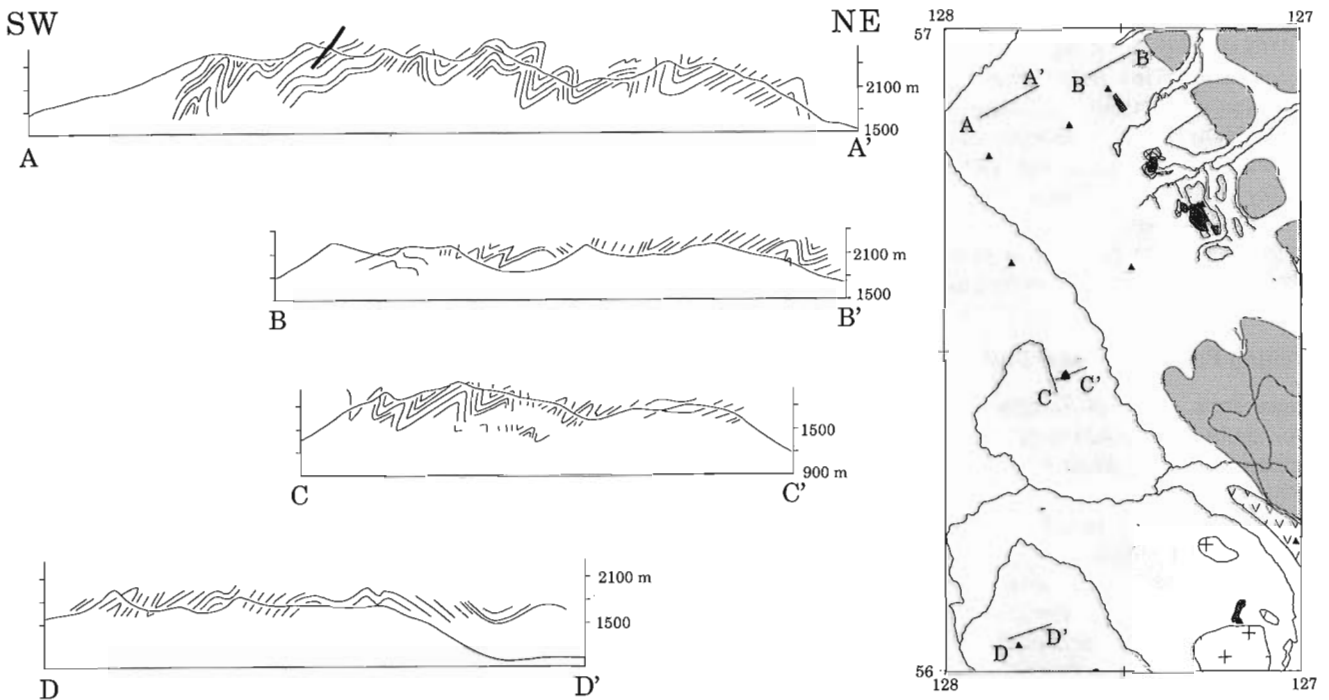


Figure 7. Cross-sections of strata in west McConnell Creek map area. No vertical exaggeration.

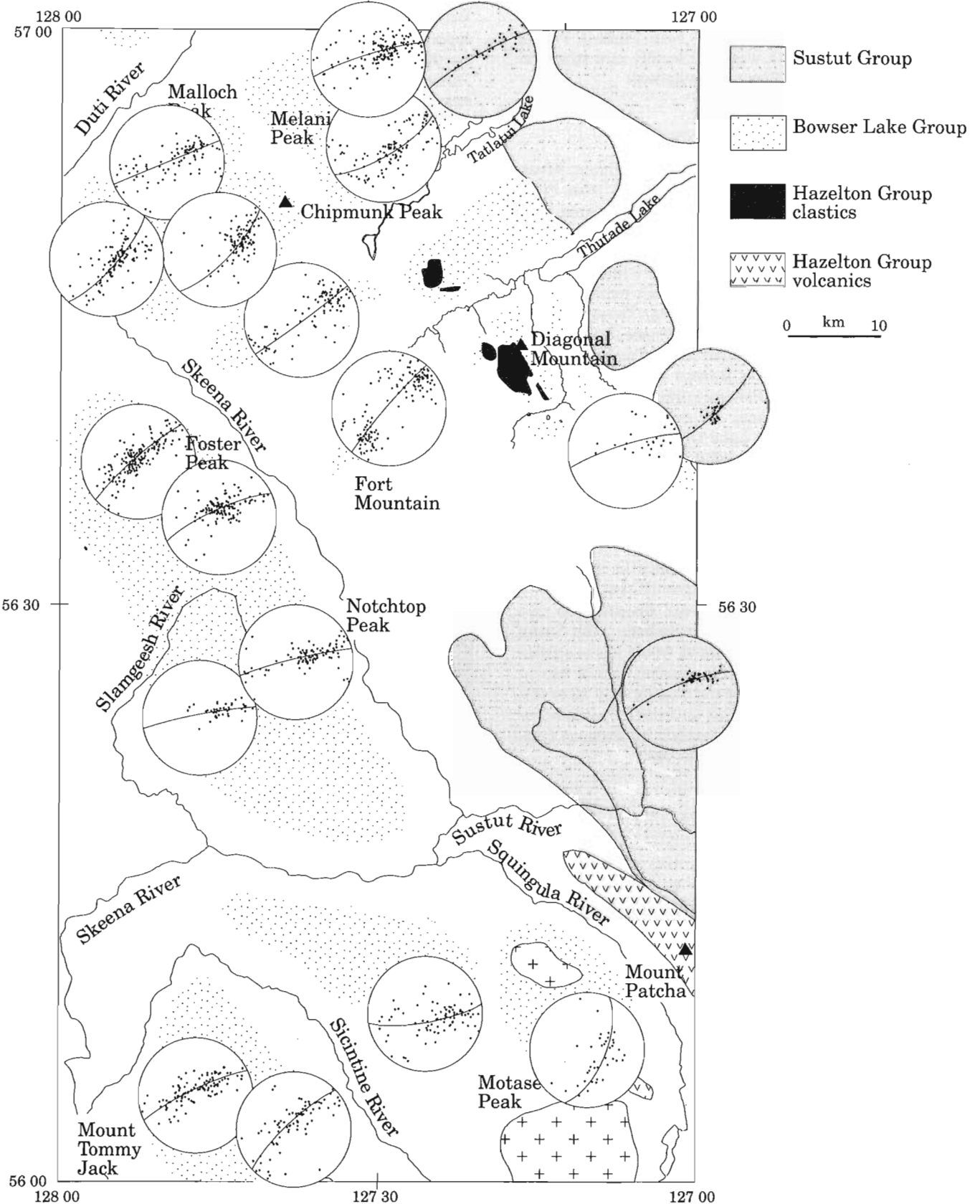


Figure 8. Lower hemisphere, equal area projections of poles to bedding for strata in west McConnell Creek map area. Shaded stereonet are for the Sustut Group.

with the same thickness of fine grained sandstone and siltstone. Ripples, crossbedding and parallel lamination are common. Coal is up to 3 m thick. Near Malloch Peak a horizon of tuff 1-4 m thick was used locally as a structural marker. Its regional significance is unknown.

Buff weathering sandstone siltstone facies

South of the Skeena River and northeast of Sicintine River, buff weathering strata are distinctly different from other Bowser Lake Group in the region. The strata were only briefly examined by us, but are about 50% medium grained poorly bedded sandstone and 50% laminated and massive siltstone and fine grained sandstone. These lithologies are interlayered in 1 to 10 m intervals, they lack marine fossils, and in at least one place, have *in situ* roots. These strata are greater than 500 m thick, and from a distance, their general appearance is more like the fluvial Tango Creek Formation of the Sustut Group than the Bowser Lake Group. The absence of detrital mica and lateral continuity with Bowser Lake Group suggest that these are not Sustut Group, but probably nonmarine Bowser Lake Group. Jeletzky (1976) considered them to be of subaerial, delta topset origin.

SUSTUT GROUP

A regional study of the Sustut Group outlines the stratigraphy and tectonic evolution of the Sustut Basin (Eisbacher, 1974). The Cretaceous, nonmarine strata are divided into two formations, each composed of two members. The Sustut Group was examined only briefly by us where it is in contact with older rocks. Sustut Group is unusual east of Mount Patcha, where Hazelton Group is overlain by only 80 to 100 m of Tango Creek Formation. This uncommonly thin lower formation of the Sustut Group is overlain by Brothers Peak Formation with at least 10 m thick intervals of tuff.

PLUTONIC ROCKS (BULKLEY INTRUSIONS)

Three plutons occur in the southern map area. They are compositionally similar granodiorite to monzodiorite and quartz monzonite, with varying amounts of potassium feldspar megacrysts, and minor hornblende and biotite. They are leucocratic, massive, medium to coarse grained, and include aplitic dykes. They have sharp intrusive contacts with the clastic country rock, and form many dykes and apophyses into the country rock. The plutons are surrounded by a rusty weathering zone up to a kilometre or more wide with quartz veins and sulphide mineralization. In the pluton southwest of Sicintine River, hornfels overprints cleavage in the Bowser Lake Group up to 100 m away from the contact, and the first appearance of randomly oriented andalusite porphyroblasts is 40 m from the contact. South of Motase Peak, garnet, andalusite, and cordierite (?) are in the 400 to 500 m wide contact aureole of the pluton. A contact aureole up to 800 m wide surrounds the pluton west of Mount Patcha. The overprinting of cleavage by hornfels, and dykes along and across fold axes indicate that these plutons are either late,

or post-tectonic with respect to structures of the Skeena Fold Belt in the immediate country rock. In some places cleavage appears to be parallel with the margins of the pluton. These are the northern limit of a belt of Late Cretaceous to Early Tertiary plutons called the Bulkley intrusions. Their age is assumed to be Late Cretaceous or Early Cretaceous based on K-Ar dates of Bulkley intrusions 80 km to the southeast (Richards, 1990). This age does not preclude younger Skeena Fold Belt structures at depth in this region.

STRUCTURAL GEOLOGY

The general structural style is depicted in cross-section (Fig. 7) and stereonet of poles to bedding (Fig. 8). As noted by Jeletzky (1976), Bowser Lake Group strata in the area



Figure 9. View northwest to overturned folds northeast of Notchtop Peak.

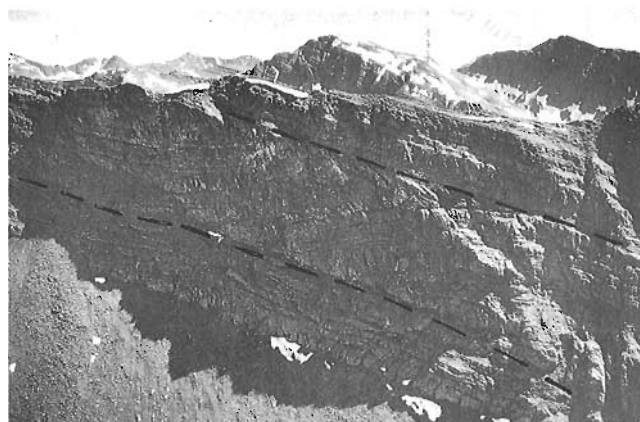


Figure 10. View southeast to bedding-parallel faults west of Notchtop Peak.

form tight folds overturned to the northeast. These folds, and others in Cretaceous and older strata are part of the Skeena Fold Belt, encompassing the entire Bowser Basin, southwest Sustut Basin, and involving underlying Hazelton Group and lower strata (Evenchick, 1991b). Most strata in west McConnell Creek area have strong closely spaced cleavage in siltstone and fine grained sandstone. Cleavage is less common in medium grained sandstone, and rare in conglomerate. Cleavage is more prevalent, and generally more intense than in the Bowser Lake map area to the west (Evenchick et al., 1993). Folds trend consistently north-northwest to northwest, and have gentle plunge (Fig. 8), consistent with neighbouring areas to the west and north (Evenchick, 1992; Evenchick et al., 1993). Folds are frequently a kilometre or less in wavelength, overturned to the northeast (Fig. 9), and consistently northeast verging (Fig. 7), in contrast to central Skeena Fold Belt (Bowser Lake map area) where domains of west vergence and many upright folds with no consistent vergence are also present. Bedding-parallel contractional faults (Fig. 10) are also present, but are only recognized where they cut upsection; they are generally of unknown magnitude of displacement. Truncation of contacts east of Bird Hill by the Sustut Group is an indication of pre-Sustut Group deformation, probably related to early history of the Skeena Fold Belt (Evenchick, 1991b).

The fine grained sandstone, siltstone facies comprises the northeastern-most exposures of Bowser Lake Group, and in a sense form the eastern "margin" of the Bowser Basin, although they are not the most proximal lithologies. The distribution of lithofacies is clearly as much a result of post-depositional contractional deformation as primary basin architecture. The result of consistent east vergence in structures in the Bowser Lake Group is exposure of deeper structural (and stratigraphic) levels to the east, an inference born out by the presence of outliers of Hazelton Group clastic rocks, and stratigraphically overlying basal Bowser Lake Group along the northeastern side of Bowser Lake Group exposure.

ACKNOWLEDGMENTS

We thank Wendy and Floyd Boyd of Suskeena Lodge on the Sustut River for their co-operation and many kindnesses throughout our work. Jim Reed of Pacific Western Helicopters transported us safely from camp to camp, and Sue Creighton and Keith Patterson provided excellent field assistance.

REFERENCES

Anderson, R.G. and Thorkelson, D.J.

1990: Mesozoic stratigraphy and setting for some mineral deposits in Iskut River map area, northwestern British Columbia; *in* Current Research, Part E; Geological Survey of Canada, Paper 90-1E, p. 131-139.

Eisbacher, G.

1974: Sedimentary and tectonic evolution of the Sustut and Sifton basins, north-central British Columbia; Geological Survey of Canada, Paper 73-31.

Evenchick, C.A.

1987: Stratigraphy and structure of the northeast margin of the Bowser Basin, Spatsizi map area, north-central British Columbia; *in* Current Research, Part A; Geological Survey of Canada, Paper 87-1A, p. 719-726.

1988: Structural style and stratigraphy in northeast Bowser and Sustut basins, north-central British Columbia; *in* Current Research, Part E; Geological Survey of Canada, Paper 88-1E, p. 91-95.

1989: Stratigraphy and structure in east Spatsizi map area, north-central British Columbia; *in* Current Research, Part E; Geological Survey of Canada, Paper 89-1E, p. 133-138.

1991a: Jurassic stratigraphy of east Telegraph Creek and west Spatsizi map areas, British Columbia; *in* Current Research, Part A; Geological Survey of Canada, Paper 91-1A, p. 155-162.

1991b: Geometry, evolution, and tectonic framework of the Skeena Fold Belt, north-central British Columbia; *Tectonics*, v. 10, p. 527-546.

1992: Bowser Basin facies and map units in southwest Toodoggone map area, British Columbia; *in* Current Research, Part A; Geological Survey of Canada, Paper 92-1A, p. 77-84.

Evenchick, C.A. and Green, G.M.

1990: Structural style and stratigraphy of southwest Spatsizi map area, British Columbia; *in* Current Research, Part F; Geological Survey of Canada, Paper 90-1F, p. 135-144.

Evenchick, C.A., Mustard, P.S., Porter, J.S., and Greig, C.J.

1993: Regional Jurassic and Cretaceous facies assemblages and structural geology in Bowser Lake map area (104 A), B.C.; Geological Survey of Canada, Open File 2582.

Jakobs, G.

1993: Jurassic stratigraphy of the Diagonal Mountain area, McConnell Creek map area, north-central British Columbia; *in* Current Research, Part A; Geological Survey of Canada, Paper 93-1A.

Jeletzky, O.L.

1976: Preliminary report on stratigraphy and depositional history of Middle to Upper Jurassic strata in McConnell Creek map-area, (94 D west half), British Columbia; *in* Report of Activities, Part A; Geological Survey of Canada, Paper 76-1A, p. 63-67.

Richards, T.A.

1976a: Takla Project (Reports 10-16): McConnell Creek map-area (94 D, East half) British Columbia; *in* Report of Activities, Part A; Geological Survey of Canada, Paper 76-1A, p. 43-50.

1976b: McConnell Creek map area (94D/east) geology; Geological Survey of Canada, Open File 342.

1990: Geology of Hazelton map area (93M); Geological Survey of Canada, Open File 2322.

Thomson, R.C., Smith, P.L., and Tipper, H.W.

1986: Lower to Middle Jurassic (Pliensbachian to Bajocian) stratigraphy of the northern Spatsizi area, north-central British Columbia; *Canadian Journal of Earth Sciences*, v. 23, p. 1963-1973.

Tipper, H.W. and Richards, T.A.

1976: Jurassic stratigraphy and history of north-central British Columbia; Geological Survey of Canada, Bulletin 270, 73 p.

Crow Lagoon tephra – new evidence of Recent volcanism in west-central British Columbia

J.G. Souther and Irene Weiland¹
Cordilleran Division, Vancouver

Souther, J.G. and Weiland, I., 1993: Crow Lagoon tephra – new evidence of Recent volcanism in west-central British Columbia; in Current Research, Part A; Geological Survey of Canada, Paper 93-1A, p. 57-62.

Abstract: Thick beds of unconsolidated basaltic tephra, uncovered during construction of a forest-access road near Crow Lagoon north of Prince Rupert, are believed to have issued from a previously unknown Quaternary centre. The tephra rests on marine clay and sand at elevations of 60 to 100 m above sea level. It consists predominantly of subaerial Plinian fallout lapilli but large ballistically emplaced bombs and accidental clasts of basement rock imply a nearby, but still unidentified source. The presence of lherzolite inclusions suggests an alkaline affinity and deep magmatic source.

Résumé : D'épaisses couches de tephra non consolidés, mises à découvert pendant la construction d'une route forestière d'accès près de la lagune Crow au nord de Prince Rupert, proviendraient d'un centre magmatique quaternaire jusqu'ici inconnu. Les tephra reposent sur des argiles et sables marins à une altitude de 60 à 100 m au-dessus du niveau de la mer. Ils se composent principalement de lapilli, qui sont les retombées subaériennes d'éruptions vulcaniennes, mais la présence de bombes volcaniques de grande taille projetées à grande distance et de clastes sporadiques provenant de roches du socle laissent supposer l'existence d'une source magmatique proche, encore non identifiée. La présence d'inclusions de lherzolite semble indiquer des affinités alcalines et l'existence d'une source magmatique de grande profondeur.

¹ P.O. Box 222, Smithers, B.C. V0J 2N0

INTRODUCTION

In the fall of 1991 a new forest-access road was contracted by the British Columbia Ministry of Forests on the south side of Khutzeymateen Inlet near Crow Lagoon. In the spring of 1992 the area was visited by Irene Weiland, a geological consultant for the Forest Service in Smithers, B.C. She identified the material exposed in new roadcuts as marine sediment overlain by recent volcanic tephra and provided samples and a location map to the Geological Survey of Canada office in Vancouver. The juxtaposition of Recent tephra deposits with the steep-sided circular depressions of Crow Lagoon and nearby Kumeon Lake raised the intriguing possibility that these anomalous circular features might be of volcanic origin. This prompted a visit to the area by J.G. Souther in September 1992 during which samples were collected for chemical analysis and radiocarbon dating. The following preliminary report incorporates observations by both authors.

REGIONAL GEOLOGICAL SETTING

Crow Lagoon is a nearly circular marine embayment connected by a narrow channel to Khutzeymateen Inlet about 40 km north of Prince Rupert. The area lies within the Coast Plutonic Complex and is shown on the regional geological map (Hutchison, 1982)

as Jurassic (?) and/or younger gneissic diorite and quartz diorite containing inclusions of paragneiss. Although Recent volcanic deposits were not previously reported at Crow Lagoon several centres of Recent volcanism occur in the general area (Fig. 1). The 220 year old Aiyansh lava flow and pyroclastic cone (Sutherland Brown, 1969) is located about 75 km to the northeast of Crow Lagoon, and a cluster of postglacial cones and flows on Behm Canal in southeast Alaska (Berg et al., 1978) are located about 80 km to the northwest.

LOCAL GEOLOGY

The Crow Lagoon area is heavily forested; the only contiguous outcrops are those along the shoreline, on steep cliffs facing the ocean, and those exposed in roadcuts along the new forest-access road (Fig. 2).

Bedrock geology

Strongly foliated quartz diorite, amphibolite, and paragneiss form all of the shoreline outcrops and cliffs facing Khutzeymateen Inlet and Crow Lagoon. No dykes which could be interpreted as feeders for the tephra deposits were found

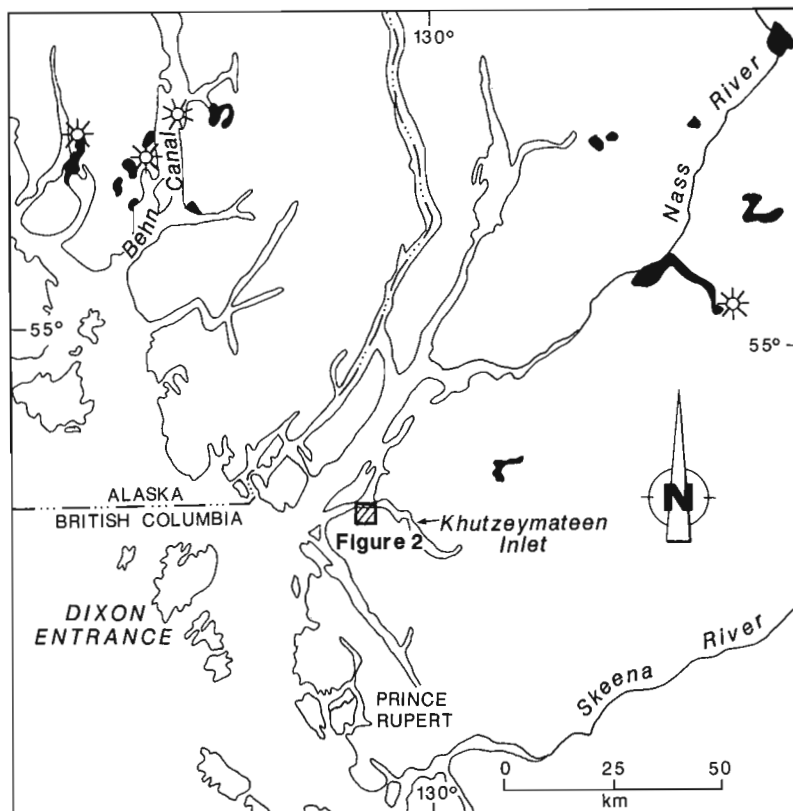


Figure 1. Index map showing the location of Crow Lagoon area (Fig. 2) and adjacent areas of Recent volcanic rocks (black). The "sunbursts" are pyroclastic cones.

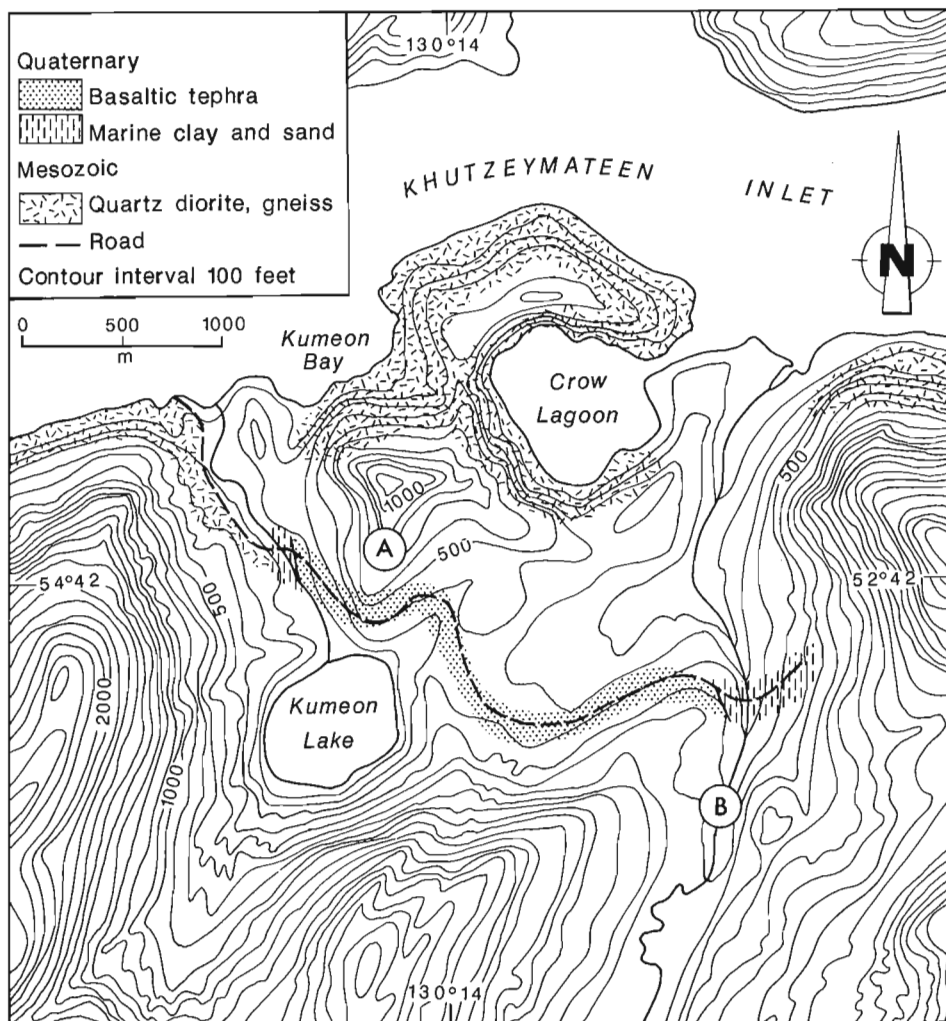


Figure 2.

Sketch map of Crow Lagoon area showing the distribution of Recent tephra and bedrock outcrops. "A" and "B" mark possible vent locations.



Figure 3.

Basaltic Plinian fallout lapilli resting on marine clay near the western end of the forest-access road.



Figure 4. Beds of plinian fallout tephra containing numerous accidental clasts of basement quartz diorite.

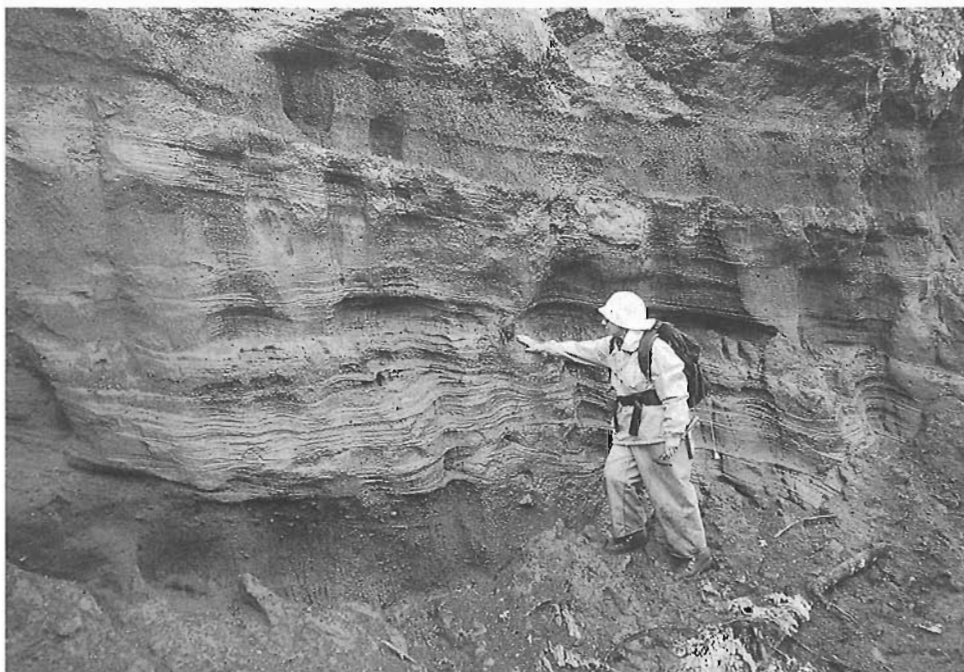


Figure 5. Thin bedded marine silt and clay overlain by a thick bed of evenly sized fallout lapilli. Geologist's hand points to buried log collected for radiocarbon dating.



Figure 6. Detail of coarse tephra containing accidental clasts of granitic rock and a small chip of carbonized wood (near white end of pen).

cutting these rocks nor was anything seen in the bedrock geology that might account for the unusual, steep-sided, circular form of Crow Lagoon and nearby Kumeon Lake.

Marine sediments

From its terminus on Kumeon Bay for a distance of about 1 km the new road exposes plutonic bedrock. At an elevation of about 60 m, the foliated quartz diorite is overlain by up to 10 m of marine clay. Farther inland, at higher elevations, this grades upwards into fine, well sorted sand of probable marine origin. Examination of the sand with a hand lens reveals no evidence of a volcanic component, suggesting that no local source of volcanic material was present prior to eruption of the overlying tephra (Fig. 3).

Basaltic tephra

For a distance of more than 2 km along the road, the marine sediments are overlain by loosely compacted beds of porous basaltic tephra. With the exception of local channelling the contact is conformable. The tephra appears to mantle the existing surface, and initial dips of the tephra, which vary from flat-lying to about 30°, are commonly parallel to the slope – apparently controlled by the underlying topography. The tephra is at least 12 m thick but its total thickness is unknown.

At low elevations, near the western end of the road, the lower 1 to 2 m of tephra display complex crosslaminations and channelling. The tephra fragments, which vary from fine lapilli to clinkers 5 cm across, are slightly abraded and have clearly been reworked by stream or wave action. Farther inland the beds are planar with normal and reverse grading

typical of subaerial Plinian fallout deposits. Accidental clasts of basement quartz diorite are present throughout the tephra deposits (Fig. 4). They are largest and most numerous where the road crosses the ridge north of Kumeon Lake. There, angular blocks of granitic rock up to half a metre across are suspended in otherwise homogeneous beds of fallout lapilli. A few breadcrust and spindle bombs up to 30 cm across were found in this same area. Some of the bombs are cored with small angular lherzolite inclusions and similar lherzolite is present within the tephra as sparse spherical inclusions up to 8 cm across. These nodules suggest an alkaline affinity and deep source for the magma.

At two localities small logs were found buried in marine sediments a short distance below the base of the tephra (Fig. 5) and at one locality small fragments of carbonized wood were recovered from a coarse, firmly compacted and cemented tephra bed (Fig. 6). All of this material has been submitted for radiocarbon dating.

SOURCE OF THE TEPHRA

The relatively large accidental clasts and bombs on the ridge north of Kumeon Lake must have been emplaced ballistically from a nearby source or rafted in by ice. Lacking any other evidence of subaqueous or subglacial origin the latter seems unlikely. However, if the pyramid-shaped hill north of Kumeon Lake was the location of the vent (site A, Fig. 2) then the pyroclastic cone must be confined to its southern flank because quartz diorite is exposed along its entire southern side.

A second possible location for the vent (site B, Fig. 2) is suggested by a pronounced knickpoint in the stream east of Crow Lagoon. Below this point the stream has cut a narrow, steep-sided valley. In contrast the stream above this point meanders across a flat, aggraded floodplain. This could be the result of temporary damming of the stream by a cinder cone.

ORIGIN OF CROW LAGOON AND KUMEON LAKE

Although the present investigation found no direct evidence of a volcanic origin for these features, their unusual morphology remains unexplained. It is difficult to visualize how such small circular depressions could be eroded to such a great depth by glacier ice. If they are of volcanic origin, either the product of phreatic explosions or collapse due to withdrawal of magma, they were clearly formed long before the nearby tephra was erupted.

ACKNOWLEDGMENTS

The authors wish to thank M.E.K. Souther for able assistance with the field work, and Glenn Woodsworth for critical review of the manuscript.

REFERENCES

- Berg, H.C., Elliott, R.L., Smith, J.G., and Koch, R.L.**
1978: Geological map of the Ketchikan and Prince Rupert quadrangles, Alaska; United States Geological Survey, Open File Report 78-73A.
- Hutchison, W.W.**
1982: Geology of the Prince Rupert-Skeena map area, British Columbia; Geological Survey of Canada, Memoir 394, 116 p.
- Sutherland Brown, A.**
1969: Aiyansh lava flow, British Columbia; Canadian Journal of Earth Sciences, v. 6, p. 1460-1468.

Geological Survey of Canada Project 770001

Geology of the northwest quadrant, Taseko Lakes map area, west-central British Columbia

Catherine J. Hickson and Shelley Higman¹
Cordilleran Division, Vancouver

Hickson, C.J. and Higman, S., 1993: Geology of the northwest quadrant, Taseko Lakes map area, west-central British Columbia; in Current Research, Part A; Geological Survey of Canada, Paper 93-1A, p. 63-67.

Abstract: The 1992 mapping of Taseko Lakes (92O) focused on the northwest quadrant, namely 92O/11, 12, 13 and the southwest corner of 92O/14. The region is largely drift covered and thick sequences of glacial fluvial deposits occupy river valleys. Flows of Chilcotin basalt are laterally extensive beneath Quaternary cover. Two porphyritic plutons were discovered of probable Late Cretaceous or early Tertiary age. One, in close association with granodiorite, resembles plutonic rocks found farther to the east. A second granodiorite body, in close association with felsic volcanic rocks, is extensively altered. West of Big Creek and roughly parallel to it, Eocene volcanic rocks are exposed that range in composition from picritic basalt to quartz-phyric rhyolite. Farther west along the ridge system of which Vedan Mountain is part, volcanic rocks of probable Early Cretaceous age are exposed. Separation of Cretaceous rocks from Eocene rocks may be along a continuation of the Little Basin Fault.

Résumé : En 1992, la cartographie de la région de Taseko Lakes (92O) a principalement porté sur le quadrant nord-ouest, notamment 92O/11, 12, 13 et le coin sud-ouest de 92O/14. La région est largement recouverte de sédiments glaciaires; d'épaisses séquences de dépôts fluvio-glaciaires occupent les vallées fluviales. Des coulées du basalte de Chilcotin occupent latéralement de grandes étendues au-dessous de la couverture quaternaire. On a découvert deux plutons porphyriques datant probablement du Crétacé tardif ou du début du Tertiaire. L'un d'eux, étroitement associé à une granodiorite, ressemble à des roches plutoniques rencontrées plus à l'est. Un second corps granodioritique, étroitement associé à des roches volcaniques felsiques, est altéré sur une grande étendue. À l'ouest de Big Creek, et presque parallèle à ce dernier, des roches volcaniques de l'Éocène affleurent dont la composition va de basaltes picritiques à une rhyolite à gros cristaux de quartz. Plus à l'ouest, le long du réseau de crêtes dont fait partie le mont Vedan, affleurent des roches volcaniques datant probablement du Crétacé précoce. La séparation des roches crétacées et des roches éocènes suit peut-être un prolongement de la faille de Little Basin.

¹ Department of Geological Sciences, Queen's University, Kingston, Ontario K7L 3N6

INTRODUCTION

Mapping of the Taseko Lakes map area (92O) started in 1990 (Hickson et al., 1991) following two weeks of reconnaissance work in 1989 (Hickson, 1990), continued in 1991 (Hickson, 1992; van der Heyden and Metcalfe, 1992), and in 1992, a traverse team, using all terrain vehicles, mapped west and north of the area covered previously. Concurrently, surficial mapping was carried out as part of the Ph.D. thesis work of David Huntley (Broster and Huntley, 1992; Huntley and Broster, 1993) and under contract to Bruce Broster. In addition, detailed stratigraphic work and mapping was continued by Brian Mahoney as part of his Ph.D. thesis (Mahoney, 1992, 1993). Mapping and detailed structural work along the Fraser and Chilcotin rivers was extended by Peter Read (Read, 1993), under contract, west of the area studied in previous years (Hickson et al., 1991; Read, 1992).

The area mapped this field season is largely drift covered with few outcrops, even along major river valleys such as the Taseko valley. Outcrop in the area is probably less than one per cent. Based on work to the east in previous summers,

reinterpretation of the region suggests that much of the outcrop mapped as Oligocene/Miocene by Tipper (Tipper, 1978) is Eocene or Early Cretaceous in age. Upper Cretaceous sediments, present in the southern part of the map area, and mapped as part of the Kingsvale Group by Tipper (Tipper, 1978) are Lower Cretaceous Jackass Mountain Group and mid-Cretaceous Silverquick formation. Major structures appear to run north-south down the Taseko River and northwest-southeast across the map area. Little evidence for the Yalakom Fault, mapped across the southeast corner of 92O/12, could be found.

STRATIGRAPHY

Quaternary and Tertiary

Miocene to Pleistocene

Chilcotin Group basalt: Flows of Chilcotin Group basalt (MPcv) are laterally extensive over much of the northwest corner of Taseko Lakes (92O) map area (Fig. 1) producing a

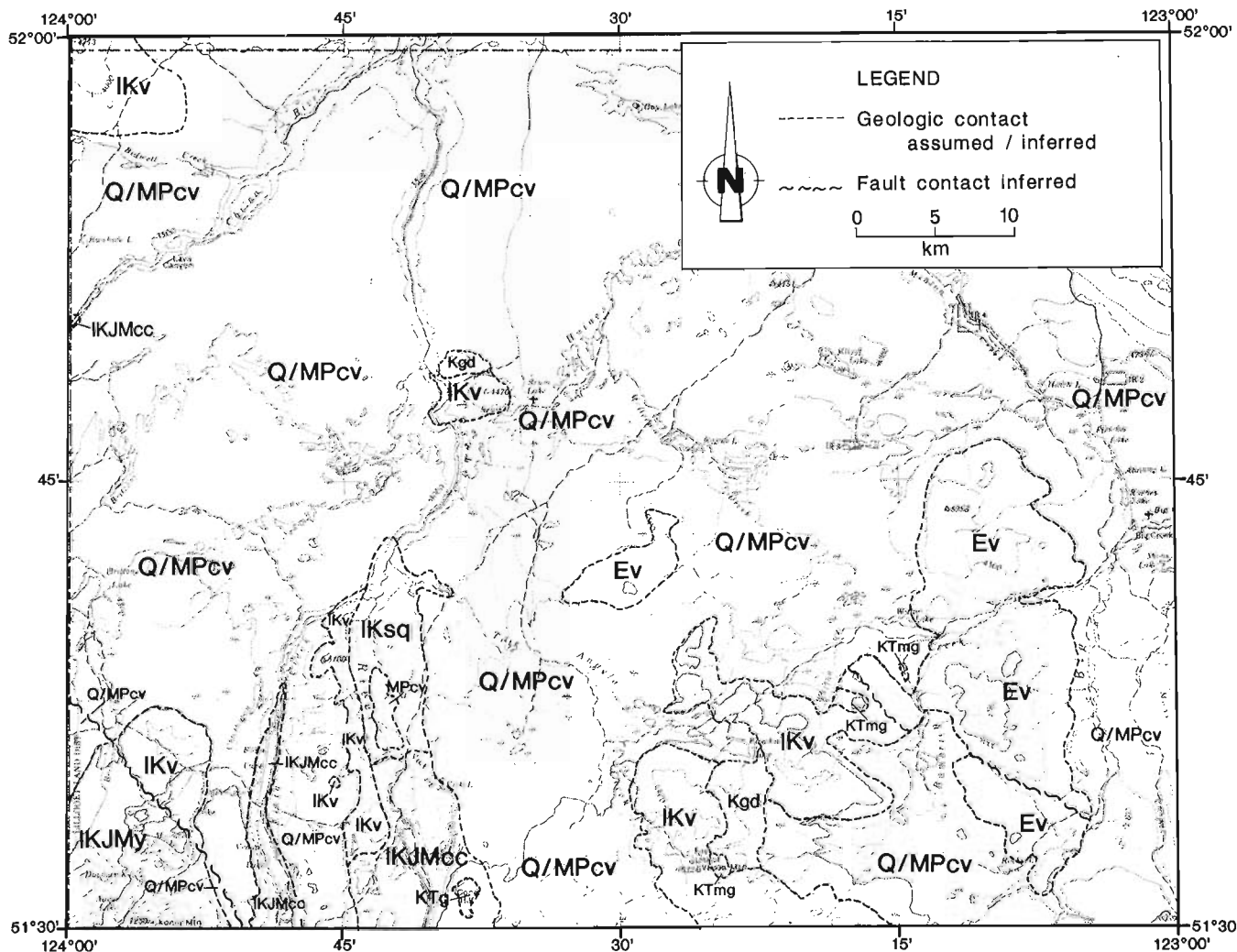


Figure 1. Geological map of the northwest quadrant, Taseko Lakes map area.

relatively flat terrain covered by meadows and bogs. Although these flows are extensive, they are generally less than 30 m in thickness. The thickest sections are in flow-filled paleovalleys where flows range up to 60 m in thickness and overlie comparable or thicker sequences of pillow lava, pillow breccia, and tuff breccia. In the extreme northwest (92O/13), evidence of Chilcotin Group basalt is found up to at least 1200 m (4000 ft.) in elevation. The land surface rises to the south toward the Coast Mountains where, in 92O/11, the plateau surface is at 1280 m (4200 ft.) and basalt flows cap ridges to 1460 m (4800 ft.) elevation. No source for these flows was found in the area mapped.

Eocene

Volcanic rocks mapped as Eocene (**Ev**; Fig. 1) in age, typically lack alteration of groundmass and phenocryst assemblages, do not have intercalated sediments, and are dominated by flows rather than breccia units. They differ from Eocene stratigraphy to the east (Hickson et al., 1991; Hickson, 1992) in that intercalated sediments were not found and the sequence is distinctly bimodal. Picritic basalt and pyroxene-phyric basalt are part of the Eocene assemblage here, but are rare in the Eocene sequence to the east (Green, 1989; Hickson et al., 1991; Hickson, 1992). In the Empire Valley area no picrites were noted (Green, 1989; Hickson et al., 1991; Hickson, 1992).

It is possible that the basalt flows are younger than Eocene age and are in fact time correlative with the basaltic flows of Flapjack Peak (20.5 Ma; N. Church in Hickson et al., 1991) and another centre on Blackdome Mountain (24 Ma; Hickson et al., 1991). Close to the basalt outcrops are glassy and fresh-appearing quartz-phyric rhyolite flows and welded tuff breccia. They may also be of Miocene age and represent the source of quartz-phyric pumiceous clasts and the thick ash layer found within Miocene sediments in the Gang Ranch area (Mathews and Rouse, 1984; Green, 1989; Hickson et al., 1991; Read, 1992). Only dating of the basalt and rhyolite flows will resolve this question.

Cretaceous to Tertiary

Several outcrops of a phenocryst-rich pluton were found (**KTmg**; Fig. 1). The exposures are confined to the Bambrick Creek map area (92O/11) and the relationship to surrounding rock units was not determined. The rock contains up to 50% phenocrysts, up to 3 cm in size, enclosed in a grey, fine grained matrix in which plagioclase and hornblende are visible. The phenocryst assemblage is: up to 25% plagioclase 0.5-3 cm in diameter, strongly zoned and commonly cored; 15% hornblende laths up to 0.5 cm in length; biotite books up to 0.5 cm in diameter approximately 5% of the rock; and minor accessory sphene. All phenocryst phases are pristine and show no evidence of alteration.

Cretaceous

Sedimentary rocks

In the southwest part of the map area (92O/12; Fig. 1) extensive green to grey sandstone of the Jackass Mountain Group (**IKJMy** and **IKJMcc**) is exposed. A 600 m (2000 ft.) section exposed on Konni Mountain is mainly green to grey, lithic rich, coarse grained sandstone (**IKJMy**). Lithic fragments are dominantly shale and, though pervasive in most sections as granule sized, angular clasts, they also form interbeds in the sandstone. Fine sand to silty interbeds are also found and become dominant to the south of Konni Mountain. The sequence as a whole coarsens upward (toward the north), but is lost under cover rocks and Pleistocene sediments north of Konni Mountain. This sequence closely resembles the Barremian to Albian, Yalakom Mountain facies (**IKJMy1**) of Schiarizza (in press). On Konni Mountain the strata are folded and stand vertically on the southern flank of the mountain.

North and east of Konni Mountain (Fig. 1), siltstone, sandstone, and conglomerate (**IKJMcc**) are exposed, closely resembling the Albian, Churn Creek facies of the Jackass Mountain Group (**IKJMcc2**) (Schiarizza, 1992). To the south and east, the Yalakom Mountain facies of the Jackass Mountain Group is in fault contact with the Churn Creek facies (Garver et al., 1989; Glover et al., 1987, 1988; Glover and Schiarizza, 1987; Schiarizza et al., 1989). Possibly the same situation exists northeast of Konni Mountain and the contact between the Yalakom Mountain facies and the Churn Creek facies marks the trace of Yalakom fault which juxtaposes the two units.

Quaternary and Tertiary	
<i>Miocene to Pleistocene</i>	
Q/MPcv	Grey olivine - and/or plagioclase-phyric subaerial basalt flows, minor interflow breccia and local pillow breccia. Scarce outcrop under Quaternary cover.
<i>Eocene</i>	
Ev	picritic basalt with olivine megacrysts; quartz-phyric rhyolite; feldsparphyric andesite
Cretaceous to Tertiary	
KTmg	Feldspar-quartz-biotite porphyry granodiorite or tonalite
Cretaceous	
Kgd	Hornblende granodiorite and diorite; chloritized hornblende; minor epidote veining
<i>Lower Cretaceous</i>	
IKsq	Silverquick formation (IKsq) Green to buff chert pebble conglomerate, green to buff sandstone; minor maroon siltstone.
IKv	Maroon to light buff feldsparphyric dacite (up to 25 % small 1 x 2 mm laths); dark grey to green aphyric andesite; welded lapilli tuff breccia; minor quartz-phyric rhyolite flows and welded lapilli tuff breccia; minor intercalated sediments.
IKJMy	Jackass Mountain Group (IKJMy and IKJMcc) <i>Yalakom Mountain facies</i> Massive green to grey lithic sandstone; minor interbedded siltstone and shale.
IKJMcc	<i>Churn Creek facies</i> Polymictic conglomerate; lithic sandstone; siltstone and shale; abundant plant fragments; marine fossils in lower siltstone.

Legend to Figure 1

The Churn Creek facies is exposed along the Taseko River and Elkin Creek (Fig. 1). The facies appears to grade upwards from black, siliceous marine siltstone to organic-debris-rich siltstone and fine grained sandstone. Above these, crossbedded green sandstone and intercalated polymictic conglomerate layers containing substantial granite and chert clast component are found. To the north and east, these units appear to grade into white weathering, crossbedded, micaceous sandstone, maroon siltstone, and chert pebble conglomerate of the Silverquick formation (**IKsq**) (late Albian to Cenomanian in age; Mathews and Rouse, 1984; Rouse et al., 1990; Mahoney et al., 1992). These sediments grade upward into more conglomeratic units which are dominated by feldsparphyric volcanic clasts, but still contain a chert clast component. The top of the section is not exposed.

Volcanic rocks

Volcanic rocks not assigned a Tertiary age are believed to be Early to mid-Cretaceous age (**IKv**). Most volcanic rocks in this unit are andesitic to dacitic in composition and distinguished from Eocene and younger volcanic rocks by their green to maroon colour, alteration of groundmass and phenocryst assemblages, ubiquitous small laths (1 x 2 mm) of altered (commonly cored and zoned) feldspar crystals, and few if any other phenocrysts.

The rocks range from maroon to light buff. Less common are dark grey to green aphyric andesite flows. Minor quartz-phyric rhyolite flows and welded dacite and rhyolite lapilli tuff and block-lapilli breccia are also found. Minor intercalated sediments are locally present (e.g., Vedan Mountain). This volcanic sequence is similar to those in the Mount Alex area and dated at 106 Ma (Hickson, 1992).

The inception of volcanism in Early Cretaceous time may be reflected in the Silverquick succession by the sudden influx of volcanic clasts. This is most clearly seen in the sections along the northern part of Churn Creek (Mahoney et al., 1992), but is also apparently reflected in the sediments mapped in 1992.

Two kilometres northwest of Scum Lake (Fig. 1) a 230 m (750 ft.) thick section of volcanic rocks (**IKv**) is exposed along the banks of the Taseko River and on a hill locally known as "Little Mountain". These rocks range in composition from andesite to rhyolite and show extensive alteration, disseminated pyrite, and quartz veins up to 15 mm in thickness. The area is held by Rea Gold Corporation and was drilled in the summer of 1991 and 1992.

Plutonic rocks

Plutonic rocks similar to those of the Mount Alex plutonic complex are found near Kloatut and Scum lakes. The rocks appear to be granodioritic in composition. Mafic phenocrysts are weakly to strongly chloritized. In one locale, quartz crystals are rod shaped and define a foliation and weak lineation. Epidote veining is common. The principle mafic phase is hornblende (up to 15%), but biotite is also present.

STRUCTURE

Due to limited outcrop, structural interpretations are poor. The Yalakom fault may separate the Yalakom Mountain facies from the Churn Creek facies of the Jackass Mountain Group, north of Konni Mountain and be responsible for the folding noted in both units. Along the Taseko River the rocks are consistently altered and veined with either quartz (Scum Lake area) or zeolites (confluence of Elkin Creek and Taseko River). No consistent structural orientation was noted. However, along the west side of the Taseko River volcanic rocks are exposed and on the east side sediments of the Silverquick formation. The sediments may have been preserved by down-dropping along a normal fault, east side down, trending roughly north. The sediments may, however, be preserved simply by paleotopography.

Along the west side of the valley of Vedan and Elkin Lake (Fig. 1), marine siltstone of the lower part of the Churn Creek facies are cut by low angle faults. The motion along these faults suggests thrusting with a southwest dip and northeast vergence. There is no evidence for major displacement. They do, however, have the same orientation as the Little Basin fault (Mahoney et al., 1992).

Evidence for the continuation of the Little Basin fault is found east of Kloatut Lake. A brecciated zone appears to juxtapose Eocene volcanic rocks against presumed Lower Cretaceous volcanic rocks. Plutonic rocks (some of which show cataclastic textures) in association with presumed Lower Cretaceous volcanic rocks are also exposed nearby (Fig. 1). Possibly they may be exposed here by movement along the Little Basin fault, or some other parallel structure. Evidence for the fault is limited.

MINERALIZATION

Little evidence of mineralization or alteration was found with the exception of the area staked and prospected around Scum Lake. However, the Gaspard Lake claims (92O/10) and Scum Lake lie close to the projection of the Little Basin fault and thus other areas along this trend, close to the plutons, may have potential. Fish Lake prospect (south of the Elkin Creek map sheet) appears to be, at least in part, structurally controlled. The pluton exposed in the area of Kloatut Lake, Scum Lake, and Fish Lake appears lithologically similar and may be similar in age.

ACKNOWLEDGMENTS

The able field assistance of Rocia Lopez is most sincerely appreciated. Useful conversations and the hospitality of P. Schiarizza, J. Riddell, and D. Mason, British Columbia Geological Survey, was most appreciated. Able helicopter piloting was provided by R. Owens, Alpen Helicopters. Bev Vanlier and G. Helmlinger helped with manuscript preparation. H.W. Tipper carefully reviewed the manuscript; his comments were most appreciated.

REFERENCES

- Broster, B.E. and Huntley, D.H.**
1992: Quaternary stratigraphy in the east-central Taseko Lakes area, British Columbia; in *Current Research, Part A*; Geological Survey of Canada, Paper 92-1A, p. 237-241.
- Garver, J.I., Schiarizza, P., and Gaba, R.G.**
1989: Stratigraphy and structure of the Eldorado Mountain area, Chilcotin Ranges, southwestern British Columbia (92O/2; 92J/15); in *Geological Fieldwork 1988*, British Columbia Ministry of Energy, Mines and Petroleum Resources, Paper 1989-1, p. 131-143.
- Glover, J.K. and Schiarizza, P.**
1987: Geology and mineral potential of the Warner Pass map sheet (92O/3); in *Geological Fieldwork 1986*, British Columbia Ministry of Energy, Mines and Petroleum Resources, Paper 1987-1, p. 157-169.
- Glover, J.K., Schiarizza P., and Garver, J.I.**
1988: Geology of the Noaxe Creek map area (92O/02); in *Geological Fieldwork 1987*, British Columbia Ministry of Energy, Mines and Petroleum Resources, Paper 1988-1, p. 105-123.
- Glover, J.K., Schiarizza, P., Umhoefer, P.J., and Garver, J.**
1987: Geology and mineral potential of the Warner Pass map sheet (92O/3); British Columbia Ministry of Energy, Mines and Petroleum Resources, Open File 1987-3.
- Green, K.C.**
1989: Geology and industrial minerals in the Gang Ranch area; British Columbia Ministry of Energy, Mines and Petroleum Resources, Open File 1989-27.
- Hickson, C.J.**
1990: A new Frontier Geoscience Project: Chilcotin-Nechako region, central British Columbia; in *Current Research, Part F*; Geological Survey of Canada, Paper 90-1F, p. 115-120.
1992: An update on the Chilcotin-Nechako project and mapping in the Taseko Lakes area, west-central British Columbia; in *Current Research, Part A*; Geological Survey of Canada, Paper 92-1A, p. 129-135.
- Hickson, C.J., Read, P., Mathews, W.H., Hunt, J.A., Johansson, G., and Rouse, G.E.**
1991: Revised geological mapping of northeastern Taseko Lakes map area, British Columbia; in *Current Research, Part A*; Geological Survey of Canada, Paper 91-1A, p. 207-217.
- Huntley, D.H. and Broster, B.E.**
1993: Glacier flow patterns of the Cordilleran Ice Sheet during the Fraser Glaciation, Taseko Lakes map area, British Columbia; in *Current Research, Part A*; Geological Survey of Canada, Paper 93-1A.
- Mahoney, J.B.**
1992: Middle Jurassic stratigraphy of the Lillooet area, south-central British Columbia; in *Current Research, Part A*; Geological Survey of Canada, Paper 92-1A, p. 243-248.
1993: Facies reconstructions in the Lower to Middle Jurassic Ladner Group, southern British Columbia; in *Current Research, Part A*; Geological Survey of Canada, Paper 93-1A.
- Mahoney, J.B., Hickson, C.J., van der Heyden, P., and Hunt, J.A.**
1992: The Late Albian-Early Cenomanian Silverquick conglomerate, Gang Ranch area: evidence for active basin tectonism; in *Current Research, Part A*; Geological Survey of Canada, Paper 92-1A, p. 249-260.
- Mathews, W.H. and Rouse, G.E.**
1984: The Gang Ranch-Big Bar area, south-central British Columbia: stratigraphy, geochronology, and palynology of the Tertiary beds and their relationship to the Fraser Fault; *Canadian Journal of Earth Sciences*, v. 21, p. 1132-1144.
- Read, P.B.**
1992: Geology of parts of Riske Creek and Alkali Lake areas, British Columbia; in *Current Research, Part A*; Geological Survey of Canada, Paper 92-1A, p. 105-112.
1993: Geology of northeast Taseko Lakes map area, southwestern British Columbia; in *Current Research, Part A*; Geological Survey of Canada, Paper 93-1A.
- Rouse, G.E., Mathews, W.H., and Lesack, K.A.**
1990: A palynological and geochronological investigation of Mesozoic and Cenozoic rocks in the Chilcotin-Nechako region of central British Columbia; in *Current Research, Part F*; Geological Survey of Canada, Paper 90-1F, p. 129-133.
- Schiarizza, P.**
in press: Geology of the Taseko-Bridge River area, NTS 92O/1,2,3; 92J/15, 16; British Columbia Ministry of Energy, Mines and Petroleum Resources.
- Schiarizza, P., Gaba, R.G., Garver, J.I., Glover, J.K., Church, B.N., Umhoefer, P.J., Lynch, T., Sajgalik, P.P., Safton, K.E., Archibald, D.A., Calon, T., MacLean, M., Hanna, M.J., Riddell, J.M., and James, D.A.R.**
1989: Geology of the Tyaughton Creek area; British Columbia Ministry of Energy, Mines and Petroleum Resources, Open File 1989-4.
- Tipper, H.W.**
1978: Taseko Lakes (92O) map-area; Geological Survey of Canada, Open File 534.
- van der Heyden, P. and Metcalfe, S.**
1992: Geology of the Piltz Peak plutonic complex, northwestern Churn Creek map area, British Columbia; in *Current Research, Part A*; Geological Survey of Canada, Paper 92-1A, p. 113-119.

 Geological Survey of Canada Project 890039-01

Aquifer mapping in the Prince George region, British Columbia: a pilot project

Brian D. Ricketts and Raelyn Crossley¹
Cordilleran Division, Vancouver

Ricketts, B.D. and Crossley, R., 1993: Aquifer mapping in the Prince George region, British Columbia: a pilot project; in Current Research, Part A; Geological Survey of Canada, Paper 93-1A, p. 69-74.

Abstract: Water well records from the Prince George area have been examined in a preliminary attempt to determine the geometry of aquifers and confining units in Quaternary deposits. Apparently there is no regionally contiguous aquifer in the area. Most aquifers are postglacial or late Fraser glacial deposits, at shallow depths. Deeper aquifers in older Pleistocene deposits tend to be thin and laterally discontinuous.

Résumé : L'examen de relevés effectués dans la région de Prince George sur des puits produisant de l'eau, a servi à une tentative de détermination de la géométrie des aquifères et des unités imperméables situées dans des dépôts d'âge quaternaire. Il semble qu'aucun aquifère n'a été décelé à l'intérieur des limites de la région. La plupart des aquifères sont des dépôts post-glaciaires ou tardiglaciaires de Fraser, situés à faible profondeur. Les aquifères plus profonds situés dans des dépôts plus anciens du Pléistocène tendent à s'amincir et à être latéralement discontinus.

¹ Department of Geological Sciences, University of British Columbia, 6339 Stores Road, Vancouver, B.C. V6T 2B4

INTRODUCTION

The Geological Survey of Canada is currently enhancing its present activities and initiating new studies in hydrogeology. In anticipation of an expanding role in this field, a pilot project has been undertaken that attempts to unravel the stratigraphic intricacies of Quaternary aquifers near Prince George, British Columbia (Fig. 1). Situated within the Fraser River drainage basin, Prince George is an important urban and industrial centre in central British Columbia.

For this aquifer study, the primary database is contained in records of water wells drilled in glaciogenic Pleistocene deposits, ranging up to 170 m in depth. Although not legally required, most water drilling companies in British Columbia file their well records with the Groundwater Section of the B.C. Ministry of Environment. The quality of well records in terms of reported lithologies, drilling rates, pump-test results

(e.g., flow rates and static levels), and water chemistry is highly variable. For example, well records that contain detailed lithological descriptions may lack data on flow rates or static levels; records with poorly recorded stratigraphy, on the other hand may have this information. Therefore, one of the principal aims of this study was to decipher and extract the useful information from the well logs in order to formulate a coherent picture of aquifer architecture in terms of 'hydrostratigraphic' units. Cross-sections have been constructed along three main transects in the map area to delineate potential aquifers and confining units (Fig. 2, 3, 4).

LOCATION

The study area (Fig. 1) is about 145 km² in the north-central part of Prince George map area (NTS 93G/15), corresponding to B.C. Ministry of Environment water well location map

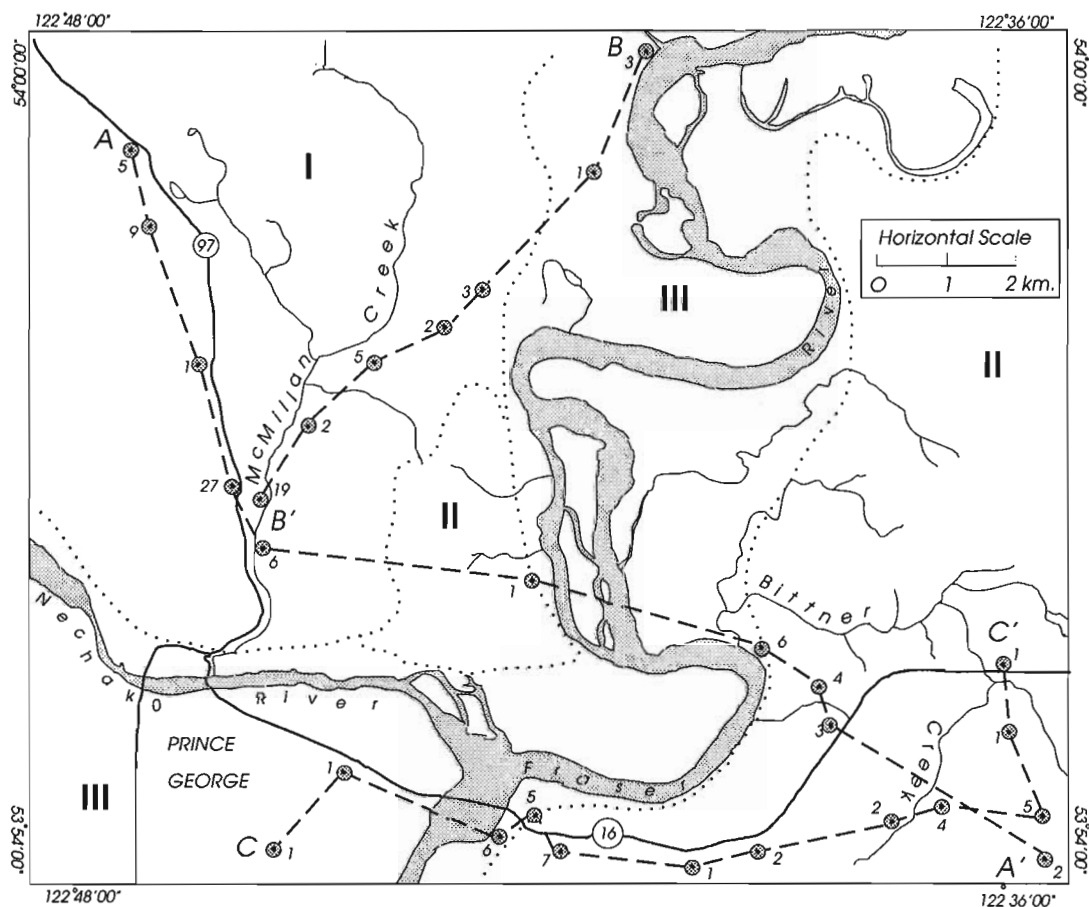


Figure 1. Location map showing surficial geology, after Leaming and Armstrong (1969), and lines of section. Map unit I (3c) = ice contact glaciofluvial drift of Fraser Glaciation; unit II (6a, b) = glaciolacustrine silt and clay, late Fraser Glaciation; unit III (7c) = sand and gravel terrace deposits, postglacial. Well numbers on transects correspond to circled numbers on stratigraphic sections in Figures 2-4.

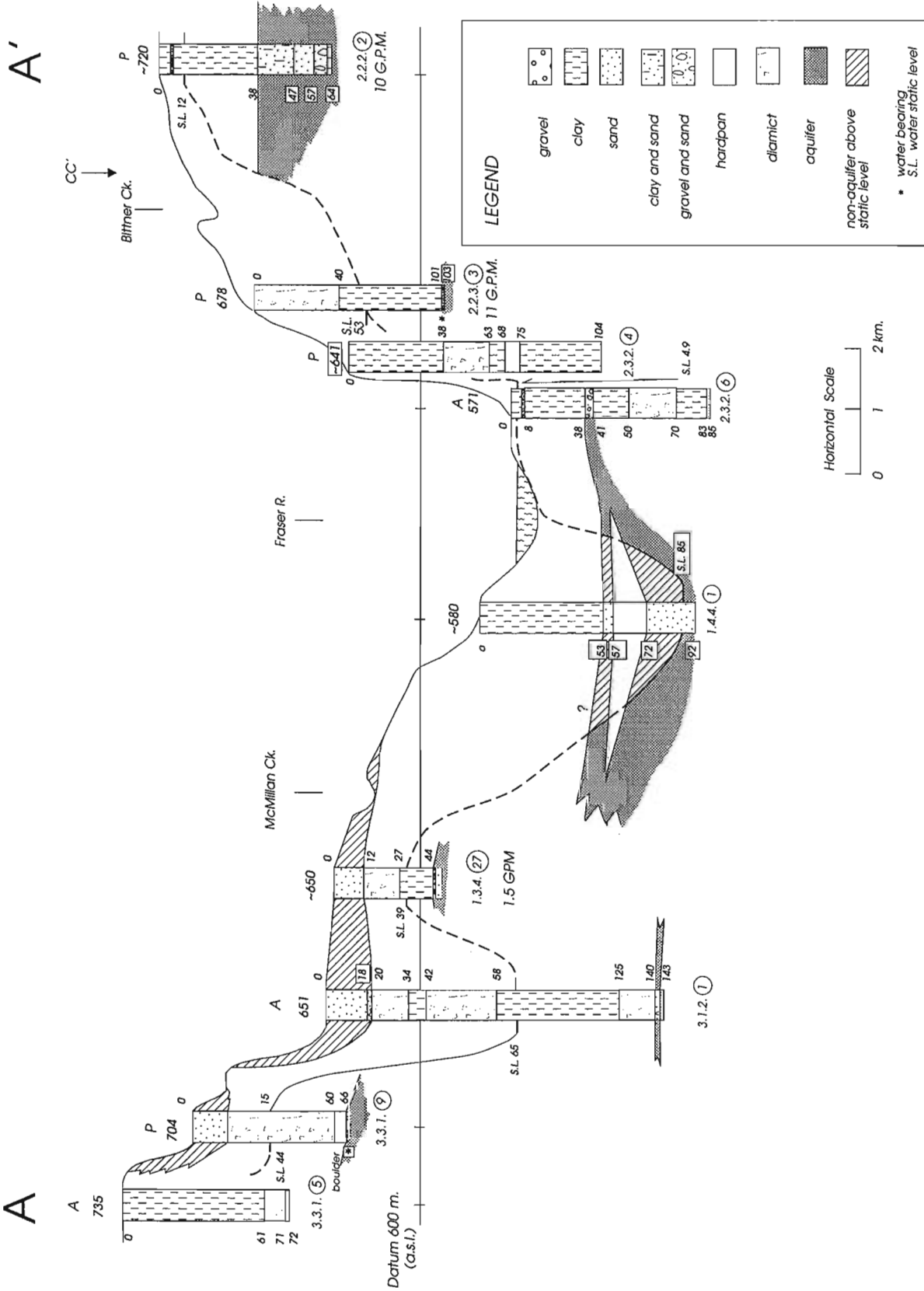


Figure 2. Stratigraphic section AA' showing well lithologies, static levels, flow rates, and inferred geometry of aquifers. 'A' and 'P' above each well indicate well status (abandoned or in production, respectively). Intersection with line CC' is indicated. Elevations, depths, and static levels are in metres. GPM = gallons/minute.

93G.097 (1:20 000). Here, the city of Prince George stands at the confluence of Fraser and Nechako rivers. North and east of this drainage the terrain is distinctly hummocky whereas to the east and south alluvial deposits underlie terraces of the Fraser River. Water well location codes are those used by the B.C. Ministry of Environment.

STRATIGRAPHIC FRAMEWORK

Three of the map units established by Leaming and Armstrong (1969) for NTS 93G are found in the Prince George area (Fig. 1). Unit I consists of Wisconsinan, stratified, ice-contact glaciofluvial sediment that underlies the hummocky topography north and east of Fraser and Nechako rivers. Glaciolacustrine clay and silt forms the bulk of unit II and constitute deposits of the late Wisconsin Fraser glacial lake system in central British Columbia (Tipper, 1971; Eyles and Clague, 1991). Unit III consists mainly of postglacial terraced fluvial deposits.

Construction of well stratigraphies required some filtering of original lithological descriptions in well records. Diamict for example, might variously be described as "till", "bouldery clay", "gravel, sand and clay", "clay with boulders" or "diamictite". We have sought to keep lithological

subdivisions simple. A diamict in this case could possess all or some of the above characteristics and might represent till or debris flow deposits.

Diamict and clay facies compose the bulk of the succession in most wells. Three diamict units are present in at least two wells (sections AA' and CC', Fig. 2, 4). Closely spaced diamict units, as in well #3.1.2 (section AA') could represent a single lodgement till with minor interfingering of subglacial clay lenses. All of these lithologies are aquicludes. Recent mapping in the Prince George area has shown that a till unit, possibly the Fraser Till, outcrops south of Bittner Creek (J.J. Clague, pers. comm., 1992). This may correspond to the uppermost diamict unit in the cross-sections (e.g., Fig. 3). If this correlation is correct an unconformity should be present at the base of the 'Fraser' diamict. Relief on the sub-Fraser unconformity would strongly influence patterns of groundwater flow.

SOME AQUIFER CHARACTERISTICS

Sand and gravel intersections in many wells are notably scarce. The thickest of these are located in shallow wells and probably are late Pleistocene or Holocene in age. Most coarse grained, porous units at depth are thin and probably laterally discontinuous. One exception to this is well #2.1.1

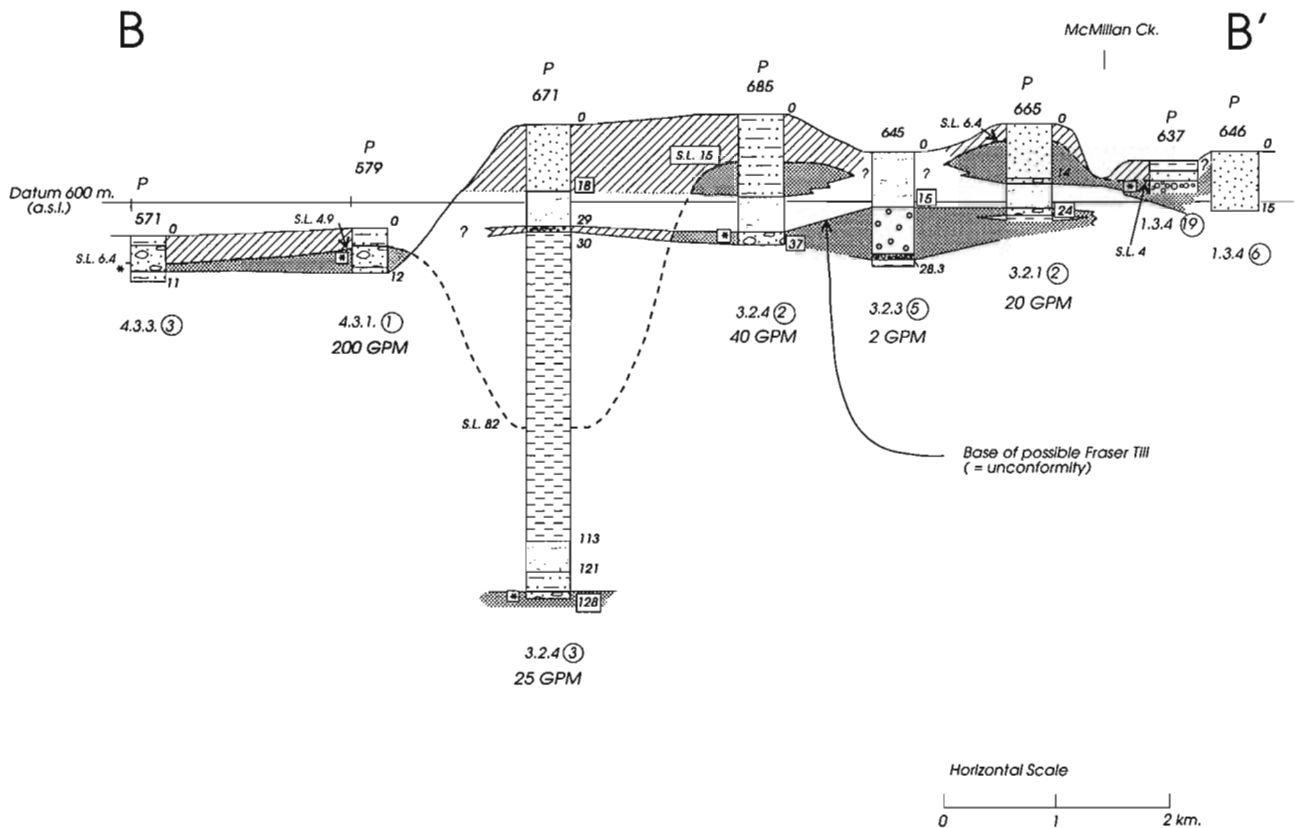


Figure 3. Stratigraphic section BB' showing well lithologies, static levels, flow rates, and inferred geometry of aquifers. Legend and symbols as for Figure 2.

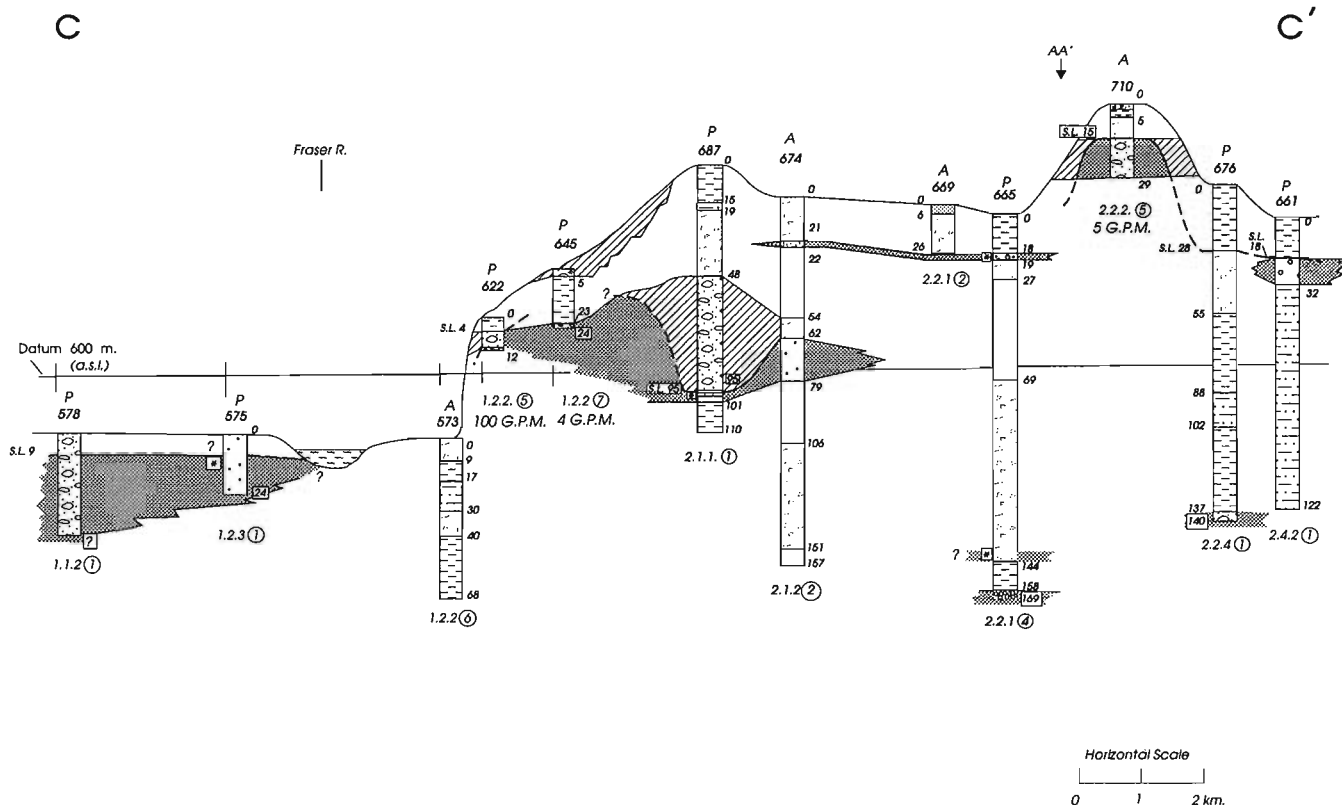


Figure 4. Stratigraphic section CC' showing well lithologies, static levels, flow rates, and inferred geometry of aquifers. Intersection with line AA' is indicated. Legend and symbols as for Figure 3.

(CC', Fig. 4) which contains 47 m of sand and gravel, most of which occurs above the reported static water level (static level refers to the equilibrium water level in a well, not necessarily coinciding with the water table). In this well, production derives from a thin sandy layer below the gravel and separated from it by a thin, impermeable layer referred to in the well log as hardpan (probably because of reduced drilling rates rather than any clear evidence of true pedological character). Plots of static levels on the stratigraphic cross-sections (Fig. 2, 3, 4) show patterns that are potentially useful for predicting saturated-zone intersections elsewhere.

It is possible to identify, in an approximate fashion, groundwater discharge and recharge areas according to criteria discussed by Freeze and Cherry (1979). As a general rule, discharge takes place in topographically low areas and recharge in areas that are topographically high. An empirical relationship between well depth and depth to static level (Fig. 5) also permits the distinction between groundwater discharge and recharge areas (Freeze and Cherry, 1979). In Figure 5 the water table is approximated by static levels in the shallow, high flow capacity wells in section BB' (Fig. 3) where the sand and gravel aquifers are either unconfined or

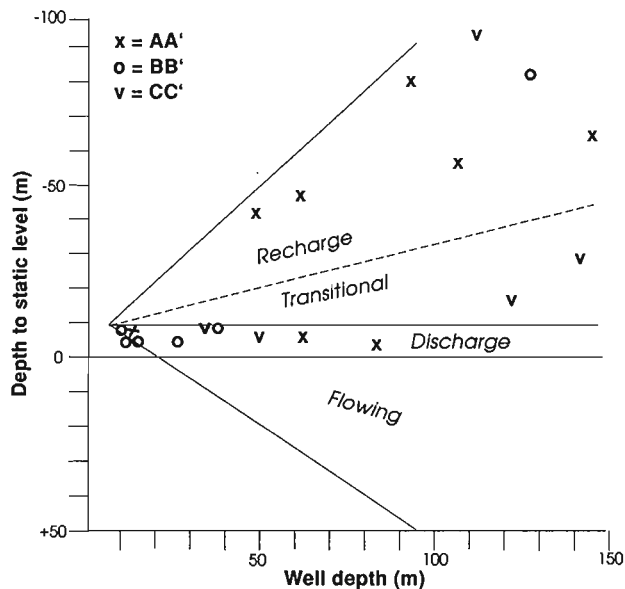


Figure 5. Plot of well depth versus depth to static water level (depths in metres). Subdivision into recharge and discharge zones after Freeze and Cherry (1979).

at very shallow depth. Most wells in section BB' plot in the groundwater discharge region of the graph. Contrasting conditions exist in section AA' where most wells plot in the groundwater recharge zone, corresponding to relatively high topography. Thus, even thick, porous sand bodies at the tops of some wells in section AA' are undersaturated. Less data are available for section CC' but those static levels that can be plotted reflect groundwater discharge or points transitional between discharge and recharge. Wells that plot in the transitional zone are more likely to be affected by seasonal variation in precipitation.

SUMMARY

Water well records have been examined from an area around Prince George. Despite the inconsistencies in recorded lithological and hydrostratigraphic information, enough useful data can be teased from the records to generate a reasonable picture of stratigraphic architecture of aquifers and confining units. Subsurface mapping of aquifers and confining units near Prince George illustrates great variability in the lateral extent and thickness of water-bearing units. No regional aquifer can be identified within the confines of the map area, at least to well depths of about 170 m. The most productive wells are in the lower areas corresponding to map

units I and III (section BB'). Preliminary interpretation suggests the areas west of McMillan Creek and east and south of Fraser River are recharge zones.

ACKNOWLEDGMENTS

Al Kohut and Rodney Zimmerman of the Groundwater Section, B.C. Ministry of Environment kindly provided well-location maps and access to well records. John Clague is thanked for discussions on the central British Columbia stratigraphy. Reviewers Lionel Jackson and John Clague are thanked for their constructive comments.

REFERENCES

- Eyles, N. and Clague, J.J.**
1991: Glaciolacustrine sedimentation during advance and retreat of the Cordilleran ice sheet in central British Columbia; *Geographie physique et Quaternaire*, v. 45, p. 317-331.
- Freeze, R.A. and Cherry, J.A.**
1979: *Groundwater*; Prentice-Hall, Inc; Englewood Cliffs, New Jersey, 604 p.
- Leaming, S.P. and Armstrong, J.E.**
1969: *Surficial Geology, Prince George, British Columbia*; Geological Survey of Canada, Map 3-1969.
- Tipper, H.W.**
1971: Glacial geomorphology and Pleistocene history of central British Columbia; *Geological Survey of Canada, Bulletin* 196, 89 p.

Lower and Middle Jurassic stratigraphy in the Treaty Glacier area and geological setting of the Treaty Glacier alteration system, northwestern British Columbia

Peter D. Lewis¹, John F.H. Thompson¹, Genga Nadaraju²,
Robert G. Anderson and Gary G. Johannson²

Cordilleran Division, Vancouver

Lewis, P.D., Thompson, J.F.H., Nadaraju, G., Anderson, R.G., and Johannson, G.G., 1993: Lower and Middle Jurassic stratigraphy in the Treaty Glacier area and geological setting of the Treaty Glacier alteration system, northwestern British Columbia; in Current Research, Part A; Geological Survey of Canada, Paper 93-1A, p. 75-86.

Abstract: Well-exposed, fossiliferous Toarcian to Middle Bajocian strata in the Treaty Glacier area include mafic and felsic flows, pillowed lava, tuff and volcanoclastic rocks, and fine- to coarse-grained clastic sedimentary rocks. Stratigraphy of the east Treaty ridge, nunatak (which hosts the Treaty Glacier prospect), and north gossan sequences are compared with regional Lower to Middle Jurassic strata. Although there is reasonable correlation of some units locally, rapid facies changes locally and regionally are indicated.

Altered, schistose rocks associated with the Treaty Glacier prospect represent a deformed advanced argillic alteration system superimposed on the Lower to Middle Jurassic rocks. The Treaty Glacier alteration system formed within 200 m of paleosurface and suggests the potential for high sulphidation epithermal mineralization; however any accompanying porphyry mineralization is likely to be at least 500 m stratigraphically below the alteration zones.

Résumé : Des strates fossilifères bien exposées, couvrant l'intervalle du Toarcien au Bajocien moyen dans la région du glacier Treaty, renferment des coulées mafiques et des coulées felsiques, des laves en coussins, des tufs et des roches volcanoclastiques, et des roches sédimentaires clastiques de granulométrie fine à moyenne. On compare la stratigraphie de la crête est de Treaty, un nunatak (qui abrite le gîte possible de Treaty Glacier), et les séquences nord à chapeau ferrugineux, aux strates régionales qui s'étendent du Jurassique inférieur au Jurassique moyen. Bien qu'il y existe, par endroits, une corrélation raisonnable entre certaines de ces unités, de rapides variations de faciès se manifestent aux échelles locale et régionale.

Des roches schisteuses altérées associées au gîte possible de Treaty Glacier représentent un système d'argilisation avancée accompagnée d'une déformation, qui est surimposé aux roches du Jurassique inférieur à moyen. Le système d'altération du glacier Treaty s'est formé à moins de 200 m de la paléosurface et laisse prévoir un potentiel élevé de minéralisation épithermale par sulfuration; cependant, toute minéralisation connexe en porphyres se situe sans doute stratigraphiquement à au moins 500 m au-dessous des zones d'altération.

¹ Mineral Deposit Research Unit, Department of Geological Sciences, University of British Columbia, 6339 Stores Road, Vancouver, B.C. V6T 1Z4

² Department of Geological Sciences, University of British Columbia, 6339 Stores Road, Vancouver, B.C. V6T 1Z4

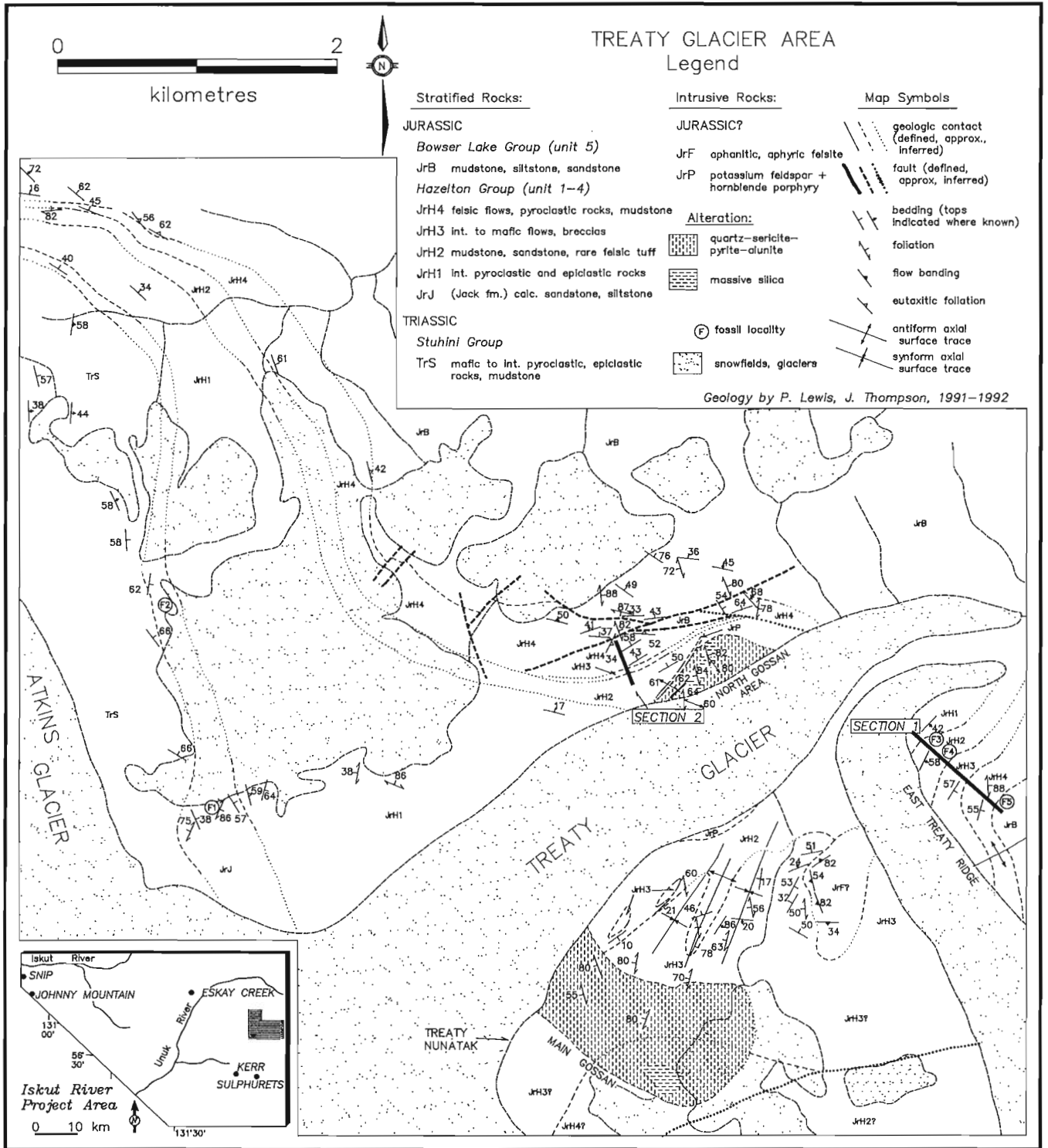


Figure 1. Geology of the Treaty Glacier area, and locations of stratigraphic sections and fossil localities described in text. Inset map shows regional location.

INTRODUCTION

Ideas concerning Jurassic stratigraphy in the Iskut River area remain controversial because of the facies changes inherent in the volcanogenic strata and the meagre (but growing) database of critical fossil and geochronological localities. An example is the Mt. Dilworth Formation, a pyroclastic felsic unit described as an important regional marker (Alldrick, 1985, 1987, 1991; Alldrick and Britton, 1988, 1991; Anderson and Thorkelson, 1990): the unit is reasonably well known in its "type" area at Troy Ridge and north along the Bowser River (Anderson and Thorkelson, 1990; Alldrick, 1991), but inclusion of all felsic pyroclastic rocks in the region within the Mt. Dilworth Formation, particularly east of the Unuk River and southwest of Treaty Creek, is problematic. Fossil control is critical to resolution of these Lower to Upper Jurassic stratigraphic problems. Benthonic, planktonic and nektonic faunas are particularly useful and occur in scattered localities (Nadaraju and Smith, 1992).

Our previous fieldwork in the Treaty Glacier area (Thompson and Lewis, 1992) focused on the general geological setting, morphology, and structural style of the main and north Treaty gossans. We concluded that the major alteration represents a deformed advanced argillic alteration system superposed on Hazelton Group volcanic and volcanoclastic rocks, but the deformation history and stratigraphic level of the host rocks was uncertain. Fieldwork in 1992 resolved these remaining uncertainties, and provided new constraints for the age and stratigraphic succession of the Hazelton Group in the eastern Iskut River area. Ammonites bracketing part of a thick section of felsic tuff previously considered part of the Mt. Dilworth Formation (Alldrick and Britton, 1988), prompted more detailed examination of the section. The sequence is unusual for felsic volcanic rocks in the Iskut River area because of its thickness and well-bedded nature, and the intercalation of fine to coarse clastic, partly marine, sedimentary rocks. The felsic strata in the Treaty Glacier area represent the best exposed and least equivocal evidence for Aalenian to Bajocian (Middle Jurassic) felsic

tuffaceous and reworked ash flow rocks. They are younger than isotopically dated Early Jurassic pyroclastic rocks correlated with the Mt. Dilworth Formation elsewhere. In addition, the transition from volcanic and sedimentary Hazelton Group strata to Bowser Lake Group rocks is well exposed in several locations in the Treaty Glacier area. The strata there represent the best Middle Jurassic reference section available in the Iskut River area.

The Treaty Glacier area occupies the eastern part of the area being studied by the Mineral Deposit Research Unit of the University of British Columbia under the project: "Metallogenesis of the Iskut River Region, Northwestern British Columbia". Access is by helicopter from Stewart, Tide Strip, Bob Quinn Lake or exploration camps in the Eskay Creek - Sulphurets region.

GEOLOGICAL SETTING

Treaty Glacier is located in northwestern British Columbia within the Sulphurets map area of Alldrick and Britton (1991), approximately 75 km north of Stewart and 10 km north of the Sulphurets camp (Fig. 1). A prominent red-brown-weathering gossan, approximately 1 km east-west by 0.5 km north-south, occurs on the northwest side of a large nunatak between Treaty and South Treaty glaciers (mineral occurrence 44, Alldrick and Britton, 1988). This, the "main gossan" in this paper, has been of interest to exploration companies for a number of years and lies at the centre of the Treaty Creek property of Tantalus Resources Limited and Teuton Resources Corporation. Alldrick and Britton (1988) reported alunite and native sulphur within the gossan. A second area of grey and locally limonite-stained bluffs on the north side of the Treaty Glacier is referred to here as the "north gossan". Natroalunite and sartorite have been reported from the north gossan (R.V. Kirkham, pers. comm., 1991).

Thompson and Lewis (1992) reviewed the general stratigraphic and structural setting of the Treaty Glacier alteration system. The Treaty Glacier area is underlain by complexly folded and faulted sedimentary rocks of the Bowser Lake Group and volcanic and epiclastic rocks of the Hazelton Group (Alldrick and Britton, 1988, 1991). Most of the Treaty nunatak, including the main and north gossans, lie on the upper plate of the southeast-directed Sulphurets thrust fault which places Hazelton Group strata over Bowser Lake Group (Alldrick and Britton, 1991). Broad northeast-trending folds and several sets of steeply-dipping faults deform these strata. Contacts of both gossans cut lithologic boundaries, but the extensive alteration obscures geological contacts within the gossans.

STRATIGRAPHY

Extensive deformation, alteration, and intrusion in the Treaty nunatak hinder reconstructing the stratigraphic succession for that area. Less disrupted and altered rocks exposed east of the South Treaty Glacier ("east Treaty ridge" in this paper, section 1 in Fig. 1), define a stratigraphic succession with

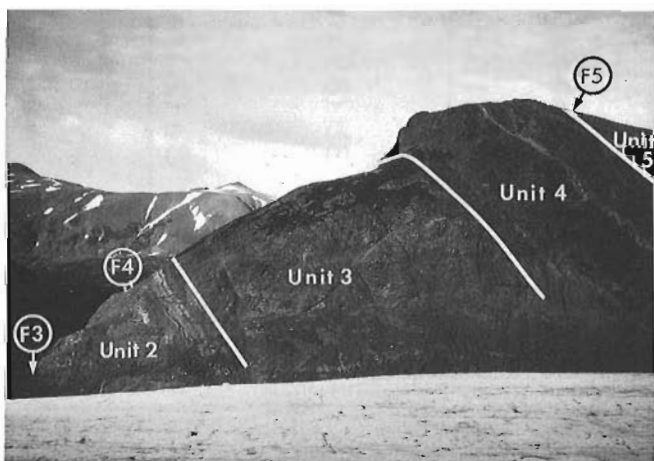


Figure 2. East Treaty ridge section, viewed looking eastward from Treaty nunatak. Fossil localities and lithology of major map units outlined described in text and in Figure 3.

EAST TREATY RIDGE STRATIGRAPHY

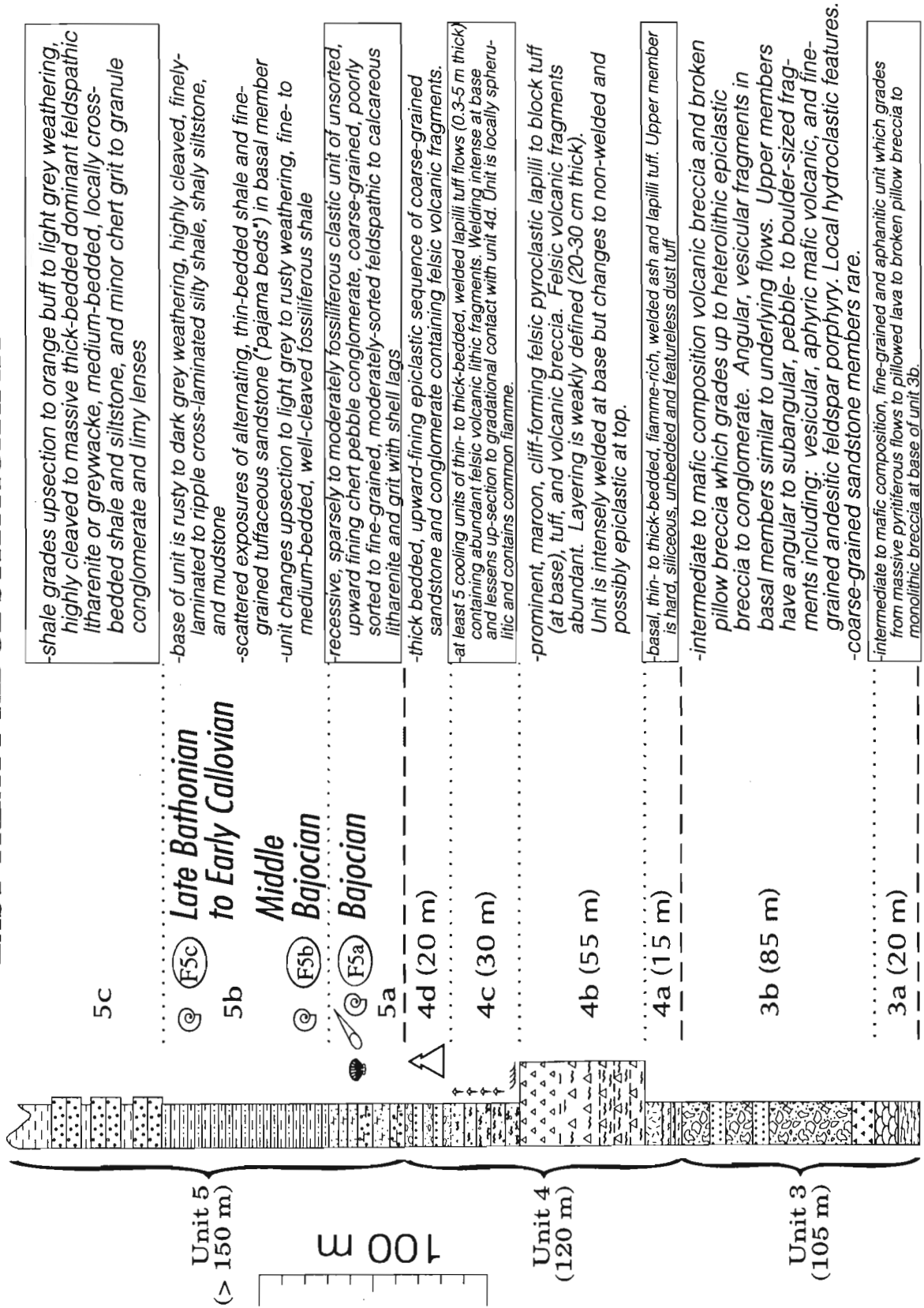
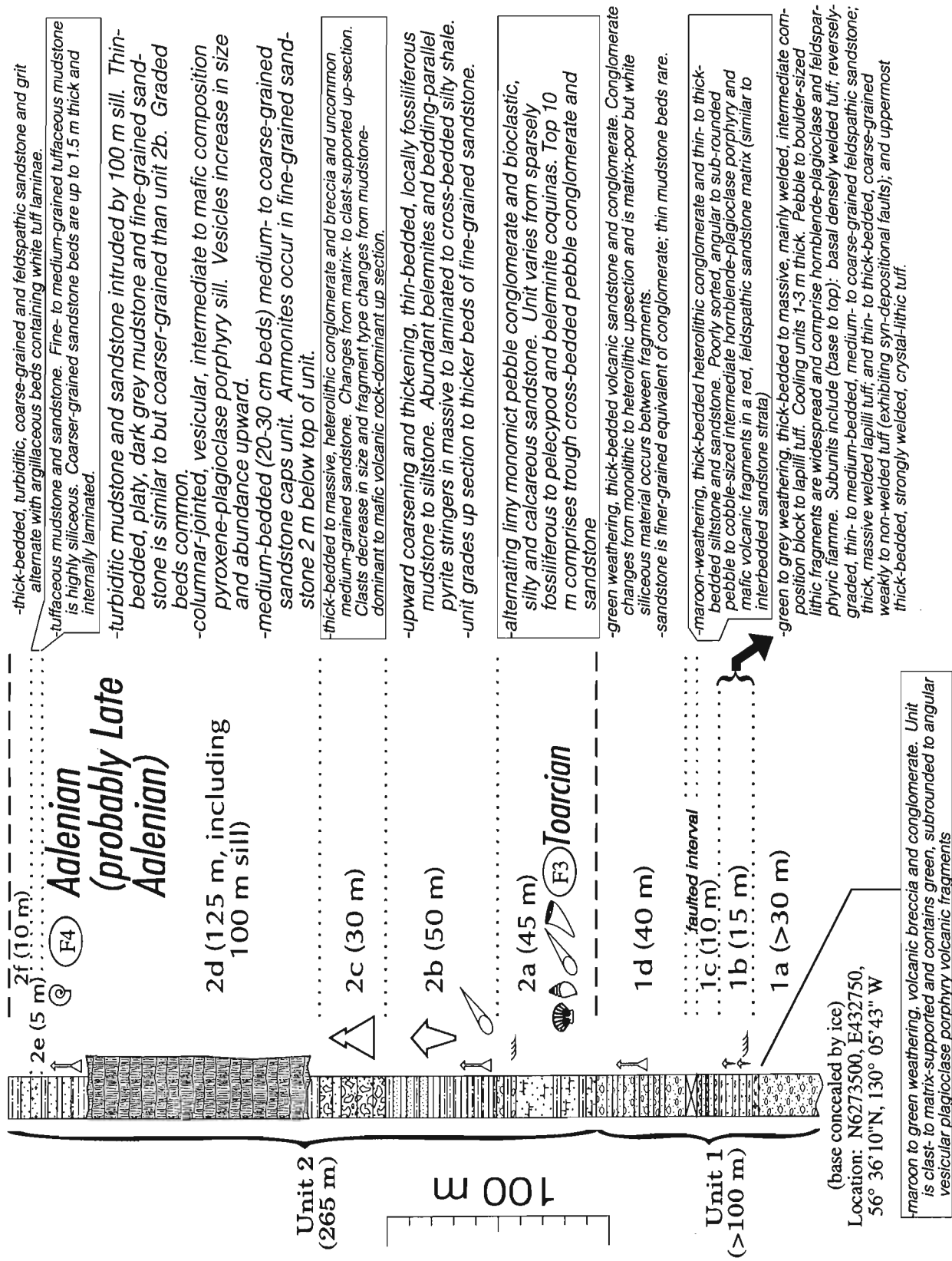


Figure 3a. Stratigraphic column and description of east Treaty ridge section.



- thick-bedded, turbiditic, coarse-grained and feldspathic sandstone and grit alternate with argillaceous beds containing white tuff laminae.
- tuffaceous mudstone and sandstone. Fine- to medium-grained tuffaceous mudstone is highly siliceous. Coarser-grained sandstone beds are up to 1.5 m thick and internally laminated.
- turbiditic mudstone and sandstone intruded by 100 m sill. Thin-bedded, platy, dark grey mudstone and fine-grained sandstone is similar to but coarser-grained than unit 2b. Graded beds common.
- columnar-jointed, vesicular, intermediate to mafic composition pyroxene-plagioclase porphyry sill. Vesicles increase in size and abundance upward.
- medium-bedded (20-30 cm beds) medium- to coarse-grained sandstone caps unit. Ammonites occur in fine-grained sandstone 2 m below top of unit.
- thick-bedded to massive, heterolithic conglomerate and breccia and uncommon medium-grained sandstone. Changes from matrix- to clast-supported up-section. Clasts decrease in size and fragment type changes from mudstone-dominant to mafic volcanic rock-dominant up section.
- upward coarsening and thickening, thin-bedded, locally fossiliferous mudstone to siltstone. Abundant belemnites and bedding-parallel pyrite stringers in massive to laminated to cross-bedded silty shale. -unit grades up section to thicker beds of fine-grained sandstone.
- alternating limy monomict pebble conglomerate and bioclastic, silty and calcareous sandstone. Unit varies from sparsely fossiliferous to pelecypod and belemnite coquinas. Top 10 m comprises trough cross-bedded pebble conglomerate and sandstone
- green weathering, thick-bedded volcanic sandstone and conglomerate. Conglomerate changes from monolithic to heterolithic upsection and is matrix-poor but white siliceous material occurs between fragments.
- sandstone is finer-grained equivalent of conglomerate; thin mudstone beds rare.
- maroon-weathering, thick-bedded heterolithic conglomerate and thin- to thick-bedded siltstone and sandstone. Poorly sorted, angular to sub-rounded pebble to cobble-sized intermediate hornblende-plagioclase porphyry and mafic volcanic fragments in a red, feldspathic sandstone matrix (similar to interbedded sandstone strata)
- green to grey weathering, thick-bedded to massive, mainly welded, intermediate composition block to lapilli tuff. Cooling units 1-3 m thick. Pebble to boulder-sized lithic fragments are widespread and comprise hornblende-plagioclase and feldspar-phryic flame. Subunits include (base to top): basal densely welded tuff; reversely-graded, thin- to medium-bedded, medium- to coarse-grained feldspathic sandstone; thick, massive welded lapilli tuff; and thin- to thick-bedded, coarse-grained weakly to non-welded tuff (exhibiting syn-depositional faults); and uppermost thick-bedded, strongly welded, crystal-lithic tuff.

Figure 3a. cont.

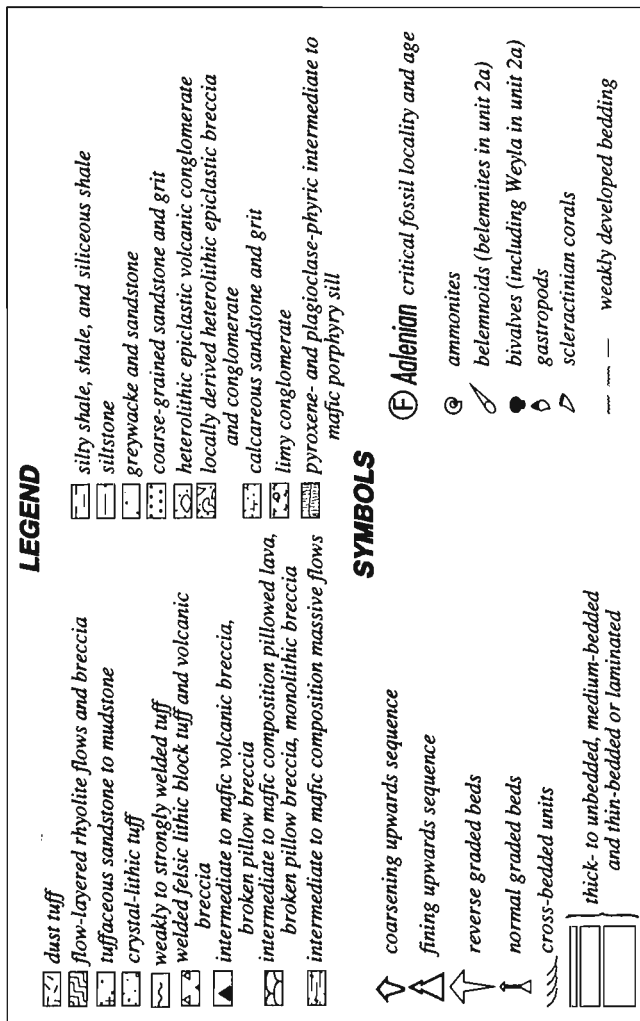


Figure 3b. Legend to accompany Figure 3a.

which the nunatak rocks can be correlated. This well-exposed section of Hazelton Group rocks contains biostratigraphic age control at four different levels. A second relatively unbroken stratigraphic succession, exposed immediately west of the north gossan (section 2 in Fig. 1) lacks the biochronological control present in the east Treaty ridge section but contains many of the same stratigraphic units.

East Treaty ridge section

A succession of pyroclastic, epiclastic, and sedimentary rocks more than 600 m thick forms the ridge south of the toe of the Treaty Glacier and is nearly continuously exposed along the ridge crest (Fig. 2). Faults, which cut the succession near its base, do not appear to have appreciable offset, nor does a sill which intrudes the middle of the section within a continuous coarsening upward sequence appear to disrupt the succession.

We define five lithostratigraphic units with sharp conformable contacts in the east Treaty ridge section and show them as map units on Figures 1 and 2. Subdivisions within these units, easily differentiated in the east Treaty ridge succession (Fig. 3a, b), lack the lateral continuity needed for mappable units. Thicknesses of stratigraphic intervals listed below and in Figure 3 were estimated during field traverses and are therefore approximate.

Lowest rocks in the east Treaty ridge section (unit 1) comprise more than 100 m of intermediate composition volcanic breccia, pyroclastic flows, and epiclastic rocks (Fig. 4a, b). Four differentiable subunits consist of a lowermost coarse volcanic breccia and conglomerate, overlying intermediate composition welded tuffs and lesser epiclastic rocks, and two upper epiclastic sandstone/conglomerate subunits.

Unit 2 is a marine sedimentary succession, 265 m thick, with a fossiliferous, coarse-grained sandstone to conglomerate base, succeeded by mudstones to siltstones, a second coarser conglomerate to breccia, and a coarsening upward mudstone to sandstone top. These lithotypes define 6 subunits, described separately in Figure 3. Near the top of unit 2, volumetrically minor felsic tuffaceous sandstone occurs within the marine sandstones and siltstones. Two important fossil collections, one from the base of the unit and one from near the top, constrain the age of the unit 2 to Toarcian-Aalenian.

Unit 3 consists of intermediate to mafic volcanic flows, breccia, and epiclastic rocks forming a sequence approximately 105 m thick. The lower part is dominantly volcanic and exhibits abundant evidence of subaqueous volcanism, including mafic to intermediate pillowed flows, broken pillow breccias, and local areas with hydroclastic textures (Hanson, 1991). Overlying epiclastic rocks grade from monolithological volcanic breccia near the base upward into heterolithic volcanic breccia to conglomerate.

Well-stratified felsic pyroclastic and epiclastic rocks of unit 4 form prominent maroon-weathering cliffs near the top of the east Treaty ridge section. Four subunits within this 120 m-thick sequence, are distinguished on the basis of clast size, thickness of stratification, and degree of welding.

Overlying the mixed volcanic and sedimentary strata of units 1-4 are thick mudstones, siltstones, and sandstones which form the lowest part of the sedimentary sequence exposed to the east in Bowser Basin. These strata comprise three subunits: a basal fossiliferous calcareous sandstone, overlying thinly-bedded mudstones and siltstones, and an upper, more thickly bedded sandstone to mudstone sections. Fossil collections from the basal subunit, from immediately above the basal subunit, and from the middle of the medial mudstone sequence date the transition from volcanism to basinal sedimentation as Bajocian.

North gossan section

Rocks exposed adjacent to the north gossan (Fig. 1) are similar to those on east Treaty ridge, but are less well exposed and cut by numerous faults. Lowest rocks in section are similar to unit 2 in the east ridge section, and are succeeded by equivalents to units 3 and 4. However, many of the subunits recognized in the north gossan section (Fig. 5) do not correlate with the subunits of the east Treaty ridge section.

Unit 2 in the north gossan section consists of two subunits with a total thickness of more than 20 m (base concealed) which are lithologically similar to the upper part of Unit 2 at east Treaty ridge. These strata are succeeded by approximately 10 m of mafic pillowed flows (unit 3), and approximately 100 m of intermediate to felsic volcanic breccia, welded pyroclastic rocks and flow breccia, tuffaceous sedimentary strata, and interstratified mudstone intervals which correlates with the mixed felsic pyroclastic and sedimentary section with unit 4 at east Treaty ridge. Overlying unit 5 mudstones are faulted against the top of unit 4 in the north gossan section, but conformably overlie it along strike.

Treaty nunatak stratigraphy

The structural complexity and alteration of rocks on the Treaty nunatak hinder identification of a representative stratigraphic section for that area. However, rocks adjacent to the main gossan strongly resemble those described above, and at least two of the five main stratigraphic units of the east Treaty ridge section occur (Fig. 5).

Northeast of the main gossan a recessive sequence of thinly-bedded turbiditic mudstones and sandstones outcrop above the Treaty Glacier. These strata contain pelecypod coquinas lithologically similar to those at the base of unit 2 on the east Treaty ridge section, as well as thinly to thickly bedded felsic tuffaceous intervals near their upper contact, correlative to those in both the east ridge and north gossan sections. Much of the northwest part of the nunatak consists of mixed fine to medium grained clastic sediments and mafic to intermediate igneous rocks lithologically similar to unit 3

in the two other sections. Although folded, the unit appears to be thicker (>100 m) than correlative strata in the east ridge and north gossan sections. Coherent mafic igneous bodies form pillowed flows (up to 20 m thick) and sills (5 to >20 m thick). Vesicularity increases upward in the sills, and upper sill contacts are irregular and locally fragmental. The bulk of the unit consists of complex mixed mafic lava and sedimentary rock. This includes disaggregated pillows in a silty matrix, irregular pillows (typically 10-30 cm across) with vesicular margins enclosed in a silt or hydroclastite matrix, and hydroclastite and peperite fragmental rocks (Fig. 6a, b). Individual beds (1-3 m thick) of coarse angular pillow breccia occur within the sequence.

Biostratigraphy

Basal Hazelton Group

The basal Hazelton Group between the north gossan and the Atkins Glacier yielded several fossil collections (made by Wes Raven, Orequest Consultants Ltd., and Jack Henderson Geological Survey of Canada, locations F1, F2 in Fig. 1).



Figure 4. Representative lithologies of unit 1 at east Treaty Ridge: **a)** coarse monolithological volcanic breccia; **b)** welded tuff with well-developed large fiamme and eutaxitic texture.

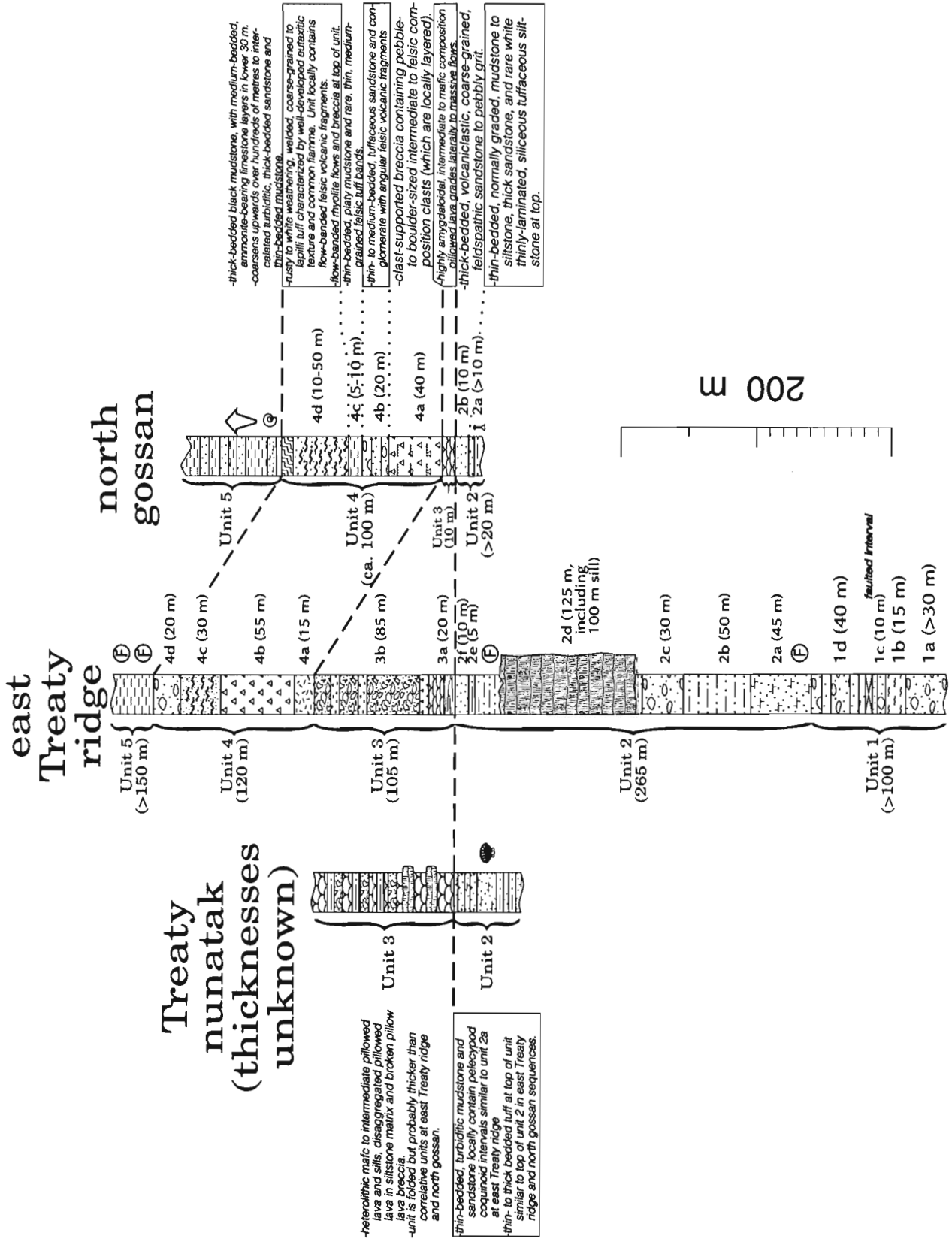


Figure 5. Stratigraphic column for north Gossan and Treaty nunatak sections, compared with simplified stratigraphy of east Treaty ridge section. Patterns and symbols as in Figure 3. Note that stratigraphic thicknesses in the Treaty nunatak section are poorly known.

Faunal assemblages include ammonites *Paracaloceras rursicostatum*, *Badouxia* cf. *canadensis*, *Canavarites* sp., and *Alsatites* sp. characteristic of the Canadense Zone, at the Hettangian-Sinemurian boundary. Benthonic forms within these assemblages include bivalves (*Weyla* and *Camptonectes*), scleractinian corals and gastropods. Geological mapping indicates that these strata lie below unit 1 and therefore provide a maximum age for the measured sections.

East Treaty ridge section (Hazelton and Bowser Lake groups)

Unit 2a fossiliferous sandstone at the east Treaty ridge section yielded *Weyla* sp. and belemnites, whose association indicates a probable Toarcian age (Report J14-1989-TPP, location F3 in Fig. 1 and 3). Higher in the section (location F4 in Fig. 1 and 3), Unit 2d mudstone and sandstone contains a relatively abundant fauna consisting of ammonites *Tmetoceras* cf. *kirki*, *Pseudolioceras* sp., *Leioceras* sp. and bivalve *Inoceramus* sp. The association of these ammonites indicates an Aalenian age, probably Late Aalenian.

Two localities from the base of unit 5 contain Bajocian ammonites (location F5 in Fig. 1 and 3). The basal calcareous sandstone (unit 5a) immediately overlying unit 4 felsic rocks yielded a poorly preserved Soniniid ammonite, and, approximately 20 m higher in unit 5b, the Middle Bajocian ammonite *Zemistephanus* sp. Nearer to the top of unit 5b, ammonites *Lilloettia* sp., and *Kepplerites* indicate a Late Bathonian to Early Callovian age.

Discussion of stratigraphy

The five lithological units defined in the Treaty Glacier area characterize a variety of volcanic and sedimentary environments. Units 1 and 4 contain several laterally continuous welded ash flow tuffs interbedded with coarse, commonly maroon weathering, volcanic breccias of mixed pyroclastic and epiclastic origin. Unit 1 is predominantly intermediate in composition whereas unit 4 is more felsic. We interpret both as subaerial deposits, although reworked parts may be locally subaqueous. Unit 2 is dominated by a coarsening upward sedimentary cycle capped by felsic tuffaceous sediments. Unit 3, in contrast, is characterized by subaqueous mafic to intermediate volcanism, which waned with deposition of epiclastic rocks higher in section. Features in this unit are typical of hydroclastic disruption resulting from the interaction of mafic lava and wet sediments (Hanson, 1991). Although the pillowed flows and pillow breccias are clearly extrusive, much of the overlying unit, especially where it is exposed on Treaty nunatak, formed by the intrusion of mafic lava into a mixture of wet sediment and a growing pile of disaggregated hydroclastite breccia. The final volcanic event in the Treaty area consists of localized rhyolite flows or flow breccias overlain by fine rhyolitic epiclastic sandstone. Similar felsic rocks occur to the west in the Eskay Creek area, but these are overlain or interbedded with mafic pillowed flows and breccias similar to unit 3 rocks in the Treaty Glacier area. This may suggest that mafic to

intermediate volcanic products formed and were preserved within intra-arc basins at different times during the late stages of Hazelton volcanism. Unit 5 marks the onset of widespread marine sedimentation within the Bowser Basin, as well as the cessation of Hazelton Group volcanism.

Possible stratigraphic correlations to named formations

The Treaty Glacier area provides an important section through Lower and Middle Jurassic strata, and form a basis for local and regional stratigraphic correlations. Of particular importance is the Aalenian to Bajocian age constraint for unit 4 felsic pyroclastic rocks, which have been traced in regional map studies westward around the McTagg Anticlinorium, and as far south as Sulphurets Creek.

The Hazelton Group in the Iskut River area traditionally has been divided into, in ascending order, the Unuk River, Betty Creek, Mt. Dilworth, and Salmon River formations. More recently, a new map unit, the Jack formation, has been proposed for a sedimentary succession at the base of the Hazelton Group, locally unconformably overlying the

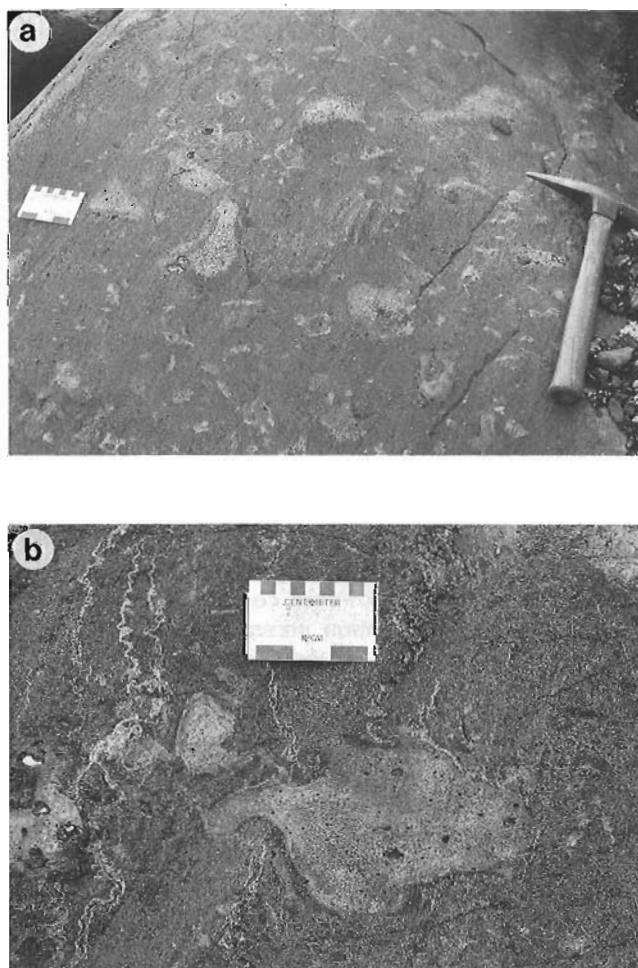


Figure 6. Representative lithologies for unit 3 hydroclastite breccia exposed on Treaty nunatak: **a)** angular to subrounded vesicular fragments in mixed volcano-sedimentary matrix; **b)** amoeboid-shaped vesicular volcanic fragments.

Stuhini Group (Henderson et al., 1992). Henderson et al. (1992) traced fossiliferous calcareous sandstone diagnostic of this unit from the type area at the toe of the Jack Glacier eastward into the Treaty Creek area, where it occurs below the strata described above (Fig. 1). This correlation is corroborated by the Hettangian to Sinemurian boundary age for ammonite collections from this unit described above.

Overlying the Jack formation in the Treaty Glacier area is a lithologically varied volcano-sedimentary sequence characterized by mafic to felsic volcanic compositions, great lateral facies variability, and indications of both subaerial and subaqueous deposition (units 1-4). Fossil collections from the underlying Jack formation, from within unit 2, and from overlying unit 5 strata indicate that this section spans a large time range, from Hettangian-Sinemurian to Bajocian. Elsewhere in the Iskut River area, similarly varied lithological succession characterize this stratigraphic interval, and although formations can be mapped locally, they are difficult to trace for more than a few kilometres. Regionally, the rocks between the Jack formation and the first significant felsic volcanic rocks are assigned to either the Unuk River or the Betty Creek formation. The lateral variability present in the Treaty Glacier area, together with the dissimilarities to Hazelton Group successions at Eskay Creek, Troy Ridge, Johnny Mountain, and elsewhere further underscores the difficulties in regional mapping of Hazelton Group formations (Lewis et al., 1992).

Felsic volcanic rocks of unit 4 are similar to rocks assigned to the Mt. Dilworth Formation elsewhere in the Iskut River area. Unit 4 is continuously exposed for over 30 km west and south of the Treaty Glacier area (Lewis, 1992), and appears to correlate with undated felsic volcanic rocks mapped as Mt. Dilworth Formation at Eskay Creek. Throughout this strike length, it occupies a position above a mixed Hazelton Group volcanic and sedimentary assemblage, and below either basinal mudstone and sandstone sediments of the Bowser Lake Group or pillowed mafic flows of the Salmon River Formation. The few age constraints in this area support this correlation: at Jack Glacier, unit 4 overlies limy fossiliferous siltstones which yield belemnites (GSC C-118980 and GSC C-118982; Gunning, 1986), tentatively dated as Toarcian (J.A. Jeletzky, written comm., 1986). However, correlation of unit 4 with the Mt. Dilworth Formation presents a contradiction to existing age assignments for these rocks, which elsewhere yield likely Upper Pliensbachian to Lower Toarcian fossil assemblages and equivalent isotopic ages. This suggests that unit 4 represents a higher stratigraphic level than the type Mt. Dilworth Formation, and that at least two felsic pyroclastic units must be distinguished regionally: a Pliensbachian to Toarcian, massive to thinly-bedded sequence of pale green pyritiferous, aphyric to feldspar-phyric pyroclastic breccia, welded tuff, and dust tuff; and an Upper Aalenian to Middle Bajocian felsic pyroclastic unit characterized by well-bedded nature and local intercalation of sedimentary rocks. The lower (older) felsic succession is missing from much of the eastern Iskut River area; the farthest north unequivocal

occurrence is at John Peaks, where the lowermost of two felsic intervals has yielded Early Jurassic isotopic ages (M.L. Bevier, unpub. data).

Unit 5 cannot be distinguished from overlying Bowser Lake Group strata, and should therefore be considered part of it. Middle Bajocian ammonites at the base of unit 5 constrain the onset of Bowser Lake Group sedimentation in the eastern Iskut River area, and are consistent with sections in the Smithers map area (Tipper and Richards, 1976), but slightly older than mainly Bathonian basal Bowser Lake Group to the northeast in the Spatsizi map area (Yorath, 1991; Ricketts et al., in press).

STRUCTURAL GEOLOGY

The Treaty Glacier area hosts several generations of folds and faults. The area lies on the upper plate of the southeast-directed Sulphurets thrust fault, which is exposed on the southwest side of the nunatak near the glacier level. There, Hazelton Group rocks override probable Bowser Lake Group siltstones and mudstones. Asymmetric folds in upper plate rocks are consistent with southeast-directed movement. Most other mappable faults are steep, strike between 070° and 120°, and have minimum apparent offsets of tens to hundreds of metres. These faults are not exposed, and unequivocal slip direction and sense indicators are lacking.

Macroscopic folds on the nunatak and east Treaty ridge trend northeasterly, are upright with subhorizontal axes, and are symmetric to slightly southeasterly vergent. Hinges are subangular to rounded and open, and typical fold wavelengths are hundreds of metres. Folds in Bowser Lake Group strata outside of the study area are upright to recumbent, and both southeast and northwest vergence is common.

Rocks in both of the Treaty Glacier alteration zones contain a strong sericitic foliation. The foliation is subvertical regionally, and strikes roughly north-south. A weak to moderate mineral elongation lineation contained in the foliation plane is oriented down-dip. In the north gossan, this foliation is parallel to compositionally layered quartz-alunite-sericite laminations and is refolded by tight angular mesoscopic folds and crenulations which have steep, northwest- to northeast-striking axial surfaces. Outside of the major alteration zones, the foliation is less well developed, but parallel to that within the altered rocks.

ALTERATION AND MINERALIZATION HISTORY

Geological mapping of areas surrounding the two major gossans demonstrates that alteration cuts across stratigraphic contacts, and most of the major units described above host alteration. At both the main and north gossan, alteration boundaries are either obscured by glacial cover or grade into surrounding unaltered host rocks (Fig. 1).

The centre of the main gossan consists of strongly foliated quartz-sericite-pyrite schist. Primary textures of the protolith are locally present throughout the gossan and become more common towards the margins where adjacent stratigraphic units may be recognized. At the north end of the main gossan, a folded sequence of mixed sedimentary and mafic volcanic rocks of units 2 and 3 strike south into the alteration zone with minor local fault offsets. South of the alteration zone, coarse epiclastic volcanic breccia or tuff and overlying felsic volcanic tuff, tentatively equated with unit 3 and possibly unit 4, strike northeast into the alteration zone. The southeastern margin of the alteration zone grades into a relatively coarse grained, likely intrusive feldspar porphyry. In the southeastern part of the gossan, zones of massive silica form a series of prominent outcrops. Rare pseudomorphed textures suggest that the silica is a replacement of volcanic fragmental units. A small zone of quartz-alunite-pyrite alteration occurs to the west, topographically below the silicification. Minor amounts of covellite are associated with this zone. Abundant float of quartz-alunite-pyrite sericite pyrophyllite-diaspore native sulphur covers the northern part of the gossan, and was probably derived from beneath the northern end of the small glacier on the nunatak. Foliation within the main gossan strikes northerly but swings to a more easterly direction in the eastern part of the zone. Boudinaged but unaltered mafic dykes also occur in the eastern part of the main gossan.

Stratigraphic reconstruction of the north gossan is hindered by complex faulting. The eastern alteration boundary is gradational into epiclastic volcanic breccia and conglomerate of the upper part of unit 2 or lower part of unit 3. The western contact is not exposed, but bedded sedimentary strata of unit 2 strike directly into the alteration boundary. To the north, a small gully separates the alteration from a feldspar megaporphyritic dyke, which cuts across strata of unit 2 and shows decreasing alteration away from the main alteration zone. The eastern and upper part of the north gossan is dominated by massive silica similar to the main gossan. The majority of the north gossan, however, consists of strongly foliated and locally crenulated quartz-alunite-pyritekaolinite rock.

Mapping, petrography, XRD analyses, mineral chemistry and limited whole rock chemistry, have refined the interpretation of the alteration zones. The important characteristics of the alteration zone are:

- Alteration cuts across and affects at least 200 m of stratigraphy. The lower contacts are not exposed. The structurally highest alteration affects the upper units of the Hazelton Group and lies 50-200 m below the highest volcanic rocks in the area.
- Both the main and north gossans contain zones of massive silicification in the highest parts of the alteration zones.
- The main zone is dominated by quartz-sericite alteration but contains small outcrops and abundant float of quartz-alunite alteration. The north gossan is dominated by quartz-alunite. Quartz-alunite in the main zone is associated locally with pyrophyllite-diaspore while kaolinite is more common in the north zone. This

mineralogical difference suggests that the north zone formed at lower temperatures, which is consistent with compositional trends in co-existing alunite (A. Thompson, pers. comm., 1992).

Thompson and Lewis (1992) suggested that the Treaty Glacier alteration zones formed in the upper part of a magmatic-hydrothermal system similar to those that occur to the south in the Sulphurets region. Additional mineralogical work and field work during 1992 supports this interpretation. As alteration affects some of the stratigraphically highest units in the Hazelton Group which represent the close of magmatism in the region, it is likely that the upper part of the system lay close to paleosurface. No evidence for the paleosurface has been found in the alteration zone but the massive silicification may represent a paleo-water table with silicification resulting from the acidification of ground water at this level. There are two implications for metallogeny:

1. Magmatic-hydrothermal alteration systems were active in the region until close to the end of Hazelton volcanism, which on the basis of the east ridge stratigraphy lies in the Middle Jurassic between the Aalenian and Bajocian stages. Jurassic magmatism, and alteration and mineralization apparently ceased with the onset of clastic sedimentation in Bowser Basin (Middle Bajocian-Bathonian.)
2. The Treaty Glacier alteration system formed within 200 m of paleosurface suggesting that there may be potential for high sulphidation epithermal mineralization. However, porphyry mineralization is likely to be at least 500 m stratigraphically below the alteration zones.

ACKNOWLEDGMENTS

P. Daubeny, J. Macdonald, and J. Moors all contributed to the fieldwork presented here. Our work benefited greatly from discussions with colleagues at the Mineral Deposit Research Unit, Geological Survey of Canada, and Orequest Consultants Ltd. Copy editing by Bev Vanlier and critical review by J. Roddick greatly improved readability of the final manuscript. This paper is Mineral Deposit Research Unit Project "Metallogenesis of the Iskut River area" (MDRU) contribution # P-012.

REFERENCES

- Alldrick, D.J.**
 1985: Stratigraphy and petrology of the Stewart mining camp (104 B/1); in Geological Fieldwork 1986; British Columbia Ministry of Energy, Mines, and Petroleum Resources, Paper 1985-1, p. 316-341.
 1987: Geology and mineral deposits of the Salmon River Valley, Stewart Area (104A, 104B); British Columbia Ministry of Mines and Petroleum Resources, Geological Survey Branch, Open File Map 1987-22.
 1991: Geology and ore deposits of the Stewart mining camp, British Columbia; Ph.D. thesis, University of British Columbia, Vancouver, 347 p.

Aldrick, D.J. and Britton, J.M.

1988: Geology and mineral deposits of the Sulphurets area (104A/5, 104A/12, 104B/8, 104B/9); British Columbia Ministry of Energy, Mines, and Petroleum Resources, Geological Survey Branch, Open File Map 1988-4.

1991: Sulphurets area geology; British Columbia Ministry of Energy, Mines, and Petroleum Resources, Geological Survey Branch, Open File Map 1991-21.

Anderson, R.G. and Thorkelson, D.J.

1990: Mesozoic stratigraphy and setting for some mineral deposits in Iskut River map area, northwestern British Columbia; *in* Current Research, Part E; Geological Survey of Canada, Paper 90-1E, p. 131-139.

Gunning, M.H.

1986: Late Triassic to Middle Jurassic (Norian to Oxfordian) volcanic and sedimentary stratigraphy and structure in the southeastern part of the Iskut River map sheet, north-central British Columbia; B.Sc. thesis, University of British Columbia, Vancouver, 85 p.

Hanson, R.E.

1991: Quenching and hydroclastic disruption of andesitic to rhyolitic intrusions in a submarine island-arc sequence, northern Sierra Nevada, California; Geological Society of America Bulletin, v. 103, p. 804-816.

Henderson, J.R., Kirkham, R.V., Henderson, M.N., Payne, J.G.,

Wright, T.O., and Wright, R.L.

1992: Stratigraphy and structure of the Sulphurets area, British Columbia; *in* Current Research, Part A; Geological Survey of Canada, Paper 92-1A, p. 323-332.

Lewis, P.D.

1992: Structural evolution of the Iskut River area: Preliminary Results; *in* Mineral Deposit Research Unit "Metallogenesis of the Iskut River Area, British Columbia", Annual Technical Report year 2, University of British Columbia, Vancouver.

Lewis, P.D., Macdonald, A.J., and Bartsch, R.D.

1992: Hazelton Group/Bowser Lake Group stratigraphy in the Iskut River area: progress and problems; *in* Mineral Deposit Research Unit "Metallogenesis of the Iskut River Area, British Columbia", Annual Technical Report year 2, University of British Columbia, Vancouver.

Nadaraju, G. and Smith, P.L.

1992: Jurassic biochronology in the Iskut River map area, British Columbia: a progress report; *in* Current Research, Part A; Geological Survey of Canada, Paper 92-1A, p. 333-335.

Ricketts, B.D., Evenchick, C.A., Anderson, R.G., and Murphy, D.C.

in press: Bowser Basin, northern British Columbia: constraints on the timing of initial subsidence and Stikinia-North America terrane interactions; Geology.

Thompson, J.F.H. and Lewis, P.D.

1992: Advanced argillic alteration at Treaty Glacier, Northwestern British Columbia; *in* Geological Fieldwork 1991, British Columbia Ministry of Energy, Mines, and Petroleum Resources, Geological Survey Branch, Paper 1992-1, p. 543-547.

Tipper, H.W. and Richards, T.A.

1976: Jurassic stratigraphy and history of north-central British Columbia; Geological Survey of Canada, Bulletin 270.

Yorath, C.J.

1991: Upper Jurassic to Paleogene assemblages; Chapter 9, *in* Geology of the Cordilleran Orogen in Canada, (ed.) H. Gabrielse and C.J. Yorath; Geological Survey of Canada, Geology of Canada, no. 4, p. 329-371.

Geological Survey of Canada Project 840046

Major lithologies and alteration of the Ajax East orebody, a sub-alkalic copper-gold porphyry deposit, Kamloops, south-central British Columbia

K.V. Ross¹, K.M. Dawson, C.I. Godwin¹, and L. Bond²
Mineral Resources Division, Vancouver

Ross, K.V., Dawson, K.M., Godwin, C.I., and Bond, L., 1993: Major lithologies and alteration of the Ajax East orebody, a sub-alkalic copper-gold porphyry deposit, Kamloops, south-central British Columbia; in Current Research, Part A; Geological Survey of Canada, Paper 93-1A, p. 87-95

Abstract: The Ajax East pit, in the Afton mine district, on the southwestern side of the sub-alkalic Iron Mask batholith, was developed on copper-gold mineralization located 600 m east of the Ajax West pit. Porphyry-style mineralization, mainly pyrite and chalcopyrite, is located at the intersection of two dioritic phases of the Iron Mask pluton.

Pit mapping at 1:750 scale and logging of representative drill core sections in 1992 resulted in the recognition of nine major lithologies and a revised chronological order: (1) Nicola volcanics, (2) picrite, (3) hybrid diorite, (4) pegmatitic hybrid diorite, (5) Sugarloaf diorite, (6) pyroxene gabbro, (7) monzonite dykes, (8) syenite dyke and (9) quartz-eye latite dykes.

Intense albitization in the Sugarloaf diorite is related both spatially and temporally to mineralization. Potassic alteration is most intensely developed in the relatively mafic hybrid diorite and Nicola volcanic units and is also related to mineralization.

Résumé : Le puits de mine d'Ajax East, dans le district minier d'Afton, sur le versant sud-ouest du batholite subalcalin d'Iron Mask, a été installé sur une minéralisation cuprifère et aurifère située à 600 m à l'est du puits de mine d'Ajax West. Une minéralisation de style porphyrique, principalement en pyrite et en chalcopyrite, se situe à l'intersection des deux phases dioritiques du pluton d'Iron Mask.

La cartographie du puits de mine à l'échelle de 1/750 et la diagraphie, en 1992, de coupes représentatives des carottes de forage, ont permis d'identifier neuf lithologies principales et de réviser l'ordre chronologique: 1) roches volcaniques de Nicola, 2) picrite, 3) diorite hybride, 4) diorite hybride pegmatitique, 5) diorite de Sugarloaf, 6) gabbro à pyroxène, 7) dykes de monzonite, 8) dyke de syénite et 9) dykes de latite oeuillée à quartz .

L'albitisation intense de la diorite de Sugarloaf est associée à la fois dans l'espace et dans le temps à la minéralisation. L'altération potassique atteint son degré maximum dans la diorite hybride relativement mafique et dans les unités volcaniques de Nicola et est également liée à la minéralisation.

¹ Mineral Deposits Research Unit, Department of Geological Sciences, University of British Columbia, 6339 Stores Road, Vancouver, B.C. V6T 2B4

² Afton Operating Corp., P.O. Box 937, Kamloops, British Columbia V2C 5N4

INTRODUCTION

The Ajax East orebody (50°37'N, 120°24'W) is one of a number of porphyry copper-gold deposits of the Afton mining district in the sub-alkalic Iron Mask batholith. This district is located 12 km west of Kamloops and 360 km northeast of Vancouver. Estimated open pit reserves in the Ajax East zone are 7 million tonnes, with a stripping ratio of 1.5:1, averaging 0.44% copper and 0.01 ounces of gold per tonne (Bond, 1987). Mining of the pit was halted in August 1991.

The Ajax East pit, situated on the southwestern side of the Iron Mask batholith at the intersection of two dioritic phases of the Iron Mask pluton, is located approximately 600 m east of the Ajax West zone (Fig. 1; Ross et al., 1992). Porphyry-style mineralization consists of pyrite and chalcopyrite with trace amounts of bornite, chalcocite and molybdenite in a gangue of calcite, albite, potassium feldspar and minor quartz. Due to the lack of feldspathoids, the Iron Mask Batholith has been reclassified as a sub-alkalic batholith (Stanley, 1992).

The objective of this study, a continuation of fieldwork started in 1991 on the Ajax West zone (Ross et al., 1992) was to determine the temporal and structural relationships of the rock units within the Ajax East pit, as well as to examine the alteration and mineralization related to these units. Mapping was conducted at 1:750 scale and core from approximately 50 drill holes was examined in detail. These data will be added to the Ajax West zone study in future descriptions of the mineralization and alteration patterns.

GEOLOGY

Pit mapping has delineated nine significantly different rock units (Fig. 2). Zircon U-Pb dating is currently underway on several of the major units. The current order, from oldest to youngest, is: Nicola volcanics, picrite, hybrid diorite, pegmatitic hybrid diorite, Sugarloaf diorite, pyroxene gabbro, monzonite dyke, syenite dyke, and quartz-eye latite dyke. Major and trace element whole rock analyses are underway. Previous field and petrographic work (Carr, 1956; Preto, 1968; Northcote, 1977; Bond, 1987; Kwong, 1987; Ross et al., 1992) is incorporated in the definition of the units. There has been a revision in the intrusive sequence; the hybrid diorite and pegmatitic hybrid diorite are mapped as older than the Sugarloaf diorite, rather than younger, as reported from the Ajax West pit (Ross et al., 1992).

The descriptions of alteration are based on field observations. A statistical study of the alteration is in progress on the data gathered from drill core samples systematically collected at two plan sections at the 860 and 940 m level, and a cross-section striking 60 degrees northwest (Fig. 2, 3). This part of the study will be supported ultimately by microprobe analyses of representative samples.

(Unit 1) Nicola volcanics, is a strongly foliated, hornfelsed screen which strikes north 40 degrees east and occurs along the hybrid diorite/Sugarloaf diorite contact throughout the length of the pit (Fig. 2, 3). The volcanics are nonmagnetic, augite phyric. Much of the augite is replaced by pale green amphibole surrounded by red-brown biotite. The Nicola is mineralized with chalcopyrite and pyrite, as foliation parallel disseminations and as veinlets crosscutting foliation. Sugarloaf diorite intrudes the screen as numerous dykes and dykelets. The hornfelsing was probably generated initially by intrusion of the hybrid diorite and later by intrusion of the Sugarloaf diorite. K-feldspar-calcite \pm epidote veins crosscut the foliation.

(Unit 2) Picrite, as designated by Cockfield (1948) and Carr (1956), is characterized by serpentinized olivine phenocrysts, relict clinopyroxene phenocrysts and up to 25% secondary magnetite (Kwong, 1987). It occurs in the northeast corner of the pit where it is in contact with Sugarloaf diorite (Fig. 2) and is also apparent as fault slices within the screen of Nicola volcanics (Fig. 3).

In hand sample picrite is a dark grey, aphanitic rock with rounded inclusions of olivine partially replaced by serpentine and magnetite. On sheared surfaces, waxy serpentine is characteristic. In thin section the corroded, serpentinized, coarse grained olivine phenocrysts are in a groundmass of aphanitic grey serpentinite and tremolite.

Disseminated pyrite and chalcopyrite occur one to two centimetres from contacts with the Sugarloaf diorite. Xenoliths of picrite within the Sugarloaf diorite appear to be affected by albite alteration.

(Unit 3) Hybrid diorite, a fine- to coarse-grained intermediate unit, with mafic to ultramafic phases, characterized by abundant disseminated magnetite, occurs on the north-western side of the pit (Fig. 2, 3). The medium- to coarse-grained phases predominate in the East pit.

In hand sample the rock is typically dark grey to green, composed of medium- to coarse-grained pyroxene, feldspar (An₃₅) and magnetite. Foliated, mineralized xenoliths of Nicola are incorporated in the unit. Chlorite and biotite replace pyroxene. The hybrid unit is only locally affected by strong albitization, but potassic alteration, characterized by hydrothermal biotite, is strongly developed. Hydrothermal biotite occurs pervasively throughout the unit and as selvages on K-feldspar-calcite-diopside \pm epidote \pm albite? veins. Pervasive and selvage biotites may differ compositionally. Propylitic alteration assemblages are intensely developed in sheared zones.

(Unit 4) Pegmatitic hybrid diorite consists of medium- to very coarse-grained pyroxene, plagioclase and magnetite. The coarse grained phase predominates, but appears to be consanguineous with the medium grained phase. Coarse grained mafic clasts occur in a finer grained more felsic matrix. This complex agmatitic unit occurs in the Ajax East pit as very localized patches of clasts in felsic matrix. However, the unit occurs in large areas north of the Ajax West and East pits (Fig. 1). Epidote alteration is common.



Figure 1. Regional geology and location of the Ajax East and West pits (see Fig. 2 for legend).

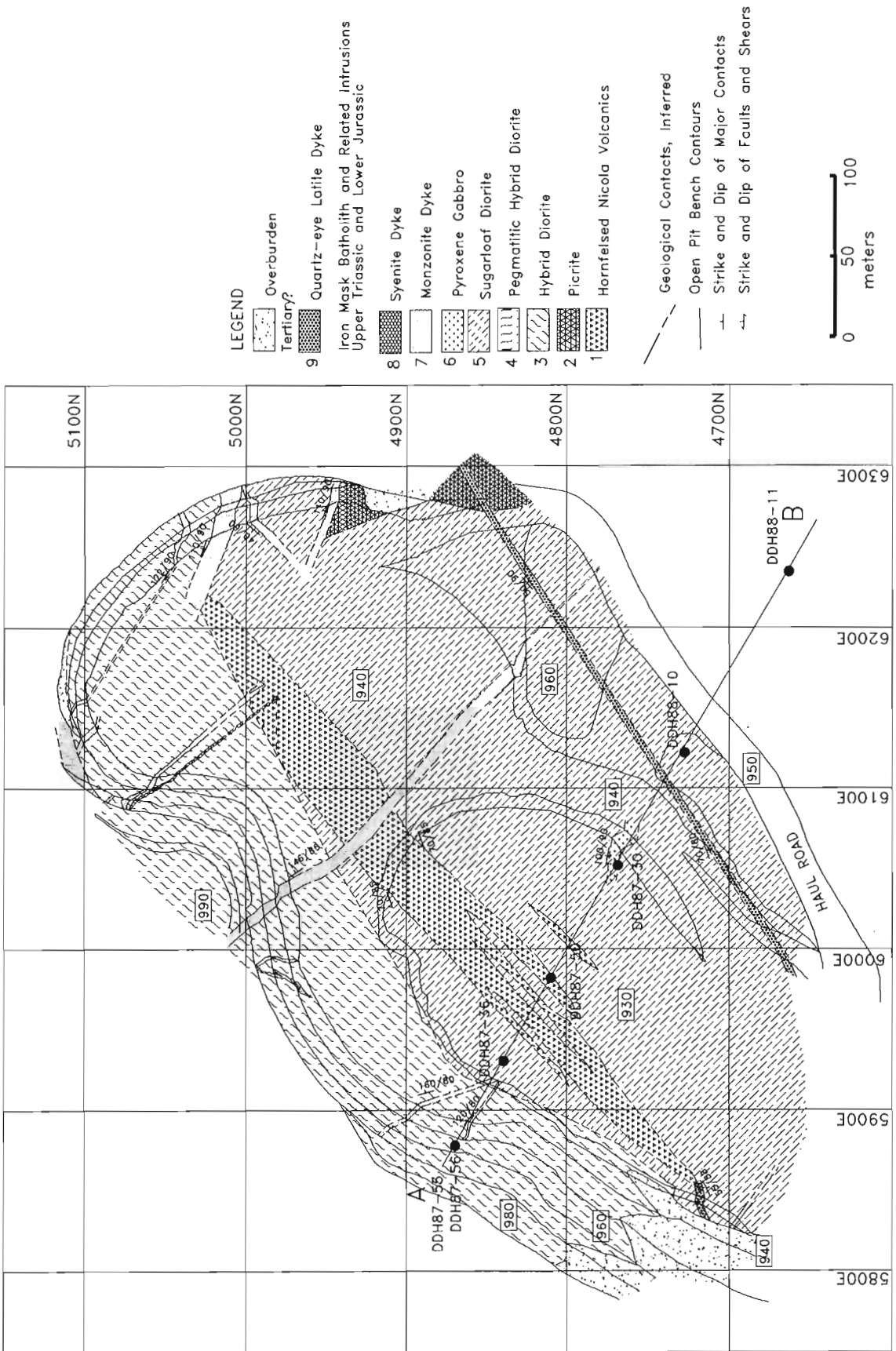


Figure 2. Geology of the Ajax East pit with location of cross-section A-B (see Fig. 3). Nine major rock units have been identified. The units are presented from youngest to oldest in legend. This order is based on field relationships.

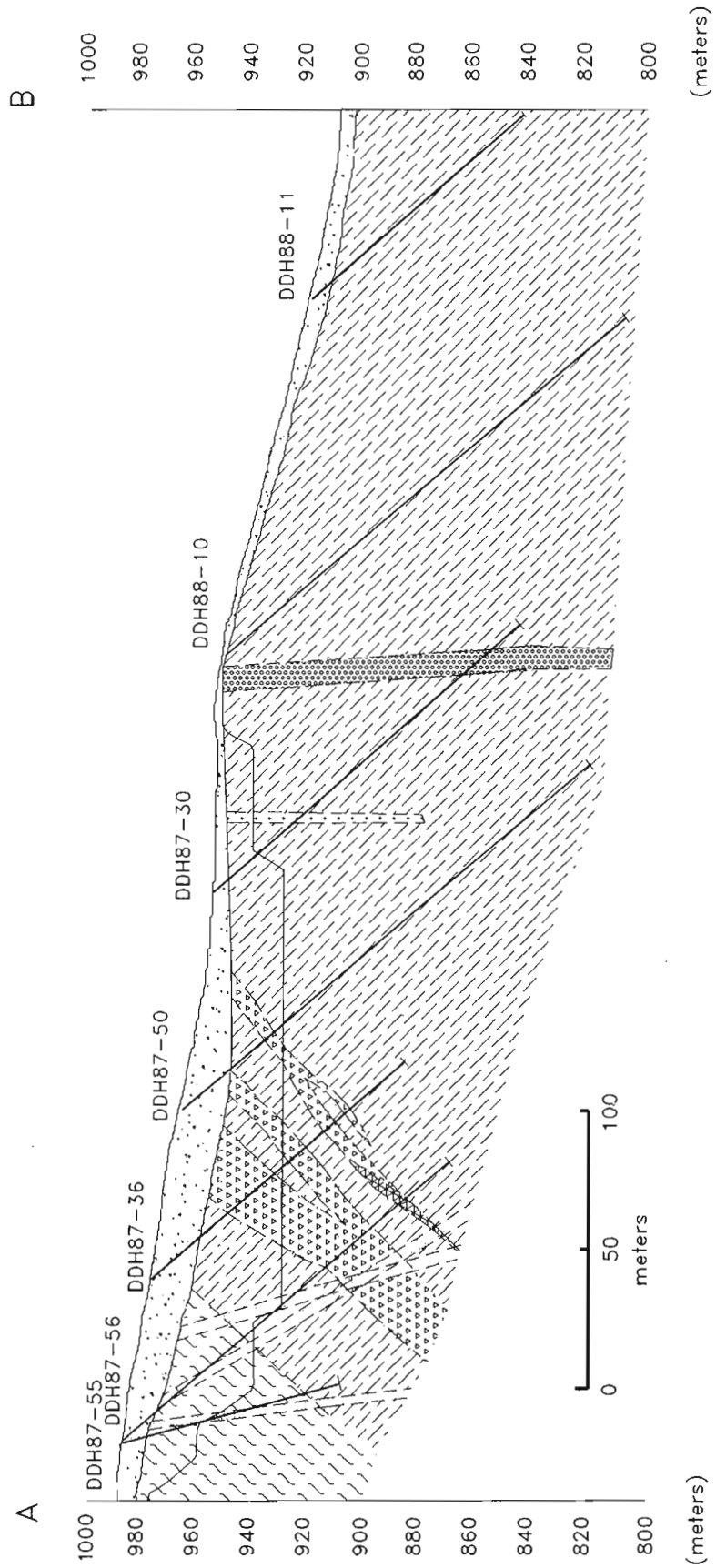


Figure 3. Cross-section A-B, Ajax East pit, striking 40° northwest and looking northeast (see Fig. 2 for location and legend).

(Unit 5) **Sugarloaf diorite**, a fine- to medium-grained porphyry, with characteristically elongate hornblende and plagioclase phenocrysts that are enclosed in a medium grey matrix. This unit, that has been mapped on a regional scale (Preto, 1968), occurs on the southeastern side of the Ajax East pit (Fig. 2, 3). This unit displays considerable textural variation, ranging from fine grained, weakly porphyritic to a medium grained crowded (phenocryst-rich) porphyry, commonly with trachytic texture.

In thin section the unit contains olive green, strongly pleochroic hornblende as prismatic crystals and needles. Feldspar makes up 55% of the rock, either as sericitized, ghostly, equant to tabular phenocrysts or as an aphanitic, sericitized ground mass.

Albitization is intensely developed and is commonly associated with mineralization. Alteration assemblages grade from weak propylitic to intense albitic. Pervasive epidote and chlorite after hornblende occur in weakly propylitized rock. Disseminated pyrite content varies from absent to several per cent. Albite envelopes are developed outward from veins containing albite-diopside-epidote. As albitization intensity increases, the envelopes coalesce to form a uniformly textured fine grained white rock. Albite-diopside-anhydrite veinlets also occur. K-feldspar-calcite-diopside \pm epidote \pm albite? veins with chlorite (after biotite?) envelopes occur within both intensely albitized rock and propylitically altered rocks. The composition of the various types of plagioclase alteration and their zonal distribution is under investigation.

(Unit 6) **Pyroxene gabbro** is a medium- to coarse-grained amphibole- and pyroxene-phyric unit with a dark grey matrix that occurs as a dyke within the Sugarloaf diorite (Fig. 2, 3). It has very limited exposure in the East pit and its orientation is uncertain.

In thin section this unit is a medium grained, crowded porphyry. Hornblende phenocrysts make up to 30% of the assemblage and may be after pyroxene. The groundmass of microcrystalline secondary hornblende and sericitized aphanitic feldspar apparently is affected locally by the albitization.

(Unit 7) **Monzonite dyke**, is a fine grained porphyry with hornblende and plagioclase phenocrysts in a feldspar matrix with approximately 2% disseminated magnetite. This unit was grouped with the Cherry Creek suite (Ross et al., 1992), but probably belongs with the Sugarloaf diorite suite. The petrographic affinity will be investigated in conjunction with a larger study on the Iron Mask units (Snyder and Russell, in progress). A major dyke traverses southeastward across the Ajax East pit, cutting the Nicola volcanics, the hybrid diorite and Sugarloaf diorite (Fig. 2). A second large dyke separates the Sugarloaf and hybrid diorites on the northeastern wall of the Ajax East pit, and a third dyke partially separates the screen of picrite in the northeastern corner of the pit from the Sugarloaf diorite. Numerous smaller dykes occur within the hybrid diorite on the northwestern wall of the pit. The dykes are typically fine grained, blue-grey to pinkish with characteristic grains of magnetite, and commonly, a pervasive epidote

alteration. The pinkish colour is due to pervasive K-feldspar alteration that occurs sporadically in some dykes and is absent in others. Disseminated chalcopyrite and pyrite occur in trace amounts. Unmineralized calcite veins crosscut mineralization.

In addition to epidote alteration in the larger dykes, and localized pervasive K-feldspar alteration, many of the smaller dykes appear to have been albitized. One dyke in particular is totally albitized though the primary texture is preserved.

(Unit 8) **Syenite dyke**, occurs parallel to a monzonite dyke (Fig. 2). Only one dyke has been noted. It is medium grained, and consists dominantly of pink potassic feldspar. Mineralization is not apparent in hand sample.

(Unit 9) **Quartz-eye latite dyke**, is hornblende, potassium feldspar and quartz phyric. These dykes cut the Sugarloaf diorite and the picrite (Fig. 2). The largest dyke is approximately 5 m wide and can be traced along the entire length of the southeastern side of the pit. A second large dyke occurs at the contact between the hybrid and the Sugarloaf diorites in the southwest corner of Ajax East pit, but could not be traced beyond the pit wall. These dykes postdate alteration, mineralization and many of the faults. Similar dykes are reported in the Afton pit (Kwong, 1987) and Ajax West pit (Ross et al., 1992).

In hand sample this unit is a uniform, fine grained, porphyritic, brownish pink rock with hornblende needles, characteristic quartz and K-feldspar phenocrysts and minor amounts of disseminated pyrite. Quartz veining, accompanied by bleaching and silicification of the host rock, is associated with these dykes.

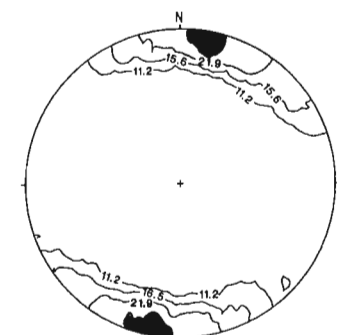
Magnetite-rich dykes (unit not defined) occur at several localities in both the Sugarloaf and hybrid diorites. These discontinuous dykes, less than a metre in width, are too small to appear on the map.

STRUCTURE

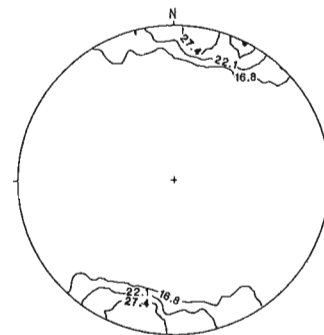
Attitudes of both mineralized and unmineralized structures in Ajax East orebody are predominantly EW/90°, oblique to principal intrusive contacts that strike northeast and dip moderately northwest. Contoured stereogram plots of poles to Ajax East mineralized and unmineralized structures are given in Figures 4 and 5 respectively. Average structural trends are given in Table 1. Intrusive contacts between older units, i.e. Nicola volcanics, picrite, Sugarloaf diorite and hybrid diorite, commonly are loci of subsequent faulting and mineralization. In contrast to Ajax East, attitudes of structures in Ajax West orebody (not illustrated) shift significantly from early, mineralized (NE/75°NW) to late, unmineralized (SE/65°SW) and moderately to shallowly dipping structures predominate. Unmineralized faults in both Ajax orebodies are concordant with the dominant southeast to east-southeast strike of regional faults, and represent a Late Mesozoic to Early Tertiary structural overprint on pre-mineralization northeast and east-west-striking structures.

Figure 4.

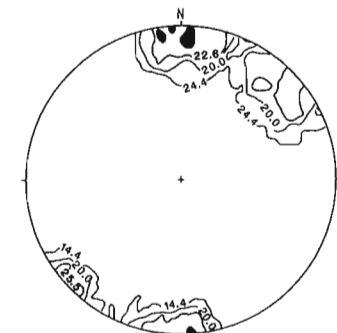
Contoured poles to planes, Schmidt projection, mineralized structures at Ajax East pit, Afton mine.



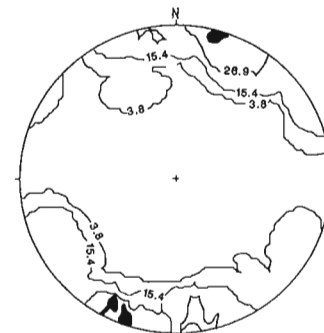
Ajax East : All Mineralized Structures; n=169



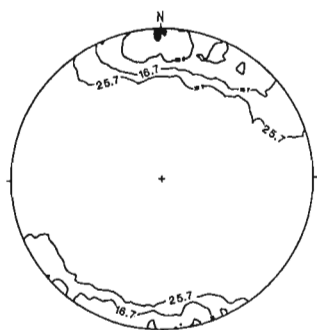
Ajax East : Mineralized Veins, Fractures; n=113



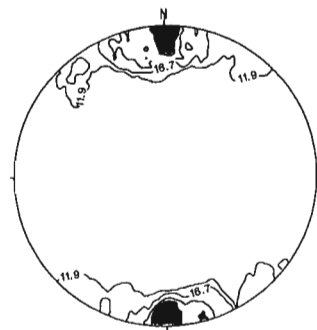
Ajax East : Mineralized Faults, Shears; n=30



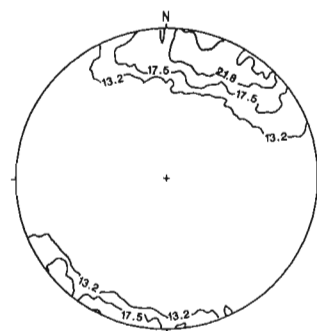
Ajax East : Mineralized Dyke Contacts; n=26



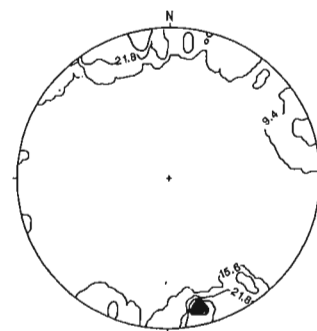
Ajax East : All Unmineralized Structures; n=205



Ajax East : Unmineralized Joints, Fractures; n=45



Ajax East : Unmineralized Faults, Shears; n=128



Ajax East : Unmineralized Dyke Contacts; n=32

Figure 5.

Contoured poles to planes, Schmidt projection, unmineralized structures at Ajax East pit, Afton mine.

Table 1. Average attitudes of structures in and adjacent to Ajax East and Ajax West pits, Afton mine

	Ajax East		Ajax West		Regional	
	mineralized	unmineralized	mineralized	unmineralized	cut Iron Mask, Nicola	cut Iron Mask, Nicola, Kamloops
Faults, shears	085/90 *140/85SW n=30	108/75SW 135/80SW n=128	062/70NW 00/55W n=75	153/75NW 030/60 NW n=55	strike 135 n=18	strike 102 n=64
Veins, fractures	115/90 105/90 n=113	090/90 n=45	145/85SW 075/85SW n=51	135/45SW n=24		
Dyke contacts	115/90 n=26	078/90 100/85S n=32	083/85N n=15	090/85N n=10		
Average of all structures	100/90 n=169	090/90 115/85S n=205	070/75NW 017/65W n=141	155/65SW 160/90 n=89		
Nicola Group volcanic, sedimentary bedding					145/70NE n=125	

* second attitude is secondary structural trend in each case

CONCLUSIONS

Detailed mapping of the Ajax East pit has delineated nine major rock units. The relative ages of these units is provisionally defined by contact relationships exposed in the pit and in drill core. Lithogeochemical trends and zircon dating of the units may refine compositional and age relationships.

Albitization is spectacularly developed within the Sugarloaf diorite and is spatially and temporally related to mineralization. Potassic alteration is more intensely developed in the relatively mafic hybrid diorite and Nicola volcanic units and may also be closely related to mineralization. Future statistical analysis of data, supported by microprobe work will help define alteration and mineralization zonation patterns.

The dominant EW/90° attitude of both mineralized and unmineralized Ajax East structures differs from that of Ajax West and regional rocks.

ACKNOWLEDGMENTS

Afton Operating Corporation, in particular Louis Tsang, helped in geological mapping problems in the pit and provided access to company files, drill core and the mine property. Research has been supported by the Geological

Survey of Canada, and the Mineral Deposit Research Unit (MDRU Contribution No. 23) through the Department of Geological Sciences, The University of British Columbia, collaborative industry-SCBC-NSERC research project, "Copper-Gold Porphyry Deposits of British Columbia." Financial support from a COSEP Grant to Ross is gratefully acknowledged.

REFERENCES

- Bond, L.**
1987: Geology and Mineralization at the Ajax Mine; unpublished company report.
- Carr, J.M.**
1956: Deposits associated with the eastern part of the Iron Mask Batholith near Kamloops, B.C.; British Columbia Department of Mines, Annual Report, p. 47-69.
- Cockfield, W.E.**
1948: Geology and mineral deposits of Nicola map-area, British Columbia; Geological Survey of Canada, Memoir 249, 164 p.
- Kwong, Y.T.J.**
1987: Evolution of the Iron Mask Batholith and its associated copper mineralization; British Columbia Ministry of Energy, Mines and Petroleum Resources, Bulletin 77, p. 1-55.
- Northcote, K.E.**
1977: Geology of the southeast half of the Iron Mask Batholith; in Geological Fieldwork, 1976; British Columbia Department of Mines and Petroleum Resources, p. 41-46.

Preto, V.A.

1968: Geology of the eastern part of the Iron Mask Batholith; in Annual Report 1967; British Columbia Ministry of Mines and Petroleum Resources, p. 137-147.

Ross, K.V., Dawson, K.M., Godwin, C.I., and Bond L.

1992: Major lithologies of the Ajax West pit, an alkaline copper-gold porphyry deposit, Kamloops, British Columbia; in Current Research, Part A; Geological Survey of Canada, Paper 92-1A, p. 179-183.

Stanley, C.R.

1992: Mineral Deposit Research Unit, Porphyry Copper-Gold Systems of British Columbia; Annual Technical Report, Section 13-1.

Teck Corporation

1990: Annual Report, 52 p.

Geological Survey of Canada Project 740098

Geochemistry of tourmalinite, muscovite, and chlorite-garnet-biotite alteration, Sullivan Zn-Pb deposit, British Columbia¹

David R. Shaw², C. Jay Hodgson³, Craig H.B. Leitch, and Robert J.W. Turner

Mineral Resources Division, Vancouver

Shaw, D.R., Hodgson, C.J., Leitch, C.H.B., and Turner, R.J.W., 1993: Geochemistry of tourmalinite, muscovite, and chlorite-garnet-biotite alteration, Sullivan Zn-Pb deposit, British Columbia; in Current Research, Part A; Geological Survey of Canada, Paper 93-1A, p. 97-107.

Abstract: The tourmalinite body underlying the western portion of the Sullivan deposit is enriched in B₂O₃, MgO, and MnO and depleted in K₂O, CaO and Na₂O and reflects replacement of feldspar and micas by tourmaline in the host sedimentary rock. The tourmalinite zone is enveloped by a zone of muscovite altered rocks which grades outward into unaltered sedimentary rock. Muscovite-altered rocks are enriched in K₂O and MnO, and depleted in CaO, Na₂O, and Fe₂O₃ due to the absence of feldspar and biotite, and increased abundance of muscovite. Chlorite-biotite-garnet alteration may represent partial chloritization of biotite-garnet-altered rocks near tourmalinite and/or Moyie gabbro intrusions. Chlorite-biotite-garnet altered rocks are enriched in Fe₂O₃, MgO, and MnO and depleted in CaO, Na₂O, and K₂O due to increased abundance of biotite, chlorite, and garnet, absence of feldspar, and decrease in muscovite relative to unaltered rocks.

Résumé : Le corps de type tourmalinite sous-jacent à la partie ouest du gisement de Sullivan est enrichi en B₂O₃, MgO et MnO et appauvri en K₂O, CaO et Na₂O, et témoigne de la substitution du feldspath et des micas par de la tourmaline dans la roche hôte sédimentaire. La zone à tourmalinite est entourée par une zone de roches altérées en muscovite, qui passe vers l'extérieur à une zone de roches sédimentaires non altérées. Les roches altérées en muscovite sont enrichies en K₂O et MnO, et appauvries en CaO, Na₂O et Fe₂O₃, en raison de l'absence de feldspath et de biotite, et de l'abondance accrue de la muscovite. L'altération en chlorite-biotite-grenat pourrait correspondre à une chloritisation partielle des roches altérées en biotite-grenat près de la tourmalinite ou des intrusions de gabbro de Moyie, ou des deux à la fois. Les roches altérées en chlorite-biotite-grenat sont enrichies en Fe₂O₃, MgO et MnO et appauvries en CaO, Na₂O et K₂O, en raison de l'abondance accrue de la biotite, de la chlorite et du grenat, de l'absence de feldspath et de la diminution de la quantité de muscovite par rapport aux roches non altérées.

¹ Contribution No. 12, Sullivan-Aldridge Project

² 8431 58th Avenue N.W., Calgary, Alberta T3B 4B4

³ Department of Geological Sciences, Queen's University, Kingston, Ontario K7L 3N6

individual analyses in Table 2. In Table 2, samples analyzed once are identified by the suffix "0" in the sample number; samples analyzed twice by the suffix "1" or "2"; control samples analysed repeatedly by a suffix "1-14". Average compositions in Table 1 include only those analyses with a suffix of "0" or "1". "Total" is the total of the XRF analysis as reported by Cominco for the major elements and LOI. The sulphide mineral content of altered rocks at the Sullivan deposit is highly variable. In our samples, sulphur abundance ranges from 0.01% to 14.9% and averages 4.7%. In contrast, the average sulphur abundance of unaltered regional Aldridge rocks is 0.25% (Fedikow, 1978). The Fe₂O₃ (total iron) abundance also displays considerable variation, ranging from 2.2% to 38.5%. In many samples, significant iron is present in iron-bearing sulphide minerals, and much of the range in iron content arises from differences in the amount of iron-bearing sulphide minerals present. In order to compare samples containing different amounts of iron-bearing sulphide minerals, the amount of iron contained in pyrrhotite, pyrite, sphalerite, chalcopyrite, and arsenopyrite was subtracted from total iron, and analyses normalized to 100% non-sulphide constituents were computed (bold numbers, Table 1).

Unless stated otherwise, major elements in altered rock types are compared on the basis of these recalculated sulphide-free analyses and Fe₂O₃ represents iron in the recalculated analysis expressed as ferric iron. These calculations yielded negative Fe₂O₃ values for four samples containing more than 9% sulphur, and these samples have been omitted from the average Fe₂O₃ concentrations in

Table 1. The exclusion of these Fe₂O₃ values, and of assumed values for boron used for calculations in samples in which boron was not analyzed, causes some of the totals for recalculated analyses to vary from 100%.

Many samples contain concentrations of minor elements below the detection limit for those elements. In order to permit the calculation of averages that will serve as a guide when comparing the minor element concentrations in altered rocks, values of one-half the detection limit for that element are reported instead of "not detected" in Table 2, and the averages calculated in Table 1 include these values (Sanford et al., in press). These values in parts per million are: 1 or 2 for Pb, 0.1 or 0.2 for Ag, 2 for Sb and Bi, 1 for As and W, and 10 for Sn and Ba.

LIMITATIONS ON THE INTERPRETATION OF CHEMICAL AND MINERALOGICAL DATA

Several concerns regarding the interpretation of chemical changes associated with alteration at the Sullivan deposit should be noted. It can be difficult to ascertain the protolith where alteration types are superposed. Arenaceous and argillaceous unaltered Aldridge rocks differ in chemistry and some differences in the chemistry of altered rocks may reflect differing sedimentary compositions. The different sulphide mineral content of different rock types causes apparent changes in the abundance of other constituents. Preservation of primary structures and textures in altered rocks is variable,

Table 2. (cont.)

Sample	SiO ₂	Al ₂ O ₃	Fe ₂ O ₃	MgO	CaO	Na ₂ O	K ₂ O	TiO ₂	P ₂ O ₅	LOI	CO ₂	TOTAL	Cu	Pb	Zn	Ag	Sb	Bi	Fe	As	W	S	Ba	Mn	Sn	B	SG	ROCK TYPE
1121-2	67.18	13.08	11.03	2.58	.37	.35	.281	.59	NA	2.81	0.03	100.80	127	430	276	0.9	2	2	6.1	1	1	2.35	220	1755	195	NA	NA	12.1
1121-1	67.05	13.08	10.99	2.57	.37	.28	2.81	.59	NA	2.82	0.13	100.56	123	450	262	1.2	2	2	4.8	1	1	2.29	217	1681	200	NA	2.8	12.1
1127-0	54.98	15.73	18.41	2.22	.81	.40	2.86	.66	NA	3.15	0.13	99.22	137	258	325	0.4	2	2	9.3	9000	12	2.06	238	4044	130	400	2.8	12.1
1220-0	51.52	10.26	22.64	1.63	.87	.67	.64	.38	.09	3.57	0.52	92.27	308	37900	1740	172.0	18	460	14.1	17	30	5.64	52	4975	76	290	3.23	12.1
1120-0	69.05	13.82	8.40	2.32	.40	.41	2.82	.63	NA	2.40	0.01	100.25	80	2570	174	7.0	2	2	4.6	1	4	1.59	229	1308	235	2900	2.7	12.2
1122-0	64.60	14.30	10.60	2.71	1.27	1.50	.57	.67	NA	1.57	0.10	97.79	50	118	295	0.1	2	2	5.1	8	4	1.44	64	1476	75	8700	2.7	12.2
1123-0	70.58	11.97	9.68	2.14	.49	.43	1.04	.55	NA	1.51	0.01	98.39	89	1160	207	3.2	2	2	5.1	8	1	2.28	95	1135	125	7850	2.6	12.2
1124-0	66.58	13.01	10.77	2.66	1.45	1.27	.19	.59	NA	1.50	0.18	98.02	85	1620	550	6.9	2	7	4.5	8	8	2.14	10	1145	85	9800	2.9	12.2
1125-0	63.24	14.07	11.31	2.66	2.04	1.47	.38	.64	NA	1.71	0.27	97.52	105	2140	730	5.4	2	6	5.8	4	1	2.58	10	1227	80	8900	2.7	12.2
1126-1	68.15	13.06	9.45	2.61	.61	.65	1.66	.60	NA	2.11	0.04	98.90	68	2500	192	7.0	2	4	4.7	1	1	1.67	143	1910	150	5300	2.9	12.2
1126-2	69.43	12.98	9.49	2.60	.61	.60	1.66	.59	NA	2.07	0.01	100.03	68	2570	193	7.0	2	7	4.8	1	1	1.65	138	1903	155	NA	NA	12.2
1107-0	70.12	7.81	10.44	1.17	2.69	.47	.96	.35	NA	1.97	0.12	95.98	85	6000	27400	12.3	2	14	7.3	150	25	5.17	41	2884	45	NA	2.9	12.3
Bleached, carbonate altered footwall rocks: 15.1 intense; 15.2 moderate; 15.3 weak.																												
1224-0	60.36	10.35	4.71	1.89	7.59	.19	3.13	.41	.11	5.73	9.05	94.47	18	194	218	0.2	2	2	3.0	29	6	1.02	793	3292	116	NA	3.33	14.0
1149-0	61.22	15.57	8.06	1.30	.57	.15	4.62	.62	.06	5.21	3.25	97.38	19	2700	450	3.8	2	2	4.7	64	4	1.12	502	1991	34	NA	2.78	15.1
1150-0	60.04	14.49	10.40	.85	.68	.16	4.47	.60	.08	6.42	3.93	98.19	31	1670	1040	2.6	2	2	6.0	339	6	3.13	478	1530	33	NA	2.86	15.1
1151-2	67.88	13.95	7.73	.86	.52	.04	3.77	.56	.09	3.36	1.37	98.76	14	270	729	0.7	2	2	4.5	28	3	1.05	392	1520	41	NA	2.78	15.2
1151-1	66.70	13.70	7.36	1.29	.52	.18	3.75	.53	.09	4.61	1.48	98.73	16	326	563	0.7	2	2	4.3	17	6	1.27	395	1484	54	NA	2.78	15.2
1152-0	58.87	20.32	7.42	1.38	.67	.16	5.97	.78	.06	3.00	0.43	98.63	13	120	235	0.4	2	2	3.0	47	6	0.77	631	2992	50	NA	2.86	15.2
1153-0	64.19	16.66	7.82	1.11	.59	.10	4.80	.67	.07	2.28	0.11	98.29	18	38	294	0.2	2	2	3.8	9	2	1.18	489	2082	35	NA	2.78	15.3

Note: Certain samples were not analysed for major elements where remaining pulp was insufficient. Major elements (SiO₂ to CO₂, Fe and S) in percent; Cu, Pb, Zn, Ag, Sb, Bi, As, W, Ba, Mn, Sn, B in ppm; NA: not analyzed; SG: specific gravity.

and the role that volume changes have played during alteration is unclear. Therefore, in this paper we focus on relative, rather than absolute chemical changes.

Biotite-facies middle greenschist metamorphism has affected both regional Aldridge rocks and altered rocks at the Sullivan deposit. Altered rock types are classified and described in terms of their present metamorphic mineralogy, and this mineralogy may be different from that which existed prior to metamorphism. The reader is cautioned that use of terms such as "muscovite-altered" does not necessarily imply that alteration produced muscovite. Muscovite may be the metamorphic equivalent of different precursor minerals formed during alteration.

UNALTERED SEDIMENTARY ROCKS

The mineralogy and geochemistry of 95 regional samples from the Aldridge Formation has been studied by Edmunds (1977). The SiO_2 , Al_2O_3 , Cu, Pb, Zn, and Mn contents were determined by colourmetric methods, and CaO, MgO, FeO, Na_2O , K_2O , and TiO_2 by atomic absorption spectrometry. Edmunds' (1977) average composition of Aldridge rocks (combining argillite and greywacke from both Lower and Middle Aldridge Formation) is used as the reference composition for comparison with the geochemistry of altered rocks from the Sullivan deposit (Table 1, alteration type 0.0). This average composition of Aldridge strata is very similar to that presented by Hamilton et al. (1982, Table 3). Values of zero reported by Edmunds were changed to one-half the detection limit for that element, FeO values reported by Edmunds were converted to Fe_2O_3 , and the arithmetic mean for each chemical constituent recalculated from the raw analytical data in Edmunds' (1977) Appendices 1.2.1 and 1.2.2.

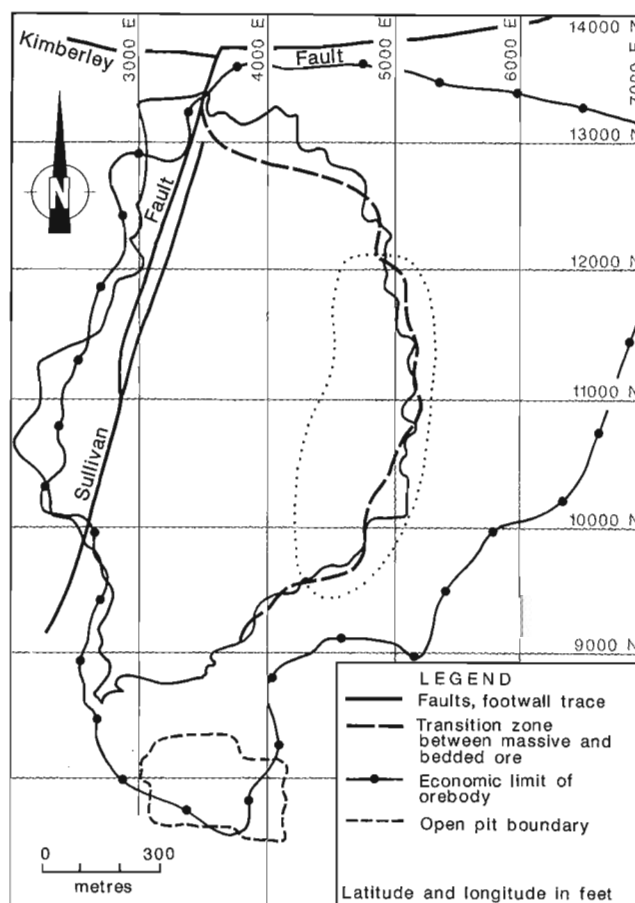
The average mineralogical composition of Aldridge rocks is 48% quartz, 20% plagioclase, 15% white mica, 11% biotite, 2.4% muscovite, 0.9% carbonate, 0.8% K-feldspar, 0.6% graphite, 0.8% iron ores, and 0.3% sphene (Edmunds, 1977). Argillaceous rocks analyzed by Edmunds ("argillite"; alteration type 0.1 in Table 1) contain more Al_2O_3 , Fe_2O_3 , MgO, CaO, K_2O , TiO_2 , Mn, Cu, and Zn and less SiO_2 , Na_2O , and Pb than do arenaceous rocks ("greywacke"; alteration type 0.2 in Table 1). Quartz and plagioclase are concentrated in arenaceous rocks; K-feldspar, biotite, white mica, graphite, iron ores, sphene, and carbonate are concentrated in argillaceous rocks. Six of the 95 samples analyzed by Edmunds are from the lower Aldridge Formation (Table 1, alteration type 0.3). They contain slightly less Fe_2O_3 and more Na_2O than do the average Aldridge Formation.

The boron concentration in 84 samples of the Prichard Formation (equivalent to Aldridge Formation) in Idaho was determined using semiquantitative spectrographic analysis by Harrison and Grimes (1970). Boron ranges from less than 10 ppm to 100 ppm, and the arithmetic mean is 22 ppm. The average Ba content of 21 samples of unaltered regional Aldridge rocks is 545 ppm (Fedikow, 1978).

FOOTWALL TOURMALINITE ALTERATION

Geology of tourmalinite

Tourmalinite is the most abundant type of altered rock underlying the Sullivan deposit (Shaw and Hodgson, 1980a,b, 1986; Hamilton et al., 1982). Tourmalinite underlies most of the western part of the orebody (Fig. 1), and the zone has the shape of a cylinder or steep-sided funnel oriented normal to bedding, with maximum lateral dimensions of 1470 m by 980 m and a vertical extent of at least 450 m. Tourmalinite resembles chert and is a dark grey, black or brown, extremely hard, lustrous rock with a pronounced conchoidal fracture. It is composed of a detrital framework of quartz, silt and sand set in a matrix of minute tourmaline needles, microcrystalline quartz and minor microcrystalline muscovite, and commonly



— extent of footwall tourmalinite
 limit of underground mapping

Figure 1. Plan view of the Sullivan orebody illustrating the lateral extent of tourmalinite underlying the sulphide body. The extent of the orebody and the location of the transition zone are shown for reference. Area of underground mapping shows location of muscovite-rich, chlorite-biotite-garnet-, and carbonate-muscovite-altered footwall sedimentary rocks discussed in this paper.

contains more than 50% tourmaline; feldspar is rare. Sedimentary structures and textures on all scales are typically well preserved.

Contact relationships between tourmalinite and tourmaline-poor rocks are well exposed in mine workings between the footwall of the orebody and about 40 m below the orebody. We refer to this as the upper tourmalinite zone. The central part of this upper tourmalinite zone (Table 1, alteration type 3.3) is characterized by tourmalinite in contact with albite-chlorite-pyrite, chlorite-pyrrhotite, and muscovite-rich rocks that formed by alteration of tourmalinite. Tourmaline-poor rocks that did not form by alteration of tourmalinite are rare. The central upper tourmalinite zone is surrounded by a fringe zone up to 275 m wide, in which sulphide-rich tourmalinite (Table 1, alteration type 3.1), sulphide-poor tourmalinite (Table 1, alteration type 3.2) and partially tourmaline-enriched rock containing abundant tourmaline and microcrystalline muscovite (Table 1, alteration type 3.0) are in contact with muscovite-altered and chlorite-garnet-biotite-altered rocks formed in part by alteration of tourmalinite.

In the deep tourmalinite zone below about 40 m from the footwall contact of the ore zone (Table 1, alteration type 3.4), a central core of tourmalinite passes outwards into a fringe zone of intercalated tourmalinite and tourmaline-poor rocks.

Chemistry of tourmalinite

The principal chemical differences between the average Sullivan tourmalinite (Table 1, alteration types 3.1-3.4) and unaltered Aldridge Formation is the high boron and very low K₂O content in the tourmalinite. This is reflected by the abundance of tourmaline and near absence of muscovite in tourmalinite. The CaO, Na₂O, and Ba contents of tourmalinite are lower than unaltered Aldridge Formation, due to the absence of plagioclase in tourmalinite. Although tourmaline is a Na- and Ca-bearing phase, its presence does not compensate for the loss of feldspar. The Fe₂O₃ (total) and sulphur contents are much higher in tourmalinite than in unaltered rocks, but when recalculated to a sulphide-free basis, tourmalinites show a reduction in Fe₂O₃. The MgO and MnO contents of tourmalinite are higher and SiO₂, Al₂O₃ and TiO₂ contents of tourmalinite are similar to unaltered rocks. The Cu, Pb, and Zn are enriched in tourmalinite reflecting the development of a sulphide network underlying the Sullivan orebody (Leitch and Turner, 1992).

Zoning in the footwall tourmalinite body

Variations in chemistry within the footwall tourmalinite zone are subtle compared to the differences between tourmalinite and unaltered rocks. When compared on a sulphide-free basis, the chemistry of sulphide-rich tourmalinites from the eastern fringe of the tourmalinite zone is similar to sulphide-poor tourmalinites from the same area. The Fe₂O₃ content appears lower and Na₂O higher in sulphide-rich

tourmalinites, however these differences may reflect inaccuracies in the calculation of Fe₂O₃ in sulphide-rich samples and uncorrected analytical interference between Na₂O and Zn in sulphide-rich samples. The MnO is enriched in sulphide-rich tourmalinite relative to sulphide-poor tourmalinite.

Within the upper tourmalinite zone, tourmalinites from the central part contain slightly more B₂O₃, Al₂O₃, Fe₂O₃, MgO, and MnO and less K₂O than upper tourmalinites from the eastern fringe of the tourmalinite zone. These differences reflect the presence of minor muscovite and less tourmaline in tourmalinite from the eastern fringe of the zone. The Pb, Zn, Ag, Sn, Sb and As are enriched in tourmalinites from the eastern fringe; Cu and Bi are enriched in samples from the centre of the zone. The Fe₂O₃ is enriched in the deep tourmalinite zone relative to the upper zone, and MgO and B₂O₃ are slightly enriched in tourmalinites from the upper tourmalinite zone.

Chemistry of partially tourmaline-enriched rock

Rocks containing abundant quartz, tourmaline, and microcrystalline muscovite occur along the margin of the footwall tourmalinite zone, concentrated at contacts between tourmalinite and muscovite-altered rocks. These partially tourmalinite-enriched rocks have higher B₂O₃, Al₂O₃, K₂O, MgO, MnO, and TiO₂ contents and lower Fe₂O₃, CaO, Na₂O, and Ba contents than unaltered Aldridge Formation. Relative to tourmalinite, partially tourmaline-enriched rock contains more Al₂O₃, K₂O, and TiO₂ and less Fe₂O₃, MgO, and B₂O₃. This suggests that partially tourmaline-enriched rock is not simply an intermediate between tourmalinite and unaltered sedimentary rock. It may be partially muscovite-altered tourmalinite transitional to muscovite-altered rocks that fringe the tourmalinite zone.

HANGING WALL TOURMALINITE

Tourmalinite also occurs above the Sullivan orebody though it is much less voluminous than footwall tourmalinite. Tourmalinite is intermittent over a 50 m stratigraphic interval from the top of the main band to the HU sulphide horizon throughout an area 900 m in diameter overlying the western part of the orebody (Fig. 2). Tourmalinite is most abundant in an arcuate zone surrounding the core of the hanging wall albite alteration zone, in the vicinity of northerly-trending Sullivan-type faults and the Main Watercourse Fault (Fig. 2). Tourmalinite is overprinted by albite-chlorite-pyrite alteration and was more extensive prior to formation of the albite-chlorite body. Hanging wall tourmalinite is similar mineralogically and texturally to footwall tourmalinite though it is locally recrystallized and less cherty in appearance adjacent to albite-chlorite-pyrite-altered rocks and Moyie gabbro sills. Relative to footwall tourmalinite, hanging wall tourmalinite appears to be depleted in SiO₂ and enriched in Al₂O₃, Fe₂O₃, MnO, K₂O, and TiO₂ (Table 1).

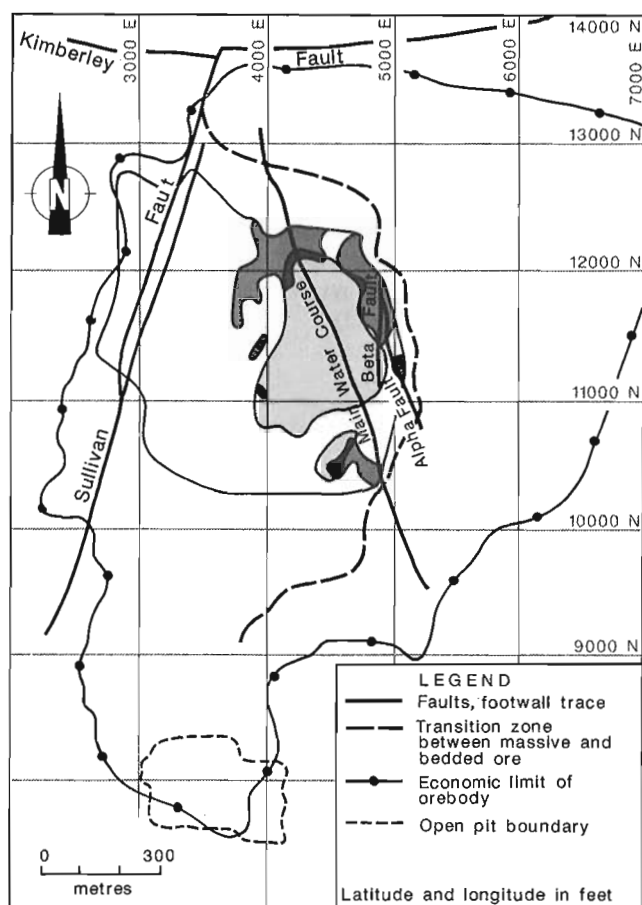
MUSCOVITE-ALTERED FOOTWALL SEDIMENTARY ROCKS

Muscovite alteration was first recognized in the hanging wall of the Sullivan orebody by Bishop (1976) and in the footwall by Shaw and Hodgson (1980a,b). Muscovite-altered rocks are common immediately below the Sullivan deposit in a crescent-shaped area along the eastern margin of the tourmalinite zone (Shaw and Hodgson, 1980b; Leitch and Turner, 1992). In this area (Fig. 1), muscovite alteration occurs in large zones of pervasively altered rock extending an unknown distance beyond the tourmalinite zone (Table 1, alteration types 2.0 and 2.1), and in distinct alteration zones several metres wide that cut tourmalinite (Table 1, alteration type 2.2). These crosscutting alteration zones are commonly associated with networks of pyrrhotite-sphalerite-galena veinlets. Muscovite-altered rocks typically consist of a detrital framework of quartz silt and very fine quartz sand set

in a matrix of microcrystalline muscovite and quartz. Feldspar and biotite are rare. Primary textures are only partly preserved, and where alteration is intense, bedding textures may be completely obliterated. Due to the subtle nature of muscovite alteration, muscovite-altered rocks can be readily mistaken in hand specimen for unaltered sedimentary rocks.

The principal chemical differences between muscovite-altered rocks and unaltered Aldridge Formation are the higher K_2O , Al_2O_3 , and MnO , and lower Na_2O , CaO and Fe_2O_3 contents of muscovite-altered rocks (Table 1, alteration types 2.0-2.2). This is due to the increased abundance of muscovite, and sharply reduced abundance of biotite and plagioclase relative to unaltered Aldridge Formation. The Cu , Pb , Zn , S , and B_2O_3 contents are enriched in muscovite-altered rocks.

Sulphide-rich muscovite-altered rocks contain more MnO and less Fe_2O_3 than do those containing less sulphide minerals. Muscovite-altered rocks from crosscutting zones in tourmalinite are depleted in SiO_2 and Na_2O and enriched in Fe_2O_3 , Al_2O_3 , MgO , and B_2O_3 relative to pervasively muscovite-altered rock.





- tourmaline present in hangingwall
-  hangingwall tourmalinite
-  hanging wall albitite

Figure 2. Plan view of the Sullivan orebody illustrating the distribution of tourmalinite in the hanging wall. The extent of the orebody and location of the transition zone are shown for reference. Also shown is the core of albitite alteration and important faults.

CHLORITE-BIOTITE-GARNET-ALTERED SEDIMENTARY ROCKS

Chlorite-biotite-garnet alteration has been well documented along the eastern margin of the footwall tourmalinite (Fig. 1; Shaw and Hodgson, 1980b, 1986), and is also found peripheral to tourmalinite in the footwall zone below muscovite alteration, and adjacent to Moyie gabbro intrusions in the most western part of the orebody. This alteration overprints tourmalinite but its relationship to muscovite-altered rocks is ambiguous. These altered rocks consist of a framework of detrital quartz grains, a matrix of chlorite, biotite, muscovite, and microcrystalline quartz, and abundant garnet and biotite porphyroblasts. Locally epidote is present. In places, fracture-controlled chlorite alteration appears to be superposed on earlier biotite-garnet alteration.

Chlorite-biotite-garnet-altered sedimentary rocks are characterized by higher Fe_2O_3 , MnO , and MgO contents and lower CaO , Na_2O , and K_2O contents than unaltered Aldridge Formation (Table 1; alteration type 12.1). This is due to the increased abundance of chlorite and garnet, and the decreased abundance of plagioclase and muscovite relative to unaltered Aldridge Formation. Chlorite-garnet-biotite-altered tourmalinite contains higher Fe_2O_3 and MnO , slightly higher MgO , CaO , Na_2O , K_2O , TiO_2 , and Al_2O_3 , and lower TiO_2 and B_2O_3 relative to unaltered tourmalinite.

CARBONATE-MUSCOVITE-ALTERED FOOTWALL ROCKS

Bleached, carbonate-muscovite-altered rocks locally cut muscovite-altered and chlorite-biotite-garnet-altered footwall rocks near the eastern margin of the tourmalinite zone. These bleached rocks are tan in colour and can be

bedded, brecciated, or foliated and are associated with steeply dipping iron-carbonate veins. These rocks are similar to muscovite-altered rocks except for the presence of porphyroblasts of carbonate and iron-chlorite. Carbonate, chlorite, and muscovite porphyroblasts locally replace garnet. Alteration of garnet and Fe-rich chlorite which is not stable in biotite-facies metamorphism suggests that carbonate-muscovite alteration postdates Middle Proterozoic regional metamorphism.

The principal differences between bleached carbonate-muscovite-altered rocks and unaltered Aldridge Formation are the higher Fe_2O_3 , Al_2O_3 , K_2O , and MnO and lower CaO and Na_2O contents of bleached rocks (Table 1). Relative to muscovite altered rocks, bleached carbonate-muscovite-altered rocks are enriched in Fe_2O_3 and CO_2 and depleted in SiO_2 and Na_2O . These chemical differences are due to replacement of the rock by carbonate (likely Fe-Mn-rich), the presence of Fe-rich-chlorite metacrysts, and the absence of plagioclase.

DISCUSSION

Chemistry of tourmalinites

Tourmalinite alteration of Aldridge Formation sedimentary rocks represents significant addition of B_2O_3 , lesser addition of MgO and MnO , and depletion of K_2O , CaO , and Na_2O . Hamilton (1984) estimated that the footwall tourmalinite zone has a mass of perhaps five billion tonnes, and Hamilton and Shaw (1986) estimate that the boron added is more than twice the total tonnage of lead and zinc in the Sullivan deposit. Enrichment in MgO and MnO reflects the abundance of tourmaline with a composition intermediate between schorl and dravite. The similar Al_2O_3 and TiO_2 contents of tourmalinite and unaltered Aldridge sedimentary rocks, as well as preservation of primary features within the tourmalinite such as delicate laminations and the detrital fabric suggest a constant volume alteration process. The little difference in silica content between tourmalinite and unaltered Aldridge Formation indicates that silicification did not accompany tourmalinite alteration, nor did tourmaline significantly replace detrital quartz. This is supported by the limited development of quartz overgrowths on detrital quartz grains (Leitch and Turner, 1991). The destruction of feldspar during tourmalinite formation suggests formation from lower pH fluids.

Based on its geochemistry, the partially tourmaline-enriched rock developed along contacts between tourmalinite and muscovite-altered rock does not appear to be simply incompletely tourmalinized Aldridge Formation. The elevated K_2O and Al_2O_3 and decreased Fe_2O_3 , MgO , and B_2O_3 contents relative to tourmalinite are more readily explained by a fringing zone of muscovite-rich rock containing less tourmalinite than the core tourmalinite body. Partially tourmaline-enriched rock may be tourmalinite partially altered to a muscovite-bearing assemblage. Muscovite-alteration commonly destroys primary rock textures, and the increase of Al_2O_3 and TiO_2 may be due to volume decrease.

Origin of tourmalinite and source of boron

Shaw and Hodgson (1980a,b) interpret footwall tourmalinite as shallow conformable syngenetic bodies overlying deeper, discordant epigenetic bodies that together comprise the tourmalinite pipe. These authors suggest that ore formation occurred during a later exhalative event, a conclusion supported by oxygen isotopic data that indicate very low temperature of formation for the tourmalinite (Nesbitt et al., 1984). However, the occurrence of tourmalinite up to the base of the orebody, and locally up to the base of the highest stratiform sulphide bed leaves open the possibility that tourmalinite formed synchronously with ore deposition, or that a number of tourmalinite- to ore-forming cycles occurred. The extensive pyrrhotite stockwork within the upper tourmalinite zone is interpreted as forming synchronously with the orebody by Leitch and Turner (1992).

Previous workers have suggested that boron in tourmalinite was derived from an undetected subjacent magma or scavenged from the sedimentary pile by connate fluids. The isotopic composition of boron from two samples from the Sullivan deposit (Palmer and Slack, 1989) is consistent with boron sourced from Aldridge sedimentary rocks, but a nonmarine evaporite borate source cannot be excluded. Slack et al. (in press) suggest that boron in tourmalinite locally associated with the stratiform Broken Hill Pb-Zn deposit was derived from evaporitic borates in a nonmarine sedimentary sequence underlying the deposit. Fluid inclusion data from the Sullivan deposit indicate high salinity fluids (15-25 wt.% $\text{NaCl}+\text{CaCl}_2$) during mineralization (Leitch, 1992).

Other alteration types

Shaw and Hodgson (1980a,b; 1986) suggested that muscovite alteration along the eastern margin of the footwall tourmalinite pipe occurred after tourmalinization during early stages of ore deposition. Leitch and Turner (1992) proposed that footwall muscovite alteration and an associated pyrrhotite-sphalerite-galena network may represent the site of late-stage fluid flow, after sealing of the central tourmalinite-pyrrhotite vent zone that formed the main stage of ore formation. Alternatively, muscovite alteration near the margin of the tourmalinite zone may be related to fluids enriched in K_2O released during tourmalinization.

The geological setting of chlorite-garnet-biotite alteration is poorly understood. It is possible that this alteration represents a stable mineral assemblage that formed after tourmalinite during hydrothermal activity associated with mineralization (Shaw and Hodgson, 1980b, 1986). Alternatively, an earlier biotite-garnet assemblage found at the periphery of the tourmalinite zone and adjacent to Moyie gabbros may have been partly altered to chlorite during later albite-chlorite-pyrite alteration (Turner and Leitch, 1992).

The timing of bleached, carbonate-muscovite alteration is uncertain but clearly postdates muscovite alteration and chlorite-biotite-garnet alteration. Textural evidence suggests this that this alteration overprints metamorphic garnet, thus it

is likely related to a younger event such as CO₂-iron metasomatism related to emplacement of Cretaceous lamprophyre dykes that cut the the Sullivan deposit.

ACKNOWLEDGMENTS

We thank Cominco Ltd. and the former and present staff of the Sullivan Mine Geology Department for their kind assistance during our field studies, and Cominco's Exploration Laboratory for performing the analyses. Critical reviews of this manuscript by Georges Beaudoin, John Hamilton, and John Slack are greatly appreciated.

REFERENCES

- Bishop, D.T.**
1976: Alteration and ore, Sullivan mine; unpublished report, Cominco Ltd.
- Edmunds, F.R.**
1977: Multivariate analysis of petrographic and chemical data from the Aldridge Formation, southern Purcell Mountains Range, British Columbia, Canada; PhD thesis, Pennsylvania State University, 368 p.
- Fedikow, M.A.F.**
1978: Geochemical and paleomagnetic studies at the Sullivan mine, Kimberley, British Columbia; M.Sc. thesis, University of Windsor, 133 p.
- Hamilton, J.M.**
1984: The Sullivan deposit, Kimberley, British Columbia – a magmatic component to genesis?; Montana Bureau of Mines and Geology, Special Publication 90, Abstracts and Summaries, Belt Symposium II, p. 58-60.
- Hamilton, J.M. and Shaw, D.R.**
1986: Evolution of source fluids and resulting deposits during genesis of the Sullivan Orebody, Kimberley, B.C., Canada (abstract); Geological Society of America, Abstracts with Programs, v. 18, no. 6, p. 626.
- Hamilton, J.M., Bishop, D.T., Morris, H.C., and Owens, O.E.**
1982: Geology of the Sullivan orebody, Kimberley, B.C., Canada; in Precambrian Sulphide Deposits; (ed.) R.W. Hutchinson, C.D. Spence, and J.M. Franklin; Geological Association of Canada, Special Paper 25, p. 597-665.
- Harrison, J.E. and Grimes, D.J.**
1970: Mineralogy and geochemistry of some Belt rocks, Montana and Idaho; U.S. Geological Survey Bulletin 1312-0, 49 p.
- Leitch, C.H.B.**
1992: A progress report of fluid inclusion studies of veins from the vent zone, Sullivan stratiform sediment-hosted Zn-Pb deposit, British Columbia; in Current Research, Part E; Geological Survey of Canada, Paper 92-1E, p. 71-82.
- Leitch, C.H.B. and Turner, R.J.W.**
1991: The vent complex of the Sullivan stratiform sediment-hosted Zn-Pb deposit, B.C.: Preliminary petrographic and fluid inclusion studies; in Current Research, Part E; Geological Survey of Canada, Paper 91-1E, p. 33-43.
1992: Preliminary field and petrographic studies of the sulphide-bearing network underlying the western orebody, Sullivan stratiform sediment-hosted Zn-Pb deposit, British Columbia; in Current Research, Part E; Geological Survey of Canada, Paper 92-1E, p. 71-82.
- Leitch, C.H.B., Turner, R.J.W., and Høy, T.**
1991: The district-scale Sullivan-North Star alteration zone, Sullivan mine area, B.C.: A preliminary petrographic study; in Current Research, Part E; Geological Survey of Canada, Paper 91-1E, p. 45-57.
- Nesbitt, B.E., Longstaffe, F.J., Shaw, D.R., and Muehlenbachs, K.**
1984: Oxygen isotope geochemistry of the Sullivan massive sulfide deposit, Kimberley, British Columbia; Economic Geology, v. 79, p. 933-946.
- Palmer, M.R. and Slack, J.F.**
1989: Boron isotopic composition of tourmaline from massive sulphide deposits and tourmalinites; Contributions to Mineralogy and Petrology, v. 103, p. 434-451.
- Sanford, R.F., Peerson, C.T., and Crovelli, R.A.**
in press: An objective replacement method for censored geochemical data; Mathematical Geology.
- Shaw, D.R. and Hodgson, C.J.**
1980a: Wall-rock alteration at the Sullivan mine, Kimberley, British Columbia (abstract); Canadian Institute of Mining and Metallurgy, Bulletin 73, no. 821, p. 75.
1980b: Wall-rock alteration at the Sullivan mine, Kimberley, British Columbia; paper presented at Fifth Annual District Six Meeting of the Canadian Institute of Mining and Metallurgy, Kimberley, B.C., October 23-25, 1980, 14 p.
1986: Wall-rock alteration at the Sullivan mine, Kimberley, British Columbia; in The Genesis of Stratiform Sediment-Hosted Lead and Zinc Deposits: Conference Proceedings, (ed.) R.J.W. Turner and M.T. Einaudi; Stanford University Publications, School of Earth Sciences, v. 20, p. 13-21.
- Shaw, D.R., Hodgson, C.J., Leitch, C.H.B., and Turner, R.J.W.**
1993: Geochemistry of albite-chlorite-pyrite and chlorite-pyrrhotite alteration, Sullivan Zn-Pb deposit, British Columbia; in Current Research, Part A; Geological Survey of Canada, Paper 93-1A.
- Slack, J.F., Palmer, M.R., Stevens, B.P.J., and Barnes, R.G.**
in press: Origin and significance of tourmaline-rich rocks in the Broken Hill district, Australia; Economic Geology.
- Turner, R.J.W. and Leitch, C.H.B.**
1992: Relationship of albitic and chloritic alteration to gabbro dykes and sills at the Sullivan deposit and nearby area, southeastern British Columbia; in Current Research, Part E; Geological Survey of Canada, Paper 92-1E, p. 95-106.

Geological Survey of Canada Project 900020

Geochemistry of albite-chlorite-pyrite and chlorite-pyrrhotite alteration, Sullivan Zn-Pb deposit, British Columbia¹

David R. Shaw², C. Jay Hodgson³, Craig H.B. Leitch, and Robert J.W. Turner

Mineral Resources Division, Vancouver

Shaw, D.R., Hodgson, C.J., Leitch, C.H.B., and Turner, R.J.W., 1993: Geochemistry of albite-chlorite-pyrite and chlorite-pyrrhotite alteration, Sullivan Zn-Pb deposit, British Columbia; in Current Research, Part A; Geological Survey of Canada, Paper 93-1A, p. 109-118.

Abstract: Chlorite-bearing assemblages represent an important suite of altered rocks at the Sullivan deposit. Chlorite-pyrrhotite-altered rocks occur along the base of the massive pyrrhotite body; they are intensely depleted in SiO₂, Na₂O, B₂O₃, and enriched in Al₂O₃, Fe₂O₃, MnO, and MgO relative to precursor tourmalinite due to abundant chlorite and destruction of quartz and tourmaline. Rocks rich in albite, chlorite, and pyrite overlie, occur within, and underlie the orebody. Albitites are enriched in Na₂O and Al₂O₃, and depleted in MgO, CaO, and K₂O, reflecting increased content of sodic plagioclase and absence of muscovite. Associated chlorite-pyrite-altered rocks are enriched in Al₂O₃, Fe₂O₃, MnO, MgO, and TiO₂, depleted in SiO₂, CaO, Na₂O, and K₂O, contain abundant chlorite and lack quartz, plagioclase, muscovite, and tourmaline.

Albitic alteration may reflect high Na/(Mg+Ca) brines that mixed with Mg-rich seawater-derived fluids to form Mg-silicate-altered rocks.

Résumé : Les assemblages contenant de la chlorite correspondent à une importante série de roches altérées à l'endroit du gisement de Sullivan. Il existe des roches altérées en chlorite et pyrrhotine le long de la base du corps massif constitué de pyrrhotine; elles sont très fortement appauvries en SiO₂, Na₂O, B₂O₃, et enrichies en Al₂O₃, Fe₂O₃, MnO et MgO par rapport à la tourmalinite précurseur, en raison de l'abondance de la chlorite et de la destruction du quartz et de la tourmaline. Les roches riches en albite, chlorite et pyrite peuvent être sus-jacentes, intérieures et sous-jacentes au corps minéralisé. Les albitites sont enrichies en Na₂O et Al₂O₃, et appauvries en MgO, CaO et K₂O, et traduisent l'accroissement du contenu en plagioclase sodique et l'absence de la muscovite. Les roches associées, qui ont été chloritisées et pyritisées, sont enrichies en Al₂O₃, Fe₂O₃, MnO, MgO et TiO₂, appauvries en SiO₂, CaO, Na₂O et K₂O, et contiennent en abondance de la chlorite mais ne contiennent pas de quartz, de plagioclase, de muscovite et de tourmaline.

L'albitisation pourrait refléter l'influence de saumures à quotient élevé Na/(Mg+Ca), qui se sont mélangées à des fluides dérivés d'eaux marines riches en Mg, et ont ainsi formé des roches altérées en silicates de Mg.

¹ Contribution No. 13, Sullivan-Aldridge Project

² 8431 58th Avenue N.W., Calgary, Alberta T3B 4B4

³ Department of Geological Sciences, Queen's University, Kingston, Ontario K7L 3N6

INTRODUCTION

The Sullivan orebody is a classic example of a stratiform sediment-hosted zinc-lead deposit (Hamilton et al., 1982). Sullivan is unique among stratiform deposits in the degree and extent of alteration associated with the orebody (Shaw and Hodgson, 1980a,b, 1986; Hamilton et al., 1982; Leitch and Turner, 1991, 1992; Turner and Leitch, 1992). For a detailed description of the geology of the deposit, the reader is referred to Hamilton et al. (1982). This paper and its companion (Shaw et al., 1993) present the geochemistry of altered rocks associated with the Sullivan deposit and focus on the relative gains and losses of constituents in altered rocks relative to unaltered sedimentary rocks of the host Aldridge Formation. This paper focuses on the geological setting and chemistry of chlorite-bearing alteration assemblages. It is based on underground mapping and sampling by Shaw from 1976 to 1979 at the Sullivan mine, as part of a Ph.D. thesis under the supervision of Hodgson at Queen's University, and ongoing work by Leitch and Turner. Geochemical data reported in this paper are based on samples collected by Shaw and analyzed by Cominco Ltd. Analytical procedures are discussed in Shaw et al. (1993).

This paper presents the results of 98 analyses of 86 samples of chlorite-pyrrhotite-altered and albite-chlorite-pyrite-altered rocks from the Sullivan deposit. Average chemical compositions are presented in Table 1 and individual analyses in Table 2. In Table 2, samples analyzed once are identified by the suffix "0" in the sample number; samples analyzed twice by the suffix "1" or "2"; control samples analyzed repeatedly by a suffix "1-14". Average compositions in Table 1 include only those analyses with a suffix of "0" or "1". "Total" is the total of the XRF analysis as reported by Cominco for the major elements and LOI. Sulphide minerals are an important component of altered rocks at the Sullivan deposit, and a significant proportion of the iron in altered rocks is present in iron-bearing sulphide minerals. In order to compare samples containing different amounts of iron-bearing sulphide minerals, the amount of iron contained in pyrrhotite, pyrite, sphalerite, chalcopyrite, and arsenopyrite was subtracted from total iron, and analyses normalized to 100% non-sulphide constituents were computed for the altered rocks (bold numbers, Table 1). Unless stated otherwise, all rock types are compared on the basis of the recalculated sulphide-free analyses, and Fe_2O_3 represents iron in the recalculated analysis expressed as ferric iron.

Many samples contain concentrations of minor elements below the detection limit for those elements. In order to permit the calculation of averages that will serve as a guide when comparing the minor element concentrations in altered rocks, values of one-half the detection limit for that element are reported instead of "not detected" in Table 2, and the averages calculated in Table 1 include these values. These values in parts per million are: 1 or 2 for Pb, 0.1 or 0.2 for Ag, 2 for Sb and Bi, 1 for As and W, and 10 for Sn and Ba.

Several concerns regarding the interpretation of chemical changes associated with alteration at the Sullivan deposit are addressed in Shaw et al. (1993). In view of these concerns, this paper will focus primarily on relative, rather than absolute, chemical changes.

Biotite-facies middle greenschist metamorphism has affected both regional Aldridge rocks and altered rocks at the Sullivan deposit. Altered rock types are classified and described in terms of their present metamorphic mineralogy, and this mineralogy may be different from that which existed prior to metamorphism. The reader is cautioned that use of terms such as "chlorite-altered" does not necessarily imply that alteration produced chlorite. Chlorite may be the metamorphic equivalent of different precursor minerals formed during alteration.

UNALTERED SEDIMENTARY ROCKS

The mineralogy and chemistry of regionally distributed unaltered host Aldridge Formation has been studied by Edmunds (1977) as discussed in Shaw et al. (1993). The average composition of Aldridge rocks is used as the reference composition for comparison with the chemistry of altered rocks at the Sullivan deposit (Table 1, alteration type 0.0). The average mineralogical composition of these Aldridge rocks is 48% quartz, 20% plagioclase, 15% white mica, 11% biotite, 2.4% muscovite, 0.9% carbonate, 0.8% K-feldspar, 0.6% graphite, 0.8% iron ores, and 0.3% sphene (Edmunds, 1977).

CHLORITE-PYRRHOTITE-ALTERED FOOTWALL TOURMALINITE

Chlorite-pyrrhotite-altered rock occurs as a semiconformable zone at the contact between the massive pyrrhotite zone of the Sullivan orebody and the footwall tourmalinite zone (Fig. 1). The chlorite-pyrrhotite zone is up to 20 m thick, is located at the centre of the footwall tourmalinite and underlies the thickest part of the western orebody. The chlorite-pyrrhotite zone is in contact with, and cuts, tourmalinite. Chlorite-pyrrhotite rocks are intensely altered and primary textures are commonly obliterated. This fabric-destructive alteration consists of massive to foliated chlorite and pyrrhotite with minor biotite, muscovite and sphene. Chlorite-pyrrhotite is north of, and contiguous with, footwall albite-chlorite-pyrite-altered rock, and together these two zones of altered rock form an elongate northerly-trending body below the sulphide deposit. Chlorite-pyrrhotite altered rock also occurs in the hanging wall zone between the massive pyrrhotite zone in the orebody and overlying albite-chlorite-pyrite (Fig. 2).

Relative to tourmalinite which chlorite-pyrrhotite replaces, there is significant depletion of SiO_2 and B_2O_3 , lesser depletion of Na_2O , significant addition of Al_2O_3 , Fe_2O_3 , MnO, and MgO, and lesser addition of K_2O and TiO_2 (see Table 1, alteration type 3.3 in Shaw et al., 1993). This is due to the abundance of chlorite and complete destruction of quartz and tourmaline in chlorite-pyrrhotite-altered rocks. The $\text{Fe}_2\text{O}_3(\text{total})$, S, Pb, Zn, Ag, Sn, and As contents of the chlorite-pyrrhotite-altered rocks are higher than in tourmalinite.

(Fig. 1). Within the ore zone, massive pyrrhotite and lead-zinc ore are altered to rocks containing abundant pyrite, chlorite, and calcite, and interbedded sedimentary rocks are altered to a chlorite-pyrite rock (Shaw and Hodgson, 1986). Alteration of the orebody is most intense in the area of the pyrite-calcite core (Fig. 3), where pyrrhotite is completely altered to pyrite; lead, zinc, and silver concentrations are below ore grade. The pyrite-calcite core is surrounded by a zone of incomplete alteration, in which lead, zinc, and silver concentrations are above ore grade and pyrrhotite is partly altered to pyrite.

In the part of the footwall zone that underlies the chlorite-pyrite-calcite alteration zone of the orebody, tourmalinite within about 20 m of the footwall contact of the orebody is discontinuously altered to albite-chlorite-pyrite in an elongate northerly-trending zone 700 m long and 350 m wide (Fig. 1). The albite-chlorite-pyrite zone in the footwall is continuous with, and extends to the south of, the chlorite-pyrrhotite zone.

Albite-chlorite-pyrite-altered rocks display strong compositional zoning, from the scale of hundreds of metres to an individual veinlet. Compositional zoning on a large scale is best developed in the hanging wall alteration zone, where a central core of albitite 430 m by 300 m in extent grades outwards to albite-chlorite-pyrite rocks. Zoning on a small scale is displayed by albitite veinlets a few millimetres thick that possess symmetrically developed chlorite-pyrite alteration envelopes. Consequently, rocks in this group display extreme variations in mineralogy and chemistry over short distances. Albitite is composed of massive granular albite with minor amounts of magnesian chlorite, sphene, pyrite, calcite, and quartz. The albite has an average composition of $An_{0.65}Ab_{98.96}Or_{0.39}$ with a range of An_0 to $An_{2.5}$ (Hamilton et al., 1982). Tourmaline is present where the albitite replaces earlier-formed tourmalinite. Chlorite-pyrite rocks contain chlorite, sphene, pyrite, muscovite, tourmaline, minor albite, and allanite. Albite-chlorite-pyrite rocks are intermediate in composition between albitite and chlorite-pyrite. Detrital quartz grains of the sedimentary protoliths are obliterated in albite-chlorite-pyrite-altered

Table 2. (cont.)

Sample	SiO ₂	Al ₂ O ₃	Fe ₂ O ₃	MgO	CaO	Na ₂ O	K ₂ O	TiO ₂	P ₂ O ₅	LOI	CO ₂	TOTAL	Cu	Pb	Zn	Ag	Sb	Bi	Fe	As	W	S	Ba	Mn	Sn	B	SG	ROCK TYPE
1131-2	28.41	17.99	28.93	14.69	.62	.27	.01	.64	.11	8.37	0.24	100.04	4	292	293	0.7	2	2	12.7	4	2	0.27	25	1888	164	50	2.94	11.1
1131-1	28.79	18.19	29.22	14.25	.64	.19	.01	.66	.11	8.50	0.01	100.56	6	279	319	0.6	2	2	16.0	5	4	0.20	35	1881	168	75	2.94	11.1
1132-0	26.25	19.77	26.29	15.38	.70	.19	.01	.97	.11	9.45	0.06	99.12	8	153	410	0.5	2	2	15.8	34	1	1.02	40	3058	230	NA	2.94	11.1
1141-2	21.38	13.22	39.27	10.82	.50	.14	.06	.64	.07	15.06	0.14	101.16	137	1710	435	8.7	2	22	25.0	452	1	13.68	27	1337	101	NA	3.13	11.1
1141-1	22.12	13.55	38.02	11.39	.51	.17	.01	.67	.07	14.38	0.21	100.89	125	1540	394	7.9	2	18	25.0	435	1	12.55	26	1372	105	NA	3.13	11.1
1154-0	28.66	21.81	23.52	9.21	1.25	.33	0.2	.85	.13	8.37	0.17	94.15	54	1920	284	7.2	2	16	13.1	383	1	5.07	49	1301	363	NA	3.33	11.1
1174-0	32.43	16.72	27.15	11.58	.39	1.12	.01	.74	.10	9.12	0.01	99.36	9	213	365	0.6	2	2	17.0	79	2	3.92	42	2498	124	NA	3.57	11.1
1155-0	66.63	11.17	10.64	4.92	.31	.35	.03	.51	.07	3.11	0.21	97.74	18	90	172	0.2	2	2	5.7	304	8	0.94	28	925	100	5100	2.78	11.2
1156-0	62.35	11.57	13.67	3.59	.42	.35	.01	.53	.06	3.60	0.10	96.14	78	220	205	0.4	2	2	8.1	243	4	3.37	36	837	108	8900	2.94	11.2
1157-0	55.33	10.50	21.17	3.78	.32	.83	.01	.41	.06	5.22	0.20	97.63	229	203	198	0.2	2	2	13.5	340	2	7.11	10	761	96	4950	2.94	11.2
1026-1	56.21	13.65	19.91	2.61	.54	1.00	.01	.56	NA	2.58	0.02	97.07	276	630	26	5.6	2	33	12.0	1200	1	8.03	50	256	40	13600	2.9	11.3
1026-2	56.83	13.75	18.92	2.79	.52	1.07	.01	.54	NA	2.80	0.01	97.22	210	600	22	5.0	2	25	10.5	1000	1	7.34	44	230	40	NA	NA	11.3
1029-0	68.36	15.13	6.52	3.13	.52	.99	.01	.53	NA	.81	0.03	95.99	4	74	35	0.6	2	2	1.8	60	4	0.52	38	596	80	14000	2.7	11.3
1030-0	73.77	13.21	4.11	2.51	.50	.80	.01	.41	NA	.41	0.01	95.72	3	57	16	0.6	2	28	0.9	90	1	0.33	41	328	40	17000	2.7	11.3
1031-2	77.94	10.45	5.07	2.05	.41	.68	.01	.40	NA	.99	0.05	98.00	3	87	15	0.5	2	2	1.9	140	4	1.27	10	334	40	NA	NA	11.3
1031-1	77.95	10.35	5.12	1.98	.41	.56	.01	.40	NA	.94	0.01	97.71	4	90	14	0.9	2	10	1.7	135	5	1.26	59	333	40	10500	2.6	11.3
1034-0	68.89	14.83	6.57	3.01	.55	.72	.01	.60	NA	.49	0.08	95.66	8	25	18	0.3	2	2	1.5	6	4	0.24	78	618	80	16500	2.8	11.3
1158-0	28.17	21.14	27.37	6.41	1.67	1.11	.01	1.03	.14	8.74	0.15	95.79	235	1280	141	3.6	2	6	15.2	1590	2	11.87	63	877	259	24700	3.70	11.3
Chlorite-pyrrhotite altered footwall tourmalinite: 13.0.																												
1229-0	24.99	17.49	28.72	16.71	.90	.12	.22	.75	.14	9.81	0.27	99.85	135	1360	950	4.3	2	11	16.6	26	3	5.26	35	5936	968	50	3.45	13.0
1230-0	37.49	13.12	25.91	12.04	.57	.17	.18	.56	.09	8.20	0.26	98.33	230	908	480	4.0	2	24	14.7	118	2	6.09	25	3553	346	300	2.70	13.0
1231-1	22.40	15.16	37.82	14.26	.70	.21	.31	.68	.13	4.78	0.16	96.45	398	537	800	2.7	2	25	23.0	152	1	9.19	35	3765	653	110	3.23	13.0
1231-2	21.92	15.12	38.17	13.39	.69	.19	.32	.67	.13	10.37	0.41	100.97	360	529	726	2.4	2	20	19.2	126	4	9.56	37	3723	649	NA	3.23	13.0
1232-0	23.62	17.23	32.87	13.19	.65	.04	.01	.81	.13	9.64	0.12	98.19	141	154	8450	0.9	2	2	18.3	3920	3	5.51	31	3663	116	600	2.78	13.0
1233-0	27.25	12.06	37.14	9.04	.43	.19	.01	.45	.12	9.13	0.05	95.82	169	17000	20500	101.0	2	287	21.0	700	2	10.69	10	2700	74	60	3.03	13.0

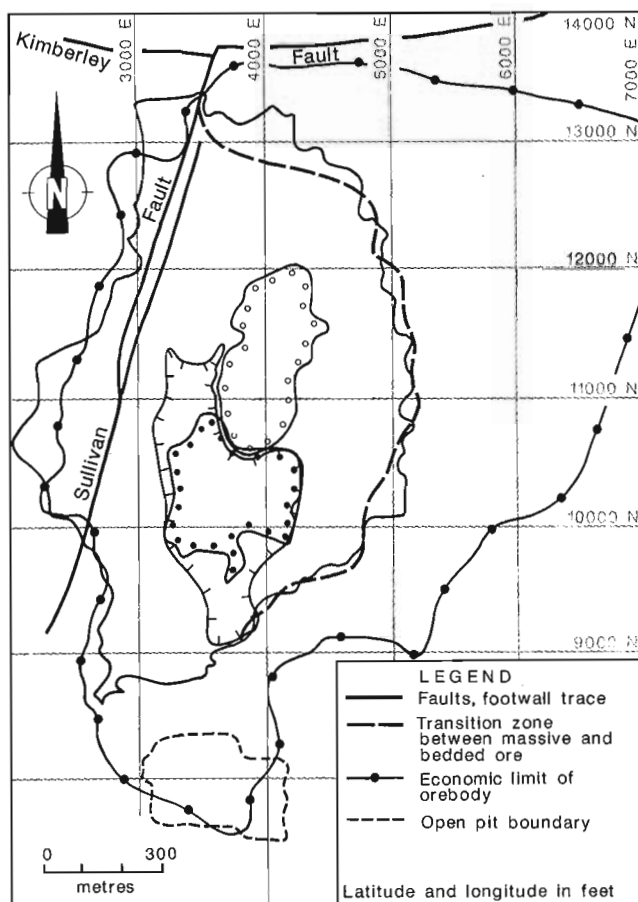
Note: Major elements (SiO₂ to CO₂, Fe and S) in percent; Cu, Pb, Zn, Ag, Sb, Bi, As, W, Ba, Mn, Sn, B in ppm; NA: not analyzed; SG: specific gravity.

rocks, albitites, and chlorite-pyrite rocks. Larger scale structures and textures such as conglomerate pebbles and bedding are locally preserved.

Albitites from the hanging wall and footwall are very similar in chemical composition, and approximate pure albite. Relative to unaltered Aldridge Formation, albitites contain substantially more Na_2O and Al_2O_3 , slightly more TiO_2 and B_2O_3 , and less Fe_2O_3 , MgO , CaO , K_2O , and Ba . These chemical differences are due to increased abundance of sodic plagioclase, the absence of muscovite, and the minor occurrence of tourmaline. Relative to precursor tourmalinite, albitites contain significantly more Na_2O , Al_2O_3 , and TiO_2 ,

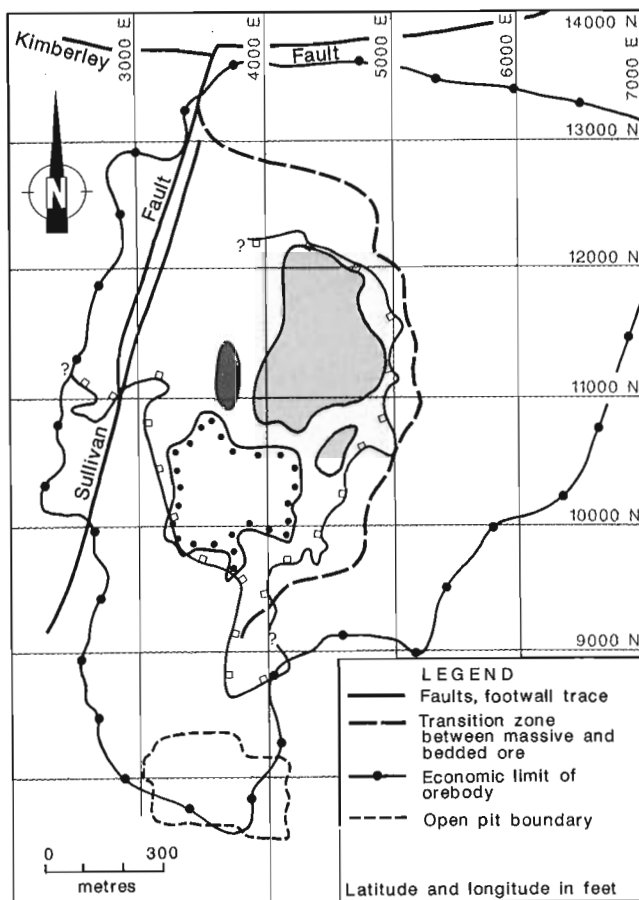
and less Fe_2O_3 , MgO , MnO , and B_2O_3 . Relative to unaltered Aldridge Formation, hanging wall albitites are enriched, and footwall albitites are depleted, in Cu , Pb , and Zn .

Chlorite-pyrite altered rocks from the hanging wall, ore zone and footwall are very similar in chemical composition, and when recalculated to a sulphide mineral-free analysis the rock composition approaches that of iron ripidolite chlorite. Relative to regional Aldridge Formation, chlorite-pyrite rocks are strongly enriched in Al_2O_3 , Fe_2O_3 , MnO , MgO , and TiO_2 and strongly depleted in SiO_2 , CaO , Na_2O , and K_2O . The Cu , Pb , Zn , and B_2O_3 are enriched and Ba depleted in chlorite-pyrite rocks relative to unaltered Aldridge Formation. Relative to precursor tourmalinite, chlorite-pyrite-altered



- ○ ○ ○ extent of footwall chlorite-pyrrhotite
- ● ● ● extent of pyrite-calcite core within sulphide body
- extent of footwall tourmalinite
- ┆┆┆┆ extent of footwall albite-chlorite-pyrite

Figure 1. Plan view of the Sullivan orebody illustrating the distribution of chlorite-pyrrhotite and albite-chlorite-pyrite alteration in rocks underlying the Sullivan orebody. The extent of the sulphide body, transition zone, pyrite-calcite core within the sulphide body, and the footwall tourmalinite zone are shown for reference. Maps are based on detailed mapping and compilation of Cominco Ltd. data by D.R. Shaw between 1976 and 1980.



- □ □ □ extent of albite-chlorite-pyrite in hanging wall
- ● ● ● chlorite-pyrrhotite in hanging wall
- ○ ○ ○ hanging wall albite
- ● ● ● extent of pyrite-calcite core within sulphide body

Figure 2. Plan view of the Sullivan orebody illustrating the distribution of albitite (after unpublished Cominco Ltd. map by S.B. Hamilton, 1962), albite-chlorite-pyrite and chlorite-pyrrhotite in rocks overlying the Sullivan orebody. The extent of the sulphide body, transition zone, and pyrite-calcite core within the sulphide body are shown for reference. Maps are based on detailed mapping and compilation of Cominco Ltd. data by D.R. Shaw between 1976 and 1980.

rocks show similar chemical changes with the exception of a strong depletion of B_2O_3 and a slight enrichment of K_2O . These chemical changes are due to the abundance of chlorite and the absence of quartz, plagioclase, and tourmaline in chlorite-pyrite-altered rocks. Albite-chlorite-pyrite rocks are intermediate both in composition and mineralogy relative to albitite and chlorite-pyrite end member alteration types.

The zone of intense albitite-chlorite-pyrite alteration in the hanging wall is overlain by an interval of slightly to moderately altered sedimentary rocks (Table 1, alteration types 9.7 to 9.9). Relative to unaltered Aldridge Formation, these slightly to moderately altered hanging wall rocks are enriched in Al_2O_3 , K_2O , and MgO , slightly enriched in Fe_2O_3 , MnO , B_2O_3 , and S , and depleted in CaO , Na_2O , Cu , Pb , and Zn . The increased K_2O , and Al_2O_3 contents and

decreased Na_2O and CaO contents reflect the occurrence of muscovite alteration (Shaw et al., 1993), and the increase in MgO , MnO , and Fe_2O_3 is due to weak chloritization.

Relative to unaltered tourmalinites from the centre of the footwall tourmalinite zone, tourmalinites partially altered to albitite-chlorite-pyrite rocks contain more Fe_2O_3 , MgO , and Na_2O , and less B_2O_3 . Apparently unaltered tourmalinites adjacent to albitite-chlorite-pyrite footwall rocks are enriched in Al_2O_3 , Fe_2O_3 , MgO , Na_2O , and B_2O_3 , and slightly depleted in SiO_2 compared to unaltered tourmalinites.

DISCUSSION

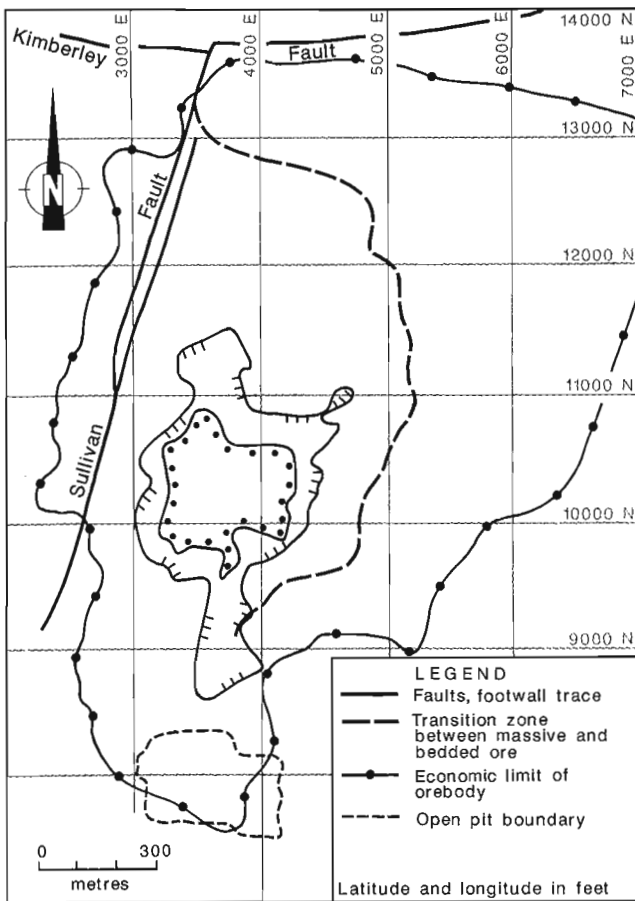
Mobility of Al_2O_3 and TiO_2 , volume changes, and absolute gains and losses during alteration

Major concerns regarding the interpretation of chemical changes associated with alteration at the Sullivan deposit are discussed in Shaw et al. (1993). Most important of these are the effect of volume change during alteration, and evidence for mobility of Al_2O_3 and TiO_2 . In strongly altered rocks (chlorite-pyrrhotite, chlorite-pyrite, albitite) primary sedimentary textures vary from partially preserved to completely destroyed. On a microscopic scale, the original detrital framework of quartz grains is completely obliterated. These observations suggest significant volume changes accompanied alteration. However, calculation of volume changes and absolute gains and losses that occurred during alteration based on an assumption of Al_2O_3 and TiO_2 immobility is problematic. Albitites containing about 18% Al_2O_3 and 0.7% TiO_2 , and chlorite-pyrite and chlorite-pyrrhotite rocks containing 20% Al_2O_3 , 1% TiO_2 and 35% SiO_2 have formed from Aldridge sediments containing 70% SiO_2 , 13% Al_2O_3 , and 0.55% TiO_2 . This requires either massive changes in volume, or mobility of Al_2O_3 and TiO_2 . The occurrence of abundant sphene in chlorite-pyrite rocks in the ore zone suggests mobility of TiO_2 , while the local preservation of delicate laminations in albitite-chlorite-pyrite-altered conglomerate pebbles suggest local volume-for-volume replacement.

Volume change during alteration implies high water-to-rock ratios during chlorite-pyrrhotite and albitite-chlorite-pyrite alteration. High water-to-rock ratios are also indicated by the similarity in chemical and mineralogical composition of albitite-chlorite-pyrite-altered rocks formed from different unaltered and tourmalinite protoliths, and the massive scale of chemical changes that accompanied alteration. This is in contrast to tourmalinite, which appears to have formed by constant-volume alteration processes (Shaw et al., 1993) characterized by lower water-to-rock ratios.

Relative timing of alteration

Chlorite-pyrrhotite and albitite-chlorite-pyrite alteration are superposed on tourmalinite and clearly postdate tourmalinitization (Shaw and Hodgson, 1980a,b, 1986; Hamilton et al., 1982; Turner and Leitch, 1992). Albitite-chlorite-pyrite alteration is superimposed on the orebody and



⋯ extent of chlorite-pyrite alteration in sulphide body
 ⋯ extent of pyrite-calcite core within sulphide body

Figure 3. Plan view of the Sullivan orebody illustrating the extent of pyrite-calcite core and maximum extent of partial chlorite-pyrite-calcite alteration within the sulphide body. The extent of the sulphide body, and location of transition zone are shown for reference. Maps are based on detailed mapping and compilation of Cominco Ltd. data by D.R. Shaw between 1976 and 1980.

clearly postdates ore deposition. Shaw and Hodgson (1986) suggest that chlorite-pyrrhotite alteration accompanied and continued after ore deposition. Replacement of pyrrhotite by pyrite near the upper margin of the hanging wall chlorite-pyrrhotite zone suggest that chlorite-pyrrhotite alteration occurred earlier than chlorite-pyrite alteration. The common zonation of albite-chlorite-pyrite-altered rocks on many scales from a central core of albitite to peripheral chlorite-pyrite implies synchronous albitization and chlorite-pyrite alteration. The occurrence of chlorite-pyrite veinlets cutting albitite, and abundant albitite fragments in a chlorite-pyrite matrix at the base of the albitite core, however, suggest that some chlorite-pyrite alteration postdated albitization, perhaps due to the collapse of the albite to albite-chlorite zone boundary late in the alteration process (Turner and Leitch, 1992).

Iron and magnesium metasomatism

The abundance of chlorite in chlorite-pyrrhotite and chlorite-pyrite alteration above, within and below the orebody is evidence of extensive iron and magnesium metasomatism of silicate minerals at the Sullivan deposit. The composition of chlorite-pyrrhotite and chlorite-pyrite rock when recalculated to a sulphide-mineral free analysis, approaches the composition of pure chlorite and reflects intense alteration and mobility of elements during alteration. Less intense iron and magnesium metasomatism is reflected by the occurrence of chlorite-biotite-garnet-altered rocks in the footwall zone (Shaw et al., 1993).

Significant addition appears to have occurred during chlorite-pyrite alteration and chlorite-pyrrhotite alteration. It is unclear whether the high iron sulphide content of chlorite-pyrrhotite and chlorite-pyrite alteration reflects the synchronous introduction of iron and sulphur during alteration, or chlorite alteration of silicates in a pyrrhotite-rich rock. Tourmalinite in close proximity to the base of the sulphide body typically contains abundant pyrrhotite (Leitch and Turner, 1992). At contacts between chlorite-pyrite and tourmalinite in the footwall zone, there is no obvious increase of sulphide content in the chloritic rock relative to the tourmalinite. Unaltered tourmalinite in the area of footwall chlorite-pyrite alteration contains 4.4% sulphur (Shaw et al., 1993). Partially altered tourmalinites and apparently unaltered tourmalinites in close proximity to chlorite-pyrite-altered and albite-chlorite-pyrite-altered tourmalinite contain 3.2% and 3.6% sulphur respectively. Footwall chlorite-pyrite rocks contain 5.1% sulphur. These geological relationships and chemical data suggest that pyrite in footwall chlorite-pyrite rocks formed by alteration of pyrrhotite in tourmalinite. Chlorite-pyrrhotite-altered footwall rocks, however, contain 7.4% sulphur and may reflect addition of both iron and sulphur.

Chlorite-pyrite and chlorite-pyrrhotite alteration reflect intense magnesium metasomatism. Formation of Mg-silicates in modern seafloor hydrothermal systems is caused by mixing of Mg-depleted silica-bearing hydrothermal fluids and Mg-bearing seawater (e.g., Seyfried et al., 1988). This Mg uptake by Mg-silicates makes it unlikely that

seawater-derived Mg will penetrate significantly into the high temperature regions of submarine geothermal systems. By analogy, chloritic alteration at Sullivan could reflect a seawater dominant system at relatively shallow depths below the seafloor (Shaw and Hodgson, 1980b; Turner and Leitch, 1992). Abundant Mg-silicates occur within iron sulphide-rich hydrothermal vent mounds in sediment-filled rifts such as Guaymas Basin and Middle Valley (e.g., Lonsdale et al., 1980; Turner et al., 1991) are interpreted to result from ingress and heating of seawater in the very shallow (<30 cm depth) subsurface (Turner et al., 1991). The concordant bodies of chlorite-pyrrhotite at the base of the Sullivan orebody may reflect a similar ingress and heating of seawater around the hydrothermal vents that formed the Sullivan orebody.

Sodium metasomatism

Extensive sodium metasomatism at the Sullivan deposit is reflected by the abundance of albite in albite-chlorite-pyrite alteration developed above and below the orebody. The composition of albitite when recalculated to a sulphide-free analysis approaches that of pure albite and reflects intense alteration and mobility of Al_2O_3 , TiO_2 , and other elements during alteration.

Experiments by Bischoff et al. (1981) monitored the reaction of greywacke with seawater and brines at 350°C and 500 bars and indicate that an assemblage of chlorite-smectite albite can form from heated seawater. However, the formation of extensive bodies of massive albite (i.e. albitite) with little chlorite likely requires brines enriched in sodium (Bischoff et al., 1981) and significantly depleted in magnesium and calcium (Seyfried et al., 1988). Sodium fixing through albitization is expected in upflow zones of seafloor hydrothermal systems in which Na- and Si-bearing, Mg-free, and Ca-depleted fluids are derived from high-temperature reactions at depth (Seyfried et al., 1988).

At Sullivan, albitite occurs along hydrothermal conduits surrounded by chlorite-rich assemblages, and locally is overprinted by late chlorite veins (Shaw and Hodgson, 1980b). Turner and Leitch (1992) suggested that albitic alteration reflects the core upflow zone of high Na/(Mg+Ca) brines. Marginal to this hydrothermal plume, mixing with Mg-rich interstitial fluids derived from seawater resulted in chlorite-dominant alteration. Turner and Leitch (1992) also suggested that waning of hydrothermal activity allowed penetration of Mg-rich seawater into the albitite body along fractures causing late chloritic alteration of albite.

ACKNOWLEDGMENTS

We thank Cominco Ltd. and the former and present staff of the Sullivan Mine Geology Department for their kind assistance during our field studies, and Cominco's Exploration Laboratory for performing the analyses. Critical reviews of this manuscript by Georges Beaudoin, John Hamilton, and John Slack are greatly appreciated.

REFERENCES
Bischoff, J.L., Radke, A.S., and Rosenbauer, R.J.

1981: Hydrothermal alteration of graywacke by brine and seawater: Roles of alteration and chloride complexing on metal solubilization at 200°C and 350°C; *Economic Geology*, v. 76, p. 659-676.

Edmunds, F.R.

1977: Multivariate analysis of petrographic and chemical data from the Aldridge Formation, southern Purcell Mountains Range, British Columbia, Canada; Ph.D. thesis, Pennsylvania State University, 368 p.

Hamilton, J.M., Bishop, D.T., Morris, H.C., and Owens, O.E.

1982: Geology of the Sullivan orebody, Kimberley, B.C., Canada; in *Precambrian Sulphide Deposits*; (ed.) R.W. Hutchinson, C.D. Spence, and J.M. Franklin; Geological Association of Canada, Special Paper 25, p. 597-665.

Leitch, C.H.B. and Turner, R.J.W.

1991: The vent complex of the Sullivan stratiform sediment-hosted Zn-Pb deposit, B.C.: Preliminary petrographic and fluid inclusion studies; in *Current Research, Part E*; Geological Survey of Canada, Paper 91-1E, p. 33-44.

1992: Preliminary field and petrographic studies of the sulphide-bearing network underlying the western orebody, Sullivan stratiform sediment-hosted Zn-Pb deposit, British Columbia; in *Current Research, Part E*; Geological Survey of Canada, Paper 92-1E, p. 61-70.

Lonsdale, P.F., Bischoff, J.L., Burns, V.M., Kastner, M., and**Sweeney, R.E.**

1980: A high-temperature hydrothermal deposit on the seabed at a Gulf of California spreading center; *Earth and Planetary Science Letters*, v. 49, p. 8-20.

Seyfried, W.E., Jr., Berndt, M.E., and Seewald, J.S.

1988: Hydrothermal alteration processes at mid-ocean ridges: Constraints from diabase alteration experiments, hot-spring fluids, and composition of the oceanic crust; *Canadian Mineralogist*, v. 26, p. 787-804.

Shaw, D.R. and Hodgson, C.J.

1980a: Wall-rock alteration at the Sullivan mine, Kimberley, British Columbia (abstract); Canadian Institute of Mining and Metallurgy, Bulletin 73, no. 821, p. 75.

1980b: Wall-rock alteration at the Sullivan mine, Kimberley, British Columbia; paper presented at Fifth Annual District Six Meeting of the Canadian Institute Mining Metallurgy, Kimberley, B.C., October 23-25, 1980, 14 p.

1986: Wall-rock alteration at the Sullivan mine, Kimberley, British Columbia; in *The Genesis of Stratiform Sediment-Hosted Lead and Zinc Deposits: Conference Proceedings*, (ed.) R.J.W. Turner and M.T. Einaudi; Stanford University Publications, School of Earth Sciences, v. 20, p. 13-21.

Shaw, D.R., Hodgson, C.J., Leitch, C.H.B., and Turner, R.J.W.

1993: Geochemistry of tourmalinite, muscovite, and chlorite-garnet-biotite alteration, Sullivan Zn-Pb deposit, British Columbia; in *Current Research, Part A*; Geological Survey of Canada, Paper 93-1A.

Turner, R.J.W. and Leitch, C.H.B.

1992: Relationship of albitic and chloritic alteration to gabbro dykes and sills at the Sullivan deposit and nearby area, southeastern British Columbia; in *Current Research, Part E*; Geological Survey of Canada, Paper 92-1E, p. 95-106.

Turner, R.J.W., Leitch, C.H.B., Ames, D.E., Hoy, T., Franklin, J.M., and Goodfellow, W.D.

1991: Character of hydrothermal mounds and adjacent altered sediments, active hydrothermal areas, Middle Valley sedimented rift, northern Juan de Fuca Ridge, northeastern Pacific: evidence from ALVIN push cores; in *Current Research, Part E*; Geological Survey of Canada, Paper 91-1E, p. 99-108.

 Geological Survey of Canada Project 900020

Surficial geology of the Queen Charlotte Basin: evidence of submerged proglacial lakes at 170 m on the continental shelf of western Canada

H.W. Josenhans, J.V. Barrie, K.W. Conway, R.T. Patterson¹,
R.W. Mathewes², and G.J. Woodsworth,³

Pacific Geoscience Centre, Sidney

Josenhans, H.W., Barrie, J.V., Conway, K.W., Patterson, R.T., Mathewes, R.W., and Woodsworth, G.J., 1993: Surficial geology of the Queen Charlotte Basin: evidence of submerged proglacial lakes at 170 m on the continental shelf of western Canada; in Current Research, Part A; Geological Survey of Canada, Paper 93-1A, p. 119-127.

Abstract: A high resolution marine seismic and sampling program in the region was carried out during a 12 day cruise aboard the research vessel *CFAV Endeavour*. Preliminary results indicate that grounded glaciers deposited sediments in the deep troughs which indent the continental shelf as far west as the shelf break. Offlapping till tongues found in the troughs indicate that ice retreated stepwise from Queen Charlotte Sound at the close of the last (Late Wisconsinan) glaciation. Detailed studies of submerged shoreline deposits define the volume and frequency of failure of steeply dipping prograde sand and gravel deposits.

Partially eroded, proglacial lake deposits found in 170 m water depth were seismically surveyed and sampled in Hecate Strait near southeastern Moresby Island. Paleolacustrine deposits at this location on the shelf imply that sea level was locally lowered by at least 170 m. Data from the cruise suggest an east to west tilt and lowering of paleoshorelines of at least 60 m vertical per 50 km horizontal.

Résumé : On a réalisé un programme de levés sismiques de haute résolution et d'échantillonnage dans la région pendant une croisière de 12 jours à bord du navire de recherche *CFAV Endeavour*. Les résultats préliminaires indiquent que des glaciers échoués ont déposé des sédiments dans de profondes fosses qui entaillent la plate-forme continentale vers l'ouest jusqu'à la marge de la plate-forme. Les langues régressives de till rencontrées dans les fosses témoignent du retrait graduel de la glace du détroit de la Reine-Charlotte à la fin de la dernière glaciation (Wisconsinien tardif). Des études détaillées des dépôts littoraux submergés ont permis de définir le volume et la fréquence de rupture des dépôts progrades fortement inclinés composés de sable et de gravier.

Les dépôts lacustres proglaciaires partiellement érodés rencontrés dans une profondeur d'eau de 170 m ont fait l'objet de levés sismiques et d'échantillonnages dans le détroit d'Hecate près du sud-est de l'île Moresby. La présence de dépôts paléolacustres situés à cet endroit sur la plate-forme continentale implique que le niveau marin s'est abaissé d'au moins 170 m à cet endroit. Les données recueillies au cours de la croisière semblent indiquer un basculement d'est en ouest et un abaissement vertical des anciennes lignes de rivage d'au moins 60 m sur des distances horizontales de 50 km.

¹ Ottawa-Carleton Geoscience Centre, Carleton University Ottawa, Ontario

² Department of Biological Sciences and Institute of Quaternary Research, Simon Fraser University, Burnaby, B.C. V5A 1S6

³ Cordilleran Division, Geological Survey of Canada, 100 West Pender Street, Vancouver, B.C. V6B 1R8

INTRODUCTION

The Queen Charlotte Basin was the focus of surficial geological studies by the Geological Survey of Canada as part of the mandate of the Frontier Geoscience Program. The results of this work indicate extremely rapid relative sea level and environmental change at the end of the last glaciation (Luternauer et al., 1989). Sea levels on the inner continental shelf were much lower (100 m) than present while at the same time areas at the heads of mainland fiords were submerged by up to 200 m. This observation implies a degree of east to west tilting in sea level. Important questions as to the timing, spatial variation, and mechanisms of these sea level changes on the western Canadian shelf are outstanding.

Onshore data suggest that parts of the Queen Charlotte Islands may have been ice free during the last glaciation (Warner et al., 1982). Questions regarding the seaward limits of the last (Fraser) glaciation on the continental shelf remain unanswered.

In view of the above mentioned gaps in what is known about this region, Cruise PGC92-004, aboard the *CFAV Endeavour*, was mounted to address objectives including (i) an investigation of the regional glacial stratigraphy, (ii) examination of the stability of steeply sloping, former

shoreline deposits, and (iii) a study of the paleoenvironments of surficial deposits to provide constraints on sea level reconstructions.

Seismic profiles were placed to determine the maximum seaward extent of glaciation and piston core samples from these glaciogenic deposits were collected to obtain dateable material to define the age and rate of ice retreat from the continental shelf. Additionally, lines were run in areas where previously collected data suggested good resolution of till sequences on the inner shelf might be obtained. These data were collected to provide insight into the mechanisms and rate of deglaciation.

Detailed site specific investigations were carried out on the eastern margin of Middle Bank in central Queen Charlotte Sound (Fig. 1) to determine the volume, composition, stability and age of a paleo-shoreline prograded spit deposit. Numerous similar large sand spits occur throughout Queen Charlotte Sound with steep prograde slopes which have failed repeatedly since their emplacement. Our objective was to acoustically image the detailed architecture of one of these features and to define the frequency and volume of slope failure at this site.

Our final area of detailed study focused on mapping and sampling a sequence of horizontally stratified, incised basin fill deposits found in the vicinity of south western Laskeek

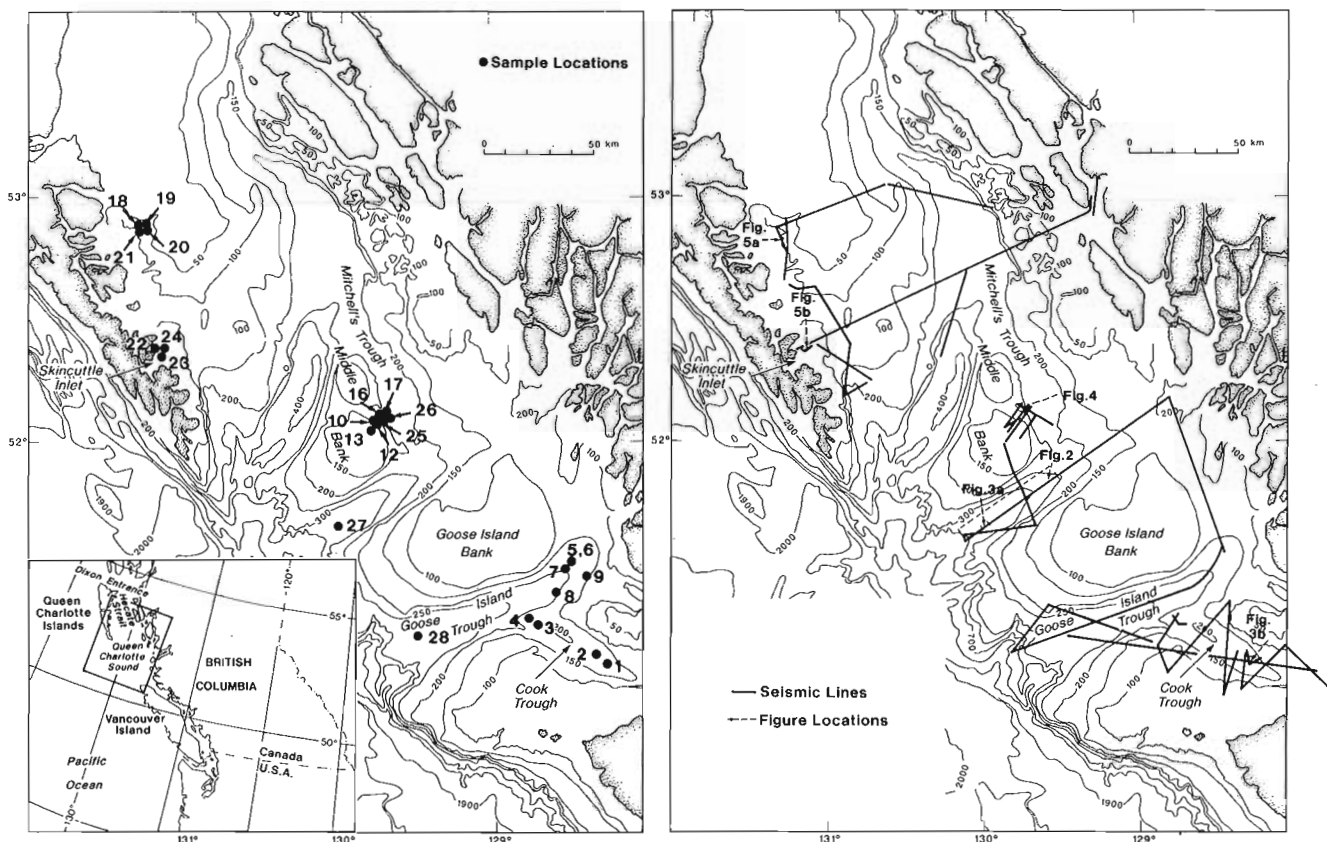


Figure 1. Bathymetry map of Queen Charlotte Sound showing location of seismic tracks and sample locations of Endeavour cruise 92A004.

Table 1. Endeavour 92-004 facts sheet

SAMPLE INVENTORY	NUMBER
PETERSON GRABS	1
BENTHOS PISTON CORES	18
VIBRACORES	5
TOTAL SAMPLES	24

DATA TYPE	KILOMETRES
3.5 KHz BATHYMETRY	180
12 KHz BATHYMETRY	1205
HUNTEC DTS	1301
SLEEVEGUN SEISMICS	1116
100 KHz SIDESCAN	1196
TOTAL LINES (#1-42)	1385

Bank off south Moresby Island in greater than 170 m water depth. Seismic profiles indicate that up to 25 m of material has been eroded from these deposits. A survey and sampling program was designed to determine the origin of the basin fill deposits and the cause of the incised relief.

The data collected during this cruise will be used to update maps of surficial geology and regional seismostratigraphy of the region published earlier by Barrie et al. (1990) and Luternauer et al. (1990), as well as to address specific questions relating to the maximum extent of glaciation and late glacial sea level history of Queen Charlotte Basin.

RESULTS

A summary listing of seismic and sample data collected in this cruise is shown in Table 1. Seismic lines and sample positions are shown in Figure 1.

Ice contact and ice retreat features

The acquired data has allowed acoustic imaging of the three dimensional distribution of glacial and postglacial sediments throughout Queen Charlotte Sound (QCS). An acoustically unstratified massive unit called "till" (Fig. 2) extends all the way to the shelf break and is interpreted to indicate that grounded glaciers flowed all the way to the shelf edge through Goose Island and Mitchell's Trough. The seismic profile illustrated in Figure 2 demonstrates the thickness and westward extent of multiple "tills" within the base of Mitchell's Trough. A piston core taken within the seismostratigraphically defined ice-proximal/ice-contact deposits associated with the uppermost "till" is illustrated in Figure 3a. The 5.5 m core sampled a poorly sorted gravelly mud at the base, which grades upwards into coarsely laminated sediments. These sedimentary features are consistent with an ice contact to ice proximal depositional setting and support the seismostratigraphic interpretation of "till".

Subsamples from core 27 (Fig. 3) were examined with a binocular microscope in an attempt to determine source terranes of the sediments. Two sand fractions were examined.

At 414-416 cm this sand consisted of quartz, feldspar, epidote, hornblende, and garnet. Some tiny lithic clasts might be shale, siltstone, or aphanitic black volcanic material. The sample from 451-453 cm consists largely of quartz, feldspar, hornblende, epidote, sphene and other minerals. A few millimetre-sized clasts of intermediate(?) volcanic rocks do not appear to be highly altered and might be Miocene or younger. Given the fine grained nature of the sediments and the absence of distinctive, diagnostic lithologies, the provenance of these samples is uncertain.

Seismic profiles collected from the troughs indicate regionally extensive "till sheets", often superimposed and typically 30 m thick. Profiles from the transition of trough to bank tops show numerous disconformities and seismic reflector truncations. The data do not clearly resolve if glacial till occurred on the bank tops although acoustically massive deposits which may represent tills are observed locally. The question of ice cover on the bank tops remains unresolved.

No evidence for young (postglacial) faulting was observed on the seismic records. The unconformity developed at the base of the glacial deposit illustrated in Figure 2 is smooth and unbroken.

A series of seismically resolved ice retreat deposits called till tongues (King et al., 1991) were found and sampled in Cook's Trough. These features were believed to have been formed by the stepwise, southward retreat of a glacier in Cook's Trough. Similar ice retreat features are resolved seismically in all the major troughs of Queen Charlotte Sound (Fig. 2). Figure 3b illustrates the seismostratigraphic setting and sedimentary features of a piston core representative of ice proximal glaciomarine sediments deposited directly at a till tongue.

Four cores were taken along the axis of Cook's Trough (Fig. 1) within similar ice-proximal till tongue settings. These cores have been subsampled and shell fragments from the ice proximal deposits will be dated to determine the rate of ice retreat from Cook's Trough.

Paleo shoreline deposits

A closely spaced grid of seismic profiles from the eastern edge of Middle Bank (Fig. 1), shows a sequence of steeply dipping prograded reflectors (Fig. 4) which extend from a depth of 110 m at the bank top to approximately 200 m in Mitchell's Trough. Vibracore samples (Fig. 4) from the top of this prograde spit sequence, indicate beach sands and well rounded gravels which must have been deposited when sea levels were at least 110 m lower than present. Four vibracores were obtained from the oldest to the youngest member of the prograded sequence. Shell fragments found within these sands and well rounded gravels will be dated to determine the age of the deposit as well as to determine the rate of progradation. Three piston cores define the lateral extent and volume of numerous slump deposits observed at the base of these shoreface deposits. Piston cores obtained from above and below a large slump deposit (Fig. 4) will be analyzed to determine the age and frequency of these slope failure events. The number of slumps observed at the base of the slope

suggest that these depositional settings may be sensitive indicators of seismicity. Experience gained in studying the three dimensional configuration and frequency of failure of these former shoreline deposits has helped to develop an appropriate methodology for studying the stability of modern high angle prograding spits such as those found off Comox, British Columbia and Port Angeles and Dungeness spits in Juan de Fuca Strait.

Proglacial lake deposits

Southeast of Moresby Island, in up to 170 m water depth, the Huntex and airgun data reveal (Fig. 5a, b) a unique seismic unit which is interpreted to represent a proglacial lake deposit. The seismic data indicate that these horizontally stratified sediments were deposited as basin fill into the localized depressions formed on the volcanics of the Masset Formation.

A regional erosional event has subsequently incised these basin fill deposits by up to 25 m, resulting in numerous (submerged) cliff sections (Fig. 5). Piston cores and vibracores were taken from the flanks of these exposures and

25 m of (Quaternary) section was sampled. At the base of the section the recovered cores contain sand- to silt-sized sediments, in what appear to be rapidly deposited rythmites. These are overlain by a fining upward sequence of rythmites and massive silty clays. Above the clays, a veneer, up to 1.5 m thick contains coarse grained sands, gravels and shell fragments. The latter unit is thought to have developed when the area was transgressed at the end of the Late Wisconsinan. In contrast to the sterile sediments found at the base, the upper part of the section includes marine shells and forams.

Pollen analysis

Preliminary results of pollen analysis from the upper 280 cm of sediments (Fig. 5a) are consistent with an interpretation of a proglacial lake deposit, grading into late-glacial muds, in turn overlain by sediments of a marine transgression. The basal varve-like rythmites contain fine organic matter and are essentially barren of pollen and spores. Between 220-250 cm, pollen and spore frequencies increase, with an abundance of pine pollen, as well as soil fungi and fresh-water plant

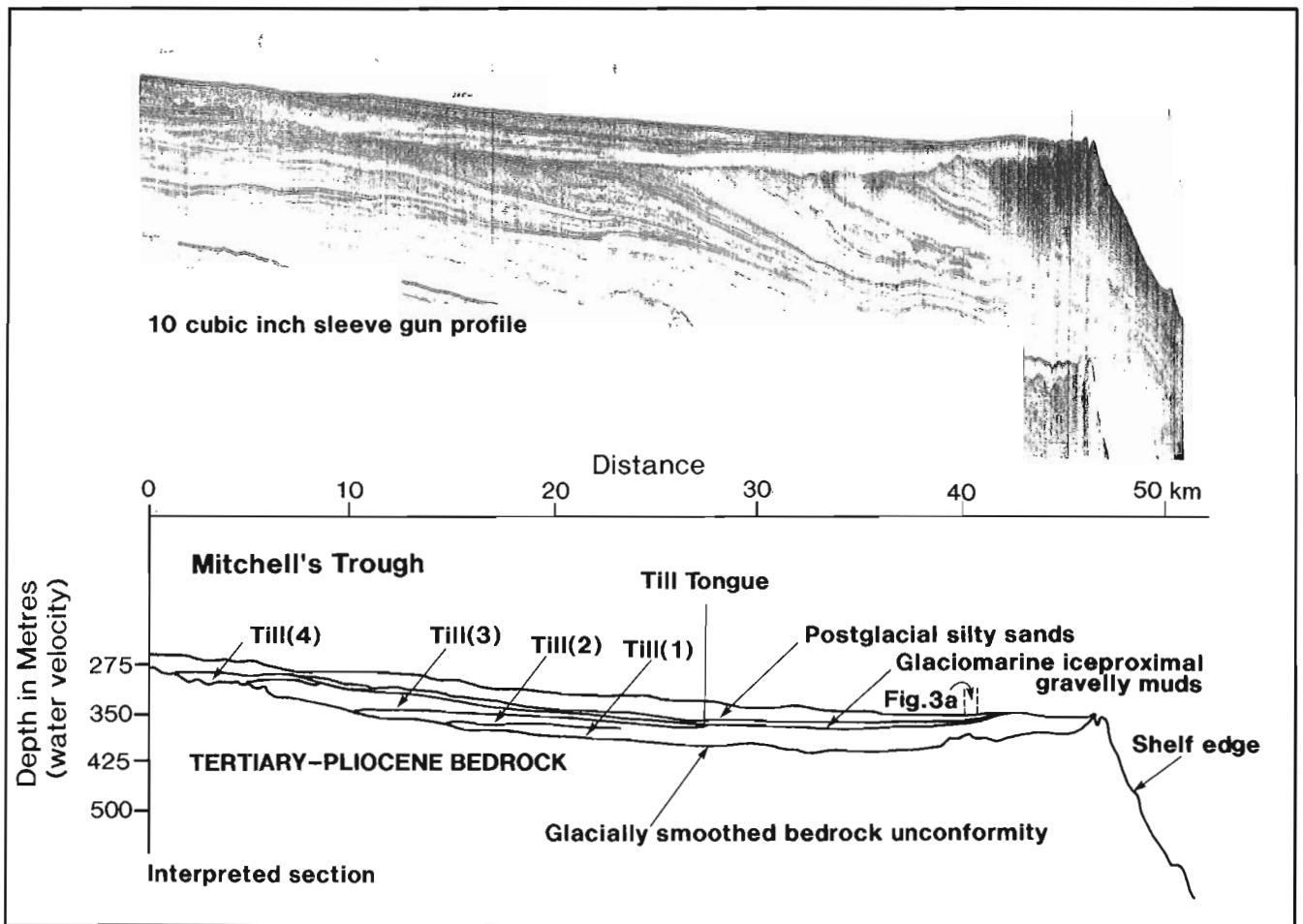
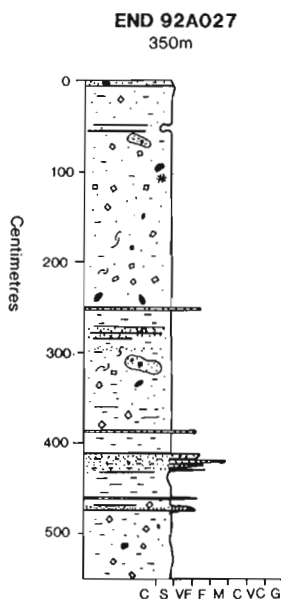
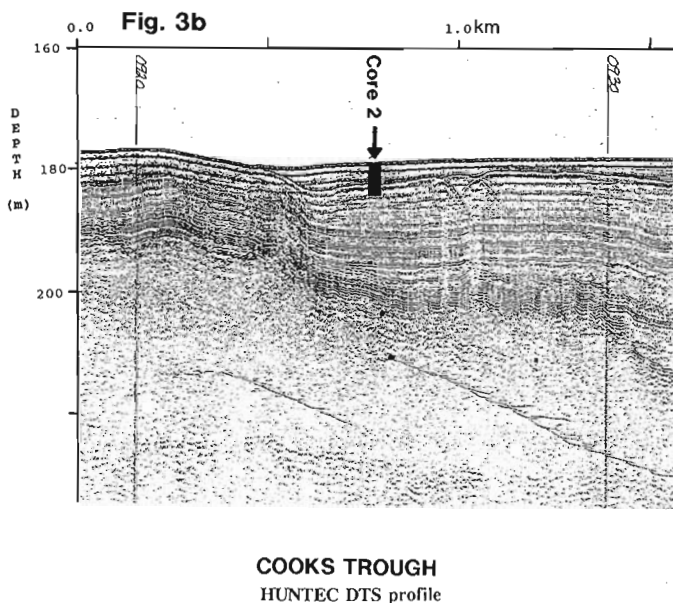
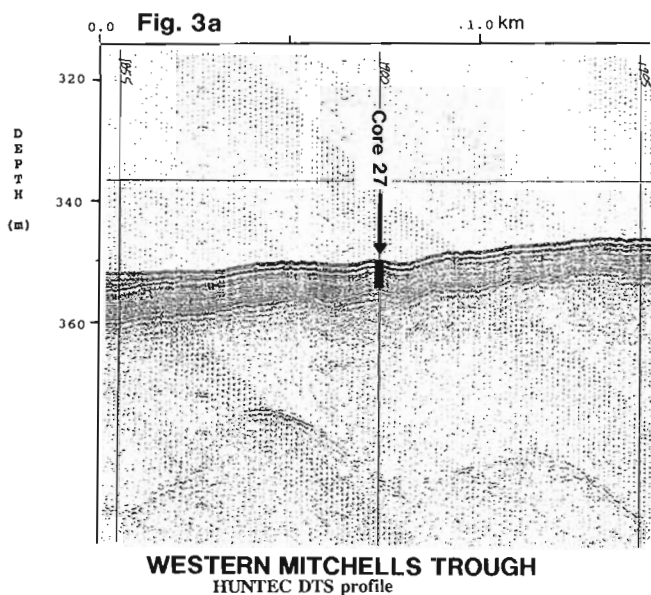


Figure 2. Sleeve gun seismic profile and interpreted section from axis of western Mitchell's Trough. The acoustically unstratified deposits above the bedrock unconformity are interpreted to represent superimposed glacial tills deposited by a waxing and waning ice margin which retreated toward the left of the diagram. For location see Figure 1.

remains. Pine pollen reaches very high values around 200 cm, and is soon joined by abundant and well preserved spruce grains by 184-186 cm. Comparison with terrestrial sequences on the Queen Charlotte Island suggests a late-glacial age of ca. 12 000 BP for initial pine expansion, and ca. 11 000 BP for the initial appearance of spruce. It appears that the sampled basin was a late-glacial fresh water lake, probably transgressed by the sea during the transition to the early Holocene.

Microfauna analysis

Twenty-seven samples from core END 92A-021 (Fig. 5a) were quantitatively examined for their foraminiferal and other microfossil group content. Fourteen of these samples contained at least some foraminifera and no sample was devoid of any useful micropaleontological specimens. Most of the non-foraminiferal bearing samples are from the Diatom



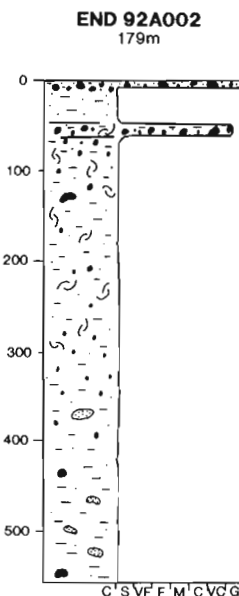
INTERPRETATION

Holocene sandy mud.

Late Wisconsinian ice-distal glaciomarine.

Late Wisconsinian ice-proximal glaciomarine.

Late Wisconsinian till.



INTERPRETATION

Late Wisconsinian gravel lags associated with lowstand of sea level.

LEGEND

- Gravel
- Sand
- - - - Silt
- Sand clast
- ⊕ Coal
- ==== Laminations
- ~ ~ ~ Shells/shell debris
- ⊙ ⚡ Burrows/bioturbation
- # # Wood fragments/organic matter
- Large wood fragment
- X X X Black streaks
- ◊◊◊◊ Rip-up clasts
- ⊙ Foraminifera

Figure 3. Huntec DTS seismic profiles interpreted to represent ice proximal stratified deposits above glacial till. The black bar indicates the actual penetration of the piston core (illustrated in the right column) with respect to the seismic profile. For location see Figure 1.

Biofacies (described below). The core could be divided into four distinct biofacies that correlated almost exactly with the various lithological units described in Figure 5a.

1. *Ostracode biofacies: 274 cm - bottom of core*

The sandy muds in the basal part of the core below 274 cm are characterized by very abundant populations of exclusively smooth walled ostracodes (probably Cypridae). This interval is also characterized by very rare centric diatoms (no pinnates were observed in this interval) and a single specimen of the foraminifera *Quinqueloculina triangularis*, a species common to neritic depths all along the Pacific coast. The

presence of the probably transported foram suggests that the ocean was not far away. The lack of fresh water indicating pennate diatoms also suggests that perhaps conditions were brackish during deposition of this interval. The lake may have been subject to periodic marine incursions at this time.

2. *Diatom biofacies: 128-274 cm*

The organic rich varved muds found between 128 and 274 cm are characterized by very abundant populations of fresh water centric and pennate diatoms, characteristic of fresh water lakes. Most of the samples from this interval are also characterized by very abundant pollen taxa also characteristic

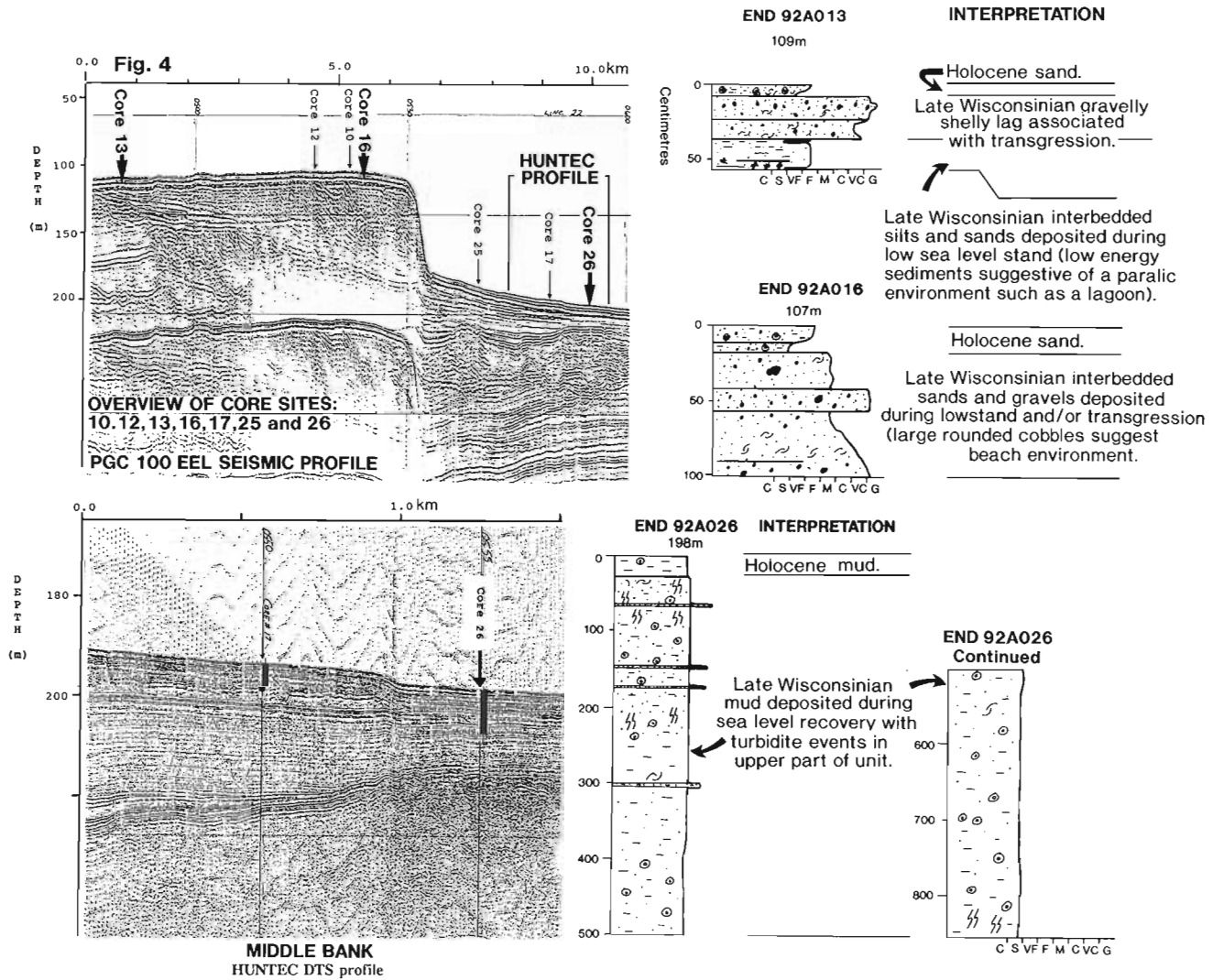


Figure 4. Sleeve gun seismic profile and Hunttec DTS high resolution profile of prograde spit deposit from Eastern Middle Bank showing the positions of cores collected in order to determine the age and rate of progradation of this feature. The Hunttec profile illustrates the acoustic character of a large slump deposit which has failed from the steep paleoshoreface. Core 92A026 has sampled horizons above and below the slump deposit and will be dated to determine the age of the failure event.

of onshore fresh water environments. The lack of bioturbation, microfossil assemblage, and the varved nature of the sediments indicate that the lake bottom had low oxygen content. One atypical interval of this biofacies found between 234 and 246 cm is characterized by a mixed lacustrine diatom and marine shelf foraminiferal fauna. In addition, specimens of the benthic fresh/brackish arcellacean *Centropyxis aculeata* are also found. The juxtaposition of these dramatically different faunas suggests again that the lake was subject to periodic marine incursions, most likely occurring during extreme storm events. However no sedimentological evidence of such a storm event is present at this horizon.

3. Shelf foraminiferal biofacies: 62-128 cm

The shelly sands found between 62 and 128 cm are characterized by an essentially modern high diversity, open shelf foraminiferal fauna. Typical species include *Buccella frigida*, *Buliminella elegantissima*, *Cribrroelphidium excavatum*, *Elphidiella nitida*, *Epistominella vitrea*, *Gavelinopsis campanulata*, *Lobatula fletcheri* and numerous others. The lack of significant proportions of cold water indicator species such as *Cassidulina reniforme* and *Cribrroelphidium excavatum* as observed elsewhere in Late Wisconsinan cores indicate water salinities and temperatures were similar to those found in the area presently (Patterson, in press). Slight abrasion and breakage of some specimens in addition to the abundant shell debris indicates minor reworking.

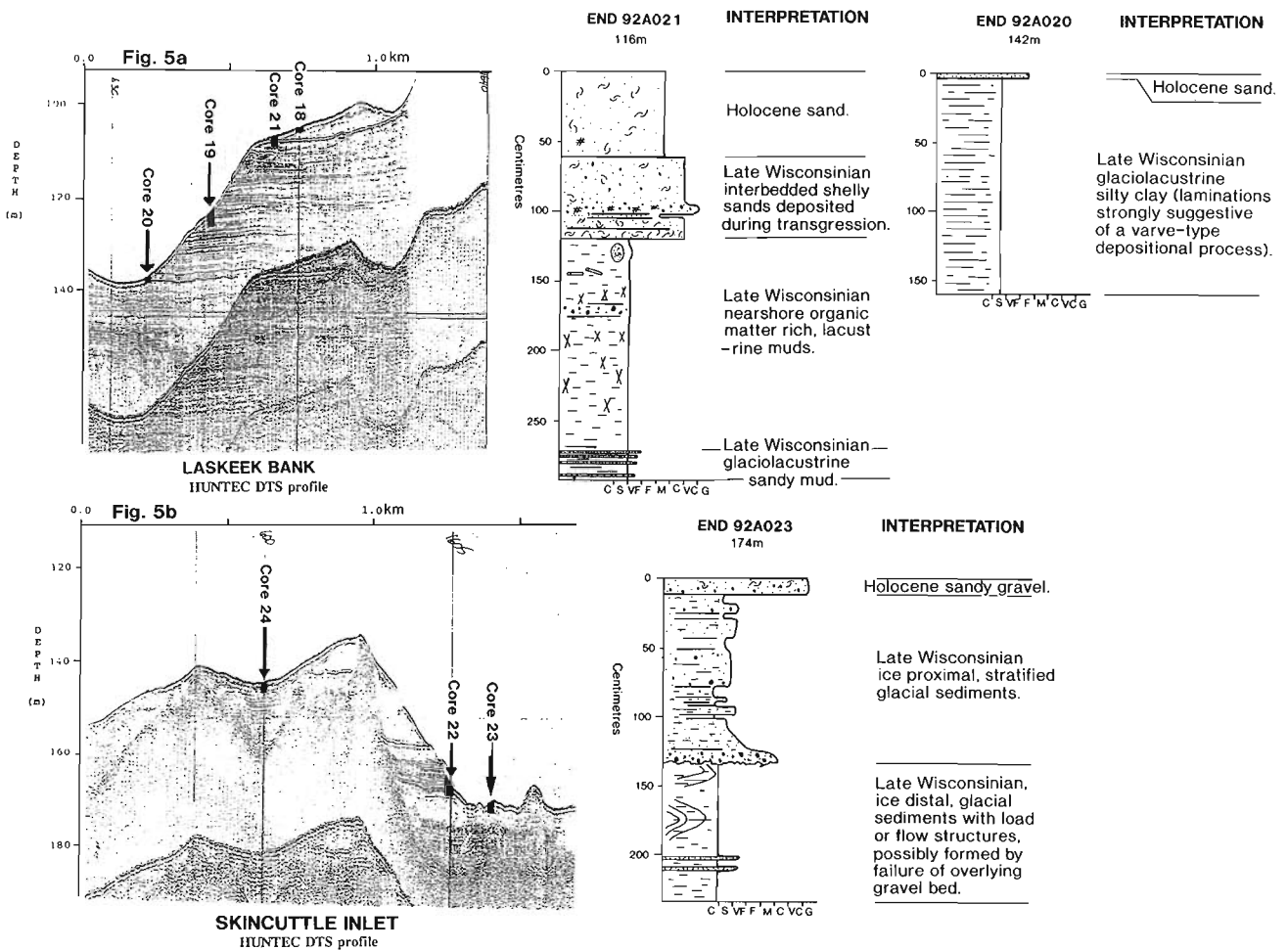


Figure 5. Huntec DTS profile of remnant horizontally stratified basin fill deposits located off Southeastern Moresby Island. For exact location refer to piston core position in Figure 1. The black bars indicate the amount of sample penetration in relation to the seismic section. Note that almost 30 m of composite section has been sampled. The origin of the erosional surface may be due to severe erosion during a transgression of the region or due to glacial erosion following emplacement of the stratified deposits.

4. *Reworked Foraminiferal Biofacies: 0-50 cm*

This biofacies is characterized by small populations of highly abraded shelf foraminiferal populations in a winnowed sand. Although essentially the same species as identified in the shelf foraminiferal biofacies, the extremely poor condition of specimens clearly differentiate the faunas found in this biofacies.

Provenance of selected samples

The sand and gravel fractions of subsamples of cores 18, 21, and 23 (Fig. 5) were examined with a binocular microscope in an attempt to determine possible source terranes for the cored sequences. The assumptions are that, if the sediments had an easterly source, they would reflect the lithologies found in the predominantly granitoid and high grade metamorphic bedrock of the Coast Mountains. If the sediments were derived from the Queen Charlotte Islands, the sediments should reflect the predominantly volcanic and sedimentary nature of the terrane. Preliminary descriptions and tentative interpretations are given below.

Core 18

The >.063 mm <2 mm (sand) fraction from 103-105 cm consists largely of quartz and feldspar grains, with subordinate hornblende and epidote. The more informative >2 mm fraction from the same interval consists mostly of dark, fine grained volcanic material or siltstone. One clast of dark green basalt has a strong textural resemblance to Upper Triassic Karmutsen basalts common on Queen Charlotte and Vancouver Islands. A small percentage of the clasts are hornblende-rich granitoid rocks. Several clasts are composed of fresh-looking, vesicular basalt, probably Miocene or younger.

The predominance of volcanic and sedimentary rocks in the lithic clasts strongly suggests that the sediments were derived from units now exposed on the Queen Charlotte Islands. The source of the the vesicular basalt is unknown; such rocks are rare on the Queen Charlotte Islands.

Core 21

Only a small amount of sample is present in the >2 mm fraction from 169-171 cm. The few large grains are dark, fine grained volcanics or siltstones. The sand fraction from 277-279 cm in the core consists largely of quartz and feldspar with significant hornblende and biotite and lesser other minerals, notably epidote.

The fact that the few large lithic clasts are volcanic or sediments, and the absence of granitoid material argues against a coast mountain origin for these sediments.

Core 23

The >2 mm fraction from 129-131 cm contains several conspicuous black, very fine grained, angular clasts that resemble hornfelsed siltstone. Most lithic clasts are grey,

unfoliated, hornblende>biotite tonalite or granodiorite. One large clast appears to be grey-green, andesite volcanic rock. The >.063 mm <2 mm fraction from the same interval is composed of feldspar with subordinate quartz, hornblende, epidote and other minerals. Lithic clasts consist of fine grained siltstone or hornfels similar to that in the coarse fraction. Some sugary aggregates of diopside(?) may have been derived from contact metamorphosed carbonate rocks.

The abundant tonalite could have been derived from either the Coast Mountains or the Queen Charlotte Islands. The absence of foliation suggests a Queen Charlotte source. Fine grained, dark sedimentary rocks are common on the Queen Charlotte Islands and rare in the Coast Mountains. The diopsidic clasts probably represent metamorphosed carbonate rocks; these are found more commonly on the Queen Charlottes but are not diagnostic.

The examined sediments were probably derived from Mesozoic units now exposed on the Queen Charlotte Islands; nothing strongly points to an easterly source.

Erosional event

Two mechanisms for eroding this regional unconformity which has dissected the basin fill deposit are proposed:

1. The transgression may have had sufficient erosive power to produce the incised relief and remove the large volumes of basin fill sediment; and
2. A glacier originating from southern Moresby Island may have advanced over the basin fill sediments and eroded and transported the material. A subsequent transgression could then have modified the existing erosional surface to produce the coarse sand and gravel veneer.

A lack of (observed) glacial till below the transgressive sands argues in favour of mechanism #1. However, a surprising lack of transgressive and younger basin fill sediments within the enclosed and incised basins has resulted from the transgression which argues in favour of mechanism #2. Detailed analysis of the core samples to define environments of deposition, provenance, age and degree of compaction are needed to constrain further interpretations.

Implications for paleo-sealevels.

The prograding spit deposit investigated on the eastern margin of Middle Bank clearly indicates that sea level must have fallen to -110 m in order to deposit the clean sands and gravels which make up the paleoshoreline feature. We infer that sealevels must have stabilized at this elevation, at least locally for an extended period (1-2 ka) to produce the observed geomorphic features and the volumes of sediment contained therein.

The lacustrine deposits sampled at a depth of 170 m from the western margin of the continental shelf indicate that sealevel had fallen to at least -170 m. The lake sediments are up to 30 m thick which implies that a lake existed at these sites for an extended period of time (several hundreds of years at least).

The proglacial basin fill site with lacustrine deposits at 170 m is approximately 50 km west of the prograde spit which was deposited near sealevel at -110 m. A minimum tilt of paleoshorelines of 60 m over a horizontal distance of 50 km is indicated.

Additional work is required to define the lower limit of lacustrine conditions and to define the lateral extent and depth of the basin into which the proglacial lake sediments were deposited.

ACKNOWLEDGMENTS

We thank the officers and crew of the "*Endeavour*" for their willing and able support at sea. We also thank the technical support staff at PGC for making it possible to collect such high quality data. Tom Vandall, Jay Stravers, John Luternauer, Olav Lian, Raelyn Crossley, Michelle Packard and Gina L'Esperance are recognized for valuable assistance at sea. The report was reviewed by T.S. Hamilton.

REFERENCES

- Barrie, J.V., Luternauer, J.L., and Conway, K.W.**
1990: Surficial geology of the Queen Charlotte Basin: Moresby Island-Queen Charlotte Sound; Geological Survey of Canada, Open File 2196, 8 maps (1: 250 000).
- Luternauer, J.L., Barrie, J.V., Conway, K.W., and Caltagirone, A.**
1990: Surficial geology of the Queen Charlotte Basin: Hecate Strait-Queen Charlotte Sound; Geological Survey of Canada, Open File 2195, 8 maps (1: 250 000).
- Luternauer, J.L., Conway, K.W., Clague, J.J., and Blaise, B.**
1989: Late Quaternary geology and geochronology of the central continental shelf of Western Canada; *Marine Geology*, v. 89, p. 57-68.
- Patterson, T.**
in press: Late Quaternary benthic foraminiferal biofacies and paleoceanography of the Queen Charlotte Sound and Southern Hecate Strait, British Columbia; *Journal of Foraminiferal Research*.
- King, L.H., Rokoengen, K., Fader, G.B.J., and Gunleiksrud, T.**
1991: Till tongue stratigraphy; *Bulletin of the Geological Society of America*, v. 103, p. 637-659.
- Warner, B.G., Mathewes, R.W., and Clague, J.J.**
1982: Ice-free conditions on the Queen Charlotte Islands, British Columbia, at the height of the Late Wisconsin Glaciation; *Science*, v. 218, p. 675-677.

Geological Survey of Canada Project 750108

Tertiary volcanic and subvolcanic rocks of central Moresby and Talunkwan islands, Queen Charlotte Islands, British Columbia

J.G. Souther

Cordilleran Division, Vancouver

Souther, J.G., 1993: Tertiary volcanic and subvolcanic rocks of central Moresby and Talunkwan islands, Queen Charlotte Islands, British Columbia; in Current Research, Part A; Geological Survey of Canada, Paper 93-1A, p. 129-137.

Abstract: Five areas of Tertiary volcanic and subvolcanic rocks were examined on central Moresby and Talunkwan islands. Each area includes basic and felsic phases ranging in composition from quartz-phyric rhyolite through andesite to basalt and diabase. However, the stratigraphy and crosscutting relationships are unique to each area and reveal no evidence of a regional paragenetic sequence. In four of the areas the eruptive rocks are associated with dyke swarms and/or sheeted intrusions comprising composite dyke complexes more than a kilometre wide and several kilometres long. Deformation of the Tertiary succession is limited to tilting, normal faulting, and local warping into open upright folds. No evidence of compressive folding or thrusting was observed in the areas examined.

Résumé : On a examiné dans la partie centrale des îles Moresby et Talunkwan cinq régions de roches volcaniques et subvolcaniques d'âge tertiaire. Chaque région contient des phases basiques et felsiques dont la composition passe de celle d'une rhyolite à gros cristaux de quartz, à celle d'une andésite puis à celle d'un basalte et d'une diabase. Cependant, les relations entre la stratigraphie et les contacts discordants sont uniques à chaque région et n'indiquent la présence d'aucune séquence paragenétique régionale. Dans quatre des secteurs, les roches éruptives sont associées à des essaims de dykes ou à des intrusions stratiformes comprenant des complexes de dykes composites de plus d'un kilomètre de large et de plusieurs kilomètres de long. La déformation de la succession du Tertiaire se limite à son basculement, à la formation de failles normales, et à des déformations en plis droits ouverts à l'échelle régionale. On n'a observé aucun indice de plissements par compression ou de chevauchements dans les secteurs examinés.

INTRODUCTION

Tertiary volcanic rocks underlie extensive areas on Graham Island (Hickson, 1991) in the northern Queen Charlotte Islands and similar strata are preserved as smaller remnants on Moresby and adjacent islands as far south as Ramsay Island (Fig. 1). In his pioneering work on the geology of the Queen Charlotte Islands, Sutherland Brown (1968) assigned all of these rocks to the Masset Formation, within which he recognized three distinct facies. The Tartu facies, which is restricted to Graham Island, was described as columnar basalt flows and rhyolitic ash flows. The Kootenay facies, which outcrops on west-central Moresby Island, was described as dominantly acid volcanics, while the Dana facies of east-central Moresby and adjacent islands was described as a complex area of mixed acid and basic intrusive and extrusive rocks. Three of the areas examined during the present study (Mount Russ, Kootenay North, and Takakia Lake) are located within Sutherland Brown's Kootenay facies and two (Redtop Mountain and Talunkwan Island) are in the Dana

facies. The Tertiary volcanic rocks on Lyell Island, also part of the Dana facies, were described in an earlier report (Souther, 1992).

KOOTENAY NORTH

The Tertiary succession north of Kootenay Inlet includes both basalt and rhyolite facies, comprising at least 600 m of volcanic flows and pyroclastic rocks associated with basic and felsic intrusive bodies (Fig. 2). An east-northeast-trending fault separates predominantly rhyolitic rocks on the south from predominantly basaltic rocks on the north.

The gently north-dipping to nearly flat-lying basaltic rocks north of the fault (Fig. 2) can be subdivided into a thick lower pile of pyroclastic rocks (KN-1) and an overlying succession of mainly basalt flows (KN-2). The pyroclastic pile is at least 300 m thick and consists mainly of thick-bedded basaltic breccias interlayered with a lesser volume of lapilli tuff and irregular flows. The breccias comprise angular to subrounded basaltic clasts randomly supported in a matrix of fine basaltic fragments and secondary alteration products. Most of the clasts are less than 10 cm across but a few are up to half a metre across. Individual beds are several tens of metres thick and a crude subhorizontal orientation of elongated clasts is the only internal expression of layering. Coarse- and fine-grained phases grade from one to another without any clear expression of bedding surfaces. All of the basalt clasts and associated flows in unit KN-1 are very fine grained to aphanitic. Most of them are aphyric or contain sparse 1 to 2 mm plagioclase phenocrysts. Quartz-epidote amygdules are locally abundant and these, plus the feldspar phenocrysts, weather out to give the deep brown weathered surface a rough, hackly texture.

The large proportion of pyroclastic rocks relative to flows in unit KN-1 suggests a proximal volcanic environment. However, no bombs or primary scoria deposits were

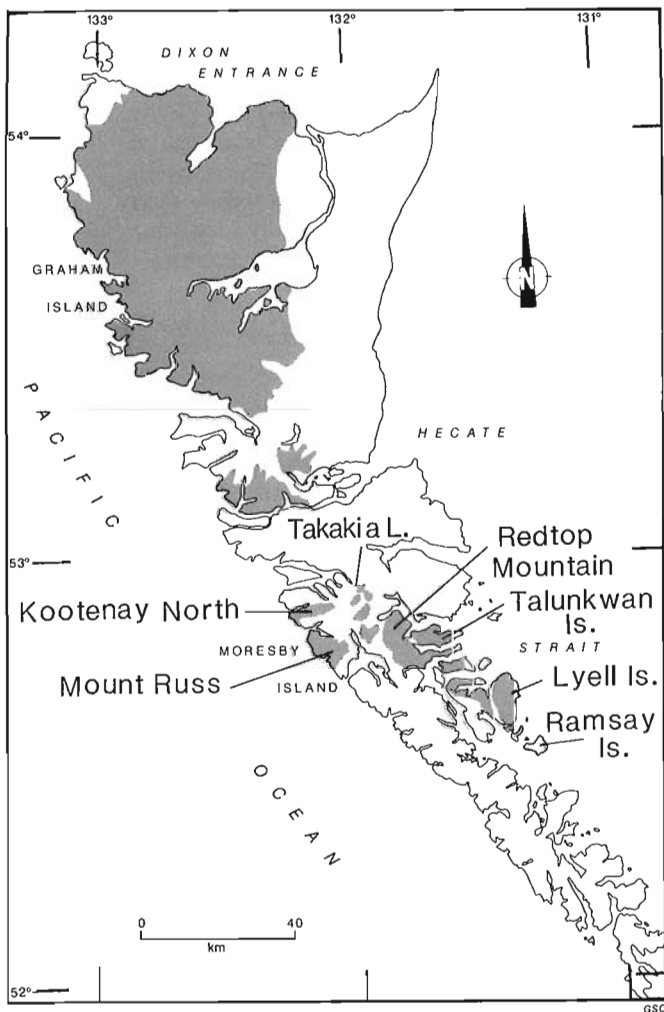


Figure 1. Index map showing the distribution of Tertiary volcanic rocks in the Queen Charlotte Islands (patterned area) and the locations of areas described in this report.

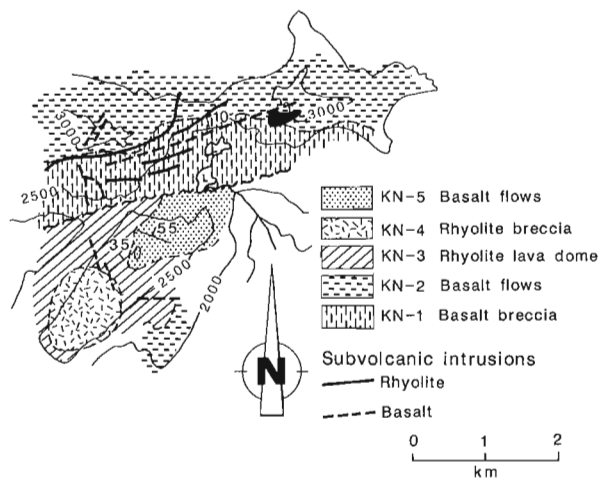


Figure 2. Sketch map of the Kootenay North area. For location see Figure 1.

observed. Instead the breccias have many features of subaqueous deposits. Pillows were seen at one locality and a 50-foot-thick succession of finely laminated tuff and carbonaceous silt are interlayered with the breccia at another. These are probably products of a lacustrine rather than a marine volcanic environment.

The basalt flows of unit KN-2 overlie the breccia succession conformably. Individual flows are 2 to 10 m thick with fairly well defined contacts. Columns are well developed locally but most of the flows have crude rectangular jointing normal to the contacts. The rock is medium grey, very fine grained, aphyric basalt.

The volcanic succession south of the fault includes both rhyolite (units KN-3, 4) and basalt (unit KN-5). The northeastern portion of the rhyolite complex consists of massive, finely flow-layered, aphyric rhyolite (unit KN-3) (Fig. 3) which exhibits the type of random, highly contorted flow folds and annealed fractures characteristic of large exogenous domes or very thick flows. The massive rhyolite of unit KN-3 grades southwesterly into rhyolite breccia



Figure 3. Flow layered rhyolite near the base of unit KN-3 (Fig. 2).



Figure 4. Rhyolite breccia from unit KN-4 (Fig. 2).

(unit KN-4) which is probably related to autobrecciation of the solidifying outer margins of the dome. The clasts are angular and mostly less than 20 cm across but clasts up to half a metre are present locally (Fig. 4). Many of the larger clasts exhibit the same fine flow-lamination that characterizes the massive rhyolite of unit KN-3 from which they were undoubtedly derived. The southern edge of the rhyolite complex is underlain by mafic flows of unknown age.

The northeast end of the rhyolite complex is overlain by steeply northeast-dipping basalt flows (unit KN-5). The basal flow of this unit is more than 15 m thick and its contact with the underlying rhyolite is sharp, displaying a well developed colonnade normal to the rhyolite surface. Overlying flows are thinner and have poorly developed rectangular cross-jointing. Like the basalt north of the fault all of these rocks are aphyric and very fine grained. The flows exhibit a steeper dip than those exposed north of the fault. The nearly vertical orientation of dykes both north and south of the fault suggests that tilting in itself cannot account for this difference. It seems likely, rather, that the flows of unit KN-5 issued from a nearby vent on the rhyolite dome and that their present attitude is due largely to steep initial dips on the steeply sloping surface of the underlying dome.

Subvolcanic intrusions are abundant throughout the Kootenay North area and are believed to be feeders for several local vents. White-weathering aphanitic rhyolite forms subvertical, east-northeast-trending tabular bodies that pinch and swell from 3 to more than 60 m thick. They are lithologically similar to the flow layered rhyolite of unit KN-4 and are probably part of the plumbing system related to the extrusive dome. Basalt dykes up to 15 m thick (Fig. 5) are present throughout the area but are best developed north of the fault. Most of them are part of an east-northeast (070°) swarm. Several dykes coalesce in the vicinity of the three major peaks in the area suggesting that these topographically high points may be erosional remnants of composite volcanoes from which the adjacent flows originated.

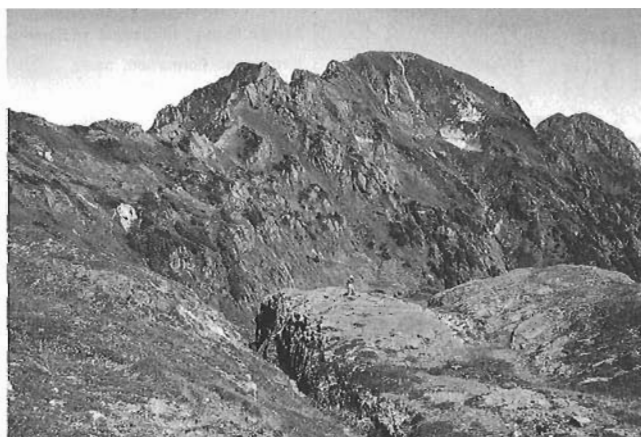


Figure 5. A 15 m basalt dyke cutting basalt flows and breccia of unit KN-1 (Fig. 2).

TAKAKIA LAKE

Sutherland Brown (1968) identified the Takakia Lake area as a major centre of Tertiary igneous activity and his map shows the complex relationship between faults and hypabyssal equivalents of the Masset Formation. The present work is in substantial agreement with Sutherland Brown's observations (Fig. 6). Medium grained diorite, which forms massive outcrops on benchlands along the east side of Takakia Lake, intrudes flaggy, rusty-weathering argillite of the Triassic/Jurassic Kunga Group. The contact, which is well exposed at several places, is generally concordant with the bedding and has moderate dips of less than 30° ; however, crosscutting relationships were also observed locally. Argillite adjacent to the contact has been baked to a hard, rusty-weathering hornfels but the adjacent massive diorite exhibits no apparent change in texture or alteration. Indeed the medium grained, massive diorite is remarkably uniform in texture and composition throughout the entire body. The only obvious internal structure is a random but pervasive network of quartz-feldspar-epidote veinlets which are probably of late stage deuteritic origin. Widely spaced subhorizontal jointing gives the rock a crudely layered aspect; these surfaces are not associated with any alteration, however, and are probably secondary (unloading) joints rather than primary igneous features.

Coarse grained diorite is exposed on the ridge north of Takakia Lake where it is in both intrusive and fault contact with Kunga Group sediments. Amygdaloidal basalt breccia, which forms small areas along the top of the ridge, also appears to be intruded by the diorite.

The ridge south of Takakia Lake is a complex of intrusive and extrusive Tertiary basaltic rocks which are spatially, and probably genetically, related to a zone of northeast-trending

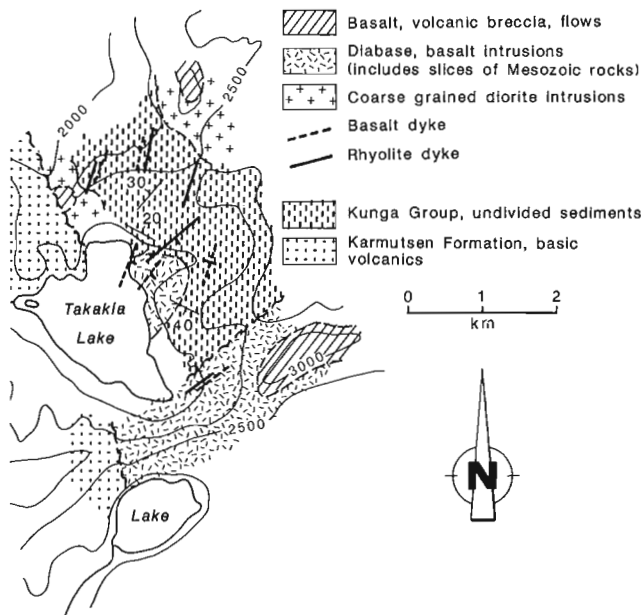


Figure 6. Sketch map of the Takakia Lake area. For location see Figure 1.

vertical faults. At the base of the succession, near the south end of Takakia Lake, massive basalt forms a succession of subhorizontal benches that resemble thick flows. However, the absence of columns or intraflow breccia suggests that these rocks are part of a subvolcanic intrusion with widely spaced, subhorizontal jointing similar to the body on the east side of the lake. Locally the massive lower basalt is cut by nearly vertical, northeast-trending dykes, faults, and slices of hornfelsed Kunga group sediments. The latter include both fault-bounded slices and inclusions up to several tens of metres across within the larger intrusive bodies (Fig. 7). Adjacent inclusions show clear evidence of relative rotation and must have been dragged a considerable distance by the rising magma. Thick tabular intrusions containing sedimentary inclusions occur up to the crest of the ridge at an elevation of 800 m. The lowest clearly extrusive volcanic breccia, followed by thick lava flows, occurs slightly higher, suggesting that only the uppermost part of the ridge is volcanic.

Basic and felsic dykes cut all of the Tertiary intrusions and adjacent country rock. The basic dykes comprise very fine grained, aphyric basalt. They are commonly from 1-3 m thick, have north-northwest trends, and dip from $60-90^\circ$ suggesting that there has been considerable post-emplacement tilting. The felsic dykes are fine grained, white-weathering rhyolite. They range from 1 m to more than 10 m thick and individual dykes can be traced along their northwesterly trends for more than 1 km. No extrusive equivalent of the felsic dykes was found in the Takakia Lake area.

The foregoing observations suggest that the Takakia Lake area was a locus of Tertiary magmatism where large successive volumes of basaltic magma rose into a northeast-trending zone of extension. The structure of the subvolcanic intrusions was controlled on the one hand by the extensional tectonic environment, giving rise to vertical tabular bodies, and by the structural anisotropy of the Kunga argillite which favoured the lateral injection of magma along bedding planes to form thick concordant sills and laccolith-like intrusions.



Figure 7. Large inclusion of Triassic(?) Kunga Group sediments in Tertiary basalt intrusion south of Takakia Lake. Vertical, sheeted basalt dykes form all but the uppermost part of peak in background. The peak itself is a mix of basaltic flows, breccia, and dykes.

MOUNT RUSS AREA

Mount Russ (elevation 860 m) is the highest point within a large area of undivided Masset volcanics which, on the regional map of the Queen Charlotte Islands (Sutherland Brown, 1968), are shown extending down to sea level on the west coast of Moresby Island. The succession dips gently toward the northwest and is at least 500 m thick. During the present study only the upper 150 m of section, the portion exposed above timberline, was examined (Fig. 8). There, the volcanic rocks comprise four distinct stratigraphic units and are underlain by several hundred metres of clastic sediments which are also believed to be part of the Tertiary succession.

The sediments, which are exposed over a broad area southeast of Mount Russ, form a well-stratified succession of thick sandstone and conglomerate beds that appear to lie conformably under the adjacent pile of Masset volcanic rocks. The succession is not folded and dips are uniformly about 15° toward the northwest. The outcrops visited during this study are predominantly coarse grained cross-stratified sandstone, in 1 to 3 m thick beds (Fig. 9). Well rounded pebbles from 2 to 6 cm across occur as isolated, randomly distributed clasts within the sands, in interbeds from 5 or 10 cm thick (Fig. 10), as well as in framework-supported conglomerate beds up to 1 m thick. The pebbles comprise a high proportion of white quartz and a variety of other lithologies, including fine grained diorite, and metasedimentary and metavolcanic rocks, which could have been derived from Yakoun or older Mesozoic rocks. Although originally mapped as Cretaceous Honna Formation (Sutherland Brown, 1968), the apparently conformable relationship between the sediments and the adjacent volcanic pile, as well as the lithological similarity between these sediments and Tertiary sediments described in

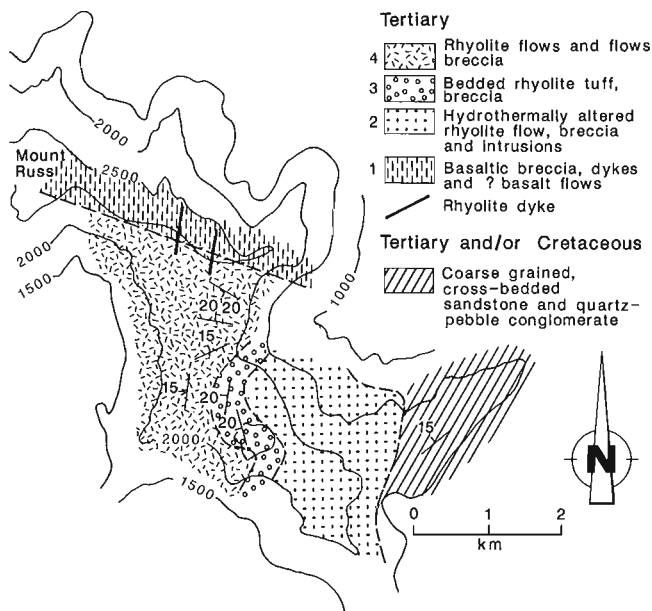


Figure 8. Sketch map of the Mount Russ area. For location see Figure 1.

a similar stratigraphic position on Mount Stapleton by Haggart et al. (1990), suggest that these rocks are part of the Tertiary succession.

The Tertiary volcanic rocks of Mount Russ area are divided into two distinct facies by a prominent west-northwest-trending lineament along the ridge southwest of Mount Russ (Fig. 8). South of the lineament rhyolite flows and pyroclastic rocks (units 2, 3, 4) predominate – indeed the only basaltic rock seen south of this lineament is a single two-foot-thick dyke. In contrast, rocks north of the lineament (unit 1) comprise basaltic breccia, mixed breccia containing basalt and minor rhyolite clasts, and extensive outcrops and cliffs of massive, fine grained, aphyric basalt. The trace of the lineament is extremely straight, suggesting that it is a vertical structure and not a stratigraphic contact within or overlying the gently northwest-dipping rhyolite succession. Basaltic rocks north of the lineament are cut in several places by northeast-trending rhyolite dykes up to 10 m thick. At one point along the lineament, the rhyolite is in contact with a large exposure (Fig. 11) of epiclastic breccia comprising randomly stacked, subrounded boulders of basalt up to 1.5 m across.



Figure 9. Cross-stratification in coarse Tertiary sandstone near the base of the Mount Russ volcanic succession.



Figure 10. Massive bed of coarse Tertiary sandstone near the base of the Mount Russ volcanic succession. Well rounded pebbles are mostly white quartz.

The lower part of the rhyolitic pile (unit 2, Fig. 8) consists almost entirely of very coarse proximal rhyolite breccia and thick rhyolite flows with well developed flow layering. The latter commonly displays convoluted flow folds with apparently random orientations. The unit is characterized by extensive fracturing and rusty weathering, which suggest a relatively high degree of hydrothermal alteration.

Unit 2 is overlain conformably by about 200 m of well bedded rhyolite tuff and tuff-breccia (unit 3), interlayered with a few spherulitic rhyolite flows (Fig. 12). Tuff beds are commonly 2 to 10 m thick and have persistent internal layering due to crude sorting of clasts ranging in size from fine grit and lapilli to angular, fracture-bounded granules of white rhyolite from 2 to 15 cm across. Many of the clasts are flat, about 1 cm thick, and were probably derived from mechanical disintegration of flow-layered rhyolite. Locally, angular clasts of flow-layered rhyolite up to a half metre across are randomly suspended within the thin-bedded, fine grained tuff sequences (Fig. 13). Individual tuff layers commonly display normal and reverse grading. They are believed to be subaerial tuffs deposited on a steeply inclined surface at or near the angle of



Figure 11. Basaltic epiclastic breccia located near the east end of the Mount Russ lineament (Fig. 8). This east-trending lineament, which separates basaltic rocks on the north from rhyolitic rocks on the south, may be a synvolcanic fault scarp.



Figure 12. View looking south at west-dipping beds of tuff (unit 3, Fig. 8) south of Mount Russ.

repose. Many of the anomalously large clasts within the tuffs were probably thrown or rolled onto the slope during periodic bursts of explosive activity.

The bedded tuff is overlain conformably by a succession of thick rhyolite flows, and flow breccia (unit 4). The flows commonly comprise varying proportions of massive rhyolite with convoluted flow layering at the base (Fig. 14), a core of spherulitic rhyolite with closely spaced bands of lithophysae (Fig. 15), and an upper zone of blocky flow breccia comprising variously deformed and bent interlocking rectangular blocks of flow layered rhyolite (Fig. 16).

Dips up to 20° in the well bedded tuff succession are probably to a large extent primary. However, some tilting has occurred and minor flexuring has produced local upright folds in the thick flows and breccias in unit 4 (Fig. 17). The west-northwest linear feature that separates basaltic rocks on the Mount Russ ridge from the rhyolitic complex farther south appears to run across the topography like a fault rather than a stratigraphic contact. Although the nature of this lineament is still unresolved, its association with basaltic epiclastic deposits suggests that it may be the trace of a synvolcanic fault scarp – either a graben boundary or a caldera margin – against which the rhyolitic assemblage was ponded.



Figure 13. Ballistic block of flow-banded rhyolite suspended in fine grained, thin-bedded tuff of unit 3 (Fig. 8).



Figure 14. Flow layered rhyolite at the base of a thick flow south of Mount Russ (unit 4, Fig. 8).



Figure 15. Large, drusy lithophysae in the central part of a thick rhyolite flow south of Mount Russ (unit 4, Fig. 8).



Figure 16. Rhyolite flow-top breccia comprising interlocking and plastically deformed blocks of flow-banded rhyolite in the upper part of a thick flow south of Mount Russ (unit 4, Fig. 8).



Figure 17. Fold in thick rhyolite flows south of Mount Russ (unit 4, Fig. 8).

REDTOP MOUNTAIN

Redtop Mountain forms a prominent, conical peak near the centre of a large area of undivided Masset Formation on northeastern Moresby Island (Fig. 18). The peak itself (Fig. 19) consists mostly of fine- to medium-grained aphyric andesite, a lesser amount of fine grained aphyric basalt, and a small proportion of quartz-feldspar-phyric rhyolite. All of these rocks occur as north-northeast-trending vertical dykes which together form a composite sheeted intrusion at least 2.5 km across. Individual dykes are from 1 m to more than 10 m thick and their orientation is remarkably consistent (015°). Indeed, the trace of the swarm is clearly visible as fine,

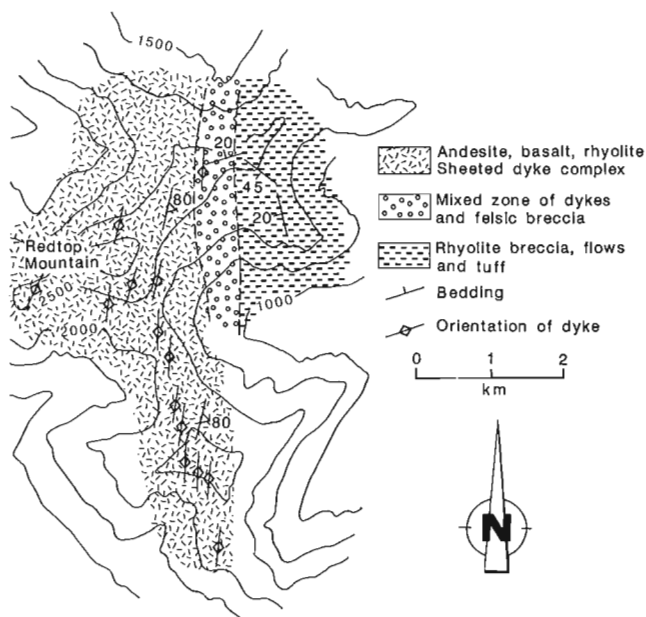


Figure 18. Sketch map of the Redtop Mountain area. For location see Figure 1.



Figure 19. View looking west to Redtop Mountain. The summit and all of the ridge visible to the left of the summit consist of vertical intrusions which form a sheeted dyke complex at least 1.5 km wide.

perfectly straight parallel lines on air photos. The complex is exposed for a length of about 7 km and extends an unknown distance into heavily forested terrane beyond the mapped area.

The internal structure of the swarm suggests a complex history of emplacement. In the central part, dykes are in mutual contact and basalt is commonly the youngest phase. However, basalt dykes are locally cut by, and form fragments within, rhyolite dykes.

Near the eastern edge of the swarm the dykes enclose isolated screens of felsic volcanic breccia, while a thick succession of similar breccia, interlayered with flow-banded rhyolite flows, forms the ridges farther east. The extrusive rocks consist entirely of rhyolite, comprising thin bedded tuff with prominent laminar bedding, thick beds of breccia containing angular clasts up to half a metre across, and banded rhyolite flows and flow-breccia with convoluted flow folds. The volcanic rocks are cut by widely spaced, 2 to 10 m thick basalt dykes which parallel the north-northeasterly trend of the adjacent sheeted complex.

The above relationships suggest that Redtop Mountain lies on the axis of a north-northeast-trending zone of Tertiary extension which served as a conduit for the successive intrusion of andesitic, basaltic, and rhyolitic magmas which erupted to form the thick piles of Masset volcanic rocks now exposed on northern Moresby Island. The orientation of the Redtop Mountain swarm is similar to that of the Tasu Inlet swarm and both contain a high proportion of basaltic dykes (Souther and Jessop, 1991). This is in contrast with the easterly trend of predominantly andesitic dykes in the adjacent Selwyn Inlet-Talunkwan swarm. The Redtop and Tasu swarms are probably related to the same regional stress field, and by inference, to the same episode of Tertiary igneous activity.

TALUNKWAN ISLAND

A cursory examination of Tertiary volcanic rocks on western Talunkwan Island (Fig. 20) reveals significant differences between that pile and the nearby Tertiary succession on Redtop Mountain. The Talunkwan section is at least 600 m thick and consists primarily of andesite flows and breccias interlayered locally with thin-bedded tuff. Although many of the rocks weather to light shades of grey, green, and brick red, freshly broken surfaces are commonly very dark green to black, suggesting a relatively basic composition. Clasts in the breccias are angular to subrounded and range in size from lapilli up to half a metre across. The majority are aphyric but 1 to 2 mm phenocrysts of white feldspar are abundant in some of the andesite clasts. The same lithologies are present in the interlayered flows. These are commonly highly fractured and lack any systematic joint pattern. Many are amygdaloidal with elliptical vesicles filled with quartz and carbonate.

The Talunkwan pile is cut by a profusion of andesite, basalt and, less commonly, felsic dykes with east-northeast trends. Most of the rocks, including many of the dykes, are

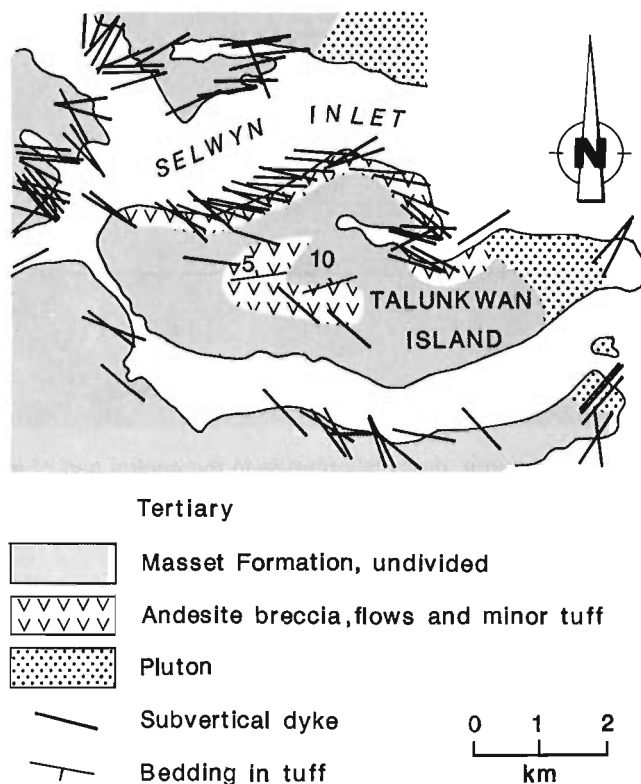


Figure 20. Sketch map showing the orientation of dykes on Talunkwan Island. For location see Figure 1.

highly fractured and veined with stockworks of quartz and carbonate. Despite this pervasive fracturing, the pile as a whole does not appear to have been significantly deformed or offset by major faults. Instead, the fracturing and veining appear to be the result of synvolcanic deformation related to intrusion and other internal forces associated with the construction of a large, subaerial volcanic edifice. In the area studied the attitude of bedded tuffs is remarkably consistent (northerly dips of 5-15°) and the dykes, though commonly fractured, are predominantly vertical. All of the pyroclastic rocks examined on Talunkwan Island are of subaerial origin. This is in marked contrast with the Lyell Island pile farther south (Souther, 1992) where subaqueous breccias predominate.

DISCUSSION

The Tertiary volcanic and associated hypabyssal rocks of central Moresby and Talunkwan islands display a wide range of compositions, from quartz-phyric rhyolite through andesite to basalt and diabase. Several of the piles are bimodal. However, no consistent temporal relationship between basic and felsic volcanism was established. Indeed the crosscutting relationships of intrusions and superposition of eruptive rocks at Kootenay North, Redtop Mountain, and Talunkwan Island suggest that repeated shifts from basic to felsic magmatism were the rule.

Four of the volcanic centres examined (Kootenay North, Redtop Mountain, Takakia Lake, and Talunkwan Island) are associated with dyke swarms or subvolcanic intrusions. In the case of Redtop Mountain and Takakia Lake, the intrusions comprise sheeted dyke complexes a kilometre or more wide, whereas dykes in the other areas are separated by screens of Tertiary volcanic or pre-Tertiary rock. The orientation of these intrusions is remarkably consistent internally but varies from area to area, suggesting that the stress fields controlling extension and dyke emplacement were of relatively local extent.

Little evidence of posteruption deformation was seen in any of the Tertiary piles examined. Normal faults in the Kootenay North and Russ Mountain areas could be the result of synvolcanic deformation related to extension or caldera formation. Similarly, the inclination of beds in the Russ Mountain and Redtop Mountain areas is probably due in part to high initial dips. Some posteruption tilting and warping of the Tertiary succession has undoubtedly occurred.

The great thickness and close proximity of Tertiary volcanic rocks on Lyell Island, Talunkwan Island, and Redtop Mountain suggest that they were originally part of a contiguous volcanic complex comprising the overlapping piles of ejecta from several discrete centres. The position of this complex is roughly coincident with the intersection of north-northeast-trending dykes of the Tasu Sound-Redtop Mountain swarm and east-trending dykes of the Selwyn Inlet-Talunkwan Island swarm (Souther and Jessop, 1991). Volcanism in the Redtop-Talunkwan region was primarily subaerial whereas farther south, on Lyell Island, the presence of subaqueous breccias (Souther, 1992) suggests that the southern edge of the volcanic complex encroached on the sea.

ACKNOWLEDGMENTS

The author wishes to thank M.E.K. Souther for able assistance with the field work, and Jim Haggart for critical review of the manuscript.

REFERENCES

- Haggart, J.W., Indrelid, J., Hesthammer, J., Gamba, C.A., and White, J.M.**
 1990: A geological reconnaissance of the Mount Stapleton-Yakoun Lake region, central Queen Charlotte Islands, British Columbia; in *Current Research, Part F*; Geological Survey of Canada, Paper 90-1F, p. 29-36.
- Hickson, C.J.**
 1991: The Masset Formation on Graham Island, Queen Charlotte Islands, British Columbia; in *Evolution and Hydrocarbon Potential of the Queen Charlotte Basin, British Columbia*, (ed.) G.J. Woodsworth; Geological Survey of Canada, Paper 90-10, p. 304-324.
- Souther, J.G.**
 1992: Geology of central Lyell Island, Queen Charlotte Islands, British Columbia; in *Current Research, Part A*; Geological Survey of Canada, Paper 92-1A, p. 343-350.
- Souther, J.G. and Jessop, A.M.**
 1991: Dyke swarms in the Queen Charlotte Islands, British Columbia, and implications for hydrocarbon exploration; in *Evolution and Hydrocarbon Potential of the Queen Charlotte Basin, British Columbia*, (ed.) G.J. Woodsworth; Geological Survey of Canada, Paper 90-10, p. 465-487.
- Sutherland Brown, A.**
 1968: Geology of the Queen Charlotte Islands, British Columbia; British Columbia Department of Energy, Mines and Petroleum Resources, Bulletin 54, 226 p.

Geological Survey of Canada Project 870070

Stratigraphy and sedimentology of the Upper Jurassic to Lower Cretaceous Longarm Formation, Queen Charlotte Islands, British Columbia

C.A. Gamba¹

Cordilleran Division

Gamba, C.A., 1993: Stratigraphy and sedimentology of the Upper Jurassic to Lower Cretaceous Longarm Formation, Queen Charlotte Islands, British Columbia; in Current Research, Part A; Geological Survey of Canada, Paper 93-1A, p. 139-148.

Abstract: Three packages are recognized within the Upper Jurassic to Lower Cretaceous Longarm Formation as presently defined. Package A comprises Upper Oxfordian to Tithonian gravelly fan delta deposits emplaced along the eastern margin of a small fault-bounded forearc basin. Upper Valanginian to Hauterivian package B comprises three progradational coarsening-upward muddy offshore to sandy shoreface sequences deposited during three relative sea-level falls or stillstands within a greatly enlarged forearc basin. Hauterivian to Aptian package C comprises a single retrogradational sandy shoreface to deep basinal fining-upward sequence deposited during a prolonged period of relative sea-level rise. The inferred northwest-southeast paleoshoreline trend derived from each package parallels the orientation of most Late Mesozoic faults exposed on the islands. Enlargement of the basin throughout Late Jurassic to mid-Cretaceous time tracked the progressive eastward migration of magmatism within the adjacent magmatic arc.

Résumé : On a identifié trois ensembles (du Jurassique supérieur au Crétacé inférieur) dans la Formation de Longarm, telle que présentement définie. L'ensemble A englobe des sédiments graveleux de cône de déjection (de l'Oxfordien supérieur au Tithonique) qui se sont accumulés sur la marge orientale d'un petit bassin d'avant-arc limité par des failles. L'ensemble B (du Valanginien supérieur au Hauterivien) englobe trois séquences négatives progradantes, des types extracôtier boueux à infratidal sableux, mises en place au cours de trois abaissements ou stabilisations relatifs du niveau de la mer dans un bassin d'avant-arc fortement agrandi. L'ensemble C (du Hauterivien à l'Aptien) englobe une seule séquence positive régressive dans laquelle les sédiments sableux de zone infratidale passent à des sédiments profonds de bassin, ces sédiments s'étant accumulés pendant une période prolongée de montée relative du niveau de la mer. L'ancienne ligne de rivage présumée, de direction nord-ouest sud-est, telle que déduite de l'examen de chaque ensemble, suit l'orientation de la plupart des failles du Mésozoïque tardif affleurant dans les îles. L'agrandissement du bassin pendant tout l'intervalle du Jurassique tardif au Crétacé moyen a suivi la migration progressive vers l'est du magmatisme survenant à l'intérieur de l'arc magmatique adjacent.

¹ Department of Geology, McMaster University, 1280 Main Street West, Hamilton, Ontario L8S 4M1

INTRODUCTION

Sutherland Brown (1968) introduced the name Longarm Formation for a succession of Late Valanginian to Barremian clastics and volcanics unconformably underlain by pre-Cretaceous strata and overlain by Albian strata of the Haida Formation (Table 1). On the basis of new macrofossil collections, Haggart (1989) tentatively expanded the Longarm Formation to include a succession of Tithonian strata exposed 2.5 km south of White Point on northwestern Graham Island, and a succession of probable lower Aptian strata exposed at Dawson Cove in western Cumshewa Inlet (Fig. 1). Haggart (1989) suggested that the Longarm Formation formed a 450 m thick fining-upwards sequence from basal Tithonian conglomerate through upper Aptian mudstone deposited during a single prolonged period of marine transgression. Haggart (1989) suggested that the Tithonian strata exposed at White Point may however reflect a separate cycle of deposition independent of that represented by Longarm strata exposed elsewhere. Reconnaissance of Hauterivian to Barremian strata exposed on southern Moresby Island by Haggart and Gamba (1990) led to the recognition of six distinct lithofacies which formed a thick transgressive (retrogradational) fining-upward sequence unconformably underlain by pre-Cretaceous strata.

Haggart (1991) suggested that a complete section of Hauterivian to Aptian Longarm strata exposed at Dawson Cove, western Cumshewa Inlet, were gradationally overlain by Lower Albian strata of the Haida Formation exposed to the east. As a result, Haggart (1991) proposed that both the Longarm and Haida formations were deposited during a single marine transgression spanning Tithonian to Turonian time. Transgression resulted in the progressive eastward onlap of marine strata onto the margins of the basin throughout this period (Haggart, 1991: Fig. 8). Haggart (1991) also noted that, contrary to Sutherland Brown (1968), no interstratified volcanics occur within the Longarm Formation.

Gamba (1991) divided the Longarm strata exposed near White Point into three distinct lithofacies assemblages: a conglomerate assemblage and a mudstone assemblage both of Tithonian age, and a sandstone assemblage of Late Valanginian to Hauterivian age (Gamba, 1991: Fig. 2). Gamba (1991) noted that the contact between the Tithonian assemblages and the Upper Valanginian to Hauterivian assemblage was faulted. He also suggested that the Tithonian assemblages represented the deposits of a gravelly shelf-type fan delta emplaced within a fault-bounded basin, while the younger Late Valanginian to Hauterivian sandstone assemblage represented two progradational shoreface sequences deposited during two episodes of relative sea-level fall or stillstand. It was concluded that, unlike Hauterivian to Aptian strata exposed elsewhere on the Charlottes, the Tithonian and Upper Valanginian to Hauterivian strata exposed near White Point did not reflect deposition under conditions of steadily rising sea level (Gamba, 1991). On the basis of new macrofossil collections retrieved from these exposures, Haggart (1992) proposed a Late Oxfordian to Tithonian age for the conglomerate assemblage. Haggart (1992) suggested that the Upper Jurassic strata were gradationally overlain by the Upper Valanginian to Hauterivian strata, and that both were deposited within a regime of steadily rising sea level.

Table 1. Previous and revised stratigraphy of the Longarm Formation

		Sutherland Brown (1968)	Thompson et al. (1991)	This paper
CRETACEOUS	Cenomanian			
	Albian	HAIDA FORMATION	HAIDA FORMATION	HAIDA FORMATION
	Aptian	? ? ?		
	Barremian	LONGARM FORMATION		
	Hauterivian		LONGARM FORMATION	C
	Valanginian			B
JURASSIC	Berriasian		LONGARM FORMATION	
	Tithonian			A
	Kimmeridgian			
	Oxfordian			

nonconformable contact
 conformable (?) contact

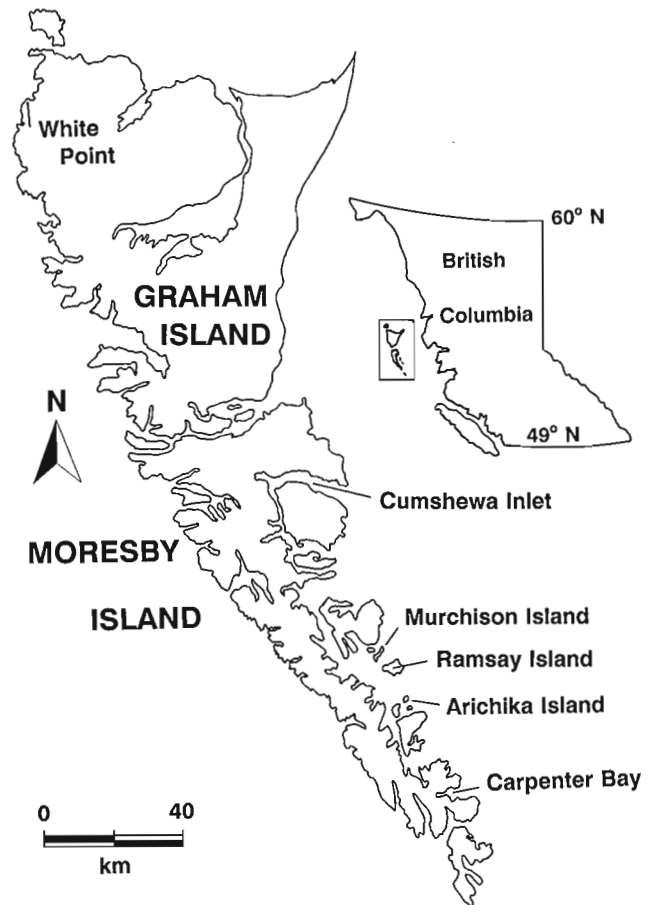


Figure 1. Location of measured sections.

As presently defined by Thompson et al. (1991) and Haggart (1991), the Longarm Formation is of Late Oxfordian to Aptian age, is unconformably underlain by pre-Late Jurassic strata and is gradationally overlain by Albian strata of the Haida Formation (Table 1). As a result of new field data collected during the 1989 through 1991 field seasons, enough sedimentological and biostratigraphic data now exist to attempt a stratigraphic analysis of the Longarm Formation. Such an analysis is necessary to: 1) account for the temporal gap contained within the Longarm Formation, 2) account for the diversity of depositional systems preserved within the Longarm Formation, and 3) to address the nature and significance of the contact between the Longarm and Haida formations.

STRATIGRAPHY OF THE LONGARM FORMATION

The Longarm Formation may be subdivided into three packages: a Late Oxfordian to Tithonian package A, a Late Valanginian to Hauterivian package B, and a Hauterivian to Aptian package C (Table 1).

Package A

Upper Jurassic strata exposed near White Point, northwest Graham Island, are assigned to package A. Arguments supporting this division are as follows. First, Upper Oxfordian to Tithonian strata and Upper Valanginian strata exposed here are not conformable and gradational as maintained by Haggart (1989, 1992), but are separated by a prominent fault (Gamba, 1991: Fig. 2). Second, Berriasian and Lower Valanginian strata linking the Upper Oxfordian-Tithonian strata to the overlying Upper Valanginian-Hauterivian strata are exposed neither at this location nor anywhere else on the Charlottes. The absence of such strata suggests that the Upper Jurassic and Lower Cretaceous strata may be separated by a nondepositional and possibly even erosional hiatus. Alternatively, as suggested by J.W. Haggart (pers. comm., 1992), strata of this age are poorly represented within western British Columbia. Third, Upper Jurassic strata exposed near White Point represent the deposits of a gravelly shelf-type fan delta emplaced adjacent to a fault-controlled margin (Gamba, 1991). Lower Cretaceous deposits of the Longarm Formation exposed elsewhere represent high-energy sandy shoreface to submarine fan deposits emplaced within a much expanded Cretaceous basin (Haggart and Gamba, 1990; Gamba, 1991). The two depositional systems, which are of completely different character, are neither temporally nor spatially linked.

Package A therefore comprises 310 m of Upper Oxfordian to Tithonian conglomerate and mudstone. The package is probably nonconformably underlain by Middle to Upper Jurassic volcanics, and is probably unconformably overlain by Upper Valanginian to Hauterivian strata of package B (Table 1).

Package B

Upper Valanginian to Hauterivian strata of the Longarm Formation are exposed near White Point on northwestern Graham Island and at Tana Point and Skidegate Narrows on southern Graham Island. At Tana Point, poorly exposed Upper Valanginian strata apparently overlie volcanics and interstratified clastics of the Middle Jurassic Yakoun Group (Sutherland Brown, 1968; Haggart, 1992). At Skidegate Narrows, poorly exposed Upper Valanginian strata are in close proximity to Lower and Middle Jurassic strata (Haggart et al., 1989).

The strata exposed at these locations are assigned to package B. Arguments supporting this division are as follows. First, Upper Valanginian to Hauterivian strata are probably nonconformably underlain by the Upper Jurassic deposits of package A. Second, Upper Valanginian strata are confined to Graham Island, and are not exposed south of Skidegate Narrows. Within the southern archipelago the oldest Longarm strata are of Hauterivian age and are unconformably underlain by pre-Cretaceous strata (Haggart and Gamba, 1990). Deposition of the Upper Valanginian part of package B was therefore confined to the Graham Island area. Third, Upper Valanginian to Hauterivian strata exposed near White Point consist of three progradational shallow marine sequences (Gamba, 1991). In contrast, Hauterivian to Aptian Longarm strata exposed elsewhere form a single, retrogradational sequence (Haggart and Gamba, 1990).

The nature of the upper boundary of package B with Hauterivian to Aptian strata of package C is unknown. In the southern islands, basal Hauterivian strata of package C consist of a conglomeratic transgressive lag which unconformably overlies pre-Cretaceous strata. It is possible that a similar transgressive lag overlies the uppermost progradational sequence within package B. Basal Hauterivian strata of package C exposed to the south may also be younger than Hauterivian strata of package B exposed to the north. The poor resolution of the Early Cretaceous biostratigraphic framework however precludes the differentiation of Lower and Upper Hauterivian strata. Finally, it is equally possible that Hauterivian strata of package B are transitional southwards into those of package C.

Package B therefore comprises 212 m of Upper Valanginian to Hauterivian mudstone and sandstone which are probably unconformably underlain by Upper Jurassic strata of package A and are overlain either nonconformably or gradationally by Hauterivian to Aptian strata of package C (Table 1).

Package C

Hauterivian to Aptian strata of the Longarm are exposed at various locations on southern Graham Island and Moresby Island (Haggart and Gamba, 1990). These strata are assigned to package C. The evidence in favour of this division were addressed above.

Package C therefore comprises a 215 m thick fining-upward sequence of Hauterivian to Aptian sandstone and mudstone which is unconformably underlain by pre-Cretaceous

strata in the southern islands and either nonconformably or gradationally underlain by Lower Valanginian to Hauterivian strata of package B in southern Graham Island (Table 1). Based upon the stratigraphic relations exposed in the Dawson Cove area of western Cumshewa Inlet, Haggart (1991) suggested that the Longarm Formation was gradationally overlain the Haida Formation. Although the actual contact between Aptian strata of the Longarm Formation and Albian strata of the Haida Formation is not exposed on the islands, several features indicate that it is nonconformable. First, the lowermost strata of the Haida Formation exposed on southern Graham and northern Moresby Island, including those exposed at Dawson Cove, are of late Early Albian age

(*Breweriaceras hulenense* zone) (Sutherland Brown, 1968; McLearn, 1972; Haggart, 1986). Lowermost Albian Haida strata are exposed only at Beresford Bay on northwestern Graham Island, where they are apparently unconformably underlain by Middle Jurassic volcanics of the Yakoun Group (Hickson and Lewis, 1990). The absence of lower Lower Albian strata in the central islands may be indicative of a non-depositional or erosional hiatus in the central islands area.

Second, recent observations made in the eastern Skidegate Narrows area by the author during the 1991 field season indicate that shallow-marine Albian sandstone of the Haida Formation are in close proximity to deep-marine Aptian mudstone of the Longarm Formation exposed 7.5 km to the

Table 2. Description and interpretation of the facies of the Longarm Formation.
HCS – hummocky cross-stratification

FACIES	DESCRIPTION	INTERPRETATION
Unstratified conglomerate	Clast-supported, poorly-sorted pebble to boulder cong., graded to ungraded, beds amalgamated, 0.2 - 2.7 m, a(p) a(l) fabric, bivalves.	High concentration turbidites, nearshore
Cross-stratified conglomerate	Clast-supported, mod. sorted pebble and cobble cong., trough or low-angle cross-stratified, sets 0.1 to 1.5 m, beds < 5.6 m.	3-d dunes and bars, shallow marine.
Channelized conglomerate	Clast-supported, poorly-sorted, pebble to boulder cong., massive, a(t) b(l) fabric, infill incised channels with up to 4.7 m relief.	Distributary channels.
Matrix-supported cong / breccia	Matrix-supported, poorly-sorted breccia, massive, beds < 0.9 m, a(p) fabric.	Debris flows, shallow marine.
Transgressive cong / breccia	Clast-supported, poorly-sorted, pebble to boulder cong / breccia, massive, beds 0.1 - 15.4 m, boulders up to 15 m, bivalve fragments.	Transgressive reworked lag, shallow shoreface.
Trough cross-stratified sandst.	Mod. sorted fine to coarse pebbly sst., sets solitary or grouped, 0.1 - 0.9 m, bivalve fragments and traces of <i>Skolithos</i> ichnofacies.	Barred sandy shoreface.
Swaley cross-stratified sandst.	Well-sorted fine to medium pebbly sst., beds 0.2 - 10.1 m, bivalve frags, inter massive clast-supported cong., beds 0.1 - 0.3 m.	Storm deposits, high-energy sandy shoreface.
Structureless bioturbated sst	Poorly-sorted, fine silty sst., heavily bioturbated, beds 0.2 - 15 m, inter HCS sst, traces of the <i>Cruziana</i> ichnofacies, bivalves.	Storm deposits, sandy offshore.
Amalgamated HCS sst	Well-sorted fine sst., beds amalgamated, 0.5 - 1.9 m, minor interbedded silty mudstone, traces of the <i>Cruziana</i> ichnofacies.	Storm deposits, transitional sandy offshore.
Massive pebbly sandstone	Poorly-sorted, fine to coarse pebbly sst., beds up to 1.6 m, oriented belemnites, abundant intraclasts with a(p) fabric.	High concentration turbidites, offshore
Channelized unstratified sst	Mod. sorted coarse pebbly sst, normally graded (Ta), with basal intraclast lag, beds highly lenticular, 0.6 to 5.6 m.	Turbidites, muddy offshore.
Interbedded mud and sandstone	Sandy mudst with inter fine-medium sst, thin (< 0.1 m) or thick (> 0.1 m) bedded, HCS, wave-rippled, or massive, beds < 0.8 m., oriented belemnites, traces of the <i>Zoophycos</i> ichnofacies.	Storm deposits, muddy offshore.
Disorganized mudstone	Matrix- to clast-supported, massive, intraclasts < 5 m, beds 2.9 - 13.2 m, rafted boulders of granite (2 m), andesite, and intraclasts.	Cohesive debris flows, muddy offshore.
Silty mudstone	Silty mudstone, in-situ bivalves, minor inter massive fine sst.	Distal muddy offshore.
Thin-bedded turbidites	Mudstone and interbedded thin (< 10 cm) fine sst., unstratified (Ta) parallel-laminated (Tb) or current-rippled (Tc), minor pebbles.	Classical turbidites submarine fan.
Pebbly sandstone turbidites	Mod. sorted, fine to medium pebbly sst., Ta, Tb, beds < 0.4 m, basal pebble lag < 0.2 m, interbedded intraclast breccias up to 1.2 m.	Submarine fan channel deposits.

northwest in Long Inlet. The occurrence of Albian Haida sandstones so close to Aptian Longarm mudstones indicates that the contact between the two formations is probably abrupt and nonconformable (i.e. Aptian offshore mudstones overlain by Albian shoreface sandstones). The absence of lower Lower Albian strata within the southern Graham-Moresby Island area may therefore reflect a relative sea-level fall accompanied by regional erosion and the westward progradation of the late Early Albian Haida shoreface. What follows is a brief discussion of the sedimentology of each of the packages.

SEDIMENTOLOGY AND DEPOSITIONAL SYNTHESIS

In this section, the previous facies schemes developed for the Longarm Formation by Haggart and Gamba (1990) and Gamba (1991) are modified. Each package is divided into facies assemblages, each comprising a variety of genetically related facies. A facies is defined on the basis of lithology, primary sedimentary structures, and type and degree of bioturbation. The assemblages of different packages may share some of the same facies. A description and interpretation of each of the facies within the Longarm Formation is presented in Table 2, while the occurrence of each facies, by package, is presented in Table 3.

Table 3. Distribution of facies within packages A, B, and C of the Longarm Formation

FACIES	A	B	C
Unstratified conglomerate	X		X
Cross-stratified conglomerate	X		X
Channelized conglomerate	X		
Matrix-supported cong / breccia			X
Transgressive cong / breccia		X	X
Trough cross-stratified sandst.	X	X	X
Swaley cross-stratified sandst.	X	X	X
Structureless bioturbated sst			X
Amalgamated hummocky cross-stratified sandstone		X	X
Massive pebbly sandstone			X
Channelized unstratified sst	X		
Interbedded mud and sandstone	X	X	X
Disorganized mudstone	X	X	
Silty mudstone			X
Thin-bedded turbidites			X
Pebbly sandstone turbidites			X

Package A

Two assemblages, comprising seven different facies, are recognized within package A: a conglomerate assemblage and a mudstone assemblage (Fig. 2). The facies of the conglomerate assemblage represent shelf-type fan delta deposits. The unstratified conglomerate facies, which form the bulk of this assemblage, represents the deposits of high concentration turbidity currents. The occurrence of interstratified swaley and hummocky cross-stratified (SCS and HCS respectively) sandstone units with these conglomerates indicates deposition within an environment situated above storm wave base. The stratified conglomerate facies represent distributary mouth bar deposits emplaced within a fan delta-front setting. The channelized conglomerate facies represent distributary channel deposits. The distribution of paleocurrent trends derived from clast imbrication within the unstratified conglomerate facies reflects radial north-northwest to south-southeast paleoflow upon the surface of the fan-shaped subaqueous delta-front from a source located to the east-northeast (Fig. 4C). The inferred package A paleoshoreline was therefore probably oriented northwest-southeast.

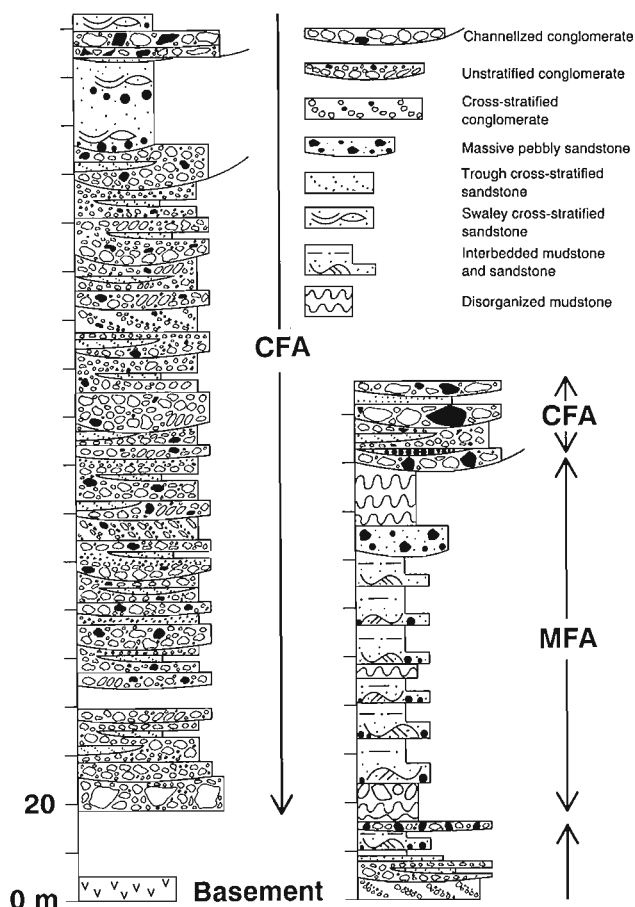


Figure 2. Stratigraphic section of package A exposed south of White Point, northwestern Graham Island. CFA – conglomerate facies assemblage, MFA – mudstone facies assemblage.

Smaller-scale cyclic packages between 10 and 22 m thick comprising a lower unit of fan delta-slope deposits overlain by a unit of fan delta-front deposits and capped by distributary channel deposits occur within the lowermost succession of the conglomerate assemblage. These cyclic packages represent the basinwards progradation of individual fan delta lobes.

The mudstone facies assemblage was deposited within a muddy slope environment located basinwards of the gravelly fan delta system and situated above storm wave base. The abrupt contact between the lower and upper conglomerate successions and the intervening mudstone succession reflects an abrupt cessation of gravelly fan delta deposition followed by a period of muddy offshore deposition followed in turn by an abrupt resumption of gravelly fan delta deposition.

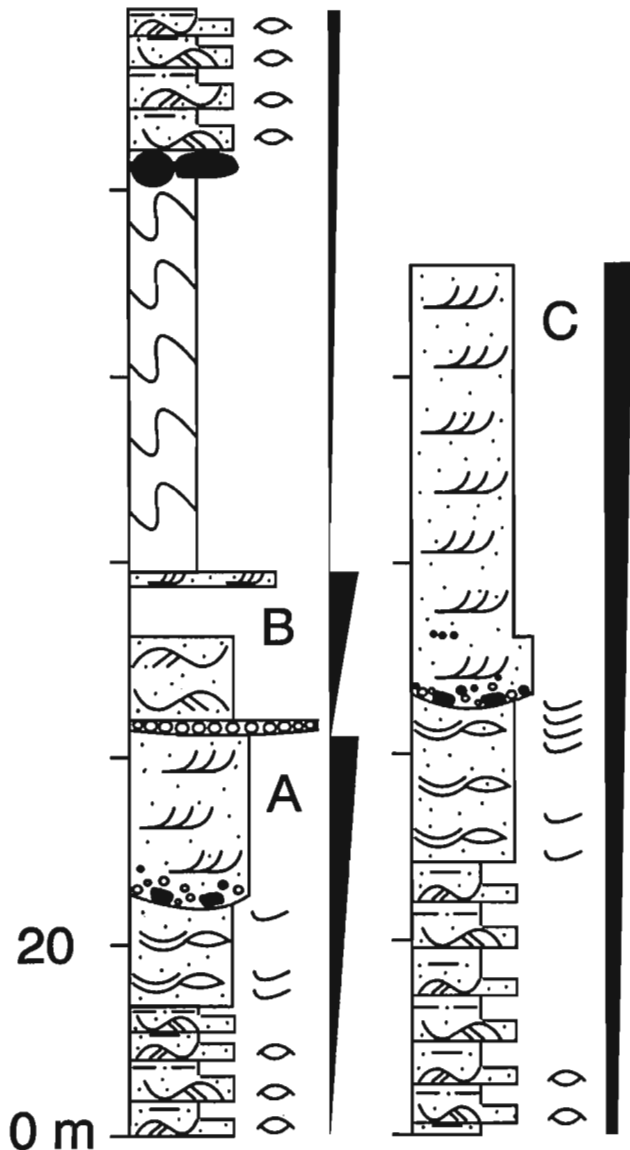


Figure 3. Stratigraphic section through package B exposed south of White Point, northwestern Graham Island.

Gravelly fan delta systems are typically situated adjacent to fault-controlled highlands (McPherson et al., 1988). The abrupt cessation and subsequent initiation of gravelly fan delta deposition may have been related to Late Jurassic movement along these faults. The absence of associated alluvial fan deposits may be attributed to the fact that the fan did not prograde basinwards to the location of the White Point exposure.

Package B

Two facies assemblages, comprising five facies, are recognized within package B: a mudstone facies assemblage and a sandstone facies assemblage. South of White Point, where the package is most completely exposed, the facies of these two assemblages form three coarsening-upwards sequences (A to C) between 16 and 116 m thick (Fig. 3).

Sequence C is the most completely exposed, and comprises a lower unit of the mudstone facies assemblage and an abruptly overlying unit of the sandstone facies assemblage. The base of the lower unit comprises a thick unit of slumped mudstone capped by boulders of mudstone, sandstone, well-rounded andesite and granodiorite. The slump is overlain by the interbedded mudstone and sandstone facies, representing deposition between fairweather and storm wave base within a muddy offshore environment. Hummocky cross-stratified sandstone beds tend to thicken and amalgamate upwards, reflecting a shoaling trend as the main source of sediment supply prograded basinwards.

The vertical arrangement of facies within the upper part of each package is from swaley cross-stratified to trough cross-stratified sandstone (Fig. 3). This reflects a transition from deposition under wave-generated oscillatory current conditions in a lower shoreface environment to deposition under fairweather wave-generated unidirectional current conditions in a shallower shoreface environment situated well above fairweather wave base. The sandstones of sequence A are overlain by a bed of the transgressive conglomerate facies at the base of sequence B. The conglomerate is interpreted as a reworked lag deposited within a shallower shoreface environment during the initial phases of transgression. This facies is abruptly overlain by deeper water deposits of sequence B.

Each coarsening-upward sequence represents the basinwards progradation of a high-energy sandy shoreface. Progradation occurred during periods of relative sea-level fall or stillstand, and was terminated by a relative sea-level rise resulting in the reworking of pebbly shoreface or nonmarine deposits into a transgressive lag and a rapid facies change into deeper water deposits. Three such relative sea-level fluctuations affected deposition during Late Valanginian through Hauterivian time.

Paleocurrents

Oriented belemnites from the interbedded mudstone and sandstone facies of sequences A and C yield a west-southwest – east-northeast axial trend, roughly parallel to the

west-northwest – east-northeast trend of parting lineation within associated hummocky cross-stratified sandstone beds (Fig. 4A). Parting lineation from hummocky cross-stratified sandstone is typically oriented perpendicular with respect to paleoshoreline, at least within Upper Jurassic and Cretaceous deposits of the Western Interior Basin (Leckie and Krystinick, 1989). The axial trend of the belemnites is probably oriented perpendicular to the package B paleoshoreline, which probably trended north-south. Trough cross-strata within the overlying sandstone assemblage of each package exhibit a fan-shaped distribution from west to northeast, oriented obliquely onshore to directly offshore of the inferred paleoshoreline trend.

Package C

Three facies assemblages, containing 14 facies, are recognized within package C: a lower sandstone assemblage, a middle mudstone assemblage, and an upper turbidite assemblage (Fig. 5). The assemblages form a 215 m thick fining-upward sequence which is completely exposed on Murchison Island.

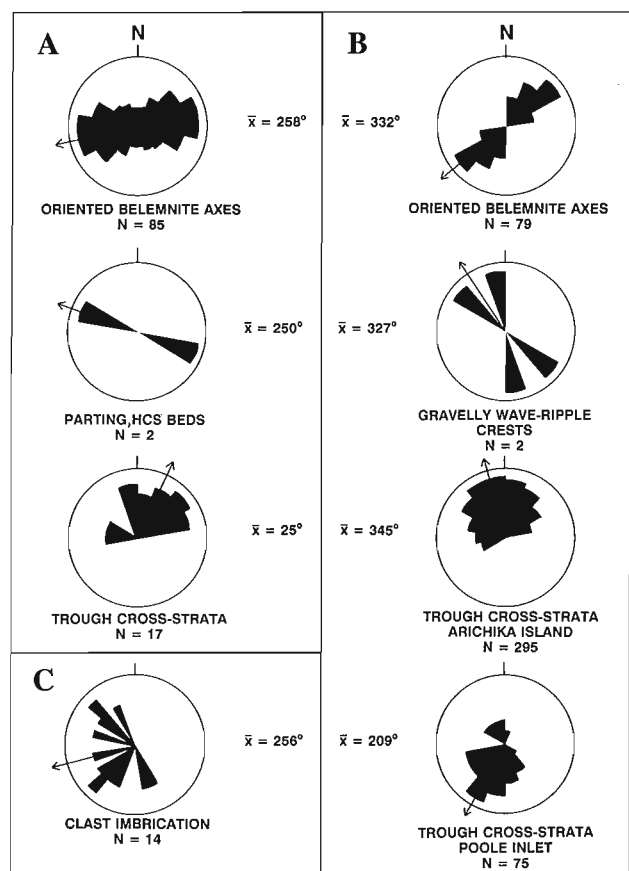


Figure 4. Synthesis of paleocurrent indicators from the Longarm Formation: **A)** package B; **B)** package C; **C)** package A. 25 measurements per station ($n = 14$) for clast imbrication from exposures of package A south of White Point.

On Moresby Island, pre-Cretaceous basement is unconformably overlain by a bed of the transgressive conglomerate facies which varies between 15.4 m at Poole Inlet to less than 0.1 m in western Cumshewa Inlet. The basal transgressive conglomerate is overlain by variably thick units of the trough cross-stratified or swaley cross-stratified sandstone facies, interpreted as sandy shoreface deposits. At Arichika Island, the trough cross-stratified sandstones are interstratified with beds of the stratified conglomerate facies, interpreted as gravelly shoreface bars. At Cumshewa Inlet, the swaley cross-stratified sandstones are overlain by 135 m of the structureless bioturbated sandstone facies, interpreted as transitional sandy offshore deposits. The sandstone assemblage thins from 180 m at Arichika Island in the south to 10 m at Ramsay Island in the north, and thickens again to 215 m at Cumshewa Inlet farther north (Fig. 5).

The deposits of the sandstone assemblage are gradationally overlain by those of the mudstone assemblage. The facies of this assemblage were deposited within a muddy offshore environment situated above storm wave base. At Murchison Island, the deposits of the mudstone assemblage are in turn gradationally overlain by those of the turbidite assemblage. In western Cumshewa Inlet, deposits of the turbidite assemblage are situated to the west of facies of the sandstone assemblage (Haggart, 1991). The facies of this assemblage were deposited within a submarine fan setting situated basinwards (southwest) of the muddy offshore environment.

As recognized by Haggart and Gamba (1990), the three assemblages form a fining-upwards sequence reflecting a transition from deposition within energetic sandy shoreface to muddy offshore and submarine fan environments. Package C therefore accumulated during a prolonged period of relative sea-level rise. The thickest accumulations of the sandstone assemblage are probably situated proximal to sources of sediment supply (i.e. near Arichika Island and Cumshewa Inlet), whereas thinner accumulations are probably situated in a more distal setting relative to source (i.e. Ramsay Island). The stratified conglomerates interbedded within this assemblage at Arichika Island also reflect proximity to a gravelly source of sediment.

Paleocurrents

The axial orientation of exhumed gravelly wave ripples within the swaley cross-stratified sandstone facies trend northwest-southeast (Fig. 4B). Wave ripple axes are typically oriented parallel to paleoshoreline (Leckie and Krystinick, 1989). This suggests that the inferred package C paleoshoreline probably trended northwest-southeast. The average axial trend of oriented belemnites from the interbedded mudstone and sandstones facies is southwest-northeast (Fig. 4B). This trend would once again appear to be oriented normal to paleoshoreline, as was the case within Package B. Paleocurrent trends from the trough cross-stratified sandstone and conglomerate facies at Arichika Island and Poole Inlet exhibit a fan-shaped distribution from northwest to northeast and from southwest to southeast respectively (Fig. 4B). The trends at Arichika Island are oriented directly alongshore and

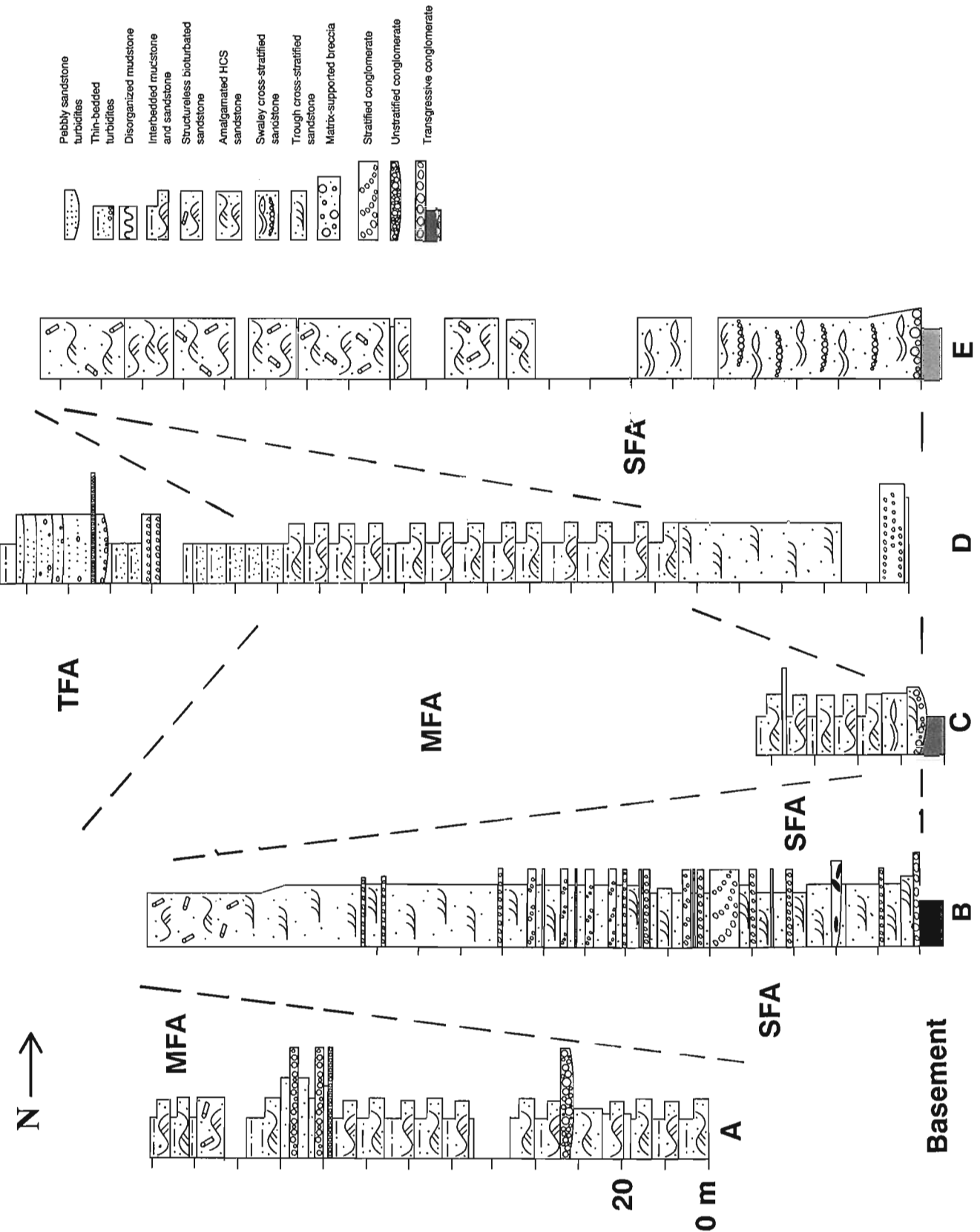


Figure 5. Stratigraphic sections of package C exposed on Moresby Island (A – Carpenter Bay, B – Arichika Island, C – Ramsay Island, D – Murchison Island, E – Dawson Cove, Cumshewa Inlet). SFA – sandstone facies assemblage, MFA – mudstone facies assemblage, TFA – turbidite facies assemblage.

directly onshore relative to the inferred northwest-southeast trend, whereas those at Poole Inlet are oriented offshore to alongshore.

DISCUSSION

During the Late Jurassic to Late Cretaceous, the Queen Charlotte Island region occupied a forearc setting located to the west of an active magmatic arc. The depositional history of the basin may be summarized as follows. In Late Oxfordian to Tithonian time, gravelly fan delta deposition occurred adjacent to the northwest-southeast trending fault-bounded eastern margin of the forearc basin. The abrupt alternation of gravelly fan delta and muddy offshore deposits reflects some element of fault-control upon sedimentation. The probable Late Jurassic age of the volcanics underlying this package indicate that active volcanism may have affected deposition, and that the basin was situated within an intra-massif setting. Isolated occurrences of similar Upper Jurassic strata in the Lyell Island – Burnaby Island area (Haggart, 1992) may have been deposited within similar fault-bounded intra-massif forearc basins (Gamba, 1991). After a probable hiatus spanning all of Berriasian time, marine deposition resumed within a greatly expanded forearc basin. Deposition during the Early Cretaceous was affected by several relative sea-level fluctuations. The deposits of package B contain three progradational high-energy sandy shoreface sequences deposited during three different periods of relative sea-level fall or stillstand in Late Valanginian to Hauterivian time. Package C comprises a single retrogradational high energy shoreface to deep basinal sequence deposited during a period of relative sea-level rise from Hauterivian to Aptian time. The evidence for fault-controlled deposition within the basin during the Early Cretaceous is not as pronounced as in Late Jurassic time.

The approximate northwest-southeast paleoshoreline trend of the forearc basin is remarkably consistent throughout Late Jurassic to Early Cretaceous time. This trend is similar to that proposed by Haggart (1991), which was based upon the progressive eastwards decrease in the age of basal Cretaceous strata on the Charlottes. The paleoshoreline orientation of the basin parallels the northwest-southeast trend of most Late Mesozoic faults mapped by Sutherland Brown (1968) and Thompson et al. (1991). Although there is no direct structural evidence for Early Cretaceous faulting (Haggart, 1992), the anomalous thickness of the shoreface sandstone assemblages within packages B and C are indicative of very rapid rates of basin subsidence. It is perhaps not inconceivable that the subsidence history of the Cretaceous forearc basin was influenced by the transtensional dextral strike slip-regime affecting the entire western Cordilleran margin throughout this period (van der Heyden, 1992; McClelland et al., 1992). The enlargement of the forearc basin throughout Late Jurassic – Early Cretaceous time probably tracked the eastward retreat of magmatism within the Coast Plutonic Complex documented by van der Heyden (1992). The progressive onlap of marine strata onto the northeast margin of the forearc basin is also observed within mid-Cretaceous deposits of the Haida and Skidegate

formations (Haggart, 1991). This trend again likely tracked the eastward retreat of magmatism within the flanking magmatic arc during this period.

CONCLUSIONS

The following conclusions can be made:

1. Three packages are recognized within the Longarm Formation as it is presently defined: a Upper Oxfordian to Tithonian package A, a Upper Valanginian to Hauterivian package B, and a Hauterivian to Aptian package C.
2. Package A comprises gravelly fan delta and muddy offshore deposits emplaced along the eastern margin of a northwest-southeast trending fault-bounded intra-massif forearc basin. Other occurrences of Upper Jurassic strata in south Moresby Island may have been deposited within similar basins.
3. Packages B and C comprise high-energy sandy shoreface to deep basinal deposits emplaced during three episodes of Late Valanginian to Hauterivian relative sea-level fall or stillstand and a prolonged episode of Hauterivian to Aptian relative sea-level rise.
4. The inferred northwest-southeast paleoshoreline orientation of the forearc basin throughout Late Jurassic and Early Cretaceous time parallels the trend of most Late Mesozoic faults and other tectonic structures on the islands.

ACKNOWLEDGMENTS

Jim Haggart is thanked for useful comments concerning an earlier version of this manuscript.

REFERENCES

- Gamba, C.A.**
1991: An update on the Cretaceous sedimentology of the Queen Charlotte Islands, British Columbia; in *Current Research, Part A*; Geological Survey of Canada, Paper 91-1A, p. 373-382.
- Haggart, J.W.**
1986: Stratigraphic investigations of the Cretaceous Queen Charlotte Group, Queen Charlotte Islands, British Columbia; Geological Survey of Canada, Paper 86-20, p. 24.
1989: Reconnaissance lithostratigraphy and biochronology of the Lower Cretaceous Longarm Formation, Queen Charlotte Islands, British Columbia; in *Current Research, Part H*; Geological Survey of Canada, Paper 89-1H, p. 39-46.
1991: A synthesis of Cretaceous stratigraphy, Queen Charlotte Islands, British Columbia; in *Evolution and Hydrocarbon Potential of the Queen Charlotte Basin, British Columbia*, (ed.) G.J. Woodsworth; Geological Survey of Canada, Paper 90-10, p. 253-277.
1992: Progress in Jurassic and Cretaceous stratigraphy, Queen Charlotte Islands, British Columbia; in *Current Research, Part A*; Geological Survey of Canada, Paper 92-1A, p. 361-365.
- Haggart, J.W. and Gamba, C.A.**
1990: Stratigraphy and sedimentology of the Longarm Formation, southern Queen Charlotte Islands, British Columbia; in *Current Research, Part F*; Geological Survey of Canada, Paper 90-1F, p. 61-66.

Haggart, J.W., Lewis, P.D., and Hickson, C.J.

1989: Stratigraphy and structure of Cretaceous strata, Long Inlet, Queen Charlotte Islands, British Columbia; in *Current Research, Part H*; Geological Survey of Canada, Paper 89-1H, p. 65-72.

Hickson, C.J. and Lewis, P.D.

1990: Geology, Frederick Island (west half), British Columbia; Geological Survey of Canada, Map 8-1990, scale 1:50 000.

Leckie, D.A. and Krystinick, L.F.

1989: Is there evidence for geostrophic currents preserved in the sedimentary record of inner to middle shelf deposits?; *Journal of Sedimentary Petrology*, v. 59, p. 862-870.

McClelland, W.C., Gehrels, G.E., and Saleeby, J.B.

1992: Upper Jurassic – Lower Cretaceous basinal strata along the Cordilleran margin: implications for the accretionary history of the Alexander – Wrangellia – Peninsular terrane; *Tectonics*, v. 11, p. 823-835.

McLearn, F.H.

1972: Ammonoids of the Lower Cretaceous Sandstone Member of the Haida Formation, Skidegate Inlet, Queen Charlotte Islands, western British Columbia; Geological Survey of Canada, Bulletin 188, 78 p.

McPherson, J.G., Shanmugam, G., and Moiola, R.J.

1988: Fan deltas and braid deltas: conceptual problems; in *Fan Deltas: Sedimentology and Tectonic Settings*, (ed.) W. Nemeč and R.J. Steel; Blackie and Sons, p. 14-22.

Sutherland Brown, A.

1968: Geology of the Queen Charlotte Islands, British Columbia; British Columbia Department of Mines and Petroleum Resources, Bulletin 54.

Thompson, R.I., Haggart, J.W., and Lewis, P.D.

1991: Late Triassic through early Tertiary evolution of the Queen Charlotte Basin, British Columbia, with a perspective on hydrocarbon potential; in *Evolution and Hydrocarbon Potential of the Queen Charlotte Basin, British Columbia*, (ed.) G.J. Woodsworth; Geological Survey of Canada, Paper 90-10, p. 3-29.

van der Heyden, P.

1992: A Middle Jurassic to Early Tertiary Andean-Sierran arc model for the Coast Belt of British Columbia; *Tectonics*, v. 11, p. 82-97.

Geological Survey of Canada Project 880038

Georgia Basin Project – geology of Vancouver map area, British Columbia

J.W.H. Monger

Cordilleran Division, Vancouver

Monger, J.W.H., 1993, Georgia Basin Project – geology of Vancouver map area, British Columbia; in Current Research, Part A; Geological Survey of Canada, Paper 93-1A, p. 149-157.

Abstract: The dominantly granitic Coast Belt in Vancouver map area (92G) is divided into five north-northwest-trending "tracts". From northeast to southwest, these comprise: (1) probable late Paleozoic to Cretaceous strata, locally metamorphosed to high grades and cut by mid- to Late Cretaceous granitic plutons; (2) Cretaceous plutons intruding and structurally imbricated with Lower Cretaceous Gambier strata; (3) Late Jurassic plutons in places overlain by Gambier strata and elsewhere cut by Cretaceous plutons; (4) Early Cretaceous plutons intruding Gambier strata; and (5) Late Jurassic and Early Cretaceous plutons cutting Late Triassic to Early Jurassic Wrangellian strata. Oldest structures are post-185 and pre-155 Ma folds in tract 5. Tracts 4 and 5 are juxtaposed across a probable Early Cretaceous normal fault. Major early Late Cretaceous deformation is manifested by southwest-vergent folds and thrust/reverse faults in tracts 1 and 2, and conjugate(?) northeast- and southwest-directed reverse faults in tracts 3 and 4.

Résumé : Dans la région cartographique de Vancouver (92G), la zone Côtière principalement granitique se subdivise en cinq «bandes» de direction nord nord-ouest. Du nord-est au sud-ouest, celles-ci comprennent : 1) des strates correspondant probablement à l'intervalle couvrant la fin du Paléozoïque au Crétacé, qui par endroits ont subi un métamorphisme intense et sont recoupées par des plutons granitiques s'échelonnant du Crétacé moyen à tardif; 2) des plutons d'âge crétacé, pénétrant les strates de Gambier du Crétacé inférieur, et structurellement imbriqués avec celles-ci; 3) des plutons datant du Jurassique tardif, par endroits recouverts par les strates de Gambier, et ailleurs recoupés par des plutons d'âge crétacé; 4) des plutons datant du Crétacé précoce, pénétrant les strates de Gambier; et 5) des plutons datant du Jurassique tardif et du Crétacé précoce, qui recoupent des strates wrangelliennes couvrant l'intervalle du Trias tardif au Jurassique précoce. Les structures les plus anciennes sont des plis datant de moins de 185 et de plus de 155 Ma dans la bande 5. Les bandes 4 et 5 sont juxtaposées de part et d'autre d'une faille normale qui date probablement du Crétacé précoce. Une importante déformation s'est manifestée au début du Crétacé tardif par des plissements de vergence sud-ouest et des failles chevauchantes et inverses dans les bandes 1 et 2, et des failles conjuguées (?) inverses de direction nord-est et sud-ouest dans les bandes 3 et 4.

INTRODUCTION

The bedrock geology of Vancouver map area (92G) was re-examined as part of Georgia Basin project, in order to better understand the nature, age and structure of the basement of eastern Georgia Basin, which includes the greater Vancouver area (Monger, 1991a). In contrast with earlier reconnaissance mapping, for which no or few isotopic dates were available, this study is enhanced by recent U-Pb dating of granitic rocks in the region, undertaken during the Lithoprobe southern Cordilleran project (Friedman and Armstrong, 1990) and as part of this project (Parrish and Monger, 1992). In addition, the relatively new techniques of strain analysis (e.g., Simpson and Schmid, 1983; Hanmer and Passchier, 1991), proved invaluable in deciphering structures in deformed granitic rocks.

Vancouver map sheet was mapped mostly at a scale of about 1:250 000 by Armstrong (1953; south-central part); Bostock (1963; west half), Roddick (1965; east half), and Roddick and Woodsworth (1979; west half). Although much of the map area is covered only by reconnaissance mapping, there are detailed studies in and near Britannia mine (e.g., James, 1929; Payne et al., 1980; Reddy, 1989), and on late Tertiary-Holocene volcanics in Garibaldi Park area (Mathews, 1958; Green et al., 1988).

Vancouver map sheet mainly encompasses the southernmost limits of the predominantly granitic Coast Belt (Fig. 1). Its southeastern corner comprises geology typical of the (North) Cascade mountains, and is separated from Coast Belt rocks by Quaternary and Tertiary strata underlying the lower Fraser River valley (Fraser Lowland), the orientation of which is in part controlled by late Tertiary northeast-trending faults (Monger, 1991a). Its southwestern corner, on Vancouver Island, is part of the Insular Belt and composed of Devonian to Jurassic rocks of Wrangellia terrane and Late Cretaceous Nanaimo Group molassic clastics, which also

overlap on to the Coast Belt (Mustard and Rouse, 1991). Geological and geophysical evidence suggest that the boundary between Insular and Coast belts, where submerged beneath Georgia Strait, lies close to the mainland, east of South Thormanby Island. It is exposed on Quadra Island in northern Georgia Strait and on islands still farther northwest (Carlisle and Suzuki, 1965; Nelson, 1979; White and Clowes, 1984; Monger, 1991b). Where exposed, the boundary is delineated by latest Middle to Late Jurassic (ca. 165-155 Ma) granitic intrusions within Wrangellian strata, east of which Jurassic, Cretaceous, and local early Tertiary granitic rocks comprise over 80% of the bedrock for a strike-normal distance of about 200 km.

The southern Coast Belt is divisible into two parts (Fig. 1). The eastern part, forming northeasternmost Vancouver map area (Fig. 2), consists of four tectonostratigraphic terranes (Harrison, Bridge River, Shuksan, and Cadwallader) in places metamorphosed to amphibolite grade, juxtaposed on major, mainly southwest-vergent, Late Cretaceous thrust faults and Late Cretaceous to earliest Tertiary dextral transcurrent faults, and intruded by Late Cretaceous and early Tertiary granitic rocks (Monger, 1986; Journeay, 1990; Lynch, 1990; Journeay and Friedman, in press). Rocks of the eastern Coast Belt can be traced southwards into the North Cascade mountains (Crickmay, 1930; Monger, 1986, 1991c). The western Coast Belt, which underlies most of Vancouver map area, is composed largely of granitic rocks ranging in age from late Middle Jurassic to early Late Cretaceous, with greenschist-grade septa and fault slices of mostly Lower Cretaceous Gambier Group (Fig. 2). Older stratified rocks, comprising Lower Jurassic Bowen Island Group and probably Upper Triassic Karmutsen and Quatsino formations (typical of Wrangellia terrane) are exposed on the west side, and Triassic Camp Cove and Jurassic Harrison Lake, Mysterious Creek, and Billhook Creek formations (comprising Harrison terrane) occur in the easternmost part of western Coast Belt, along Harrison Lake (Fig. 2; Monger, 1991b). Rocks correlative with those in western Coast Belt are known in the North Cascades only in the structural window north of Mount Baker, low in the stack of thrust sheets comprising the Northwest Cascades System (Monger, 1991c, and references therein).

As first recognized by Crickmay (1930), rocks of western Coast Belt acted as a (relatively) rigid block (or foreland) during major Late Cretaceous and earliest Tertiary compression and transpression featuring west-vergent thrust faults concentrated in eastern Coast Belt and the North Cascades (Monger 1986, 1991a; Journeay, 1990; Journeay and Friedman, in press). Detritus eroded mostly from the uplifted eastern Coast Belt and the North Cascades comprises the Late Cretaceous Nanaimo Group and early Tertiary Chuckanut, Burrard, Kitsilano, and Huntingdon formations and possibly younger, unnamed strata which are the molassic sedimentary fill of Georgia Basin (Johnson, 1984; England and Calon, 1991; Mustard, 1991; Mustard and Rouse, 1991; Monger, 1991a). These rocks are preserved around the present Georgia Strait mostly by Neogene and Recent differential uplift of the Coast Belt and Vancouver Island (Parrish, 1983; Hohdahl et al., 1989).

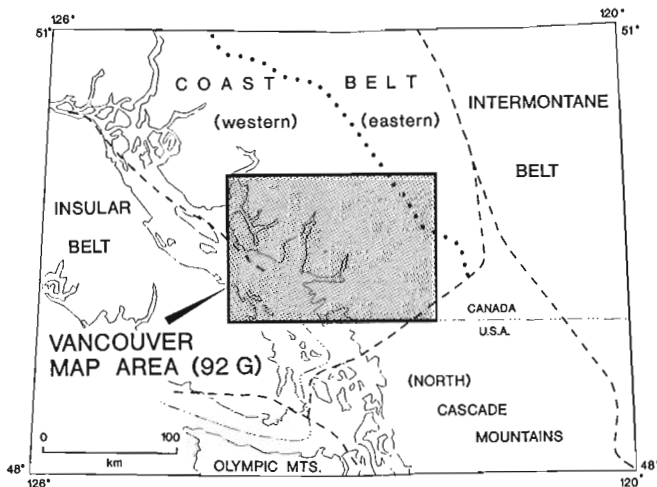


Figure 1. Index map showing location of Vancouver map area within the geological provinces of southwestern British Columbia and adjacent part of Washington State.

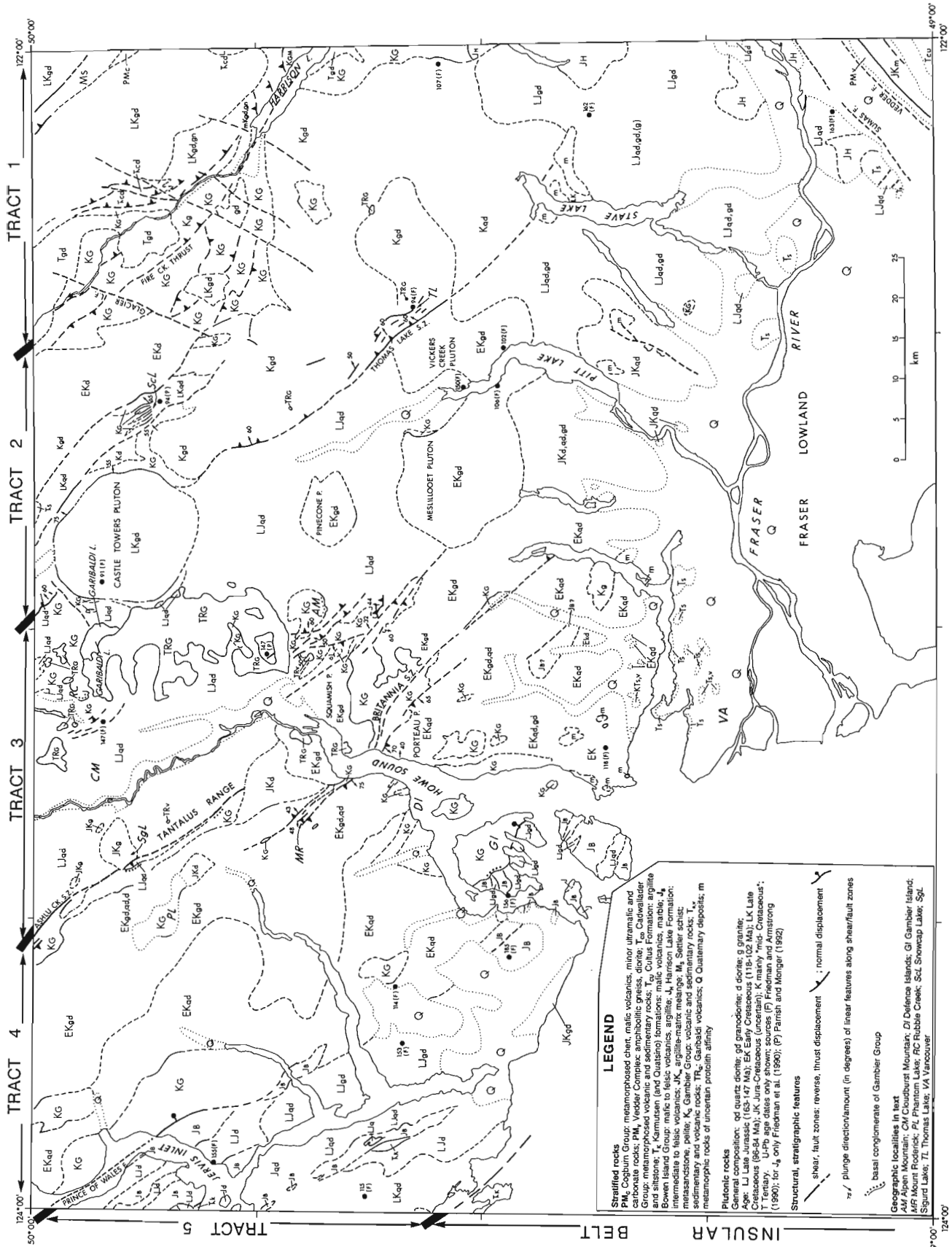


Figure 2. Sketch map showing geology of Vancouver (92G) map area (with exception of southwesternmost part), with emphasis on ages of rock units and structures.

ROCK UNITS AND STRUCTURES, VANCOUVER MAP AREA

Distribution, ages and structures of rock units in Vancouver map area are shown on Figure 2. Crystallization ages of the dominant granitic rocks are known with confidence only where U-Pb dates exist, and elsewhere are inferred from intrusive relationships to dated granitic rocks and from intrusive and locally stratigraphic relationships to dated strata. On the sketch map (Fig. 2) six age categories of granitic rocks are identified: Late Jurassic (U-Pb date range, 163-147 Ma); Early Cretaceous (118-102 Ma), Late Cretaceous (96-84 Ma), Jura-Cretaceous (uncertain), Cretaceous (late Early Cretaceous-early Late Cretaceous), and Tertiary. Composition of the granitic rocks cannot be used as a guide to age; within each age bracket lithologies range from predominant quartz diorite and lesser granodiorite to local diorite, and rare gabbro and granite. An extensive K-Ar dating program is being undertaken to supplement the limited number of available U-Pb dates, as it has been found in this area that where both U-Pb and new K-Ar dates exist, the latter mostly differ from the former by only a few million years, and thus can be used as a relatively inexpensive guide to crystallization age.

Monger (1991b) divided the Coast Belt in Vancouver map area into four north-northwest-trending, orogen-parallel, "tracts" based on known or inferred ages of mainly Jurassic and Cretaceous rocks and structures within each. This division is adhered to herein, except that the former "Squamish River tract" is further subdivided into eastern and western parts, and tract names are abandoned for numbers (1 to 5 from northeast to southwest; Fig. 2). Young volcanic rocks of the Garibaldi Group occur mainly in the north-central map area, but probable correlative plugs and dykes are scattered across tracts 2, 3, and 4).

Tract 1: (former Central Coast Belt - Northwest Cascades System of Monger, 1991b)

Rocks and structures in Tract 1 in Vancouver map area were mapped most recently by Journeay and Czontos (1989), Journeay (1990), Lynch (1990), and Journeay and Friedman (in press) and are the north-northwest along-strike extension of rocks exposed on both sides of Harrison Lake, southwestern Hope map area (Monger, 1989) and in the North Cascade mountains to the south (Monger, 1991c). They comprise Lower Cretaceous (Berriasian, Valanginian, Hauterivian, and Albian; Arthur, 1986) sedimentary and volcanic rocks, respectively Peninsula and Brokenback Hill formations (Crickmay, 1930), and are correlative with the Fire Lake Group of Roddick (1965), and the Gambier Group (Armstrong, 1953) farther west near Howe Sound; herein they are included in the Gambier Group. Fault slices of more metamorphosed strata are correlated with the Cogburn Group (=? Mississippian to Jurassic Bridge River terrane), Triassic Cadwallader Group (Cadwallader terrane), and Mesozoic (Jura-Cretaceous?) Settler schist (=? Shuksan terrane) of southwestern Hope map area (Lynch, 1990). Intrusive rocks include Late Cretaceous granitic rocks (correlative with

intrusions along strike to southeast (96 ± 1 Ma and 84 ± 1 Ma; Parrish and Monger, 1992), local gneiss, and minor Tertiary intrusions. The rocks are complexly deformed, with initial post-Gambier (Fire Lake) southeast-directed thrusts, folds associated with mainly southwest-directed high-angle thrusts, and northeast-trending, mid- to Late Tertiary(?) dextral-normal faults (Lynch, 1990). The Cretaceous structures are part of the Coast Belt Thrust System (Journeay and Friedman, in press) dated between 91 and 96 Ma, mostly from relationships of faults to dated plutons.

Tract 2: (northeastern part of former Squamish River tract)

Tract 2 is distinguished mainly by the presence of abundant granitic rocks, of mainly late Early to early Late Cretaceous ages (Fig. 2; U-Pb dates: 113 ± 2 , 94 ± 2 , 94 ± 2 , 107 ± 2 Ma; Friedman and Armstrong, 1990; Journeay and Friedman, in press) with local Middle Jurassic granitic rocks (162-163 Ma) in the southeast. Local septa and/or fault slices within the granitic rocks appear to be mainly variably metamorphosed and deformed Gambier (or Twin Island) equivalents, based on lithologies which include the local presence of granite cobble conglomerate. In places, such as north of Snowcap Lake, granitic rocks dated at 94 ± 0.5 Ma (Parrish and Monger, 1992) both intrude metasedimentary (with conglomerate) and volcanic rocks, and are structurally imbricated with them on northeast-dipping (ca. 50° - 70°) structures with northeast plunging, downdip stretching lineations. Elsewhere, mylonite zones occur within the granitic rocks, but have not been traced for any distance.

The southwestern boundary of Tract 2 is the Thomas Lake shear zone (Monger, 1990). North of the map area, it crosses Highway 99 about 2 km southwest of the settlement of Whistler. Southwest of this it is exposed on Corrie Ridge (5 km north northwest of Garibaldi Lake) where undated granitic rocks are emplaced on the Lower Cretaceous Helm Formation (of the Garibaldi Group) with strong northeast plunging (60°) northeast-side-up linear fabrics developed in the shear zone (Fig. 3). The zone is interrupted by the Castle Towers Pluton (U-Pb dated at 91 ± 3 Ma; Friedman and Armstrong, 1990) but southwest of this can be traced more-or-less continuously for 40 km, to the area south of Thomas Lake, where it is about 1 km wide. From there, a strong linear extends along Tingle Creek as far as the north end of Stave Lake. Along the shear zone, a strong northeast-dipping fabric is developed in granitic rocks (Fig. 4), with northeast-side-up movement indicators and linear fabrics that plunge northeastwards at 50 - 60° . In the hanging wall of the shear zone are mainly Cretaceous granitic rocks (dated at Thomas Lake as 94 ± 2 Ma; R.M. Friedman, pers. comm., 1992). In the footwall (Tract 3), are mostly Late Jurassic granitic rocks with local Lower Cretaceous Gambier strata and Early Cretaceous plutons (e.g., Vickers Creek pluton; 106 ± 2 , 102 ± 2 Ma; Friedman and Armstrong, 1990). The shear zone is considered by Journeay and Friedman (in press) to be the basal thrust of their Coast Belt Thrust System, and it moved in early Late Cretaceous time (between? 94-91 Ma).

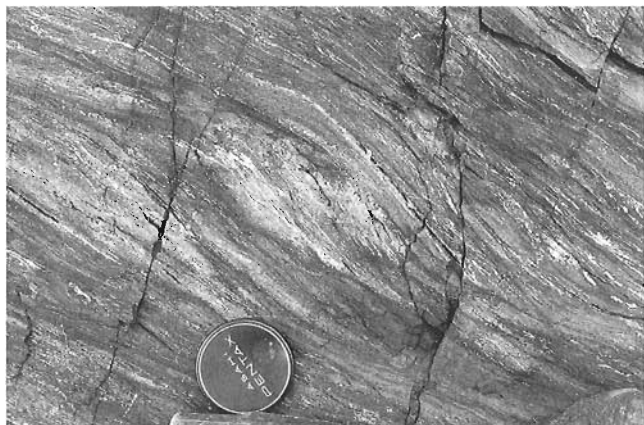


Figure 3. Sigmoidal structure in foliated amphibolite indicating movement to southwest (top to left on photo). From metamorphosed Gambier Group(?), on Corrie Ridge, 6.5 km east-northeast of The Black Tusk, Garibaldi Park, and about 100 m below contact with granitic rock, overthrust to southwest on Thomas Lake shear zone.



Figure 4. Strongly foliated quartz diorite in Thomas Lake shear zone, 1.5 km northwest of west end of Thomas Lake.

Tract 3: (southwestern part of former Squamish River tract)

As noted above, Tract 3 consists of mainly Late Jurassic quartz diorite and includes the Cloudburst quartz diorite of Mathews (1958). These granitic rocks are overlain locally by Gambier strata, and intruded by granodioritic-quartz dioritic plutons of mid-Cretaceous age.

Late Jurassic (U-Pb dates of $164 \pm 3/-6$, 162 ± 2 , 150 ± 2 , 147 ± 0.5 , 145 ± 2 Ma; Friedman and Armstrong, 1990; Parrish and Monger, 1992; R.M. Friedman, pers. comm., 1992) granitic rocks extend more-or-less continuously from the northern boundary of the map area, between Ashlu Creek and Cheakamus River to the southern (exposed) limits of the Coast Belt near Fraser River. They are predominantly quartz diorite, although the southeasternmost ones are granodiorite. Locally, as between Cheakamus and Squamish rivers, they have a gneissic fabric, and elsewhere, as in the Cheakamus canyon, a strong mylonitic fabric has been superimposed on

them. In many places, as in the Cheakamus, Mamquam, and Pitt River valleys, they contain numerous intrusions including dark, fine grained mafic dykes, and distinctive hornblende feldspar porphyry and fine grained green feldspar porphyry, quartz feldspar porphyry, and local "quartz-eye" porphyry dykes and intrusions. In places, abundant pyrite is associated with these intrusions. The quartz-eye porphyry and quartz feldspar porphyry bodies in the Pitt River watershed, mapped by Roddick (1965) as Harrison Lake Formation, appear to be intrusions. The porphyritic intrusions may be feeders to Gambier Group volcanics. Local brown-weathering andesitic dykes are probably correlative with the late Tertiary-Recent Garibaldi volcanics.

Clastic rocks of the Gambier Group stratigraphically overlie Late Jurassic rocks in at least three localities: south of Rubble Creek (Mathews, 1958); on Alpen Mountain (Lynch, 1991); and near Sigurd Lake in the Tantalus Range (this report). The basal Gambier Group includes shallow marine, crossbedded arkosic sandstone (Fig. 5), as well as conglomerate locally with large quartz diorite clasts (Fig. 6). From this unit, called the Cheakamus Formation in the area north of Rubble Creek near the Black Tusk, Mathews (1958) collected the pelecypod *Inoceramus*. Re-collection of these fossils in 1991 with W.H. Mathews, and their re-identification by J. Haggart (GSC loc. 187629) suggests they are of Hauterivian age (131-124 Ma). They also are found in the mainly volcanic Brokenback Hill Formation on the west side of Harrison Lake. North of Black Tusk area, these rocks pass apparently stratigraphically upwards into a heterogenous unit called the Empetrum Formation by Mathews (1958), that is composed of volcanic breccia, coarse diorite and granite cobble conglomerate, and olistostromes containing large carbonate blocks. In the same area, the Empetrum Formation is apparently overlain stratigraphically by the Helm Formation (Mathews, 1958), comprising pyritic argillite with interbedded graded sandstone beds. A similar three-part sequence occurs south of Sigurd Lake in the northwestern Tantalus Range, although there the probable equivalent of the Empetrum is a breccia with abundant volcanic fragments. In the Alpen Mountain-Mamquam River-Howe Sound area,

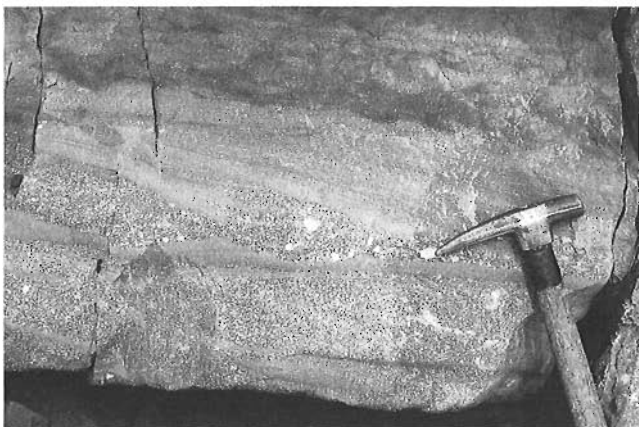


Figure 5. Crossbedding in coarse arkosic sandstone of the Lower Cretaceous Cheakamus Formation (Gambier Group); on ridge 0.75 km northwest of The Black Tusk, Garibaldi Park.



Figure 6. Boulder of quartz diorite in basal Gambier conglomerate and sandstone sequence stratigraphically overlying probable Late Jurassic quartz diorite, 0.5 km west-southwest of Sigurd Lake, northwest Tantalus Range.

Lynch (1991), drawing in part on the work of others, found far more volcanic rock in the section; above basal sedimentary rocks, two composite volcanic complexes are separated by sedimentary rocks of Albian age.

Early and Late Cretaceous intrusions (U-Pb dates 91 ± 3 , 102 ± 2 , 106 ± 2 Ma; Friedman and Armstrong, 1990) form the clearly defined Castle Towers and Vickers Creek plutons that lie within the matrix of Late Jurassic granitic rocks. The undated Pinecone pluton appears to be similar. They are typically fresh granodioritic to quartz dioritic bodies, and contain relatively few dykes; those are either mafic or brown-weathering, Garibaldi(?) andesite.

In places Tract 3 contains both southwest-vergent and northeast-vergent, steeply dipping shear zones that range from either well developed mylonites, as in Cheakamus Canyon, to the typically brittle and irregular fabrics seen in the Mamquam River area. The southwestern boundary of Tract 3 is the Ashlu Creek shear zone, which clearly displays southwest-side-up fabrics near Ashlu Creek, on the northern margin of the map area (Fig. 2; contrary to what was said by the writer in 1991!). The probable continuation of this zone near Sigurd Lake brings Late Jurassic quartz diorite and overlying Gambier Group over an undated but probably younger granodioritic pluton. The zone is difficult to trace as a continuous feature along the remainder of the Tantalus Range, although fabrics indicate strong deformation locally. To the southwest, near Mamquam River, Lynch (1991) mapped the southwestern boundary of Tract 3 as a structurally complex area of east- and west-vergent shear zones.

Tract 4: (former Howe Sound tract)

Rocks within Tract 4 appear to be of entirely of Cretaceous age. In addition to granitic rocks, they include well-studied, deformed Gambier strata in and adjacent to the Britannia shear zone (Payne et al., 1980; Heah, 1982; McColl, 1987) as well as septa exposed in the walls of Howe Sound of known Albian age, and on Gambier and Anvil islands, and those southwest of the Tantalus Range and near Jervis Inlet. U-Pb

dates from hosting granitic rocks are late Early Cretaceous (118 ± 2 , 114 ± 2 , 102 ± 2 Ma; north of map-sheet), and in this tract the granitic rocks appear to form regionally extensive bodies, rather than discrete small Cretaceous plutons as in tract 3. They typically have no fabrics and few dykes, but in places show probable intrusive fabrics (foliated but with intact crystals and flat and elongate xenoliths) or mylonites or sheared granites (with broken grains).

With the exception of strata in and near the Britannia shear zone, Gambier rocks in this tract mostly have well-preserved primary fabrics, including ripple markings exposed on bedding surfaces in the septum near Phantom Lake. Metamorphic grade in these septa is mostly low greenschist facies, with andalusites widespread in argillaceous strata in the southwest end of the Tantalus Range and in the area east of Vancouver Bay on Jervis Inlet. Some small septa within the predominant granitic rock, such as those on the west side of Howe Sound north of Defence Islands, have a completely reconstituted fine grained, granulitic metamorphic texture and locally contain small garnets.

In places, the granitic rocks are clearly involved in deformation affecting Gambier strata. On the west side of Howe Sound, the apparent northwest extension of the Britannia shear zone includes a 1 km wide exposure of Gambier Group with southwest-dipping foliation. The northern contact, with the Squamish Pluton, appears to be intrusive but is slightly faulted. The southern contact dips southwest at 70° and has a strong, southwest-side-up mylonitic fabric, as recognized by Lynch (1991) from the northern margin of the Porteau pluton on the east side of Howe Sound. The extension of this zone to the northwest is entirely within granitic rock, and is exposed near the summit of Mount Roderick. There, southwest-dipping, southwest-side-up (at $55\text{--}60^\circ$) mylonite zones occur within granitic rock (Fig. 7) for a distance of nearly 2 km across strike, in apparent conjugate relationship with northeast-dipping ($45\text{--}65^\circ$), northeast-side-up ultramylonite (or pseudotachylite) zones (Fig. 8, 9).

The southwestern boundary of this tract appears to be at least in part a syn-Gambier, northeast-side-down normal fault with local intrusions and dykes along it, herein called Prince of Wales Fault (Monger, 1991b). It extends south-southwestwards from Brittain River, along Prince of Wales Reach on Jervis Inlet, then onland at least as far south as Narrows Inlet. A possible comparable structure is a normal fault juxtaposing Gambier Group to the northeast with Jurassic granite to the southwest on Gambier Island (Lynch, 1991).

Tract 5: (former Sechelt tract)

Tract 5 contains metavolcanic and metasedimentary rocks of the Lower Jurassic Bowen Island Group (U-Pb date $185 \pm 8/3$ Ma; Friedman et al., 1990) as well as local marbles and metabasalts correlated with the Quatsino and Karmutsen formations, and Late Jurassic (U-Pb dates of 156 ± 2 , 155 ± 3 , 155 ± 2 Ma) and local Early Cretaceous (115 ± 2 , 114 ± 2 Ma) granitic rocks (Friedman and Armstrong, 1990). Rocks of the Lower Jurassic Bowen Island Group were tightly to isoclinally folded prior to intrusion of 155 Ma granitic rocks (Monger, 1991b).

STRUCTURAL HISTORY

Oldest structures recognized are tight to isoclinal folds and penetrative cleavage in the Lower Jurassic Bowen Island Group in Tract 5, and are post-185 Ma, pre-155 Ma in age.

An episode of syn-Gambier extension probably is manifested by the Prince of Wales Fault along Jervis Inlet and by intrusions, including dyke swarms, spatially associated with this fault. In addition, widespread dyking possibly related to Gambier volcanism occurs widely within Late Jurassic plutons in Tract 3, between Cheakamus and Pitt rivers. Rapid uplift and erosion to expose Late Jurassic quartz diorite (ca. 147 Ma), prior to Hauterivian (ca. 135 Ma) Gambier deposition may also be related to extension. Facies changes seen in Gambier sedimentary rocks, from basal shallow water sandstone and



Figure 7. Northwest extension of Britannia shear zone exposed on Mount Roderick; northeast-vergent, southwest-dipping zones of mylonite/sheared granitic rock in probable Early Cretaceous quartz diorite; barely visible, but circled, asymmetric feldspar grain indicates left-side-up movement.

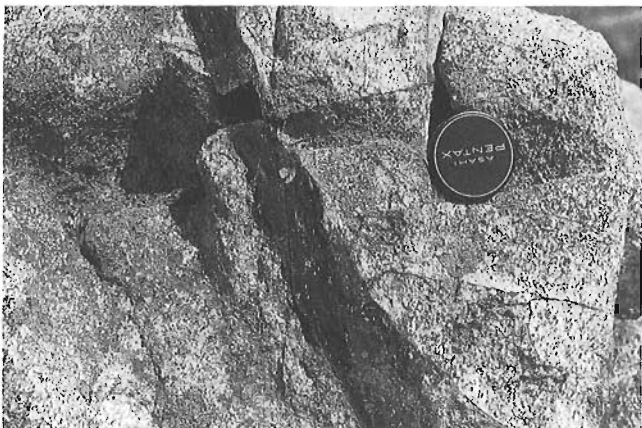


Figure 8. Northwest extension of the Britannia shear zone, on Mount Roderick; strike-normal view of pseudotachylite (ultramylonite) dyke in quartz diorite; these dykes dip to northeast and have southwest-vergence, in apparent conjugate relationship with mylonite zones in same area (Fig. 7).



Figure 9. Pseudotachylite dyke, Mount Roderick; view in plane of dyke, showing steep, downdip fabric.

conglomerate, through olistoliths, to deeper water turbidites, may record rapid vertical movements, but whether these are related to extension is unknown.

Early Late Cretaceous contraction is the major deformation in the area. It is dated most precisely in the map area on the Thomas Lake shear zone at between ca. 91-94 Ma. This shear zone is considered by Journeay and Friedman (in press) to be the basal thrust of their Coast Belt Thrust System, which is well developed in the northeast part of the map area (Tract 1 and parts of Tract 2). The thrust system there is regionally penetrative, contains a local early phase of southeast-directed contraction (Lynch, 1990), overprinted by dominant southwest-directed high-angle thrust faulting. In the remainder of the map area, regional contraction is manifested mainly by discrete zones in granitic rocks that may be mylonitic, brittle, or rarely ultramylonitic. Since this deformation overlaps with the time of granitic intrusion in the region, the style of structure developed may reflect rock temperature during deformation. Vergence during this contraction is to the southwest in the northeastern part of the map area, but in the northern Howe Sound-Mamquam River-Ashlu Creek areas, deformation is directed both to the southwest and northeast. With the exception of the northeast part of the map area, no major crustal shortening appears to have taken place. Shear zones are steep, many appear to be discontinuous, and Gambier Group strata occur across much of the map area.

Eocene contractional deformation occurs on Vancouver Island (England and Calon, 1991), in early Tertiary strata on the mainland (in Washington; Johnson, 1991), and latest(?) Cretaceous-early Tertiary dextral transpressional and Early Tertiary dextral transcurrent movements are known mainly east of the map area, in the eastern Coast Belt (Journeay, 1990; Monger, 1991a). Except possibly in the Harrison Lake area, structures formed in this time interval have not been identified in the southern Coast Belt.

Northeast-trending structures in the southeastern part of the map area include the concealed Vedder and Sumas faults in Fraser Lowland (southeastern Vancouver map area, Fig. 2), between which Paleogene clastics are downropped, and also structures outlined by small northeast-trending bodies of

mid- to Late Tertiary granitic and volcanic rocks (Monger, 1991a; Coish and Journeay, 1992). During this study, other northeast-trending linears were examined for evidence of late movement, but most appear to be eroded, aligned joint systems. For example, a prominent northeast-trending linear extends from the south end of Coquitlam Lake, across the head of Pitt Lake and along Vickers Creek, where it is apparently cut off by the Thomas Lake shear zone. Northeast of this, along trend, bedrock along the trend of the linear is exposed and features small dykes of fresh, brown-weathering Garibaldi(?) andesite which intrude northeast-trending joint sets (Fig. 10). Orientation of the head of Howe Sound appears to be controlled by joints developed within the Squamish Pluton. Origin of the northeast-trending joint sets is unknown.

Latest movements in the map area appear to be over 2 km of regional uplift in the last 10 million years (assuming a land surface at sea level 10 million years ago; Parrish, 1983) and contemporary vertical uplift of 1 mm/a, with a subsidence rate of 1 mm/a south of Vancouver (Hohdahl et al., 1989).

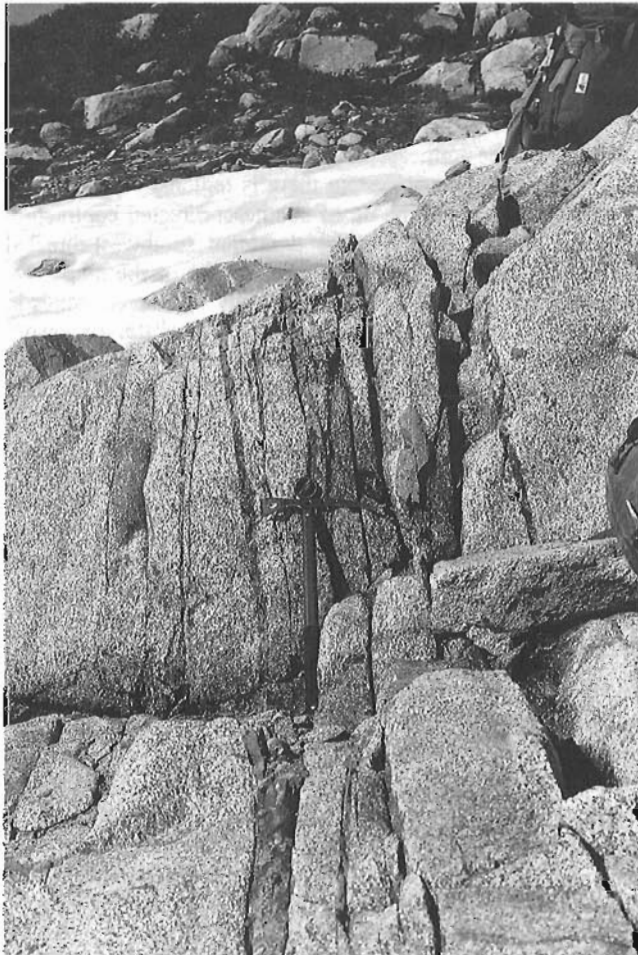


Figure 10. Dykelets, probably related to Gambier Group volcanics, intrude northeast-trending joints; northeast of head of Vickers Creek. A prominent linear extends for about 30 km to southwest of this to the south end of Coquitlam Lake.

ACKNOWLEDGMENTS

The mountaineering expertise of my assistant, Bertrand Groulx, was invaluable in helping me carry out field work in 1992. Thanks are also due to the Greater Vancouver Water District (Mr. R.G. Jones), and to the British Columbia Ministry of Parks (Mr. A. Midnight) for permission to carry out field studies in the water district and in Garibaldi Park. Richard Friedman freely permitted use of his U-Pb data funded by Lithoprobe.

REFERENCES

- Armstrong, J.E.**
1953: Preliminary map, Vancouver north, British Columbia; Geological Survey of Canada, Paper 53-28, 7 p.
- Arthur, A.J.**
1986: Stratigraphy along the west side of Harrison Lake, southwestern British Columbia; in *Current Research, Part B*; Geological Survey of Canada, Paper 86-1B, p. 715-720.
- Bostock, H.H.**
1963: Geology Squamish (Vancouver, west half map-area), British Columbia; Geological Survey of Canada, Map 42-1963.
- Carlisle, D. and Suzuki, T.**
1965: Structure, stratigraphy and paleontology of an Upper Triassic section on the west coast of British Columbia; *Canadian Journal of Earth Sciences*, v. 2, p. 442-484.
- Coish, R.A. and Journeay, J.M.**
1992: The Crevasse Crag Volcanic Complex, southwestern British Columbia: structural control on the geochemistry of arc magmas; in *Current Research, Part A*; Geological Survey of Canada, Paper 92-1A, p. 95-103.
- Crickmay, C.H.**
1930: The structural connection between the Coast Range of British Columbia and the Cascade Range of Washington; *Geological Magazine*, v. 67, p. 482-491.
- England, T.J.D. and Calon, T.J.**
1991: The Cowichan fold and thrust system, Vancouver Island, southwestern British Columbia; *Geological Society of America Bulletin*, v. 103, p. 336-362.
- Friedman, R.M. and Armstrong, R.L.**
1990: U-Pb dating, southern Coast Belt (49°-51°), southwestern British Columbia; *Proceedings of Lithoprobe Southern Canadian Cordillera Transect Workshop*, University of Calgary, Alberta, p. 146-155.
- Friedman, R.M., Monger, J.W.H., and Tipper, H.W.**
1990: Age of the Bowen Island Group, southwestern Coast Mountains, British Columbia; *Canadian Journal of Earth Sciences*, v. 27, p. 1456-1461.
- Green, N.L., Armstrong, R.L., Harakal, J.E., Souther, J.G., and Read, P.B.**
1988: Eruptive history and K-Ar geochronology of the late Cenozoic Garibaldi volcanic belt, southwest British Columbia; *Geological Society of America Bulletin*, v. 100, p. 563-579.
- Hanmer, S. and Passchier, C.**
1991: Shear-sense indicators: a review; Geological Survey of Canada, Paper 90-17, 72 p.
- Heah, T.S.T.**
1982: Stratigraphy, geochemistry and geochronology of the Lower Cretaceous Gambier Group, Sky Pilot area, southwestern British Columbia; B.Sc. thesis, University of British Columbia, Vancouver, 97 p.
- Hohdahl, S.R., Faucher, F., and Dragert, H.**
1989: Contemporary vertical motion in the Pacific Northwest, in *Slow Deformation and Transmission of Stress in the Earth*, (ed.) S.C. Cohen, and P. Vanicek; American Geophysical Union/International Union of Geodesy and Geophysics Geophysical Monograph, 49, v. 4, p. 17-29.
- James, H.T.**
1929: Britannia Beach map area, British Columbia; Geological Survey of Canada, Memoir 128, 139 p.

Johnson, S.Y.

1984: Stratigraphy, age and paleogeography of the Eocene Chuckanut Formation, northwest Washington; *Canadian Journal of Earth Sciences*, v. 21, p. 92-106.

1991: Sedimentation and tectonic setting of the Chuckanut Formation, northwest Washington; *Washington Geology*, v. 19, no. 4, p. 12-13.

Journey, J.M.

1990: A progress report on the structural and tectonic framework of the southern Coast Belt, British Columbia; in *Current Research, Part E*; Geological Survey of Canada, Paper 90-1E, p. 183-195.

Journey, J.M. and Czontos, L.

1989: Preliminary report on the structural setting along the southeast flank of the Coast Belt, British Columbia; in *Current Research, Part E*; Geological Survey of Canada, Paper 89-1E, p. 177-187.

Journey, J.M. and Friedman, R.M.

in press: Structural setting and geochronometry of the Coast Belt Thrust System, southwestern British Columbia; *Tectonics*.

Lynch, J.V.G.

1990: Geology of the Fire Lake Group, southeast Coast Mountains, British Columbia; in *Current Research, Part E*; Geological Survey of Canada, Paper 90-1E, p. 197-204.

1991: Georgia Basin Project: stratigraphy and structure of Gambier Group rocks in the Howe Sound-Mamquam River area, southwest Coast Belt, British Columbia; in *Current Research, Part A*; Geological Survey of Canada, Paper 91-1A, p. 49-57.

Mathews, W.H.

1958: Geology of the Mount Garibaldi area, southwestern British Columbia; *Geological Society of America Bulletin*, v. 69, p. 161-178.

McCull, K.M.

1987: Geology of Britannia Ridge, east section, southwest British Columbia; M.Sc. thesis, University of British Columbia, Vancouver, 207 p.

Monger, J.W.H.

1986: Geology between Harrison Lake and Fraser River. Hope map area, southwestern British Columbia; in *Current Research, Part B*; Geological Survey of Canada, Paper 86-1B, p. 699-706.

1989: Geology of Hope and Ashcroft map-areas; Geological Survey of Canada, Maps 41-1989, 42-1989, scale 1:250 000.

1990: Georgia Basin: Regional setting and adjacent Coast Mountains geology, British Columbia; in *Current Research, Part F*; Geological Survey of Canada, Paper 90-1F, p. 95-107.

1991a: Late Mesozoic to Recent evolution of the Georgia Strait-Puget Sound region, British Columbia and Washington; *Washington Geology*, v. 19, no. 4, p. 3-7.

1991b: Georgia Basin Project: structural evolution of parts of southern Insular and southwestern Coast belts, British Columbia; in *Current Research, Part A*; Geological Survey of Canada, Paper 91-1A, p. 219-228.

Monger, J.W.H. (cont.)

1991c: Correlation of Settler Schist with Darrington Phyllite and Sliuksan Greenschist and its tectonic implications, Coast and Cascade Mountains, British Columbia and Washington; *Canadian Journal of Earth Sciences*, v. 28, p. 447-458.

Mustard, P.S.

1991: Stratigraphy and sedimentation of the Georgia Basin, British Columbia and Washington State; *Washington Geology*, v. 19, no. 4, p. 7-9.

Mustard, P.S. and Rouse, G.E.

1991: Sedimentary outliers of the eastern Georgia Basin margin, British Columbia; in *Current Research, Part A*; Geological Survey of Canada, Paper 91-1A, p. 229-240.

Nelson, J.L.

1979: The western margin of the Coast Plutonic Complex on Hardwicke and West Thurlow Islands, British Columbia; *Canadian Journal of Earth Sciences*, v. 16, p. 1166-1175.

Parrish, R.R.

1983: Cenozoic thermal evolution and tectonics of the Coast Range of British Columbia; I. Fission track dating, apparent uplift rates, and patterns of uplift; *Tectonics*, v. 2, p. 601-631.

Parrish, R.R. and Monger, J.W.H.

1992: New U-Pb dates from southwestern British Columbia; in *Radiogenic Age and Isotope Studies: Report 5*, Geological Survey of Canada, Paper 91-2, p. 87-108.

Payne, J.G., Bratt, J.A., and Stone, B.G.

1980: Deformed Mesozoic volcanogenic Cu-Zn sulfide deposits in the Britannia District, British Columbia; *Economic Geology*, v. 75, p. 700-721.

Reddy, D.G.

1989: Geology of the Indian River area, southwestern British Columbia; M.Sc. thesis, University of British Columbia, Vancouver, 166 p.

Roddick, J.A.

1965: Vancouver North, Coquitlam, and Pitt Lake map-areas, British Columbia, with special emphasis on the evolution of the plutonic rocks; Geological Survey of Canada, Memoir 335, 276 p.

Roddick, J.A. and Woodsworth, G.J.

1979: Geology of Vancouver west half, and mainland part of Alberni; Geological Survey of Canada, Open File 611.

Simpson, C. and Schmid, S.M.

1983: An evaluation of criteria to deduce the sense of movement in sheared rocks; *Geological Society of America Bulletin*, v. 94, p. 1281-1288.

White, D.J. and Clowes, R.M.

1984: Seismic investigation of the Coast Plutonic Complex-Insular Belt boundary beneath Georgia Strait; *Canadian Journal of Earth Sciences*, v. 21, p. 1033-1049.

Geology of northeast Taseko Lakes map area, southwestern British Columbia¹

P.B. Read²

Cordilleran Division, Vancouver

Read, P.B., 1993: Geology of northeast Taseko Lakes map area, southwestern British Columbia; in Current Research, Part A; Geological Survey of Canada, Paper 93-1A, p. 159-166.

Abstract: The map area straddles the dextral strike-slip Fraser Fault. East of the fault, the Cache Creek Complex consists of massive limestone of the Marble Canyon Formation and overlying Western Belt of siliceous phyllite, ribbon chert, thin limestone beds, and basic metavolcanics, totalling 1000 m and ranging from Permian to Upper Triassic. West of the fault, ribbon chert and metavolcanics of Farwell slice range from Lower Permian to uppermost Triassic and correlate with the Cache Creek Complex. On both sides of the fault, a siltstone-greywacke unit, devoid of chert, structurally and(?) stratigraphically overlies the complex. Equivalents to the Carboniferous metavolcanics of Thaddeus slice, the Upper Permian felsic to basic metavolcanics, and the massive limestone of the Marble Canyon Formation are absent across the fault. The Miocene Chilcotin River had a flow direction and position similar to the present. It joined the north-flowing Miocene Fraser River a few kilometres north of its present confluence.

Résumé : La région cartographique recouvre en partie la faille de Fraser, qui est un décrochement dextre. À l'est de la faille, le complexe de Cache Creek se compose de calcaires massifs de la Formation de Marble Canyon et de la zone occidentale sus-jacente, composée de phyllite siliceuse, de chert zoné, de minces couches calcaires et de roches métavolcaniques basiques, qui au total ont 1 000 m d'épaisseur et qui couvrent l'intervalle du Permien au Trias supérieur. À l'ouest de la faille, le chert zoné et les roches métavolcaniques du lambeau de charriage de Farwell s'échelonnent du Permien inférieur à la partie supérieure du Trias et peuvent être corrélés avec le complexe de Cache Creek. Des deux côtés de la faille, une unité composée de siltstone et grauwacke et dépourvue de chert, recouvre structuralement et (?) stratigraphiquement le complexe. Les équivalents des roches métavolcaniques d'âge carbonifère du lambeau de charriage de Thaddeus, des roches métavolcaniques felsiques à basiques du Permien supérieur, et du calcaire massif de la Formation de Marble Canyon, sont absents de part et d'autre de la faille. Au Miocène, la rivière Chilcotin avait la même direction d'écoulement et la même situation qu'aujourd'hui. À cette époque, elle rejoignait le fleuve Fraser qui s'écoulait vers le nord, à quelques kilomètres au nord de son confluent actuel.

¹ Contribution to the Frontier Geoscience Program Chilcotin-Nechako Hydrocarbon Province

² Geotex Consultants Limited, #1200 – 100 West Pender Street, Vancouver, B.C. V6B 1R8

INTRODUCTION

The work reported in this paper comes from the third year of a four-year geological investigation of the northeast corner of the Taseko Lakes map area (92O) at the southern end of the Chilcotin-Nechako Hydrocarbon Province (Hickson, 1990). Although still in progress, this year's geological mapping at a scale of 1:50 000 extends to the northern boundary of Taseko Lakes area at latitude 52°N and lies between longitudes 122°05' and 122°30' (Fig. 1).

West of Fraser Fault, earlier mapping (Read, 1992) indicated that Middle Jurassic and older rocks form three or more northeasterly-directed thrust sheets of which the thickest is Farwell slice. The slice consists of Farwell Pluton and its wall rocks of ribbon chert, grey and green phyllite, and metavolcanics correlated with the Cache Creek Complex (Cordey and Read, 1992). East of Fraser Fault, a similar stratigraphic sequence, belonging to the Western Belt of the Cache Creek Complex, stratigraphically overlies massive limestone of the Marble Canyon Formation. On both sides of the fault, a thick succession of grey siltstone with minor greywacke structurally, and possibly stratigraphically, overlies rocks of the Cache Creek Complex. Although Mortimer (1987) followed Trettin (1980) in placing similar rocks in the 'Pavilion beds', and Monger and McMillan (1989) relegated them to the Western Belt of the complex, Cordey and Read (1992) suggested that they may form an overlap assemblage.

STRATIGRAPHY

Cache Creek Complex

East of Fraser Fault, the complex consists of paleontologically dated rocks ranging from Permian to Late Triassic. West of the fault, the complex includes correlative rocks of the same age range. Recent paleontological results (Table 1) have improved our understanding of the ages of some of the units.

East of Fraser Fault, fairly continuous sections along Alkali Creek and the Fraser River expose the entire width of the Western Belt and some of the underlying Marble Canyon Formation (**Pmcc**) (Fig. 1). Northward along the Fraser River from its confluence with Doc English Gulch and in Springhouse Hills east of the river, a southwesterly dipping panel of light grey, unbedded limestone of the Marble Canyon Formation diminishes northwesterly from an outcrop width of 3.5 km on Peavine Mountain to 500 m in Sword Creek. A second panel extends from south of Mount Pablo and crosses the Fraser River north of the map area before disappearing under Miocene basalt flows. Where the limestone is hundreds of metres thick, its upper contact defines the top of the Marble Canyon Formation, but where the limestone is a hundred metres or less in thickness, uncertainty exists as to whether it should be included within the Marble Canyon Formation. Herein, the thin limestones have been excluded and placed with the overlying rocks. The formation is undated in the northeast corner of Taseko Lakes map area, but 80 km to the south near Jesmond, it is Late Permian and Early Triassic (Beyers and Orchard, 1989).

Legend for Figure 1

CENOZOIC	
Quaternary and Tertiary	
Pleistocene	
Pvb	CHILCOTIN GROUP (Pv to Ms) Grey olivine- and/or plagioclase-phyric subaerial basalt flows
Tertiary	
Pliocene	
Pvb	Grey olivine- and/or plagioclase-phyric subaerial basalt flows
Ps	Unconsolidated fluvial sandstone and pebble to boulder conglomerate
Miocene	
Mvb	Grey olivine- and/or plagioclase-phyric subaerial basalt flows
Ms	Fraser Bend Formation Unconsolidated fluvial sediments; minor rhyolite ash; rare diatomaceous earth
Eocene	
Es	Conglomerate, sandstone; minor siltstone and shale
Evb	Dark grey olivine basalt flows
Eva	Aphyric grey dacite and andesite flows; minor breccia
Evd	Plagiophyric dacite breccia and flows
Evr	Rhyolite tuff, ash and breccia; rare flows
MESOZOIC	
Jurassic	
Middle to Upper Jurassic	
mJcg	South of Bald Mountain: Red sparsely plagioclase-phyric volcanic conglomerate overlying nonbedded quartz-bearing feldspathic sandstone
mJscg	North of Bald Mountain: Interbedded grey-green volcanic chip conglomerate and nonbedded quartz-bearing feldspathic sandstone
JKdi	Chloritized hornblende diorite and quartz diorite
Middle and Lower Jurassic	
Jpw	Grey siltstone, shale; minor grey lithic wacke
Lower Jurassic	
IJs	Grey noncalcareous siltstone with thin sandstone laminae; minor thin limestone
Triassic	
Middle to Upper Triassic	
Urs	Grey nonlimy siltstone and minor interbedded thin calcareous sandstone
Urc	Nonbedded light to medium grey micritic limestone
PALEOZOIC	
Permian	
Late Permian	
lPfqm	FARWELL PLUTON Leucoquartz monzonite, quartz monzonite, granodiorite
rdi	Chloritized and locally foliated metadiorite and quartz metadiorite
Upper Permian	
UPv	Grey-green and locally maroon porphyritic (plagioclase, quartz) dacite and rhyolite flows and tuffs, felsite- and quartz-feldspar porphyry-bearing tuff; minor green metabasalt flows
Permian to Triassic	
Lower Permian to Upper Triassic	
rv	CACHE CREEK COMPLEX (rv to Pmcc) Western Belt: Meta-andesite and metabasalt breccia and flows
Prf	Western Belt: Grey phyllite, siliceous phyllite, and grey to green ribbon chert; thin limestone layers and lenses
Prp	Western Belt: Red siliceous phyllite and siltstone
Pmcc	Marble Canyon Formation Grey unbedded micritic limestone
Mississippian and Pennsylvanian	
Lower Mississippian and Pennsylvanian	
MPv	Grey-green and green greenstone; minor limestone lenses

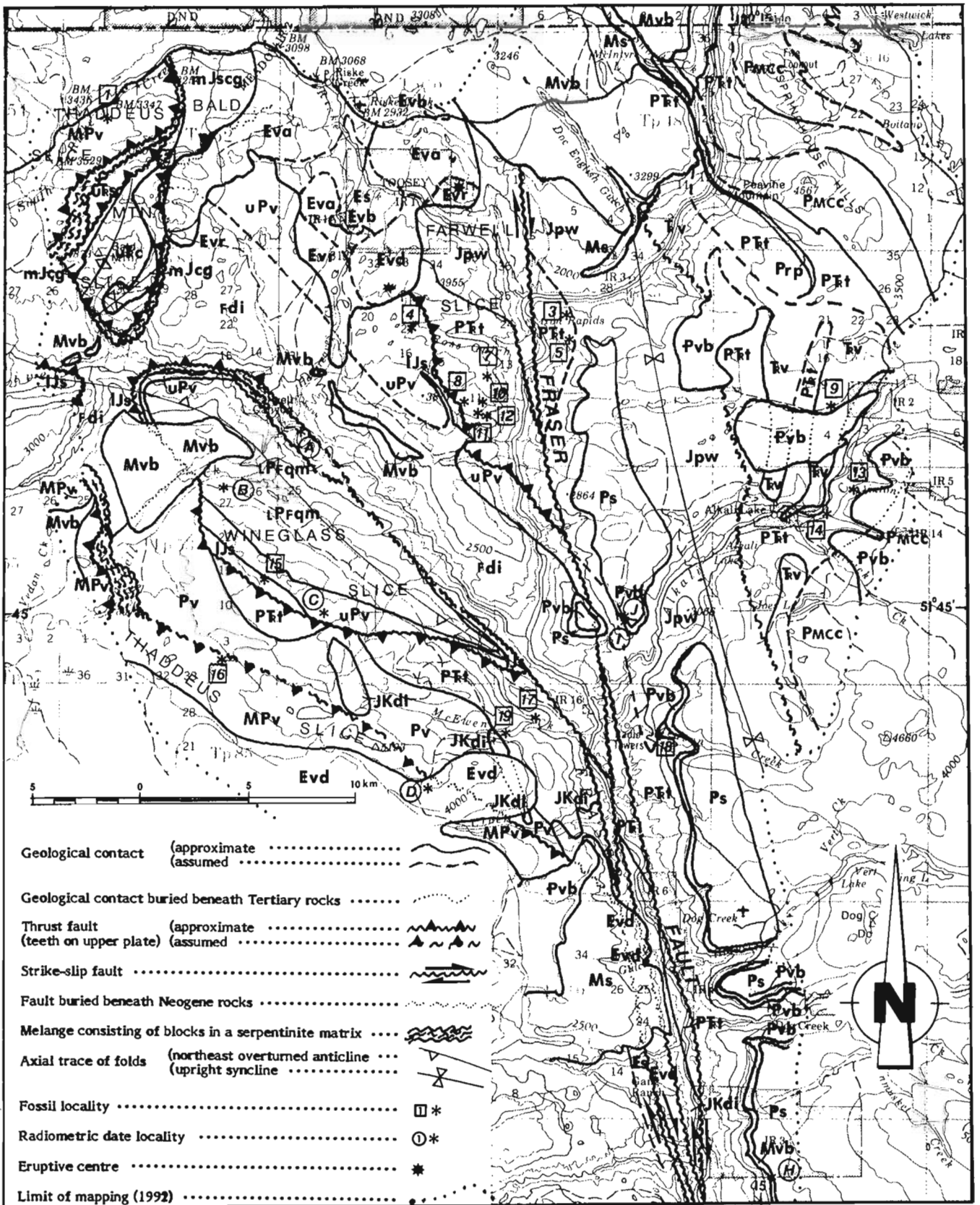


Figure 1. Preliminary geological map of parts of Dog Creek (920/9), Riske Creek (920/15), and Alkali Lake (920/16) map areas.

Table 1. Recent fossil and radiometric date localities, northeast corner of Taseko Lakes map area (920)

Symbol	Easting	Northing	Age (Reference)
1*	521850	5756130	Pennsylvanian (Orchard, unpubl. data)
2	524130	5754130	Late Triassic (Tozer and Tipper, unpubl. data)
3	543000	5746870	Early Triassic (Orchard, unpubl. data)
4	535850	5746250	Pennsylvanian to Early early Permian (Orchard, unpubl. data)
5	543170	5745550	Late Triassic, Late Carnian or Early Norian (Cordey & Read, 1992)
6	539250	5744000	Late Triassic, Late Norian (Cordey & Read, 1992)
7	537700	5743000	Triassic, early Ladinian to Early Carnian (Cordey & Read, 1992)
8	553880	5742930	Triassic, Ladinian to Carnian (Cordey & Read, 1992)
9	555450	5742750	Late Triassic, Carnian to Norian (Orchard, unpubl. data)
10	538730	5742350	Middle Triassic, late Anisian or early Ladinian (Cordey & Read, 1992)
11	539250	5742080	Late Triassic, Early Carnian (Cordey & Read, 1992)
12	541710	5740860	Late Triassic, Early or Middle Norian (Cordey & Read, 1992)
13	556300	5739000	Permian (Orchard, unpubl. data)
14	554970	5737800	Triassic, possibly early Ladinian to Late Carnian (Cordey & Read, 1992)
15	529000	5734870	Late Toarcian (Hickson, 1990)
16	529630	5730480	Mississippian, Tournaisian (Orchard, unpubl. data)
17	541800	5728250	Triassic, early Ladinian to Late Carnian (Cordey & Read, 1992)
18	546920	5728120	upper Paleozoic to mid-Triassic (Orchard, unpubl. data)
19	540930	5727750	Early Permian, late Asselian to late Sakmarian (Cordey & Read, 1992)
A**	530080	5741810	258 ± 5 Ma - U-Pb Zircon (Friedman & van der Heyden, 1992)
B	527250	5738850	254 ± 1.2 Ma - U-Pb Zircon (GSC, unpubl. data)
C	530950	5733200	259 ± 2 Ma - U-Pb Zircon (GSC, unpubl. data)
D	536470	5725270	47.4 ± 0.7 Ma - K-Ar whole-rock (GSC, unpubl. date)
E	530660	5722440	50.5 ± 2.1 Ma - K-Ar whole-rock (GSC, unpubl. date)
F	535640	5721770	48.2 ± 0.8 Ma - K-Ar whole-rock (GSC, unpubl. date)
G	535270	5718750	43.5 ± 1.1 Ma - K-Ar whole-rock (GSC, unpubl. date)
H	552220	5707400	8.40 ± 0.27 Ma - K-Ar whole-rock (GSC, unpubl. date)
I	545300	5733100	3.20 ± 0.15 Ma - K-Ar whole-rock (GSC, unpubl. date)
J	545450	5733000	2.46 ± 0.14 Ma - K-Ar whole-rock (GSC, unpubl. date)

* Fossil Collection localities shown as numbered boxes on Figure 1.
** Radiometric date localities shown as lettered circles on Figure 1.

Overlying the Marble Canyon Formation is a sequence of grey and minor green phyllite, siliceous phyllite, and ribbon chert with locally bedded limestone of unit **PTt**, grey-green metavolcanic breccia and dark green phyllitic greenstone locally pillowed of unit **Tv**, and a very distinctive red siliceous phyllite-siltstone (**Prp**). This succession, about a thousand metres thick, outcrops along Alkali Creek east of Alkali Lake and along the Fraser River north of its confluence with Doc English Gulch. It forms the eastern limb of a northerly-trending syncline from Joes Lake northward along the Fraser River. The west limb of the syncline underlies a narrow strip on the east side of Fraser Fault extending from southeast of the mouth of Riske Creek to south of Dog Creek. The top of the succession lies at the base of a structurally and stratigraphically(?) higher grey siltstone-greywacke package devoid of chert. Although the succession is strongly deformed and extensively recrystallized, the combination of conodont and radiolarian dating (Table 1, localities 3, 4, 9, 13, and 14) indicates that Permian and Lower, Middle, and Upper Triassic rocks are present. The sequence between the Marble Canyon Formation and the siltstone-greywacke is similar to Trettin's

(1980) and Mortimer's (1987) Western Belt, but differs from Monger and McMillan's (1989) Western Belt which includes the siltstone-greywacke succession which I, along with Trettin and Mortimer, have excluded.

West of Fraser Fault in Farwell slice, the complex contains a tectonically thickened assemblage of ribbon chert, siliceous grey and green phyllite, and intercalated massive to bedded limestone layers of unit **PTt**. It outcrops south of Ross Gulch and in the middle to lower few kilometres of Word and McEwen creeks, where the limestone beds are absent. Radiolarian dating shows that the ribbon cherts range from Early Permian to Late Triassic near McEwen Creek (Table 1, localities 17 and 19) where greenstone probably structurally and possibly stratigraphically underlies the ribbon chert assemblage. Near Ross Gulch, the range is Middle to latest Triassic (Table 1, localities 6-8 and 10-12). The base of the unit lies at the downward disappearance of significant ribbon chert and the top lies at the top of the highest ribbon chert. Cordey and Read (1992) correlated this chert-bearing assemblage and the underlying metavolcanic rocks exposed in McEwen and Word creeks with the Cache Creek Complex.

Unnamed Upper Paleozoic volcanic units (MPv and uPv)

West of Fraser Fault, the remainder of the metavolcanic rocks and minor lenticular limestones compose parts of two thrust slices, not presently correlated with other upper Paleozoic to lower Mesozoic units.

North of Bald Mountain and in the upper part of Word Creek, Thaddeus slice consists of massive greenstone (MPv) with a few limestone lenses that yield Pennsylvanian and Mississippian conodonts (Table 1, localities 1 and 16). Because the early Mississippian (Tournaisian) age is considerable older than those from the southern Cache Creek, but similar to the oldest dated chert of the Bridge River complex (Cordey and Schiarizza, in press), rocks of Thaddeus slice are not correlated with either complex.

Restricted to Wineglass slice, texturally well-preserved metadacite flows and lapilli tuff, and overlying meta-andesite and metabasalt flows of unit uPv range from a hundred to probably less than a thousand metres thick. East of Farwell Creek and on the sides of Chilcotin River valley 2-5 km downstream from the mouth of Big Creek, the metadacite volcanics grade downward through dykes of metadacite and felsite into a marginally porphyritic leucoquartz monzonite. Although the contact of the metavolcanic rocks with the overlying fossiliferous Lower Jurassic (Late Toarcian) sediments is unexposed, felsic clasts in the sediments imply an unconformity, not a fault. Based on the felsic composition of the volcanics, which is atypical of the Cache Creek Complex, and the overlying fossiliferous sediments, Read (1992) erroneously placed the volcanics in the Lower Jurassic. U-Pb zircon-dating of the metadacite and adjacent leucoquartz monzonite, however, yielded Late Permian ages of 259 ± 2 Ma and 254 ± 1.2 Ma respectively (Table 1, localities A and B) and supports a cogenetic relationship between the intrusion and felsic volcanics. Because the Permian to Late Triassic ribbon chert assemblage, typical of the Cache Creek Complex, is absent between the Late Permian volcanics and immediately overlying Lower Jurassic sediments, the Permian volcanics have not been correlated with the complex.

Unnamed siltstone-greywacke unit (Jpw)

A grey siltstone-phyllite-greywacke unit (Jpw), with thin grit- to pebble-conglomerate layers, outcrops on both sides of Fraser Fault. Siliceous beds and turbidites are common, but tuffaceous beds are rare, and chert absent. East of the fault, the unit is well exposed on the north side of Alkali Creek, up and downstream from Alkali Lake. West of the fault, it underlies the slopes northwest of the mouth of Riske Creek. It certainly overlies, structurally and possibly stratigraphically, the ribbon chert of the complex.

East of the fault, the basal contact is buried beneath a 200 m-wide gap in outcrop on the north side of Alkali Creek where a road from Alkali Ranch zigzags up the slope and exposes faulted and isoclinally folded ribbon chert of the Cache Creek Complex. On the northeast side of Doc English Gulch, a hydrothermally altered chert fault-breccia and buff-weathering siliceous phyllite form the outcrop edge on the

metavolcanics and limestones of the complex. The nearest siltstone outcrop is a few hundred metres away. Bedding attitudes and facing directions indicate that the siltstone-greywacke unit occupies the core of an upright, closed syncline that extends for at least 30 km subparallel to Fraser Fault. It appears from under the Chilcotin lavas north of Harpers Creek, trends north-northwest across Alkali Creek and the Fraser River, and disappears under the lavas to the north.

West of the fault, the basal contact appears folded a few kilometres south of Toosey Indian Reservation 1, but to the south of Ross Gulch, where the ribbon chert and intercalated limestone layers are truncated along the base of the siltstone-greywacke unit, shattered siltstone outcrops favour a faulted contact. Near peak 3955' south of Toosey Indian Reservation 1, an angular chert grit and fine chert breccia lie in contact with ribbon chert and mark the lower contact of the siltstone-greywacke unit. Although the grit and breccia are viewed as the basal sediments of the unit, an outcrop gap of 200 m exists between them and the first grey siltstone outcrop; faults may be present. In summary, the basal contact probably is a faulted unconformity.

Even though the siltstone-greywacke unit is presently undated in the map area, a post-Triassic age would be consistent with the unit overlying latest Triassic ribbon chert west of Fraser Fault. The characteristic dominance of siltstone and greywacke in the unit and the absence of chert are typical of the radiolaria-bearing clastic rocks of Early and Middle Jurassic age which Cordey et al. (1987) dated about 100 km to the south in Kelly Creek and Monger and McMillan (1989) included in the Western Belt of the Cache Creek Complex. Cordey and Read (1992) noted the lithologic similarity between the Cayoosh Assemblage and the siltstone-greywacke unit of the map area, but removed the latter from the Cache Creek Complex and treated it as an overlap assemblage.

Unnamed Lower Jurassic sediments (IJs)

Green unbedded tuff, grey massive limestone, pebble conglomerate, and fossiliferous grey shale and siltstone form up to 100 m of Lower Jurassic sediments. U-Pb zircon-dating of the volcanic rocks underlying the sediments, show that the volcanics, formerly placed in the Lower Jurassic (Read, 1992), are actually Late Permian (Table 1, locality B) and now are excluded from the unit. Because fossils occur in the sediments at only one locality (Table 1, locality 15), all other occurrences are based on lithologic correlation.

Unnamed Eocene volcanic (Evr, Evd, Eva, and Evb) and sedimentary units (Es)

Eocene volcanic and particularly sedimentary rocks form widely scattered outcrops which extend northward from the head of Hargreaves Creek, through and west of Toosey Indian Reservation 1 to the eastern flank of Bald Mountain and northward beyond the map area. The rhyolite tephra of unit Evr consists of white ash southwest of peak 3955' south of Toosey Indian Reservation 1, lapilli tuff immediately east of

the reservation, and breccia together with flows a few kilometres south and west of the southwest corner of the reservation. East of the reservation, 200 m of steep-dipping, layered tuff with angular rhyolite blocks up to 0.5 m in diameter may mark a rhyolite eruptive centre.

Within and south of the reservation, porphyritic dacite flows and intercalated breccias of unit **Evd**, with 5 to 20% plagioclase crystals up to 3 mm, are up to 150 m thick, form peak 3955' and the surrounding hills, and overlie the rhyolite ash. Grey, aphyric andesite and dacite flows and locally breccias of unit **Eva** compose the western half of the Eocene succession and extend eastward where they locally overlie the rhyolite. Vesicular to amygdaloidal basalt flows of unit **Evb**, volumetrically insignificant, are exposed in roadcuts on the western edge of Toosey Indian Reservation 1 and on Highway 20 north of the northeast corner of the reservation.

Along the re-routed forestry access road west of Toosey Indian Reservation 1, a few slumped roadcuts of conglomerate, tuffaceous sandstone, and leaf-bearing siltstone of unit **Es** expose an indeterminate thickness of Eocene sediments within the volcanic succession. A few more outcrops suggest that they may extend up to 3 km to the west.

*Chilcotin Group (units **Mvb** and **Ms**)*

Remnants of a broad sheet of vesicular olivine basalt flows (unit **Mvb**) extend westward for 20 km from the west valley wall of the Fraser River to the village of Riske Creek and northward beyond the map area. A few small areas of flows of **Mvb** remain along the northeast wall valley of the Chilcotin River near and downstream from Hargreaves Creek. Here and there fluvial sediments of unit **Ms** fill paleochannels buried by the flows.

On the north side of the Fraser River from 3 to 6 km upstream from the mouth of Riske Creek, scattered outcrops of friable sandstone, fine (2-5 cm) sedimentary breccia composed of grey siltstone clasts from unit **Jpw**, and silica-cemented and veined, rhyolite ash and tuff lie between 1950' and 2800' elevation. These rocks are a facade plastered against an easterly-trending paleovalley wall. Within 15 m of the overlying basalt flows near Doc English Gulch, volcanic conglomerate and diatomaceous earth outcrop near the edge of and within a 3 km long basalt block slide. North in Sword Creek valley, Highway 20 cuts through slumped basalt tephra immediately beneath the basalt flows, and a new fence line 200 m southwest of the unnamed lake on Sword Creek exposes diatomaceous earth under the basalt. The maximum thickness of sediments is 130 m and they belong to the Fraser Bend Formation of Late Miocene age (Rouse and Mathews, 1979).

From Hargreaves Creek downstream along the Chilcotin River, pebble to cobble conglomerate up to 20 m thick underlies the basalt flows. The subrounded to angular clasts are mainly volcanic in contrast to the conglomerate along the Fraser River where quartzite clasts are important. Imbrication of the clasts indicates a southeastward current direction, and together with their position, implies that the present

course and flow-direction of the Chilcotin River are subparallel to those in the Miocene. Near the river mouth, the outcrop distribution shows that the paleochannel and confluence of the Chilcotin River with the Fraser River lay up to 2 km north of its present position. This distribution would be expected if the paleoflow of the Fraser River were northward.

Between Riske and Sword creeks, vesicular olivine basalt flows and basal breccia of unit **Mvb** are up to 150 m thick. Basalt breccia is rare in the Chilcotin Group, but occurs at Canoe and Dog creeks (Mathews and Rouse, 1986) and in the present area at the base of the succession where the lavas flowed into water. The base of the cliffs on the southwest side of Doc English Gulch, expose 60 m of pillow lava, pillow breccia, and palagonitic tuff and breccia with broken glassy margins on some of the clasts. About 3 km to the northeast these deposits thin and disappear, only to reappear on the north side of Sword Creek and continue beyond the north edge of the map area. North of Sword Creek, the breccia and tuff are coarsely bedded with east- to southeasterly-dipping foreset beds implying water near the present position of the Fraser River. At Doc English Gulch, thin felsic airfall tuffs are intercalated with the lower basalt flows. The combination of felsic tuffs, a thick basal section of palagonitic tuff and breccia, and the underlying sediments has created an extensive, postglacial, basalt block slide, 3 km long, which crossed the river terraces and reached the Fraser. Based on a single K-Ar whole-rock date of 10.0 ± 1.2 Ma (Mathews, 1989), the olivine basalt is probably Late Miocene.

Olivine basalt flows (**Mvb**) along the northeast side of the Chilcotin River near and downstream from Hargreaves Creek, do not exceed 80 m and lack a basal breccia. Three K-Ar whole-rock dates of 7.9 ± 0.6 , 8.5 ± 0.3 , and 9.2 ± 0.4 Ma (Mathews, 1989) for the Beaumont locality, 8 km west of the map area, probably indicate a valid Late Miocene age for the flow remnants in the map area.

INTRUSIONS

*Farwell Pluton (units **IPFqm** and **Fdi**)*

Farwell Pluton consists mainly of two compositional ranges: a leucoquartz monzonite to granodiorite (unit **IPFqm**) and a chloritized hornblende-biotite quartz diorite to diorite (unit **Fdi**). The former has 20% or less mafics and the latter 25% or more. Although not entirely mapped, the leucoquartz monzonite to granodiorite commonly forms the southwestern side of the intrusion and the quartz diorite to diorite, the northeastern half of the intrusion. Wineglass Fault forms the contact between the two at the north end of the pluton but the nature of the remainder of the contact is unknown. Two U-Pb zircon dates, 258 ± 5 Ma (Friedman and van der Heyden, 1992) and 254 ± 1.2 Ma (this report), were obtained from granodiorite and leucoquartz monzonite respectively in the southwestern half of the pluton. The northeastern half is undated.

STRUCTURE

West of Fraser Fault, Jurassic and older rocks are stacked in a series of three or more folded thrust slices, with each slice separated by mylonitized rocks and here and there sheared serpentinite. Because of U-Pb zircon dating, the lowest slice, Wineglass slice, is now known to contain Lower Jurassic sediments overlying Late Permian volcanics that have been intruded by the Late Permian Farwell Pluton. Wineglass slice probably extends northeast to include the intruded, locally felsic volcanics (**uPv**) on the northeast side of Chilcotin River near peak 3817'. Farwell slice incorporates an undated chloritized metadiorite (**Fdi**), ribbon cherts with intercalated limestone (**PTt**), and a structurally overlying siltstone-greywacke unit (**Jpw**). The succession faces and dips northeasterly. Because Eocene and younger units cover the northern extension of Farwell Fault, the extent of the slice is speculative, but its eastern truncation along Fraser Fault is not.

East of Fraser Fault, bedding attitudes outline a north-northwesterly-trending syncline with its western limb obliquely truncated along the fault. The eastern limb of the syncline exposes a duplication of the southwesterly-dipping Marble Canyon Formation with one limestone panel passing through Peavine Mountain and a second through Mount Pablo. Whether this results from a pair of isoclinal, northwesterly-plunging anticlines separated by a syncline, or from fault duplication is uncertain, but the distinctive red siltstone horizon above the limestone is apparently not repeated.

DISCUSSION

New radiometric and micropaleontologic dating results defined the ages of some of the stratified and plutonic rock units but enigmas remain. For example, Wineglass slice contains fossiliferous Lower Jurassic sediments (**IJs**) overlying U-Pb zircon-dated Late Permian volcanics (**uPv**) intruded by Late Permian cogenetic intrusions (**LPFqm**). The overlying Farwell slice has a 3000 m tectonically thickened succession of Lower Permian to Upper Triassic ribbon chert (**PTt**) which is absent in Wineglass slice implying that the two slices came from widely separated sources. An enigma is that both slices contain chloritized metadiorite (**Fdi**) of unknown but presumed Permian age which suggests that they never were widely separated.

Another enigma is that the pre-upper Jurassic rocks west of Fraser Fault are correlative in part with the Cache Creek Complex and similar in part to the Bridge River Complex or overlying Cayoosh Assemblage. The Cache Creek Complex consists of thick, unbedded limestone of the Marble Canyon Formation, and overlying thin limestones, ribbon chert, grey and green phyllite and siliceous phyllite, and basic metavolcanic rocks which comprise the Western Belt. Structurally, and possibly unconformably, overlying these rocks is a thick turbiditic siltstone-greywacke unit which I do not consider to be part of the complex. While the ribbon chert

and siltstone-greywacke unit can be correlated across Fraser Fault, the Marble Canyon Formation has no counterpart west of the fault, and the basic volcanic-rich succession of Carboniferous age, which composes Thaddeus slice west of the fault, is absent east of it. Ribbon chert (**PTt**) on both sides of the fault correlate with the Cache Creek Complex, while the siltstone-greywacke unit (**Jpw**) on both sides appear to correlate with the Cayoosh Assemblage which, according to Journey and Northcote (1992), conformably overlies the Bridge River Complex. Although Carboniferous rocks are absent from the Cache Creek Complex in the south, they are present in the Bridge River Complex.

Along the Chilcotin River, remnants of Upper Miocene fluvial sediments indicate that the Miocene paleochannel was subparallel to the present course of the Chilcotin in the map area and flowed southeastward. Although paleocurrent indicators are absent from Upper Miocene sediments along the Fraser upstream from Riske Creek, the flow was probably northward along a course subparallel to the present course. The quartzite-rich clast composition of the Miocene fluvial conglomerate exposed on Fiftyseven Creek near Clinton (Read, in press) and in the Gang Ranch area (Mathews and Rouse, 1984; Hickson et al., 1991) implies that these two areas separated by 70 km, are part of a common northward-flowing Miocene drainage system. The absence of quartzite clasts in the Miocene conglomerate in the lower part of the Chilcotin River indicates that the Miocene Fraser River did not flow northwestward along the Chilcotin River, but rather that the two Miocene rivers joined and flowed northward near the site of the present Fraser River.

ACKNOWLEDGMENTS

The kind assistance of Grant Hoffman of the Cotton Ranch and the Bonners of Deer Park Ranch are most appreciated. Dr. C.J. Hickson of the Geological Survey of Canada funded this project through the Chilcotin-Nechako Hydrocarbon Province Project, under contract #23254-2-0143/01-XSB. Drs. F. Cordey and M.J. Orchard provided radiolarian and conodont dates, respectively, from these fossil-poor rocks, and the Geochronology Section of the Survey, K-Ar and U-Pb dates, that made geological interpretations possible in this area of sparse outcrop and complex geology. Dr. J.A. Roddick critically reviewed and improved the manuscript.

REFERENCES

- Beyers, J.M. and Orchard, M.J.
1989: Permian-Triassic boundary beds in the Cache Creek Group, Marble Range, near Jesmond, British Columbia; in *Current Research, Part E; Geological Survey of Canada, Paper 89-1E*, p. 127-132.
- Cordey, F. and Read, P.B.
1992: Permian and Triassic radiolarian ages from the Cache Creek Complex, Dog Creek and Alkali Lake areas, southwestern British Columbia; in *Current Research, Part E; Geological Survey of Canada, Paper 92-1E*, p. 41-51.
- Cordey, F. and Schiarizza, P.
in press: A long-lived Panthalassic remnant: the Bridge River accretionary complex, Canadian Cordillera; *Geology*.

Cordey, F., Mortimer, N., DeWever, P., and Monger, J.W.H.

1987: Significance of Jurassic radiolarians from the Cache Creek terrane, British Columbia; *Geology*, v. 15, p. 1151-1154.

Friedman, R.M. and van der Heyden, P.

1992: Late Permian U-Pb dates for the Farwell and Northern Mount Lytton plutonic bodies, Intermontane Belt, British Columbia; in *Current Research, Part A*; Geological Survey of Canada, Paper 92-1A, p. 137-144.

Hickson, C.J.

1990: A new Frontier Geoscience Project: Chilcotin-Nechako region, central British Columbia; in *Current Research, Part F*; Geological Survey of Canada, Paper 90-1F, p. 115-120.

Hickson, C.J., Read, P., Mathews, W.H., Hunt, J.A., Johansson, G., and Rouse, G.E.

1991: Revised geological mapping of northeastern Taseko Lakes map area, British Columbia; in *Current Research, Part A*; Geological Survey of Canada, Paper 91-1A, p. 207-217.

Journey, J.M. and Northcote, B.R.

1992: Tectonic assemblages of the Eastern Coast Belt, southwest British Columbia; in *Current Research, Part A*; Geological Survey of Canada, Paper 92-1A, p. 215-224.

Mathews, W.H.

1989: Neogene Chilcotin basalts in south-central British Columbia: geology, ages, and geomorphic history; *Canadian Journal of Earth Sciences*, v. 26, p. 969-982.

Mathews, W.H. and Rouse, G.E.

1984: The Gang Ranch – Big Bar area, south-central British Columbia: stratigraphy, geochronology, and palynology of the Tertiary beds and their relationship to Fraser Fault; *Canadian Journal of Earth Sciences*, v. 21, p. 1132-1144.

Mathews, W.H. and Rouse, G.E. (cont.)

1986: An Early Pleistocene proglacial succession in south-central British Columbia; *Canadian Journal of Earth Sciences*, v. 23, p. 1796-1803.

Monger, J.W.H. and McMillan, W.J.

1989: Geology, Ashcroft, British Columbia; Geological Survey of Canada, Map 42-1989, sheet 1, scale 1:250 000.

Mortimer, N.

1987: Geological map of parts of NTS 92I/13; British Columbia Ministry of Energy, Mines and Petroleum Resources, Open File 1987-18.

Read, P.B.

1992: Geology of parts of Riske Creek and Alkali Lake areas, British Columbia; in *Current Research, Part A*; Geological Survey of Canada, Paper 92-1A, p. 105-112.

in press: Tertiary geology and industrial minerals, south-central British Columbia; British Columbia Ministry of Energy, Mines and Petroleum Resources, Bulletin.

Rouse, G.E. and Mathews, W.H.

1979: Tertiary geology and palynology of the Quesnel area, British Columbia; *Bulletin of Canadian Petroleum Geology*, v. 27, p. 418-445.

Trettin, H.P.

1980: Permian rocks of the Cache Creek Group in the Marble Range, Clinton area, British Columbia; Geological Survey of Canada, Paper 79-17, 17 p.

Geological Survey of Canada Project 890039-06

Glacier flow patterns of the Cordilleran Ice Sheet during the Fraser Glaciation, Taseko Lakes map area, British Columbia

David H. Huntley¹ and Bruce E. Broster¹
Cordilleran Division

Huntley, D.H. and Broster, B.E., 1993: Glacier flow patterns of the Cordilleran Ice Sheet during the Fraser Glaciation, Taseko Lakes map area, British Columbia; in Current Research, Part A; Geological Survey of Canada, Paper 93-1A, p. 167-172.

Abstract: Patterns of glacier flow associated with the advance of the Cordilleran Ice Sheet during the Fraser Glaciation are described for the Taseko Lakes area, British Columbia. Landforms, striae, and sediment sequences suggest that during early stages of the Fraser Glaciation, valley glaciers flowing from the Camelsfoot and Marble ranges blocked the Fraser River in the southern portion of the study area. As a result, proglacial lake systems developed in the major valleys of the central interior of British Columbia. Three major ice streams from the Camelsfoot, Chilcotin and Pacific ranges advanced north and north-eastward over the Fraser Plateau and eventually coalesced with west and southwestward flowing Cariboo Mountain ice along the Fraser River valley south of Williams Lake. Relict periglacial landforms above 1980 m delineate the ice surface over the Fraser Plateau prior to retreat.

Résumé : On a décrit les configurations d'écoulement de la glace, associées à l'avancée de l'inlandsis de la Cordillère au cours de la glaciation de Fraser dans la région des lacs Taseko en Colombie-Britannique. Les formes de relief, les stries et les séquences sédimentaires semblent indiquer que pendant les phases initiales de la glaciation de Fraser, les glaciers de vallée s'écoulant des chaînons Camelsfoot et Marble ont bloqué le Fraser dans la partie sud de la région à l'étude. De ce fait, des réseaux de lacs proglaciaires se sont formés dans les principales vallées de la région centrale de l'intérieur de la Colombie-Britannique. Trois grandes langues de glace issues des chaînons Camelsfoot, Chilcotin et Pacific ont progressé vers le nord et le nord-est au-dessus du plateau de Fraser et ont finalement fusionné avec les glaces de Cariboo Mountain qui s'écoulaient vers l'ouest et le sud-ouest dans la vallée du Fraser au sud du lac Williams. Des formes de relief périglaciaires résiduelles situées au-dessus de 1 980 m délimitent la surface couverte par les glaces au-dessus du plateau de Fraser, avant le recul de ces glaces.

¹ Department of Geology, University of New Brunswick, P.O. Box 4400, Fredericton, New Brunswick E3B 5A3

INTRODUCTION

Over large parts of British Columbia's Interior Plateau, drumlinized and fluted till records the diverse flow pattern of the Cordilleran Ice Sheet during the late Wisconsin Fraser Glaciation. The generalized glacier flow pattern in the Taseko Lakes area (NTS 920; Fig. 1) has been documented by Tipper (1971) and Heginbottom (1972). As part of a wider study, the Quaternary history of this area has been re-examined, and observations pertinent to the variable pattern of glacier flow are summarized here.

SETTING

Three principal physiographic elements are recognized in the study area (Broster and Huntley, 1992): mountains; upland and plateau areas; and valleys. The Fraser Plateau occupies the northern two-thirds the study area. East of the Fraser River, the Fraser Plateau gives way to the Green Timber Plateau. These plateaux consist largely of rolling to level upland, dissected by the deeply incised valleys of the Fraser

River and its tributaries. The Fraser Plateau is bordered on the south by the Marble, Camelsfoot, Chilcotin and Pacific ranges (Fig. 2a).

FIELD METHODS

Glacier flow directions were determined from drumlins, crag and tail, roches moutonnées and flutes observed on 1:20 000 (1967) and 1:60 000 (1987) scale air photos. These landforms, as well as striae and rattails on bedrock outcrops, were also examined in the field. However, because of poor bedrock exposure and extensive weathering, interpretations rely heavily on sediment sequences and directional landforms.

PATTERNS OF GLACIER FLOW DURING THE FRASER GLACIATION

Prominent drumlin fields and fluted terrain were mapped over much of the Fraser Plateau. Figure 2b is a synopsis of ice flow patterns determined from directional glacial landforms and combines earlier work (Tipper, 1971; Heginbottom, 1972) with data collected by the senior author in 1991 and 1992.

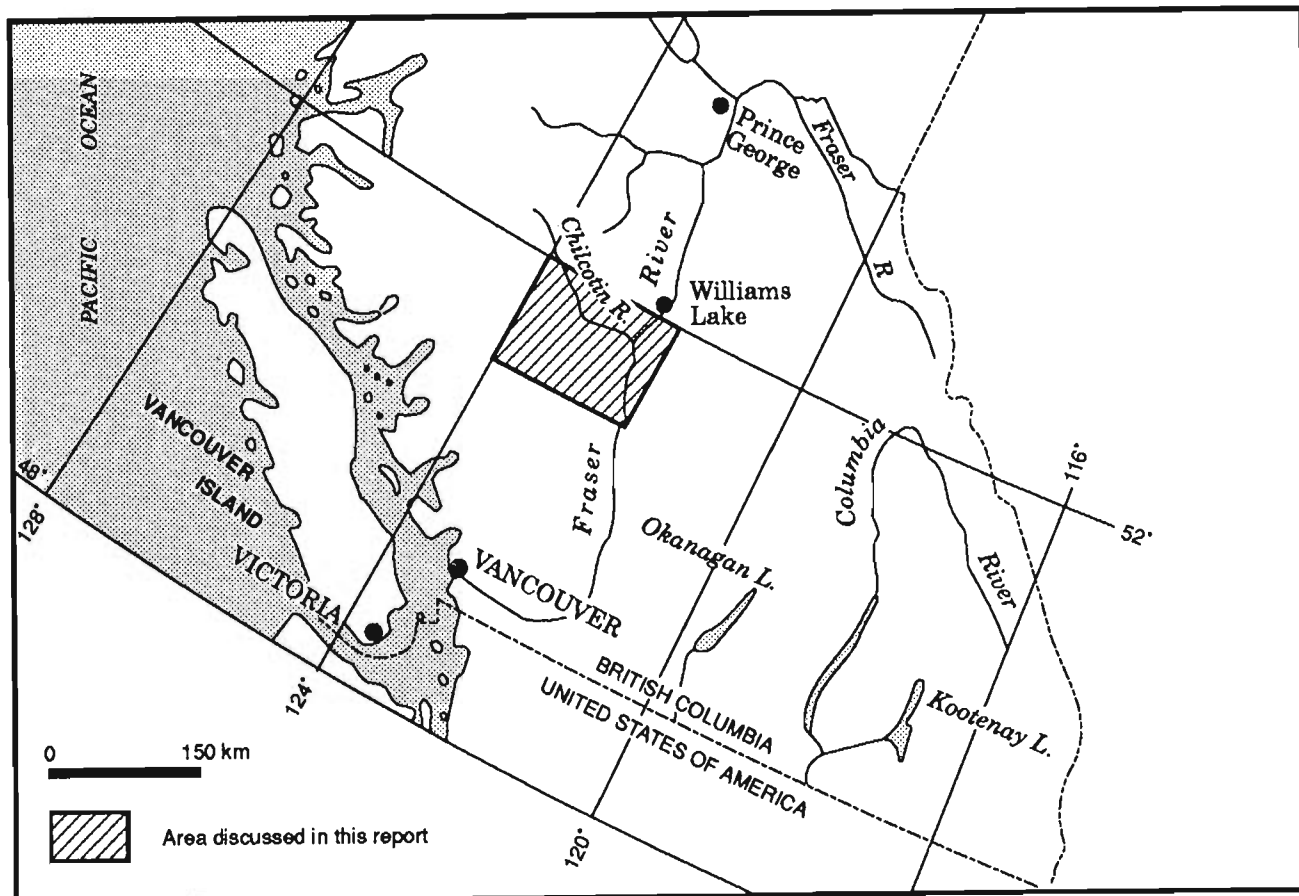


Figure 1. Location of Taseko Lakes map sheet (NTS 920).

Early during the Fraser Glaciation, as elsewhere (e.g., Kerr, 1934; Davis and Mathews, 1944), alpine glaciers grew in high mountain areas in southern portions of the study area. As glaciation intensified, piedmont lobes from these centres advanced across the Interior Plateau and coalesced to form the Cordilleran Ice Sheet (Clague, 1981). There were several centres of ice dispersal in the Taseko Lakes area (Tipper, 1971; Heginbottom, 1972). In the south, ice flowed from the Camelsfoot and Marble ranges; to the west, the Chilcotin and Pacific ranges were the main source; and east of the Fraser River, ice flowed mainly from the Cariboo Mountains. The geographical distribution of these sources indicates that ice from southern and western sources likely entered the study area before ice from the east.

Camelsfoot and Marble ranges

Cirques are present on most major peaks in the Camelsfoot Range. Their orientation is dominantly northwest to northeast. Northwestern flowing ice from the western Camelsfoot Range (e.g., Red and Poison mountains; Fig. 2b)

entered the upper Churn Creek basin where it was deflected northeastward by ice flowing out of the eastern Chilcotin Range (Fig. 2b). Glaciers in northeast- and east-trending valleys (e.g., Lone Cabin, South French Bar and Ward creeks) coalesced with valley glaciers flowing from the Marble Range (e.g., Big Bar Creek) to produce a U-shaped glacial trough in the Fraser River valley. Ice blocked the Fraser River valley in this area, ponding an extensive proglacial lake. Thick glaciolacustrine sediments subsequently accumulated in this lake system (Eyles and Clague, 1991). Ice from more distant sources advanced into and eventually overrode this lake.

South-facing cirques in the vicinity of Nine Mile Ridge indicate the presence of a former ice divide. Glaciers from these cirques flowed southeastward into the Fraser River valley south of the study area.

Chilcotin and Pacific ranges

Cirques in the Chilcotin and Pacific ranges, are generally oriented north and northeast, although there are exceptions in the higher southwest sector (e.g., Mount Tatlow). Several ice

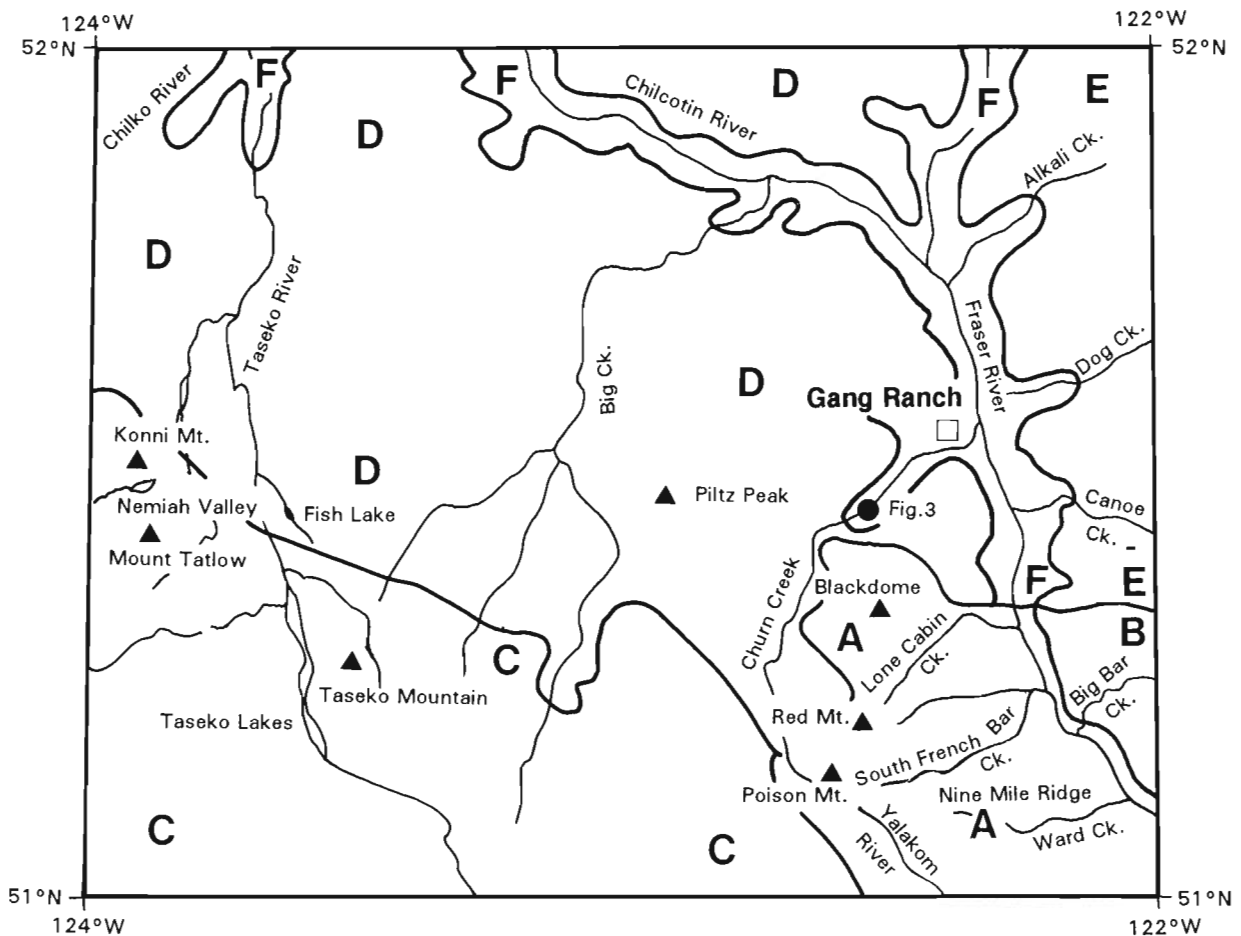


Figure 2a. Map of study area. Major physiographic regions: A - Camelsfoot Range; B - Marble Range; C - Chilcotin and Pacific ranges; D - West Fraser Plateau; E - East Fraser and Green Timber plateaux; F - Major river valleys (modified from Valentine et al., 1987). Solid triangles - peaks. Solid circles - reference location of text figures.

divides are recognized in this area (Fig. 2b). Striae and crag-and-tail features in the Nemiah Valley suggest that there was an ice divide west of Mount Tatlow and Konni Mountain (Fig. 2b). East of the divide, ice flowed northeastward across the Fraser Plateau after coalescing with major valley glaciers flowing from the southwest portion of the Taseko Lakes area.

West Fraser Plateau

Ice from the Camelsfoot, Chilcotin and Pacific ranges advanced across the Fraser Plateau and coalesced with Cariboo Mountain ice over the Fraser River valley (Fig. 2b; Tipper, 1971). Three major ice lobes followed the main valleys draining the Chilcotin and Camelsfoot ranges. Two westerly lobes extended over the plateau from the Taseko River and Big Creek valleys. The orientation of drumlins and flutes indicates northward ice flow with crude radial dispersal, likely produced as ice spilled across the low undulating surface of the Fraser Plateau. This pattern is especially

conspicuous near Fish Lake (Fig. 2a, b). A third lobe extended in a northeasterly direction along Churn Creek, entering the Fraser River valley south of Gang Ranch (Fig. 2b).

Ice advance sequences were examined at several sites in the west Fraser Plateau. Near Big Creek (UTM co-ordinates E034 N300; NTS 92O/10), glacial deformation structures were observed in advance glaciofluvial sediments. These structures were produced during the advance of ice over the area in the early part of Fraser Glaciation.

In upper Churn Creek valley, upwards of 50 m of bedded glaciofluvial gravels and ice-contact stratified and massive diamicts were deposited during ice advance (Fig. 3). These sediments are transitional with glaciolacustrine sediments towards Gang Ranch and Fraser Valley. Both sequences were partly eroded and drumlinized as ice advanced along Churn Creek into the ponded Fraser River valley. Retreat glaciofluvial and glaciolacustrine sediments were subsequently deposited over the earlier sediments (Fig. 3).

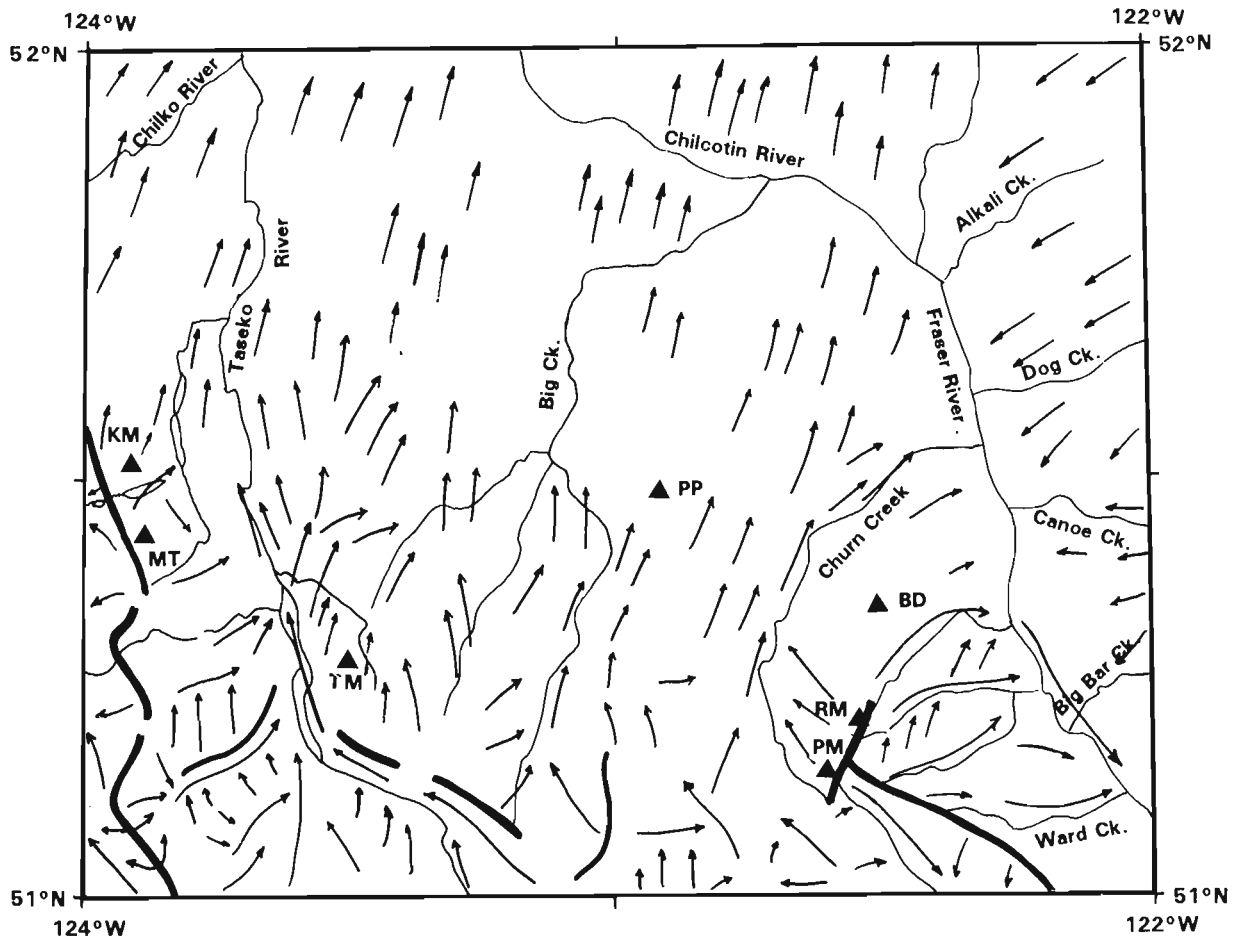


Figure 2b. Simplified pattern of ice flow and location of former ice divides in the Taseko Lakes area, from Tipper (1971), Heginbottom (1972) and this study. Arrows indicate directions of ice flow as determined herein. Bold lines mark approximate positions of ice divides. KM - Konni Mountain; MT - Mount Tatlow; TM - Taseko Mountain; PP - Piltz Peak; BD - Blackdome; RM - Red Mountain; PM - Poison Mountain.

Striae are rare or absent on many peaks, isolated uplands and the Fraser Plateau, notably Piltz Peak and Blackdome Mountain (Fig. 2a). Instead, there is widespread felsenmeer and relict patterned ground, and tors occur along some ridge crests. These observations suggest that periglacial conditions prevailed above 1980 m in these areas during Fraser Glaciation. Although this may not reflect the maximum elevation of the Cordilleran Ice Sheet on Fraser Plateau during Fraser Glaciation, it does represent a stable limit prior to ice retreat.

East Fraser and Green Timber plateaux

Ice from the Cariboo Mountains advanced over the east Fraser and Green Timber plateaux. Here, drumlins record west to southwest glacier flow east the Fraser River (Fig. 2b). In contrast to the situation west of the Fraser River, ice advance sequences were not observed in eastern valleys. This suggests that sediments may have been removed or reworked during the later phases of glaciation.

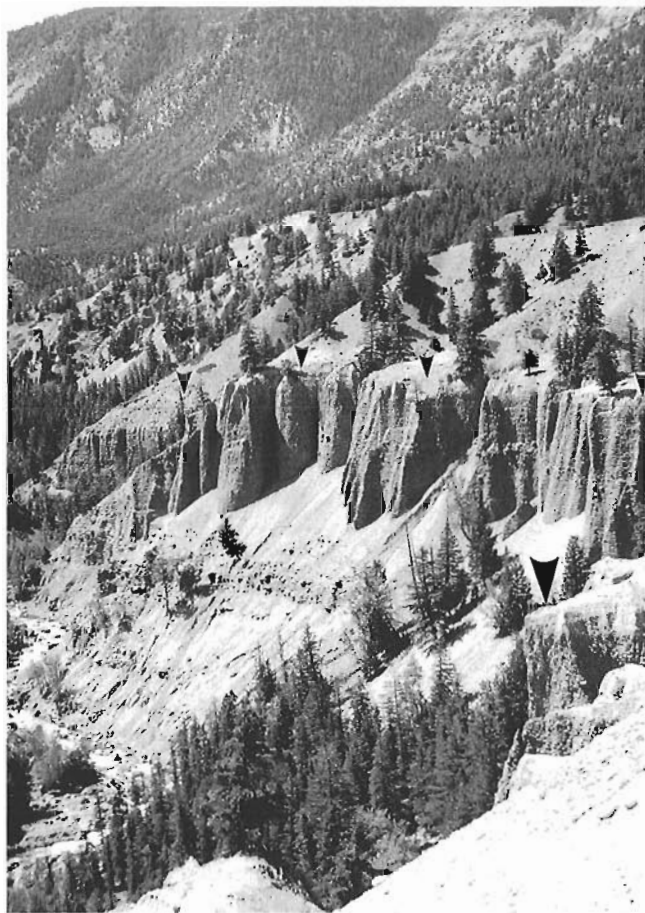


Figure 3. Advance and retreat glaciofluvial sediments in upper Churn Creek valley (contact indicated by arrows). The advance sequence is gradational with glaciolacustrine sediments exposed in the Gang Ranch area.

CONCLUSIONS

An ice flow history is proposed for the Late Wisconsinan advance of the Cordilleran Ice Sheet in the Taseko Lakes area. Key conclusions are:

1. During an early stage of Fraser Glaciation, valley glaciers flowing from the Camelsfoot and Marble ranges blocked Fraser River south of Big Bar Creek.
2. Due to this blockage, a proglacial lake system developed within the Fraser River valley and its tributaries. Thick glaciolacustrine sediments accumulated in this lake system.
3. Several ice divides were present in the Camelsfoot, Chilcotin and Pacific ranges. Three major ice lobes from these source areas advanced north-northeastward over the Fraser Plateau. This ice mass eventually coalesced with west-southwestward flowing Cariboo Mountain ice along the Fraser River valley south of Williams Lake.
4. Flow patterns (Fig. 2b) in the Taseko Lakes area suggest that lobes continued to function as discrete ice streams within the Cordilleran Ice Sheet as it flowed across the Fraser Plateau.
5. Relict periglacial landforms above 1980 m indicate a stable upper limit of glaciation prior to ice retreat.

ACKNOWLEDGMENTS

Logistical and financial assistance for fieldwork was provided by C.J. Hickson. Support for travel and preparation of this report was received from Supply and Services Canada, Contract No. 23254-1-0145/01-XSB. Assistance in the field was provided by Irene Alarie. Thanks are extended to Larry and Bev Ramstead and the staff of Gang Ranch for their co-operation during the 1991 and 1992 seasons. Informative and enlightening discussions were provided by Catherine Hickson, Peter Bobrowsky and Peter van der Heyden. A review by J.J. Clague significantly improved the final manuscript.

REFERENCES

- Broster, B.E. and Huntley, D.H.**
1992: Quaternary stratigraphy in the east-central Taseko Lakes area, British Columbia; in *Current Research, Part A*; Geological Survey of Canada, Paper 92-1A, p. 237-241.
- Clague, J.J.**
1981: Late Quaternary geology and geochronology of British Columbia. Part 2; Summary and discussion of radiocarbon-dated Quaternary history; Geological Survey of Canada, Paper 80-35, 41 p.
- Davis, N.F.G. and Mathews, W.H.**
1944: Four phases of glaciation with illustrations from southwestern British Columbia; *Journal of Geology*, v. 52, p. 403-413.
- Eyles, N. and Clague, J.J.**
1991: Glaciolacustrine sedimentation during advance and retreat of the Cordilleran Ice Sheet in central British Columbia; *Géographie physique et Quaternaire*, v. 45, p. 317-332.

Heginbottom, J.A.

1972: Surficial geology of Taseko Lakes map area, British Columbia; Geological Survey of Canada, Paper 72-14, 9 p.

Kerr, F.A.

1934: Glaciation of northern British Columbia; Transactions of the Royal Society of Canada, v. 28, Sec. IV, p. 17-32.

Tipper, H.W.

1971: Glacial geomorphology and Pleistocene history of central British Columbia; Geological Survey of Canada, Bulletin 196, 89 p.

Valentine, K.W.G., Watt, W., and Bedwany, A.L.

1987: Soils of the Taseko Lakes area, British Columbia; Agriculture Canada, British Columbia Soil Survey, Report No. 36, 131 p.

Geological Survey of Canada Project 890039-03

Facies reconstructions in the Lower to Middle Jurassic Ladner Group, southern British Columbia

J. Brian Mahoney¹

Cordilleran Division, Vancouver

Mahoney, J.B., 1993: Facies reconstructions in the Lower to Middle Jurassic Ladner Group, southern British Columbia; in Current Research, Part A; Geological Survey of Canada, Paper 93-1A, p. 173-182.

Abstract: The Lower to Middle Jurassic Ladner Group comprises the argillaceous Boston Bar Formation and the overlying volcanoclastic Dewdney Creek Formation. The latter is subdivided into a proximal, eastern facies and a distal, western facies. The proximal facies comprises pyroclastic rocks and lava flows, coarse grained lithic sandstone and conglomerate, and fine grained sandstone, siltstone, and argillite. This facies was deposited in a subaerial to subwave-base environment on a steep, west-dipping volcanoclastic apron by subaqueous pyroclastic flows and mass sediment gravity flows. The distal facies comprises two lithofacies: coarse grained sandstone and conglomerate and thin-bedded sandstone, siltstone and argillite. The distal facies is the product of subwave-base mass sediment flows and hemipelagic deposition on the distal portions of a volcanoclastic apron. The Middle Jurassic Lillooet Group is correlated with the western distal facies, and represents a slice of the Ladner Group offset along the dextral Fraser Fault.

Résumé : Le Groupe de Ladner, qui couvre l'intervalle du Jurassique inférieur à moyen, englobe la Formation de Boston Bar, composée de strates argileuses, et la Formation de Dewdney Creek sus-jacente, composée de roches volcanoclastiques. Cette dernière est subdivisée en un faciès est de type proximal et un faciès ouest de type distal. Le faciès proximal englobe des roches pyroclastiques et des coulées de laves, un grès lithique grossier et un conglomérat, et un grès, un siltstone et une argilite à grain fin. Ce faciès sédimentaire s'est accumulé dans un milieu subaérien passant à un milieu situé au-dessous de la base des vagues, sur une plaine d'épandage volcanoclastique de fort pendage ouest, par des coulées pyroclastiques subaquatiques et des glissements gravitaires des sédiments. Le faciès distal englobe deux lithofaciès: un grès et un conglomérat grossiers, et un grès, un siltstone et une argilite finement lités. Ce faciès distal est le produit des glissements gravitaires des sédiments au-dessous de la base des vagues et de la sédimentation hémipélagique sur les portions distales d'une plaine d'épandage volcanoclastique. Le Groupe de Lillooet du Jurassique moyen peut être corrélé avec le faciès ouest de type distal, et représente une tranche des couches décalées le long d'une faille dextre, à savoir la faille de Fraser.

¹ Department of Geological Sciences, University of British Columbia, 6339 Stores Road, Vancouver, B.C. V6T 1Z4

INTRODUCTION

The Ladner Group is a Lower to Middle Jurassic clastic succession exposed in southwestern British Columbia east of the Fraser fault system. The succession was deposited on the eastern margin of the Intermontane Belt in the Jurassic-Cretaceous Methow basin (Fig. 1). The group is subdivided into: 1) Sinemurian? to Upper Toarcian(?) Boston Bar Formation, a thick section of thin bedded argillite; and 2) Upper Toarcian to Upper Bajocian Dewdney Creek Formation, a sequence of coarse grained volcanoclastic rocks and lava flows (O'Brien, 1986, 1987).

Two distinct facies belts may be mapped within the Dewdney Creek Formation throughout its outcrop belt (Fig. 1). Delineation of these facies belts allow direct correlations to be made between the Ladner Group and Middle Jurassic Lillooet Group, exposed to the north near Lillooet on the opposite side of Fraser fault. This correlation adds additional constraints on the magnitude of transcurrent offset along the Fraser fault system (Fig. 1), and permits restoration of the original facies configuration of the Ladner Group.

This investigation is part of a regional analysis of Jurassic stratigraphy and basin configuration undertaken as a doctoral research project under the joint sponsorship of the Geological Survey of Canada and the University of British Columbia. Fieldwork in 1992 was completed under the auspices of the Chilcotin-Nechako Project, a regional mapping program in the south-central Intermontane Belt (Hickson, 1992). Field work in 1992 concentrated on a narrow outcrop belt of Jurassic strata situated between the Coast and Intermontane belts, in the Hope (92H), Pemberton (92J), and Taseko Lakes (92O) map areas.

GEOLOGICAL SETTING

The Boston Bar Formation of Ladner Group lies unconformably on oceanic greenstone and chert of the Triassic Spider Peak Formation, interpreted to be the basement of the Methow basin (Cairnes, 1924; Ray et al., 1985; Ray, 1986, 1990). Boston Bar Formation is overlain by volcanogenic sedimentary rocks of the Dewdney Creek Formation of Ladner Group. Dewdney Creek Formation is turn locally overlain unconformably by sandstone and conglomerate of the Upper Jurassic Thunder Lake sequence and the Lower Cretaceous Jackass Mountain Group (Monger, 1970; Coates, 1974; O'Brien, 1986).

Methow basin strata comprise Lower Jurassic to Upper Cretaceous rocks exposed east of the Yalakom and Hozameen fault systems (Garver, 1992), and west of the Pasayten Fault. The Pasayten Fault separates Jurassic and Cretaceous basinal sediments from gneisses and plutonic rocks of the Late Permian-Triassic Mount Lytton Complex and the Late Jurassic Eagle Plutonic complex (Greig, 1989; Friedman and van der Heyden, 1992) (Fig. 1). The eastern limit of Jurassic strata is the Chuwanten fault, an east-vergent thrust fault that places Jurassic strata over Cretaceous rocks

(Monger, 1989) (Fig. 1). The western limit of Methow basin strata south of Boston Bar is the Hozameen fault system, which separates Methow strata from Permian to Jurassic oceanic greenstones and chert of Hozameen Group (Monger, 1970, 1989; Ray, 1986, 1990).

North of Lytton, black siltstone, argillite, sandstone and conglomerate of the Aalenian to Bajocian Lillooet Group are exposed west of the Fraser fault system. Lillooet Group is unconformably overlain by strata of the Cretaceous Jackass Mountain Group (Kleinspehn, 1982; Schiarizza et al., 1989, 1990; Mahoney, 1992); the base of the Lillooet Group is not exposed. The western limit of the Lillooet Group is the Yalakom Fault, which separates an imbricate stack of Triassic, Jurassic, and Cretaceous clastic rocks on the northeast from the oceanic greenstone and chert of the Mississippian to Jurassic Bridge River Group (Schiarizza et al., 1989, 1990).

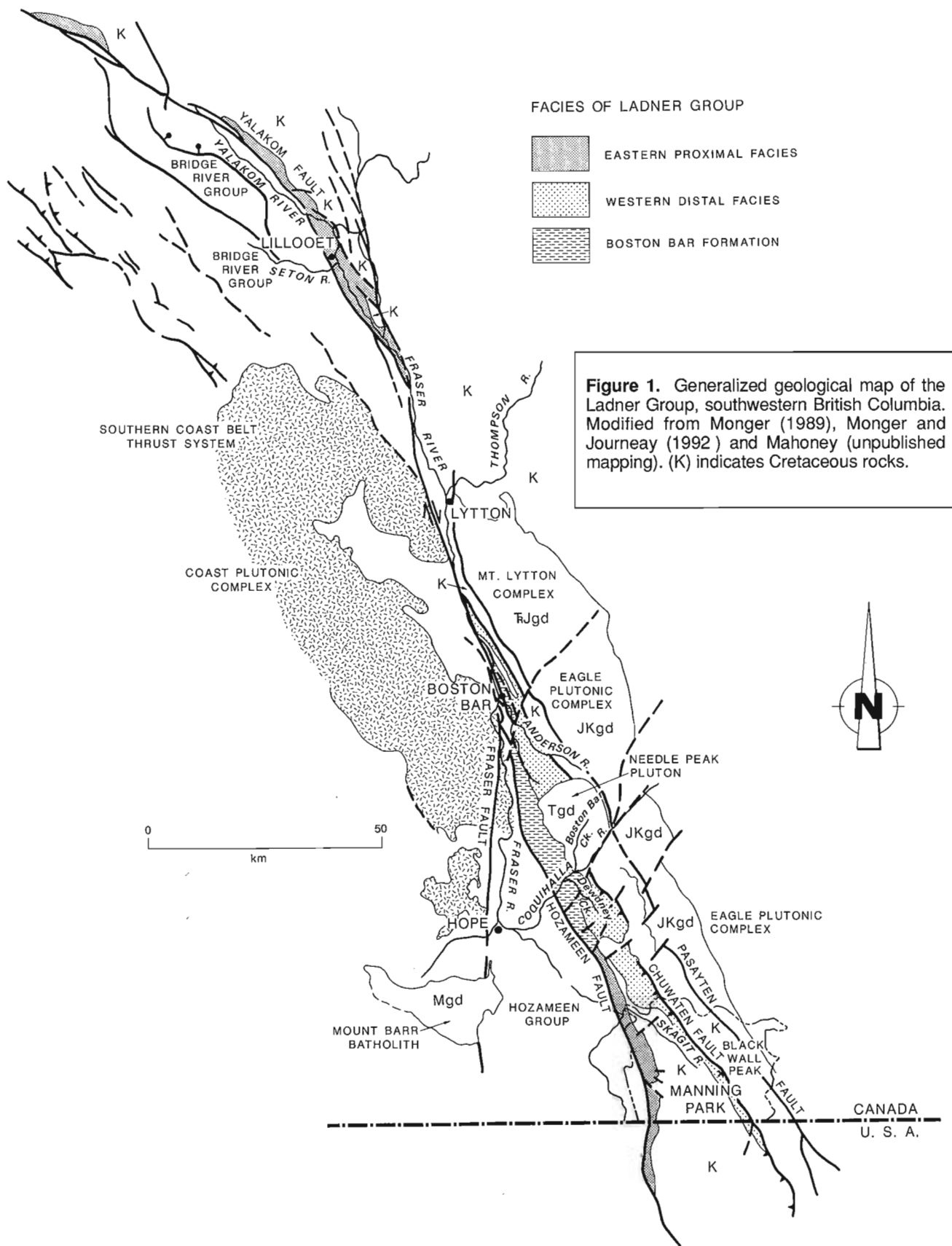
PREVIOUS WORK

Nomenclature of Jurassic rocks of the Methow basin has a long and complex history, primarily due to the lack of well exposed sections, poor age control, and complex structural relations. Significant strides in biostratigraphy, particularly by Coates (1974) and O'Brien (1986, 1987) have delineated the range and distribution of units, although disagreements still exist (Ray, 1990).

Cairnes (1924, 1944) named the Ladner Group for a thick sequence of slate and tuffaceous greywacke exposed along Ladner Creek northeast of Hope. Dewdney Creek Group was named for a sequence of coarse grained volcanogenic strata exposed in the Dewdney Creek area, and tentatively assigned a Late Jurassic to Early Cretaceous age (Cairnes, 1924, 1944).

Coates (1974) applied the name Ladner Group to rocks of Sinemurian(?), Toarcian, and Bajocian age that lie disconformably or with slight angular unconformity beneath rocks of Late Jurassic age in the Manning Park area. He subdivided the Ladner Group into an eastern and western outcrop belt, and established two reference sections for the group (Lookout section in the eastern belt; Divide section in the western belt). Coates (1974) correlated Upper Jurassic (Oxfordian to Portlandian) volcanogenic siltstone, sandstone, and rounded pebble conglomerate overlying Ladner Group with the Dewdney Creek Group of Cairnes (1924, 1944).

O'Brien (1986, 1987) significantly revised the nomenclature of Jurassic strata in the region based on new paleontological control in the Coquihalla and Anderson River areas (Fig. 1). O'Brien (1986) found that the type area of the "Upper Jurassic to Lower Cretaceous" Dewdney Creek Group of Cairnes (1924, 1944) consisted of Middle Jurassic strata, which she interpreted to lie conformably above Jurassic strata of Ladner Group. Consequently, O'Brien (1986, 1987) incorporated all Lower and Middle Jurassic rocks of the region into the Ladner Group, and subdivided the group into Lower Jurassic Boston Bar Formation and the overlying Middle Jurassic Dewdney Creek Formation. Upper Jurassic and Lower Cretaceous clastic strata disconformably



above Ladner Group, including the Dewdney Creek Group as defined in Manning Park (Coates, 1974), were renamed the Thunder Lake assemblage.

Ray (1986) mapped and described the stratigraphy of Ladner Group in Coquihalla River area in detail, documented the basal unconformity between the group and the underlying Spider Peak Formation, and analyzed the deformation of the group. Ray (1990) found Late Jurassic *Buchia* bivalves in fine grained siltstone lithologically indistinguishable and apparently conformable with argillaceous strata of the lower Ladner Group. On this basis, Ray (1990) disagreed with the subdivisions of O'Brien (1987), and mapped both Lower and Upper Jurassic siltstone and argillite as Ladner Group.

Ray (1990) mapped coarse grained volcanogenic strata overlying argillaceous rocks of Ladner Group as Jura-Cretaceous Dewdney Creek Group. The presence of Middle Jurassic ammonites in these overlying rocks suggests this assignment is incorrect. However, the applicability of the stratigraphy defined by O'Brien (1987) and described in this paper to the area mapped by Ray (1990) north of the Coquihalla River remains in dispute.

Mahoney (1992) reviewed the previous work and described the stratigraphy and depositional setting of Middle Jurassic volcanogenic strata of Lillooet Group near Lillooet (Fig. 1).

LADNER GROUP STRATIGRAPHY

Boston Bar Formation

Boston Bar Formation comprises strongly deformed and metamorphosed argillite, siltstone, lithic sandstone and minor conglomerate exposed in the west-central part of the Ladner Group outcrop belt, from south of the Coquihalla River northward to north of Boston Bar, where it is truncated by the Fraser fault system. The western limit of exposure is the Hozameen Fault, and the eastern boundary is the contact with the Dewdney Creek Formation or the Tertiary Needle Peak pluton (Monger, 1989) (Fig. 1).

O'Brien (1986) and Monger (1989) showed the Boston Bar Formation extending along the western edge of the Jurassic outcrop belt as far south as the International Border. Mapping during 1992 indicates that the unit does not extend south of Mt. Dewdney, and that all Lower and Middle Jurassic strata in Manning Park should be included in Dewdney Creek Formation. Fine grained strata mapped as Boston Bar Formation in Manning Park contains abundant coarse grained volcanic detritus and Late Toarcian to Middle Bajocian fossils, characteristics of the distal facies of Dewdney Creek Formation. Undated strata of Twisp Formation in Methow Valley, in Washington State, are lithologically similar to the Boston Bar Formation, but definitive correlation awaits age control.

Argillaceous strata characterize the Boston Bar Formation, although siltstone is equally abundant. The formation grades upward over a few hundreds of metres from a basal conglomerate and sandstone section into the siltstone

and argillite that dominate the section (Ray, 1990). New mapping in the Anderson River area demonstrates that the formation coarsens upward into medium- to coarse-grained sandstone and limestone-bearing volcanic conglomerate in the upper 200 m of section, near the contact with the overlying Dewdney Creek Formation.

The Boston Bar Formation unconformably overlies Triassic Spider Peak Formation (Ray, 1990). Matrix supported, polymict pebble to boulder conglomerate at the base of the formation contains subangular to rounded clasts of greenstone, quartz diorite, syenite, limestone, sandstone, and siltstone in a matrix of fine grained sand and silt. O'Brien et al. (1992) reported a 235 ± 10 Ma quartz diorite clast from this basal conglomerate and suggested it was derived from the Late Permian Mount Lytton Complex to the east. This correlation, if correct, indicates that the Methow basin has been adjacent to Quesnellia since its inception (O'Brien et al., 1992).

The upper contact of Boston Bar Formation is not exposed, but is believed to be gradational with the overlying Dewdney Creek Formation (O'Brien, 1986, 1987). The age of Boston Bar Formation is poorly constrained by sparse fossils as Sinemurian(?) to Toarcian(?) (Monger, 1989). The stratigraphic position of the Late Jurassic *Buchia* bivalves reported by Ray (1990) remains unclear.

Structural features in Boston Bar Formation consists of strong near-bedding-parallel cleavage, tight to isoclinal mesoscopic and macroscopic scale folds, and abundant bedding-parallel faults. Deformation increases significantly adjacent to both the Needle Peak pluton and to major faults, particularly the Fraser fault system (Fig. 1). The rocks are locally metamorphosed to hornblende hornfels facies. Structural and metamorphic alteration in the Boston Bar Formation is locally much higher than in the overlying Dewdney Creek Formation. These differences may be the result of pre-Toarcian deformation or may be apparent features created by competency differences in units adjacent to major faults and intrusions.

Dewdney Creek Formation

The Upper Toarcian to Upper Bajocian Dewdney Creek Formation is a heterogeneous package of coarse grained sandstone, conglomerate, siltstone, pyroclastic rocks, and volcanic flows with considerable lateral and vertical variation throughout the outcrop belt. It is exposed in a 200 km-long northwest trending outcrop belt extending from south of the International Border to north of Boston Bar (Fig. 1). The formation is exposed in two distinct outcrop belts contained in the limbs of a broad synclinerium situated between Hozameen and Chuwanten faults (Coates, 1974) (Fig. 1).

Dewdney Creek Formation comprises an eastern proximal facies assemblage and a western distal facies assemblage (Fig. 2, 3a). This distinction, first recognized by Coates (1974) in the Manning Park area, is herein extended throughout the entire Middle Jurassic part of the Methow basin.

Eastern proximal facies

This assemblage comprises three distinct lithofacies: 1) fine- to coarse-grained pyroclastic rocks and lava flows; 2) coarse grained lithic sandstone and conglomerate lithofacies; and 3) fine grained sandstone, siltstone, and minor argillite. These lithofacies are interbedded with one another in varying proportions throughout the area, but a very general fining upward sequence in the order of thousands of metres is generally recognized along the length of the outcrop belt (Fig. 2).

The volcanic lithofacies consists of coarse grained andesitic to dacitic breccia, tuff-breccia, lapilli tuff, lithic crystal tuff, crystal tuff, vitric tuff, and rare andesitic lava flows. Coarse pyroclastic rocks are typified by andesitic breccia exposed at Blackwall Peak in the Lookout section in Manning Park, where the breccia consists of matrix-supported pebble to boulder sized angular to subangular clasts of green hornblende crystal tuff in a fine grained plagioclase-bearing matrix. The most voluminous pyroclastic lithology in the formation is medium to very thick bedded (0.3 to 2 m) andesitic tuff-breccia and lapilli tuff.

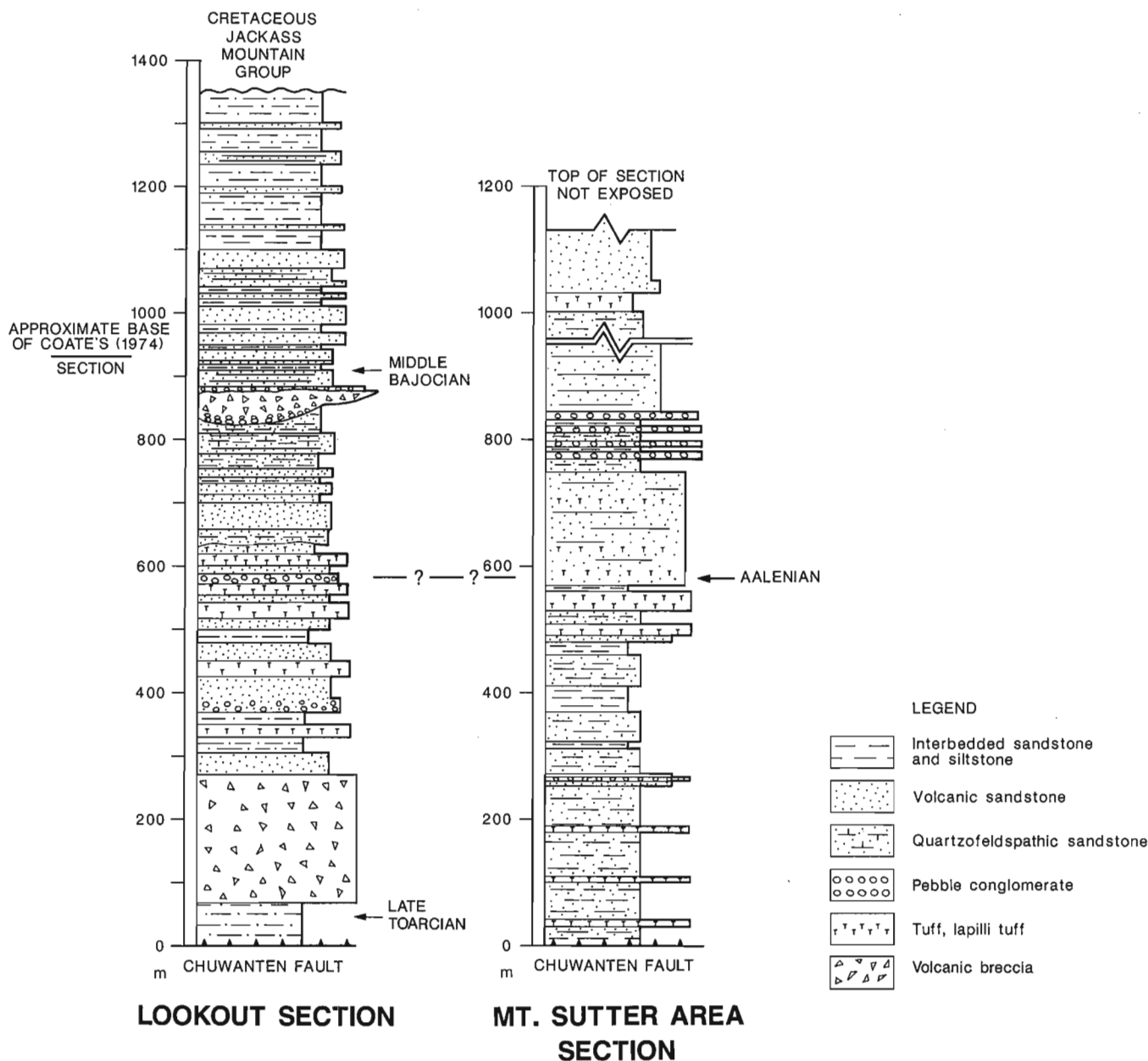


Figure 2. Partial stratigraphic sections of the eastern proximal facies of Dewdney Creek Formation. The Lookout section is in Manning Park, south of Blackwall Peak, with the base of the section at co-ordinates (10U, 663200mE, 5440600mN). The upper portion of the section is a revision of the Lookout section of Coates (1974). The Mt. Sutter section is a composite section measured on the east and west flanks of Mt. Sutter, and on the ridge above Mt. Tulameen. The base of the section is at (10U, 638700mE, 5477300mN).

These beds commonly show crude normal and reverse grading, parallel laminae, and locally contain siltstone rip-up clasts and other accidentals, including rare bioclasts. Many of the coarser pyroclastic beds are lenticular and, in the Lookout section, tuff-breccia fills submarine channels. Fine grained lithic crystal tuff, crystal tuff and vitric tuff is common in the upper third of the formation, and tends to be thin to medium bedded (3-30 cm), parallel laminated, and laterally continuous. These tuffs locally aggregate to 10-25 m.

Rare andesitic lava flows occur along the eastern margin of the outcrop belt in the Anderson River area (Fig. 1). The flows are generally green, aphanitic to porphyritic, with hornblende phenocrysts in an aphanitic matrix. Calcite and zeolite amygdules are common near the base and tops of flows, and the flows are commonly highly altered.

The coarse grained sandstone and conglomerate lithofacies consists of medium to thick bedded (0.1 to 0.8 m), medium to coarse grained lithic feldspathic wacke and arenite interbedded with minor fine to medium grained arenite and siltstone. Sandstone beds amalgamate to 2-25 m. The sandstone commonly contains siltstone rip-up clasts in the basal few centimetres, and generally exhibit normal grading and crude parallel laminae. Scour features, channel cuts, soft-sediment deformation and granule conglomerate stringers are locally abundant. Woody debris is common, and a medium bedded shelly lag deposit was noted at one locality. Coarsening and thickening and fining and thinning upward sequences (1-10 m thick) are common. The majority of the sandstone is volcanic, with plagioclase the most abundant clastic component, and lesser volcanic lithics, chloritized mafic grains, and quartz, all indicating a first-cycle volcanic source. One 40+ m thick section within the Lookout section of Manning Park contains abundant quartzofeldspathic arenite of unknown derivation. Pebble to boulder, matrix and clast-supported conglomerate with angular to subrounded volcanic clasts form lenticular horizons throughout the section, but are more common in the lower portions of the formation.

Fine grained sandstone, siltstone, and argillite lithofacies is characterized by thin bedded, thin laminated, fine to very fine grained, well sorted, lithic feldspathic arenite, medium to coarse grained laminated siltstone, and minor argillite. The unit contains abundant sedimentary structures, including parallel laminae, cross laminae, graded bedding (normal and reverse), flaser bedding, scour features, load casts, pinch and swell features, ripple marks, climbing ripples, and convolute laminae. Partial Bouma sequences are locally evident. This lithofacies commonly gradationally overlies thick sandstone sequences, but also forms thick (10-100 m) sequences, particularly near the upper portion of the section.

Depositional environment

The volcanic lithofacies was deposited by a combination of pyroclastic flows, debris flows, and air fall. Thick bedded (0.75-2 m) lapilli tuff that fine upwards from a basal rip-up horizon into lithic crystal tuff with inversely graded pumice

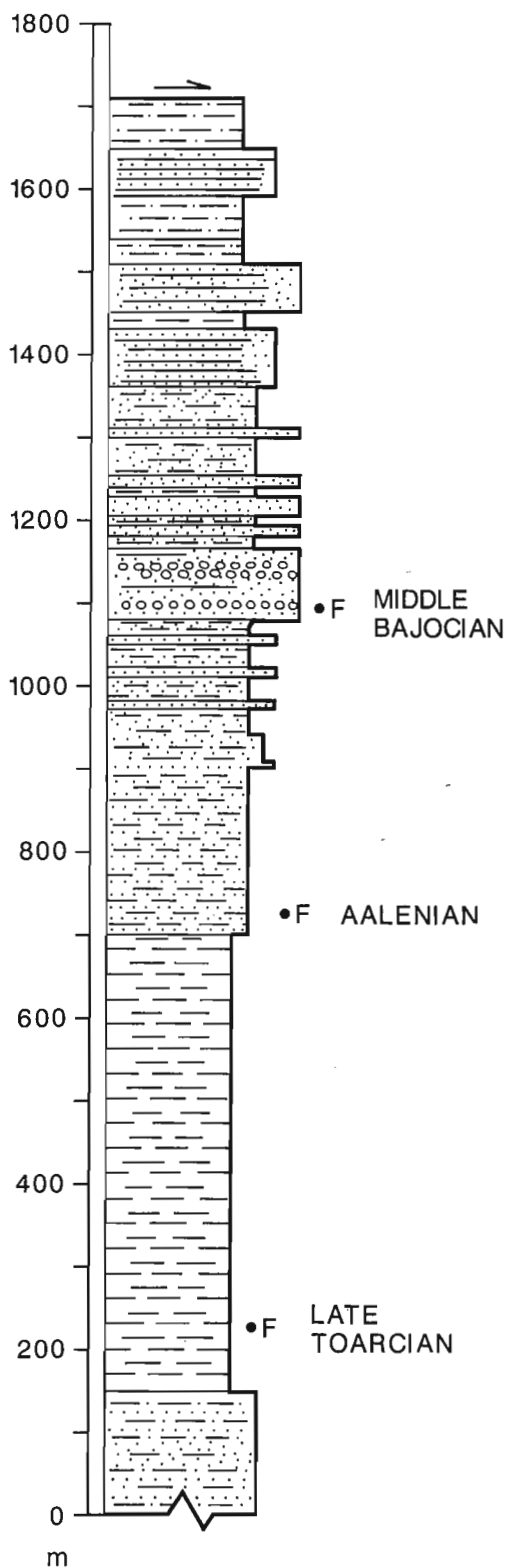
clasts near the upper contact are interpreted as subaqueous pyroclastic flows (Fisher and Schmincke, 1984). Thick bedded tuff-breccia and lapilli tuff with inversely graded bases overlain by normally graded crudely laminated medium bedded lapilli tuff and lithic crystal tuff may also indicate subaqueous pyroclastic flows. Thin, normally graded crystal tuffs with irregular lower contacts, randomly oriented plagioclase crystals and reworked tops are believed to be air fall deposits. Thick, lenticular, and locally channel-filling breccia and tuff-breccia with rare clast alteration rinds represent lahars. Non-pillowed lava flows in the Anderson River drainage indicate a nearby subaerial vent region.

The coarse grained sandstone and conglomerate lithofacies was primarily deposited by subaqueous mass flow mechanisms. Thick (0.6-2 m), structureless to crudely laminated sandstone and granule conglomerate with abundant basal rip-up clasts dominates the facies, and is the product of high-concentration turbidity currents. Intercalated thin-bedded siltstone represent low-concentration partial turbidites. Lenticular pebble to boulder conglomerate within fine grained facies indicates subaqueous channelized flow in the eastern part of the outcrop belt.

Fine grained sandstone and siltstone lithofacies is the product of low concentration turbidity currents, hemipelagic suspension sedimentation, and tractional sediment transport. Thin bedded, bottom-cut-out partial Bouma sequences (TCDE, TDE) are normally associated with thick bedded sandstone successions, and represent deposition in the waning stages of high concentration mass sediment flows. However, parallel laminated sandstone, siltstone and argillite locally aggregate to 10-25 m, and are believed to be the result of both low concentration turbidity currents and tractive sedimentation. Tractive sedimentation is indicated by locally abundant sedimentary structures, and by parallel and crosslaminated fossil-rich lag deposits near the eastern boundary of the outcrop belt. Thick sequences (5-15 m) of black argillite are the product of hemipelagic sedimentation.

The eastern proximal facies was deposited rapidly in shallow to intermediate depth (below normal wave base) water adjacent to an energetic andesitic to dacitic volcanic system. Deposition occurred on a volcaniclastic apron characterized by episodic pyroclastic influx and subaqueous mass sediment gravity flows. The apron shallowed to the east, as evidenced by an increase in bioclastic debris, woody debris, coarse volcanic breccia and lava flows toward the eastern edge of the outcrop belt. A steep gradient is implied by the proximity of high concentration turbidites and subaerial(?) lava flows, and by the overall coarse grain size of the sediment. Sediment transport was dominantly to the west, as indicated by the east-to-west proximal-distal transition, and by rare paleocurrent indicators. Rapid lateral facies changes suggest an uneven bottom topography, and the presence of quartzofeldspathic rocks in Manning Park suggest multiple source areas. The abundance of convolute laminae, ball and pillow structures, overturned flame structures, and lack of biogenic structures suggest deposition was rapid.

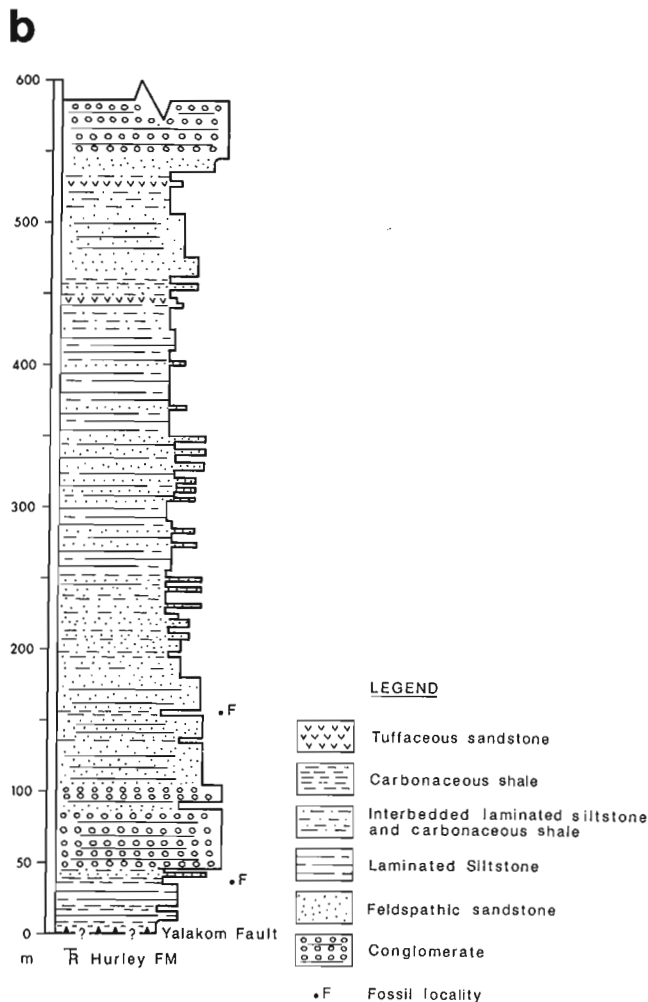
a UPPER JURASSIC
THUNDER LAKE SEQUENCE



DIVIDE SECTION

Figure 3.

a) Partial stratigraphic section of the western distal facies of the Dewdney Creek Formation. The Divide section is in Manning Park, on the ridge between Skagit River and Twenty-six Mile Creek. The base of the section is at (10U 647700mE, 5447200mN). The section is an expansion and revision of the section of Fربولd et al. (1969). **b)** Stratigraphic section of the Lillooet Group, measured upstream from the confluence of Blue Creek and Yalakom River north of Lillooet. The base of the section is at (10U, 537800mE, 565370mN). This section is from Mahoney (1992). Note difference in scale between the two sections. F=lower and upper fossil localities are Vaalenian and Bajocian, respectively.



LILLOOET GROUP

Western distal facies

The western distal facies may be subdivided into two lithofacies: 1) a coarse grained sandstone and conglomerate lithofacies and 2) a fine grained facies of thin bedded sandstone, siltstone and argillite. The thin bedded lithofacies is volumetrically dominant, but it weathers recessively, creating prominent ribs of sandstone and conglomerate that appear to dominate the section. Figure 3a contains a partial stratigraphic section of the western distal facies.

The thin bedded lithofacies consists of rhythmically interbedded 2-5 cm thick fine- to very fine-grained sandstone, siltstone, and argillite. Thin-bedded, fine grained sandstone and gradationally overlying siltstone form thin (3-8 cm) couplets that give the outcrop a banded appearance. Sedimentary structures consist of parallel lamination, with subordinate crosslaminae, convolute laminae, and graded bedding, organized into partial and complete Bouma sequences. Bioturbation is locally evident. Cyclicity is common, with fine sandstone beds alternately coarsening and thickening, then fining and thinning upward on a 10-50 m scale. Thin bedded carbonaceous argillite is intercalated throughout the section, and locally forms 0.5 to 1 m beds.

Coarse grained sandstone and conglomerate lithofacies consists of medium to very coarse grained lithic feldspathic arenite and wacke and granule to pebble volcanic conglomerate. The sandstone and conglomerate is medium to very thickly bedded, structureless to crudely laminated, and commonly contains fine grained rip-up clasts at the base. Sandstone and conglomerate beds are gradationally overlain by, and intercalated with, the fine grained lithofacies. Granule to pebble conglomerate is generally matrix-supported, crudely graded, and commonly forms thin "stringers" within sandstone-dominated sections. Medium and thick bedded sandstone and conglomerate beds occur in 50-80 m thick sequences, which commonly display coarsening and thickening upward and fining and thinning upward cyclicity.

Depositional environment

The western distal facies is the product of subaqueous mass sediment flow and hemipelagic deposition in a subwave-base marine environment. The thin bedded lithofacies was deposited by low concentration turbidity currents. This interpretation is based on the abundance of both complete and bottom-cut-out partial (T_{BCDE} , T_{CDE} , T_{DE}) Bouma sequences and the uniform, laterally continuous bedding. Homogeneous argillite sequences are the product of hemipelagic sedimentation, as shown by minor normal grading, lack of tractive sedimentary features, and the preservation of ammonite fauna. Episodic increases in clastic influx, perhaps due to migrating distributary lobes or the progradation of a clastic wedge, introduced coarse clastic debris into the basin. The coarse grained lithofacies is the product of unchanneled, high concentration turbidity current deposition during these periods of high clastic influx. This interpretation is supported by the abundance of thick to

very thick bedded, structureless to crudely graded sandstone beds, inferred to be amalgamated mass sediment gravity flows, enveloped in fine grained hemipelagic sediments.

The western distal facies is thought to have been deposited farther from the volcanic highland than the eastern proximal facies due to its overall finer grained nature, lack of primary pyroclastic debris and lava flows, lack of channels, abundance of organized turbidite features, and the absence of wood and shallow water shelly debris. The western distal facies is believed to have been deposited at the base of a volcanoclastic apron which received sediment from the east.

Age

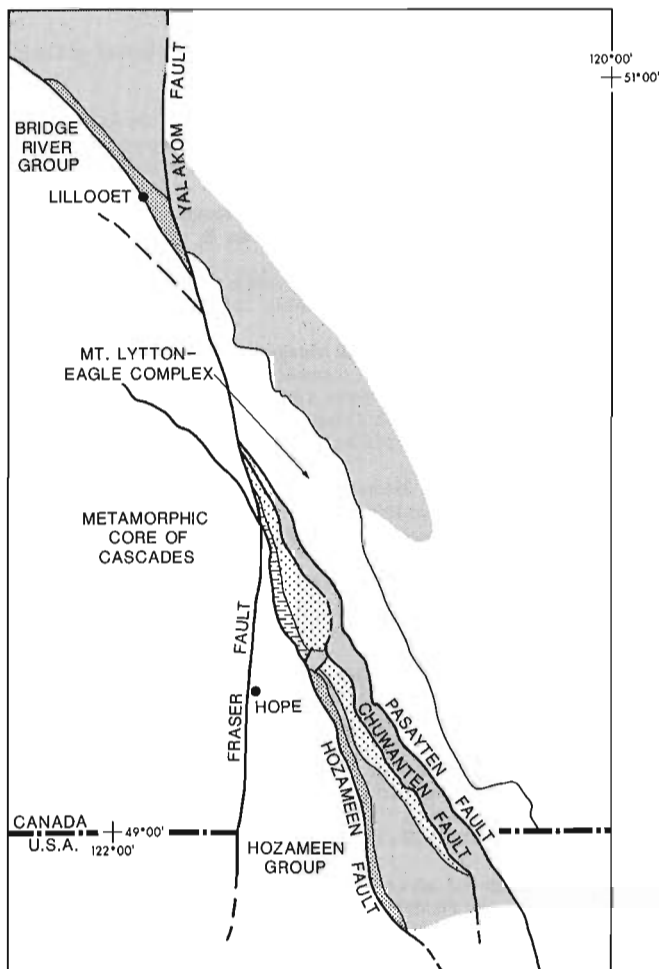
The age of Dewdney Creek Formation is constrained as Late Toarcian to Late Bajocian (O'Brien, 1986; this study), although the age of the upper and lower contacts is unknown. Five new fossil localities were discovered during 1992, including the oldest and youngest fossils yet found in the eastern outcrop belt. A well-preserved ammonite, *Zemistephanus richardsoni*, of late Early Bajocian to early Late Bajocian age from the Anderson River area extends the known age range of the formation (H.W. Tipper, pers. comm., 1992). The association of *Tmetoceras* with Trigonid pelecypods and brachiopods in volcanic strata suggests sediments east of the Anderson River are Early Aalenian or older, indicating that volcanism was active from at least Early Aalenian to Late Bajocian time. A Toarcian(?) to Aalenian initiation of volcanism is indicated by a thick sequence of lapilli tuffs and tuff stratigraphically below an Aalenian(?) ammonite discovered by O'Brien (1986), on the east flank of Mt. Sutter.

The Early Bajocian ammonite identified by O'Brien (1987) from below the breccia of Blackwall Peak is problematic. Frebold et al. (1969) noted a Late Toarcian ammonite from the same section, and the fine grained nature of the sediments preclude reworking to account for this contradiction. The discovery of Aalenian ammonites stratigraphically above the breccia of Blackwall Peak supports a Late Toarcian age for the breccia (Coates, 1974), suggesting volcanism was active as early as Late Toarcian. The ammonite discovered by O'Brien (1987) may indicate structural duplication along a strand of the Chuwanten Fault.

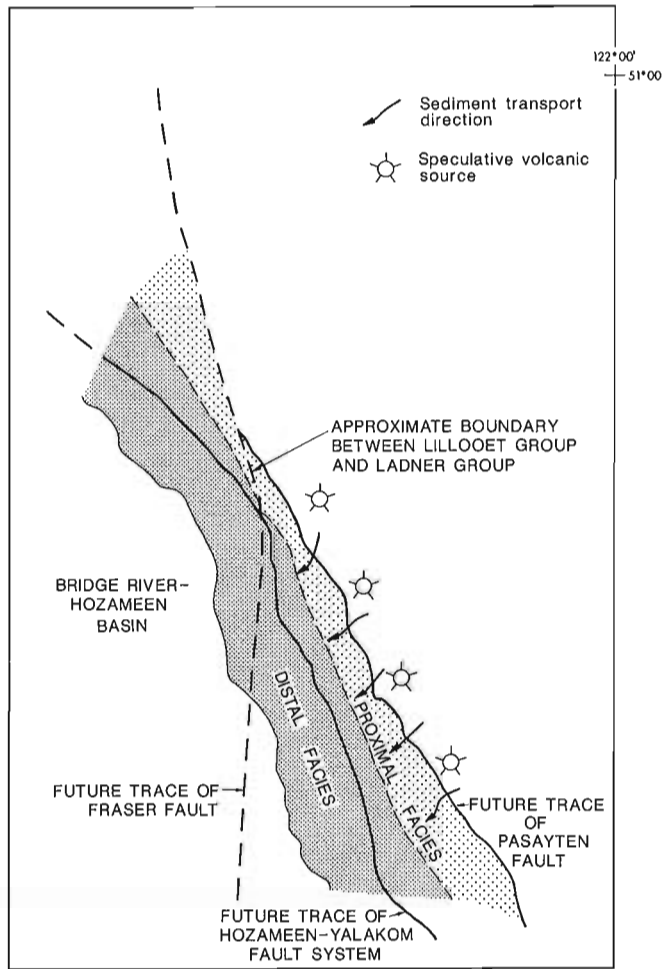
Lillooet Group

The Aalenian to Bajocian Lillooet Group consists of 800+ m of fine grained sandstone, siltstone, argillite, and lesser conglomerate exposed west of the Fraser fault system (Mahoney, 1992, and references therein) (Fig. 1). The age, lithology, sediment transport direction, faunal types, inferred depositional environment, and stratigraphic and structural position of the Lillooet Group (Fig. 3b) is similar to that of the western distal facies of Dewdney Creek Formation (Mahoney, 1992).

Examination of facies distribution on a regional scale shows that the western distal facies of Dewdney Creek Formation does not extend north of the Eocene Needle Peak



PRESENT



MIDDLE JURASSIC

Figure 4. Diagrammatic reconstruction of the facies assemblages of the Dewdney Creek Formation, with offset on the Fraser Fault System restored. See Figure 1 for legend; light grey = Cretaceous rocks.

Pluton. The entire formation north of the pluton consists of the eastern proximal facies, with the distal facies missing. However, the western margin of Dewdney Creek Formation is truncated north of Boston Bar by the Fraser fault system. Displacement estimates on the Tertiary Fraser fault system range from 80-150 km, based on the offset of the Hozameen/Yalakom fault system, displacement of the Jackass Mountain Group, and correlation of the Permian Farwell Pluton and the Mount Lytton Complex (Kleinspehn, 1982; Monger, 1985; Friedman and van der Heyden, 1992; Monger and Journeay, 1992). Restoration of this magnitude places the Lillooet Group adjacent and west of the proximal facies of Dewdney Creek Formation (Fig. 4). I suggest that the Lillooet Group may be directly correlated with the western distal facies of Dewdney Creek Formation based on sedimentologic, stratigraphic, and structural grounds, and that Lillooet Group therefore represents a slice of the Ladner Group offset along the dextral Fraser Fault System. It is

further suggested that the name Lillooet Group be abandoned, and those rocks be assigned to Dewdney Creek Formation of Ladner Group.

ACKNOWLEDGMENTS

Darcy McDonald provided excellent assistance in the field, and is gratefully acknowledged for his motivation and good cheer. Time spent in the field with P.K. Link in the Dewdney Creek area proved invaluable, as always. I thank C.J. Hickson for her support and interest in the project. Reviews by R.M. Bustin, J.V. Ross, J.W.H. Monger, P.S. Mustard and G.J. Woodsworth were extremely helpful, as were numerous conversations with J.W.H. Monger concerning the stratigraphy and tectonics of the region. Bev Vanlier's help with the manuscript is much appreciated. This study was partially supported by EMR Research Agreement 111-4-92.

REFERENCES

Cairnes, C.E.

1924: Coquihalla area, British Columbia; Geological Survey of Canada, Memoir 139.

1944: Hope, British Columbia; Geological Survey of Canada, Map 737A.

Coates, J.A.

1974: Geology of the Manning Park area, British Columbia; Geological Survey of Canada, Bulletin 238, 177 p.

Fisher, R.V. and Schmincke, H.-U.

1984: Pyroclastic Rocks; Springer-Verlag, Berlin, 472 p.

Frebold, H., Tipper, H.W., and Coates, J.A.

1969: Toarcian and Bajocian rocks and guide ammonites from southwestern British Columbia; Geological Survey of Canada, Paper 67-10, 55 p.

Friedman, R.M. and van der Heyden, P.

1992: Late Permian U-Pb dates for the Farwell and Northern Mt. Lytton plutonic bodies, Intermontane Belt, British Columbia; in *Current Research, Part A*; Geological Survey of Canada, Paper 92-1A, p. 137-144.

Garver, J.I.

1992: Provenance of Albian-Cenomanian rocks of the Methow and Tyaughton basins, southern British Columbia: a mid-Cretaceous link between North America and the Insular terrane; *Canadian Journal of Earth Sciences*, v. 29, no. 6, p. 1274-1295.

Greig, C.J.

1989: Geology and geochronometry of the Eagle Plutonic Complex, Coquihalla area, southwestern British Columbia; M.Sc. thesis, University of British Columbia, Vancouver, 423 p.

Hickson, C.J.

1992: An update on the Chilcotin-Nechako project and mapping in the Taseko Lakes area, west-central British Columbia; in *Current Research, Part A*; Geological Survey of Canada, Paper 92-1A, p. 129-135.

Kleinspehn, K.L.

1982: Cretaceous sedimentation and tectonics, Tyaughton-Methow Basin, southwestern British Columbia; Ph.D. thesis, Princeton University, New Jersey, 184 p.

Mahoney, J.B.

1992: Middle Jurassic stratigraphy of the Lillooet area, south-central British Columbia; in *Current Research, Part A*; Geological Survey of Canada, Paper 92-1A, p. 243-248.

Monger, J.W.H.

1970: Hope map-area, west half, British Columbia; Geological Survey of Canada, Paper 69-47, 75 p.

1985: Structural evolution of the southwestern Intermontane Belt, Ashcroft and Hope map areas, British Columbia; in *Current Research, Part A*; Geological Survey of Canada, Paper 85-1A, p. 349-358.

Monger, J.W.H. (cont.)

1989: Geology, Hope, British Columbia; Geological Survey of Canada, Map 41-1989, sheet 1, scale 1:250 000.

Monger, J.W.H. and Journeay, J.M.

1992: Guide to the geology and tectonic evolution of the southern Coast Belt; field guide to accompany Penrose Conference on "Tectonic Evolution of the Coast Mountains Orogen", 92 p.

O'Brien, J.

1986: Jurassic stratigraphy of the Methow Trough, southwestern British Columbia; in *Current Research, Part B*; Geological Survey of Canada, Paper 86-1B, p. 749-756.

1987: Jurassic biostratigraphy and evolution of the Methow trough, southwestern British Columbia; M.Sc. thesis, University of Arizona, Tucson, 150 p.

O'Brien, J.A., Gehrels, G.E., and Monger, J.W.H.

1992: U-Pb geochronology of plutonic clasts from conglomerates in the Ladner and Jackass Mountain groups and the Peninsula Formation, southwestern British Columbia; in *Current Research, Part A*; Geological Survey of Canada, Paper 92-1A, p. 209-214.

Ray, G.E.

1986: Geology of the Hozameen Fault between Boston Bar and the Coquihalla River; British Columbia Ministry of Energy, Mines and Petroleum Resources, Open File 1986-1, scales 1:20 000 and 1:6 000.

1990: The geology and mineralization of the Coquihalla gold belt and Hozameen fault system, southwestern British Columbia; British Columbia Ministry of Energy, Mines and Petroleum Resources, Bulletin 79, 97 p.

Ray, G.E., Coombes, S., MacQuarrie, D.R., Niels, R.J.E.,**Shearer, J.T., and Cardinal, D.G.**

1985: Precious metal mineralization in southwestern British Columbia; in *Field Guides to Geology and Mineral Deposits in the Southern Canadian Cordillera*, (ed.) D.J. Tempelman-Kluit; Geological Society of America Cordilleran Section Field Guide, Vancouver, B.C., p. 9.1 - 9.31.

Schiarizza, R., Gaba, R.G., Coleman, M., Garver, J.I., and**Glover, J.K.**

1990: Geology and mineral occurrences of the Yalakom River area; in *Geological Fieldwork 1989*, British Columbia Ministry of Energy, Mines and Petroleum Resources, Paper 1990-1, p. 53-72.

Schiarizza, R., Gaba, R.G., Glover, J.K., and Garver, J.I.

1989: Geology and mineral occurrences of the Tyaughton Creek area; in *Geological Fieldwork 1988*, British Columbia Ministry of Energy, Mines and Petroleum Resources, Paper 1989-1, p. 115-143.

 Geological Survey of Canada Project 890039-02

New Middle Cambrian fossil and geological data from the Brussilof magnesite mine area, southeastern British Columbia

W.H. Fritz and G.J. Simandl¹

Institute of Sedimentary and Petroleum Geology

Fritz, W.H. and Simandl, G.J., 1993: New Middle Cambrian fossil and geological data from the Brussilof magnesite mine area, southeastern British Columbia; in Current Research, Part A; Geological Survey of Canada, Paper 93-1A, p. 183-190.

Abstract: In the Brussilof mine area in southeastern British Columbia, the magnesite-bearing Cathedral Formation is overlain by the Stephen Formation, which contains *Ptychagnostus gibbus* Zone fossils. Sixty-five kilometres to the northwest, in the Field area, the Field member of the overlying Eldon Formation belongs to the same zone. Correlation between the two areas suggests an unconformity in the Brussilof area at the Cathedral/Stephen contact. The time-rock equivalents of the two lowest Eldon members and an older, rock-equivalent of the Stephen Formation in the Field area are probably missing at this contact.

The proposed sub-Stephen unconformity in the Brussilof area represents adequate time for evaporite formation and/or ground preparation suitable for ore deposition. A later, abrupt transgression is recorded by the *P. gibbus* fauna in the Stephen Formation. The fossils and their mode of preservation indicate an open ocean level of salinity and deposition below wave base.

Résumé : Dans la région de la mine Brussilof dans le sud-est de la Colombie-Britannique, la Formation de Cathedral qui contient de la magnésite est recouverte par la Formation de Stephen, laquelle contient des fossiles de la zone à *Ptychagnostus gibbus*. À 65 km plus au nord-ouest, dans la région de Field, le membre de Field qui fait partie de la Formation d'Eldon sus-jacente appartient à la même zone. La corrélation entre les deux secteurs semble indiquer l'existence d'une discordance dans la région de Brussilof au contact entre les formations de Cathedral et de Stephen. Les équivalents chronostratigraphiques des deux membres basaux d'Eldon et un équivalent lithostratigraphique plus ancien de la Formation de Stephen dans la région de Field manquent probablement au niveau de ce contact.

La discordance proposée au-dessous de la Formation de Stephen dans la région de Brussilof représente un intervalle de temps suffisant pour avoir permis la formation d'évaporites et la préparation du sol propices à la mise en place du minerai. La faune à *P. gibbus* présente dans la Formation de Stephen témoigne d'une transgression ultérieure abrupte. Les fossiles et leur mode de conservation indiquent un taux de salinité correspondant à celui de la pleine mer, et une sédimentation se produisant au-dessous de la base des vagues.

¹ British Columbia Ministry of Energy, Mines and Petroleum Resources, Victoria, British Columbia V8V 1X4

INTRODUCTION

The Brussilof mine is located in the southern Canadian Rocky Mountains (Fig. 1). By 1990, 1,015,200 metric tons of magnesite had been produced (British Columbia Ministry of Energy, Mines and Petroleum Resources, 1990) at this mine. The magnesite at the mine site and three other showings in the area was discovered during the mapping of the Kananaskis Lakes areas by G.B. Leech (1979). Later research on the magnesite has been published by Simandl and Hancock, 1991, and Simandl et al. (in press).

The magnesite is hosted by the Middle Cambrian Cathedral Formation near the formation's westernmost margin. The overlying Stephen Formation is thin compared to the Stephen to the northwest, where it also overlies Cathedral platform carbonate rocks. The depositional relationship between the Cathedral and the Stephen in the Brussilof mine area has not been discussed previously, despite the large number of magnesite showings a short distance below the Cathedral/Stephen contact.

Recognition of the Middle Cambrian formations in the Brussilof area is based upon their lithologies, relative positions in alternating clastic and carbonate pairs (Grand Cycles of Aitken, 1966), and their presence in nearby areas. In this paper we focus on the Cathedral/Stephen and the Stephen/Eldon contacts, which we accept as being valid as currently mapped. However, the identification of fossils, collected recently across the Stephen/Eldon contact, in the Brussilof Mine area, date the contact as considerably younger than the same contact to the northwest. In this report, we assess the age of this contact, and the thinness of the Stephen Formation, in terms of their possible relationship to the ore deposits.

GENERAL GEOLOGY

Near the west margin of the Cathedral Formation (Fig. 2) an assumed fault (north trending) divides the area into two distinct subareas. The subarea west of the (?) fault is underlain by the thin bedded, slope and basal deposits of the Chancellor Formation. These Middle and lower Upper Cambrian strata are folded and belong to the outer detrital belt (see Fritz, 1991, for depositional belts). To the east of the (?) fault nearly flat-lying inner detrital and middle carbonate belt strata occur. These strata are generally thicker bedded and less deformed, and are (except for the Lower Cambrian Gog Group) of Middle Cambrian age. These formations and their local thicknesses are as follows (Simandl and Hancock, 1991; in ascending order): Gog Group, upper 250 m exposed; Naiset Formation, 65-70 m; Cathedral Formation, 340 m; Stephen Formation, approximately 16 m; undivided Eldon and Pika formations, approximately 500 m, with basal black limestone unit, approximately 50 m; Pika Formation, not measured; Arctomys Formation, not measured.

Near the Brussilof mine the Cathedral Formation is predominantly dolomite (Simandl and Hancock, 1991; Simandl et al., in press). Textures suggest that some of the dolomite originally contained gypsum disks. Brecciated areas have

been cemented with coarse, white dolomite. Pyrite is common, either in disseminated form or in pods and veins. Sparry carbonate is present in the Cathedral, Eldon, and Pika formations. The high-grade sparry magnesite was found in the Cathedral Formation adjacent to the formation's western margin.

The stratigraphic section shown in Figures 2 (location) and 3 contains only one prominent shale unit (Stephen Formation), and only one fossiliferous interval that starts 3.5 m below the top of the Stephen and extends 2.0 m into the Eldon. Described sections in the southern part of the area, near Miller Pass (Stewart, 1991, Section 12), and in the northern part of the area and 37 km to the northwest (Aitken, in press, composite sections AC 102-AC103 and AC 53-AC55), illustrate a similar stratigraphic succession, with the Stephen between the Cathedral and Eldon formations.

PALEONTOLOGY AND CORRELATION

The fossils from the Mt. Brussilof section (Plate 1) are identified as follows: *Diagoniella* sp., *Ehmaniella* sp., *Elrathina* sp., *Lingulella* sp., *Lejopyge seminula* (Whitehouse), *Peronopsis fallax* (Linnarsson), *Peronopsis interstricta* (White), *Peronopsis amplaxis?* Robison, and *Ptychagnostus gibbus* (Linnarsson).

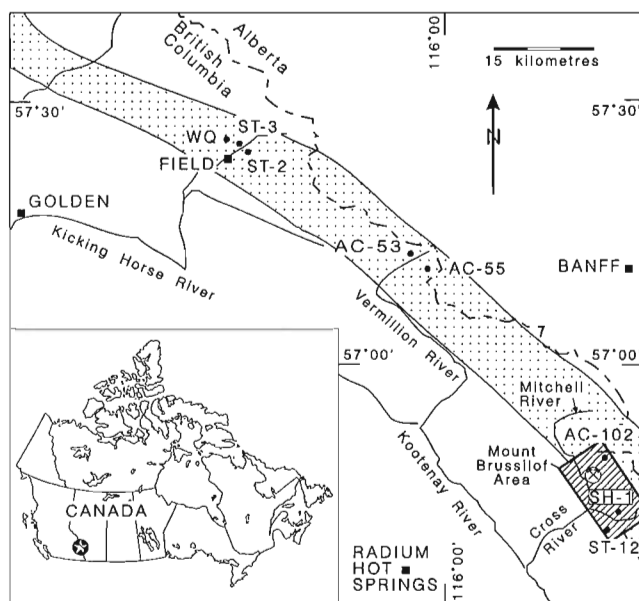


Figure 1. Locality map showing the Brussilof magnesite mine area, and its position relative to the Kicking Horse Rim (stippled pattern). Abbreviated localities are: WQ, Walcott's Burgess Shale Quarry; ST2 and ST3, sections measured by Stewart (1991) in the Field area; AC102-AC103 and AC53-AC55, and AC103, composite section measured by Aitken (in press, AC103 is off the map and a short distance to the east); ST12, section by Stewart (1991); SH1, section shown in Figure 3.

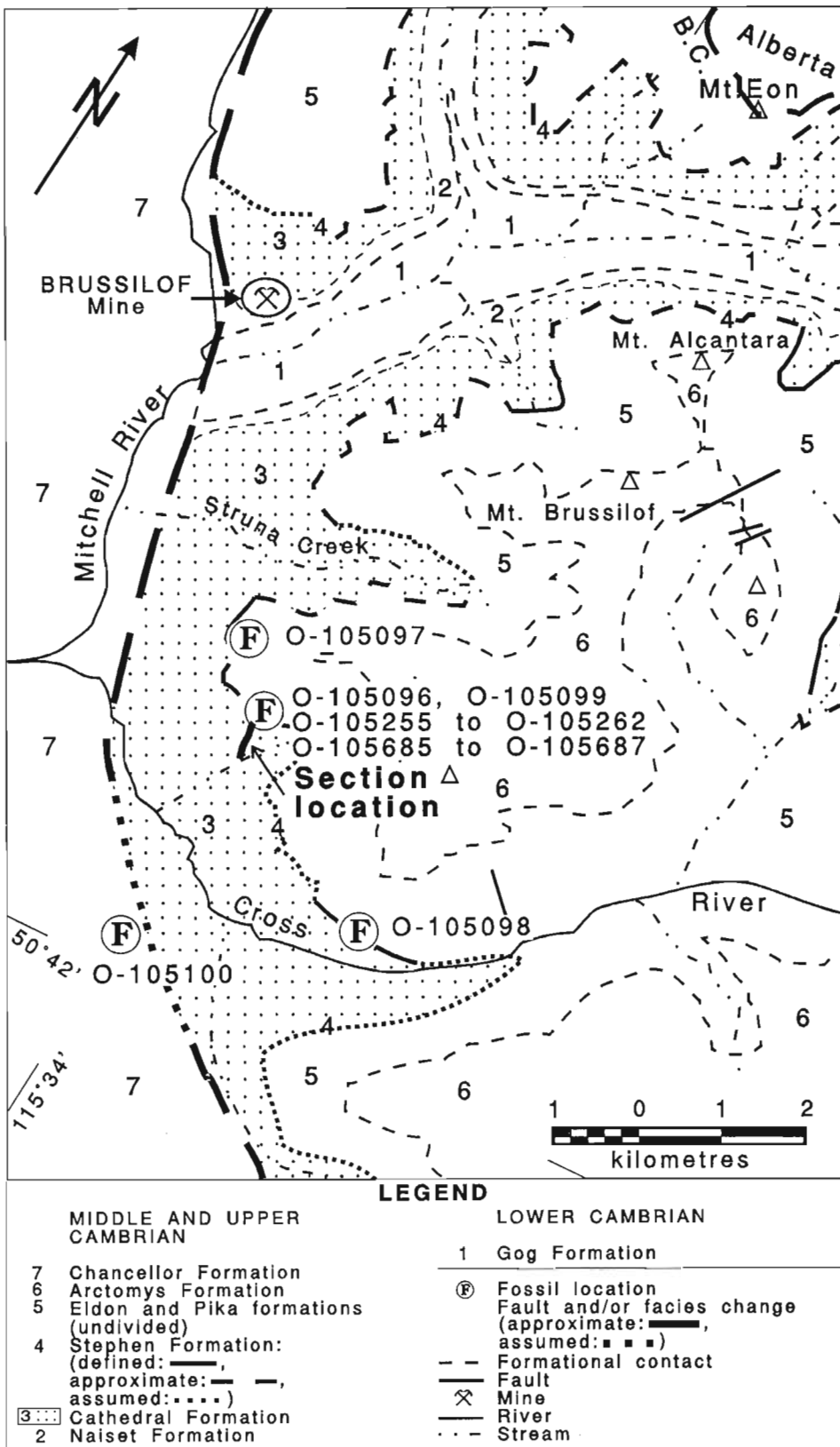


Figure 2. Geological map of the Brussilof magnesite mine area. Map units are: 1 – Gog Group; 2 – Naiset Formation; 3 – Cathedral Formation; 4 – Stephen Formation; 5 – Eldon-Pika formations; 6 – Arctomys Formation; 7 – Chancellor Formation. (Map adapted from Simandl and Hancock, 1991.)

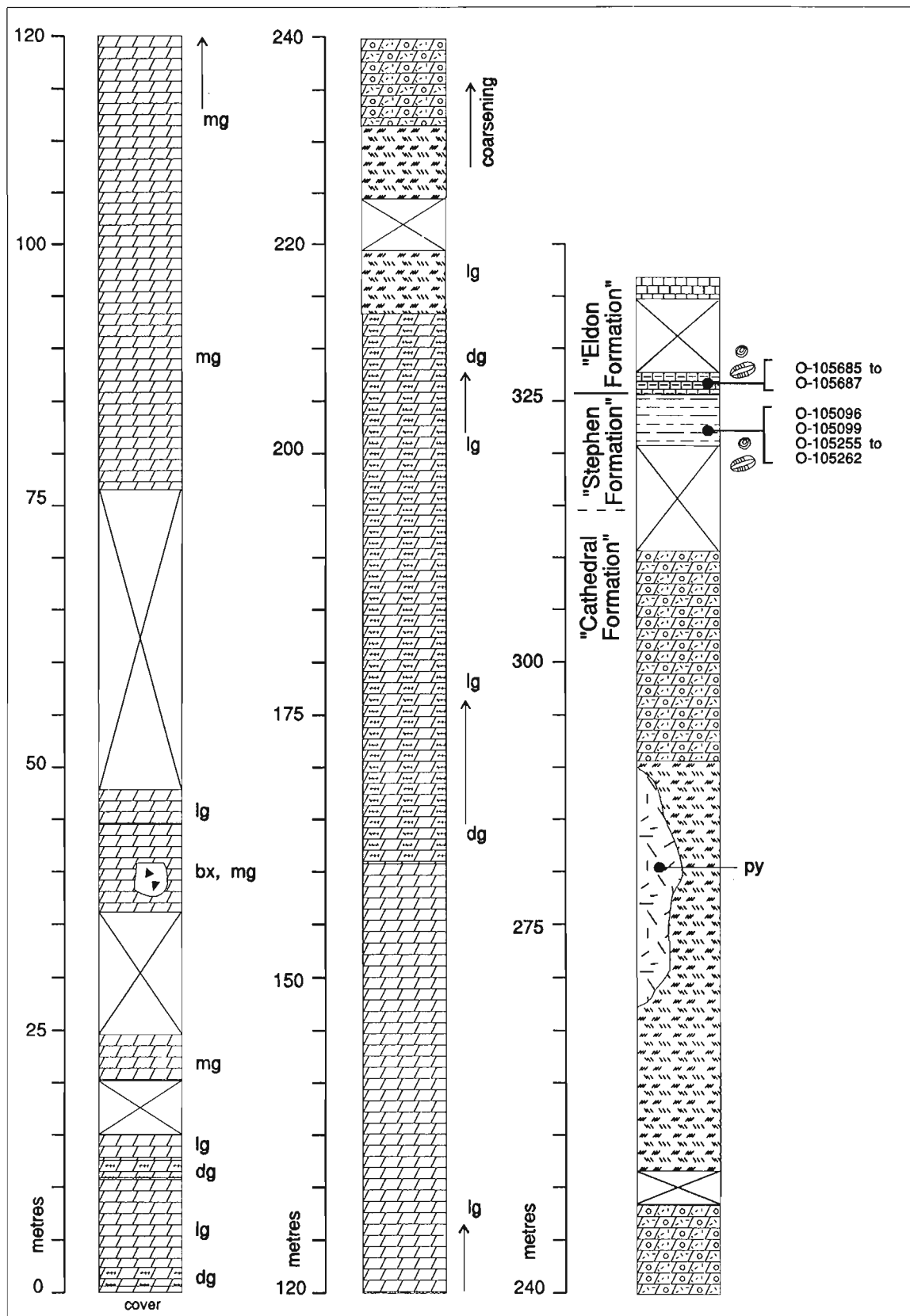
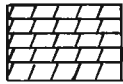
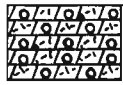


Figure 3. Stratigraphic section. Location shown on Figure 2. *Ptychagnostus gibbus* Zone fossils are from the interval 3.5 m below to 2.0 m above the Stephen/Eldon formational contact. Geological Survey of Canada localities from this interval are O105096 to O105099, O105255 to O105262, and O105685 to O105687.

LEGEND for Fig. 3

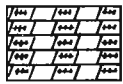
dolomite



sugary dolomite



fenestral dolomite

dolomite with
sparry carbonate

limestone



interbedded limestone



shale



sparry carbonate



trilobite

inarticulate
brachiopod

lg

light grey

mg

medium grey

dg

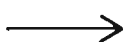
dark grey

bx

dissolution breccia

py

pyritiferous



gradation

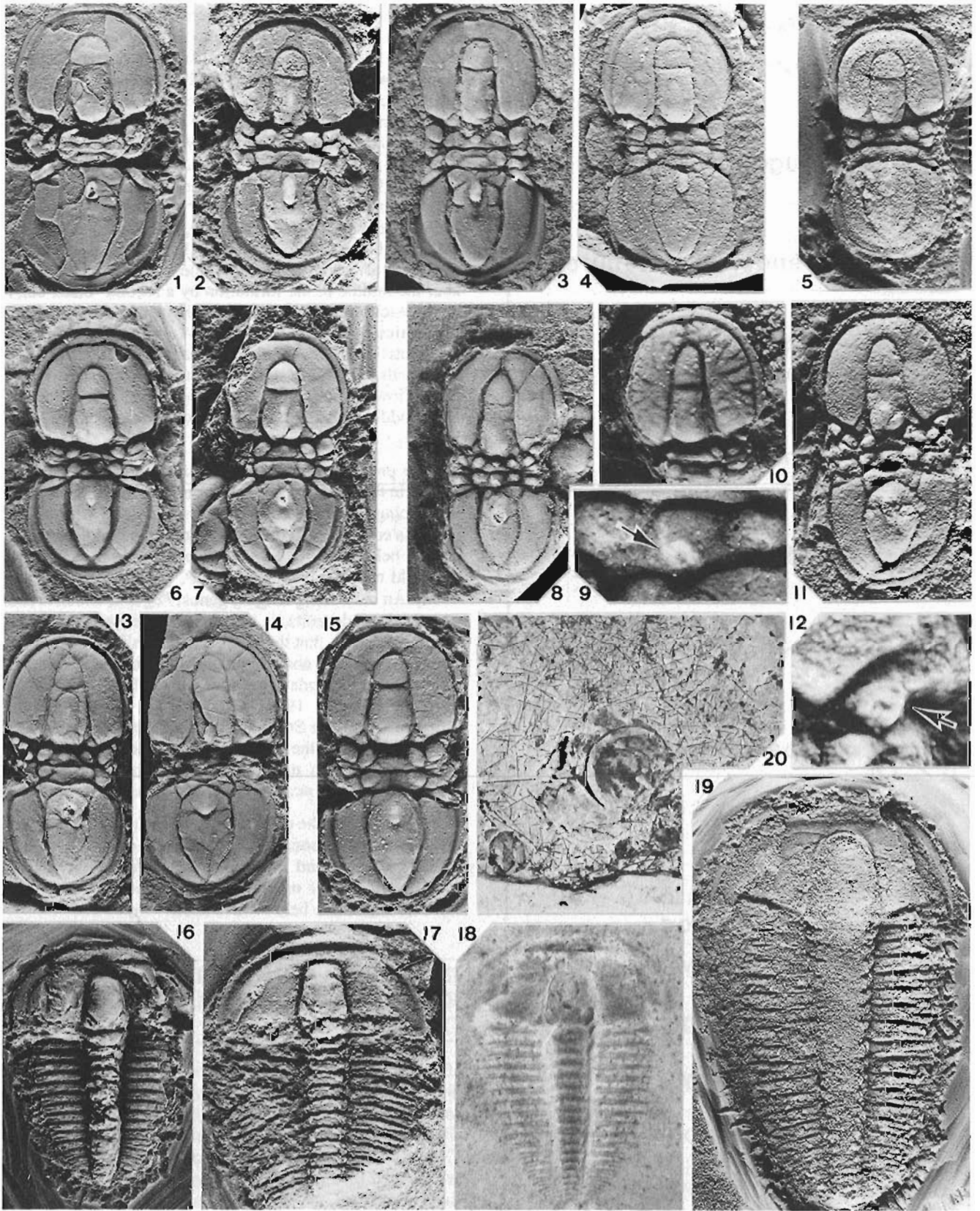
The Field area, located 65 km northwest of the Brussilof mine area, offers the best opportunity for correlating Brussilof fossils, as its fossil succession has been studied in detail (Rasetti, 1951; Fritz, 1971; unpub. GSC reports). Lithological units and faunas, in the Field area, bearing upon the present correlation are shown in Figure 4. The upper Stephen, to be formally named the Waputik member (Aitken, in press), contains the *Ehmainella burgessensis* fauna (Rasetti, 1951). The overlying lower Eldon nodular limestone unit, herein referred to as the "lower black band", contains the *Bathyriscus adaeus* fauna (Rasetti, 1951; amended by Fritz, 1971). Above the lower black band is a considerable thickness of barren Eldon dolomite that is in turn overlain near the middle of the formation by a second "black band", to be described formally as the Field member of the Eldon Formation (Aitken, in press). A gross environmental interpretation of the above units, based upon their lithology and fossils, is as follows: Waputik member, inner detrital belt; Eldon "lower black band", upper slope; Eldon lower dolomite unit, middle carbonate belt; and Eldon Field member, upper slope.

The presence of *Lejopyge seminula* and *Ptychagnostus gibbus* in the Brussilof collections is considered justification for placing them in the basinal *Ptychagnostus gibbus* Zone, which is equivalent to the upper part of the middle and inner detrital belt *Bathyriscus-Elrathina* Zone. In the Field area, the Field member belongs to the *P. gibbus* Zone (Robison, 1982). An older, long ranging genus, *Pagetia*, which is common in slope deposits, is absent from the Brussilof collections, suggesting that these fossils occur above the range of *Pagetia*. *Pagetia* is absent from the Field member as well, but is present in the underlying lower black band and Waputik member (Rasetti, 1951; Fritz, 1971). In the Field and Brussilof areas, the Stephen/Eldon contact is gradational. In the Brussilof area, the *P. gibbus* fauna is equally abundant in the upper Stephen medium brownish grey shale (typical Stephen lithology) and the lower Eldon dark grey limestone.

The facts that the exoskeletons of many of the agnostoid trilobites and associated ptychoparioid trilobites have remained intact, and that the *Diagoniella* sponge spicules have retained their orientation with respect to each other, indicate deposition below wave base.

INTERPRETATION OF THE STEPHEN/ ELDON AND CATHEDRAL/STEPHEN CONTACTS

If the fossiliferous Stephen/Eldon boundary strata in the Brussilof section are indeed equivalent to the Field member in the Field area, and if the underlying (12.5 m) portion of the Stephen is the same age, then a hiatus exists at the Cathedral/Stephen contact (Fig. 4). The missing time represented by this hiatus is equivalent to the time required, in the Field area, for the deposition of the Waputik member, the Eldon lower black band, and the overlying Eldon dolomite member (pre-Field member). In addition, if an unconformity exists in the Field area between the Waputik member and the Cathedral Formation, as suggested by Deiss (1940), Rasetti



(1951), McIlreath (1977), and Fritz (1971, 1990, 1991), then a further increment of depositional time is probably missing below the Stephen Formation in the Brussilof area.

It could be argued that the *Ptychagnostus gibbus* Zone fossils are "facies fossils" and that the strata below these fossils are equivalent to the zone elsewhere, where the range is fully extended in strata deposited under optimal, basinal conditions. The lower black band, however, was deposited under conditions similar to those associated with the Field member, but carries a different (older) fauna, including the older agnostis *Peronopsis columbiensis* Rasetti.

It could also be argued that the time equivalent of the three missing units in the Brussilof Mine area is represented by the (thus far) barren 12.5 m of Stephen Formation below the *Ptychagnostus gibbus* fauna. This cannot be refuted, but seems unlikely to the authors.

Finally, it could be argued that, in the Brussilof mine area, the upper Cathedral Formation is younger than in the Field area, and that this younger part of the Cathedral Formation is the time-rock equivalent of the three Field stratigraphic units considered as "missing" in the unconformity interpretation. This also seems unlikely on the grounds of regional relationships. The strata and their mutual relationships (shown in

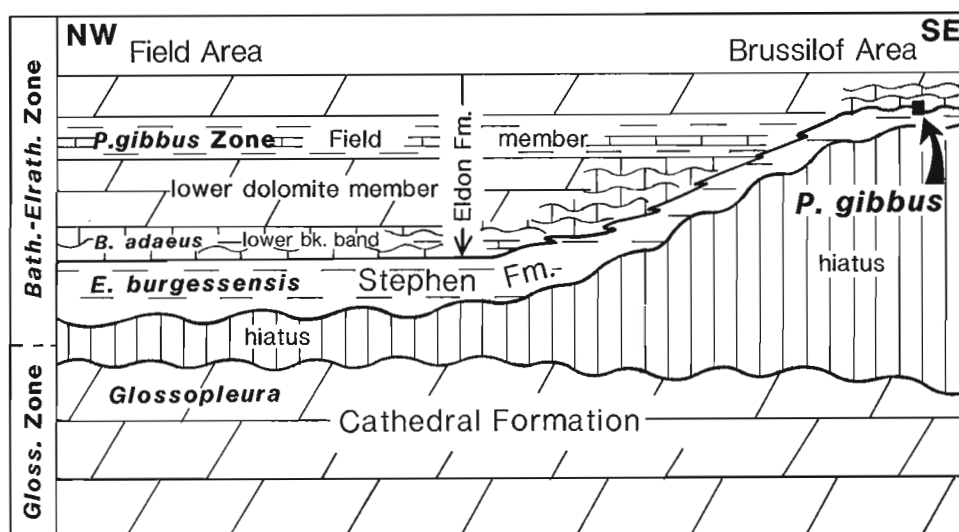


Figure 4. Schematic cross-section showing the correlation between the Field and Brussilof magnesite mine areas. The *Ptychagnostus gibbus* Zone (basinal zone), and the *Bathyriscus adaeus* and *Ehmaniella burgessensis* faunas are within the *Bathyriscus Elrathina* Zone in the Field area. In the Brussilof area, *P. gibbus* Zone fossils are shown to cross a younger Stephen/Eldon contact than is present in the Field area. Thicknesses not to scale.

Plate 1 (left)

Figures 1-4, *Peronopsis fallax* (Linnarsson); 1 x 5.2, GSC no. 106092; 2 x 5.0, GSC no. 106093; 3 x 4.0, GSC no. 106094; 4 x 3.9, GSC no. 106095.

Figure 5, *Peronopsis amplaxis?* Robison, x5.1, GSC no. 106096.

Figures 6, 7, 15, *Peronopsis interstricta* (White) 6 x 5.3, GSC no. 106097; 7 x 4.1, GSC no. 106098; 15 x 5.6, GSC no. 106104.

Figures 8-12, *Ptychagnostus gibbus* (Linnarsson); 8 x 5.8, GSC no. 106099; 9 x 28.7, part of Figure 8 enlarged; 10 x 10.8, GSC no. 106100; 11 x 5.6, GSC no. 106101; 12 x 21.1, part of Figure 11 enlarged.

Figures 13, 14, *Lejopyge seminula* (Whitehouse); 13 x 5.7, GSC no. 106102; 14 x 3.8, GSC no. 106103.

Figures 16, 17, *Ehmaniella* sp.; 16 x 3.6, GSC no. 106105; 17 x 4.5, GSC no. 106106.

Figures 18, 19, *Elrathina* sp.; 18 x 6.1, GSC no. 106107; 19 x 2.9, GSC no. 106108.

Figure 20, *Diagoniella* sp. with pygidium of *P. fallax* near centre, x2.8, GSC no. 106109.

Figured specimens are from the following GSC field localities in the stratigraphic section (Text-fig. 3): 1, 14, GSC loc. 105099; 2-4, 6, GSC loc. 105258; 5, 15, GSC loc. 105686; 7, GSC loc. 105260; 8-10, 16, GSC loc. 105685; 11, 12, GSC loc. 105255; 13, GSC loc. 105262; 18, 20, GSC loc. 105261. Figured specimens 17 and 19 are from GSC loc. 105100 in the southern part of the area (Text-fig. 2).

Fig. 4) change to the southeast toward the Montania High, so that it is far more likely that the upper surface of the Cathedral would be eroded in that direction. If not eroded, then the time-rock equivalents of the Stephen and lower Eldon in the field area would be expected to be represented by inner detrital clastic rocks, and not by the clean carbonate rocks of the Cathedral Formation, which clearly belong to the middle carbonate belt.

ORIGIN OF MAGNESITE

Currently, two hypotheses are being considered by the Geological Survey Branch of the British Columbia Ministry of Energy, Mines and Petroleum Resources to explain the Brussilof magnesite mine area ore deposits. They are: 1) formation of magnesite and/or magnesite precursors in an evaporitic environment, as illustrated by modern examples such as Coorong Lakes of South Australia (Warren, 1990) or Sebkhah El Melah in Tunisia (Perthuisot, 1980); and 2) formation of magnesite by replacement of dolomitic rocks that may or may not have contained gypsum. The replacement may be late diagenetic or epigenetic, depending on the source of the fluids (Simandl and Hancock, 1991; Simandl et al., in press).

In either case, pre-Stephen lowstand conditions would have provided a beneficial environment for magnesite formation. In the second hypothesis, karsting would serve as ground preparation, as described by Sangster (1988) for Mississippi Valley-type lead-zinc deposits. Slumping and fracturing of the Cathedral formation near the Cathedral's seaward margin (Stewart, 1991) may also have contributed to ground preparation.

ACKNOWLEDGMENTS

Parts of our manuscript were discussed with B. Grant, J.K. Rigby, R.A. Robison, and D.K. Sangster. It was read by M.J. Copeland and B.S. Norford. K.D. Hancock assisted Simandl with fieldwork and part of the illustrations. The remaining illustrations were prepared by H. McLaughlin. We thank those mentioned above, and remain responsible for any errors or omissions.

REFERENCES

- Aitken, J.D.**
1966: Middle Cambrian to Middle Ordovician cyclic sedimentation, Southern Rocky Mountains of Alberta; Bulletin of Canadian Petroleum Geology, v. 14, no. 4, p. 405-441.
- Aitken, J.D.** (cont'd.)
in press: Middle Cambrian stratigraphy of the Southern Rocky Mountains, Canada; Geological Survey of Canada, Bulletin 398.
- British Columbia Ministry of Energy, Mines and Petroleum Resources**
1990: British Columbia mineral statistics, annual summary tables, historical mineral production to 1990; British Columbia Ministry of Energy, Mines and Petroleum Resources, 86 p.
- Deiss, C.**
1940: Lower and Middle Cambrian stratigraphy of southwestern Alberta and southeastern British Columbia; Geological Society of America Bulletin, v. 51, p. 731-794.
- Fritz, W.H.**
1971: Geological setting of the Burgess Shale; Proceedings of the North American Paleontological Convention, September 1969, Part 1, p. 1155-1170.
1990: Comment: in defense of the escarpment near the Burgess Shale fossil locality; Geoscience Canada, v. 17, no. 2, p. 106-110.
1991: Cambrian assemblages; in Geology of the Cordilleran Orogen in Canada, (ed.) H. Gabrielse and C. Yorath; Geological Survey of Canada, Geology of Canada, no. 4, p. 155-184 [Also Geological Society of America, The Geology of North America, v. G2].
- Leech, G.B.**
1979: Kananaskis Lakes (82 J, W 1/2); Geological Survey of Canada, Open File 634.
- McIlreath, I.A.**
1977: Stratigraphic and sedimentary relationships at the western edge of the Middle Cambrian carbonate facies belt, Field, British Columbia; Ph.D. thesis, University of Calgary, Calgary, Alberta, 259 p.
- Perthuisot, J.P.**
1980: Sebkhah El Melah near Zarzis: a recent paralic salt basin (Tunisia); in Evaporite Deposits; Editions Technip, Paris, p. 1217.
- Rasetti, F.**
1951: Middle Cambrian stratigraphy and faunas of the Canadian Rocky Mountains; Smithsonian Miscellaneous Collections, v. 116, no. 5, 277 p.
- Robison, R.A.**
1982: Some Middle Cambrian angostoid trilobites from western North America; Journal of Paleontology, v. 56, p. 132-160.
- Sangster, D.**
1988: Breccia-hosted lead-zinc deposits in carbonate rocks; in Paleokarst, N.P. James and P.W. Choquette (ed.); Springer-Verlag, New York Inc., p. 102-116.
- Simandl, G.J. and Hancock, K.D.**
1991: Geology of the Mount Brussilof Magnesite deposits, southeastern British Columbia (82 J/12, 13); British Columbia Ministry of Energy, Mines and Petroleum Resources, Paper 19911, p. 269-278.
- Simandl, G.J., Hancock, K.D., Paradis, S., Hora, Z.D., and MacLean, M.**
in press: Mount Brussilof sparry magnesite deposit, southeastern British Columbia, Canada; Canadian Mining and Metallurgy Bulletin.
- Stewart, W.D.**
1991: Stratigraphy and sedimentology of the Chancellor succession (Middle and Upper Cambrian), southeastern Canadian Rocky Mountains; Ph.D. thesis, University of Ottawa, Ottawa, Ontario, 534 p.
- Warren, J.K.**
1990: Sedimentology and mineralogy of dolomitic Coorong Lakes, South Australia; Journal of Sedimentary Petrology, v. 60, p. 843858.

Geological Survey of Canada Project 650024

Geology of the Illecillewaet synclinorium in the Durrand/Dismal glaciers area, western Selkirk Mountains, British Columbia

Maurice Colpron¹ and Raymond A. Price¹
Cordilleran Division

Colpron, M. and Price, R.A., 1993: Geology of the Illecillewaet synclinorium in the Durrand/Dismal glaciers area, western Selkirk Mountains, British Columbia; in Current Research, Part A; Geological Survey of Canada, Paper 93-1A, p. 191-198.

Abstract: Detailed mapping of the Illecillewaet synclinorium in the Durrand/Dismal glaciers area has documented regional south-to-north facies change in rocks of Lardeau Group. This facies change coincides with rapid thickening of the Badshot Formation and is interpreted as the expression of a fundamental structural feature that controlled the configuration of the sedimentary basin.

The structure of the area is dominated by northwest-trending, southwest-verging folds and faults that define the Illecillewaet synclinorium, and that have deformed an older pervasive schistosity and older east-verging thrust faults. Four plutons of Middle Jurassic age intrude these rocks along a discordant west-northwest trend. Structural relationships around the granitic stocks suggest that they were emplaced during the development of the regional southwest-verging structures, and that these structures continued to develop after the solidification of the plutons.

Résumé : La cartographie détaillée du synclinorium d'Illecillewaet, dans la région des glaciers Durrand et Dismal, a révélé un changement régional de faciès du sud vers le nord au sein des roches du Groupe de Lardeau. Ce changement de faciès correspond à un épaississement rapide de la Formation de Badshot, et est interprété comme étant le reflet d'un élément structural majeur qui contrôlait la configuration du bassin sédimentaire.

La structure de la région est dominée par des plis et des failles d'orientation nord-ouest et de vergence sud-ouest qui délimitent le synclinorium d'Illecillewaet. Ces structures déforment une schistosité ancienne et des chevauchements précoces de vergence est. Quatre plutons, datant du Jurassique moyen recourent ces roches le long d'un axe discordant d'orientation ouest-nord-ouest. Les relations structurales autour des massifs granitiques suggèrent qu'ils ont été mis en place durant la période de formation des structures régionales de vergence sud-ouest, et que ces structures ont continué à se développer après la solidification des plutons.

¹ Department of Geological Sciences, Queen's University, Kingston, Ontario K7L 3N6

INTRODUCTION

The Illecillewaet synclinorium is a west-facing fold in the southwest flank of the Selkirk Fan structure (Wheeler, 1963), a segment of the zone of structural divergence that follows the Omineca crystalline belt and straddles the suture zone between North America and Intermontane "superterrane" (Fig. 1; Price, 1986). The stratigraphic succession involved in the Illecillewaet synclinorium consists of the Eo-Cambrian Hamill Group (Walker and Bancroft, 1929), the Lower Cambrian Badshot Formation (Walker and Bancroft, 1929) and conformably overlying Lade Peak Formation (Fyles and Eastwood, 1962; Zwanzig, 1973), and the Lardeau Group (Walker and Bancroft, 1929; Fyles and Eastwood, 1962; Wheeler, 1963; Zwanzig, 1973). Preliminary results, obtained during the summer of 1991, established that the Lardeau Group in the Illecillewaet synclinorium is gradationally intercalated, and therefore conformable, with the underlying miogeoclinal sequence comprising the Lade Peak and Badshot formations and Hamill Group (Colpron and Price, 1992). These relationships are incompatible with the hypothesis that the Lardeau Group is tectonically inverted (Smith and Gehrels, 1992a) and structurally juxtaposed over the Hamill Group and Badshot Formation (Wheeler and McFeely, 1991; Smith and Gehrels, 1992b).

This paper presents the preliminary results of additional detailed mapping (1:20 000) in the northern part of the Illecillewaet synclinorium during the summer of 1992. The Durrand/Dismal Glaciers area (NTS sheets 82N/5 and 4) is located northeast of Revelstoke and north of the Trans-Canada Highway. It is defined, approximately, to the west and east by the limits of Mount Revelstoke and Glacier National parks (respectively), and to the north by latitude 51°24'N.

STRATIGRAPHIC RELATIONS

The stratigraphic relations within the Lardeau Group in the Durrand/Dismal Glaciers area are summarized in Figure 2. Three simplified stratigraphic columns outline variations among three broad geographic areas: 1) the Jumping Creek syncline between Illecillewaet River and Mount Moloch; 2) the vicinity of Fidelity Mountain; and 3) the Downie Lake area (Fig. 3).

Illecillewaet River – Mount Moloch

The Jumping Creek syncline in the area between Illecillewaet River and Mount Moloch is bounded to the southwest and northeast by the Albert Canyon anticline and the Fortitude Mountain fault (Zwanzig, 1973), respectively (Fig. 3). The stratigraphy of the Lardeau Group in this area was described, in part, by Colpron and Price (1992; Fig. 2). Along both flanks of the Jumping Creek syncline, the Lardeau Group comprises three mappable units: a lower black graphitic phyllite (L1), a middle green phyllite and quartzite (L2), and an upper sequence of intercalated grits and black phyllite (L3).

These three units are gradationally intercalated, and therefore conformable, with each other and with the Lade Peak Formation (LP).

Wheeler (1963) and Zwanzig (1973) tentatively correlated the lower unit (L1) of the Lardeau Group in the Illecillewaet synclinorium with the Index Formation in the Ferguson area (Fyles and Eastwood, 1962). They also correlated our middle and upper units (L2 and L3, respectively) with the Broadview Formation in the Ferguson area (Fyles and Eastwood, 1962). Alternatively, Read (1975) and Sears (1979) suggested that the whole of the Lardeau Group in the Illecillewaet synclinorium is a lateral equivalent of the Index Formation of the Kootenay Arc. We concur with Read (1975) and Sears (1979).

Talc and chlorite schists, as well as a few greenstone bodies, occur locally in the area (not shown in Fig. 3). The greenstone occurrences are limited to a few localities along the northwest side of Tangier River and west of Tumbledown Mountain, and to the middle unit (L2) of the Index Formation. Talc and chlorite schists are not restricted to a specific stratigraphic horizon, nor are they restricted to a specific structure. They occur locally in the lower (L1), middle (L2), and upper (L3) units of the Index Formation. Talc and chlorite schists locally appear to be gradational into each other. Their origin is enigmatic, but they do not appear to be slices of ophiolitic ultramafic rocks.

Fidelity Mountain

The Lardeau Group in the Fidelity Mountain area occupies the northeast flank of the Lanark Peak anticline (Zwanzig, 1973), and forms the multiple fault slices and folds that define the Corbin Peak syncline (Fig. 3). In contrast with the area between Illecillewaet River and Mount Moloch, the Lardeau Group in the vicinity of Fidelity Mountain comprises only the graphitic phyllite of the "Lower" Index Formation (L1) and the grits and argillites of the "Upper" Index Formation (L3; Fig. 2). The "lower" and "upper" members of the Index Formation are gradationally intercalated, and the grits of the "upper" member display spectacular flame structures. These sedimentary structures confirm that the grits are conformable with, and stratigraphically overlie the black phyllite of the Index Formation.

Downie Lake

The rocks overlying the Badshot Formation (B) in the Downie Lake area, north of Mount Moloch, are significantly different from those to the south (Fig. 2). Near Downie Lake, the Lade Peak Formation (LP) is typically a dark grey dolomitic limestone that contains buff weathering dolomitic nodules. The contact between individual beds of light-coloured dolostone, typical of the Badshot Formation, and dark grey limestone, typical of the Lade Peak Formation, is generally sharp, but the two rock types are gradationally intercalated; and therefore, the two formations are conformable.

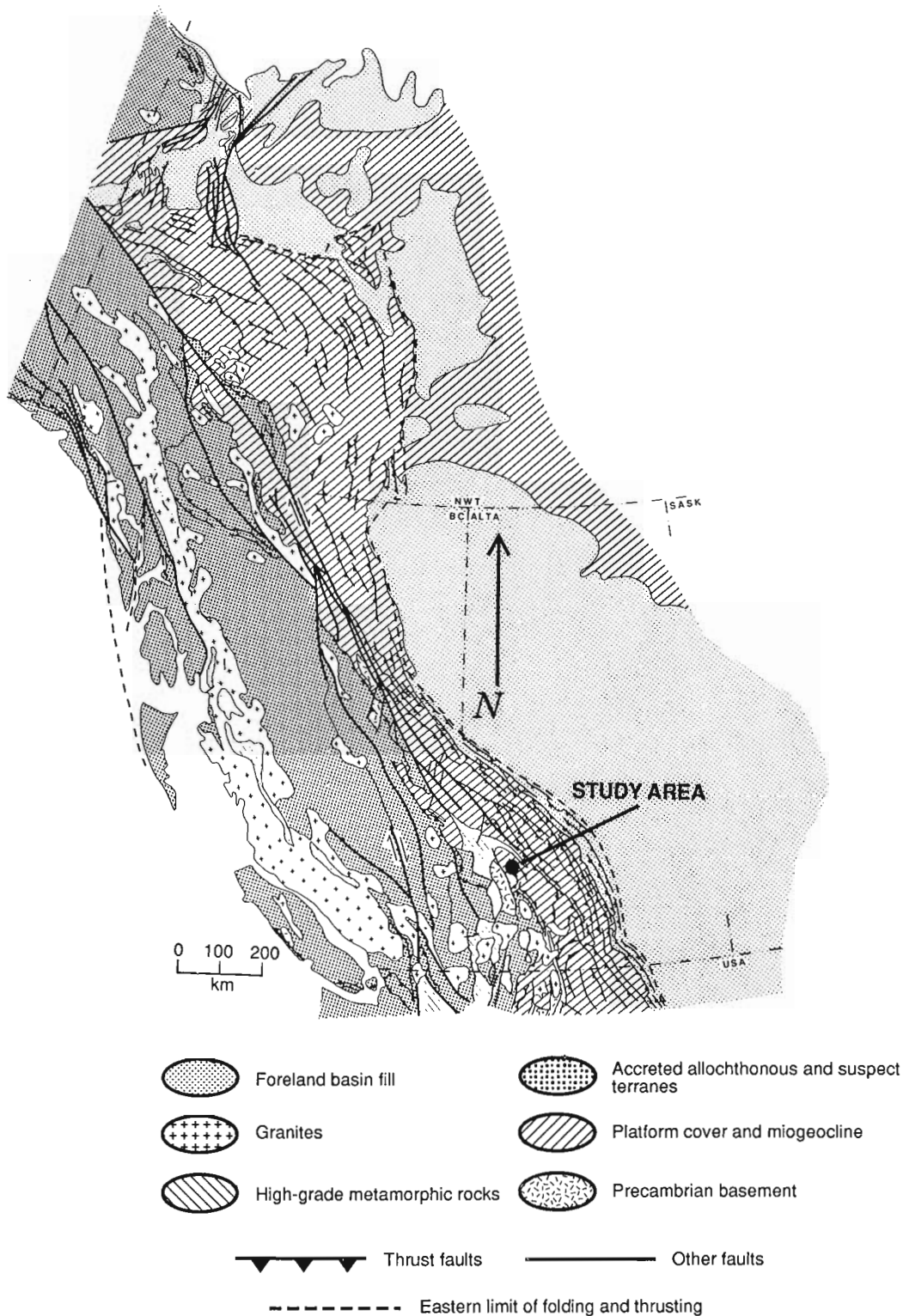


Figure 1. Tectonic sketch map of the Canadian Cordillera showing the location of the Durrand/Dismal Glaciers area (modified after Douglas, 1968, and Price, 1986).

**Illecillewaet River -
Mt. Moloch**
(Colpron & Price, 1991)

**Fidelity
Mountain**

**Downie
Lake**

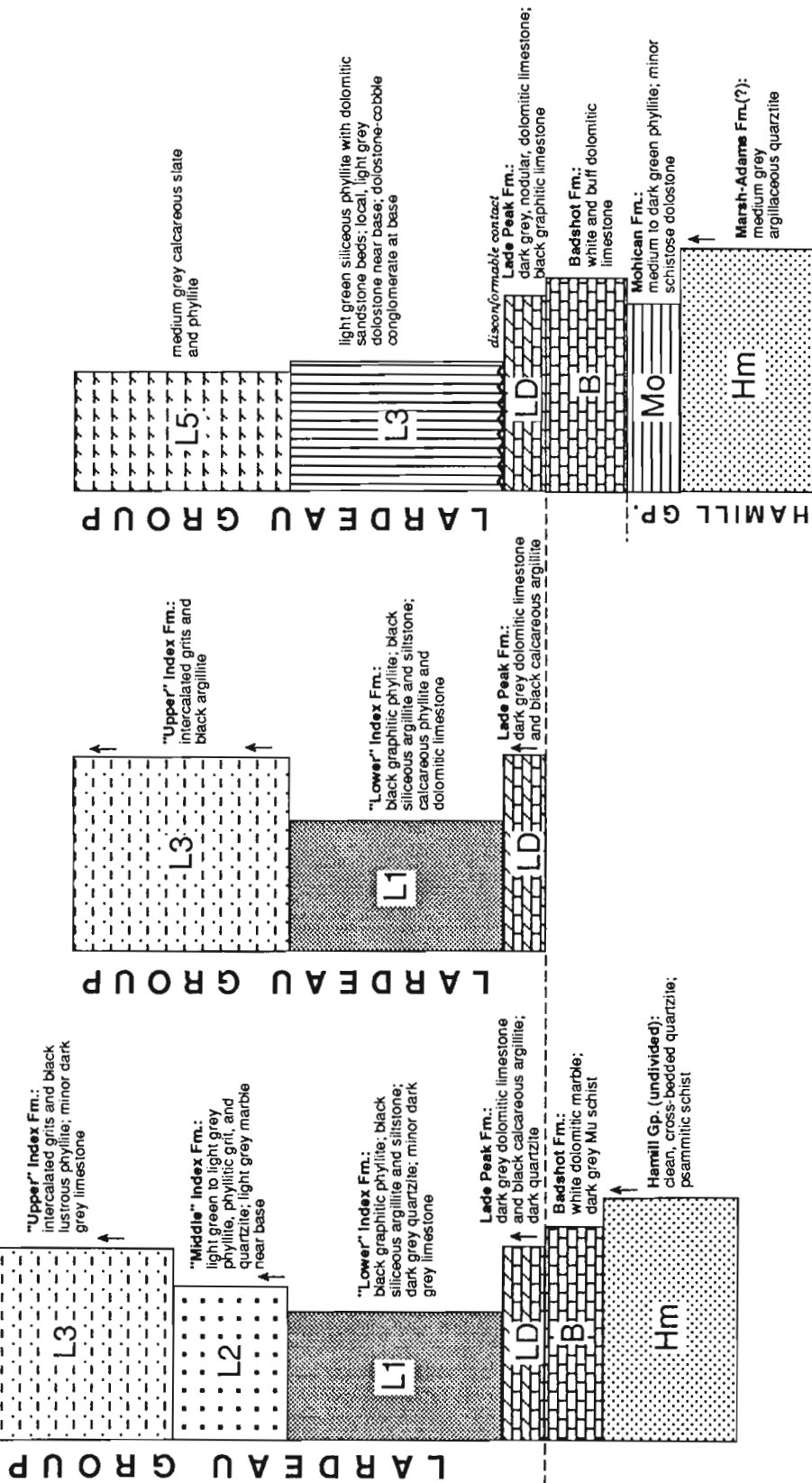


Figure 2. Simplified stratigraphic relationships for the Durrand/Dismal Glaciers area. Unit designators (Hm, B, LD, etc...) and patterns for the "Middle" Index Formation (L2; Jumping Creek syncline), the Mohican Formation (Mo) and unit L4 of the Lardeau Group (Downie Lake) correspond to those used on the map in Figure 3. Small arrows indicate relative position of observed topping indicators. All contacts are gradational unless otherwise stated. No thickness relationships implied.

MC '92



Figure 3. Simplified geological map of the Durrand/Dismal Glaciers area. Unit designators and patterns are as in Figure 2. Random dash pattern: Middle Jurassic granitic plutons. Structural data shown are strike and dip of dominant foliation and trend and plunge of dominant fold axes. Thrust faults have barbs on upthrown side; overturned thrust faults have ticks on lower plate. Other faults are steeply to moderately east-dipping. Geology to the north of Downie Lake is modified in part from unpublished mapping by R.L. Brown. Geology north of Mount Graham Lake is modified after Wheeler (1963), and that of the Albert Canyon anticline, after Zwanzig (1973). **SCF:** Standfast Creek fault; **DCF:** Downie Creek fault; **FMF:** Fortitude Mountain fault; **ACA:** Albert Canyon anticline; **JCS:** Jumping Creek syncline; **LPA:** Lanark Peak anticline; **FS:** Fang Stock; **TS:** Tangier Stock; **CS:** Corbin Stock; **LS:** Lanark Stock; **Dgn:** Devonian granodiorite gneiss (Clachnacudainn gneiss); **ms:** undivided metasedimentary rocks.

The Lade Peak Formation is laterally discontinuous in the Downie Lake area (Fig. 3). It is overlain by a distinctive assemblage of dolostone-cobble conglomerate, dolomitic sandstone, and medium to dark green chloritic and calcareous schist (base of L4). The conglomerate unit, although unrecognized elsewhere in the Durrand/Dismal Glaciers area, appears to be a common unit at the base of the Lardeau Group to the east, in the Downie Creek map area (Brown, 1991). The conglomerate is overlain by light green siliceous and dolomitic phyllite (L4) which is in turn overlain by medium grey calcareous slate (L5; Fig. 2, 3). A thin and discontinuous, light grey dolostone unit occurs locally near the base of the light green phyllite unit (L4). In places, as on the west side of Downie Lake, the light green phyllite (L4) lies directly on the Badshot Formation, with no intervening Lade Peak Limestone. This relationship, and the presence of the conglomerate unit, suggest that, in the Downie Lake area, the Lardeau Group is disconformable over the Lade Peak and Badshot formations.

DISCUSSION

Throughout most of the Durrand/Dismal Glaciers area, the Badshot Formation is generally less than 300 m thick; however, in the vicinity of Mount Moloch, it is apparently more than 2500 m thick. This change in thickness may be due partly to structural repetition, but it coincides with the conspicuous south-to-north facies change in the Lardeau Group. This facies change is presumably the expression of a fundamental structural feature that controlled the configuration of the sedimentary basin, and probably the thickness of the Badshot Formation as well.

INTRUSIVE ROCKS

Four plutons intrude the Illecillewaet synclinorium (Fig. 3). They are aligned along a west-northwest trend that is discordant with regional structures. As noted by Wheeler (1963, p. 17), the larger stocks exposed on the west side of Tangier River (Fang Stock, underneath Dismal Glacier; and Tangier Stock, north of Fang Rock) are uniform hornblende-biotite porphyritic granites which contain 35-40% microcline phenocrysts larger than 2 cm. Those east of Tangier River (Corbin and Lanark stocks, respectively north and east of Fidelity Mountain), are medium-grained hornblende-biotite quartz monzonite, in which microcline phenocrysts constitute 20-60% of the rock, and rarely exceed 1 cm. All four stocks contain primary epidote and sphene. The largest (Fang Stock) yielded an U-Pb zircon age of 168 ± 2 Ma (Brown et al., 1992).

Fang and Corbin stocks both have contact aureoles characterized by retrograded andalusite porphyroblasts. Along the southern margin of Fang Stock, relict andalusites are commonly larger than 5 cm long. Along the southern margin of Tangier Stock, marbles of the Lade Peak Formation contain an actinolite + talc(?) assemblage.

A few diabase and lamprophyre dykes occur in the Durrand/Dismal Glaciers area. Those south of Mount Durrand are of lamprophyric composition, contain biotite phenocrysts, and generally strike east-northeast. Those northeast of Mount Durrand are fine grained diabase, and they trend north-northwest. The diabase and lamprophyre dykes postdate all nearby structures.

Light green dykes, containing up to 30% plagioclase phenocrysts, are present in several locations around Downie Lake. These dykes are generally well foliated and locally boudinaged.

STRUCTURAL RELATIONS

The structure of the Durrand/Dismal Glaciers area is dominated by the northwest-trending, southwest-verging folds and faults that define the Illecillewaet synclinorium (Fig. 3). These structures deformed an older pervasive schistosity which is locally accompanied by mesoscopic isoclinal folds. They also deformed older east-verging thrust faults that outline map-scale structures near Fidelity Mountain. The northwest-trending, southwest-verging folds change abruptly to an east-northeast orientation around the larger Middle Jurassic plutons (Fang and Tangier stocks; Fig. 3).

Along the east flank of the Jumping Creek syncline, in the footwall of the southwest-verging Fortitude Mountain fault (Zwanzig, 1973), the dominant foliation, which parallels the axial surfaces of the southwest-verging folds, flattens and becomes moderately west-dipping. This suggests that the Fortitude Mountain fault postdates the development of the penetrative fabric and, therefore, that it formed during the latter part of the evolution of the Jumping Creek syncline. The northwest-trending Downie Creek fault (Brown, 1991) shows a similar temporal relationship. In its hanging wall, near Downie Creek, it truncates east-trending folds which apparently originated as northwest-trending, southwest-verging folds, and subsequently were rotated around the northern margin of the Fang Stock (Fig. 3). However, farther south the Downie Creek fault dies out in the core of the Durrand Glacier anticline, which is part of the southwest-verging fold train that defines the Illecillewaet synclinorium. Thus the Downie Creek fault is concordant with the southwest-verging folds at its south end, but truncates deformed southwest-verging folds farther north.

In the Downie Lake area, the dominant easterly-trending folds deform a previously overturned stratigraphic sequence; and they, in turn, are truncated by northwest-trending, southwest-verging thrust faults (Fig. 3).

Younger west-northwest trending, steeply to moderately dipping crenulation cleavage and open folds are superposed on the northwest trending structures, and are most strongly developed adjacent to the Fang, Tangier and Corbin stocks.

RELATIONSHIP BETWEEN PLUTON EMPLACEMENT AND REGIONAL DEFORMATION

The relationship between the granitic intrusions of the Durrand/Dismal Glacier area and the regional deformation, and, particularly, the change in orientation of the dominant structures around these plutons, is critical to the understanding of the tectonic evolution of the Illecillewaet synclinorium. Wheeler (1963, p. 26) suggested that the plutons postdate the regional deformation and that the deflection of structures reflects forceful emplacement of the granites. Alternatively, Reesor (1963) proposed that perhaps the plutons were emplaced early in the tectonic history, and acted as competent, resistant masses during subsequent deformation. More recently, Brown et al. (1992) argued that the Middle Jurassic plutons postdate the dominant phase of deformation and that the deflection of structures may possibly be explained by later "rigid body rotation of the plutons".

Our observations indicate that the granitic plutons were emplaced, consolidated and then behaved as rigid bodies, all during the progressive deformation that resulted in the development of the dominant, regional, northwest-trending, southwest-verging folds and thrust faults. The plutons truncate southwest-verging fold structures and the dominant northwest-striking foliation in their immediate wall rocks; but the axial surfaces of the southwest-verging folds are deflected conspicuously between and around the larger plutons as a result of strain that occurred after the plutons had consolidated. The axial surface of the Lanark Peak anticline, one of the main regional folds within the Illecillewaet synclinorium (Zwanzig, 1973), can be traced northwest from Tangier River into the anticline on the southwest side of Fang Rock (Fig. 3). This anticline, which is cored by limestone of the Badshot Formation, is wrapped around the northwest end of the Tangier Stock, and rotated into a northeast-southwest trend in the narrow gap between Tangier and Fang stocks.

Boudinaged granitic dykes along the northern margin of Fang Stock, as well as incipient shear zone development along its southern margin, and strain shadows around the andalusite porphyroblasts, all suggest that significant penetrative strain has occurred in the surrounding rocks after the plutons have solidified. The Lanark Stock is cut by several late, brittle faults.

Perhaps the most significant relationship is that between the southwest-verging Downie Creek fault and the east-trending folds north of Fang Stock (Fig. 3). These transverse folds are discordant with the dominant regional northwest-trending structures, and they must have been rotated into their east-west orientation prior to the development of the Downie Creek fault. However, as discussed above, the Downie Creek fault extends into, and is congruent with the Durrand Glacier anticline, which is a major component of the northwest-trending, southwest-verging Illecillewaet synclinorium.

Thus, the granitic plutons are synkinematic with the earlier stages of the development of the northwest-trending, southwest-verging folds and faults of the Illecillewaet synclinorium. But they are pre-kinematic, and acted as rigid

inclusions during the later stages in the development of some of the same regional fold and fault structures of the Illecillewaet synclinorium.

SUMMARY

South-to-north facies changes in the Lardeau Group appear to coincide with the rapid thickening of the Badshot Formation near Mount Moloch. This suggests that deposition of the Lardeau Group, and probably the Badshot Formation, was controlled by a fundamental structural feature within the sedimentary basin.

Structural relationships around the Middle Jurassic granitic stocks suggest that they were emplaced during the development of the regional southwest-verging structures, and that these structures continued to develop after the solidification of the plutons.

ACKNOWLEDGMENTS

Financial support for this study was provided by EMR Research Agreement #028-4-92 and NSERC Grants #CRD117288 and #OGP0092418 to R.A. Price, and Queen's University Graduate Travel Grant, GSA Research Grant, and FCAR postgraduate scholarship to M. Colpron. Thanks to Rob Whelan for his assistance in and out of the field and his invaluable mountaineering skills. Allen Dennis of Revelstoke kindly provided us with a roof while out of the field. Discussions in the field with Jim Crowley and Dick Brown (Carleton University), and Dugald Carmichael and Marian Warren (Queen's University) are greatly appreciated and were most stimulating. Special thanks to Dick Brown for making available his unpublished map of the Downie Lake area. J.A. Roddick critically read the manuscript.

REFERENCES

- Brown, R.L.**
1991: Geological map and cross-section, Downie Creek map area (82M/8), British Columbia; Geological Survey of Canada, Open File Map 2414.
- Brown, R.L., McNicoll, V.J., Parrish, R.R., and Scammell, R.J.**
1992: Middle Jurassic plutonism in the Kootenay Terrane, northern Selkirk Mountains, British Columbia; in *Radiogenic Age and Isotopic Studies: Report 5*; Geological Survey of Canada, Paper 91-2, p. 135-141.
- Colpron, M. and Price, R.A.**
1992: Preliminary results on the stratigraphy and structure of the Lardeau Group in the Illecillewaet synclinorium, western Selkirk Mountains, British Columbia; in *Current Research, Part A*; Geological Survey of Canada, Paper 92-1A, p. 157-162.
- Douglas, R.J.W.**
1968: Geological map of Canada; Geological Survey of Canada, Map 1374A.
- Fyles, J.T. and Eastwood, G.E.P.**
1962: Geology of the Ferguson area, Lardeau District, British Columbia; British Columbia Department of Mines and Petroleum Resources, Bulletin No. 45, 92 p.

Price, R.A.

1986: The southeastern Canadian Cordillera: thrust faulting, tectonic wedging, and delamination of the lithosphere; *Journal of Structural Geology*, v. 8, p. 239-254.

Read, P.B.

1975: Lardeau Group, Lardeau map-area, west half (82K west half), British Columbia; in *Report of Activities, Part A*; Geological Survey of Canada, Paper 75-1A, p. 29-30.

Reesor, J.

1963: Fang Stock; in *Age Determinations and Geological Studies (including isotopic ages - Report 4)*, (ed.) G.B. Leech, J.A. Lowdon, C.H. Stockwell and R.K. Wanless; Geological Survey of Canada, Paper 63-17, p. 18.

Sears, J.W.

1979: Tectonic contrasts between the infrastructure and suprastructure of the Columbian orogen, Albert Peak area, western Selkirk Mountains, British Columbia; Ph.D. thesis, Queen's University, Kingston, Ontario, 154 p.

Smith, M.T. and Gehrels, G.E.

1992a: Stratigraphic comparison of the Lardeau and Covada groups: Implications for revision of the stratigraphic relations in the Kootenay Arc; *Canadian Journal of Earth Sciences*, v. 29, p. 1320-1329.

Smith, M.T. and Gehrels, G.E. (cont'd.)

1992b: Structural geology of the Lardeau Group near Trout Lake, British Columbia: implications for the structural evolution of the Kootenay Arc; *Canadian Journal of Earth Sciences*, v. 29, p. 1305-1319.

Walker, J.F. and Bancroft, M.F.

1929: Lardeau map-area, British Columbia: *General Geology*; in *Lardeau map-area, British Columbia*, (ed.) J.F. Walker, M.F. Bancroft and H.C. Gunning; Geological Survey of Canada, Memoir 161, p. 1-16.

Wheeler, J.O.

1963: Rogers Pass map-area, British Columbia and Alberta (82N W¹/₂); Geological Survey of Canada, Paper 62-32, 32 p.

Wheeler, J.O. and McFeely, P.

1991: Tectonic assemblage map of the Canadian Cordillera and adjacent parts of the United States of America; Geological Survey of Canada, Map 1712A.

Zwanzig, H.V.

1973: Structural transition between the foreland zone and the core zone of the Columbian orogen, Selkirk Mountains, British Columbia; Ph.D. thesis, Queen's University, Kingston, Ontario, 158 p.

Geological Survey of Canada Research Agreement 028-4-92

New correlations of the Hadrynian Windermere Supergroup in the northern Selkirk Mountains, British Columbia

Stephen E. Grasby¹ and Richard L. Brown¹
Cordilleran Division, Vancouver

Grasby, S.E. and Brown, R.L., 1993: New correlations of the Hadrynian Windermere Supergroup in the northern Selkirk Mountains, British Columbia; in Current Research, Part A; Geological Survey of Canada, Paper 93-1A, p. 199-206.

Abstract: The Horsethief Creek Group in the northern Selkirk Mountains, is subdivided into six informal map units: Semipelite-Amphibolite, Middle Marble, Basal Pelite, Comedy Creek, Clastic, and Upper Pelite. The Comedy Creek unit in the northern Selkirk Mountains is correlated with the Old Fort Point Formation of the Miette Group, "the marker" in the Kaza Group, and the Baird Brook division in the Horsethief Group of the Purcell Mountains. These correlations help define the Windermere basin, and place constraints on the southern extent of the Pleasant Valley Thrust. The correlations also require that the succession between the Middle Marble unit and the Cambrian thin 2 km between Cherub Mountain and Mount Shaughnessy.

Résumé : Le Groupe de Horsethief Creek situé dans le nord des monts Selkirk est subdivisé en six unités cartographiques informelles, qui sont: l'unité à semipélite-amphibolite, l'unité intermédiaire de marbre, l'unité basale pélitique, l'unité de Comedy Creek, l'unité clastique et l'unité supérieure pélitique. L'unité de Comedy Creek dans le nord des monts Selkirk peut être corrélée avec la Formation d'Old Fort Point qui fait partie du Groupe de Miette, «l'unité repère» du Groupe de Kaza, et la division de Baird Brook dans le Groupe de Horsethief situé dans les monts Purcell. Ces corrélations aident à définir le bassin de Windermere, et à délimiter le prolongement sud du chevauchement de Pleasant Valley. Ces corrélations impliquent également que la succession comprise entre l'unité intermédiaire de marbre et le Cambrien s'amincit de 2 km entre le mont Cherub et le mont Shaughnessy.

¹ Department of Earth Sciences at Ottawa-Carleton Geoscience Centre, Carleton University, Ottawa, Ontario K1S 5B6

INTRODUCTION

Three nomenclature schemes are applied to Windermere strata in south-central British Columbia and adjacent Alberta: Miette Group in the Rocky Mountains, Horsethief Creek Group in the Purcell, Selkirk, and Monashee mountains, and Cariboo and Kaza groups in the Cariboo Mountains (Fig. 1). Local markers facilitate correlation of strata within each mountain range; however lack of stratigraphic continuity and paleontological control inhibit correlations between ranges.

Ross and Murphy (1988) were the first to correlate a distinctive tripart unit in the Miette Group (the Old Fort Point Formation) with a similar unit in the Kaza Group ("the marker"), and interpreted it as a time stratigraphic marker, representing a basin wide rapid transgression. The existence of a regional time stratigraphic marker was supported by Kubli (1990) who correlated the Baird Brook division in the Horsethief Creek Group of the Purcell Mountains with the Old Fort Point Formation and "the marker".

A tripart sequence mapped in the Cherub Mountain region of the northern Selkirks (this report) (Fig. 2) correlates with the Old Fort Point Formation, the Baird Brook division, and "the marker". This allows Horsethief Creek Group strata in this area to be correlated with Windermere strata in the Rocky, Purcell, Monashee, and Cariboo mountains.

STRATIGRAPHY OF THE CHERUB MOUNTAIN AREA

Horsethief Creek Group strata in the northern Selkirk Mountains have been traditionally divided into three members: lower pelitic, middle marble, and upper pelitic (Brown et al., 1978). More detailed mapping demonstrates there are six distinct and mappable units, named informally (from base to top): Semipelite-Amphibolite unit (= lower pelitic member), Middle Marble unit (= middle marble member), Basal Pelite unit (= lower subdivision of upper pelitic member), Comedy Creek unit (new), Clastic unit (= middle subdivision of upper pelitic member), and Upper Pelite unit (= upper subdivision of the upper pelitic member) (Fig. 3). All six units can be traced from Ventego Creek north to the Adamant pluton. All contacts examined are a mixed gradation, except for the abrupt upper and lower contacts of the Comedy Creek unit. The base of Horsethief Creek Group was not observed in the map area. The top of Horsethief Creek Group is defined by a sharp contact with overlying massive quartzites belonging to Hamill Group.

Brief descriptions of the six units are presented below.

Semipelite-Amphibolite unit

The Semipelite-Amphibolite unit is characterized by thinly interbedded silver-grey semipelite and pelite, minor pink to grey fine grained quartzites, and occasional layers of

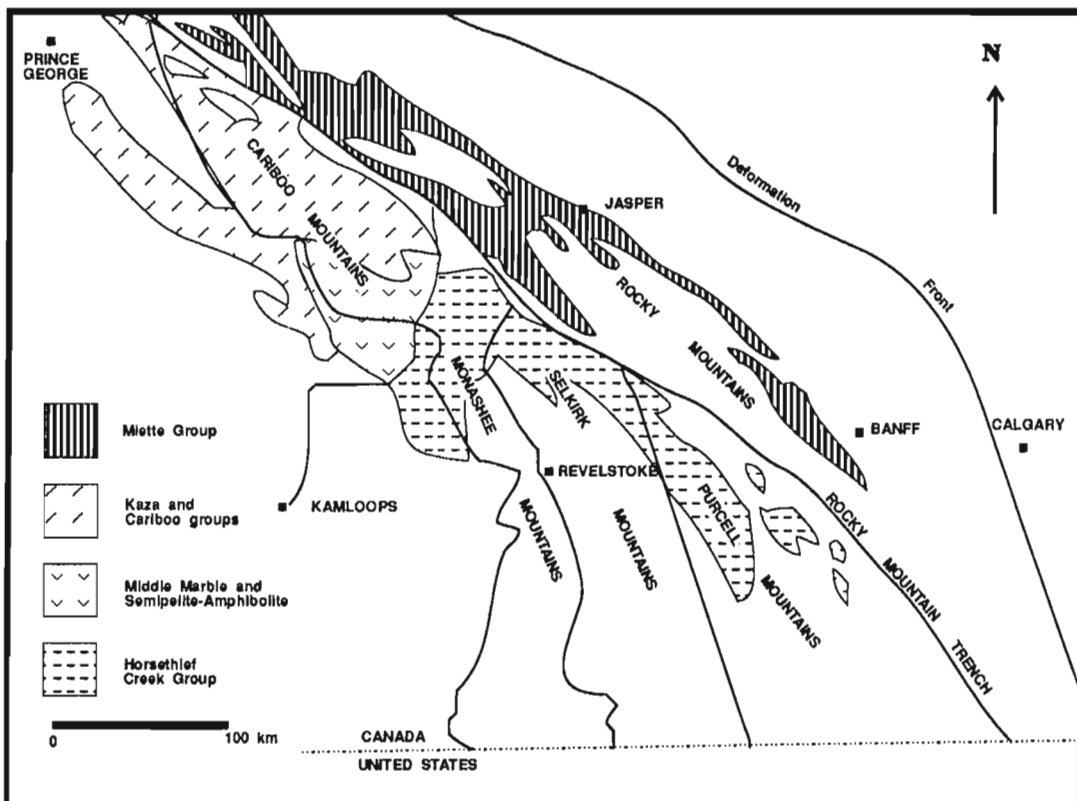


Figure 1. Regional map showing exposures of Windermere Supergroup strata with the local terminology.

amphibolite. Semipelitic layers have a characteristic platy cleavage, with a micaceous sheen. Amphibolite layers are either concordant or discordant with respect to bedding. Tippet (1976) suggested concordant amphibolites, which tend to be rich in biotite and garnet, may be a metamorphosed dolomitic carbonate, and discordant amphibolites are metamorphosed basalt. Sevigny (1988) used rare-earth element patterns, immobile-incompatible-element ratios, and characteristic element abundances, as the bases for suggesting amphibolites in the Semipelite-Amphibolite unit in the Monashee Mountains are metamorphosed alkaline and tholeiitic basalts.

The exposed thickness of the Semipelite-Amphibolite unit is approximately 900 m. The base was not observed in the study area, however it was mapped by Poulton and Simony (1980) immediately to the southeast. Here the Semipelite-Amphibolite unit is underlain by a grey pelite, and then a grit dominated unit. The upper contact is a mixed gradation, approximately 100 m thick, with the overlying marble unit. For mapping purposes, the upper contact is defined by the first appearance of persistent carbonate-rich horizons.

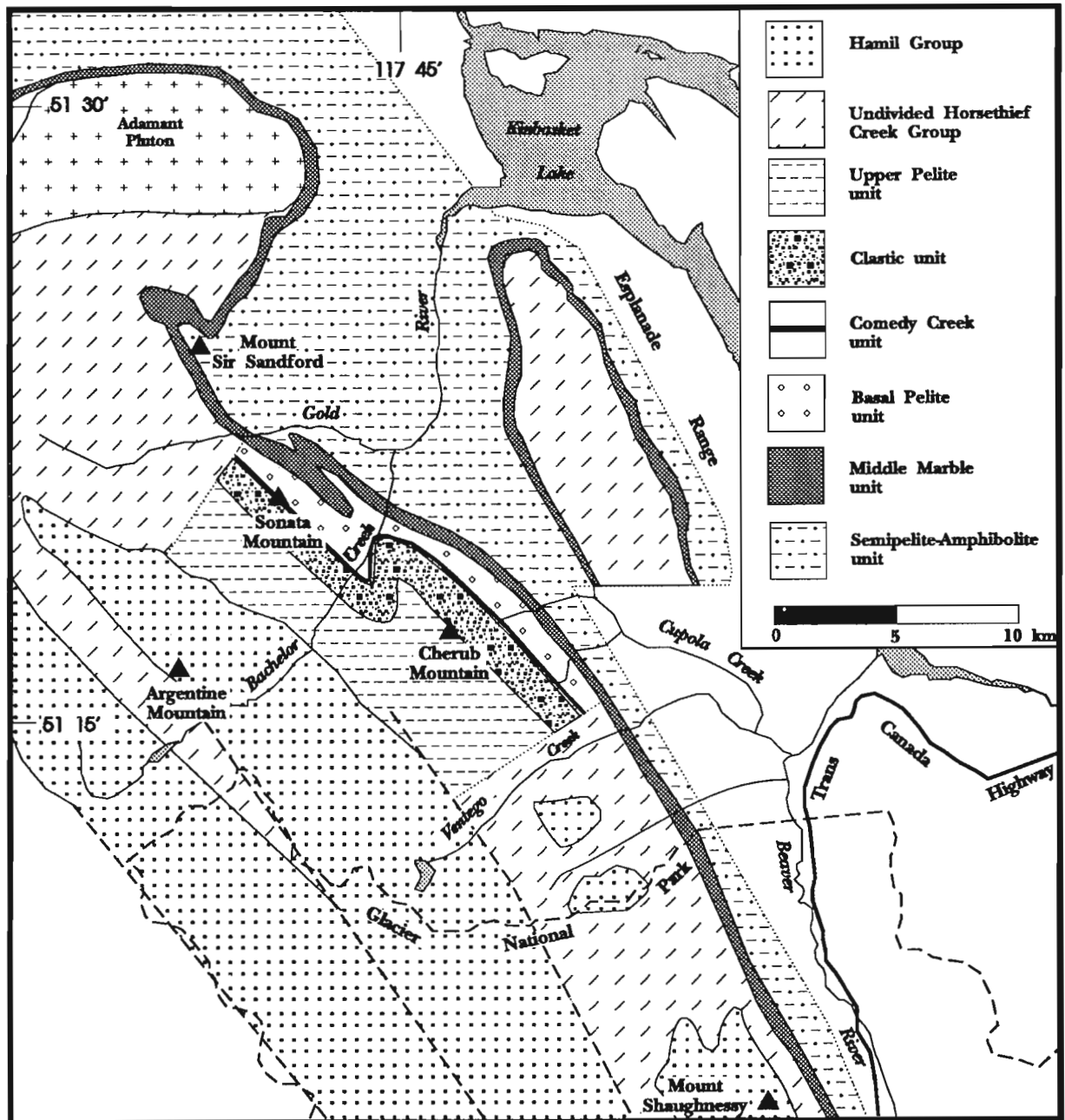


Figure 2. Geology of the Cherub Mountain area.

Middle Marble unit

The Middle Marble unit is characterized by thick grey calcite marble bands. Internally the unit is composed of zones rich in rusty pelites, semipelite, calcsilicates, and pure and impure marbles. The upper contact is a mixed gradation; for mapping purposes it is defined as the last bed of light grey calcitic marble. The unit's structural thickness is approximately 2000 m.

Basal Pelite unit

The Basal Pelite unit consists of 1000 m of interbedded brown weathering psammite and rusty weathering, silver grey pelite. The psammites carbonate content increases towards the Middle Marble unit. Pelite beds contain abundant biotite and garnet, unlike pelites of the Semipelite-Amphibolite unit that

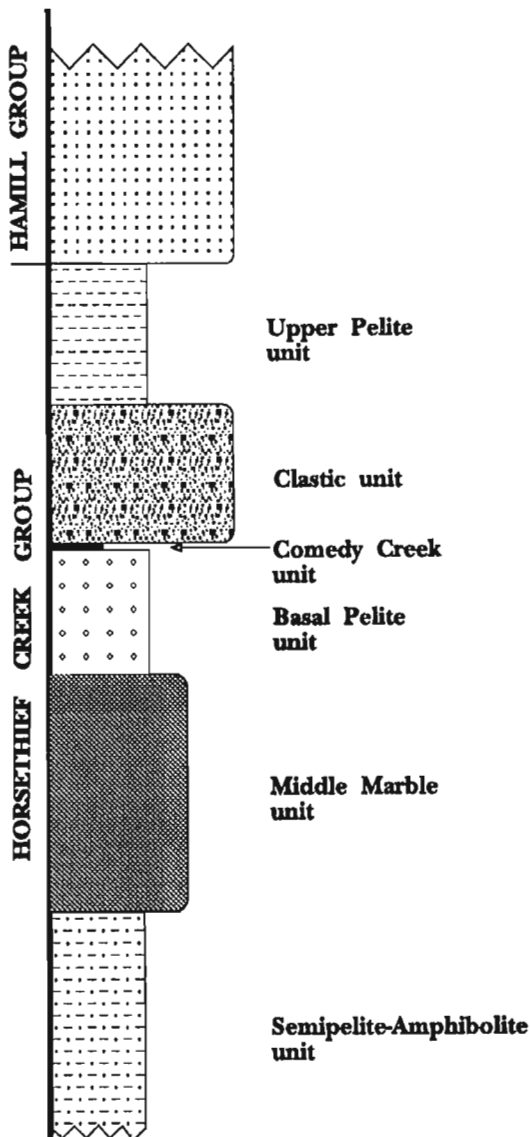


Figure 3. Schematic stratigraphic section of the Horsethief Creek Group in the Cherub Mountain area.

are at equivalent metamorphic grade (based on index minerals in adjacent lithologies). Grit beds, up to 5 m, are rare.

Comedy Creek unit

The Comedy Creek unit is named after its excellent exposures in Comedy Creek valley. Comedy Creek unit is easily recognized in the field, and forms a lithologically and stratigraphically unique succession. It can be traced continuously for more than 40 km along strike, always in the same relative stratigraphic position.

Comedy Creek unit consists of three distinctive and sequential members (from base to top): lower pelite, banded carbonate, and upper pelite. The lower pelite member has a silver-grey micaceous sheen, and a characteristic slaty cleavage. Laminations of semi-pelite are common. The upper contact is a mixed gradation with brown weathering calcareous bands 5 to 10 cm thick. For mapping purposes, the contact with the overlying banded carbonate member is defined at the base of the first carbonate band >5 cm. Total thickness of this member is approximately 40 m.

The banded carbonate member is very distinctive, and easily recognized. Glacial moraines containing banded carbonate blocks can be traced to the outcrop source. The base of the banded carbonate member is characterized by interbedded green-grey pelite with brown weathering calcareous layers on a scale of 5 to 10 cm. Layers of orange weathering carbonate (1-2 cm), and white weathering biotite rich semipelite, are progressively more abundant upward in the succession. Banding occurs at the centimetre scale. Near the top of this member the carbonate layers become thicker (10-15 cm) and more abundant. The member is approximately 50 m thick.

The contact with the overlying upper pelite member is abrupt. The pelite is graphitic, black, and contains abundant disseminated pyrite; semipelitic laminations are common near its base. The upper pelite member is approximately 20 m thick.

Clastic unit

The Clastic unit consists of approximately equal proportions of grits interbedded with rusty weathering green-grey pelites. The grits are massive to graded and consist of quartzite, vein quartz, feldspar and minor carbonate clasts, 2 to 8 mm in diameter. Scours are common, providing abundant tops. The clastic unit forms an overall fining upward succession approximately 1000 m in thickness. At Sonata Mountain, the base is marked by a lenticular horizon of pebble to boulder conglomerate. This horizon is not present in the Cherub Mountain area.

Upper Pelite unit

The Upper Pelite unit is characterized by rhythmically laminated pelites having a silver-grey micaceous sheen. Thin brown layers (1-2 mm) of calcareous siltstone are common.

Grits, medium grained quartzites, and psammites beds are common near the base of the unit. These beds thin and decrease in abundance upwards. The unit is approximately 1200 m thick.

A similar sequence of pelites is present along the eastern base of the Esplanade Range.

REGIONAL CORRELATIONS

Comedy Creek unit allows correlations to be made between the northern Selkirk and the Rocky, Monashee, Cariboo, and Purcell mountains (Fig. 4). These correlations are discussed below.


COLUMBIA MOUNTAINS			ROCKY MOUNTAINS			
CARIBOO MOUNTAINS (Pell, 1984)	NORTHERN SELKIRKS (this study)	PURCELLS (Kubli, 1990)	MOUNT ROBSON	SOUTHERN SELWYN RANGE (Grasby, 1991)	LAKE LOUISE AREA (Aitken, 1969)	
CARIBOO GROUP	YANKEE BELLE FORMATION	UPPER CLASTIC DIVISION	UPPER MIETTE GROUP	UPPER CLASTIC UNIT		
	CUNNINGHAM FORMATION	CARBONATE DIVISION		BYNG 		CARBONATE UNIT
	ISAAC FORMATION	UPPER PELITE UNIT		SLATE DIVISION		SLATE UNIT
KAZA GROUP	UPPER KAZA	UPPER GRIT DIVISION	MIDDLE MIETTE GROUP	UPPER MIDDLE MIETTE GROUP	HECTOR FORMATION	
	"MARKER"	COMEDY CREEK UNIT		BAIRD BROOK DIVISION	OLD FORT POINT FORMATION	OLD FORT POINT FORMATION
	MIDDLE KAZA	BASAL PELITE UNIT		LOWER GRIT DIVISION	LOWER MIDDLE MIETTE GROUP	LOWER MIDDLE MIETTE GROUP
	LOWER KAZA					
	MARBLE UNIT	MID-MARBLE UNIT		LOWER MIETTE GROUP	LOWER MIETTE GROUP PELITE	
	SEMIPELITE AMPHIBOLITE UNIT	SEMIPELITE AMPHIBOLITE UNIT			LOWER MIETTE GROUP GRIT	
	PELITE UNIT					
	GRIT UNIT					

Figure 4. Regional correlations of Windermere Supergroup strata, using the Old Fort Point Formation as a datum (not to scale).

Correlation with the Rocky Mountains

A number of lines of evidence support the correlation of Horsethief Creek Group in the northern Selkirks with Miette Group. Most striking are the similarities in lithology and stratigraphic associations of Comedy Creek unit and Old Fort Point Formation. Both are unique to the exposed Horsethief Creek Group and Miette Group, respectively. Lithologies and stratigraphic sequences are identical. Like the Comedy Creek unit, Old Fort Point Formation is characterized by a basal silty pelite member, a middle member of interbedded carbonate, dolomitic siltstone and pelite bands, and an upper graphitic black pelite member containing disseminated pyrite.

Both Comedy Creek unit and Old Fort Point Formation are stratigraphically overlain by a thick succession of interbedded grit and pelite (Clastic unit and upper middle Miette Group respectively). In both areas the dominance of grit units is replaced over a short gradational interval by rhythmically laminated pelite containing occasional bands of quartzite and grit (Upper Pelite unit and upper Miette Group respectively). These pelite successions are overlain by massive Cambrian quartzites (Hamill and Gog groups respectively).

There are some noticeable differences in strata overlying the Old Fort Point Formation and Comedy Creek unit. The grits in the Clastic unit in the northern Selkirks are finer grained and less abundant than typically found in middle Miette Group. This is consistent with observations in the southern Selwyn Range, where grit units in middle Miette Group thin and become subordinate to pelites, going west towards the southern Rocky Mountain Trench (Grasby, 1991). The Clastic unit in the northern Selkirks may be a more distal equivalent of the middle Miette Group.

The strata underlying Comedy Creek unit and Old Fort Point Formation are markedly different. There is no widespread marble in lower Miette Group equivalent to Middle Marble unit. However local carbonate units have been described by Carey and Simony (1985), and there is indirect evidence in the lower Miette Group for the temporal existence of a carbonate platform. Large channels in lower Miette Group pelite are commonly filled with quartzite pebble conglomerates that contain large intrabasinal carbonate blocks up to 2.5 m across (Grasby, 1991). These blocks may have been derived from carbonates equivalent to Middle Marble unit.

As well, there is no equivalent of the Semipelite-Amphibolite unit in lower Miette Group. However, this unit is known to have only local extent (Sevigny, 1988; Poulton and Simony, 1980). Amphibolite layers are most abundant in the northern Monashees (Raeside and Simony, 1983) and become progressively less abundant to the south, and are rare near the Trans-Canada Highway. Similarly, there is a decrease in the abundance of amphibolite layers going north to the Cariboods (Pell and Simony, 1987). The absence of amphibolites in the Miette Group may be related to the lack of volcanic activity in the parts of the Windermere basin that are now east of the Rocky Mountain Trench.

The lithological similarities between Comedy Creek unit and Old Fort Point Formation, the fact that they are unique features in the exposed Windermere strata in both areas, and the similarity of the overlying stratigraphic succession, are strong support for the correlation of these two units. Stratigraphic variation between the two areas is thought to reflect variations in sedimentary environment and distribution of volcanic activity within Windermere basin.

Correlation with the Monashee Mountains

The Middle Marble and Semipelite-Amphibolite units may be confidently traced from the northern Selkirks, across Columbia River, into the Monashee Mountains near Mica Dam (Simony et al., 1980). However, a succession similar to the Comedy Creek unit has not been reported in the Monashees. The Upper Clastic division of Scrip Range (Raeside and Simony, 1983) is the highest stratigraphic level exposed in the Monashees, and closely resembles lower Kaza Group (P.S. Simony, pers. comm., 1992). This implies that if a Comedy Creek unit equivalent had existed in the Monashees, it was likely eroded.

Correlations with the Cariboo Mountains

Pell and Simony (1987) traced the Middle Marble and Semipelite-Amphibolite units from the northern Selkirks, across the Monashees, and into the southern Cariboods, providing a primary stratigraphic link between the three mountains ranges. Ross and Murphy (1988) correlated "the marker" in the Cariboods with Old Fort Point Formation. This implies Comedy Creek unit is correlative with "the marker", providing further stratigraphic control.

Comedy Creek unit and "the marker" both overlie Middle Marble unit, and occur below a clastic dominated sequence (Clastic unit and upper Kaza Group respectively), that is overlain by a thick sequence of rhythmically laminated pelite (Upper Pelite unit and Isaac Formation respectively).

The main difference between the succession in the Cariboods and the northern Selkirks, is that the clastic unit is thinner, and the grits within it are not as abundant as in the upper Kaza. As well, there are no equivalents in the study area of the Cunningham and Yankee Belle formations, that overlie Isaac Formation in the Cariboods. This implies that in the northern Selkirks there is a sub-Cambrian stratigraphic omission greater than 1600 m, relative to the Cariboods.

Correlations with the Purcell Mountains

Kubli (1990) correlated a tripart sequence in the grit division of the Purcell Mountains (the Baird Brook division) with Old Fort Point Formation and "the marker", based on lithological similarities and a common stratigraphic sequence. This implies that Comedy Creek unit is correlative with Baird Brook division. This correlation is supported by the similarity of the stratigraphic succession above the two units.

Comedy Creek unit and Baird Brook division are both overlain by a grit dominated unit (Clastic unit and upper grit division respectively), that are both overlain by a thick sequence of laminated pelite with minor clastics (Upper Pelite unit and slate division respectively). The carbonate division in the Purcells, which overlies the slate division, was mistakenly correlated with the Middle Marble unit in the northern Selkirks by Poulton and Simony (1980) and Pell and Simony (1987). There are no equivalents of the carbonate division in the study area.

The strata underlying the Baird Brook division and Comedy Creek unit are markedly different. There are no equivalents of the Middle Marble and Semipelite-Amphibolite units in the strata underlying Baird Brook division. Kubli (1990) suggested that boulder size clasts of dolomite in the basal pelitic division in the Purcells indicates the proximity of a carbonate platform. This may be a Middle Marble unit equivalent. The absence of amphibolites in the Purcells is not surprising, considering they become progressively less abundant south of the Monashees.

DISCUSSION

Pleasant Valley Thrust

Struik (1986a,b, 1987) proposed that a west verging thrust (Pleasant Valley Thrust) places Kaza Group structurally above Middle Marble and Semipelite-Amphibolite units in the southern Cariboo. He correlated the Middle Marble unit with a Paleozoic carbonate exposed in the Cariboo lake area (Struik, 1982). If his interpretation, and the above correlations, are correct, it implies that the Middle Marble unit in the northern Selkirks is Paleozoic, and that Pleasant Valley Thrust should occur in the zone overlying the Middle Marble unit. This zone was examined carefully, and there was no evidence of a fault. We therefore conclude that Pleasant Valley Thrust does not extend southward at this stratigraphic level. Our data indicate that the Middle Marble and underlying Semipelite-Amphibolite unit are indeed part of the Hadrynian Horsethief Creek Group.

Lateral variations in the Horsethief Creek Group

In the Cherub Mountain area, there are approximately 3 km of strata separating Cambrian quartzites from the Middle Marble unit. Near Mount Shaughnessy, 25 km to the southwest, this separation is less than 800 m. Work by Poulton and Simony (1980) suggests that strata between the Cambrian and Middle Marble unit near Mount Shaughnessy include equivalents of the Basal Pelite unit, Clastic unit, and some portion of the Upper Pelite unit. As noted above, the grit units in the Cherub Mountain area are thinner, finer grained, and less abundant than equivalent units having the same stratigraphic position in other mountain ranges. Thinning and fining of the succession between the Middle Marble unit and the Cambrian can be attributed to a greater distance from the source. Some of the stratigraphic omission may also be related sub-Cambrian erosion.

CONCLUSIONS

The Horsethief Creek Group in the northern Selkirks may be divided into six units. The Comedy Creek unit is confidently correlated with Old Fort Point Formation in the Rockies, "the marker" in the Cariboo, and Baird Brook division in the Purcells. An Old Fort Point Formation equivalent has not been reported in the Monashees.

The above correlations place some preliminary constraints on the geometry of the Windermere basin: 1) grits associated with Comedy Creek unit are less abundant, and finer grained, suggesting that Windermere strata in the northern Selkirks was deposited in a more distal setting; 2) igneous activity that formed the extensive amphibolites deposits in the Monashees and northern Selkirks was limited to strata exposed west of the Rocky Mountain Trench; 3) Pleasant Valley Thrust does not extend south into the northern Selkirks; and 4) Windermere strata in the northern Selkirks form a conformable stratigraphic sequence.

ACKNOWLEDGMENTS

Helicopter support and expediting by Don McTighe was greatly appreciated. This project was funded by EMR Research Agreement no. 017492 and NSERC research grant A2693 to R.L. Brown. Discussions with P. Simony helped improve this paper. Helpful comments by R.I. Thompson are greatly appreciated.

REFERENCES

- Aitken, J.D.
1969: Documentation of the sub-Cambrian unconformity, Rocky Mountain Main Ranges, Alberta; Canadian Journal of Earth Science, v. 6, p. 193-200.
- Brown, R.L., Tippett, C.R., and Lane, L.S.
1978: Stratigraphy, facies changes, and correlations in the northern Selkirk Mountains, southern Canadian Cordillera; Canadian Journal of Earth Science, v. 15, p. 1129-1140.
- Carey, J.A. and Simony, P.S.
1985: Stratigraphy, sedimentology and structure of Late Proterozoic Miette Group, Cushing Creek area, B.C.; Bulletin of Canadian Petroleum Geology, v. 33, p. 184-203.
- Grasby, S.E.
1991: Stratigraphy of the Miette Group and tectonic history of the southern Selwyn Range, western Main Ranges, British Columbia; M.Sc. thesis, McGill University, Montreal, Quebec, 121 p.
- Kubli, T.
1990: Geology of the Dogtooth Range, northern Purcell Mountains, British Columbia; Ph.D. thesis, University of Calgary, Alberta, 324 p.
- Pell, J.
1984: Stratigraphy, structure and metamorphism of the Hadrynian strata in the southeastern Cariboo Mountains, B.C.; Ph.D. thesis, University of Calgary, Alberta.
- Pell, J. and Simony, P.S.
1987: New correlations of Hadrynian strata, south-central British Columbia; Canadian Journal of Earth Science, v. 24, p. 302-313.
- Poulton, T.P. and Simony, P.S.
1980: Stratigraphy, sedimentology, and regional correlations of the Horsethief Creek Group (Hadrynian, Late Precambrian) in the northern Purcell and Selkirk mountains, British Columbia; Canadian Journal of Earth Science, v. 17, p. 1708-1724.

Raeside, R.P. and Simony, P.S.

1983: Stratigraphy and deformational history of the Scrip Nappe, Monashee Mountains, British Columbia; *Canadian Journal of Earth Science*, v. 20, p. 639-650.

Ross, G.M. and Murphy, D.C.

1988: Transgressive stratigraphy, anoxia, and regional correlations within the late Precambrian Windermere grit of the southern Canadian Cordillera; *Geology*, v. 10, p. 139-143.

Sevigny, J.H.

1988: Geochemistry of Late Proterozoic amphibolites and ultramafic rocks, southeastern Canadian Cordillera; *Canadian Journal of Earth Science*, v. 25, p. 1323-1337.

Simony, P.S., Ghent, E.D., Graw, D., Mitchell, W., and Robins, D.B.

1980: Structural and metamorphic evolution of northeast flank of Shuswap Metamorphic Complex, southern Canoe River area, British Columbia; in *Cordilleran Metamorphic Core Complexes*, (ed.) M.D. Crittenden, Jr., P.J. Coney, and G.H. Davies; Geological Society of America, Memoir 153, p. 445-461.

Struik, L.C.

1982: Snowshoe Formation (1982), central British Columbia; in *Current Research, Part B*; Geological Survey of Canada, Paper 82-1B, p. 117-124.

Struik, L.C. (cont.)

1986a: A regional east-dipping thrust places Hadrynian onto probable Paleozoic rocks in Cariboo Mountains, British Columbia; in *Current Research, Part A*; Geological Survey of Canada, Paper 86-1A, p. 589-594.

1986b: Imbricated terranes of the Cariboo gold belt with correlations and implications for tectonics in southeastern British Columbia; *Canadian Journal of Earth Science*, v. 23, p. 1047-1061.

1987: The ancient western North American margin: an alpine rift model for the west-central Canadian Cordillera; Geological Survey of Canada, Paper 87-15, 19 p.

Tippett, C.R.

1976: A structural and stratigraphic cross-section through the Selkirk Fan Axis, Selkirk Mountains, southeastern British Columbia; M.Sc. thesis, Carleton University, Ottawa, Ontario, 166 p.

Energy, Mines and Resources Research Agreement No. 017492

Evidence for Cretaceous deformation in the Kootenay Arc based on U-Pb and $^{40}\text{Ar}/^{39}\text{Ar}$ dating, southeastern British Columbia

Alain D. Leclair, Randall R. Parrish, and Doug A. Archibald¹
Continental Geoscience Division

Leclair, A.D., Parrish, R.R., and Archibald, D.A., 1993: Evidence for Cretaceous deformation in the Kootenay Arc based on U-Pb and $^{40}\text{Ar}/^{39}\text{Ar}$ dating, southeastern British Columbia; in Current Research, Part A; Geological Survey of Canada, Paper 93-1A, p. 207-220.

Abstract: The late-synkinematic Baldy Pluton and postkinematic Midge Creek Stock intrude multiply deformed and metamorphosed rocks in the central Kootenay Arc. U-Pb zircon systematics display the combined effects of inheritance from Precambrian xenocrystic zircons and probable postemplacement (<100 Ma) Pb loss, and consequently yield imprecise crystallization ages of 100-150 Ma for these intrusions. U-Pb dates on titanite and allanite provide emplacement ages of $117 \pm 4/-1$ Ma for the Baldy Pluton and 111 ± 5 Ma for the Midge Creek Stock. $^{40}\text{Ar}/^{39}\text{Ar}$ age spectra for amphibole from the aureoles of these intrusions and the deformed "tail" of the Nelson Batholith also support a mid-Cretaceous age for these intrusions and elevated temperature at this time. These ages are consistent with geological field evidence, and imply that the penetrative deformational event, at this crustal level, culminated with the emplacement of these intrusions in mid-Cretaceous time.

Résumé : Le pluton syncinématique tardif de Baldy et le massif intrusif postcinématique de Midge Creek pénètrent des roches très souvent déformées et métamorphosées dans la région centrale de l'arc de Kootenay. La classification des roches obtenue à l'aide de la méthode U-Pb sur le zircon témoigne des effets combinés de l'héritage laissé par des zircons xéno-cristallins d'âge précambrien et par la perte probable en Pb s'étant produite après la mise en place (<100 Ma), et ne permet donc qu'une détermination imprécise des âges de cristallisation, soit de 100 à 150 Ma, dans le cas de ces intrusions. Les âges déterminés à l'aide de la méthode U-Pb sur la titanite et l'allanite établissent que la mise en place a eu lieu il y a $117 \pm 4/-1$ Ma dans le cas du pluton de Baldy, et il y a 111 ± 5 Ma dans le cas du massif intrusif de Midge Creek. Les âges établis à l'aide de la méthode $^{40}\text{Ar}/^{39}\text{Ar}$ sur les amphiboles recueillies des auréoles de métamorphisme associées à ces intrusions et de la «queue» déformée du batholite de Nelson confirment eux aussi, pour le moment, l'âge crétacé de ces intrusions et la présence de températures élevées. Ces âges correspondent aux données géologiques relevées sur le terrain et laissent supposer que l'épisode de déformation pénétrative, à ce niveau de la croûte, s'est terminé par la mise en place de ces intrusions au Crétacé moyen.

¹ Department of Geological Sciences, Queen's University, Kingston, Ontario K7L 3N6

INTRODUCTION

The structural/metamorphic history of the central Kootenay Arc is characterized by regional, contact, and retrograde metamorphic events and at least three phases of deformation, spanning the interval from mid-Paleozoic to Eocene time (Fyles, 1967; Crosby, 1968; Read and Wheeler, 1976; Höy, 1980; Glover, 1978; Klepacki and Wheeler, 1985; Leclair, 1988 and references therein). It is punctuated by three main periods of igneous activity which provide critical time constraints for these metamorphic and deformation events and have important implications for the tectonics of the southeastern Canadian Cordillera (e.g., Archibald et al., 1983, 1984). Late-synkinematic and postkinematic granitoid intrusions of the Nelson and Bayonne Granitic suites (Reesor, 1983; Leclair, 1986) in the Midge Creek Area (Fig. 1) intrude a sequence of Helikian to Triassic strata that have experienced polyphase deformation and metamorphism. Two of these intrusions, Baldy Pluton and Midge Creek Stock, were chosen for U-Pb geochronology. Based on field and microstructural relationships, the emplacement of the Baldy Pluton occurred in the latter part of the penetrative deformation (Phase II) and regional metamorphism, whereas the Midge Creek Stock clearly truncates regional metamorphic zones and Phase II structures and was emplaced after Phase III deformation and regional uplift (Leclair, 1988). In this context, the geochronological results bear on the temporal relationships between plutonism, metamorphism, and deformation in the Kootenay Arc.

The U-Pb zircon geochronology of the Baldy Pluton and Midge Creek Stock was first studied as part of the Ph.D. thesis by Leclair (1988). The initial zircon results, which are summarized below, reveal a pattern of discordance that did not yield precise emplacement ages for either of the intrusions. In an effort to better define these ages, a follow-up U-Pb study was done using igneous minerals such as titanite and allanite, which are free of inheritance. This paper describes the setting and age of the Baldy Pluton and Midge Creek Stock and discusses their significance with respect to the protracted tectono-metamorphic history of the central Kootenay Arc. Also, the $^{40}\text{Ar}/^{39}\text{Ar}$ ages of hornblende from six samples and biotite from one sample are reported.

GEOLOGICAL SETTING AND FIELD RELATIONS

The Kootenay Arc of the southeastern Canadian Cordillera is essentially a west-facing homocline of metamorphic rocks, with an aggregate thickness of about 20 km (Fig. 1). Neoproterozoic to Triassic strata, which comprise the stratigraphic sequence, have been complexly deformed, regionally metamorphosed, and intruded by granitoid plutons during the Jura-Cretaceous Columbian Orogeny (see Price, 1981; Archibald et al., 1983; references therein). In the regional tectonic framework, the Kootenay Arc is roughly coincident with the boundary zone linking the paleocontinental margin of North America to the leading edge of allochthonous terranes (see Wheeler and McFeely, 1991). The Midge Creek Area (Leclair, 1986; Fig. 1) includes the

narrowest, central segment of the Kootenay Arc, suggesting that it is perhaps the most highly deformed and attenuated part of this arcuate tectonostratigraphic element (Leclair, 1983). It is characterized by intense penetrative deformation associated with tight to isoclinal coaxial folds and intermediate-pressure regional metamorphism (0.55-0.70 GPa) locally superimposed by lower-pressure contact aureoles related to mesozonal granitoid intrusions of the Nelson and Bayonne Granitic suites (Leclair, 1988). These intrusions and/or their contact aureoles crosscut major north-northeast-striking faults such as the Seaman Creek and Midge Creek faults (Fig. 2). The Seaman Creek Fault is part of a composite fault zone extending along the Kootenay Arc for at least 150 km. It has been interpreted as the basal detachment of a large-scale thrust nappe that separates the autochthonous North American Terrane on the east from the parautochthonous Kootenay Terrane to the west (Leclair, 1984, 1990).

Baldy Pluton

The Baldy Pluton, considered by Little (1960) to be part of the Jurassic Nelson Granitic Suite, is a 35 km long and structurally concordant, sill-like intrusive body that extends obliquely across the Midge Creek area (Fig. 2). It intrudes lower Paleozoic strata of the Hamill and Lardeau groups. The contact zone of the pluton contains numerous lenticular inclusions of country rocks several metres long. The northern part of the pluton, at least, is bordered by a narrow sillimanite zone, with the common assemblage garnet-sillimanite-biotite-muscovite-quartz-plagioclase. A foliation within the pluton, which is defined by ellipsoidal segregations of fine grained quartz and plagioclase and the alignment of biotite flakes and flattened mafic clots, parallels the main fabric (S_2) in enclosing strata. Both field and microstructural relationships suggest that emplacement of the Baldy Pluton occurred late-synkinematically with respect to the penetrative deformation (Phase II) and sometime after the intermediate-pressure regional metamorphic event (Leclair, 1988). Mineral assemblages in the contact aureole suggest emplacement at crustal levels commensurate with paleopressures between 0.35 and 0.55 GPa.

Midge Creek Stock

The Midge Creek Stock of the Bayonne Granitic Suite is a structurally discordant, teardrop-shaped pluton which covers a 12 km² area and has a high magnetic relief signature. It is clearly emplaced athwart the regional structural grain and cuts or deforms the strong and pervasive north-northeast-trending fabric (S_2) in enclosing stratified rocks of the Windermere Supergroup and Hamill Group (Fig. 2). Only the north-westernmost margin of the stock displays a well developed foliation which is concordant with the trend of structures in adjacent Hamill Group strata. The sharp contact of the stock dips steep to vertical, cutting across layering in the country rocks at a high angle. Rare metasedimentary inclusions and pegmatite dykes occur along the margin. The Midge Creek Stock truncates regional-metamorphic isograds, superimposing a lower-pressure contact aureole containing andalusite and sillimanite on the regionally metamorphosed

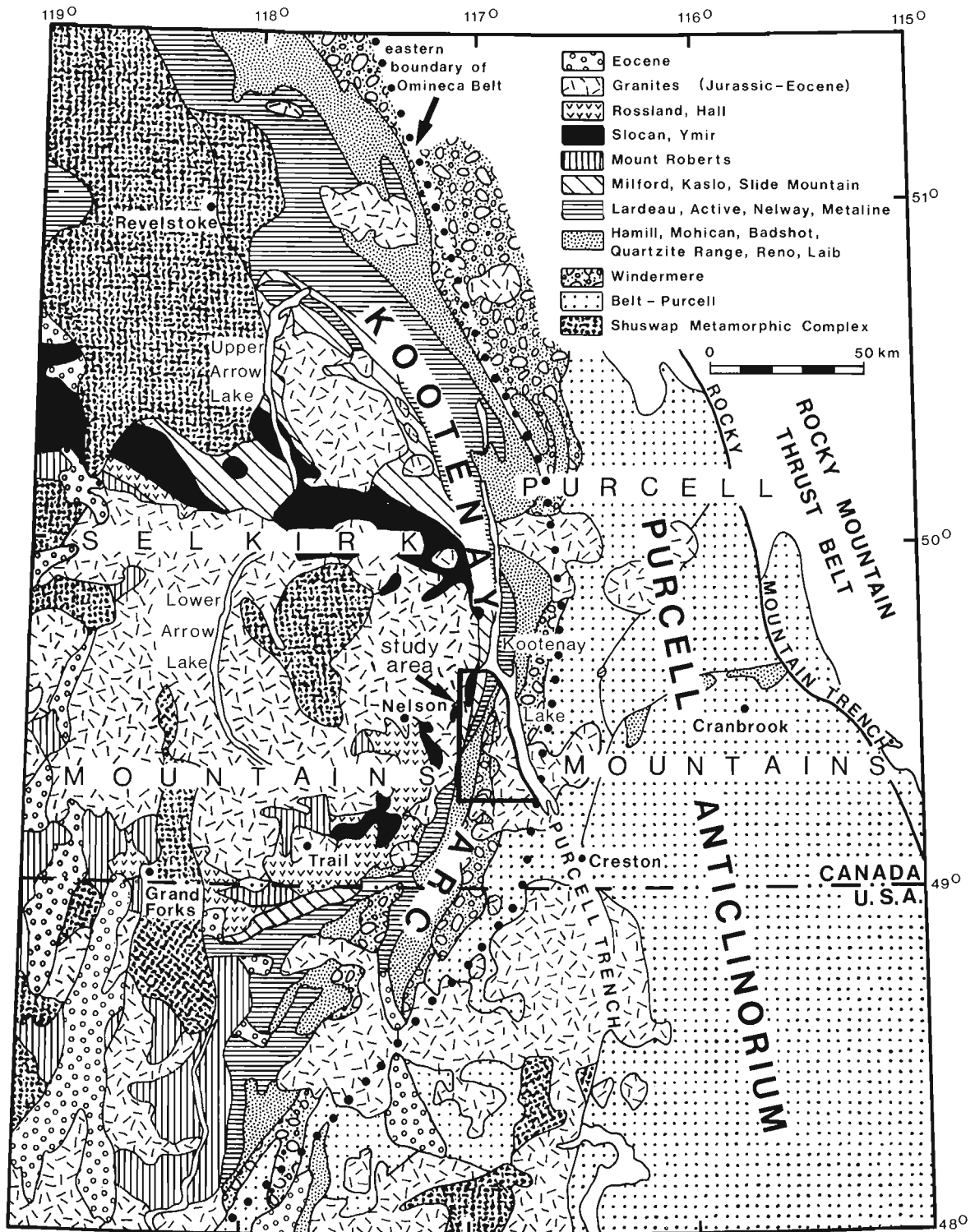


Figure 1. Generalized geological map of the Kootenay Arc and surrounding area showing the distribution of tectonostratigraphic assemblages and the main structural elements of the southeastern Canadian Cordillera (after Tipper et al., 1981; Wheeler and McFeely, 1991). The Midge Creek area is outlined.

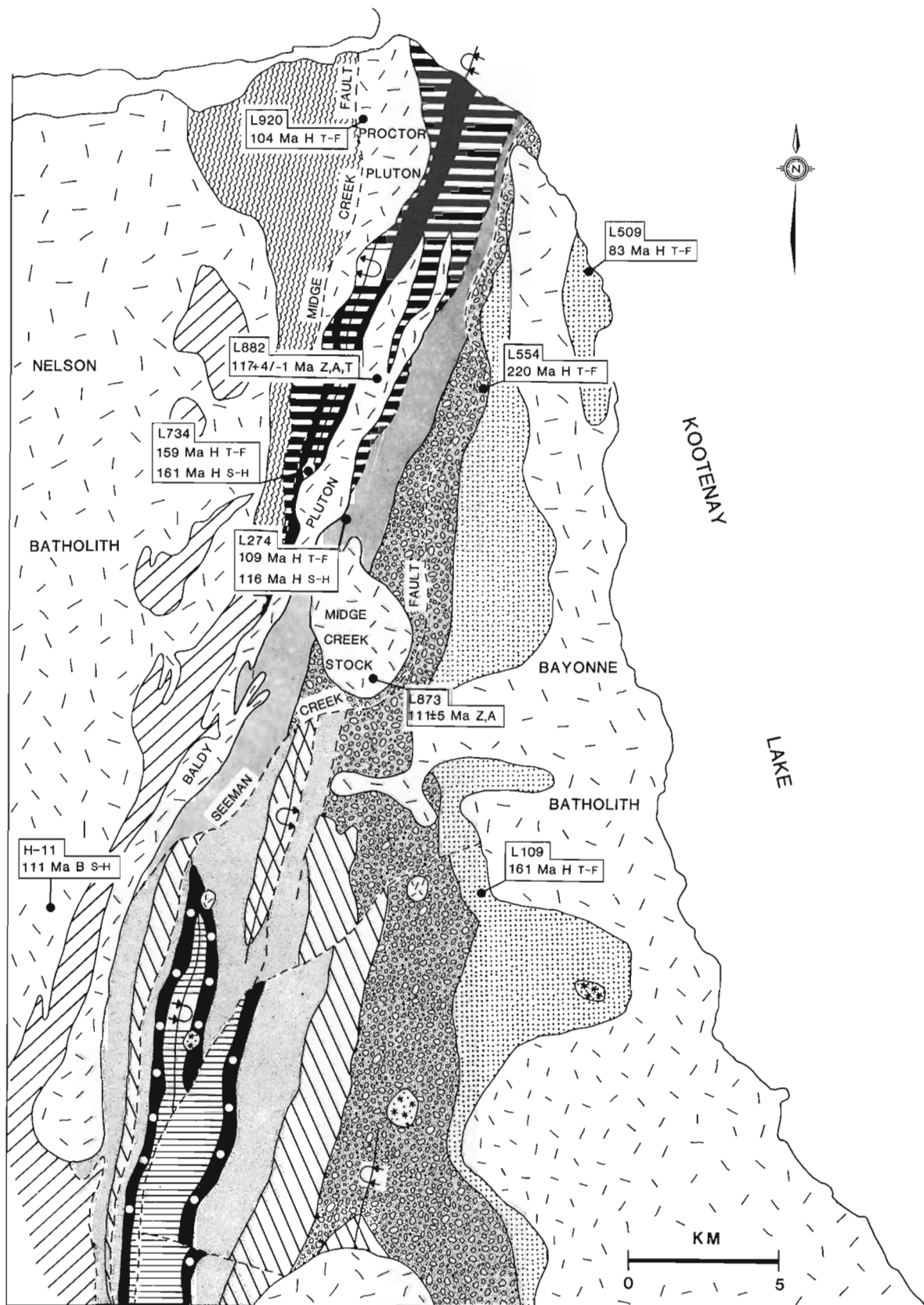


Figure 2. Simplified geological map of the Midge Creek area, central Kootenay Arc (Leclair, 1986; as modified from Rice, 1941; McAllister, 1951; Little, 1985). The locations and ages of U-Pb and $^{40}\text{Ar}/^{39}\text{Ar}$ samples are shown. Annotations for U-Pb samples are: Z=zircon, A=allanite and T=titanite. Annotations for $^{40}\text{Ar}/^{39}\text{Ar}$ samples are: H=hornblende, B=biotite, T-F=total-fusion age and S-H=step-heating integrated age. See text for discussion.

country rocks. Porphyroblast-matrix microstructural relationships suggest that contact-metamorphic minerals crystallized in a tectonically dormant environment at crustal levels within the 0.25-0.35 GPa range (Leclair, 1988). A period of regional cooling (~100°C) and uplift (7-10 km), concurrent with Phase III deformation, is inferred to have occurred before the emplacement of the Midge Creek Stock.

U-Pb GEOCHRONOLOGY

Sample descriptions

Baldy Pluton

The dominant phases of the Baldy Pluton are strongly foliated, leucocratic, medium grained biotite granodiorite and tonalite. They have an allotriomorphic texture with minor myrmekite, and display some degree of recrystallization in the form of polygonal subgrains of quartz and plagioclase. Common K-feldspar megacrysts are locally augen-shaped and normally 2 cm long, but may reach 5 cm. Plagioclase grains, 2-3 mm long, exhibit a weak preferred orientation.

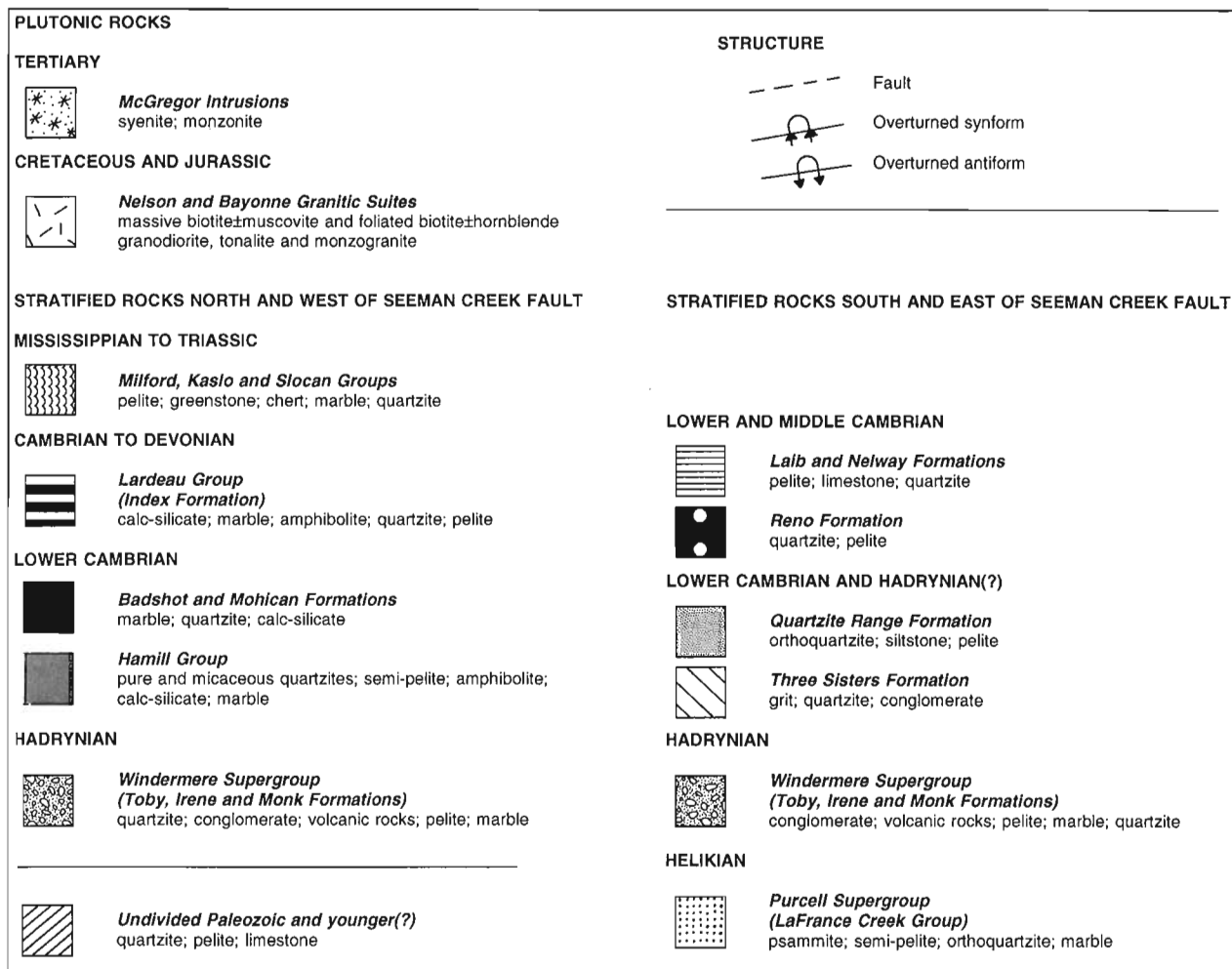
They have a composition around An_{30} and are slightly sericitized. Quartz occurs as discrete irregular phenocrysts, averaging 0.5-2.0 mm in diameter, or as small grains (<0.3 mm) in segregations with plagioclase. Potassium feldspar consists mainly of interstitial anhedral less than 1.5 mm in diameter with good cross-hatched twinning. Mafic clots are composed of chlorite-altered biotite, poikilitic epidote, and minor sphene. Allanite cores with epidote rims, zircon, apatite, calcite, and opaques together make up less than 1% of the rock. Muscovite and garnet are rare.

The U-Pb dating sample (L882RA-1-83) of the Baldy Pluton lies in the northern part of the pluton (Fig. 2). It is a medium grained, foliated leucotonalite with about 15% biotite, rare 3 cm long K-feldspar megacrysts, and elongated clots of biotite, epidote, and titanite that define a shallow south-southwest plunging lineation.

Midge Creek Stock

The Midge Creek Stock consists mainly of massive, medium- to coarse-grained leucogranodiorite with biotite, muscovite, epidote, and minor titanite and allanite. It shows strong

LEGEND Figure 2



mineralogical and compositional affinities to the Bayonne Batholith which is part of the same suite of granitic rocks. The granodiorite has a hypidiomorphic granular texture with rare phenocrysts of plagioclase, quartz and/or K-feldspar. Plagioclase occurs as subhedral laths, 0.5 to 5 mm long, which are normally zoned from An₄₀ to An₂₇ and slightly altered to sericite and epidote. Quartz is anhedral, 0.1 to 4 mm in diameter and weakly strained. Interstitial K-feldspar grains, up to 7 mm long, display minor perthitic textures and may include quartz and plagioclase. Slightly chlorite-altered biotite forms clusters with muscovite, epidote, and titanite.

Muscovite flakes (<1 mm long) are commonly enclosed in plagioclase, but also occur in the groundmass. Discrete anhedral of epidote are spatially associated with biotite. Accessory minerals include apatite, coarse titanite, allanite, zircon, opaques, and local garnet.

The dated rock sample (L873RA-1-83) of the Midge Creek Stock was collected about 500 m from its southeastern contact (Fig. 2). It is a weakly foliated, fine- to medium-grained leucogranodiorite including approximately 20% muscovite, biotite, and epidote.

Table 1. U-Pb analytical data for Baldy Pluton and Midge Creek stock

sample,** analysis	wt.## (mg)	U, (ppm)	Pb,+ (ppm)	²⁰⁶ Pb* ²⁰⁴ Pb	Pb _c ,# (pg)	²⁰⁸ Pb+ ²⁰⁶ Pb	²⁰⁶ Pb++ ²³⁸ U	²⁰⁶ Pb++ ²³⁸ U (Ma)	²⁰⁷ Pb++ ²³⁵ U	²⁰⁷ Pb++ ²³⁵ U (Ma)	²⁰⁷ Pb++ ²⁰⁶ Pb	corr. coef.	²⁰⁷ Pb*** ²⁰⁶ Pb (Ma)
Baldy Pluton, sample L882RA-1-83													
<i>titanite</i>													
T1,clr	0.104	78.80	1.803	111	106	0.36	0.01890 ± 0.30	120.7 ± 0.7	0.1280 ± 1.06	122.3 ± 2.4	0.04910 ± 0.89	0.67	153 ± 42
T2,clr	0.219	88.94	1.898	119	224	0.31	0.01830 ± 0.42	116.9 ± 1.0	0.1199 ± 1.38	114.9 ± 3.0	0.04752 ± 1.13	0.69	75 ± 53
T3,cdy	0.361	82.41	1.720	106	392	0.28	0.01825 ± 0.61	116.6 ± 1.4	0.1228 ± 1.90	117.6 ± 4.2	0.04881 ± 1.54	0.69	139 ± 73
T4,clr,sa	0.138	85.33	1.871	121	132	0.34	0.01833 ± 0.46	117.1 ± 1.1	0.1218 ± 1.53	116.7 ± 3.4	0.04819 ± 1.27	0.68	109 ± 59
T5,clr,sa	0.115	68.58	1.656	85	139	0.46	0.01852 ± 0.70	118.3 ± 1.6	0.1245 ± 2.30	119.2 ± 5.2	0.04878 ± 1.88	0.69	137 ± 88
<i>allanite</i>													
A1	0.307	186.4	36.81	41	3058	11.06	0.01883 ± 2.43	120.2 ± 5.8	0.1193 ± 8.23	114.4 ± 17.8	0.04596 ± 6.79	0.69	-4 ± 332
A2	0.290	171.8	33.24	39	2868	10.75	0.01893 ± 2.60	120.9 ± 6.2	0.1201 ± 8.65	115.1 ± 18.8	0.04600 ± 7.10	0.69	-2 ± 347
A3	0.335	199.5	36.35	40	3652	10.11	0.01884 ± 2.49	120.3 ± 5.9	0.1180 ± 8.36	113.3 ± 17.9	0.04544 ± 6.87	0.69	-32 ± 338
<i>zircon</i>													
A	0.367	1029	45.87	9091	115	0.087	0.04407 ± 0.15	278.0 ± 0.8	0.5397 ± 0.17	438.2 ± 1.2	0.08884 ± 0.04	0.97	1400 ± 1.6
B	0.184	933.2	30.02	9787	36	0.064	0.03292 ± 0.15	208.8 ± 0.6	0.3298 ± 0.17	289.4 ± 0.8	0.07255 ± 0.04	0.97	1004 ± 1.6
C	0.210	900.8	29.67	16844	23	0.080	0.03318 ± 0.15	210.4 ± 0.6	0.3420 ± 0.17	298.7 ± 0.8	0.07475 ± 0.04	0.97	1062 ± 1.6
D	0.192	877.6	30.27	15343	24	0.074	0.03478 ± 0.16	220.4 ± 0.8	0.3775 ± 0.17	325.2 ± 1.0	0.07872 ± 0.04	0.98	1165 ± 1.6
E	0.574	790.3	34.57	3410	83	0.092	0.04335 ± 0.20	273.6 ± 1.0	0.5095 ± 0.20	418.1 ± 1.1	0.08524 ± 0.06	0.95	1321 ± 2.2
F	0.879	738.2	24.17	3410	145	0.086	0.03284 ± 0.20	208.3 ± 0.8	0.3548 ± 0.20	308.3 ± 0.8	0.07835 ± 0.06	0.95	1156 ± 2.0
G	0.580	1046	38.95	14453	98	0.085	0.03723 ± 0.19	235.6 ± 0.8	0.3995 ± 0.20	341.3 ± 1.2	0.07782 ± 0.04	0.98	1142 ± 1.6
Midge Creek Stock, sample L873RA-1-83													
<i>allanite</i>													
A1	0.127	282.7	39.72	34	2588	8.01	0.01790 ± 3.66	114.4 ± 8.3	0.1258 ± 21.1	120 ± 48	0.05096 ± 19.1	0.61	240 ± 975
A2	0.179	269.6	39.64	34	3557	8.46	0.01783 ± 3.04	113.9 ± 6.9	0.1314 ± 9.9	125 ± 23	0.05345 ± 8.2	0.65	348 ± 380
<i>zircon</i>													
A	0.496	1271	43.22	3763	86	0.092	0.03383 ± 0.20	214.5 ± 0.8	0.3674 ± 0.20	317.7 ± 0.8	0.07876 ± 0.06	0.95	1166 ± 2.0
B	1.406	1338	43.00	8989	125	0.082	0.03224 ± 0.20	204.5 ± 0.8	0.3471 ± 0.20	302.5 ± 0.8	0.07809 ± 0.06	0.95	1149 ± 2.0
C,a	0.652	1884	59.47	8062	301	0.093	0.03142 ± 0.19	199.4 ± 0.8	0.3243 ± 0.20	285.2 ± 1.0	0.07488 ± 0.04	0.98	1065 ± 1.6
D	0.034	1447	36.39	3754	22	0.051	0.02612 ± 0.18	166.2 ± 0.6	0.2498 ± 0.19	226.4 ± 0.8	0.06935 ± 0.06	0.95	909 ± 2.4
E	0.271	1440	46.60	20500	39	0.080	0.03255 ± 0.16	206.5 ± 0.6	0.3437 ± 0.17	300.0 ± 0.8	0.07659 ± 0.04	0.98	1110 ± 1.6
F	0.367	1246	41.52	21452	44	0.090	0.03316 ± 0.16	210.3 ± 0.6	0.3572 ± 0.17	310.1 ± 1.6	0.07813 ± 0.04	0.98	1150 ± 1.6
G,cdy	0.130	3156	100.9	1791	46	0.101	0.03171 ± 0.15	201.2 ± 0.6	0.3151 ± 0.18	278.1 ± 0.8	0.07208 ± 0.09	0.88	988 ± 3.4

** a, abraded; sa, strongly abraded to less than 0.5 of original crystal diameter; clr, clear; cdy, cloudy; all other fractions are unabraded

Weighing error = 0.001 mg.

+ Radiogenic Pb.

* Measured ratio, corrected for spike, and Pb fractionation of 0.09% +/- 0.03%/AMU

Total common Pb in analysis corrected for fractionation and spike.

++ Corrected for blank Pb and U, and common Pb (Stacey-Kramers model Pb composition equivalent to the interpreted age of the rock); errors are 1 standard error of the mean in percent for ratios and 2 standard errors of the mean when expressed in Ma.

*** Corrected for blank and common Pb, errors are 2 standard errors of the mean in Ma.

Analytical procedures

Zircon, titanite, and allanite were extracted from the crushed rock samples by conventional mineral separation techniques using a Wilfley table, heavy liquids, and a Frantz isodynamic separator. Hand picking of minerals ensured 100% purity of the mineral concentrates. Seven multigrain fractions of zircon were hand picked from each rock sample, five of which consist of clear, euhedral, crack-free crystals. Two fractions of zircons with clearly visible cores (inherited zircons) were analyzed. Some crystals were abraded using the technique of Krogh (1982), as indicated in Table 1. Zircon fractions were chemically dissolved and analyzed following procedures outlined in Parrish et al. (1987). Several multigrain fractions of titanite and allanite were also analyzed, using procedures outlined in Parrish et al. (1992); a few of the titanite fractions were strongly abraded, as discussed below. Analytical blanks during the study ranged from 15 to 40 picograms Pb and <30 picograms U, except for a few of the earliest analyses of zircon which were somewhat higher. Common lead corrections utilized the Stacey and Kramer (1975) two-stage model, with a model Pb age of 115 Ma. Data is tabulated in Table 1 and shown in concordia plots of Figures 4 and 5, below.

Results

The zircon population in each sample consists of colourless to light brown, euhedral to subhedral, equant to elongate prismatic, clear zircons with some crystals containing a high percentage of core material (Fig. 3). The data sets are generally quite similar. In each case, all seven zircon points are notably discordant and noncolinear within analytical uncertainty, with both abraded and non-abraded fractions plotting along, or close to, the same array. There is no doubt that even the "clear" zircons contained substantial amounts of inherited core material. The zircons have discordant U-Pb ages of 208-438 Ma for the Baldy Pluton and 166-318 Ma for the Midge Creek Stock. The data sets form scattered arrays reflecting inheritance of Precambrian zircon, with no apparent correlation between degree of inheritance and percentage of visible core material (compare Fig. 3 and 4). We consider the effects of radiation-damage Pb loss to be quite minor.

The preponderance of an inherited component and the scattered array precludes determining a precise crystallization age from zircon for either sample. A regression of the most colinear zircon data points from each sample produces a discordia line with lower intercept ages of 144 ± 24 Ma for the Baldy Pluton and 112 ± 20 Ma for the Midge Creek Stock, as initially stated in Leclair (1988). These ages were provisionally considered the approximate time of emplacement of the two intrusions, and though imprecise, they appear to be consistent with the field relationships. The average age of inherited Pb from an older crustal component is in the 1.5-2.2 Ga range.

The additional, more recently obtained, U-Pb data from titanite and allanite remove some of the uncertainty about the magmatic age of these two intrusions. In both cases, almost all mineral fractions consisted of clear and euhedral grains,

with minor inclusions. All of the five titanite fractions and three allanite fractions from both the Baldy Pluton and Midge Creek Stock are concordant within analytical error (Fig. 4 and 5). In both rocks, initial U-Pb dates on titanite had a range in age from about 115-120 Ma, suggesting that intrusion was of mid-Cretaceous age. This conclusion is at odds with the assignment of the Baldy Pluton to the Middle Jurassic (ca. 165-170 Ma) Nelson Suite by Little (1960) and later by Wheeler and McFeely (1991). Two explanations are possible, either the Baldy Pluton is mid-Cretaceous in age or a thermal event reset titanite U-Pb systematics during mid-Cretaceous time.

Baldy Pluton

To determine which of these interpretations was correct, allanite, which has a higher closure temperature than titanite (Heaman and Parrish, 1991), was analyzed to see if it was older. Additionally, two fractions of titanite were strongly abraded to less than half of their initial size to also see if a trend towards older ages could be discerned and therefore assess the "thermal resetting" hypothesis. As indicated on Figures 4a and 4b, the titanite and allanite analyses from the Baldy Pluton fall between 115-125 Ma. All titanites except analysis T5 are in agreement with an age estimated at 117 ± 1 Ma. The allanite analyses are essentially identical and plot somewhat above concordia, which can be explained by excess amounts of ^{206}Pb from initially incorporated ^{230}Th , in a manner analogous to Th-rich minerals such as monazite (Schärer, 1984; Parrish, 1990). The average $^{206}\text{Pb}/^{238}\text{U}$ age and standard error of the three allanite analyses are 120.5 ± 3.5 Ma. If the Th/U ratio of the Baldy Pluton is near the average of normal igneous rocks, approximately 3, the correction for this excess ^{206}Pb decreases the $^{206}\text{Pb}/^{238}\text{U}$ age by about 3.5 Ma for these allanites (see Schärer, 1984 or Parrish, 1990). The corrected $^{206}\text{Pb}/^{238}\text{U}$ age and standard error are therefore 117.0 ± 3.5 Ma, which is in perfect agreement with the titanite age of 117 ± 1 Ma. There is no evidence for significant dispersion of these U-Pb data toward an older, presumably Jurassic age, and we therefore conclude that the Baldy Pluton crystallized at 117 ± 1 Ma, which takes into account the different uncertainties of titanite and allanite U-Pb data.

Midge Creek Stock

Allanite from the Midge Creek Stock has larger U-Pb age uncertainties due to the higher correction for common Pb (Table 1; Fig. 5). Two analyses are in agreement with the mean $^{206}\text{Pb}/^{238}\text{U}$ age and standard error of 114 ± 5 Ma. These allanites have lower Th/U ratios relative to the Baldy Pluton allanites, and the corresponding correction for excess ^{206}Pb is about 2.8 Ma, assuming a whole rock Th/U ratio of 3. Therefore, the corrected $^{206}\text{Pb}/^{238}\text{U}$ mean age is 111 ± 5 Ma, rounded to the nearest 1 Ma. We infer that this age best approximates the crystallization age. This slightly younger age is consistent with the field relationships which indicate that the Midge Creek Stock intruded after the Baldy Pluton.

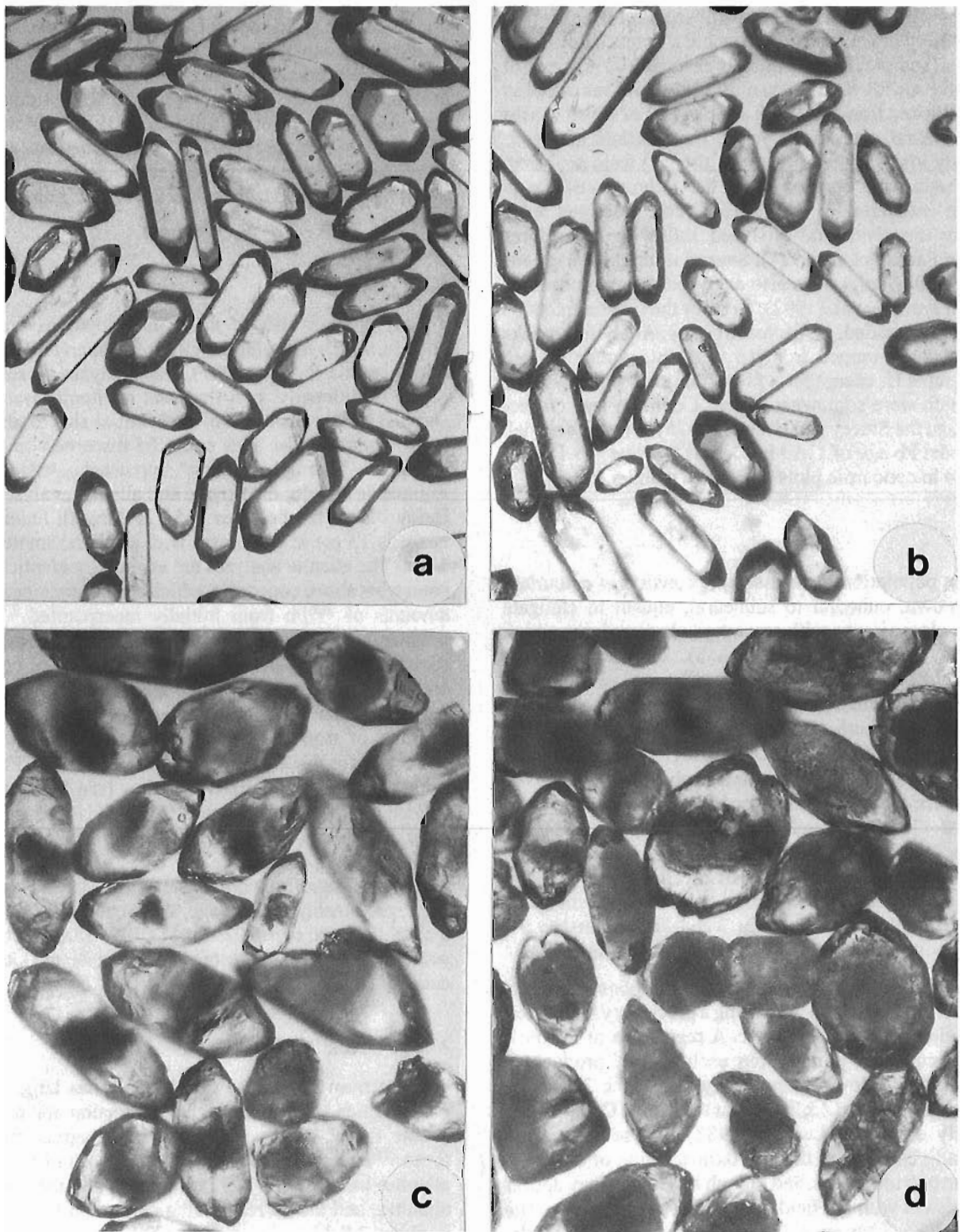


Figure 3. Photomicrographs of zircons from the Baldy Pluton. a) -105+74 μm fraction; clear, euhedral, long-prismatic zircons with no cores (analysis D); b) -105+74 μm fraction; clear, euhedral, long-prismatic zircons with faint to very faint cores (analysis C); c) +105 μm fraction; subhedral zircons with 30-50% snowball cores (analysis B); d) +105 μm fraction; subhedral to anhedral zircons with more than 60% snowball cores (analysis A).

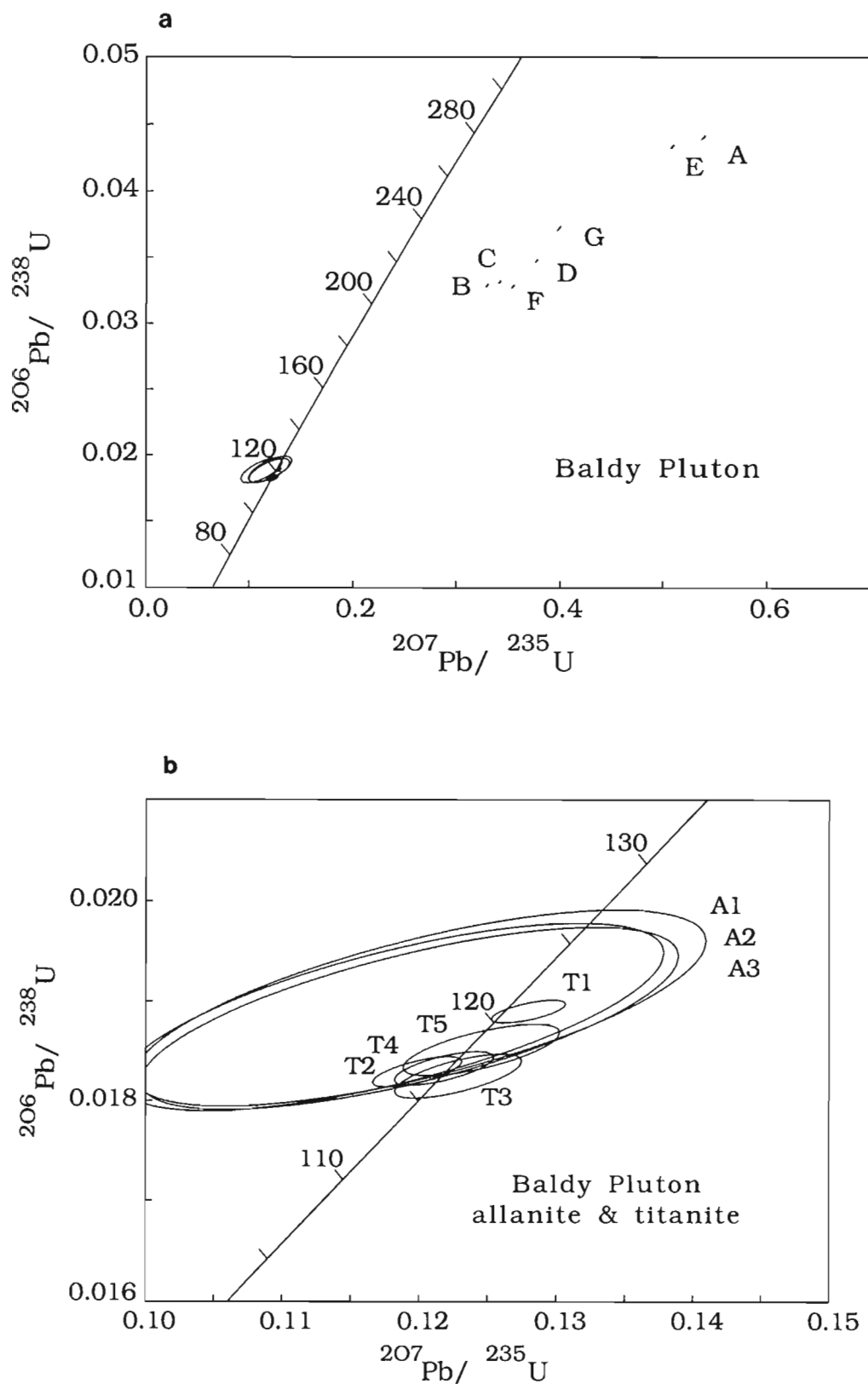


Figure 4. U-Pb concordia diagram for zircons from the biotite leucotonalite sample of the Baldy Pluton. Letter/numerical labels beside data points refer to analysis numbers of zircon fractions in Table 1. Error ellipses reflect analytical uncertainty at the 95% confidence level. (a) concordia diagram for all data; (b) concordia diagram for allanite and titanite data.

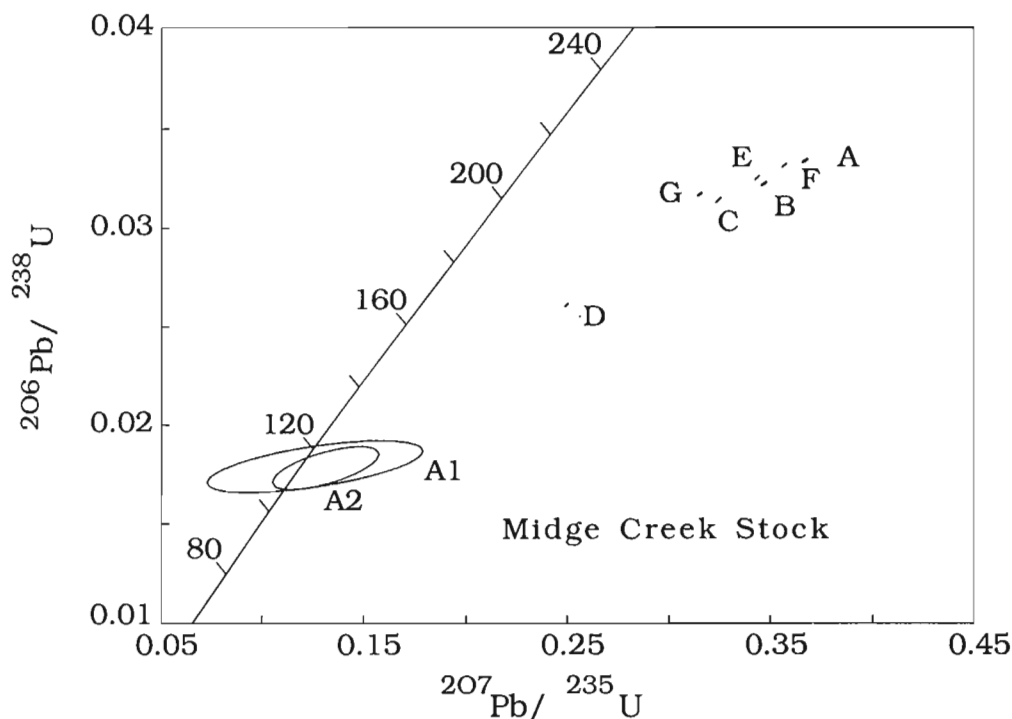


Figure 5. U-Pb concordia diagram for zircons from the leucogranodiorite of the Midge Creek Stock. Letter/numerical labels beside data points refer to analysis numbers of zircon fractions in Table 1. Errors shown indicate the analytical uncertainty at the 95% confidence level.

$^{40}\text{Ar}/^{39}\text{Ar}$ DATING

Analytical procedures

Hornblende was separated from six samples for $^{40}\text{Ar}/^{39}\text{Ar}$ dating to ascertain patterns of regional cooling. Three were collected from amphibolite dykes, two from stratigraphic amphibolite units, and one from the Procter Pluton. A detailed description of the samples and their geological setting is available elsewhere (Leclair, 1988). Biotite from the strongly foliated and linedated "tail" of the Nelson Batholith (i.e. southern part) on the western boundary of the area was also analyzed (see Fig. 2 for sample locations).

Mineral separates were prepared using a Frantz magnetic separator, heavy liquids and, where appropriate, by hand-picking to >99.9% purity. Samples and five flux monitors (standards) were irradiated with fast neutrons in position 5C of the McMaster Nuclear Reactor (Hamilton, Ontario) for 29 hours in two different irradiations. The monitors were distributed throughout the irradiation container, and J-values for individual samples were determined by interpolation for step-heated samples and, because of a low flux gradient, using the mean value for total-fusion analyses ($J = 0.007359$).

Both step-heating experiments and total-fusion analysis of the monitors and samples were done in a quartz tube heated using a Lindberg tube furnace. The bakeable, UHV, stainless-steel argon extraction system is operated on-line to a substantially

modified, A.E.I. MS-10 mass-spectrometer run in the static mode. Measured mass-spectrometric ratios were extrapolated to zero-time, corrected to an $^{40}\text{Ar}/^{36}\text{Ar}$ atmospheric ratio of 295.5, and corrected for neutron induced ^{40}Ar from potassium, and ^{39}Ar and ^{36}Ar from calcium. Dates and errors were calculated using formulae given by Dalrymple et al. (1981), and the constants recommended by Steiger and Jäger (1977). Errors represent the analytical precision only (i.e., error in J value = 0). The flux monitors which were used were LP-6 biotite at 128.5 Ma and DA-83-48-BB biotite at 97.5 Ma. A table of analytical data is available from the authors upon request.

Results

Except for a hornblende date of 220 Ma, which was obtained from a sample with low K_2O content, the total-gas ages are within the range of conventional K-Ar dates (75-160 Ma) reported for metamorphic amphiboles from adjacent areas in the central Kootenay Arc (Archibald et al., 1983). The resulting ages fall in the 83-161 range, corroborating a complex cooling history in the interval between mid-Jurassic and mid-Cretaceous time. This range could be caused by argon loss or gain, or by different cooling histories. Further discussion of the results can be found in Leclair (1988). To aid in the interpretation of total fusion ages, two amphiboles from the aureoles of the Midge Creek Stock and Baldy Pluton,

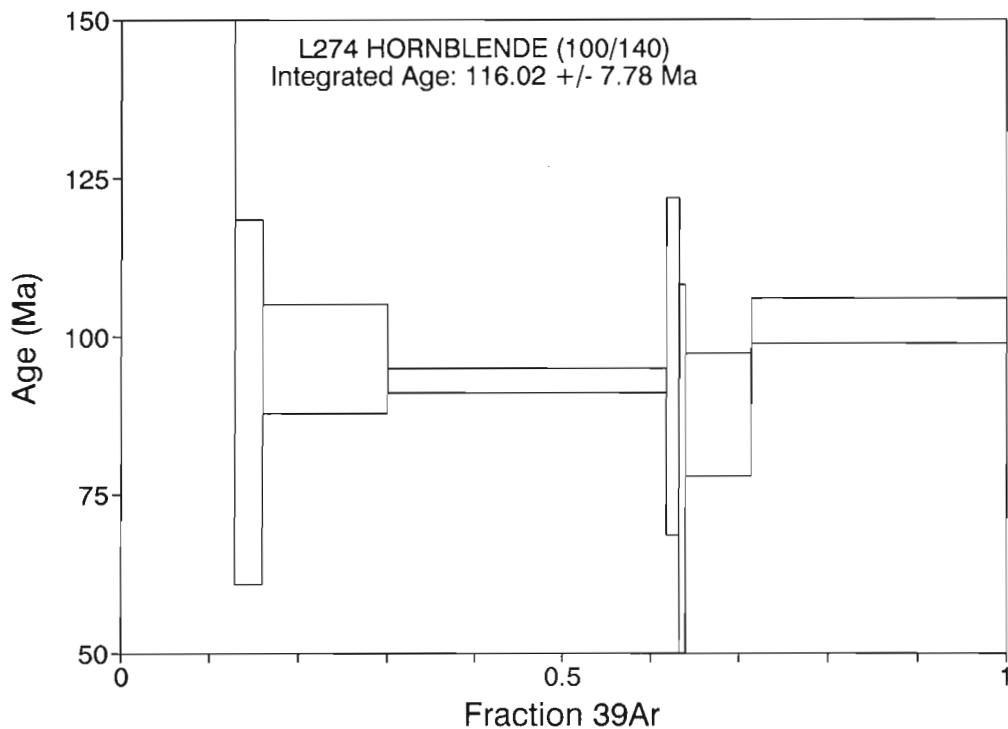


Figure 6. $^{40}\text{Ar}/^{39}\text{Ar}$ step-heating age spectra for L274 hornblende from the aureole of the Midge Creek Stock. See text for discussion.

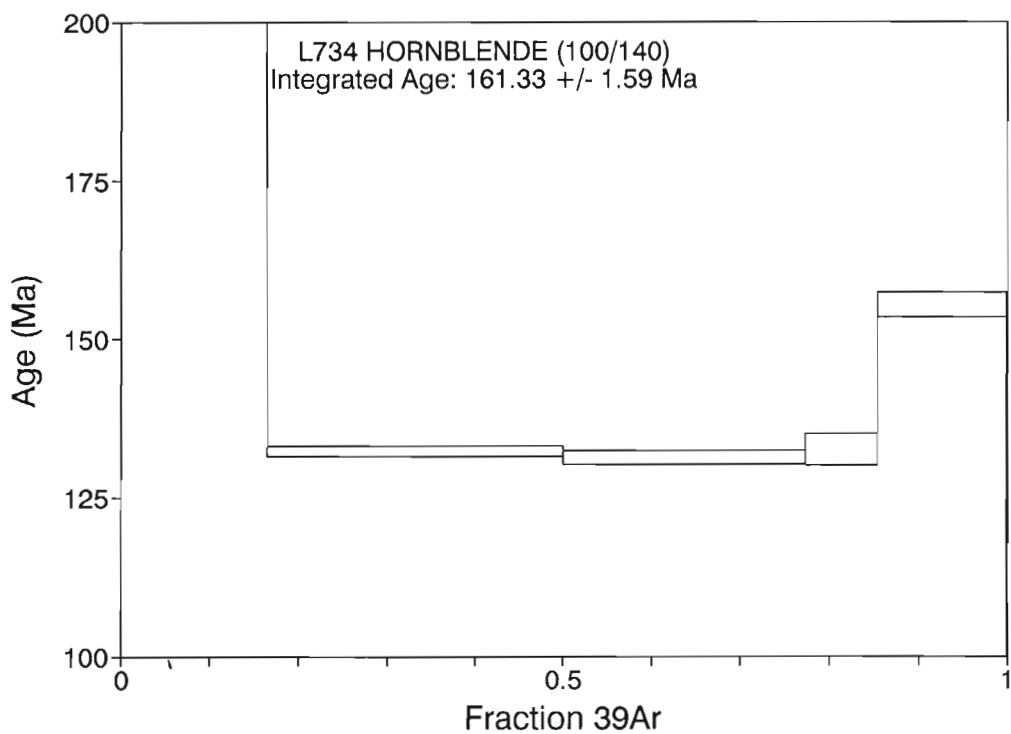


Figure 7. $^{40}\text{Ar}/^{39}\text{Ar}$ step-heating age spectra for L734 hornblende from the aureole of the Baldy Pluton. See text for discussion.

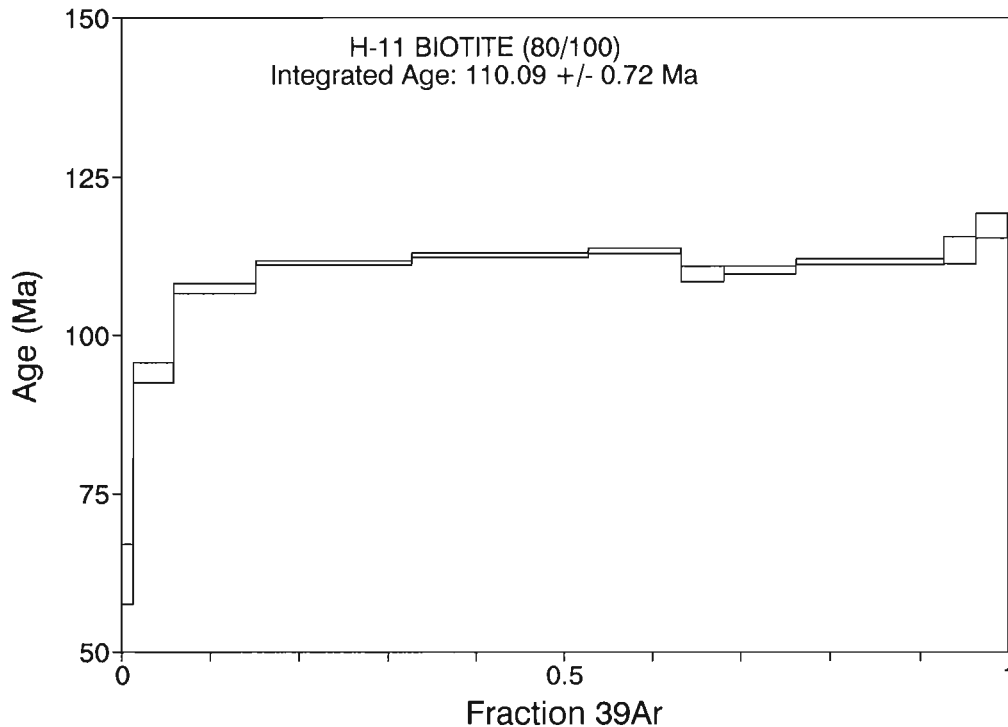


Figure 8. $^{40}\text{Ar}/^{39}\text{Ar}$ step-heating age spectra for H-11 biotite from the deformed "tail" of the Nelson Batholith. See text for discussion.

as well as a biotite from the Nelson Batholith on the western margin of the area were step-heated. These age spectra are shown in Figures 6, 7, and 8.

Hornblende L274 from the aureole of the Midge Creek Stock yielded a complex spectrum with a two-pulsed release of ^{39}Ar (Fig. 6). The most precise low and high temperature steps have dates of 93 ± 2 Ma and 102 ± 4 Ma, respectively. Although the significance of the two dates is unclear, it is probable that cooling of this amphibole through the closure temperature to Ar diffusion took place between 91 and 106 Ma, which closely followed the 111 ± 5 Ma emplacement age of the Midge Creek Stock.

Hornblende L734 from the aureole of the Baldy Pluton has a "U-shaped" spectrum typical of amphiboles that contain excess argon (Fig. 7). Although the integrated date (161 ± 2 Ma) suggests a mid-Jurassic age, the minimum date (131 ± 1 Ma from 3 steps representing 69% of the gas) is a better estimate of the time of cooling of this sample. This date is older than the U-Pb titanite and allanite dates and is considered to be a maximum for cooling through the hornblende closure temperature.

Biotite H-11 (previously dated by Archibald et al., 1983) is from the strongly deformed "tail" of the Nelson Batholith and yielded a disturbed age spectrum with an integrated date of 110 ± 0.7 Ma (Fig. 8). The low temperature step indicates thermal overprinting in late Cretaceous or later time. It is difficult to estimate the true cooling age of this sample but the

highest dates (113 and 117 Ma) imply that this area cooled through the closure temperature of biotite in mid-Cretaceous or earlier time.

DISCUSSION

The U-Pb zircon data for the Baldy Pluton and Midge Creek Stock show the effects of large degrees of inheritance of older zircons and perhaps more recent (<100 Ma) secondary Pb loss. The inherited Pb component originates from xenocrystic zircons of Precambrian age, which may themselves be discordant. These zircons may have been derived from sediments with a cratonic source or from Precambrian basement rocks that might have underlain the area at the time of emplacement. It appears that all zircon crystals in these samples possess inherited cores, whether visible or not; this is obvious from very small zircon fractions (10-20 crystals) which had petrographically clear zircons.

The U-Pb titanite and allanite data provide more exact emplacement ages for these two intrusions. The $117 + 4/-1$ Ma age for the Baldy Pluton is much younger than its previously postulated Jurassic age inferred from the U-Pb zircon data. The allanite age (111 ± 5 Ma) of the Midge Creek Stock falls within the uncertainty of its zircon age (112 ± 20 Ma). It is similar to ages of related plutonic rocks of the Kootenay Arc and neighbouring regions (Archibald et al., 1983, 1984; Höy, 1988), with comparable geological settings and field relations.

The improved ages for the two intrusions remain compatible with field relations; however, it is necessary to reconsider the constraints they place on the timing of metamorphic and deformational events in the central Kootenay Arc. Combined with the geological field relations, the data for Baldy Pluton imply that penetrative deformation (Phase II) culminated in mid-Cretaceous time. The Midge Creek Stock, which is about 7 Ma younger, postdates much of this deformation event. The emplacement of this high-level intrusion into regionally metamorphosed rocks (≥ 0.55 GPa) indicates minimum decompression of 0.20 GPa between the regional- and contact-metamorphic events (Leclair, 1988). This period of decompression may be relatively local and related to east-west shortening in this section of the Kootenay Arc during its east-directed transport on lower thrusts of the foreland. $^{40}\text{Ar}/^{39}\text{Ar}$ results support a mid-Cretaceous age for these two plutons and imply that the area was still at moderate-to-high temperatures in mid-Cretaceous time. Part of the shortening and attenuation of strata may also be of this age. Resetting or final cooling of the "tail" of the Nelson Batholith can now be rationalized.

The mid-Cretaceous age proposed here for the culmination of penetrative ductile deformation (D_2) and regional amphibolite-facies metamorphism within the Kootenay Arc postdates previously suggested constraints of Jurassic age (see Smith and Gehrels, 1992). This may imply diachronous deformation along the Kootenay Arc between different structural levels.

ACKNOWLEDGMENTS

This study was originally undertaken as part of A.D.L.'s Ph.D. thesis at Queen's University, while under the supervision of Hewart Helmstaedt and Dugald Carmichael. Fieldwork was carried out with financial and logistical support from the Geological Survey of Canada under the direction of J.E. Reesor during remapping of part of the Nelson sheet. A.D.L. received financial assistance from Natural Sciences and Engineering Research Council of Canada (NSERC), Ontario Graduate Scholarship and Queen's University. $^{40}\text{Ar}/^{39}\text{Ar}$ dates were obtained in the Geochronology Laboratory at Queen's University which is funded by an NSERC operating grant to Ed Farrar. Vicki McNicoll reviewed the manuscript.

REFERENCES

- Archibald, D.A., Glover, J.K., Price, R.A., Farrar, E., and Carmichael, D.C.
1983: Geochronology and tectonic implications of magmatism and metamorphism, southern Kootenay Arc and neighbouring regions, southeastern British Columbia. Part I: Jurassic to mid-Cretaceous; Canadian Journal of Earth Sciences, v. 20, p. 1891-1913.
- Archibald, D.A., Krogh, T.E., Armstrong, R.L., and Farrar, E.
1984: Geochronology and tectonic implications of magmatism and metamorphism, southern Kootenay Arc and neighbouring regions, southeastern British Columbia. Part II: Mid-Cretaceous to Eocene; Canadian Journal of Earth Sciences, v. 21, p. 567-583.
- Crosby, P.
1968: Tectonic, plutonic and metamorphic history of the central Kootenay Arc, British Columbia, Canada; Geological Society of America, Special Paper 99, 94 p.
- Dalrymple, G.B., Alexander, E.C., Jr., Lanphere, M.A., and Kraker, G.P.
1981: Irradiation of samples for $^{40}\text{Ar}/^{39}\text{Ar}$ dating using the Geological Survey TRIGA Reactor; U.S. Geological Survey, Professional Paper 1176, 55 p.
- Fyles, J.T.
1967: Geology of the Ainsworth-Kaslo Area, British Columbia; British Columbia Department of Mines and Petroleum Resources, Bulletin 53, 125 p.
- Glover, J.K.
1978: Geology of the Summit Creek map-area, southern Kootenay Arc, British Columbia; Ph.D. thesis, Queen's University, Kingston, Ontario, 143 p.
- Heaman, L. and Parrish, R.R.
1991: U-Pb geochronology of accessory minerals; in Applications of radiogenic isotope systems to problems in geology, short course handbook; (ed.) L. Heaman and J.N. Ludden; Mineralogical Association of Canada, v. 19, p. 59-102.
- Höy, T.
1980: Geology of the Riondel Area, central Kootenay Arc, southeastern British Columbia; British Columbia Department of Mines and Petroleum Resources, Bulletin 73, 89 p.
1988: Geochemistry, geochronology, and tectonic implications of two quartz monzonite intrusions, Purcell Mountains, southeastern British Columbia; Canadian Journal of Earth Sciences, v. 25, p. 106-115.
- Klepacki, D.W. and Wheeler, J.O.
1985: Stratigraphic and structural relations of the Milford, Kaslo and Slocan Groups, Goat Range, Lardeau and Nelson map-areas, British Columbia; in Current Research, Part A; Geological Survey of Canada, Paper 85-1A, p. 277-286.
- Krogh, T.E.
1982: Improved accuracy of U-Pb zircon ages by the creation of more concordant systems using air abrasion technique; Geochimica et Cosmochimica Acta, v. 46, p. 637-649.
- Leclair, A.D.
1983: Stratigraphy and structural implications of central Kootenay Arc rocks, southeastern British Columbia; in Current Research, Part A; Geological Survey of Canada, Paper 83-1A, p. 235-240.
1984: Comparison of stratigraphy and structure across the Seaman Creek Fault, a major tectonic boundary in the central Kootenay Arc, southeast British Columbia; Geological Association of Canada, Program with Abstracts, v. 9, p. 83.
1986: Geology of the Midge Creek Area, Nelson (82F/7,10) map-area, southeastern British Columbia; Geological Survey of Canada, Open File 1352.
1988: Polyphase structural and metamorphic histories of the Midge Creek Area, southeast British Columbia: Implications for tectonic processes in the central Kootenay Arc; Ph.D. thesis, Queen's University, Kingston, Ontario, 264 p.
1990: Tectonostratigraphy, structure and collision at the leading edge of allochthonous terranes in the central Kootenay Arc, southeastern British Columbia; Geological Association of Canada, Program with Abstracts, v. 15, p. A74.
- Little, H.W.
1960: Nelson map-area, west half, British Columbia; Geological Survey of Canada, Memoir 308, 205 p.
1985: Geological map and notes, Nelson (west half) map-area, British Columbia; Geological Survey of Canada, Open File 1195.
- McAllister, A.L.
1951: Ymir map-area, British Columbia; Geological Survey of Canada, Paper 51-4, 58 p.
- Parrish, R.R.
1990: U-Pb dating of monazite and its application to geological problems; Canadian Journal of Earth Sciences, v. 27, p. 1431-1450.
- Parrish, R.R., Bellerive, D., and Sullivan, R. W.
1992: U-Pb chemical procedures for titanite and allanite in the Geochronology Laboratory, Geological Survey of Canada; in Radiogenic Age and Isotopic Studies; Report 5; Geological Survey of Canada, Paper 91-2, p. 187-190.

Parrish, R.R., Roddick, J.C., Loveridge, W.D., and Sullivan, R.W.

1987: Uranium-lead analytical techniques at the geochronology laboratory, Geological Survey of Canada; in Radiogenic Age and Isotopic Studies: Report 1; Geological Survey of Canada, Paper 87-2, p. 3-7.

Price, R.A.

1981: The Cordilleran foreland thrust and fold belt in the southern Canadian Rocky Mountains; in Thrust and nappe tectonics, (ed.) N.J. Price and K. MacClay; Geological Society of London, Special Publication v. 9, p. 427-448.

Read, P.B. and Wheeler, J.O.

1976: Geology, Lardeau west-half, British Columbia; Geological Survey of Canada, Open File 432.

Reesor, J.E.

1983: Nelson map-area, east half, British Columbia; Geological Survey of Canada, Open File 929.

Rice, H.M.A.

1941: Nelson map-area, east half, British Columbia; Geological Survey of Canada, Memoir 228, 86 p.

Schärer, U.

1984: The effect of initial ^{230}Th disequilibrium on young U-Pb ages: the Makalu case, Himlaya; Earth and Planetary Science Letters, v. 67, p. 191-204.

Smith, M.T. and Gehrels, G.E.

1992: Structural geology of the Lardeau Group near Trout Lake, British Columbia: implications for the structural evolution of the Kootenay Arc; Canadian Journal of Earth Sciences, v. 29, p. 1305-1319.

Stacey, J.S. and Kramer, J.D.

1975: Approximation of terrestrial lead isotope evolution by a two-stage model; Earth and Planetary Science Letters, v. 26, p. 207-221.

Steiger, R.H. and Jäger, E.

1977: Subcommission on Geochronology: Convention on the use of decay constants in geo- and cosmochemistry; Earth and Planetary Science Letters, v. 36, p. 359-362.

Tipper, H.W., Woodsworth, G.J., and Gabrielse, H.

1981: Tectonic assemblage map of the Canadian Cordillera; Geological Survey of Canada, Map 1505A.

Wheeler, J.O. and McFeely, P.

1991: Tectonic map of the Canadian Cordillera and adjacent parts of the United States of America; Geological Survey of Canada Map 1712A, scale 1:2 000 000.

Geological Survey of Canada Project 830006

Tectonic assemblages of the Eastern Coast Belt, southwestern British Columbia: implications for the history and mechanisms of terrane accretion

J.M. Journeay

Cordilleran Division, Vancouver

Journeay, J.M., 1993: Tectonic assemblages of the Eastern Coast Belt, southwestern British Columbia: implications for the history and mechanisms of terrane accretion; in Current Research, Part A; Geological Survey of Canada, Paper 93-1A, p. 221-233.

Abstract: The Eastern Coast Belt straddles the boundary between the Insular and Intermontane superterranes in southwestern British Columbia. It is made up of fault-bounded terranes and associated basin successions of late Paleozoic to late Mesozoic age, and crosscutting plutons of Late Cretaceous to Early Tertiary age. Stratified rocks include oceanic assemblages of the Bralorne-East Liza and Bridge River complexes (Bridge River Terrane), island arc assemblages of the Cadwallader Group (Cadwallader Terrane), and associated Jura-Cretaceous fine grained clastic successions of the Relay Mountain, Cayoosh, Brew, Ladner and Taylor Creek groups. Preliminary stratigraphic linkages between these clastic successions and older tectonic elements of the Eastern Coast Belt suggest that rocks of the Cadwallader and Bridge River terranes were overlapped by an upward-coarsening clastic succession prior to deposition of the Albian Taylor Creek Group and the onset of deformation in mid- and Late Cretaceous time.

Résumé : La zone de la côte orientale chevauche la limite entre le superterrane insulaire et le superterrane intermontagné dans le sud-ouest de la Colombie-Britannique. Elle se compose de terranes limités par des failles et de successions de bassin associées dont l'âge couvre l'intervalle s'étendant de la fin du Paléozoïque à la fin du Mésozoïque, et de plutons transversaux dont l'âge se situe entre le Crétacé tardif et le Tertiaire précoce. Les roches stratifiées comprennent des assemblages océaniques des complexes de Bralorne-East Liza et de Bridge River (terrane de Bridge River), des assemblages d'arc insulaire du Groupe de Cadwallader (terrane de Cadwallader), et les successions clastiques associées, de granulométrie fine et d'âge jurassique-crétacé, des groupes de Relay Mountain, de Cayoosh, de Brew, de Ladner et de Taylor Creek. Les liens stratigraphiques préliminaires établissent entre ces successions clastiques et des éléments tectoniques plus anciens de la zone côtière orientale semblent indiquer que les roches des terranes de Cadwallader et de Bridge River ont été en partie recouvertes par une séquence clastique négative antérieure à la sédimentation du Groupe de Taylor Creek (Albien) et le commencement de la déformation au cours du Crétacé moyen et tardif.

INTRODUCTION

Stratigraphic linkages between tectonic assemblages of the Eastern Coast Belt provide important insights on the history and mechanisms of terrane accretion along the inboard margin of Wrangellia, and bear directly on currently debated interpretations for the evolution of the Coast Belt orogen as a whole (Fig. 1, 2). There is general agreement that Late

Jurassic and older assemblages of the Eastern Coast Belt (Fig. 2), which include the Bralorne-East Liza and Bridge River complexes (Bridge River Terrane), the Cadwallader and Tyaughton groups (Cadwallader Terrane) and parts of the Relay Mountain Group and Cayoosh Assemblage were stratigraphically linked by mid-Cretaceous time (110-100 Ma). Each is unconformably overlain by fluvial and/or shallow marine clastic rocks of Albian age (Taylor Creek

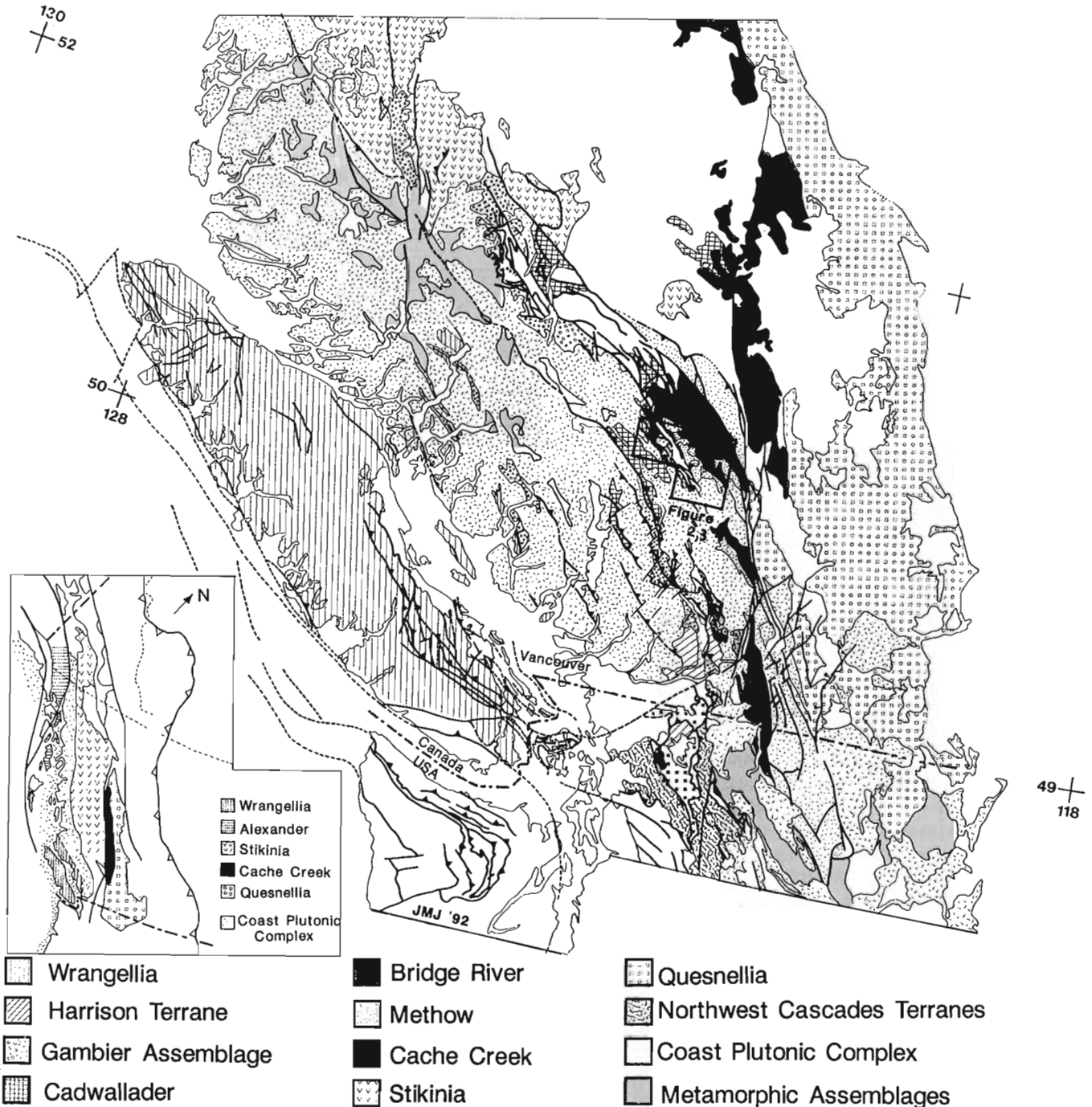


Figure 1. Terranes of the southern Coast Belt.

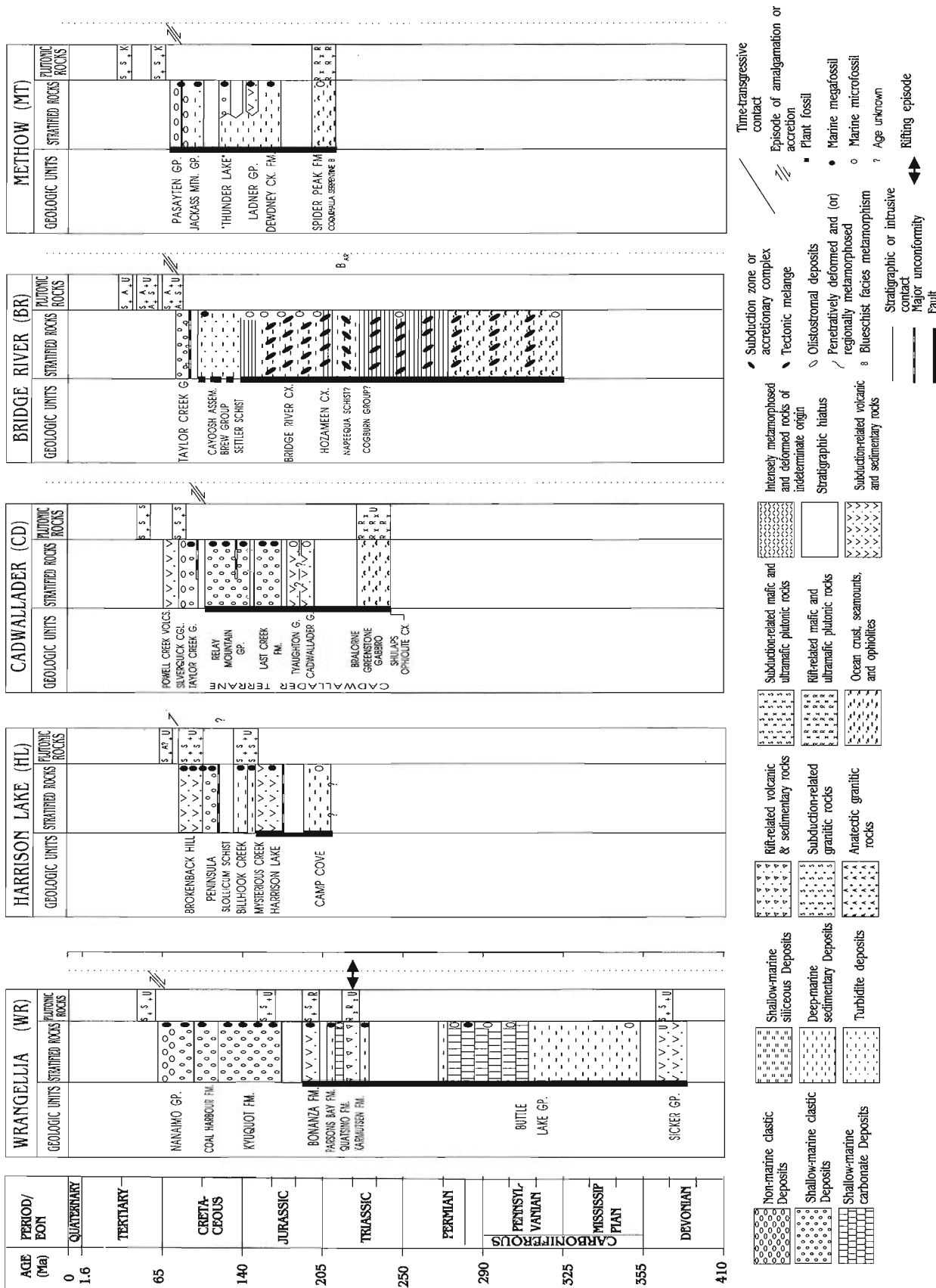


Figure 2. Tectonic assemblages of the southern Coast Belt. Modified from Monger and Journeay (1992) See text for discussion.

Group), derived in part from emergent thrust sheets of the Bridge River Complex during late Early Cretaceous contractional deformation (Garver, 1991). Pre-Albian linkages between these terranes are more tenuous.

Middle Jurassic and younger clastic rocks, which include the Relay Mountain and Taylor Creek groups (Fig. 2), are widely distributed in the Cadwallader and Chilcotin ranges of the Eastern Coast Belt, and record a relatively simple history of deformation. They are structurally interleaved with fault-bounded island arc assemblages of the Cadwallader Terrane and with imbricated oceanic rocks of the Bridge River Terrane, both of which record a history of polyphase deformation. These observations led Rusmore et al. (1988) to conclude that terranes of the Eastern Coast Belt were amalgamated and structurally interleaved along the boundary between the Intermontane and Insular superterranes in Middle Jurassic time, prior to deposition of the Relay Mountain Group, which they interpreted as a tectonic overlap assemblage.

Recent stratigraphic and structural studies in the Chilcotin Range (Schiariizza et al., 1989, 1990; Garver, 1991) have shown that contacts between the Relay Mountain Group and older terranes of the Eastern Coast Belt, previously assumed to be part of a regional unconformity, are instead structural discontinuities marked by arrays of contractional and/or strike-slip faults. In addition, there is no evidence of widespread Middle Jurassic deformation in the southern Chilcotin or Cayoosh ranges of the Eastern Coast Belt (Schiariizza et al., 1990; Journeay et al., 1992). Lower Jurassic shales of the Last Creek Formation and overlying Middle Jurassic and younger clastic rocks of the Relay Mountain Group share the same history of deformation.

Variations in structural style that exist between the Relay Mountain Group and older terranes, and which have been cited as evidence of Middle Jurassic deformation (Rusmore et al., 1988), are also documented in pre-Middle Jurassic rocks of the Bridge River Complex and in overlying Jura-Cretaceous rocks of the Cayoosh Assemblage (Journeay et al., 1992), both of which record a history of imbricate faulting and inhomogeneous deformation. Documented stratigraphic ties between oceanic rocks of the Bridge River Complex and unconformably overlying fine grained clastic successions of the Cayoosh Assemblage indicate that parts of the "Bridge River ocean" remained open to marine sedimentation until Early Cretaceous time (Journeay and Northcote, 1992). These observations argue against a Middle Jurassic history of terrane accretion (as suggested by Rusmore et al., 1988), but do not rule out the possibility that Cadwallader, Bridge River and Methow terranes may have been stratigraphically linked along the inboard margin of Wrangellia prior to final amalgamation and imbricate thrusting in late Early Cretaceous time.

To test this hypothesis, I have focused on the stratigraphy and structural setting of Jura-Cretaceous basin successions that overly oceanic rocks of the Bridge River Complex and island arc assemblages of the Cadwallader Group. Fieldwork during the 1992 season included 1:50 000 and 1:25 000 scale

mapping of tectonic assemblages and bounding faults in the Cadwallader, Bendor and Cayoosh ranges (92J/10 and 92J/9, see also Mahoney and Journeay, 1993).

STRUCTURAL FRAMEWORK

The Bralorne Fault Zone (Fig. 3) is one of several major thrust faults in the Eastern Coast Belt (Rusmore, 1985; Journeay et al., 1992). The basal detachment of this fault roots north-eastward beneath disrupted oceanic rocks of the Bridge River Terrane (Fig. 4), and is out-of-sequence with respect to the main detachment of the Coast Belt Thrust System (Journeay et al., 1992).

In its footwall are Triassic and Early Jurassic island arc assemblages of the Cadwallader Terrane (Cadwallader and Tyaughton groups), and several arc-related successions of uncertain age and correlation. I have named these sections according to geographic location and describe them separately in the text. They include interlayered volcanic and volcanoclastic rocks of the Birkenhead and Grizzly Pass sections, and fine grained turbidites and overlying coarse clastic rocks of the Noel Mountain Section (Fig. 3).

The imbricate zone of the Bralorne Fault is a tectonic mélange comprising footwall slivers of the Cadwallader Group, and hanging wall slivers derived both from the Bridge River Terrane (Bralorne-East Liza and Bridge River complexes), and from overlying basin successions of the Cayoosh Assemblage. Fault-bounded clastic rocks of uncertain correlation occur both in the mélange belt and in the upper plate of the Bralorne Fault Zone. Stratigraphically coherent sections were measured along McGillivray Creek, Standard Ridge, Mt. McGillivray and Connel Creek (Fig. 3, 4), and are described in detail below.

TECTONO-STRATIGRAPHIC ASSEMBLAGES

Bralorne-East Liza complex

Fault slivers of ultramafic rock and associated greenstone-gabbro, interpreted to be part of a dismembered ophiolite, are restricted to the mélange belt and upper plate of the Bralorne Fault Zone (Fig. 5). Mafic and ultramafic rocks are well-exposed in the northern Cadwallader Range, along the headwaters of President, Crazy, Plutus and Chism creeks. They include thick sections of altered dunite, harzburgite and peridotite (President ultramafic suite; Cairnes, 1937), in which primary compositional layering and igneous cumulate textures are locally well-preserved. Along fault zones, these ultramafic rocks are penetratively deformed and hydrothermally altered to serpentinite and talc-carbonate schist.

Greenstones of the Bralorne-East Liza Complex include pillowed flows and flow breccias, lapilli tuffs and fine grained amygdaloidal basalts and basaltic andesites. Geochemical signatures of these rocks suggest that they may have formed

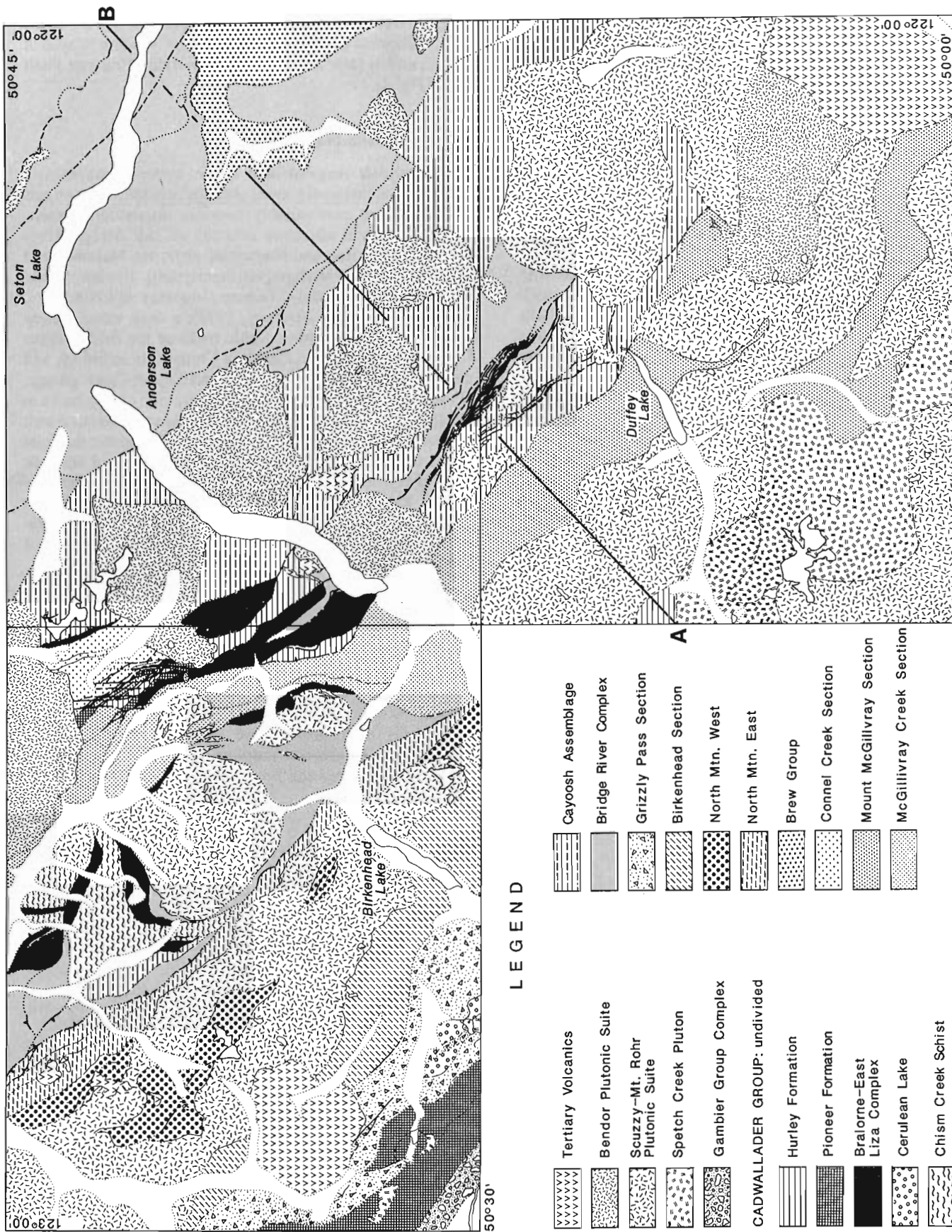


Figure 3. Regional geology of the Eastern Coast Belt (92J/8, 9 10). Based on results of this study and previous mapping by Journeay and Northcote (1992), Journeay et al. (1992), Roddick and Hutchison (1973), Woodsworth (1977), and Rusmore (1985).

either as island arc tholeiites (IAT) or as mid-ocean ridge basalts (MORB; Rusmore, 1985; Leitch, 1989). In the Bralorne mining district, these metavolcanic greenstones and associated rocks of the President ultramafic suite are intruded by Early Permian (~270 Ma) hornblende-quartz diorite and plagiogranite (soda granite) of the Bralorne suite (U-Pb zircon; Leitch, 1989).

Bridge River Complex

The Bridge River Complex is an assemblage of greenstone and bedded chert with subordinate siltstone, greywacke, metavolcanic tuff, limestone and sheared serpentinite (Roddick and Hutchison, 1973; Schiarizza et al., 1990; Journeay and Northcote, 1992). Two distinct mélangé belts are recognized in the Bridge River Complex. The eastern Bridge River mélangé ranges in age from Mississippian to late Middle Jurassic (Callovian; F. Cordey, pers. comm., 1992) and is made up primarily of sheared greenstone, serpentinite, chert and fine grained volcanoclastic rock. It is bounded to the east by the Fraser River Fault, and to the west by the Downton Creek Fault (Fig. 4; Journeay et al., 1992). The western Bridge River mélangé is similar in both composition and structural complexity to its eastern counterpart, but is undated. It is structurally interleaved with Permian and older mafic and ultramafic rocks of the Bralorne-East Liza Complex, and includes thick sections of sheared greenstone and chert, previously mapped as part of the Chism Creek Schist (Rusmore, 1985; Woodsworth, 1977; Journeay and Northcote, 1992).

Situated between these two mélangé belts, in the upper plate of the Bralorne Fault, is a relatively coherent, but undated section of the Bridge River Complex, comprising massive and pillowed greenstone, calcareous greenschist and bedded chert interlayered with subordinate siltstone, limestone and fine grained volcanoclastic sandstone (Journeay and Northcote, 1992). Rocks that define this section are

penetratively deformed and are well-exposed along the limbs of a southwest-verging syncline in the western Cayoosh Range, and in fault slivers of the underlying Bralorne Fault Zone (Fig. 4).

Cayoosh Assemblage

The Cayoosh Assemblage is an upward-coarsening succession of metamorphosed phyllitic argillite, siltstone and sandstone that conformably overlies interbedded greenstone, chert and siliceous siltstone of the Bridge River Complex (Journeay and Northcote, 1992; see Mahoney and Journeay, 1993 for stratigraphic description). It is interpreted to be part of the Methow Terrane (Journeay and Northcote, 1992; Mahoney and Journeay, 1993); a deep water marine succession that overlaps oceanic rocks of the Bridge River Complex, and that includes Jura-Cretaceous turbidites and clastic successions of the Ladner and Taylor Creek groups. Upward-coarsening volcanic and quartz-rich clastic rocks in the upper part of the Cayoosh Assemblage are correlated with the Brew Group and are interpreted to record either the final stages of terrane amalgamation or the emergence of volcanic arc and crystalline basement terranes in the Upper Jurassic and/or Early Cretaceous. There are no demonstrable stratigraphic ties between the Cayoosh Assemblage and Jura-Cretaceous clastic successions of the Tyaughton Group, Last Creek Formation or Relay Mountain Group.

Cadwallader Group

The Cadwallader Group is a Late Triassic island arc assemblage consisting of intermediate and mafic metavolcanic flows (Pioneer Formation) and associated fine grained volcanoclastic rocks (Hurley Formation; Rusmore, 1985). Greenstones of the Pioneer Formation are characterized by green to purplish-weathering, massive and feldsparphyric flows and flow breccias. Locally, these flows

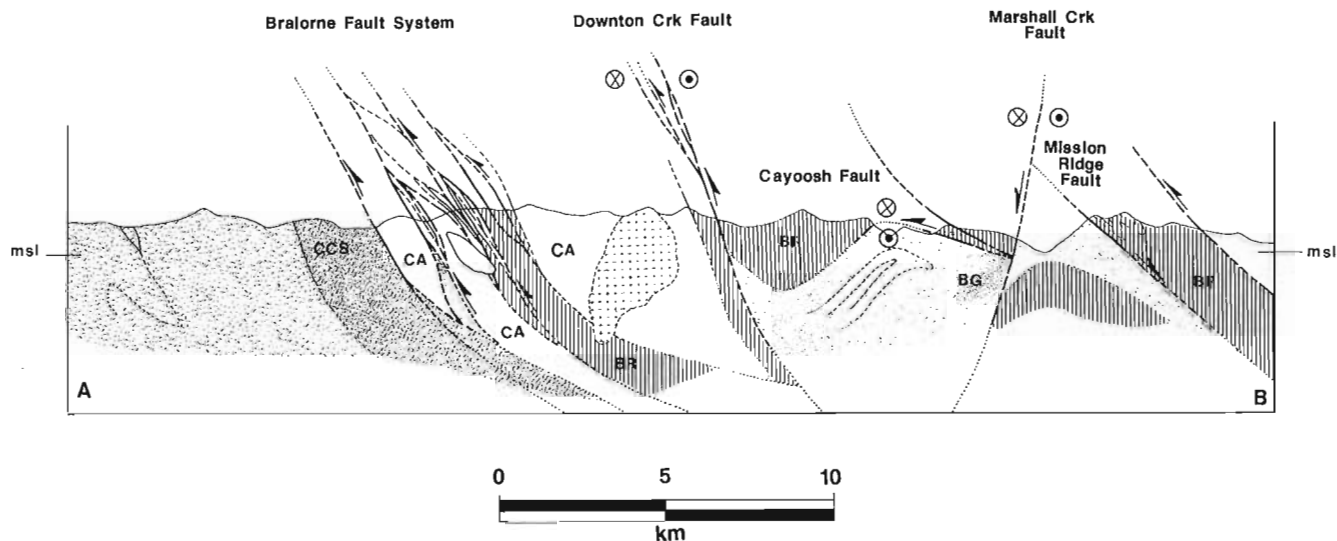
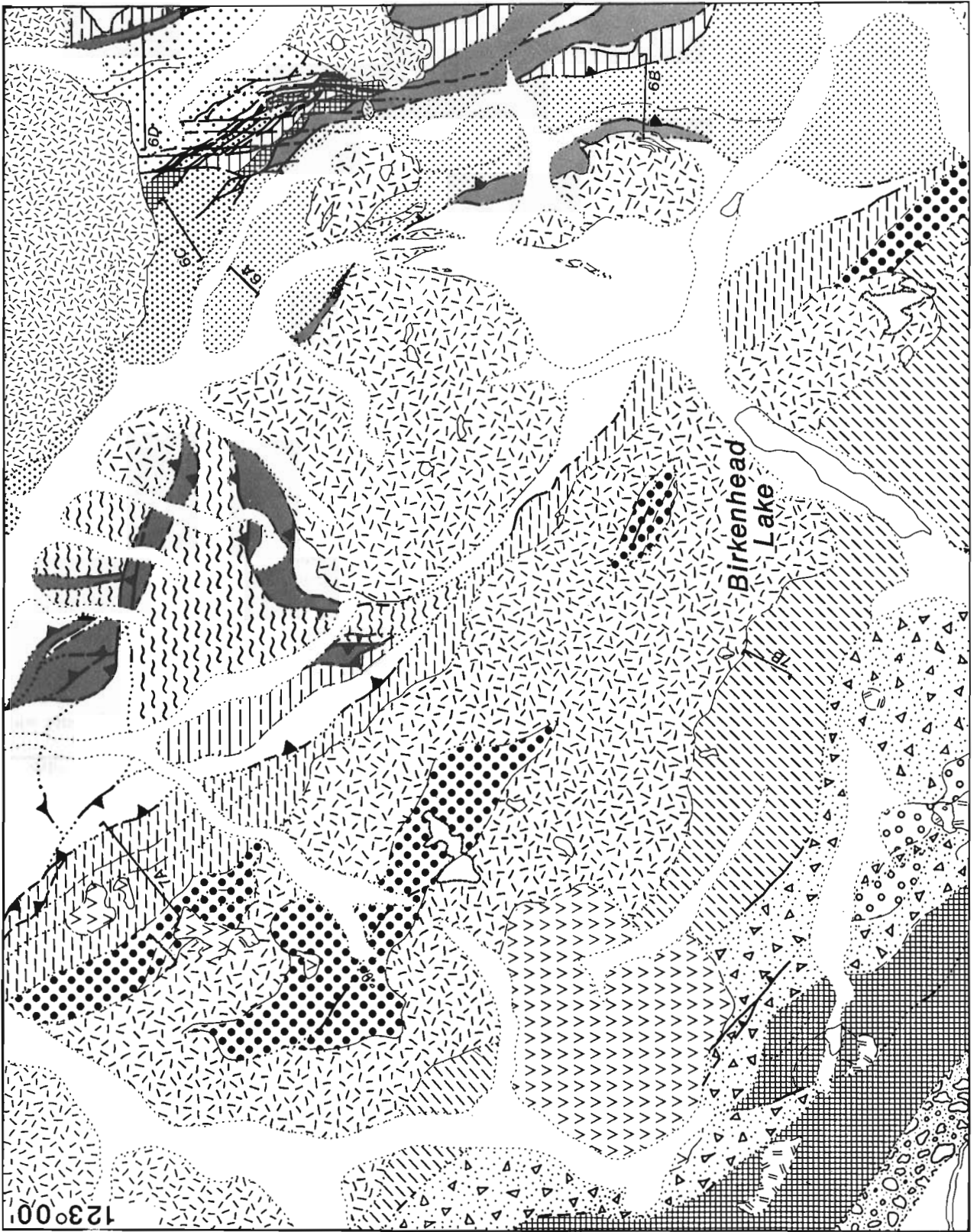


Figure 4. Geological cross-section of the Eastern Coast Belt. See Figure 3 for location of section line.



50° 30'

are intercalated with fragmental lithic and crystal-lithic tuffs. Major and trace element geochemical signatures are transitional between modern island arc tholeiites and mid-ocean ridge basalts. Conformably overlying these volcanic rocks is an upward fining sequence of thin-bedded volcanoclastic wacke, greywacke/siltstone turbidite, and calcareous siltstone (Hurley Formation), locally containing greenstone and fragmental metavolcanic flows near its base, and distinctive limestone-volcanic-plutonic clast conglomerates throughout. Fossils collected from limestones near the contact between the Pioneer and Hurley formations range in age from late Carnian to middle Norian (Rusmore, 1985).

Rocks of the Cadwallader Group occur in fault-bounded slivers throughout the Eastern Coast Belt, both in the upper and lower plates of the Bralorne Fault Zone (Fig. 5). They are structurally interleaved with older oceanic rocks of the Bralorne-East Liza Complex, and with Lower Jurassic clastic successions of the Tyaughton Group, Lower and Middle Jurassic shales and siltstones of the Last Creek Formation (Rusmore, 1985; P. Schiarizza, pers. comm., 1991) and Jura-Cretaceous siltstones and sandstones of the Relay Mountain Group. There are, however no documented stratigraphic contacts between the Cadwallader Group and these other assemblages.

Chism Creek Schist

The Chism Creek Schist is a metamorphosed tectonic *mélange* comprising imbricated slivers of chert, greenstone, amphibolite, mafic and ultramafic rock, phyllite, micaceous schist, and quartz-rich feldspathic sandstone derived in part from Cadwallader, Bridge River and Methow terranes (Rusmore, 1985). It is on strike with and interpreted to be part of a system of high-grade thrust nappes that includes the Cogburn Group *mélange* and Settler Schist (Journeay, 1990; Journeay and Northcote, 1992).

To resolve stratigraphic and structural relationships in the Chism Creek Schist, I have subdivided it into its components (compare Fig. 4 and 5). What remains is a *mélange* of structurally interleaved mafic and ultramafic rocks (Bralorne-East Liza Complex), metachert (Bridge River Complex) and metasedimentary rocks, the boundaries of which could not be resolved at a scale of 1:50 000 (Fig. 5). Metamorphic isograds, defined by the first appearance of biotite, garnet and staurolite (Rusmore, 1985), cut across the boundaries between these tectonic assemblages, and are late-kinematic with respect to structures of the Bralorne Fault Zone.

STRATIGRAPHIC ASSEMBLAGES OF UNCERTAIN CORRELATION

Thick sections of metavolcanic and metasedimentary rocks occur in both upper and lower plates of the Bralorne Fault Zone (Fig. 4, 5). Stratigraphic linkages between these rocks and pre-Middle Jurassic terranes of the Eastern Coast Belt are uncertain at this stage of investigation.

Hanging wall assemblages

McGillivray Creek section

The McGillivray Creek section, previously mapped as part of the Chism Creek Schist, is a coherent succession of thin-bedded phyllitic siltstones, metavolcanic schists and volcanoclastic sandstones. Detailed structural sections were measured along the ridge crest northeast of Blackwater Creek (Fig. 6B) and along Standard Ridge (Fig. 6A). Compositional layering throughout this section is isoclinally folded and transposed parallel to a penetrative schistosity.

Interlayered black graphitic shales and dark grey phyllitic siltstones at the base of the succession (~300 m) are characterized by thin (millimetre-scale) laminae of sandy siltstone, light grey tuffaceous and calcareous siltstone. These rocks grade upwards into a thick succession (200-300 m) of light grey and green metavolcanic (tuffaceous?) schist and calcareous phyllitic siltstone. These metavolcanic rocks are interdigitated with and apparently grade northward, along Prospector Peaks and Standard Ridge, into calcareous volcanoclastic sandstones and thin-bedded greywacke/siltstone turbidites (Fig. 6A). Interlayered with this clastic succession, at the north end of Standard Ridge, are matrix- and clast-supported conglomerates. Clasts include rounded pebbles and boulders of unfoliated granite, granodiorite, chert and angular fragments of dark siltstone and light grey felsic metavolcanics (locally feldsparphyric). Calcareous pebbly mudstone horizons near the top of this section contain both chert fragments and boulders of dark grey limestone.

Mt. McGillivray section

The Mt. McGillivray section is more than a kilometre wide and consists primarily of interlayered volcanoclastic wacke, dark grey and black graphitic siltstone, tuffaceous siltstone, and thin-laminated siliceous siltstone (Fig. 6C). These rocks resemble the upper volcanoclastic facies of the McGillivray Creek section, but are distinguished from the latter by the occurrence of quartz-rich feldspathic arenites and interlayered couplets of massive dark greenstone and thin-banded phyllitic "quartzite". Quartzite bands are 1-5 cm thick and are rhythmically interlayered with thin (millimetre-scale) laminae of phyllitic siltstone. They are isoclinally folded, thoroughly recrystallized and may represent either phyllitic quartz-rich arenite, siliceous metavolcanic tuff and/or meta-chert.

Connel Creek section

The Connel Creek section is a fault-bounded and structurally thickened assemblage of interlayered siltstone and volcanoclastic sandstone. It is contiguous with and believed to be part of the Cayoosh Assemblage (Fig. 3). However, structural complexities preclude direct correlation of these two sections. Reversals in dip direction and the repetition of distinct stratigraphic horizons define what appear to be regional antiformal and synformal culminations (Fig. 6D, E).

The antiformal culmination at the head of Connel Creek is cored by a thick (~400 m) succession of interlayered dark grey siltstone/greywacke turbidites and thinly laminated sandy and tuffaceous siltstones, locally containing lenses of massive and fragmental metavolcanic flows. These rocks resemble those in the lower argillite/siltstone facies of the Cayoosh Assemblage at the head of Melvin Creek (see Mahoney and Journeay, 1993). They are structurally overlain, both to the northeast and to the southwest, by an assemblage of interlayered amphibolite (metavolcanic

flows), thin-banded quartzite (felsic meta-tuffs and/or quartz-rich metasandstone) and phyllitic siltstone, locally containing thin, but distinctive lenses of granite-chert-volcanic pebble conglomerate. These rocks resemble the greenstone/quartzite lithofacies of the Mt. McGillivray section, and interlayered greenstones and quartz-rich metavolcanic sandstones of the Cayoosh Assemblage.

The section is interrupted along the flanks of Whitecap Mountain by steep, northeast-dipping imbricate faults marked by altered mafic and ultramafic rock of uncertain

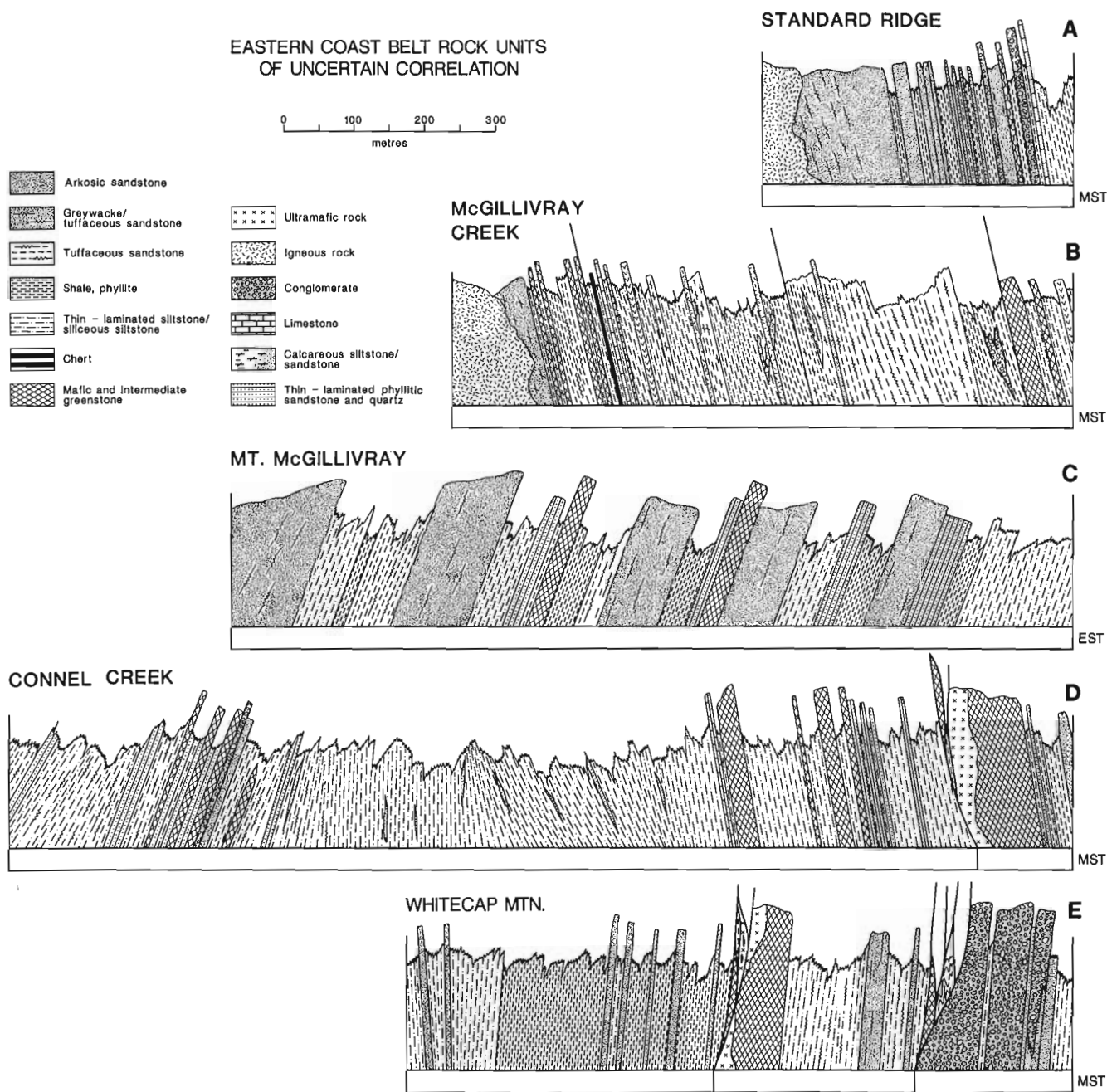


Figure 6A-E. Clastic successions of uncertain correlation in the imbricate zone and upper plate of the Bralorne Fault Zone. See Figure 3 for location of section lines.

correlation. Overlying these mafic rocks with apparent conformity is a section of dark grey and black siltstones and laminated meta-tuffaceous siltstones containing transposed lenses of greywacke/siltstone turbidite and metavolcanic greenstone (Fig. 6D, E). This section resembles the transition zone between the upper Bridge River Complex and the Cayoosh Assemblage. It is cut by a steep, southwest-dipping imbricate fault zone, in the footwall of which is a thick succession of interlayered arkosic wacke and shaly siltstone containing thick lenses of both pebble and boulder conglomerate. Conglomerates are matrix-supported and contain rounded clasts of foliated and unfoliated granodiorite, dark grey limestone and siltstone. The age of these conglomerates is uncertain.

Footwall assemblages

Noel Mountain section

The Noel Mountain section is a coherent northeast-dipping panel of sedimentary rocks comprising an eastern assemblage of siltstones and fine grained volcanoclastic sandstones, and a western assemblage of interlayered coarse clastic sandstones, siltstones and conglomerates (Fig. 7A). The section is locally cut by bedding-parallel faults and is interpreted to be structurally overturned.

The eastern assemblage is undated, but believed to be part of the Cadwallader Group (Hurley Formation; Rusmore, 1985). It comprises a thick (350-400 m) succession of thin-bedded dark grey slaty siltstones containing feldspathic and calcareous wacke horizons and thin, but distinctive lenses of dark grey limestone, limestone pebble conglomerate and calcareous siltstone. Sandstone horizons thicken to the west and are interlayered with both calcarenite and dark grey limestone. These rocks grade westward, across what appears to be a minor west-dipping fault panel, into a succession of dark grey and black shales, phyllites and siltstones containing thin horizons of light grey tuffaceous siltstone, calcareous and feldspathic wacke and discontinuous lenses of granite-limestone-siltstone conglomerate. These rocks grade westward into interlayered siltstones and pebbly sandstones of the western assemblage.

The western assemblage comprises a thick succession of interlayered siltstone, sandstone and conglomerate. The section is undated, but interpreted to be part of the Cretaceous (Albian) Taylor Creek Group (Woodsworth, 1977; Rusmore, 1985). Sandstone and conglomerate horizons are well-distributed throughout the section. Sandstones include both thin- and thick-bedded greywacke and quartz-rich feldspathic arenite. Distinctive thin laminated sandstone/siltstone turbidites are locally abundant and very similar in appearance to those of the upper Cayoosh Assemblage (see Mahoney and Journeay, 1993). Coarse clastic rocks include thin pebbly mudstone horizons and thick cobble and boulder conglomerates. These conglomerates are typically heterolithic and dominated by clasts of chert, granite and recrystallized quartz-rich sandstone. In general, chert clasts become less abundant and volcanic clasts more abundant from east to

west. At the west end of the section, these conglomerates are interleaved with quartz- and feldspar-phyric metavolcanic flows, volcanoclastic sandstones and siltstones. Adjacent to and within pendants of the Mt. Rohr Pluton, these rocks are metamorphosed to upper greenschist and lower amphibolite facies and contain porphyroblastic phases of garnet, staurolite, andalusite, biotite and hornblende.

Birkenhead section

The Birkenhead section is a northeast-dipping panel of interlayered massive and fragmental metavolcanic flows and associated fine grained volcanoclastic rocks. The base of the section in the northern Lillooet Range (Fig. 7C) is characterized by massive and fragmental metavolcanic flows that grade upwards into fine grained volcanoclastic sandstones and siltstones. The lower metavolcanic sequence consists primarily of dark green and maroon feldsparphyric flows, flow breccias and both light and dark grey fragmental lithic tuffs. These rocks are similar in appearance to metavolcanic greenstones of the Late Triassic Pioneer Formation. At the top of this metavolcanic sequence is a 200 m thick succession of interlayered felsic metavolcanic flows, recrystallized limestone and calcareous sandstone. These rocks grade upwards into fine-grained dark grey volcanoclastic sandstones, sandy limestones and siltstones, similar in appearance to those of the Hurley Formation. This section is structurally overlain by fossiliferous Lower Jurassic sandstones and siltstones of the Tyaughton Group (Fig. 7D; Woodsworth, 1977), and is repeated east of Eight Mile Creek (Fig. 7E) along what is interpreted to be a high-angle reverse fault.

In the Cadwallader Range, intermediate and felsic metavolcanic flows and associated fragmental metavolcanic rocks occur at the east end of the section and appear to be structurally overturned (compare Fig. 7B and 7C). They are interlayered with and grade westward into a succession of thin- and thick-bedded volcanoclastic sandstone, arkosic wacke and siltstone.

Grizzly Pass section

The Grizzly Pass section overlies Middle Triassic greenstone and fossiliferous metasedimentary rocks of the Cadwallader Group in the Tenquille Lake region of the western Cadwallader Range. It consists primarily of fragmental intermediate and felsic metavolcanic rocks, feldspar and quartz-phyric metavolcanic flows and associated fine grained volcanoclastic rocks. Although undated, these rocks are interpreted to be part of the transitional facies of the Hurley Formation (Riddell, 1991). Other possible correlations are with Upper Jurassic volcanics of the Billhook Creek Formation and Lower Cretaceous volcanics of the Brokenback Hill Formation. Both of these sections are characterized by thick accumulations of intermediate and felsic fragmental volcanic rocks and are known to occur in fault slivers of the Coast Belt Thrust System along strike to the southeast (Journeay and Friedman, in press).

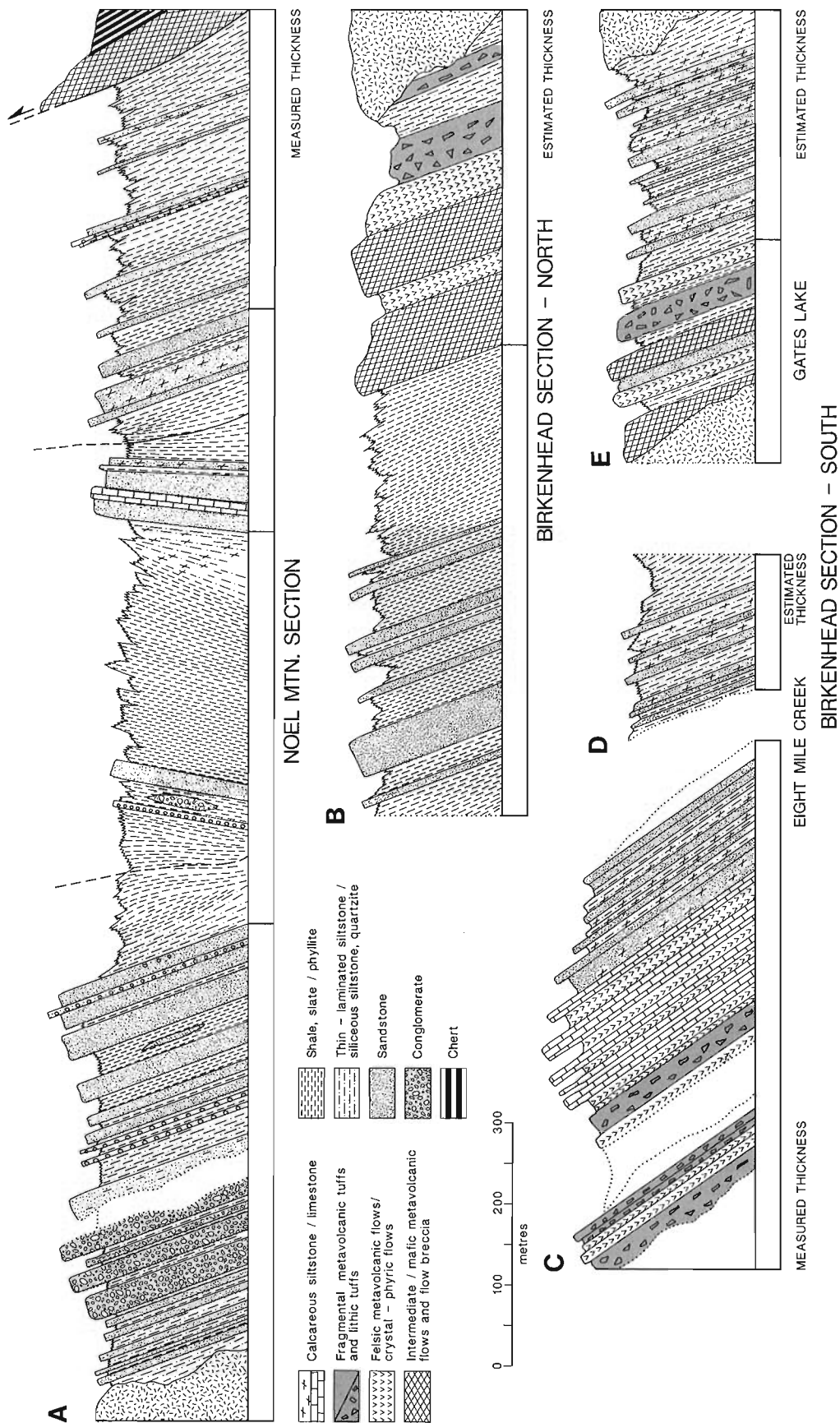


Figure 7A-E. Clastic successions of uncertain correlation in the lower plate of the Bralorne Fault Zone. See Figure 3 for legend and Figure 3 for location of section lines.

DISCUSSION AND CONCLUSIONS

The Bralorne Fault Zone represents a fundamental tectonic boundary in the Eastern Coast Belt. The magnitude of displacement across the Bralorne Fault is unknown. The absence of matching hanging wall/footwall cut-offs in structural sections indicate minimum displacements of several tens of kilometres (Fig. 4). Crustal sections, based on the integration of near-surface geological data and Lithoprobe seismic reflection data indicate that cumulative displacement across the Bralorne Fault Zone may be an order of magnitude greater (Varsek et al., in press). However, similarities in the Jura-Cretaceous clastic successions that overlie the Bridge River and Cadwallader terranes suggest that they were stratigraphically linked prior to the onset of large-scale crustal imbrication in early- to mid-Cretaceous time.

Clastic successions that occur in the imbricate zone and upper plate of the Bralorne Fault are tentatively correlated with the Cayoosh Assemblage. The Connel Creek and Mt. McGillivray sections both contain thick accumulations of volcanoclastic sandstone and a distinctive greenstone/quartzite lithofacies. Stratigraphic similarities suggest that these two sections are part of the lower argillite/siltstone and volcanic sandstone succession of the Cayoosh Assemblage (Mahoney and Journeay, 1993). The McGillivray Creek section has a higher proportion of felsic metavolcanic rocks, but is otherwise very similar to the Connel Creek and Mt. McGillivray sections. It grades upward into coarse chert-bearing boulder conglomerates and is contiguous with metamorphosed quartz-rich clastic rocks of the Cayoosh Assemblage (previously mapped as Chism Creek Schist). These correlations imply that clastic successions that overlie oceanic rocks of the Bridge River Complex were widespread in the Eastern Coast Belt prior to the onset of thrust imbrication in mid- to Late Cretaceous time.

Lower plate clastic successions are tentatively interpreted to be part of the Cadwallader Terrane. Metavolcanic flows and flow breccias in the Tenquille Lake region are interlayered with fragmental metavolcanic flows, limestones and volcanoclastic rocks of Late Triassic age, and are correlated with the Pioneer Formation (Riddell, 1991). Undated metavolcanic flows, flow breccias and lithic tuffs of the Birkenhead section grade upwards into interlayered limestones and calcareous volcanoclastic sandstones, and are interpreted to be part of the transitional facies between Pioneer and Hurley formations (Woodsworth, 1977). They are structurally overlain by coarse clastic rocks of the Tyaughton Group. Calcareous siltstones and volcanoclastic rocks of the eastern Noel Mountain section are similar in appearance and are tentatively correlated with rocks of the Hurley Formation in the Eldorado Creek region (Rusmore, 1985). These rocks are gradational westward into a thick succession of shales and siltstones that most likely correlate with Lower Jurassic rocks of the Last Creek Formation. Interlayered siltstones and chert-pebble conglomerates at the west end of this section may represent the transition into Middle Jurassic and younger clastic rocks of the Relay Mountain and/or Taylor Creek Group.

Interlayered boulder conglomerates, sandstones and siltstones occur in clastic successions associated with both the Cadwallader and Bridge River terranes. Conglomerates are characterized by the presence of granite and granodiorite boulders, chert and greenstone clasts and a variety of intermediate and felsic volcanic clasts. In the eastern Cayoosh and Lillooet ranges, these conglomerates overly fossiliferous early Cretaceous calcarenites of the Brew Group (interpreted to be part of the Cayoosh Assemblage; Journeay and Northcote, 1992), and contain granite boulders of Late Jurassic age (V. Coleman, pers. comm., 1992). Conglomerates that overlie Triassic rocks of the Cadwallader Group and Upper Jurassic volcanic rocks of the Gambier Assemblage (Billhook Creek Formation) also contain granite boulders of Late Jurassic age (Friedman and Armstrong, 1990; Riddell, 1991), and are interpreted to be part of an overlap assemblage that bridged Wrangellia and assembled terranes of the Eastern Coast Belt (Cadwallader, Bridge River and Methow terranes) prior to Late Cretaceous thrusting and crustal imbrication.

The possibility of older stratigraphic ties between Wrangellia and terranes of the Eastern Coast Belt remains, but can not be proven at this stage of investigation. Jura-Cretaceous rocks that overlie the Cadwallader Group and Bridge River Complex (western Noel Mountain section and Cayoosh Assemblage, respectively) are both characterized by an upward-coarsening clastic succession of feldspathic arenites and quartz-rich sandstones, locally containing significant proportions of intermediate and felsic volcanic rocks. I interpret these quartz-rich clastic rocks to be part of an overlap assemblage that records the final stages of terrane amalgamation and/or the emergence of volcanic arc and crystalline basement terranes in the Late Jurassic and Early Cretaceous. The age and provenance of these quartz-rich clastic rocks are currently under investigation.

ACKNOWLEDGMENTS

Fieldwork was carried out in collaboration with Carlo Sanders, Jan-Henk van Konijnenburg and Monique Jaasma from the University of Amsterdam, and with Bruce Miller from the University of British Columbia. I thank them for their contributions and assistance throughout the summer. My understanding of Eastern Coast Belt geology has evolved through stimulating discussions with Jim Monger, Glenn Woodsworth, Margi Rusmore, Paul Schiarizza, Jean Pautier, Brian Mahoney and Bill McClelland. I thank them for sharing their ideas and experience. Helicopter and logistical support were provided by John and Patricia Goats of Pemberton Helicopters.

REFERENCES

- Cairnes, C.E.
1937: Geology and mineral deposits of the Bridge River mining camp, British Columbia; Geological Survey of Canada, Memoir 213, 140 p.

- Friedman, R.M. and Armstrong, R.L.**
1990: U-Pb dating, southern Coast Belt; in *Lithoprobe Southern Canadian Cordillera Workshop Report*, p. 146-156.
- Garver, J.I.**
1991: Kinematic analysis and timing of structures in the Bridge River Complex and overlying Cretaceous rocks, Cinnabar Creek area, southwestern British Columbia (92J/15); in *Geological Fieldwork 1990*, British Columbia Ministry of Energy, Mines and Petroleum Resources, Paper 1991-1, p. 65-75.
- Journeay, J.M.**
1990: A progress report on the structural and tectonic framework of the southern Coast Belt, British Columbia; in *Current Research, Part E*; Geological Survey of Canada, Paper 90-1E, p. 183-195.
- Journeay, J.M. and Northcote, B.R.**
1992: Tectonic assemblages of the Eastern Coast Belt, southwest British Columbia; in *Current Research, Part A*; Geological Survey of Canada, Paper 92-1A, p. 215-224.
- Journeay, J.M., Sanders, C., Van-Konijnenburg, J.-H., and Jaasma, M.**
1992: Fault systems of the Eastern Coast Belt, southwest British Columbia; in *Current Research, Part A*; Geological Survey of Canada, Paper 92-1A, p. 225-235.
- Journeay, J.M. and Friedman, R.M.**
in press: The Coast Belt Thrust System: evidence of Late Cretaceous shortening in the Coast Belt of SW British Columbia; *Tectonics*.
- Leitch, C.H.B.**
1989: Geology, wall-rock alteration and characteristics of the ore fluid at the Bralorne mesothermal gold-vein deposit, southwestern British Columbia; PhD. thesis, University of British Columbia, Vancouver, 483 p.
- Mahoney, J.B. and Journeay, J.M.**
1993: The Cayoosh Assemblage, southwestern British Columbia: last vestige of the Bridge River Ocean; in *Current Research, Part A*; Geological Survey of Canada, Paper 93-1A.
- Monger, J.W.H. and Journeay, J.M.**
1992: Guide to the Geology and Tectonic Evolution of the Southern Coast Belt: A Field guide to accompany the Penrose Conference on the "Tectonic evolution of the Coast Mountain Orogen", May, 1992.
- Riddell, J.M.**
1991: Geology of the Mesozoic volcanic and sedimentary rocks east of Pemberton, British Columbia; in *Current Research, Part A*; Geological Survey of Canada, Paper 91-1A, p. 245-254.
- Roddick, J.A. and Hutchison, W.W.**
1973: Pemberton (east half) map-area, British Columbia; Geological Survey of Canada, Paper 73-17, 21 p.
- Rusmore, M.E.**
1985: Geology and tectonic significance of the Upper Triassic Cadwallader Group and its surrounding faults, southwestern British Columbia; PhD. thesis, University of Washington, Seattle, 170 p.
- Rusmore, M.A., Potter, C.J., and Umhoefer, P.J.**
1988: Middle Jurassic terrane accretion along the western edge of the Intermontane Superterrane, southwestern British Columbia; *Geology*, v. 16, p. 891-899.
- Schiarizza, P., Gaba, R.G., Coleman, M., Garver, J.I., and Glover, J.K.**
1990: Geology and mineral occurrences of the Yalakom River area (920/1,2, 92J/15,16); in *Geological Fieldwork 1989*, British Columbia Ministry of Energy, Mines and Petroleum Resources, Paper 1990-1, p. 53-73.
- Schiarizza, P., Gaba, R.G., Glover, J.K., and Garver, J.I.**
1989: Geology and mineral occurrences of the Tyaughton Creek area (920/2, 92J15,16); in *Geological Fieldwork 1988*, British Columbia Ministry of Energy, Mines and Petroleum Resources, Paper 1989-1, p. 115-130.
- Varsek, J.L., Cook, F.A., Clowes, R.M., Journeay, J.M., Monger, J.W.H., Parrish, R.R., Kanasevich, E.R., and Spencer, C.S.**
in press: Lithoprobe crustal reflection structure of the southern Canadian Cordillera II: Coast Mountains transect; *Tectonics*.
- Woodsworth, G.J.**
1977: Pemberton (92J) map area, British Columbia; Geological Survey of Canada, Open File 482.

Geological Survey of Canada Project 890036

The Cayoosh Assemblage, southwestern British Columbia: last vestige of the Bridge River Ocean

J.B. Mahoney¹ and J.M. Journeay
Cordilleran Division, Vancouver

Mahoney, J.B. and Journeay, J.M., 1993: The Cayoosh Assemblage, southwestern British Columbia: last vestige of the Bridge River Ocean; in Current Research, Part A; Geological Survey of Canada, Paper 93-1A, p. 235-244.

Abstract: The Cayoosh Assemblage is a coherent succession of fine grained clastic metasedimentary rocks that conformably overlies oceanic assemblages of the Bridge River Terrane in southwestern British Columbia. Thin-bedded phyllitic siltstones near the base of the Cayoosh Assemblage are intercalated with sandy and tuffaceous siltstones, thin-bedded greywacke and limestone. These rocks grade upwards into a succession of siltstones, fragmental metavolcanic rocks and associated volcanoclastic sandstones. Phyllitic siltstones and pyritiferous shales of the upper Cayoosh Assemblage grade upwards into a succession of interlayered thin- and thick-bedded feldspathic arenites, quartz-rich feldspathic arenites and phyllitic sandstones. This upper siltstone/sandstone lithofacies is correlated on the basis of rock type with Lower Cretaceous fossiliferous rocks of the Brew Group. These rocks provide a record of Jura-Cretaceous sedimentation in the Eastern Coast Belt and offer a means of reconstructing the evolution of the Bridge River 'ocean,' and the history of terrane interactions along the boundary between the Intermontane and Insular superterranes.

Résumé : L'assemblage de Cayoosh est une succession cohérente de roches métasédimentaires clastiques à grain fin qui recouvrent en concordance les assemblages océaniques du terrane de Bridge River dans le sud-ouest de la Colombie-Britannique. Des siltstones graphiteux finement lités, proches de la base de l'assemblage de Cayoosh, sont interstratifiés avec des siltstones sableux et tufacés, et avec une grauwacke et un calcaire finement lités. Ces roches passent vers le haut à une succession de siltstones, de roches métavolcaniques détritiques et de grès volcanoclastiques associés. Les siltstones phylliteux et les shales pyriteux de la partie supérieure de l'assemblage de Cayoosh passent vers le haut à une succession d'arénites feldspathiques à lits fins et à lits épais, d'arénites feldspathiques riches en quartz et de grès phylliteux. Ce lithofaciès supérieur à siltstone et grès peut être mis en corrélation, en fonction du type lithologique, avec les roches fossilifères du Crétacé inférieur qui font partie du Groupe de Brew. Ces roches constituent une colonne stratigraphique jurassique-crétacée de la zone de la côte orientale dont l'étude permettra aux chercheurs de reconstituer l'évolution de l'«océan» de Bridge River et d'établir les interactions successives des terranes qui se sont produites sur la limite entre le superterrane intermontagneux et le superterrane insulaire.

¹ Department of Geological Sciences, University of British Columbia, 6339 Stores Road, Vancouver, B.C. V6T 1Z4

INTRODUCTION

The Bridge River Complex is a Mississippian to Middle Jurassic assemblage of greenstone, chert and fine-grained clastic rocks that occurs along the boundary between the Insular and Intermontane superterrane of the southern Coast Belt. It is conformably overlain by Jura-Cretaceous clastic rocks of the Cayoosh Assemblage and is structurally interleaved with other terranes of the southern Coast Belt along an array of contractional and strike-slip faults that range in age from Late Cretaceous to Early Tertiary (Fig. 1, 2).

Evolution of the Bridge River 'ocean' and its linkage to adjacent terranes of the Insular and Intermontane belts prior to the onset of crustal imbrication, are fundamental to an understanding of the Coast Belt orogen, and to the history of superterrane accretion in the southern Canadian Cordillera (Monger and Journeay, 1992). Estimates for the timing of terrane accretion in the southern Coast Belt range from Middle Jurassic (Rusmore et al., 1988; van der Heyden, 1992) to Early Cretaceous (Monger et al., 1982). There is no direct evidence for the timing or mechanism of terrane accretion in

the Bridge River Complex. However, conformably overlying fine-grained clastic successions of the Cayoosh Assemblage are gradational upwards into Lower Cretaceous quartz-rich sandstones and conglomerates of the Eastern Coast Belt (Journeay and Northcote, 1992). These rocks record Jura-Cretaceous sedimentation in the region, and may provide a means of reconstructing the terminal history of the Bridge River 'ocean' and the history of terrane accretion in the Eastern Coast Belt.

This study focuses on the stratigraphy of the Cayoosh Assemblage in its type locality (Fig. 1, 3), and explores potential linkages with clastic successions in adjacent parts of the southern Coast Belt. Stratigraphic studies by Mahoney are part of a PhD dissertation jointly sponsored by the Geological Survey of Canada and the University of British Columbia.

GEOLOGICAL SETTING

The Bridge River Complex is an oceanic assemblage of greenstone, chert, siliceous siltstone and serpentinite, locally interleaved with lesser greywacke, limestone, and ultramafic

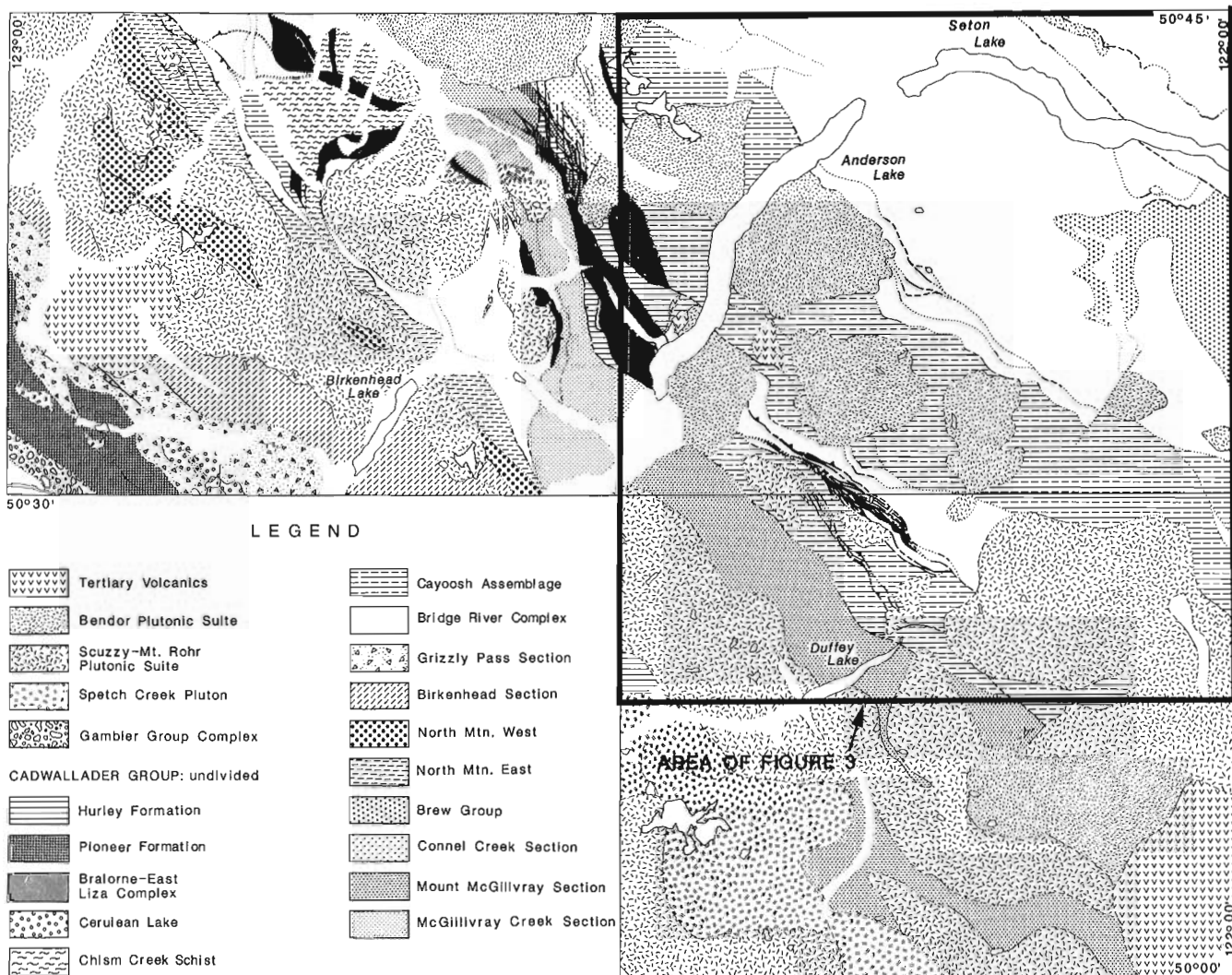


Figure 1. Regional Geology of the Eastern Coast Belt. See Journeay (1993) for map credits.

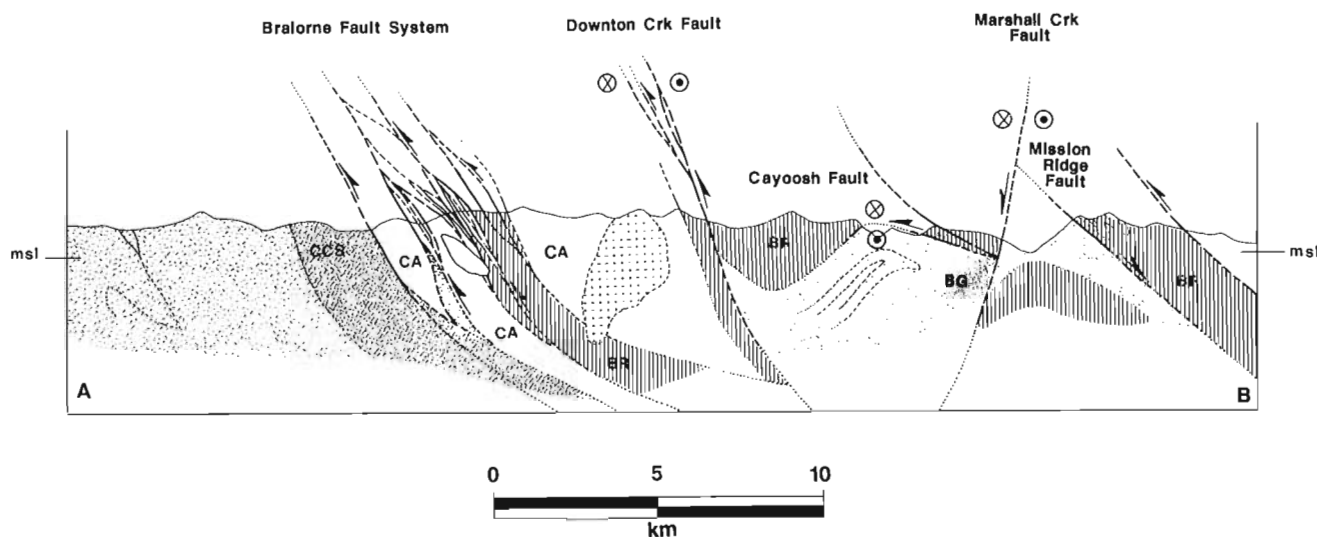


Figure 2. Geological cross-section of the Eastern Coast Belt. See Figure 3 for location of section line.

rock (Schiariizza et al., 1989, 1990; Journeay et al., 1992; Journeay, 1993). Two distinct zones of structural imbrication (tectonic mélangé) are recognized in the Bridge River Complex (see Journeay, 1993). The eastern mélangé zone is well-exposed in the eastern Cayoosh and Chilcotin ranges. It is flanked by the Downton Creek and Fraser Fault systems, and contains dismembered cherts and greenstones that range in age from Mississippian to late Middle Jurassic (Cordey, 1988, 1990). The western mélangé belt, well-exposed in the eastern Cadwallader Range, is similar in composition to its eastern counterpart, and is cut by high angle imbricate faults of the Bralorne Fault Zone. Situated between these two mélangé belts, in the upper plate of the Bralorne Fault and in the lower plate of the Downton Creek Fault, is a deformed but coherent succession of Bridge River greenstone, thin-bedded ribbon chert, calcareous greenschist, graphitic siltstone and fine grained volcanoclastic sandstone (Fig. 1, 2; Journeay and Northcote, 1992).

The Cayoosh Assemblage is a Jura-Cretaceous succession of fine grained clastic metasedimentary rocks that conformably overlies interbedded greenstone, chert and siliceous siltstone of the Bridge River Complex (Journeay and Northcote, 1992). The type section is characterized by thin-bedded siltstone and sandstone, quartz-rich feldspathic arenite, laminated phyllitic arenite and volcanoclastic sandstone, and is well exposed in alpine ridges of the western Cayoosh Range. It is flanked to the west by the Bralorne Fault and to the east by the Downton Creek Fault (Fig. 3).

The Brew Group (Duffell and McTaggart, 1952) is a fault-bounded sequence of argillite, siltstone, greywacke, quartz-rich sandstone and conglomerate, locally containing fossiliferous sandstone of Early Cretaceous (Early Neocomian) age. It is flanked by the Cayoosh Creek Fault and, as presently mapped, includes a sequence of interlayered greenstone, greenschist and associated fine grained volcanoclastic sandstone and siltstone of uncertain age and correlation.

CAYOOSH ASSEMBLAGE STRATIGRAPHY

The Cayoosh Assemblage, previously mapped as part of the Bridge River Group (Roddick and Hutchison, 1973; Woodworth, 1977), comprises a thick succession of fine grained metasedimentary rocks. At its type locality, the Cayoosh Assemblage conformably overlies interlayered greenstone, chert and fine grained siltstone/sandstone couplets of the Bridge River Complex. It occupies the core of a southwest-verging syncline, the limbs of which are cut by southwest-directed thrusts of the Bralorne and Downton Creek fault zones (Fig. 2). Primary sedimentary structures and stratigraphic relationships are preserved, but have been modified by the effects of penetrative deformation and regional metamorphism.

Rocks of the Bridge River Complex and overlying Cayoosh Assemblage share the same history of penetrative deformation and metamorphism. Compositional layering is isoclinally folded (locally transposed and disrupted) and is cut by a penetrative slaty cleavage containing lower greenschist grade metamorphic assemblages. In contact aureoles adjacent to crosscutting plutons, these rocks are recrystallized and contain lower amphibolite grade assemblages of garnet, hornblende, biotite, staurolite \pm andalusite. Structural styles vary with rock type and record a history of inhomogeneous strain. Competent sandstone and greywacke beds are only weakly deformed, whereas thin-bedded siltstone/shale and argillite successions are isoclinally folded and locally transposed. Bedding parallel shear zones are common, particularly along the boundaries between competent and incompetent horizons. However, they do not significantly disrupt the stratigraphic succession, and are interpreted to have accommodated relatively small amounts of displacement.

These structural and metamorphic complexities negate any attempt to estimate primary stratigraphic thicknesses or to reconstruct detailed patterns of sedimentation in the

Cayoosh Assemblage. However, continuity of individual map units and preservation of regional facies relationships lead us to conclude that the Cayoosh Assemblage, although deformed and metamorphosed, is stratigraphically coherent and preserves a record of Jura-Cretaceous sedimentation in the Eastern Coast Belt. For the purposes of discussion, we use sedimentary terminology and vertical rock columns (Fig. 4, 5) to describe stratigraphic relationships in the Cayoosh Assemblage. These columns were compiled from measured structural sections and should not be used to infer primary stratigraphic thickness.

Sections that were examined during the 1992 field season (Fig. 4) include the upper transitional facies of the Bridge River Complex and the lower fine grained clastic succession of the Cayoosh Assemblage. Both sections occur on the

upright lower limb of the Cayoosh syncline and are well-exposed along ridge crests adjacent to Melvin Creek (Fig. 3). The upper part of the Cayoosh Assemblage is exposed in the core of the syncline, along strike to the southeast in the Lillooet Range (Journey and Northcote, 1992).

The Cayoosh Assemblage comprises five lithofacies, including: 1) an argillite/siltstone succession; 2) volcanic tuff/tuff-breccia; 3) volcanic sandstone; 4) a siltstone/quartz-rich sandstone succession; and 5) granitoid-bearing conglomerate.

Argillite/siltstone succession

The base of the Cayoosh Assemblage is well-exposed along steep ridges flanking the northern headwaters of Melvin Creek (54910mE, 559540mN; Fig. 3). At this locale,

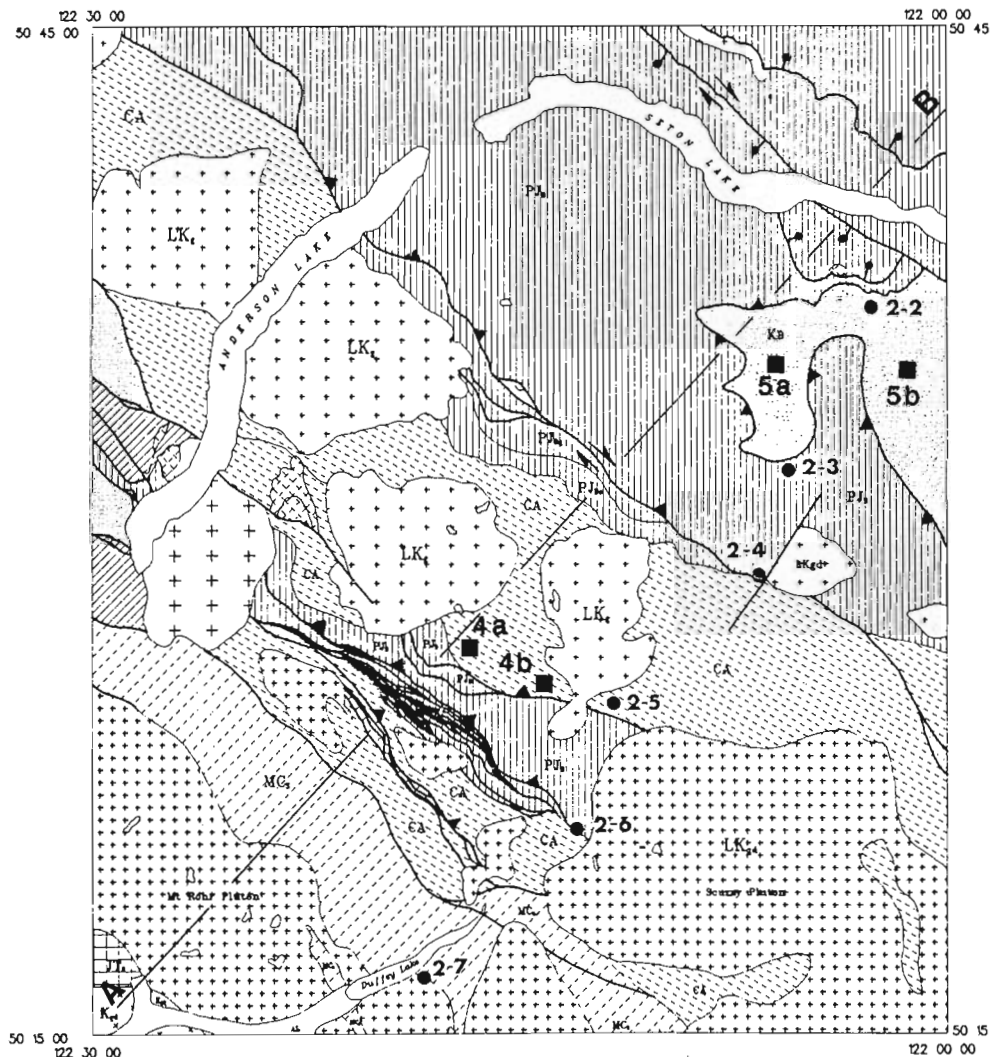


Figure 3. Geological map of the Cayoosh Range (92J/9 map area) showing the distribution and regional structural setting of the Cayoosh Assemblage and the location of measured structural sections. Field trip stops from Monger and Journey (1992). Section locations include: 4a=Melvin Creek section; 4b=Cayoosh Creek section; 5a=lower Brew Group section; 5b=upper Brew Group section. Map symbols include: CA= Cayoosh Assemblage; KB=Brew Group; MCs=Chism Creek Schist; PJb=Bridge River Complex; cross pattern= intrusive rock.

interbedded greenstones, ribbon cherts, and black siliceous argillites of the Bridge River Complex are conformably overlain by a thick sequence of dark grey to black, thin bedded argillite and siltstone of the Cayoosh Assemblage. The contact is sharp, and is placed at the top of the stratigraphically highest chert horizon in the Bridge River Complex (Fig. 4).

The basal portion of the Cayoosh Assemblage is approximately 350 m thick and comprises a monotonous succession of dark grey to black, thin-bedded and laminated phyllitic argillite, argillaceous siltstone, siltstone, and sandy siltstone, locally interlayered with discontinuous horizons of thin and medium bedded greywacke and limestone. Thin (2-5 cm) sandy siltstone beds form resistant horizons within

more recessive argillite, and have the appearance of thin-bedded turbidites. Greywacke beds are light grey, thin to medium bedded (5-25 cm), fine grained feldspathic wackes with sharp upper and lower contacts, parallel laminae and locally developed graded bedding. Limestone beds are thin to medium bedded, blue grey, locally sandy and everywhere recrystallized. Greywacke and limestone beds comprise less than 10% of the section near its base, but become increasingly more abundant upsection. A distinctive unit in the argillite/siltstone succession is a mottled, phyllitic argillite characterized by irregular, light grey elongate lenses. When viewed down-plunge, these lenses appear as discontinuous thin (<0.5 cm) light grey to white laminae in a matrix of folded

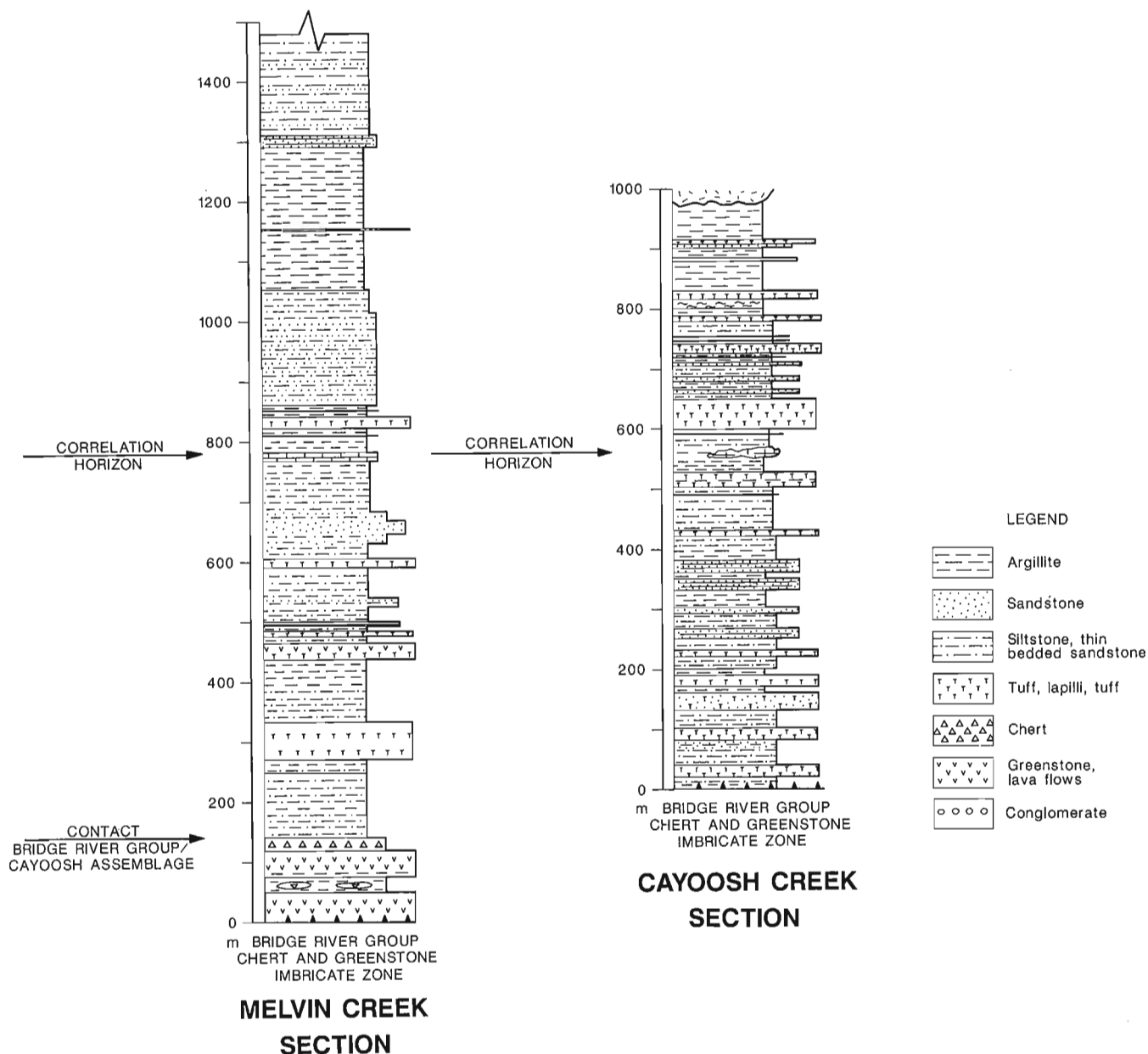


Figure 4. Structural sections of the Cayoosh Assemblage in its type locality of the western Cayoosh Range. See Figure 3 for location of sections.

dark grey argillite. They are interpreted to be thin ash horizons that have been isoclinally folded and transposed parallel to the dominant schistosity.

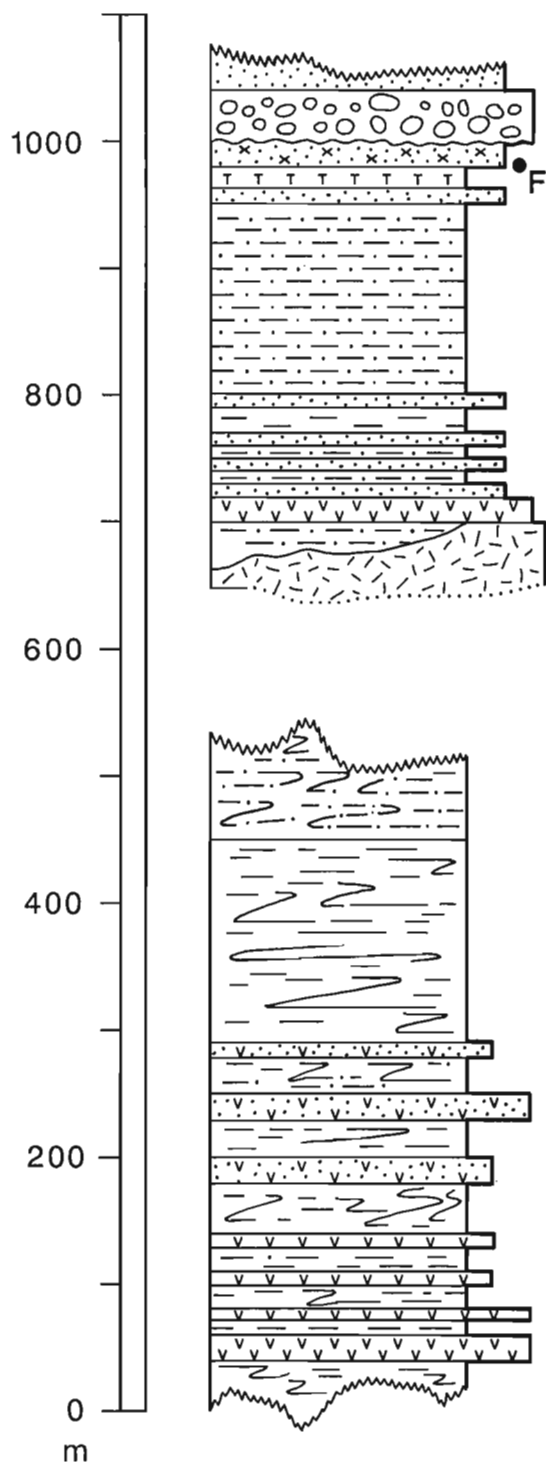
Volcanic tuff/tuff-breccia succession

Thin-bedded argillites and siltstones of the basal Cayoosh Assemblage are locally interlayered with thick (2-60 m) horizons of light to dark green, medium and thick bedded tuff, lapilli tuff, and tuff-breccia (Fig. 4). These horizons are characterized by sharp upper and lower contacts and form laterally continuous and resistant blocky outcrops. The majority of the tuffaceous units are medium bedded, fine grained tuffs and lapilli tuffs consisting of plagioclase grains set in a green, aphanitic matrix. Parallel and wavy lamination and thin (2-5 cm) lenses of dark grey argillite occur locally. Lithic clasts are stretched and consist primarily of fine grained tuff. Coarsening upward sequences are locally evident, with fine grained vitric and crystal tuff coarsening upward into lapilli tuff and tuff-breccia. Rare andesitic(?) flows, locally containing stretched pillows and remnant devitrification structures (spherulites) are also present. These volcanic rocks represent a minor (10-25%) but stratigraphically important component of the lower Cayoosh Assemblage. They represent distinct pulses of volcanic activity in a basin characterized by thick accumulations of fine grained sediments.

Volcanic sandstone succession

Fine grained siltstone, greywacke and associated tuffaceous volcanic rocks grade upwards into a thick (approximately 500-600 m) sequence of fine to coarse grained volcanic sandstone and siltstone (Fig. 4). This volcanoclastic succession consists primarily of interlayered lithic feldspathic arenite and greywacke with thin laminated siltstone. The ratio of sandstone to siltstone varies from 4/1 to 1/2. Sandstone is light grey to light brown on weathered surfaces, thin to medium bedded, fine to coarse grained, and generally well sorted. Parallel laminations, graded bedding, scour features, rip-up clasts, and flame structures are locally well preserved. Sandstone beds commonly have sharp basal contacts, and gradational upper contacts into overlying siltstone beds. Sandstone and siltstone beds are arranged in both coarsening and thickening upward, and fining and thinning upward sequences that range from 5 to 50 m thick (Fig. 4). Sandstone intervals vary in thickness and lateral extent on a scale of 1-2 km. They are interpreted to be lenticular in cross-section and lobate in plan view.

Sandstone units are composed primarily of subangular plagioclase grains and subrounded volcanic lithic fragments, with variable amounts of quartz (5-15%). The quartz content



COMPOSITE STRUCTURAL SECTION OF BREW GROUP

Figure 5. Composite structural section of the Brew Group. The lower part of the section is compiled from exposures along the Cayoosh River, in the footwall of the Cayoosh Creek Fault. The upper part of the section represents the lower upright limb of an antiformal syncline exposed along the south flank of Mount Brew and includes rocks initially defined as part of the Brew Group by Duffell and McTaggart (1952). See Figure 4 for legend. F = Lower Neocomian fossil locality.

increases upwards, with the sandstones in the upper portion of the Cayoosh Assemblage distinctly more quartz-rich than those in the lower portion. Rare thin-bedded, reddish weathering quartz-rich feldspathic arenite occurs throughout the section, and suggests the Cayoosh Assemblage received detritus from multiple source regions.

Siltstone/quartz-rich sandstone succession

The volcanic sandstone succession is gradationally overlain by a thick (200-300 m) sequence of argillite, siltstone and sandstone (Fig. 4). Tuffaceous volcanic horizons occur locally near the base of the sequence, but decrease in abundance upwards. Thin light grey to white laminae, interpreted as tuffaceous ash layers, are locally abundant and attest to continued volcanic activity. Pyritiferous shales and siltstones grade upwards into feldspathic sandstones, similar in appearance to those of the lower argillite/siltstone succession, but containing much higher proportions of detrital quartz. These sandstones consist primarily of thin to thick bedded, fine to coarse grained quartz-rich feldspathic arenite and thin-bedded phyllitic quartzite. Feldspathic arenite beds are 5-8 m thick, locally graded and contain basal shale rip-up clast horizons.

This clastic succession is stratigraphically and compositionally similar to interbedded sandstone, siltstone and shale of the lower portion of the Brew Group (Journeay and Northcote, 1992). Similarities in sandstone composition, interbedded volcanic units, and coarsening upwards stratigraphy suggest a correlation between the Cayoosh Assemblage and the Brew Group. We interpret the Cayoosh Assemblage to be laterally equivalent to and gradationally overlain by rocks of the Brew Group, which suggests that the Cayoosh Assemblage and Brew Group formed a coherent, widespread stratigraphic succession that was dismembered by large-scale crustal imbrication in the Late Cretaceous and early Tertiary.

The lower portion of the Brew Group consists of interbedded dark grey argillite and siltstone, thin-bedded greywacke, thin and thick bedded quartz-rich sandstone, and minor tuffaceous intervals (Fig. 5). Amphibolite lenses near the bottom of the sequence are interpreted to be metavolcanic flows (Journeay and Northcote, 1992). These rocks grade upwards into a distinctive clastic facies of interlayered siltstones, quartz-rich feldspathic arenites and thin laminated phyllitic quartzites. Sandstones become thicker bedded and compositionally and texturally less mature upwards, and are interlayered with tuffaceous siltstones and calcarenites. Calcareous sandstones at the top of this succession contain bivalves of Early Neocomian age (Duffell and McTaggart, 1952).

Conglomerate

Overlying the quartz-rich clastic facies of the Brew Group is a 100-150 m thick section of boulder conglomerate (Fig. 5). The conglomerate cores a southwest-verging antiformal syncline (Mustard, 1983), and represents an important marker horizon in the Brew Group. Well-rounded cobbles and boulders consist primarily of granite and granodiorite, argillite, felsic and intermediate volcanic rock, chert, quartzite, and foliated gneissic rock. One of these granodiorite boulders yielded Middle Jurassic zircons (V. Coleman, pers. comm., 1992).

AGE OF THE CAYOOSH ASSEMBLAGE

The age of the Cayoosh Assemblage is poorly constrained. No macrofossils have been recovered, and due to the structural and metamorphic overprint, it is unlikely that any will be. Microfossil (radiolaria and conodonts) recovery has been unsuccessful. Felsic volcanics from the middle portion of the assemblage are being processed for zircon.

Age constraints for the Cayoosh Assemblage are provided by its relationship with other units in the region. The assemblage must be younger than greenstones and cherts of the Bridge River Complex, which it conformably overlies. Radiolaria as young as Callovian have been recovered from several localities in the eastern imbricate zone, although the majority of dates are Late Triassic (Anisian to Late Norian) and Early to Middle Jurassic (Pliensbachian to Bajocian) (Cordey, 1988, 1990; P. Schiarizza, pers. comm., 1992). No radiolaria have yet been recovered from the western imbricate zone or the central coherent section of the Bridge River Complex. The structural complexity and uncertainty about original basin configuration make it entirely possible that chert deposition in the west either ended before or continued after the cessation of chert deposition in the eastern Bridge River Complex. The age of the transition zone between the Bridge River Complex and overlying Cayoosh Assemblage is therefore unknown.

Fossiliferous greywacke underlying the granite-bearing boulder conglomerate that caps the Brew Group succession yield the bivalve *Buchia crassicollis* of Early Neocomian (Berriasian?) age. Assuming the correlation between the upper Cayoosh Assemblage and the Brew Group is valid, it follows that the majority of the Cayoosh Assemblage/Brew Group stratigraphy must be older than Early Neocomian. As a working hypothesis, we postulate that rocks of the Cayoosh Assemblage and correlative rocks of the Brew Group are part of a widespread clastic succession that ranges in age from Middle(?) Jurassic to Early Cretaceous, with the majority of the unit being Middle(?) to Late Jurassic.

EQUIVALENT ROCKS OF THE SOUTHERN COAST BELT

Structural complexities and the absence of timing constraints from the Cayoosh Assemblage preclude a direct correlation with other clastic successions of the southern Coast Belt. However, the assemblage overlies the Bridge River Complex, which is locally as young as Middle Jurassic, and contains Early Neocomian fossils near the top of the succession, arguing against correlation with pre-Middle Jurassic strata, such as the Triassic Cadwallader and Tyaughton groups (Rusmore et al., 1988; Umhoefer, 1989). Jura-Cretaceous clastic and volcanic successions of the southern Coast Belt that may be in part correlative with the Cayoosh Assemblage include the Harrison Lake Formation, the Gambier Assemblage, the Relay Mountain Group, and the Ladner Group (Fig. 6). Metamorphosed clastic rocks of the Cayoosh Assemblage are recognized in the Settler and Chism Creek schist units of the Coast Belt Thrust System (Journeay, 1990; Monger, 1991).

Harrison Lake Formation/Gambier Assemblage

The Harrison Lake Formation, exposed on the west side of Harrison Lake and in fault slivers of the Coast Belt Thrust System, comprises a thick succession of rhyolitic to andesitic volcanic flows and pyroclastic rocks of probable Toarcian to Bajocian age (Fig. 6). The Harrison Lake Formation is overlain by a sequence of Lower Callovian shale and thin bedded sandstone (Mysterious Creek Formation), which are, in turn, overlain by volcanoclastic rocks of the Oxfordian Billhook Creek Formation. These units are unconformably overlain by coarse sandstone and granitoid-bearing conglomerate of the Berriasian Peninsula Formation (Arthur, 1986) and volcanic arc sequences of the Brokenback Hill Formation of the Gambier Assemblage.

Relay Mountain Group

The Middle Jurassic to Lower Cretaceous (Callovian to Hauterivian) Relay Mountain Group is well-exposed in the Chilcotin Range, west of the Yalakom Fault and east of the Downton Creek Fault. It lies unconformably above fine grained volcanoclastic sandstone, siltstone, and minor conglomerate of the Lower to Middle Jurassic (Hettangian to Bajocian) Last Creek Formation (Fig. 6; Umhoefer, 1989). The Relay Mountain Group consists predominantly of volcanoclastic thin bedded siltstone and medium to thick bedded sandstone. Primary volcanic rocks are absent in both the Last Creek Formation and Relay Mountain Group, with the exception of probable thin ash beds in the Last Creek Formation. The Relay Mountain Group is unconformably overlain by conglomerate of the Taylor Creek Group (Garver, 1989).

Ladner Group

Ladner Group is exposed on the east side of the Fraser Fault System, and in tectonic slivers along the west side of the fault (Monger, 1986; Mahoney, 1993). Lower Jurassic argillite and thin-bedded siltstone of the Boston Bar Formation is gradationally overlain by the Toarcian to Bajocian Dewdney Creek Formation, which is a thick volcanoclastic unit that consists of an eastern proximal facies and a western distal facies (O'Brien, 1986; Mahoney, 1993). Ladner Group is disconformably overlain by the Thunder Lake sequence, a thin feldspatholithic sandstone of Oxfordian to Tithonian age (O'Brien, 1986), and by quartz-bearing lithic feldspathic sandstone and granitoid-bearing conglomerate of the Hauterivian(?) to Albian Jackass Mountain Group (Kleinspehn, 1985).

TENTATIVE CORRELATIONS

We interpret the Cayoosh Assemblage to be both laterally equivalent to and gradationally overlain by rocks of the Brew Group. Together, these rocks represent a coherent Jura-Cretaceous clastic succession that conformably overlies oceanic rocks of the Bridge River Complex and is capped by Early Cretaceous and younger conglomerates. Three lithofacies in the Cayoosh Assemblage/Brew Group succession are considered distinct enough to be useful in regional correlation, including: 1) volcanic tuff and tuff-breccia; 2) quartz-rich clastic rocks, and 3) granitoid-bearing conglomerates. Although undated, these distinctive lithofacies provide the basis for lithostratigraphic correlation with other clastic successions of the southern Coast Belt.

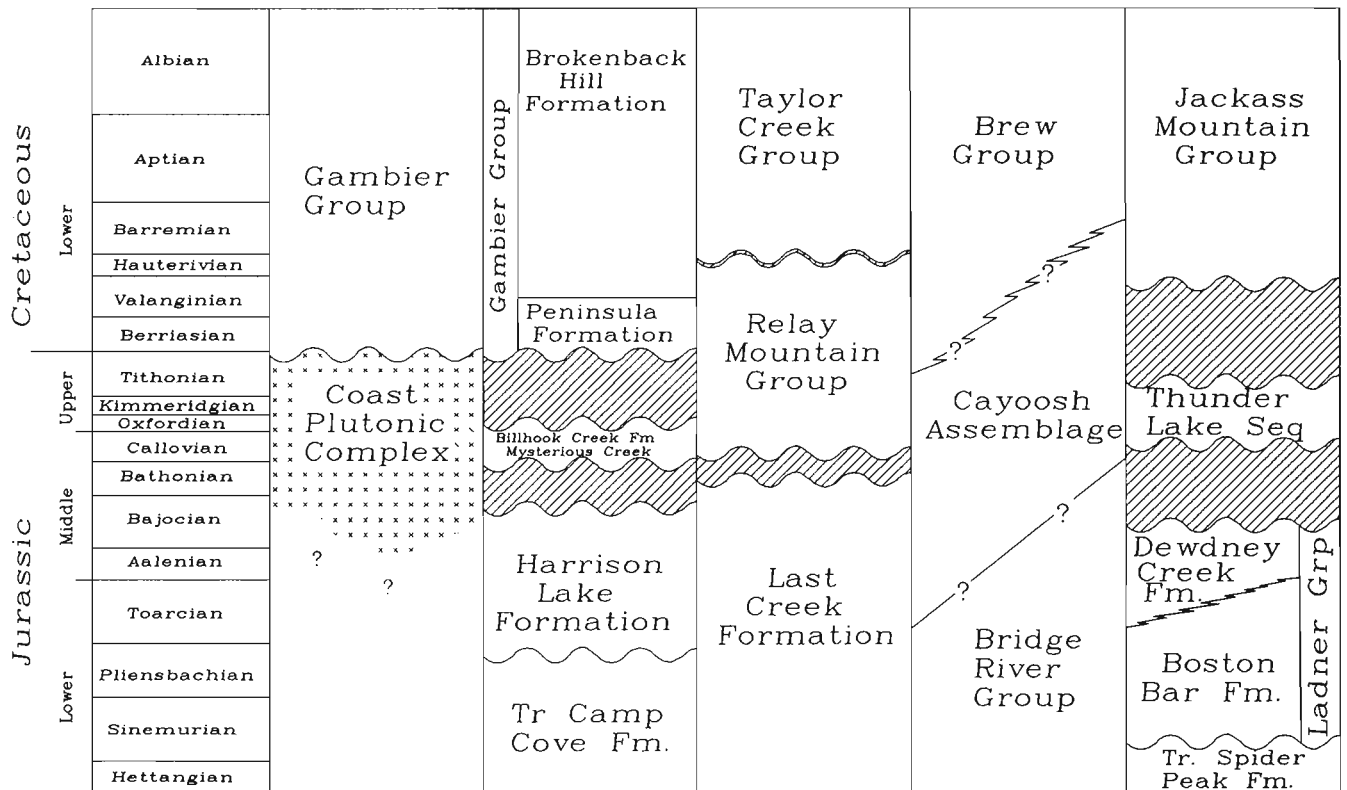


Figure 6. Correlation chart of Jura-Cretaceous units in the southern Coast Belt. Data from Arthur (1986); O'Brien (1986); Umhoefer (1989); Lynch (1991); Mahoney (1993).

Volcanic/volcaniclastic facies

Volcanic and volcaniclastic rocks of the Cayoosh Assemblage are interlayered with thick accumulations of siltstone/greywacke turbidite, graphitic siltstone and shale. The presence of fragmental volcanic flows and abundant tuffaceous detritus suggest a proximal source. These volcanics could be westerly derived, from Middle and Upper Jurassic volcanic flows and pyroclastic rocks of the Harrison Lake Formation and overlying Billhook Creek Formation, or easterly derived, from Middle Jurassic volcanic and volcaniclastic rocks of the Dewdney Creek Formation (Ladner Group) (Fig. 6). The Relay Mountain Group lacks primary volcanic rocks. Harrison Lake Formation and overlying units provide a source for volcanic material, but are lacking in quartz-rich detritus. The association of volcaniclastic rocks and overlying quartz-rich feldspathic sandstone in the Middle Jurassic Ladner Group and younger rocks is similar to that of the Cayoosh Assemblage, and suggests a possible correlation between the two.

Quartz-rich clastic facies

The quartz-rich clastic facies of the Cayoosh Assemblage conformably overlies the volcanic lithofacies and is overlain by the Lower Cretaceous conglomerate lithofacies.

In the Harrison Lake area, volcanic and volcaniclastic rocks of the Harrison Lake Formation are overlain by sandstone and siltstone of the Mysterious Creek Formation and volcaniclastic sediments of the Billhook Creek Formation, which are in turn overlain by granitoid-bearing conglomerate of the Peninsula Formation. Harrison Lake Formation contains abundant quartz-bearing rhyolitic volcanic rocks, but quartz-rich detritus is absent. The detrital component of both the Mysterious Creek and Billhook Creek formations are distinctly quartz poor.

Quartz detritus is minimal in the Relay Mountain Group, although Upper Jurassic (lower Oxfordian) sandstone in the lower Relay Mountain Group contains up to 17% detrital quartz of inferred plutonic origin (Umhoefer, 1989). However, these quartzofeldspathic sandstones are overlain by a thick sequence of quartz-poor volcaniclastic rocks of the middle and upper Relay Mountain Group.

The Dewdney Creek Formation of Ladner Group contains an anomalous sequence of quartzofeldspathic sandstone of inferred Aalenian age that interrupts the predominantly volcaniclastic succession (Mahoney, 1993). The source of this sandstone is unknown. The formation also contains quartz-bearing tuffs and lapilli tuffs. The Thunder Lake assemblage and lower Jackass Mountain Group lie above the volcaniclastic Dewdney Creek Formation, and below granitoid bearing conglomerate of the Jackass Mountain Group. These strata display an increase in plutonic debris over the underlying units, but do not constitute a "quartz-rich" facies. The transition from volcaniclastic rocks with minor quartz-rich detritus in the Dewdney Creek Formation to feldspathic sandstones and conglomerates of the Thunder Lake Sequence and lower Jackass Mountain Group is similar to that observed in the upper Cayoosh Assemblage, and may be correlative.

Lower Cretaceous granitoid-bearing conglomerate

Lower Cretaceous granitoid-bearing conglomerates form an important marker horizon in the southern Canadian Cordillera. They represent the first definitive tie between the Insular and Intermontane superterranes. Granitoid-bearing conglomerates containing granitic clasts of Middle to Late Jurassic age are known from the Lower Cretaceous Gambier Group of the Insular Terrane (Lynch, 1991), from the Berriasian Peninsula Formation of the Harrison Lake Terrane (Arthur, 1986; O'Brien et al., 1992), from the Lower Cretaceous(?) Brew Group of the Bridge River Terrane (Duffell and McTaggart, 1952; Journeay and Northcote, 1992), and from the Hauterivian to Albian Jackass Mountain Group of the Methow Terrane (Kleinspehn, 1985). These conglomerates probably represent a clastic pulse related to uplift and erosion of arc assemblages either during or after terrane amalgamation.

The top of the Cayoosh Assemblage/Brew Group succession is marked by a granitoid-bearing conglomerate containing Middle Jurassic plutonic clasts that overlies Lower Neocomian fossiliferous sandstone. We interpret this conglomerate to be part of a Lower Cretaceous overlap assemblage that includes coarse clastic rocks of the Gambier Assemblage and the Jackass Mountain Group.

The correlation of the granitoid-bearing conglomerate in the upper Cayoosh Assemblage/Brew Group with a regional Lower Cretaceous overlap assemblage is important. The stratigraphy of the Cayoosh Assemblage/Brew Group consists of pelagic sediments overlain by volcaniclastic to quartz-rich clastic sediments, capped by granitoid-bearing conglomerate. We suggest that this stratigraphy records the cessation of pelagic sedimentation in the Bridge River "ocean", the initiation of Middle(?) to Late(?) Jurassic arc volcanism associated with basin closure, and the eventual uplift and erosion of this arc in Early Cretaceous time.

ONGOING INVESTIGATIONS

Our geological understanding of the Cayoosh Assemblage and its tectonic implications is in its infancy. Critical questions currently under investigation:

1. What is the age of the Cayoosh Assemblage? How does the age of this clastic assemblage fit into the established Mesozoic basin framework (Garver, 1989; Umhoefer, 1989; Mahoney, 1992, 1993)?
2. What is the affinity/derivation/source of the volcanic rocks in the Cayoosh Assemblage? The isotopic and geochemical signatures of these rocks may allow for correlations with other Mesozoic volcanic arcs in southern British Columbia.
3. What is the source of the granitic clasts found in the conglomerate, and how does this conglomerate relate to similar units in the region?
4. Finally, can the Cayoosh Assemblage be definitively correlated with other units in the region, thus providing a stratigraphic framework that places constraints on the tectonic evolution of the region?

ACKNOWLEDGMENTS

Fieldwork was carried out in collaboration with Bill McClelland, who has undertaken a pilot U-Pb study of detrital zircons and felsic flows to help constrain the age and provenance of the Cayoosh Assemblage. We thank him for his astute observations and contributions in the field and for many stimulating and entertaining discussions of Coast Belt and cosmic geology. Our understanding of Jura-Cretaceous stratigraphy in the southern Coast Belt has evolved through discussions with Jim Monger, Glenn Woodsworth and Paul Schiarizza. We thank them for sharing their ideas and experience. Helicopter and logistical support were provided by John and Patricia Goats of Pemberton Helicopters.

REFERENCES

- Arthur, A.J.**
1986: Stratigraphy along the west side of Harrison Lake, southwestern British Columbia; in *Current Research, Part A*; Geological Survey of Canada, Paper 86-1B, p. 715-720.
- Cordey, F.**
1988: Etude des radiolaires Permians, Triassiques et Jurassiques des complexes ophiolitiques de Cache Creek, Bridge River et Hozameen (Columbie Britannique, Canada): implications paleographiques et structurales; Phd. thesis, Université Pierre et Marie Curie, Paris, France.
1990: Radiolarian age determinations from the Canadian Cordillera; in *Current Research, Part E*; Geological Survey of Canada, Paper 90-1E, p. 121-126.
- Duffell, S. and McTaggart, K.C.**
1952: Ashcroft map area, British Columbia; Geological Survey of Canada, Paper 67-10, 55 p.
- Garver, J.I.**
1989: Basin evolution and source terranes of Albian-Cenomanian rocks in the Tyaughton Basin, southern British Columbia: implications for mid-Cretaceous tectonics in the Canadian Cordillera; Phd. thesis, University of Washington, Seattle.
- Journey, J.M.**
1990: A progress report on the structural and tectonic framework of the southern Coast Belt, British Columbia; in *Current Research, Part E*; Geological Survey of Canada, Paper 90-1E, p. 183-195.
1993: Tectonic assemblages of the eastern Coast Belt, British Columbia: Implications for the history and mechanisms of terrane accretion; in *Current Research, Part A*; Geological Survey of Canada, Paper 93-1A.
- Journey, J.M. and Northcote, B.R.**
1992: Tectonic assemblages of the Eastern Coast Belt, southwest British Columbia; in *Current Research, Part A*; Geological Survey of Canada, Paper 92-1A, p. 215-224.
- Journey, J.M., Sanders, C., van-Konijnenburg, J.-H., and Jaasma, M.**
1992: Fault systems of the Eastern Coast Belt, southwest British Columbia; in *Current Research, Part A*; Geological Survey of Canada, Paper 92-1A, p. 225-235.
- Kleinspehn, K.L.**
1985: Cretaceous sedimentation and tectonics, Tyaughton-Methow Basin, southwestern British Columbia; *Canadian Journal of Earth Sciences*, v. 22, p. 229-233.
- Lynch, J.V.G.**
1991: Georgia Basin Project: stratigraphy and structure of Gambier Group rocks in the Howe Sound-Mamquam River area, southwest Coast Belt, British Columbia; in *Current Research, Part A*; Geological Survey of Canada, Paper 91-1A, p. 49-57.
- Mahoney, J.B.**
1992: Middle Jurassic stratigraphy of the Lillooet area, south-central British Columbia; in *Current Research, Part A*; Geological Survey of Canada, Paper 92-1A, p. 243-248.
1993: Facies reconstructions in the Lower to Middle Jurassic Ladner Group, southern British Columbia; in *Current Research, Part A*; Geological Survey of Canada, Paper 93-1A.
- Monger, J.W.H.**
1986: Geology between Harrison Lake and Fraser River, Hope map area, southwestern British Columbia; in *Current Research, Part B*; Geological Survey of Canada, Paper 86-1B, p. 699-706.
1991: Correlation of Settler schist with Darrington Phyllite and Shuksan Greenschist and its tectonic implications, Coast and Cascade Mountains, British Columbia and Washington; *Canadian Journal of Earth Sciences*, v. 28, p. 447-458.
- Monger, J.W.H., Price, R.A., and Tempelman-Kluit, D.J.**
1982: Tectonic accretion and the origin of two major metamorphic and plutonic belts in the Canadian Cordillera; *Geology*, v. 10, p. 70-75.
- Monger, J.W.H. and Journey, J.M.**
1992: Guide to the geology and tectonic evolution of the southern Coast Belt; field guide to accompany Penrose Conference on "Tectonic Evolution of the Coast Mountains Orogen", 92 p.
- Mustard, J.F.**
1983: The geology of the Mount Brew area, Lillooet, British Columbia; M.Sc. thesis, University of British Columbia, Vancouver, 74 p.
- O'Brien, J.A.**
1986: Jurassic stratigraphy of the Methow Trough, southwestern British Columbia; in *Current Research, Part B*; Geological Survey of Canada, Paper 86-1B, p. 749-756.
- O'Brien, J.A., Gehrels, G.E., and Monger, J.W.H.**
1992: U-Pb geochronology of plutonic clasts from conglomerates in the Ladner and Jackass Mountain groups and the Peninsula Formation, southwestern British Columbia; in *Current Research, Part A*; Geological Survey of Canada, Paper 92-1A, p. 209-214.
- Roddick, J.A. and Hutchison, W.W.**
1973: Pemberton (east half) map-area, British Columbia; Geological Survey of Canada, Paper 73-17, 21 p.
- Rusmore, M.E., Potter, C.J., and Umhoefer, P.J.**
1988: Middle Jurassic terrane accretion along the western edge of the Intermontane superterrane, southwestern British Columbia; *Geology*, v. 16, p. 891-894.
- Schiarizza, P., Gaba, R.G., Glover, J.K., and Garver, J.I.**
1989: Geology and mineral occurrences of the Tyaughton Creek area (92O/2, 92J/15,16); in *Geological Fieldwork 1988*, British Columbia Ministry of Energy, Mines and Petroleum Resources, Paper 1989-1, p. 115-130.
- Schiarizza, P., Gaba, R.G., Coleman, M., Glover, J.K., and Garver, J.I.**
1990: Geology and mineral occurrences of the Yalakom River area (92I/1,2, 92J/15,16); in *Geological Fieldwork 1989*, British Columbia Ministry of Energy, Mines and Petroleum Resources, Paper 1990-1, p. 53-73.
- Umhoefer, P.J.**
1989: Stratigraphy and tectonic setting of the Upper Cadwallader Terrane and overlying Relay Mountain Group, and the Cretaceous to Eocene structural evolution of the eastern Tyaughton Basin, British Columbia; Phd. thesis, University of Washington, Seattle, 186 p.
- van der Heyden, P.**
1992: A Middle Jurassic to early Tertiary Andean-Sierran arc model for the Coast Belt of British Columbia; *Tectonics*, v. 11, p. 82-97.
- Woodsworth, G.J.**
1977: Pemberton (92J) map area, British Columbia; Geological Survey of Canada, Open File 482.

Holocene foraminiferal faunas from cores collected on the Fraser River delta, British Columbia: a paleoecological interpretation

R. Timothy Patterson¹ and John L. Luternauer
Cordilleran Division, Vancouver

Patterson, R.T. and Luternauer, J.L., 1993: Holocene foraminiferal faunas from cores collected on the Fraser River delta, British Columbia: a paleoecological interpretation; in Current Research, Part A; Geological Survey of Canada, Paper 93-1A, p. 245-254.

Abstract: Interpretation of sedimentary environments are made based on the foraminiferal faunas recovered from four cores (FD90-A, FD90-B, FD91-1, and FD91-2) collected on the Fraser delta. These relatively short cores (<55 m) are primarily comprised of prodelta sands overlying ancestral Strait of Georgia mud and silt. The muds and silts are characterized by a low diversity foraminiferal fauna, dominated by *Buccella frigida*, *Criboelphidium excavatum*, and *Elphidiella hannai*. This fauna is typical of low salinity, neritic depth conditions. Foraminifera are virtually absent from the prodelta sands as the winnowing conditions prevalent during deposition of this unit made colonization difficult.

Résumé : On a réalisé l'interprétation des milieux sédimentaires en fonction des faunes de foraminifères recueillies dans quatre carottes (FD90-A, FD90-B, FD91-1, et FD91-2) prélevées dans le delta du Fraser. Ces carottes relativement courtes (<55 m) sont principalement composées de sables prodeltaïques recouvrant les boues et silts du détroit de Georgia ancestral. Ces derniers sont caractérisés par une faune peu diversifiée de foraminifères, contenant surtout *Buccella frigida*, *Criboelphidium excavatum* et *Elphidiella hannai*. Cette faune est caractéristique d'un milieu néritique de faible salinité. Les foraminifères sont virtuellement absents des sables prodeltaïques, étant donné que les conditions de déflation qui ont régné tout au long de la période de sédimentation de cette unité, ont rendu toute colonisation difficile.

¹ Ottawa-Carleton Geoscience Center and Department of Earth Sciences, Carleton University, Ottawa, Ontario K1S 5B6

INTRODUCTION

In response to growing concern over the potential for a devastating mega-thrust earthquake affecting the highly urbanized Fraser River delta, the Geological Survey of Canada has initiated multi-disciplinary geological research. These studies, coordinated by the GSC Cordilleran Geoscience Division, have involved many agencies from around the continent. Emphasis of research on the subaerial and subsurface parts of the delta has focused on acquiring data useful for assessing earthquake damage from both liquefaction and ground motion amplification (Luternauer, 1990; Clague et al., 1991).

Previous micropaleontological research has identified a large number of discrete and recognizable biofacies present on the delta (Williams, 1989; Patterson, 1990; Patterson and Cameron, 1991; Jonasson and Patterson, in press). This data is indispensable for the identification and interpretation of late Quaternary marine and glaciomarine deposits and provides a significant resource for the analysis of paleoenvironments not readily recognizable by sedimentological means alone. The purpose of the ongoing micropaleontological research is to refine our knowledge of foraminiferal and arcellacean distribution patterns associated

with particular sedimentological facies. In this paper we present the preliminary results of the foraminiferal analysis of four cores collected in 1990 and 1991 from various localities on the southern delta (Fig. 1). These results corroborate the results obtained from the analysis of two other cores, the 367 m core FD87-1 collected from the southern part of the delta and the 122.4 m core FD88-1 collected from the western part of Lulu Island. Detailed sedimentological and micropaleontological analyses of both these previously examined cores is provided elsewhere (Luternauer et al., 1991; Patterson and Cameron, 1991).

FRASER DELTA FORAMINIFERAL BIOFACIES CONTROLS

To date, nine different foraminiferal and arcellacean biofacies have been identified from recent and fossil Fraser delta sediments. While most of these biofacies are found in the subsurface some do not fossilize well and are thus restricted to modern environments (Patterson, 1990; Jonasson and Patterson, in press). This is particularly true of the marshy areas where acidic conditions caused by the rotting of vegetation result in poor preservation of calcareous taxa. Under these conditions only agglutinated taxa preserve well. Conversely, due to late Quaternary climatic and oceanographic changes, several biofacies identified in the subsurface have no modern counterparts (Patterson and Cameron, 1991). Glaciomarine foraminiferal faunas identified at the base of core FD87-1 are presently found only in glaciated bays surrounding Spitzbergen Island (Sejrup and Guilbault, 1980). Sedimentological regime also plays an important role in determining the type of foraminiferal fauna found. For example, all of the cores examined thus far have been obtained from the southern part of the delta. Due to Coriolis effect, this area has experienced primarily sandy deposition since initiation of prodelta development. This flow regime deposits siltier and muddy sediments typical of a less active sedimentological regime on the northern part of the delta (Johnson, 1921; Mathews and Shepard, 1962; Thompson, 1981). This region, where a richer fossil fauna is expected, has not been examined for its foraminiferal fauna.

METHODS AND MATERIALS

Fifty-five samples were obtained from four Geological Survey of Canada cores collected using a Sonic Dilling Ltd. (Vancouver) rig from various stations around the Fraser delta (Fig. 1). Core FD90-A was collected from the western part of Sea Island; core FD90-B was collected from the northwest corner of the intersection of Francis Street and Railway Avenue in Richmond on the western margin of Lulu Island; core FD91-1 was collected from adjacent to the Vancouver International Airport Main Terminal; and core FD91-2 was collected from the eastern part of Lulu Island.

All samples were processed by the method described by Patterson and Cameron (1991) and rinsed using 63 μm screens. Thirty-three of the 55 samples were found to contain

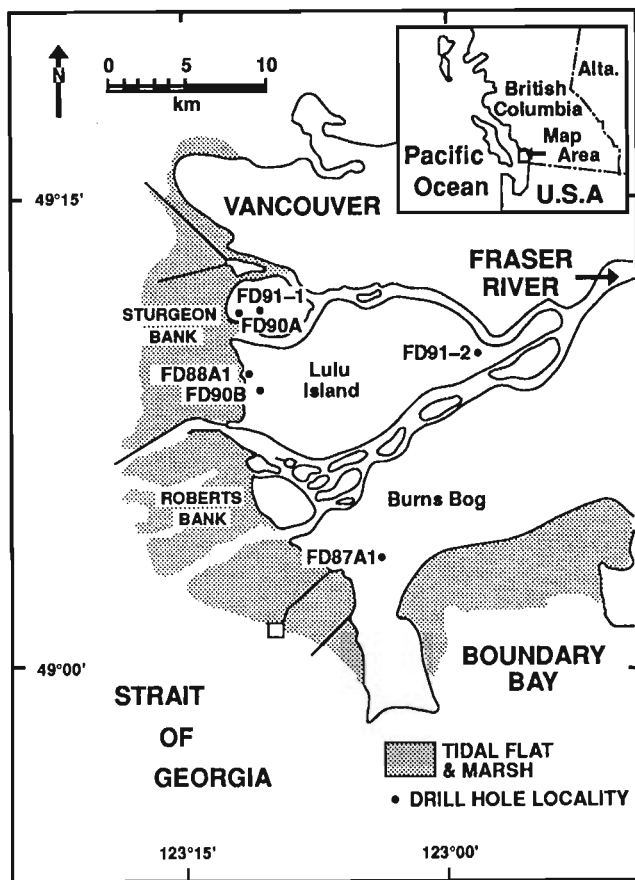


Figure 1. Location map showing position of various geographical landmarks and cores discussed in this paper.

foraminifera, and 23 of these samples (Tables 1 and 2) contained populations large enough for statistical analysis (see Patterson and Fishbein, 1989). Twenty-one species of benthic foraminifera are identified in this study. The per cent error was calculated using the standard error equation (s_{x_i}):

$$s_{x_i} = 1.96 \sqrt{\left[\frac{X_i [1 - X_i]}{N} \right]}$$

where (N) is the total number of counts, and (X) is the fractional abundance of a species (Patterson and Fishbein, 1989).

Conventional radiocarbon (^{14}C) dating was performed on bryophytes, mollusc shells and plant material at the Radiocarbon Laboratory of the Geological Survey of Canada. Accelerator mass spectrometry radiocarbon dating was

conducted at the IsoTrace Laboratory of the University of Toronto and by the Radio-Isotope Direct Detection Laboratory of McMaster University.

INTERPRETATION OF CORES

Core FD90-A

The 40 m core FD90-A was collected from the western part of Sea Island (Fig. 1). Only a single statistically significant low diversity foraminiferal fauna (Patterson and Fishbein, 1989), found between the 31.09 and 36.12 m interval of the core, was observed (Fig. 2; Table 1). The sedimentology of this interval is interbedded silts and sands overlying a diamicton. Both contain a foraminiferal fauna that is primarily comprised of up to 46.0% *Buccella frigida* (Cushman, 1922), up to 95.2% *Criboelphidium excavatum* (Terquem, 1876), and up to 54.5% *Elphidiella hannai*

Table 1. Foraminiferal occurrences in samples from cores FD90-A and FD90-B

Species/Sample	3062	3063	3064	3065	3066	3067	3068	3069	3045	3046	3047	3048	3049
Core	FD90A	FD90A	FD90A	FD90A	FD90A	FD90A	FD90A	FD90A	FD90B	FD90B	FD90B	FD90B	FD90B
Total Number of Specimens	0	276	0	1437	429	225	953	22	0	0	0	0	0
Depth in Core (m)	17.37	31.09	32.6	34.59	34.84	35.17	36.12	36.88	1.52	4.27	4.57	5.79	7.47
Percent Sample Examined	100.0	100.0	100.0	100.0	100.0	100.0	100.0	100.0	100.0	100.0	100.0	100.0	100.0
<i>Buccella frigida</i>		46.0		16.1	6.1	5.3	0.3						
<i>Bullminella elegantissima</i>		0.4		0.1			0.1						
<i>Cassidulina reniforme</i>		0.4						18.2					
<i>Criboelphidium excavatum</i>		30.1		46.1	84.1	42.7	95.2	4.5					
<i>Criboelphidium groenlandicum</i>				8.4	2.6			22.7					
<i>Criboelphidium tumidum</i>				1.9									
<i>Elphidiella hannai</i>		9.8		30.8	6.8	50.7	1.4	54.5					
<i>Epistominella pacifica</i>							0.1						
<i>Epistominella vitrea</i>						0.9							
<i>Fissurina vureola</i>				0.1									
<i>Gavelinopsis campanulata</i>							0.2						
<i>Islandiella norcrossi</i>							0.1						
<i>Nonionella stella</i>		10.5			0.5		1.3						
<i>Quinqueloculina seminulum</i>						0.4							
<i>Siphonaperta stalkerii</i>							1.3						
<i>Spirosigmoidina tenuis</i>							0.1						
<i>Stainforthia sp.</i>		2.9		0.1									

Species/Sample	3050	3051	3052	3053	3054	3055	3056	3057	3058	3059	3060	3061
Core	FD90B	FD90B	FD90B	FD90B	FD90B	FD90B	FD90B	FD90B	FD90B	FD90B	FD90B	FD90B
Total Number of Specimens	0	0	253	141	81	38	17	30	133	80	32	0
Depth in Core (m)	10.82	11.28	18.75	18.90	19.29	19.35	19.57	20.30	21.49	31.24	42.06	53.95
Percent Sample Examined	100.0	100.0	100.0	100.0	100.0	100.0	100.0	25.0	100.0	25.0	100.0	100.0
<i>Buccella frigida</i>			60.1	55.3	51.9	57.9	29.4	66.7	54.9	11.3	12.5	
<i>Bullminella elegantissima</i>												
<i>Cassidulina reniforme</i>												
<i>Criboelphidium excavatum</i>			26.5	17.7	18.5	10.5	35.3	20.0		20.0	31.3	
<i>Criboelphidium groenlandicum</i>												
<i>Criboelphidium tumidum</i>			0.4	0.7		2.6			42.9			
<i>Elphidiella hannai</i>			11.5	26.2	28.4	28.9	35.3	13.3		67.5	53.1	
<i>Epistominella pacifica</i>												
<i>Epistominella vitrea</i>												
<i>Fissurina vureola</i>												
<i>Gavelinopsis campanulata</i>									1.5			
<i>Islandiella norcrossi</i>												
<i>Nonionella stella</i>			1.2							1.3	3.1	
<i>Quinqueloculina seminulum</i>												
<i>Siphonaperta stalkerii</i>												
<i>Spirosigmoidina tenuis</i>												
<i>Stainforthia sp.</i>									0.8			
<i>Siphonaperta stalkerii</i>												

(Cushman and Grant, 1927); identified as *Elphidiella nitida* Cushman, 1941, in Patterson and Cameron (1991). This assemblage is referable to the *Criboelphidium excavatum* Biofacies of Patterson and Cameron (1991). This overall assemblage has been associated with neritic depths and reduced salinities (Patterson and Cameron, 1991; Sloan, 1980). These are the conditions that would be expected – as they exist today – in the ancestral Strait of Georgia silts off the front of the Fraser delta. Based on a ^{14}C date from a shell, the area was over ridden by prodelta sands by about 9180 BP. As this area shallowed during the gradual transition from ancestral Strait of Georgia sediments to the coarser sediments characteristic of the delta front the proportions of the species making up the foraminiferal populations also changed. As a result of these continually changing conditions some species variation is recognizable, and expected, even within the *Criboelphidium excavatum* Biofacies. For example, *Elphidiella hannai* typically dominates lower diversity *Criboelphidium excavatum* Biofacies at the deep water, or more open marine, end of the biofacies range (Sloan, 1980). As the environment continues to shallow and freshen with the increasing proximity of the delta front *Criboelphidium excavatum* begins to dominate the biofacies (Sloan, 1980). In this core the proportions of these key indicator species vary considerably up core. The high variability in the proportions of the dominant foraminiferal species in adjacent samples and the interbedded, sand/silt, nature of the sediments suggests some minor reworking. Since the foraminiferal fauna found in this interval do not show evidence of abrasion, this transport was probably minor.

Part of the foraminiferal fauna of this interval is found in an underlying diamicton of unknown age. Due to the chaotic nature of diamictons, it is probable that this fauna has also been reworked. In fact many specimens from this interval show evidence of transport induced abrasion. This unit may be related to a diamicton reported by Patterson and Cameron (1991) to be associated with penultimate (Semiahmoo) or older glacial event.

Core FD90-B

This 55 m core was collected from the northwest corner of the intersection of Francis Street and Railway Avenue in Richmond on the western margin of Lulu Island (Fig. 1). Sedimentologically this core is quite different from FD90-A. The basal part of this core is characterized by extensive muds and silts beneath the 20 m mark, and is overlain by prodelta sands which are similar to those observed in FD90-B (Fig. 3). Statistically significant populations of foraminifera (Patterson and Fishbein, 1989) were only recovered from the silty and muddy intervals of the core between 18.75 and 53.95 m (Table 1). Again the foraminiferal fauna is overwhelmingly dominated by *Buccella frigida* (11.3-66.7%), *Criboelphidium excavatum* (10.5-45.9%), and *Elphidiella hannai* (up to 67.5%). Although much of the lower part of the core was not sampled, these muds and silts are interpreted to have been deposited offshore on the floor of the ancestral Strait of Georgia. The low diversity foraminiferal fauna again developed in response to low

Table 2. Foraminiferal occurrences in samples from cores FD91-1 and FD91-2

Species/Sample	91-1-79	91-1-26	91-1-32	3194	3195	91-1-41A	3196	91-1-46	91-1-71	91-1-75	91-1-78	91-1-50	3197	3198	3199
Core	FD91-1	FD91-1	FD91-1	FD91-1	FD91-1	FD91-1	FD91-1	FD91-1	FD91-1	FD91-1	FD91-1	FD91-1	FD91-1	FD91-1	FD91-1
Total Number of Specimens	0	87	89	25	64	0	7	0	0	0	0	0	3	5	3
Depth in Core (m)	8.39	12.24	13.5	13.93	14.69	15.12	15.12	17.78	20.32	21.76	23.03	23.48	25.1	26.68	30.48
Percent Sample Examined	100.0	100.0	100.0	100.0	100.0	100.0	100.0	100.0	100.0	100.0	100.0	100.0	100.0	100.0	100.0
<i>Ammonia beccarii</i>							14.3								
<i>Buccella frigida</i>		19.5	21.3	28.0	15.6		28.6							20.0	33.3
<i>Criboelphidium excavatum</i>		71.3	74.2	68.0	71.9		14.3						66.7	20.0	66.7
<i>Criboelphidium gunteri</i>														40.0	
<i>Criboelphidium tumidum</i>															
<i>Elphidiella hannai</i>		6.9	4.5	4.0	12.5		42.9						33.3	20.0	
<i>Favulina melo</i>															
<i>Nonionella stella</i>															
<i>Quinqueloculina seminulum</i>		1.1													
<i>Rosalina columbiensis</i>															
<i>Siphonaperta stalker</i>															

Species/Sample	91-1-83	91-1-61	91-1-64	91-1-67	91-2-41	91-2-52	3201	3202	3203	3204	3205	3206	3207	3208	3200
Core	FD91-1	FD91-1	FD91-1	FD91-1	FD91-2	FD91-2	FD91-2	FD91-2	FD91-2	FD91-2	FD91-2	FD91-2	FD91-2	FD91-2	FD91-2
Total Number of Specimens	0	0	1	0	0	0	67	582	99	291	7	406	392	892	1750
Depth in Core (m)	31.52	32.53	33.44	34.45	11.53	17.68	24.35	24.5	24.8	25.58	25.79	29.94	32.53	36.02	44.08
Percent Sample Examined	100.0	100.0	100.0	100.0	100.0	100.0	100.0	25.0	100.0	25.0	100.0	100.0	100.0	25.0	100.0
<i>Ammonia beccarii</i>															
<i>Buccella frigida</i>							10.4	9.3	9.1	4.8	28.6	14.5	1.5	0.3	0.2
<i>Criboelphidium excavatum</i>							82.1	79.7	82.8	80.0	57.1	78.1	91.1	94.3	95.3
<i>Criboelphidium gunteri</i>															
<i>Criboelphidium tumidum</i>								1.2							
<i>Elphidiella hannai</i>							7.5	9.6	8.1	14.1		6.2	4.3	2.2	
<i>Favulina melo</i>											14.3				
<i>Nonionella stella</i>									0.3				0.3		0.2
<i>Quinqueloculina seminulum</i>															
<i>Rosalina columbiensis</i>															
<i>Siphonaperta stalker</i>			100.0					0.2		0.7		1.2	2.8	3.1	4.3

salinity conditions caused by the freshening influence of the nearby Fraser River. Deposition at the core site changed from clays to silts as the prograding delta front neared. In response to decreasing salinities the relative proportion of the more marine *Elphidiella hannai* declined and the proportion of the more freshwater tolerant *Criboelphidium excavatum* increased. However, this trend was sharply reversed at this site for a short interval around 6210 BP., just prior to deposition of prodelta sands. In a very short interval the proportion of *Elphidiella hannai* increased dramatically and the proportion of *Criboelphidium excavatum* declined

suggesting a return to more marine conditions (Sloan, 1980). This faunal shift may indicate that the mouth of the Fraser River migrated further away for a short time.

Core FD91-1

This 55.5 m core was collected adjacent to the Vancouver International Airport Main Terminal (Fig. 1). Statistically significant populations of foraminifera were restricted to a single interval of core FD91-1 (Fig. 4; Table 2). This fauna

CORE FD90-A

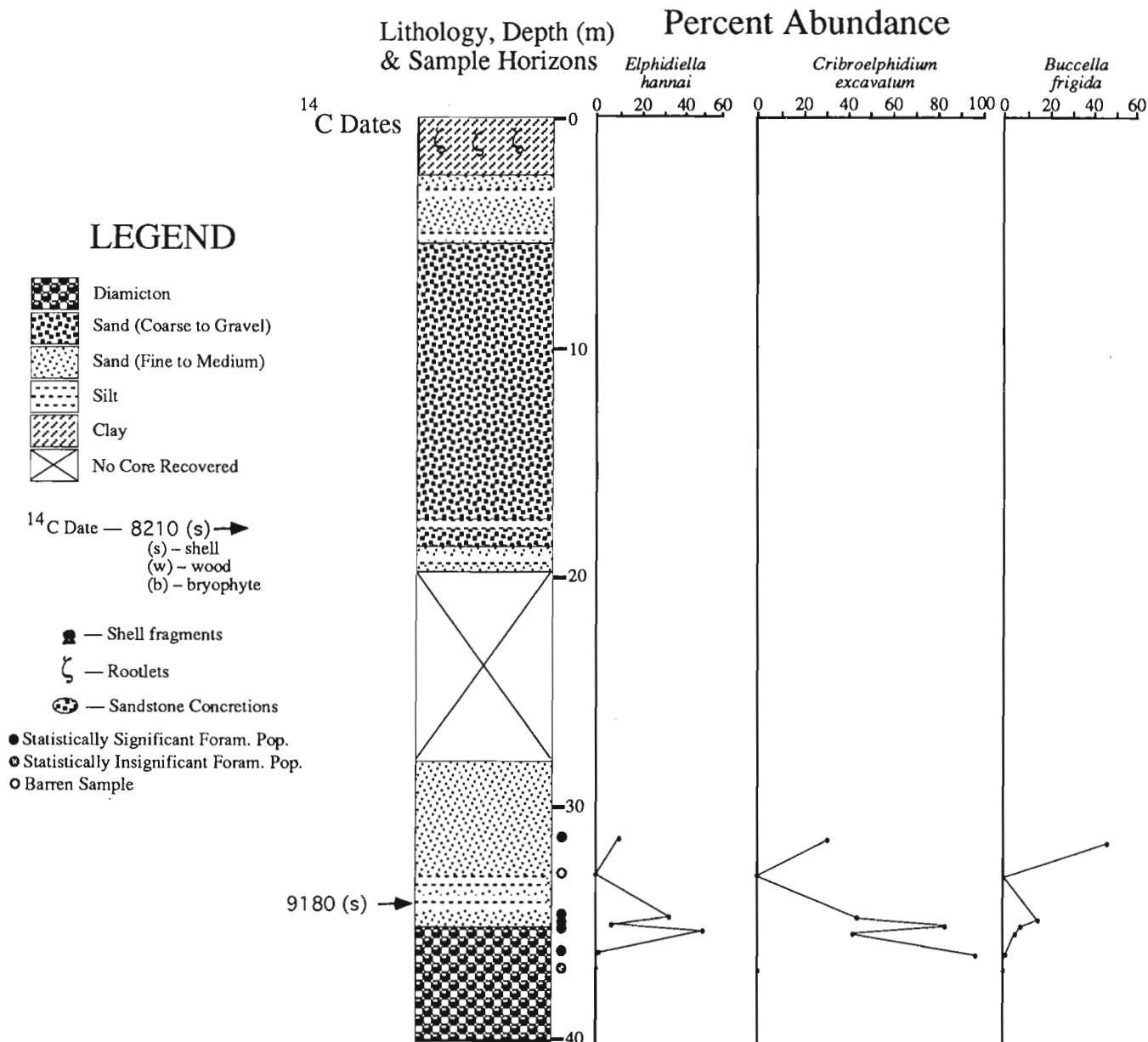


Figure 2. Lithology, ¹⁴C dates, and relative abundances of the dominant foraminiferal species in core FD90-A.

CORE FD90-B

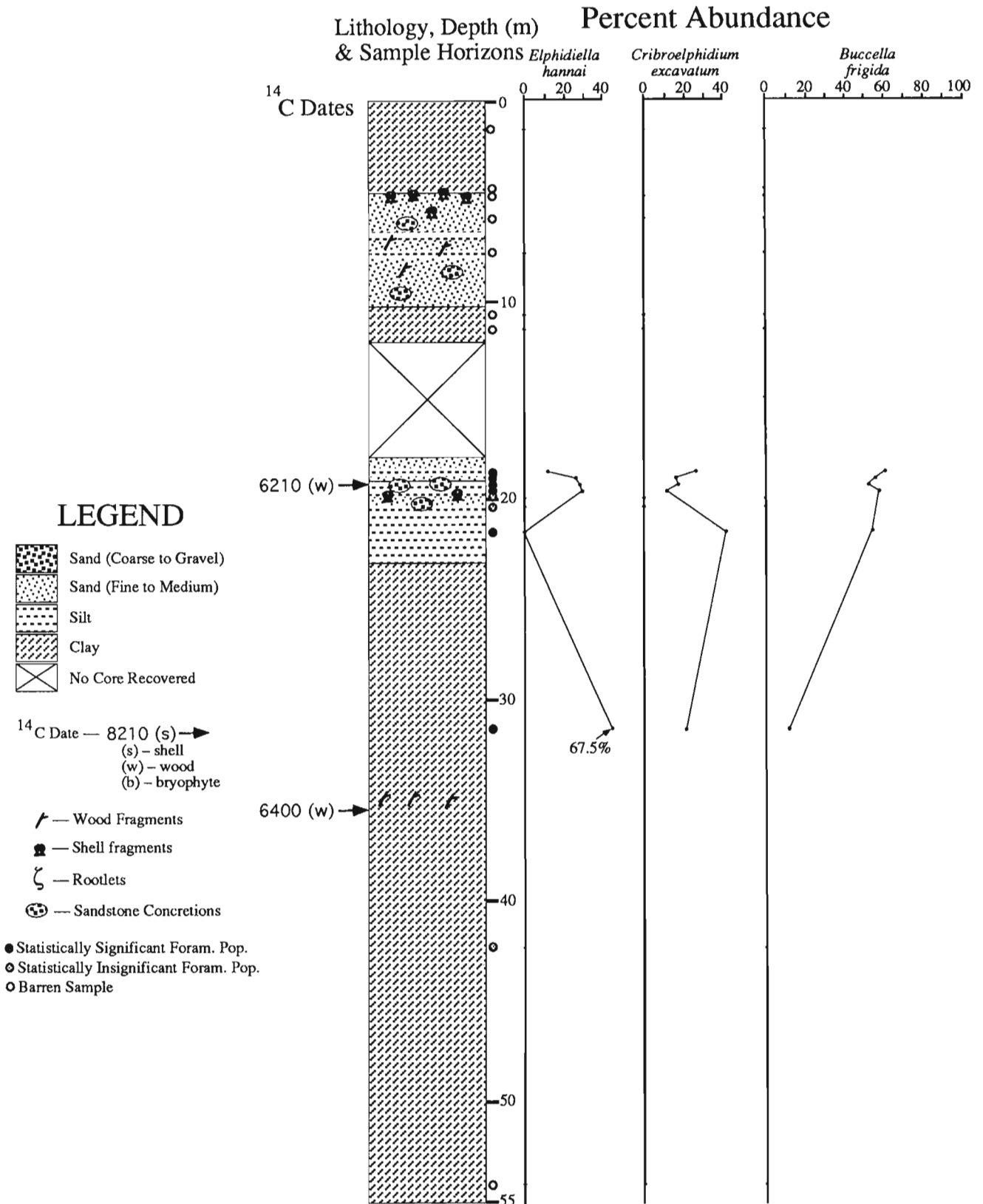


Figure 3. Lithology, ¹⁴C dates, and relative abundances of the dominant foraminiferal species in core FD90-B.

CORE FD91-1

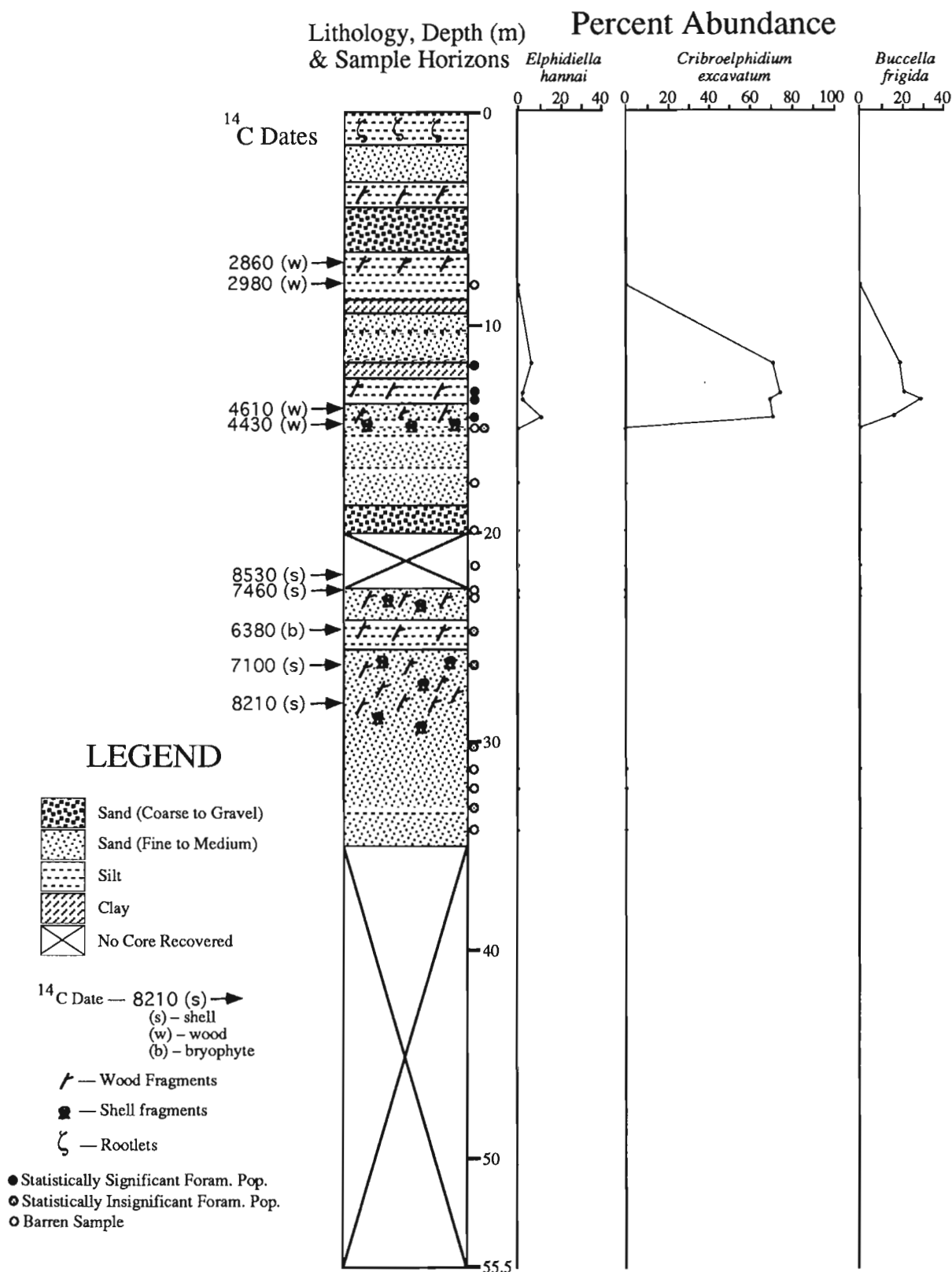


Figure 4. Lithology, ¹⁴C dates, and relative abundances of the dominant foraminiferal species in core FD91-1.

CORE FD91-2

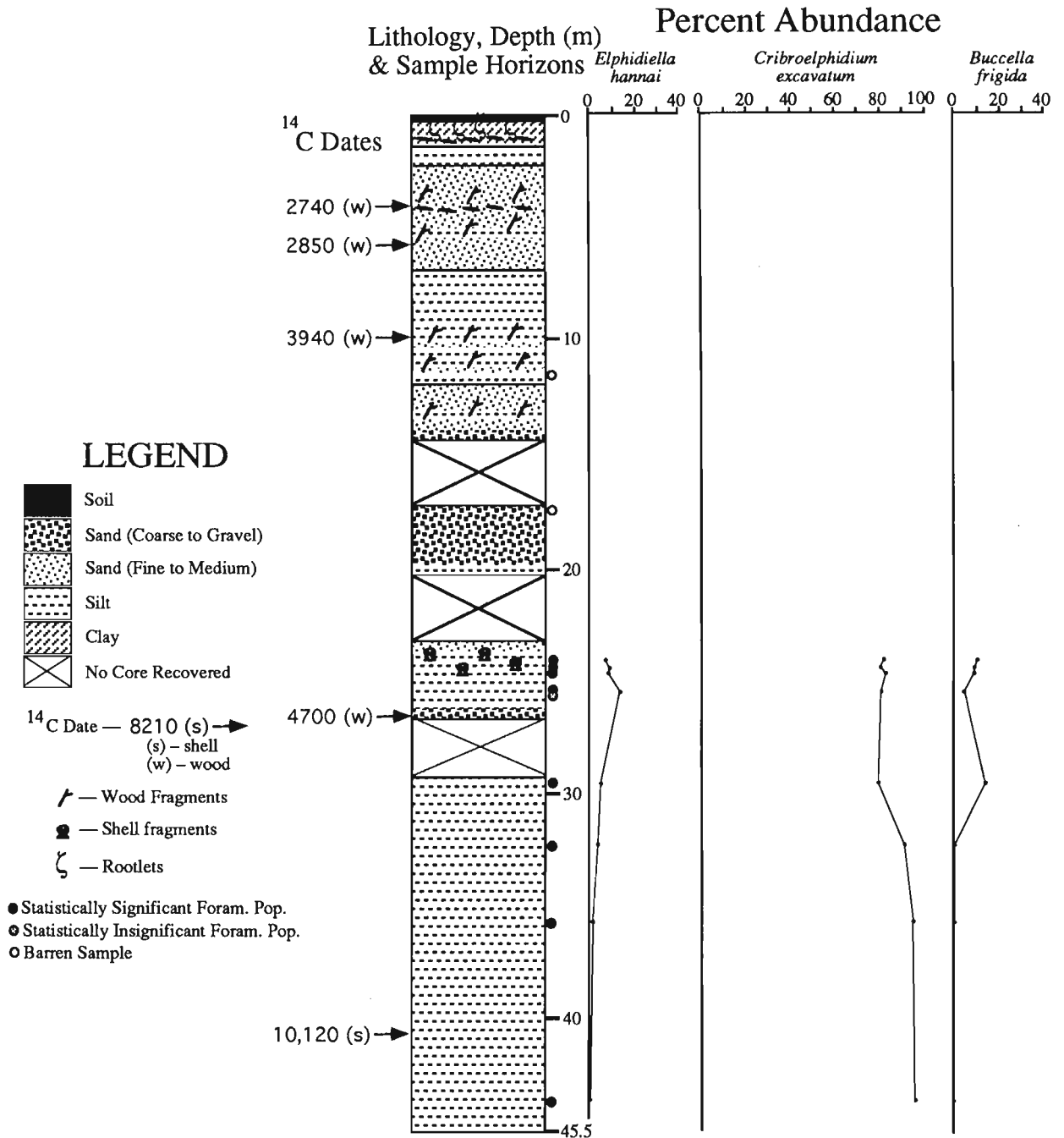


Figure 5. Lithology, ¹⁴C dates, and relative abundances of the dominant foraminiferal species in core FD91-2.

is exclusively again referable to a reduced diversity *Criboelphidium excavatum* Biofacies (Patterson and Cameron, 1991).

The *Criboelphidium excavatum* biofacies bearing interval of the core (12.4 and 14.7 m) is overwhelmingly dominated by *Criboelphidium excavatum* (68.0-74.2%). Lesser proportions of *Buccella frigida* (15.6-28.0%) and *Elphidiella hannai* (4.0-12.5%) are also typically found; again characteristic of relatively shallow (neritic depths) and lower salinity water conditions. The foraminiferal fauna is found in silts and clays, bracketed above and below, by prodelta sand and coarse sand. The features observed in this interval are interpreted as being the result of a secondary depositional event with the foraminiferal fauna being reworked from nearby pre-existing sediments. This interpretation is supported by the presence of somewhat poorly preserved and marginally statistically significant foraminiferal populations in these samples. Total faunal counts were generally low, varying between 25-89 specimens. In addition, many of the foraminiferal tests are darkly stained and have been partially oxidized, probably in response to exposure to the environment and to acids released by the organic debris concentrated in this interval. Evidence of reworking also was recorded in a nearby core FD90-A (see above). Calcareous specimens found in the organic-rich marshes of the Fraser delta often have a similar appearance. However, the fauna observed here is not referable to a marsh fauna (Patterson, 1990).

A few samples found between 15.12 and 34.45 m had a few specimens of various shallow water foraminiferal species. These specimens, often found with organic debris in sandy units, were very abraded and often broken, suggesting considerable reworking.

Core FD91-2

This 45.5 m core was collected from the eastern part of Lulu Island (Fig. 1). The interval found beneath 24.35 m is generally characterized by statistically significant foraminiferal populations again all attributable to a low diversity *Criboelphidium excavatum* dominated fauna (Fig. 5; Table 2; Patterson and Fishbein, 1989). As has been observed for all the other cores, this fauna is characteristic of relatively shallow (neritic depths) and brackish water conditions. This interval is older than 4500 BP (base on ¹⁴C date), comprised primarily of silts, and interpreted to be ancestral Strait of Georgia sediments adjacent to a considerable freshening influence from the Fraser River – as indicated by the dominance of *Criboelphidium excavatum* in all foraminifera-bearing samples. The relatively large foraminiferal populations found in this interval and the good condition of the specimens indicate that the fauna is probably in situ. Conditions suitable for colonization by this foraminiferal fauna terminated by sometime after 4700 BP with the initiation of prodelta sand deposition.

CONCLUSIONS

This study has resulted in the recognition of paleo-environmental facies not readily characterized by sedimentological techniques alone. The results also underline the importance of a multidisciplinary approach to understanding the depositional history of the Fraser delta. Future foraminiferal studies will be invaluable to furthering our knowledge on the history and current status of the delta.

ACKNOWLEDGMENTS

This research was supported by NSERC operating grant OGPOO41665 as well as contracts from the Geological Survey of Canada to R.T.P. We would like to thank M. Johns, and H. Elizabeth Patterson for critically reviewing the manuscript.

REFERENCES

- Clague, J.J., Lichti-Federovich, S., Guilbault, J.-P., and Mathews, R.W.**
1991: Holocene sea level change, south-coastal British Columbia; in Current Research, Part A; Geological Survey of Canada, Paper 91-1A, p. 15-21.
- Cushman, J.A.**
1922: Results of the Hudson Bay expedition, 1920; I - The foraminifera. Canada, Biological Board of Canada; Contributions of Canadian Biology (1921), no. 9, p. 135-147.
- Cushman, J.A. and Grant, U.S.**
1927: Late Tertiary and Quaternary *Elphidium*s of the west coast of North America; San Diego Society of Natural History Transactions, v. 5, p. 69-82.
- Johnson, W.A.**
1921: Sedimentation of the Fraser River delta; Geological Survey of Canada, Memoir 125, 46 p.
- Jonasson, K. and Patterson, R.T.**
in press: Preservation potential of marsh benthic foraminifera from the Fraser River Delta, British Columbia; Micropaleontology.
- Luternauer, J.L.**
1990: 1989 field activities and accomplishments of geophysical and geotechnical land-based operations and marine/fluvial surveys, Fraser River delta, British Columbia; in Current Research, Part E; Geological Survey of Canada, Paper 90-1E, p. 235-237.
- Luternauer, J.L., Clague, J.J., and Feeney, T.D.**
1991: A 367 m core from southwestern Fraser river delta, British Columbia; in Current Research, Part E; Geological Survey of Canada, Paper 91-1E, p. 127-134.
- Mathews, J.P. and Shepard, F.P.**
1962: Sedimentation of Fraser River delta, British Columbia; American Association of Petroleum Geologists Bulletin, v. 46, p. 1426-1438.
- Patterson, R.T.**
1990: Intertidal benthic foraminiferal biofacies on the Fraser River Delta, British Columbia: modern distribution and paleoecological importance; Micropaleontology, v. 36, p. 229-244.
- Patterson, R.T. and Cameron, B.E.**
1991: Paleoenvironmental significance of the foraminiferal biofacies succession in the late Quaternary sediments of the Fraser River delta, British Columbia; Journal of Foraminiferal Research, v. 21, p. 228-243.
- Patterson, R.T. and Fishbein, E.**
1989: Re-examination of the statistical methods used to determine the number of point counts needed for micropaleontological quantitative research; Journal of Paleontology, v. 63, p. 245-248.
- Sejrup, H.-P. and Guilbault, J.-P.**
1980: *Cassidulina reniforme* and *C. obtusa* (Foraminifera), taxonomy, distribution, and ecology; Sarsia, v. 65, p. 79-85.

Sloan, D.

1980: Foraminifera of Sangamon (?) estuarine deposits beneath central San Francisco Bay, California; in *Quaternary Depositional Environments of the Pacific Coast*, (ed.) M.E. Field, R.G. Douglas, A.H. Bouma, J.C. Ingle, and I.P. Coulburn; Pacific Coast Paleogeography Symposium 4, April 9, 1980, p. 1-12.

Terquem, O.

1876: Essai sur le classement des animaux qui vivent sur la plage et dans les environs de Dunkerque, pt. 1; *Mémoires de la Société Dunkerquoise pour l'Encouragement des Sciences des Lettres et des Arts (1874-1875)*, v. 19, p. 405-457.

Thompson, R.E.

1981: Oceanography of the British Columbia coast; Canadian Special Publication of Fisheries and Aquatic Sciences, v. 56, 291 p.

Williams, H.F.L.

1989: Foraminiferal zonations on the Fraser River delta and their application to paleoenvironmental interpretations; *Paleogeography, Paleoclimatology, Paleoecology*, v. 73, p. 39-50.

Geological Survey of Canada Project 860022

Implications of ^{137}Cs sediment profiles for sediment accumulation rates on the Fraser River delta foreslope, British Columbia

T.F. Moslow¹, R.W. Evoy¹, and J.L. Luternauer
Cordilleran Division, Vancouver

Moslow, T.F., Evoy, R.W., and Luternauer, J.L., 1993: Implications of ^{137}Cs sediment profiles for sediment accumulation rates on the Fraser River delta foreslope, British Columbia; in Current Research, Part A; Geological Survey of Canada, Paper 93-1A, p. 255-261.

Abstract: Sediment accumulation rates calculated for ^{137}Cs sediment profiles from piston cores in the Fraser River delta foreslope vary widely both between core locations and within individual cores. However, two general trends are apparent in the data set: sediment accumulation rates (1) decrease through time in all five piston cores; and (2) generally increase towards the Sand Heads sea valley.

The entire assayed length of piston core VEC89A-03, flanking the Sand Heads sea valley, is interpreted to be post-1963, which necessitates a minimum sedimentation rate of 4.1 cm/a adjacent to the main channel. Additional evidence of the large-scale downslope transport of sediment to the delta front includes: (1) the documentation of sediment failure up-channel from VEC89A-03; (2) an increase in ^{137}Cs concentration in the upper two sample increments of this core.

Résumé : Les taux de sédimentation calculés pour les profils sédimentaires ^{137}Cs à partir de l'examen d'échantillons prélevés par carottier à piston sur le prodelta du Fraser varient largement à la fois entre les sites de carottage et à l'intérieur même des carottes individuelles. On observe toutefois deux tendances générales dans l'ensemble de données: les taux de sédimentation 1) ont diminué avec le temps, comme l'indique l'examen de chacune des cinq carottes et, 2) ont généralement augmenté en direction de la vallée marine de Sand Heads.

Selon les interprétations, toute la longueur analysée de l'échantillon VEC89A-03 recueilli par carottier à piston, en bordure de la vallée océanique de Sand Heads, daterait d'une période postérieure à 1963, indiquant ainsi un le taux de sédimentation minimum de 4,1 cm/a à proximité du chenal principal. Les indices supplémentaires d'un important transport sédimentaire en aval jusqu'au front du delta, comprennent : 1) des preuves de la rupture des sédiments en amont du chenal, à partir de VEC89A-03 et, 2) un accroissement de la concentration de ^{137}Cs dans les deux portions supérieures échantillonnées de cette carotte.

¹ Department of Geology, University of Alberta, #1-26 Earth Sciences Building, Edmonton, Alberta T6G 2E3

INTRODUCTION

This study presents a preliminary interpretation of sediment accumulation rates in the Fraser River delta foreslope as determined from Cs-137 profiles. The database consists of subsamples from piston cores collected during a 1989 research cruise of the **CSS Vector**, and constitutes one aspect of the Geological Survey of Canada's ongoing research into environmental and geohazards assessment of the Fraser River delta slope. The specific objective of this study was to determine temporal and spatial variability in rates and patterns of sediment accumulation on the delta slope. Where previous studies have focused on Holocene accretion of the delta (Williams and Roberts, 1988, 1990; Clague et al., 1991; Hart et al., 1992) and diurnal to annual fluctuations in sediment dynamics (Kostaschuk et al., 1989), this study focuses on patterns and variations in sediment accumulation rates over a 36 year period from 1954 through 1989 (Moslow et al., 1991).

The study area for this project consists of a 20 km by 7.5 km section of the delta foreslope (Fig. 1), and overlaps with previous studies by Kostaschuk et al. (1992) and Hart et al. (in press). Water depths within this area range from less than 50 m to greater than 200 m over approximately 3.0 km horizontal distance, and at an average gradient exceeding 3.0°. Concern over the stability of this slope in response to seismic and/or sediment loading has provided the impetus for this and related studies aimed at improving the database necessary for informed development or environmental decisions.

PREVIOUS WORK: Cs-137 SEDIMENT ACCUMULATION RATES

Cesium-137 is a radiogenic isotope produced as a byproduct of the testing of nuclear weapons, and is not known to occur naturally. Global distribution of Cs-137 in surface sediments therefore represents fallout from atmospheric testing.

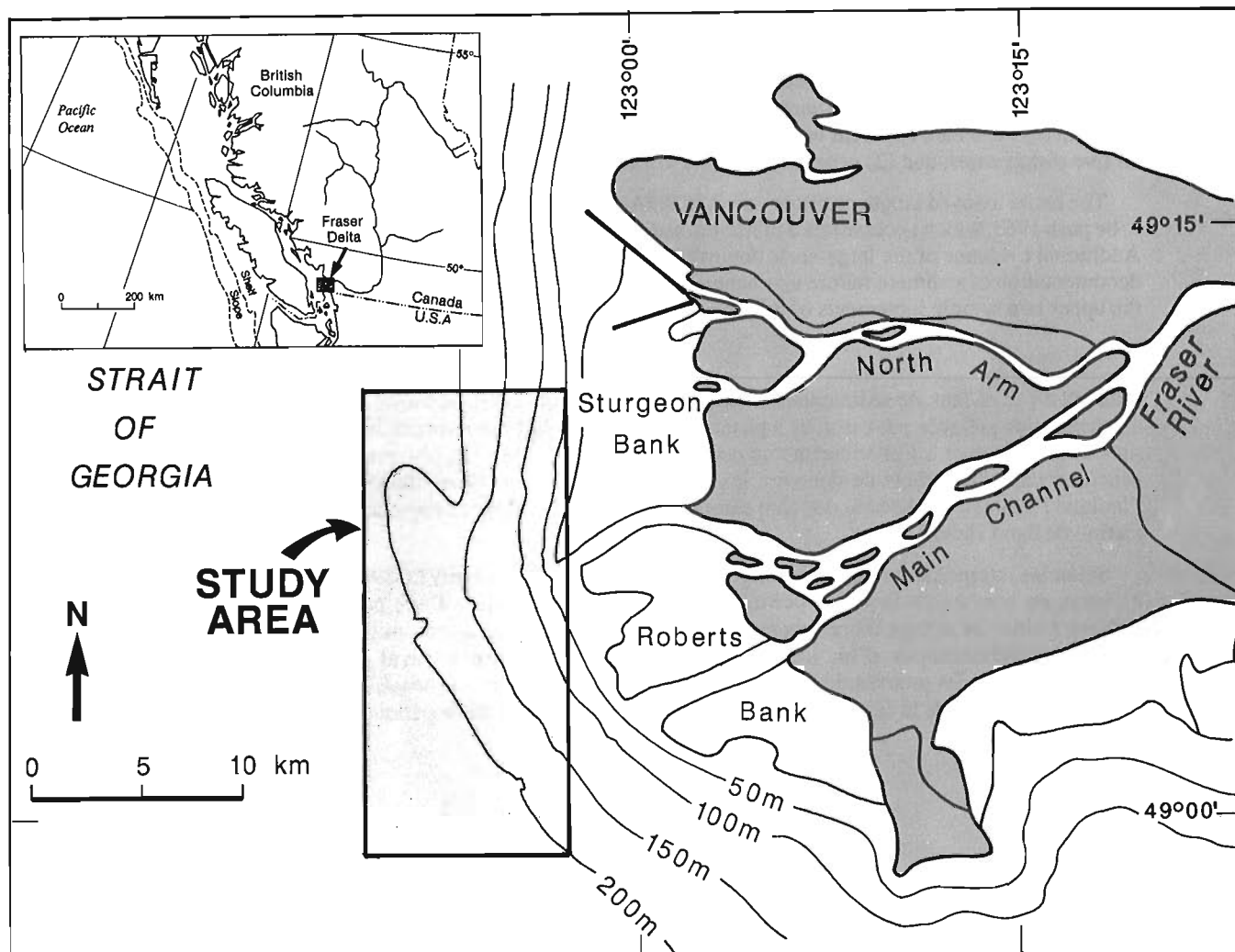


Figure 1. Study area location map. Area enclosed within rectangular box is detailed in Figure 2. (Modified from Moslow et al., 1991; Kostaschuk et al., 1992).

Vertical accretion rates of recent sediments in the Fraser delta foreslope can thus be approximated based on Cs-137 distribution in soil profiles.

The assumptions made in calculating sedimentation rates are:

1. first appearance of Cs-137 represents the initiation of widespread atmospheric testing in 1954;
2. peak Cs-137 concentrations reflect the resumption of testing in 1963 after a brief hiatus; and
3. tailing effects of relatively low concentrations due to bioturbation are negligible in the study area.

From detailed sedimentological descriptions of piston cores used in this study, it was observed that the cored intervals selected are conformable, with no reduction due to erosion, and were essentially nonburrowed (Moslow et al., 1991).

METHODOLOGY

Five of 18 piston cores collected from the Fraser River delta foreslope during the **CSS Vector** 1989 cruise were selected for subsampling and analyzed for Cs-137 content. The cores selected represent a variety of depositional settings and sedimentation rates in the area. Sediment subsampling began at the sediment-water interface, and was continued to the estimated maximum depth at which concentrations of Cs-137 could be anticipated. With the exception of core VEC89A-03, all samples were counted until at least one barren core increment, which was not sand-rich, was encountered. This ensured that all cores except VEC89A-03 were sampled through the first appearance of Cs-137.

Analytical work for this study was carried out by the Saskatchewan Institute of Pedology, University of Saskatchewan, following the methodology of DeJong et al. (1982). Cs-137 counting equipment consisted of a high-purity Ge-crystal coupled to a 4096 Multichannel Analyzer (MCA). Equipment was calibrated using a certified solution of Cs-137 in a carrier solution of CsCl in HCl. Soil standards were prepared by mixing known amounts of the water standard with Cs-137 free soils or peat.

Counting efficiency depends on detector efficiency and the amount of radiation reaching the detector, which in turn depends on self-adsorption and is a function of sample volume and density. Compositionally similar sediment was encountered in all intervals sampled, it was therefore possible to pack all samples to approximately the same volume and density. The gamma radiation adsorption coefficient is thus effectively constant.

Cs-137 concentrations are reported as histograms of activity (Bq/kg) per unit interval. Sedimentation accumulation rates were then calculated based on first appearance and maximum concentrations of Cs-137, which represent 1954 and 1963, respectively. Histograms were compared to lithology and sediment texture to test for any depositionally mediated controls over concentration.

As the sample intervals chosen exceeded annual sedimentation rates, it was not possible to exactly position either 1954 or 1963. Consequently, sedimentation rates were calculated from the midpoint of the intervals representing first appearance and maximum accumulation, with the sediment-water interface as the 1989 datum. This obviates the necessity of presenting all sedimentation rates as ranges.

RESULTS: SEDIMENT PROFILES

VEC89A-03

Core VEC89A-03 was collected from the flank of the Sand Heads' Channel at a water depth of 190 m (Fig. 2), and constitutes two distinct coarsening- and thickening-upward cycles resulting from channel migration. Only the upper cycle was subsampled for Cs-137 analysis. Samples were collected at 5 cm intervals to a depth of 105 cm (base of cycle 1). This core consists of graded fine- to medium-grained sands exhibiting wavy and lenticular bedding and containing rafted organic material and clayey-silt interbeds (Fig. 3).

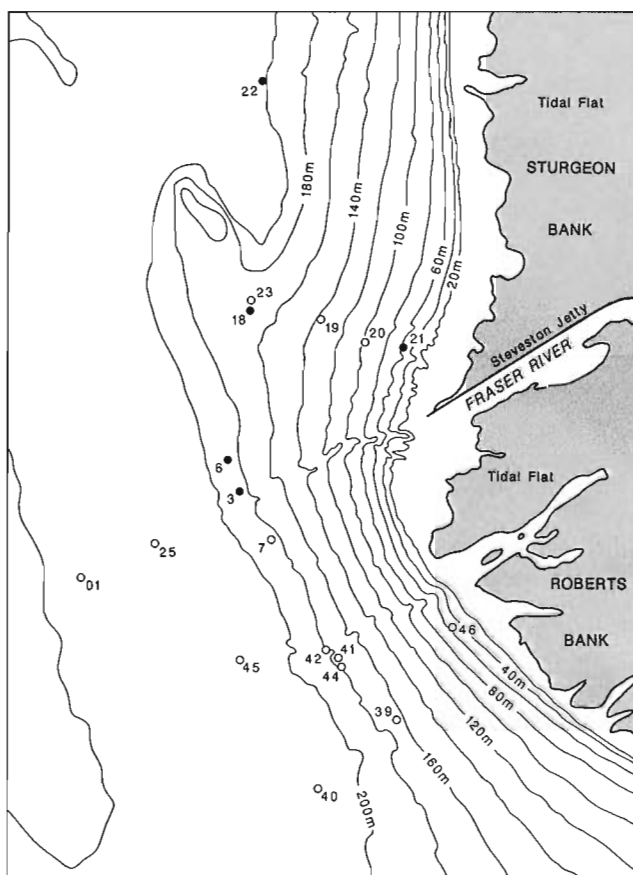


Figure 2. Detailed bathymetry and piston core site locations in the study area. Piston core sites with Cs-137 data available are represented with closed circles.

The sampled interval did not penetrate the base of the Cs-137 horizon, consequently only a minimum sedimentation rate over the interval can be calculated. Assuming that the top of the core represents a 1989 datum,

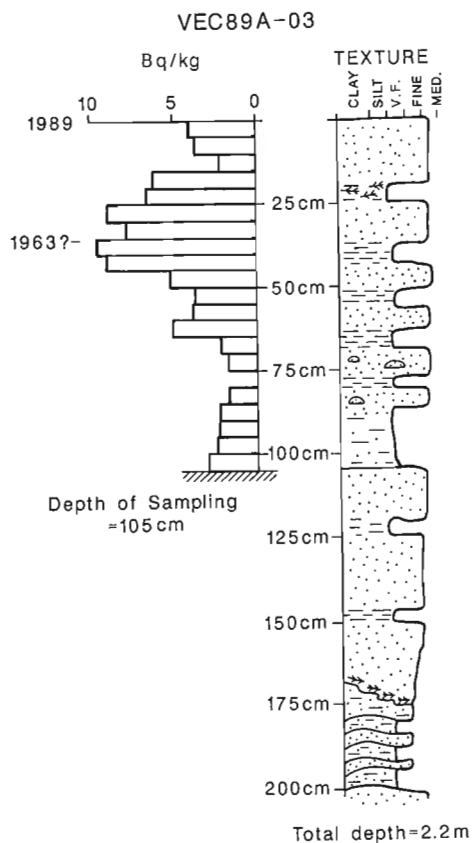


Figure 3. Cs-137 sediment profiles and sedimentological log for piston core VEC89A-03.

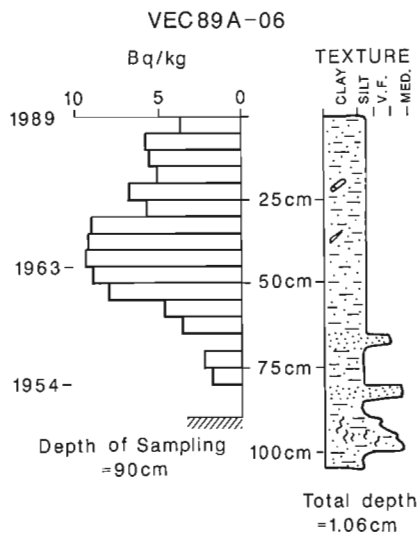


Figure 4. Cs-137 sediment profiles and sedimentological log for piston core VEC89A-06.

accumulation of 105 cm of sediment during the past 36 years (1954 to 1989) necessitates sedimentation rates in excess of 2.92 cm/a.

If the maximum concentration encountered in the core represents the 1963 value, the underlying 65 cm of sediment must have accumulated over a maximum 9 year period. This results in a calculated minimum sediment accumulation rate exceeding 7.22 cm/a. An increase in Cs-137 concentration

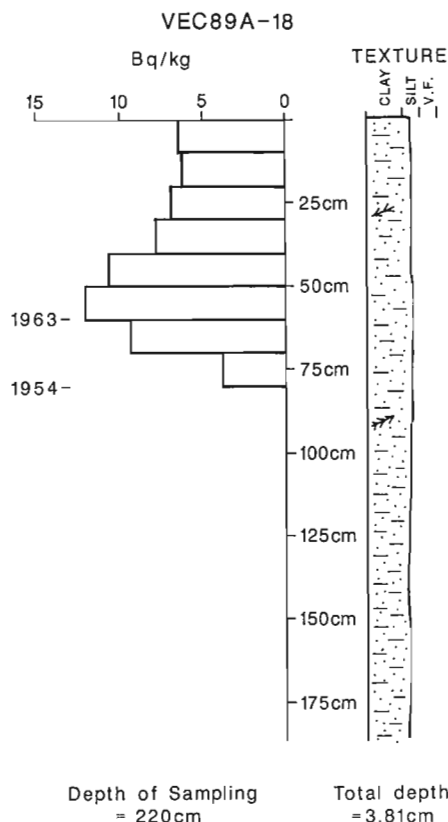
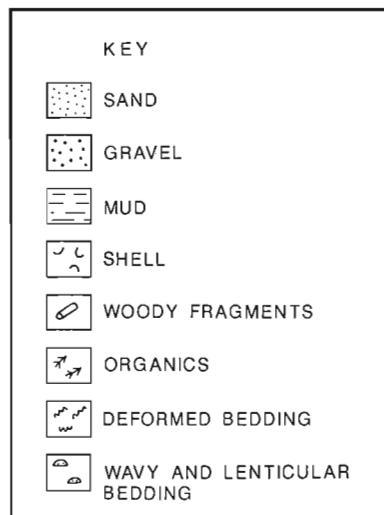


Figure 5. Cs-137 sediment profiles and sedimentological log for piston core VEC89A-18.



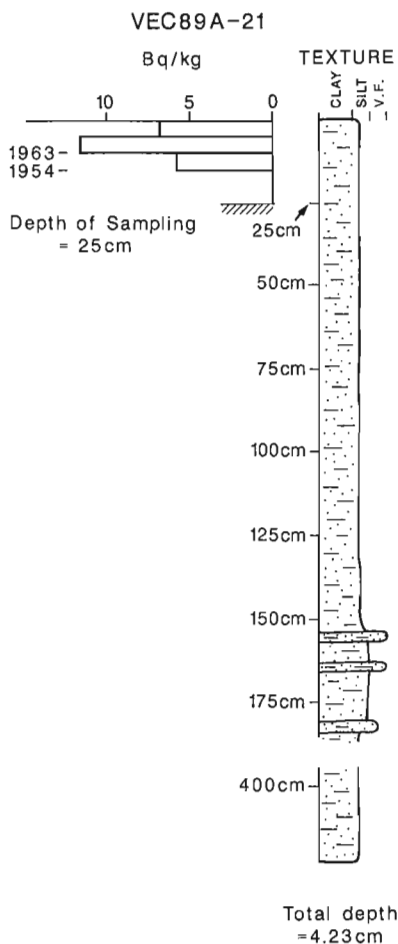


Figure 6. Cs-137 sediment profiles and sedimentological log for piston core VEC89A-21.

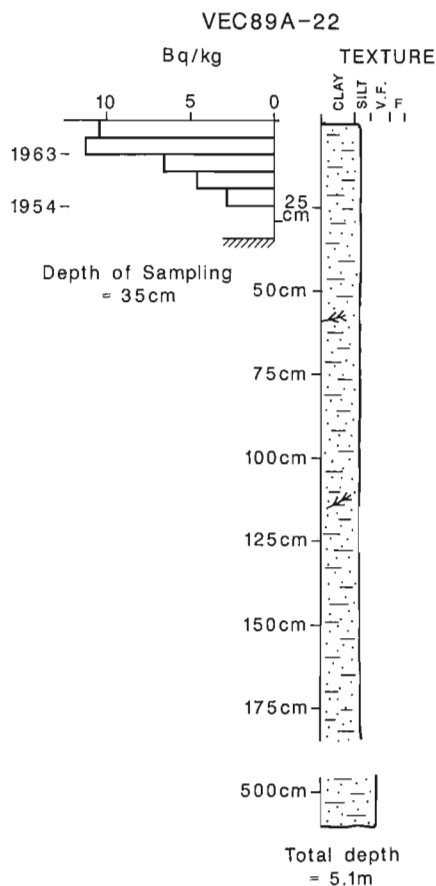


Figure 7. Cs-137 sediment profiles and sedimentological log for piston core VEC89A-22.

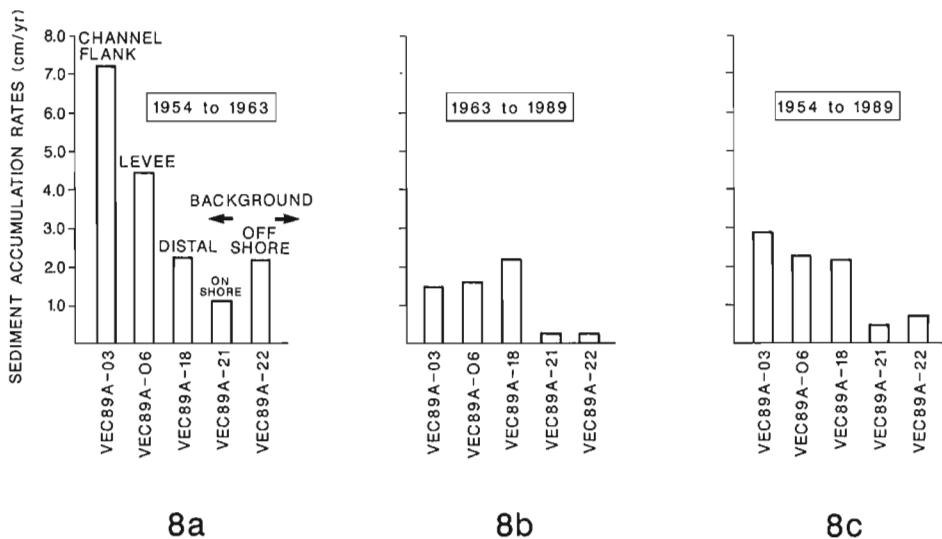


Figure 8. Histograms plotting variation in sediment accumulation rates from selected sites on the Fraser River delta through time. Note overall decrease in sediment accumulation rates through time and general decrease laterally away from the Sand Heads sea valley. **a)** Sediment accumulation rates for time period 1954 to 1963. **b)** Sediment accumulation rates for time period 1963 to 1989. **c)** Cumulative sediment accumulation rate, 1953 through 1989.

was noted in the upper two sample increments (10 cm) of the core, and is atypical of sediment profiles in the Fraser River delta area to date. This anomaly may reflect redeposition of older sediment from upslope via sediment-gravity flow processes, as proposed by Kostaschuk et al. (1992) and Hart et al. (in press).

VEC89A-06

Core VEC89A-06 was collected from a water depth of approximately 190 m, some 800 m north of VEC89A-03 and the Sand Heads valley (Fig. 2). This core consists primarily of massive silty-clay and clayey-silt with thin, silty, very fine- to fine-grained sands which exhibit graded bases and abrupt tops (Fig. 4), and the entire interval constitutes a poorly defined fining upward cycle interpreted as a sequence of levee and overbank flow deposits associated with breaching of the main channel levees.

The core was subsampled at 5 cm intervals to a depth of 90 cm; base of detectable Cs-137 concentration occurs at a depth of either 80 or 85 cm. The reason for this uncertainty is that the barren interval from 80 to 85 cm is composed predominantly of fine quartz sand. Other intervals of similar grain size and lithology show a marked suppression of Cs-137 values. The strongest correlation between Cs-137 and grain size and composition in the study area is the barren interval between 65-70 cm in this core. This interval consists of very fine sand composed predominantly of quartz with lesser mafic fragments and feldspar and subordinate mica. Clay minerals are virtually absent in this interval.

A minimum sedimentation rate of 2.29 cm/a can be calculated for core VEC89A-06 (Table 1). Peak Cs-137 concentration in the core was encountered in the increment from 40 to 45 cm and is interpreted as the 1963 peak. Accumulation of 40 to 45 cm of sediment between 1963 and 1989 represents a sedimentation rate of 1.57 cm/a.

Sediment in the basal portion of the subsampled core interval includes a minor component of coarser grained material, likely resulting from overbank flow or unconfined turbidity currents breaching the Sand Heads sea valley. The calculated rate of accumulation for the period 1954 to 1963 is 4.44 cm/a.

VEC89A-18

Deposition of core VEC89A-18 occurred in a slight saddle on the lower delta foreslope in a water depth of 170 m (Fig. 2). This core consists of a dense and compacted, black clayey-silt with few shell fragments and minor disseminated organic matter (Fig. 5). Samples collected for Cs-137 analysis in VEC89A-18 were taken over 10 cm intervals, the only samples at this increment in the study. The base of measurable Cs-137 concentrations occurs at a depth of either 70 to 80 cm or 80 to 90 cm. This uncertainty reflects a possible "trace" Cs-137 reported by the laboratory in the latter interval.

This core represents the first of the five sampled to be analyzed for Cs-137; results have been discussed previously (Moslow et al., 1991). Sediment accumulation rates, recalculated using the 1954 datum for first appearance, are a constant 2.22 cm/a throughout.

VEC89A-21

Core VEC89A-21 was deposited in an interchannel or levee environment in relatively shallow water (50 m) on the upper foreslope (Fig. 2). This core consists of massive silty clay with rare silty laminations. The section subsampled for Cs-137 represents deposition of sediment from suspension. The base of the subsampled interval is at 25 cm (Fig. 6); basal Cs-137 concentration occurs at a depth of 15 to 20 cm. Minimum sedimentation rate for the period 1954 to 1989 is 0.49 cm/a.

Maximum Cs-137 concentration occurs in the interval 5 to 10 cm, reflecting much slower accumulation rates post-1963 (0.28 cm/a) as opposed to the period 1954 through 1963 (1.11 cm/a). There is no sedimentological evidence to support a change in sediment accumulation pattern or rate in core from this interval, and we suggest that finer sample increments are necessary to resolve sedimentation rates.

VEC89A-22

Core VEC89A-22 accumulated in a prodelta to basinal environment in a water depths of 206 m (Fig. 2). Internal sedimentary structure consists of massive silty clay to clayey-silt with rare silty laminations and minor rafted organic debris (Fig. 7). The depositional process was settling of sediment from suspension.

Samples collected for Cs-137 analysis were taken over 5 cm increments to a depth of 35 cm. The basal Cs-137 concentration occurs at a depth of 25 to 30 cm; therefore minimum sedimentation rate for the period 1954 to 1989 is 0.76 cm/a. Maximum concentration, as in VEC89A-21, occurs in the interval 5 to 10 cm, reflecting low post-1963 accumulation rates (0.28 cm/a). Accumulation rates for the period 1954 through 1963 are calculated to be 2.22 cm/a.

Table 1. Calculated sediment accumulation rates for piston cores from the Fraser River delta foreslope

Piston core	1954-1963	1963-1989	1954-1989
VEC89A-03	7.22 cm/a	1.48 cm/a	2.92 cm/a
VEC89A-06	4.44 cm/a	1.57 cm/a	2.29 cm/a
VEC89A-18	2.22 cm/a	2.22 cm/a	2.22 cm/a
VEC89A-21	1.11 cm/a	0.28 cm/a	0.49 cm/a
VEC89A-22	2.22 cm/a	0.28 cm/a	0.76 cm/a

DISCUSSION

Sediment accumulation rates calculated for cores from the Fraser delta foreslope exhibit a wide degree of variation both between piston core locations, and through time. Two general temporal/spatial patterns are evident in the data set. Sediment accumulation rates typically decrease through time, and generally increase towards the Sand Heads' valley (Fig. 8).

In piston core VEC89A-03, the peak Cs-137 concentration was encountered in the increment from 35 to 40 cm (Fig. 3). Global peak concentrations represent fallout from 1963 testing (Ashley, 1977; Pennington et al., 1973). The accumulation of 40 cm of sediment over a 27 year period from 1963 to 1989 requires a minimum sediment accumulation rate of 1.48 cm/a, a relatively low value. However, this interval corresponds to the thickest, coarsest sequence recovered, and should be anticipated to reflect the highest sedimentation rates in the entire study area.

Two possible explanations for this may be postulated. If the entire assayed assemblage is post-1963, this would necessitate a minimum sedimentation rate of 4.1 cm/a since 1963, which is realistic given the calculated accumulation rate for the pre-1963 sequence (7.22 cm/a). Alternatively, the top of the upper interval may have been reduced by erosion. Evidence in support of the latter includes the documentation of large scale sediment failures which have moved up to 10^6 m^3 of sediment in individual events up-channel from the core site (McKenna and Luternauer, 1987; Kostaschuk et al., 1992).

With the exception of piston core VEC89A-18, there is a marked decrease in sediment accumulation rates post-1963. This pattern holds true in the upper foreslope (site 21), proximal to the Sand Heads sea valley in the lower delta foreslope (sites 03, 06), and in the prodelta (site 22). The significance of this observation is not evident, and requires further study to test for any positive correlation with cultural constraints. The regional nature of this observation argues against a local explanation for this related to avulsion in the Sand Heads sea valley.

ACKNOWLEDGMENTS

Numerous comments and criticisms by Bruce Hart and Tark Hamilton have helped to improve and clarify this manuscript, and are gratefully acknowledged. Funding was provided by EMR and NSERC grants to T.F.M. (Research Agreement No. 034 4 92).

REFERENCES

- Ashley, G.M.**
1977: Sedimentology of a freshwater tidal system. Pitt River-Pitt Lake, British Columbia; Ph.D. dissertation, University of British Columbia, Vancouver, 234 p.
- Clague, J.J., Luternauer, J.L., Pullan, S.E., and Hunter, J.A.**
1991: Postglacial deltaic sediments, southern Fraser River delta, British Columbia; Canadian Journal of Earth Sciences, v. 28, p. 1386-1393.
- DeJong, E., Villar, H., and Bettany, J.R.**
1982: Preliminary investigations on the use of ^{137}Cs to estimate erosion on Saskatchewan; Canadian Journal of Soil Science, v. 62, p. 673-683.
- Hart, B.S., Prior, D.B., Barrie, J.V., Currie, R.G., and Luternauer, J.L.**
in press: A river mouth submarine channel and failure complex, Fraser Delta, Canada; Sedimentary Geology.
- Hart, B.S., Prior, D.B., Hamilton, T.S., Barrie, J.V., and Currie, R.G.**
1992: Patterns and styles of sedimentation, erosion and failure, Fraser Delta slope, British Columbia; in Geotechnique and Natural Hazards: Proceedings of First Canadian Symposium on Geotechnique and Natural Hazards; Canadian Geotechnical Society, p. 365-372.
- Kostaschuk, R.A., Luternauer, J.L., McKenna, G.T., and Moslow, T.F.**
1992: Sediment transport in a submarine channel system: Fraser River Delta, Canada; Journal of Sedimentary Petrology, v. 62, p. 273-282.
- Kostaschuk, R.A., Stephan, B.A., and Luternauer, J.L.**
1989: Sediment dynamics and implications for submarine landslides at the mouth of the Fraser River, British Columbia; in Current Research, Part E; Geological Survey of Canada, Paper 89-1E, p. 207-212.
- McKenna, G.T. and Luternauer, J.L.**
1987: First documented large failure at the Fraser River delta front, British Columbia; in Current Research, Part A; Geological Survey of Canada, Paper 87-1A, p. 919-924.
- Moslow, T.F., Luternauer, J.L., and Kostaschuk, R.A.**
1991: Patterns and rates of sedimentation on the Fraser River delta slope, British Columbia; in Current Research, Part E; Geological Survey of Canada, Paper 91-1E, p. 141-145.
- Pennington, W., Cambray, R.S., and Fisher, E.M.**
1973: Observations on lake sediments using fallout ^{137}Cs as a tracer; Nature, v. 242, p. 324-326.
- Williams, H.F.L. and Roberts, M.C.**
1988: Holocene sea-level change and delta growth: Fraser River delta, British Columbia; Canadian Journal of Earth Sciences, v. 26, p. 1657-1666.
- 1990: Two middle Holocene marker beds in vertically accreted floodplain deposits, lower Fraser River, British Columbia; Geographie physique et Quaternaire, v. 44, p. 27-32.

Geological Survey of Canada Project 860022

A delta topset sheet sand and modern sedimentary processes in the Fraser River delta, British Columbia

P.A. Monahan¹, J.L. Luternauer, and J.V. Barrie²
Cordilleran Division, Vancouver

Monahan, P.A., Luternauer, J.L., and Barrie, J.V., 1993: A delta topset sheet sand and modern sedimentary processes in the Fraser River delta, British Columbia; in Current Research, Part A; Geological Survey of Canada, Paper 93-1A, p. 263-272.

Abstract: Borehole data in the Fraser River delta demonstrate that a nearly continuous unit of sand, generally 10 to 20 m thick, underlies the surficial silts of the subaerial delta plain. The sand is arranged into one or more sharp-based fining-upward sequences, and is interpreted to be a complex of distributary channel deposits. Historically, distributary channel migration to accommodate the accumulation of channel sands has only been recorded where distributaries cross the tidal flats. However, stratigraphic sequences that represent channel migration across both the tidal flats and the subaerial delta plain have been tentatively identified in cores.

Résumé : Les données fournies par les sondages effectués dans le delta du Fraser démontrent qu'une unité presque continue de sable, généralement de 10 à 20 m d'épaisseur, est recouverte par les silts superficiels de la plaine deltaïque subaérienne. Les sables sont disposés selon une ou plusieurs séquences à granulométrie normale dont la base est très nettement délimitée, et que l'on considère un complexe alluvial qui se serait accumulé dans des défluent. Au cours des temps historiques, on a noté que la migration des défluent suite à l'accumulation des sables fluviaux ne se produisait qu'aux endroits où ces défluent traversent l'estran. Toutefois, on a cherché à identifier provisoirement dans les carottes les séquences stratigraphiques qui représentent la migration des défluent à travers l'estran et à travers la plaine deltaïque subaérienne.

¹ School of Earth and Ocean Sciences, University of Victoria, P.O. Box 1700, Victoria, B.C. V8W 2Y2

² Pacific Geoscience Centre, Sidney

INTRODUCTION

Subsurface geological mapping of the Holocene Fraser River delta was initiated in part to provide a long term perspective of the sedimentary processes operating on the delta. Since the sediments are the result of these processes, they should provide a record consistent with processes observed and inferred from geomorphological evidence. The objective of this preliminary report is to demonstrate that distributary channel sand deposits form a nearly continuous composite sand unit underlying the subaerial delta plain and thus are much more extensive than previously recognized, and to comment on the implications of this conclusion.

SETTING

The Fraser River is the largest river on Canada's west coast and has constructed a delta with a topset area of 1000 km². The delta plain includes the southern portions of the Greater Vancouver urban area as well as key industrial and transportation facilities. Recent investigations of this important area have focused on the effects of human activities on deltaic processes and on geological hazards that could affect the region.

The modern delta appears to be entirely Holocene in age (Clague et al., 1983; Williams and Roberts, 1989). It comprises: a subaerial plain that extends 23 km west from a gap in the Pleistocene uplands at New Westminster and is mantled by silt and peat; a band of dominantly sandy tidal flats up to 9 km wide; and a foreslope that descends at an average slope of 1.5° to depths of 300 m in the Strait of Georgia (Fig. 1) and that is dominantly silty to the north and sandy to the south of the Main Channel (Fig. 1; Clague et al., 1983, 1991). The river divides into four distributaries where it crosses the delta plain. The annual sediment load is reported to be 12 to 30 million tons, of which 40% is sand (Milliman, 1980).

PREVIOUS WORK

Although the Fraser delta has been extensively studied (Johnston, 1921; Mathews and Shepard, 1962; Clague et al., 1983; Luternauer, 1980; Hart et al., 1992, in press), there have been few investigations of the subsurface stratigraphy. Clague et al. (1983) incorporated subsurface data into their interpretation, but no cone penetration tests (CPTs) were available at the time. Roberts et al. (1985) reported on a shallow coring program that focused on the southern part of

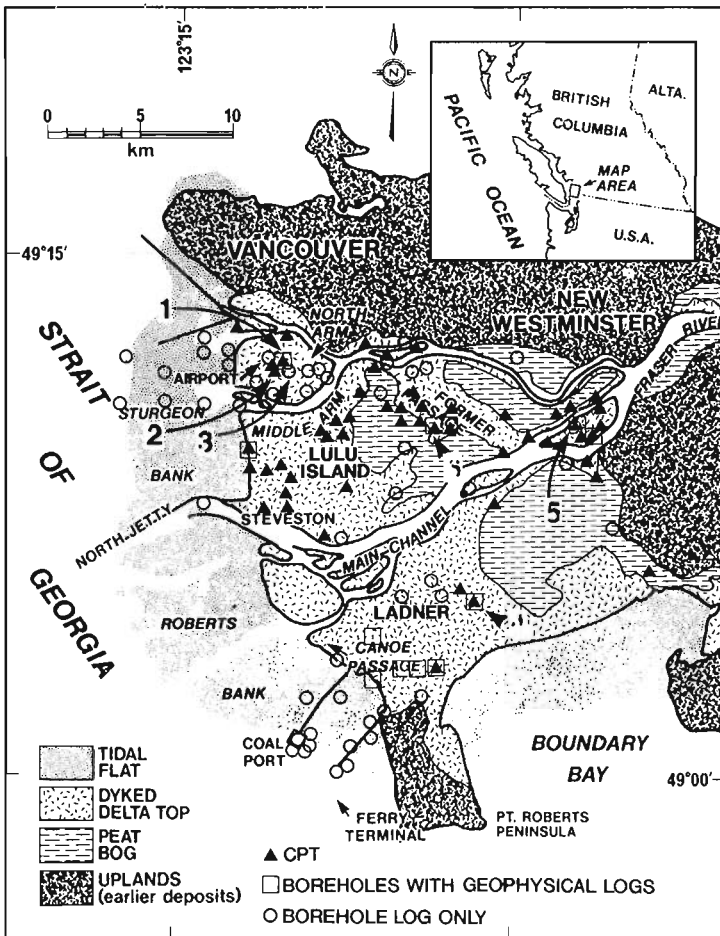


Figure 1.

Location and sedimentary setting of the Fraser River delta, showing the location of borehole data and of sites referred to in this paper: 1, location of borehole in Figure 2; 2, location of borehole in Figure 3; 3, location of borehole in Figure 4; 4, location of borehole east of Ladner; 5, location of Figure 8; 6, location of borehole in Figure 9.

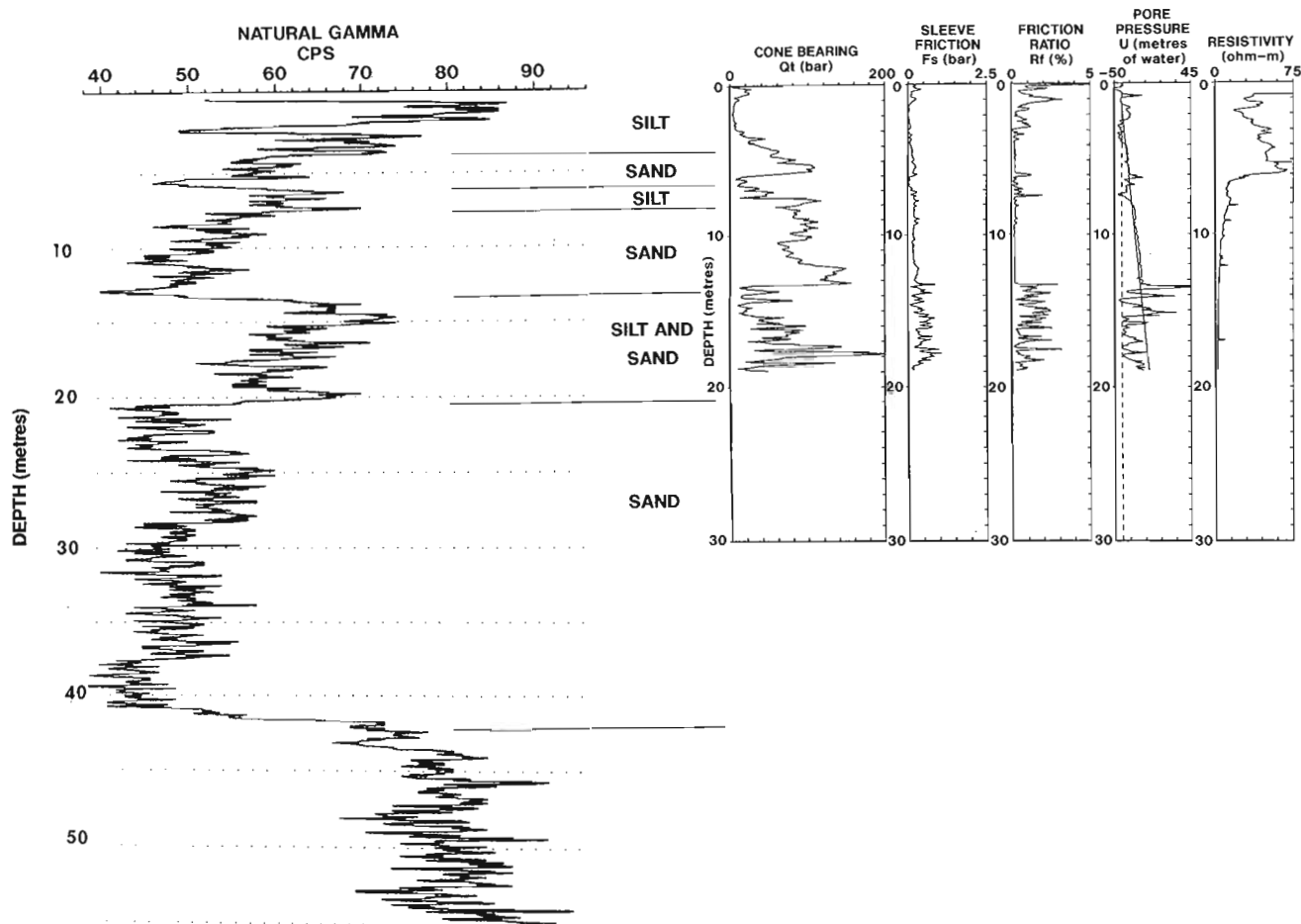


Figure 2. Comparison of a Cone Penetration Test and a gamma ray log from an adjoining borehole at the Vancouver International Airport. Vertical scale in metres. See Figure 1 for location.

the delta. Williams and Roberts (1989, 1990) investigated the topset deposits in Lulu Island in a series of shallow boreholes, and documented the chronology of the mid- to late Holocene sea-level rise from the depth and thickness of floodplain silts. In the southernmost portion of the delta, the Geological Survey of Canada and Simon Fraser University have drilled ten boreholes and acquired 45 km of seismic reflection data (Clague et al., 1991; Jol and Roberts, 1988, 1992; Luternauer, 1988, 1990; Luternauer et al., 1986, 1991; Pullan et al., 1989; Patterson and Cameron, 1991). In recent years, these drilling programs have been expanded to other areas of the delta. Furthermore, the Geological Survey of Canada has acquired CPTs and seismic refraction data at selected sites to contribute to the assessment of the regional liquefaction potential in the delta (Finn et al., 1989; Hunter et al., 1991, 1992). Recently, Watts et al. (1992) published a CPT cross-section demonstrating the utility of this data for stratigraphic purposes.

DATABASE

This study is based primarily on boreholes drilled by Geological Survey of Canada and engineering test holes, in particular cone penetration tests (CPTs; Fig. 1). The GSC has drilled 17 boreholes throughout the delta since 1986. Of those 13 have been logged by geophysical methods - including gamma ray - and the last 9 have been continuously cored. These boreholes provide excellent data, but they are unevenly distributed across the delta. A large number of engineering test holes exist (see Mustard and Roddick, 1992, for those drilled prior to 1973), but most have been discontinuously sampled. In contrast, CPTs, which have been conducted since the early 1980s (Finn et al., 1989), continuously and consistently record various physical properties of the sediment penetrated. Combined with data from adjoining boreholes they provide consistent and correlatable stratigraphic data (Campanella et al., 1983). We have obtained CPTs at over 50 sites widely distributed across the delta. Although some of these were acquired by the GSC, most were acquired for engineering purposes.

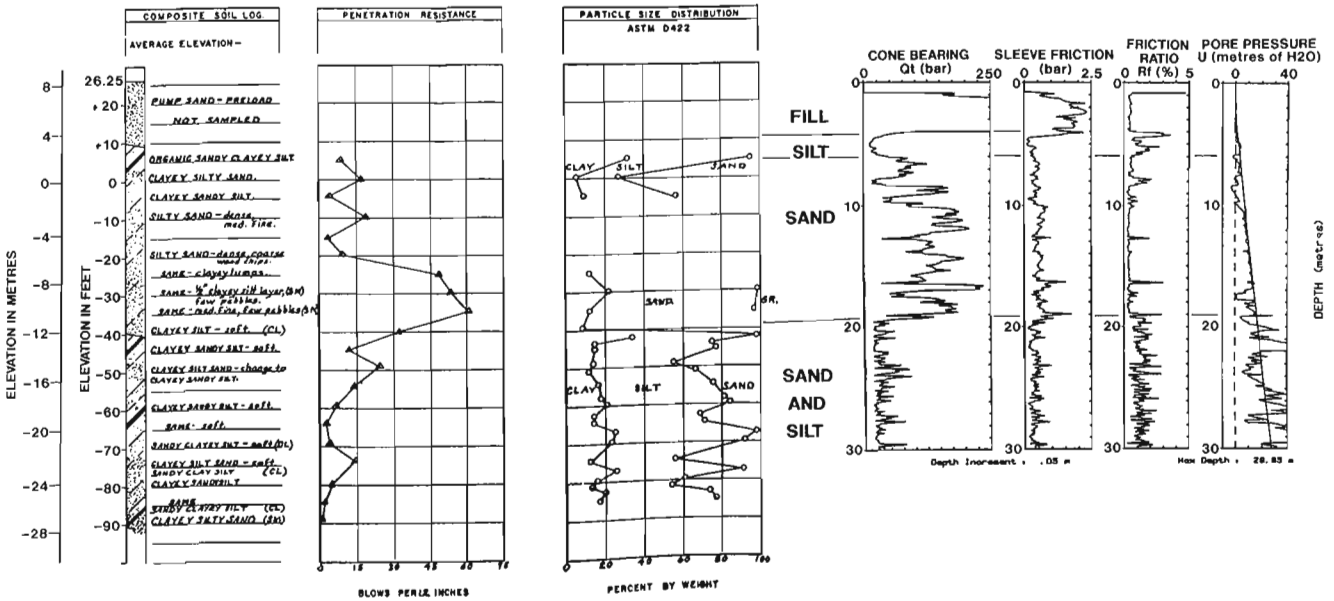


Figure 3. Comparison of a Cone Penetration Test and data from an offsetting borehole, Main terminal Building, Vancouver International Airport. Scale of the CPT in metres: note original scale of the borehole log in feet. Courtesy of Transport Canada and the Vancouver Airport Authority. Grain size data from sieve analysis. See Figure 1 for location.

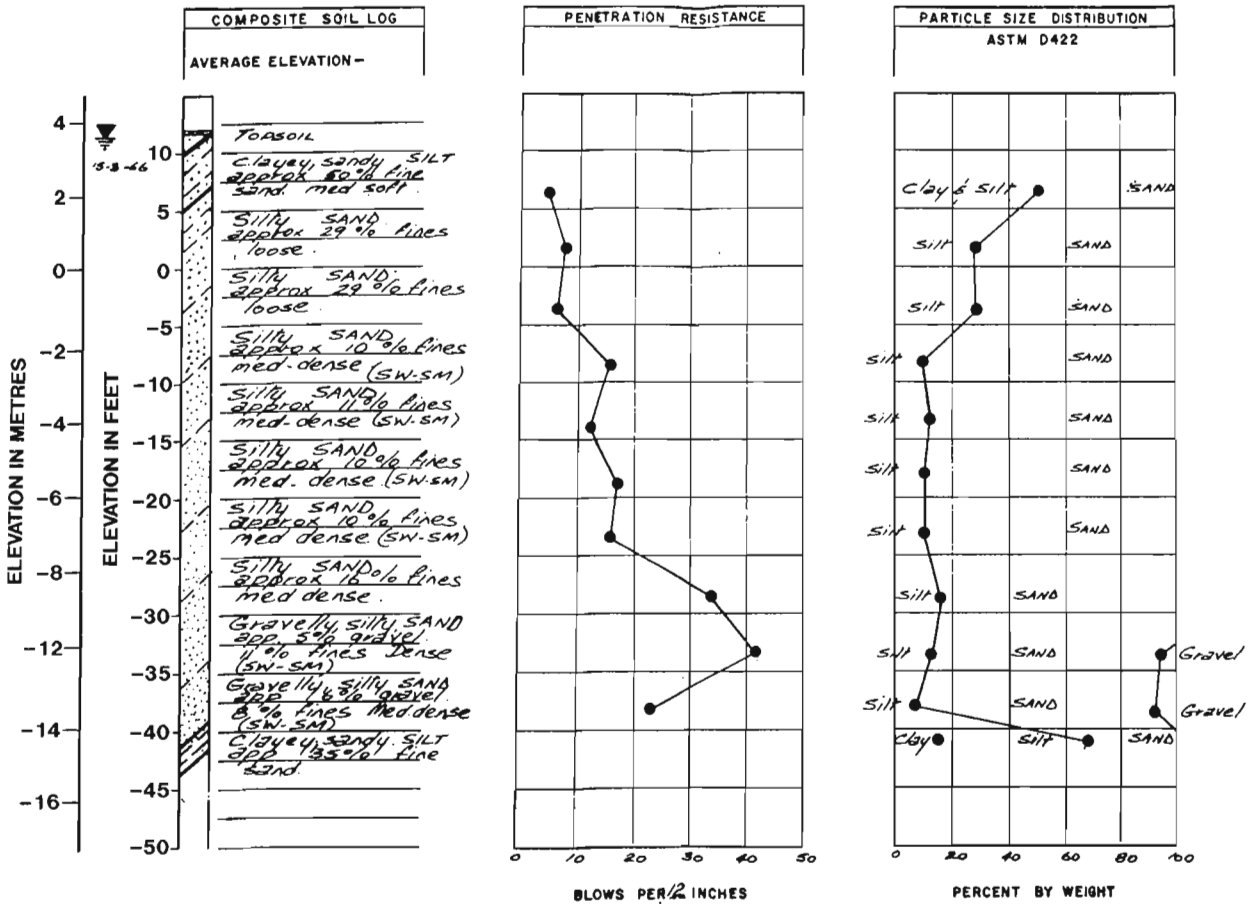


Figure 4. Borehole log, Sewer Pumphouse, Vancouver International Airport. Note original scale in feet. Courtesy of Transport Canada and the Vancouver Airport Authority. Grain size data from sieve analysis. See Figure 1 for location.

RESULTS

Cone penetration tests can be used for stratigraphic interpretations in a manner comparable to geophysical borehole logs. A comparison of a CPT and a gamma ray log from an adjoining GSC borehole at the Vancouver International Airport is shown in Figure 2. The sand and silt units observed in the borehole can be readily recognized on the gamma ray log as well as on the "cone bearing" and "friction ratio" curves on the CPT. In particular, the "friction ratio" is similar to the gamma ray curve, with sands having low values and finer sediments causing deflections to the right. At this site, the core, the gamma ray log, and the CPT demonstrate that the sands in the upper 15 m are arranged into two sharp-based fining-upward sequences. Pebbles were observed in this core at the base of these sequences.

A similar sharp-based fining-upward sequence can be recognized in a CPT and an older borehole log from a nearby site at the Airport (Fig. 3), which in this case was sampled closely enough to record the abrupt base of the sand unit. Here too, there is a gravel component in the lower part of the sand. Another borehole log from the Airport (Fig. 4) also records the sharp base of the sand unit and the upward fining, from sand with gravel at the base to silty sands at the top.

The sand in the delta topset is arranged into one or, less commonly, more fining-upward sequences in nearly every borehole and log in the subaerial delta plain. The sand thus forms a nearly continuous unit that is generally 10 to 20 m

thick and that has a sharp base with several metres of local relief (Fig. 5 and 6). The sands range from fine to coarse, and commonly have a gravel component.

The east-west cross-section (Fig. 6) also shows how the sand unit climbs and the overlying upper tidal flat and floodplain silt unit thins from east to west, reflecting the rise in sea level as the delta prograded westward (Williams and Roberts, 1989). In the second log from the east end of this section, an upper sharp-based fining-upward sand unit also occurs near the top between 4 and 12 m. In the easternmost log the upper and lower sands observed in the log to the west have merged to form an unbroken sand unit 40 m thick. Gravel was reported in nearby boreholes in the lower 5 m of the sand.

DISCUSSION

The arrangement of sands into sharp based fining-upward sequences is typical of channel deposits. The sharp irregular base indicates an erosional contact. In contrast, surficial deposits at the present delta front appear to grade down from sands on the tidal flats to silts on the foreslope (Luternauer and Murray, 1973; Hart et al., in press). The delta topset sands are interpreted to be distributary channel sands rather than tidal channel deposits. Coarse sand and gravel size material occur in distributary channels and not normally in other environments (Clague et al., 1983). Furthermore, the overall thickness is generally consistent with the depth of distributary channels. The sand unit at the top of the second

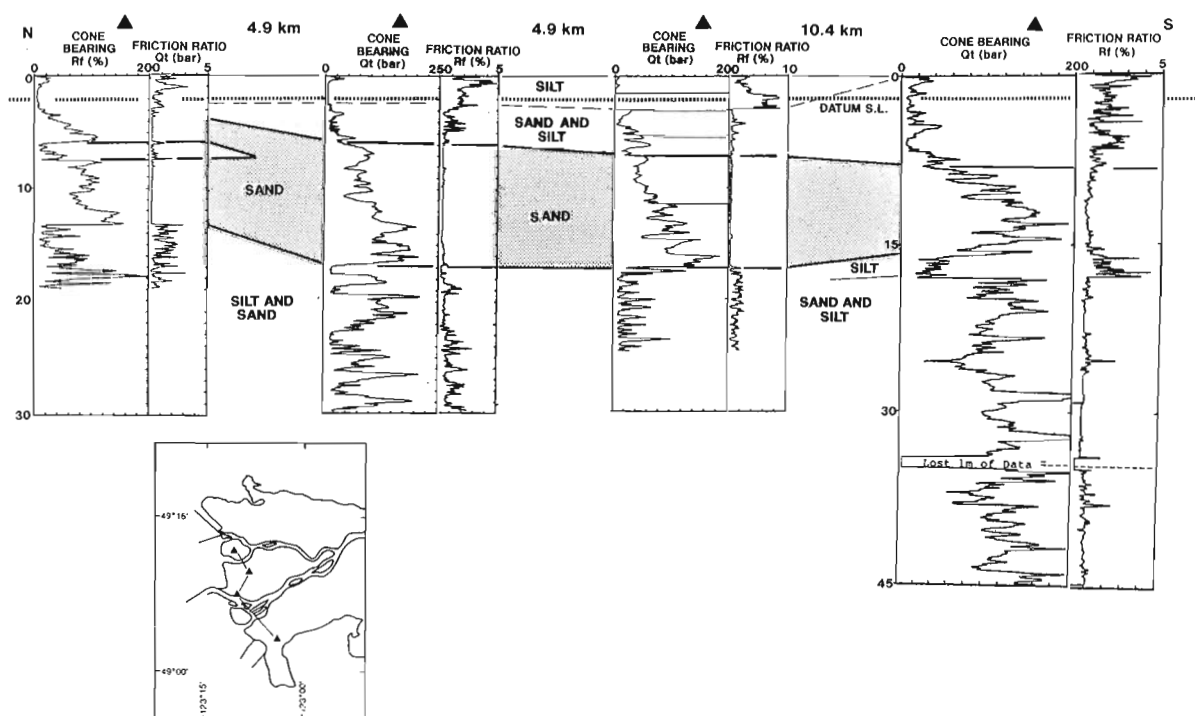


Figure 5. Fraser delta: north-south CPT cross-section along western margin of subaerial plain. The southernmost log directly offsets GSC borehole 87-1, reported by Luternauer et al. (1991), and Clague et al. (1991). Vertical scale in metres.

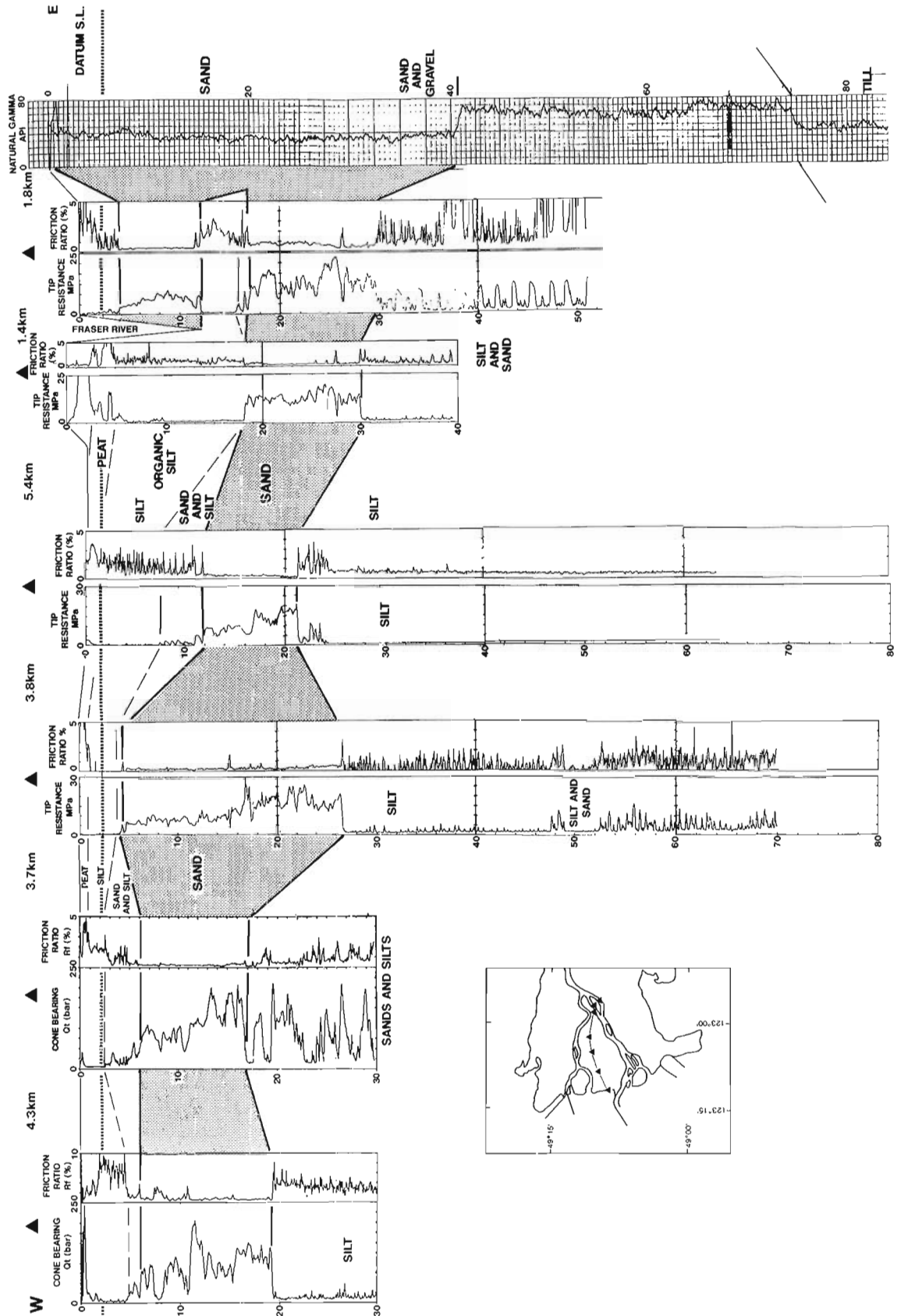


Figure 6. Fraser delta: east-west CPT cross-section across subaerial delta plain. Vertical scale in metres. The easternmost log is a gamma ray log.

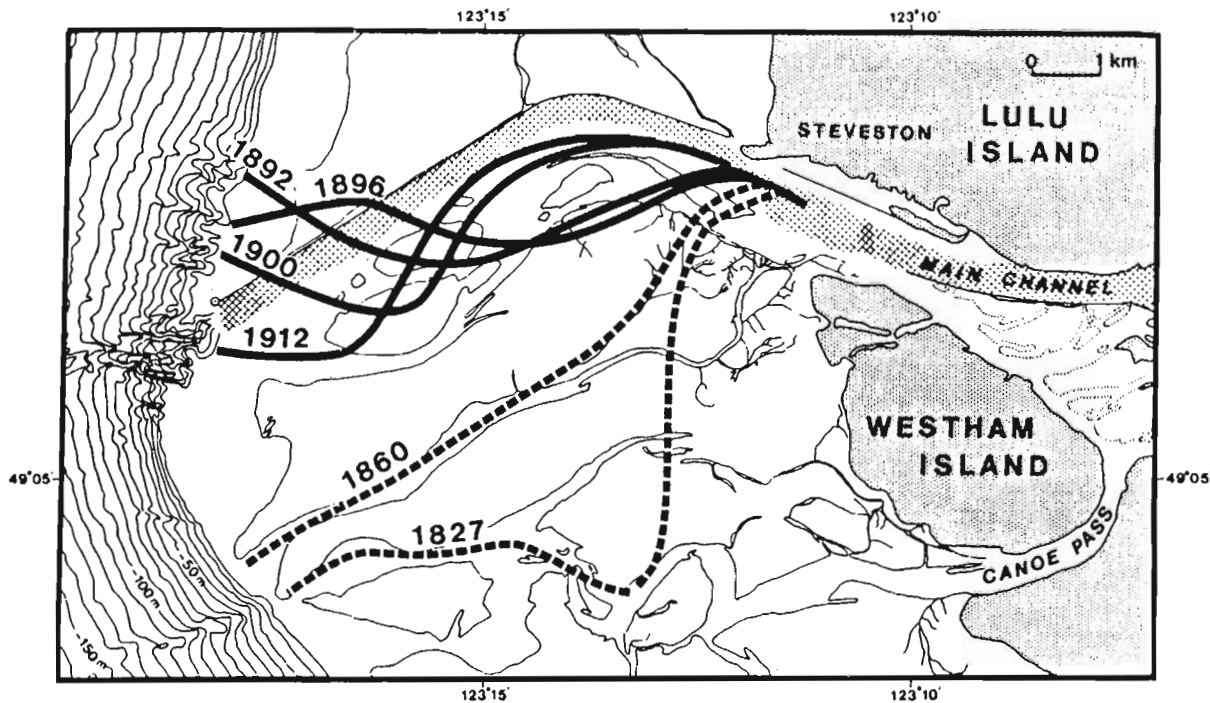


Figure 7. Changes in channel position at the mouth of the Main Channel, 1827 to present. Former channel positions have been obtained from old charts and maps. The present channel is indicated by a cross-hatched pattern and the north side is bounded by a jetty. Land areas are stippled. From Clague et al. (1983).



Figure 8. Photograph of a trench in a beach beside an active distributary channel at the head of the delta. Note the interbedding of coarse sand and laminated silts and sands. Depth of trench about 0.5 m. See Figure 1 for location.



Figure 9. Photograph of split core from a site in central Lulu Island. Note interbedding of medium grained sands and laminated sands and silts. Between 11 and 11.2 m. See Figure 1 for location.

log from the east of Figure 6 can be confidently attributed to a distributary channel, since it occurs immediately beside an active distributary channel, which is incised to almost the same depth as the base of the sand.

Consequently, the borehole data demonstrate that the subaerial plain is underlain by a nearly continuous unit of distributary channel sands. The entire subaerial topset has been reworked by channel migration, which has eroded the original upper foreslope and tidal flat deposits.

PATTERNS OF CHANNEL MIGRATION

Historically, channel migration to accommodate the accumulation of channel sands has been only reported where the distributaries cross the tidal flats. Figure 7 shows the migration of the Main Channel that has been recorded over a 100 year period prior to construction of the jetties which now control its position (Milliman, 1980; Clague et al., 1983). During that period, a significant portion of the tidal flat area appears to have been reworked.

A stratigraphic sequence that is interpreted to represent channel migration across the tidal flats has been observed in a continuous core taken near Ladner in the southern delta (Fig. 1). There, the topset sand is 23 m thick and consists of fine- and medium-grained sands with occasional pebbles, disarticulated whole shells, and clasts of silt. It is directly overlain by burrowed silts and sands interpreted to be tidal flat deposits. Pebbles and shells occur in sands at the base of the present Main Channel where it crosses the tidal flats (unpublished borehole data).

Extensive channel migration and abandonment on the subaerial plain has not been directly observed, but has been inferred from geological and geomorphological evidence. The linear gap in the peat bogs in eastern Lulu Island has been interpreted to be an abandoned former distributary (Fig. 1; Clague et al., 1983), and sloughs beside the major channels indicate that some channel migration has occurred. Channel migration on the delta plain has probably not been as important as channel migration across the tidal flats, since the upper foreslope deposits have been entirely eroded, and thick floodplain silts are preserved in the eastern delta.

Subaerial delta plain channel sands may perhaps be recognized by the absence of shell debris, and the presence of unburrowed laminated silt interbeds at the top - such as those observed in a shallow trench we dug on a beach beside an active distributary channel at the head of the delta (Fig. 8). Similar interbedded sands and laminated silts have been recognized at the top of channel sands in several boreholes (Fig. 9).

CONCLUSIONS AND IMPLICATIONS

Distributary channel migration in the Fraser delta has produced a nearly continuous composite unit of sand generally 10 to 20 m thick underlying the surficial silts of the subaerial delta plain. Although most of the recent channel migration (i.e. prior to jetty construction) occurred where the channels cross the tidal flats, channel migration on the delta plain can also be recognized in the sedimentary record, and may have been more significant in the past.

There are several implications to this conclusion. Firstly, much of the bedload of the river has been stored in channel deposits in the topset. The effect of artificial channellization of the Main Channel across the tidal flats is to impede channel migration, and thus curtail this process.

Secondly, thick sheet-like sands in large deltas are generally associated with wave dominated settings (Wright, 1985), but the predominance of channel sand deposits in the topset attests to the importance of the river's influence. The extent of channel migration in forming a nearly continuous sand is unusual and has probably been determined by the high proportion of sand in the sediment load. Thus, the extensive topset channel sand of the Fraser delta, with its erosional and diachronous base and occasional marine fossils, is potentially a useful stratigraphic model. However, in order to properly

develop the model, more work is required to understand the evolution of the sand and to confirm the environmental signatures.

Finally, subsurface mapping of a modern delta can be successfully used to highlight important modern processes that operate on a time scale longer than direct scientific observation.

ACKNOWLEDGMENTS

The authors gratefully acknowledge the generous assistance of the Ministry of Transportation and Highways Geotechnical and Materials Engineering Branch, the Ministry of Environment Groundwater Section, B.C. Hydro, B.C. Rail, Vancouver Airport Authority, Vancouver Port Corporation, Public Works Canada, Greater Vancouver Regional District, the City of Richmond, the Corporation of Delta, School District 38 (Richmond), School District 37 (Delta), ConeTec Investigations Ltd., Klohn Leonoff Ltd., Geopacific Consultants Ltd., Macleod Geotechnical Ltd., HBT Agra Ltd., Triton Consultants Ltd., Golder Associates, Cook Pickering and Doyle Ltd., the Dominion Company, R.G. Campanella of the Department of Civil Engineering of the University of British Columbia, and J.A. Hunter of the Terrain Sciences Division of the GSC in providing the data that was necessary for this study; the dedicated efforts of Sonic Drilling Ltd. and T.D. Feeney in the field; the drafting and preparation of the figures by L. Bedard and R. Franklin; generation of log output by Brian Roth and Richard Chadwick; and the constructive discussions with J.J. Clague, B.S. Hart, P.S. Mustard, J.A. Hunter, and D. Lister, who reviewed this paper. The CPT's illustrated here were generated by ConeTec Investigations Ltd. and the Ministry of Transportation and Highways. P.A. Monahan is being supported by a University of Victoria Fellowship.

REFERENCES

- Campanella, R.G., Robertson, P.K., and Gillespie, D.**
1983: Cone penetration testing in deltaic soils; *Canadian Geotechnical Journal*, v. 20, p. 23-35.
- Clague, J.J., Luternauer, J.L., and Hebda, R.J.**
1983: Sedimentary environments and postglacial history of the Fraser River Delta and lower Fraser Valley, British Columbia; *Canadian Journal of Earth Sciences*, v. 20, p. 1314-1320.
- Clague, J.J., Luternauer, J.L., Pullan, S.E., and Hunter, J.A.**
1991: Postglacial deltaic sediments, southern Fraser River Delta, British Columbia; *Canadian Journal of Earth Sciences*, v. 28, p. 1386-1393.
- Finn, W.D.L., Woeller, D.J., Davies, M.P., Luternauer, J.L., Hunter, J.A., and Pullan, S.E.**
1989: New approaches for assessing liquefaction potential of the Fraser River Delta, British Columbia; *in Current Research, Part E; Geological Survey of Canada, Paper 89-1E*, p. 221-231.
- Hart, B.S., Prior, D.B., Barrie, J.V., Currie, R.G., and Luternauer, J.L.**
in press: A river mouth channel and failure complex, Fraser delta, Canada; *Sedimentary Geology*, v. 81.
- Hart, B.S., Prior, D.B., Hamilton, T.S., Barrie, J.V., and Currie, R.G.**
1992: Patterns and styles of sedimentation, erosion and failure, Fraser delta slope, British Columbia; *in Geotechnique and Natural Hazards, A symposium sponsored by the Vancouver Geotechnical Society and the Canadian Geotechnical Society, May 6-9, 1992*, p. 365-372.
- Hunter, J.A., Luternauer, J.L., Neave, K.G., Pullan, S.E., Good, R.L., Burns, R.A., and Douma, M.**
1992: Shallow shear wave velocity-depth data in the Fraser River delta from surface refraction measurements, 1989, 1990, 1991; Geological Survey of Canada, Open File 2504.
- Hunter, J.A., Woeller, D.J., and Luternauer, J.L.**
1991: Comparison of surface, borehole, and seismic cone penetrometer methods of determining the shallow shear wave velocity structure in the Fraser River delta, British Columbia; *in Current Research, Part A; Geological Survey of Canada, Paper 91-1A*, p. 23-26.
- Johnston, W.A.**
1921: Sedimentation of the Fraser River Delta; Geological Survey of Canada, Memoir 125, 46 p.
- Jol, H.M. and Roberts, M.C.**
1988: The seismic facies of a delta onlapping an offshore island: Fraser River Delta, British Columbia; *in Sequences, Stratigraphy, Sedimentology: Surface and Subsurface*, (ed.) D.P. James and D.A. Leckie; Canadian Society of Petroleum Geologists, Memoir 15, p. 137-142.
- 1992: The seismic facies of a tidally influenced Holocene delta: Boundary Bay, Fraser River delta, B.C.; *Sedimentary Geology*, v. 77, p. 173-183.
- Luternauer, J.L.**
1980: Genesis of morphologic features on the western delta front of the Fraser River, British Columbia - status of knowledge; *in The Coastline of Canada*, (ed.) S.B. McCann; Geological Survey of Canada, Paper 80-10, p. 381-396.
- 1988: Geoarchitecture, evolution, and seismic risk assessment of the southern Fraser River delta, B.C.; *in Current Research, Part E; Geological Survey of Canada, Paper 88-1E*, p. 105-109.
- 1990: 1989 field activities and accomplishments of geophysical and geotechnical land-based operations and marine/fluvial surveys, Fraser River delta, British Columbia; *in Current Research, Part E; Geological Survey of Canada, Paper 90-1E*, p. 235-237.
- Luternauer, J.L. and Murray, J.W.**
1973: Sedimentation of the Fraser River Delta; *Canadian Journal of Earth Sciences*, v. 10, p. 1642-1663.
- Luternauer, J.L., Clague, J.J., and Feeney, T.D.**
1991: A 367 m core from southwestern Fraser River delta, British Columbia; *in Current Research, Part E; Geological Survey of Canada, Paper 91-1E*, p. 127-134.
- Luternauer, J.L., Clague, J.J., Hamilton, T.S., Hunter, J.A., Pullan, S.E., and Roberts, M.C.**
1986: Structure and stratigraphy of the southwestern Fraser River delta: a trial shallow seismic profiling and coring survey; *in Current Research, Part B; Geological Survey of Canada Paper 86-1B*, p. 707-714.
- Mathews, W.H. and Shepard, F.P.**
1962: Sedimentation of the Fraser River Delta; *Bulletin of the American Association of Petroleum Geologists*, v. 46, p. 1416-1463.
- Milliman, J.D.**
1980: Sedimentation in the Fraser River and its estuary, southwestern British Columbia (Canada); *Estuarine and Coastal Marine Science*, v. 10, p. 609-633.
- Mustard, P.S. and Roddick, J.A.**
1992: Vancouver subsurface information data bank for the period 1913 to 1972. A re-release of Open File 382 (1976, J.R. Bélanger and J.E. Harrison) in a DOS database format; Geological Survey of Canada, Open File 3182.
- Patterson, R.T. and Cameron, B.E.B.**
1991: Foraminiferal biofacies succession in the late Quaternary Fraser River delta, British Columbia; *Journal of Foraminiferal Research*, v. 21, p. 228-243.
- Pullan, S.E., Jol, H.M., Gagné, R.M., and Hunter, J.A.**
1989: Compilation of high resolution "optimum offset" shallow seismic reflection profiles from the southern Fraser River delta, British Columbia; Geological Survey of Canada, Open File 1992.
- Roberts, M.C., Williams, H.F.L., Luternauer, J.L., and Cameron, B.E.B.**
1985: Sedimentary framework of the Fraser River delta, British Columbia: preliminary field and laboratory results; *in Current Research, Part A; Geological Survey of Canada, Paper 85-1A*, p. 717-722.

Watts, B.D., Seyers, W.C., and Stewart, R.A.

1992: Liquefaction susceptibility of Greater Vancouver area soils; *in* Geotechnique and Natural Hazards, A symposium sponsored by the Vancouver Geotechnical Society and the Canadian Geotechnical Society, May 6-9, 1992, p. 145-157.

Williams, H.F.L. and Roberts, M.C.

1989: Holocene sea-level change and delta growth: Fraser River Delta, British Columbia; Canadian Journal of Earth Sciences, v. 26, p. 1657-1666.

Williams, H.F.L. and Roberts, M.C. (cont.)

1990: Two middle Holocene marker beds in vertically accreted floodplain deposits, lower Fraser River, British Columbia; Geographie Physique et Quaternaire, v. 44, p. 27-32.

Wright, L.D.

1985: River deltas; *in* Coastal Sedimentary Environments, Second Revised, Expanded Edition, (ed.) R.A. Davis; Springer-Verlag, New York, p. 1-76.

Geological Survey of Canada Project 860022

Sedimentology and lithofacies associations of the Fraser River delta foreslope, British Columbia

Richard W. Evoy¹, Thomas F. Moslow¹, and John L. Luternauer
Cordilleran Division, Vancouver

Evoy, R.W., Moslow, T.F., and Luternauer, J.L., 1993: Sedimentology and lithofacies associations of the Fraser River delta foreslope, British Columbia; in Current Research, Part A; Geological Survey of Canada, Paper 93-1A, p. 273-280.

Abstract: Five lithofacies were recognized from piston cores examined for this study. These lithofacies are: 1) massive silty clay with minor organics and rare parallel laminations, 2) silty clay to clayey silt with rare parallel silt and very fine sand laminations, 3) clayey silt with silt or very fine sand interbeds, 4) silty, very fine- to medium-grained sand units with less than 10% thin clay or silt interbeds, and 5) debris flow. Facies 4 can be subdivided based on the presence or absence of silty-clay interbeds, and individual sand bed thicknesses.

Lithofacies distribution patterns suggest that the Fraser delta foreslope is dissected by a number of both active and inactive channels. These channels serve as a mechanism for sediment bypassing across the foreslope. It is hypothesized that they debouche as a series of prodelta depositional lobes.

Résumé : On a identifié cinq lithofaciès en examinant des échantillons recueillis avec un carottier à piston, aux fins de la présente étude. Ces lithofaciès sont : 1) une argile silteuse massive accompagnée de petites quantités de matière organique et de quelques rares laminations parallèles, 2) une argile silteuse ou un silt argileux à rares laminations parallèles de silt et de sable très fin, 3) un silt argileux à intercalations de silt ou de sable très fin, 4) des unités de sable silteux, très fin à moyen, dont moins de 10 % se composent de minces intercalations d'argile ou de silt, et 5) des coulées de débris. Le faciès 4 se laisse subdiviser selon la présence ou l'absence d'intercalations d'argile silteuse, et l'épaisseur des couches individuelles de sable.

Les modes de distribution des lithofaciès semblent indiquer que le prodelta du Fraser est disséqué par plusieurs chenaux actifs et chenaux inactifs. Ces derniers permettent le détournement des sédiments à travers le prodelta. On suppose qu'ils débouchent en formant une série de lobes sédimentaires prodeltaïques.

¹ Department of Geology, University of Alberta, #1-26 Earth Sciences Building, Edmonton, Alberta T6G 2E3

INTRODUCTION

This study documents preliminary sediment distribution patterns and lithofacies associations in the Fraser River delta foreslope. These data constitute part of the GSC's ongoing research into environmental and geohazards assessment of the Fraser River delta slope, the specific objectives of which include: 1) documentation of rates and patterns of sedimentation, and 2) analysis of sediment stability conditions on the delta slope. This study focuses on sediment dispersion patterns by detailing eighteen piston cores collected from the Fraser delta foreslope aboard the research vessel **CSS Vector** during 1989. All cores were described using a process sedimentologic approach to identify sedimentary facies and genetically related stratigraphic units. Selected half-slab intervals were subsequently X-radiographed to test for fine-scale structure in massive clayey-silt units, and to look for evidence of bioturbation (Moslow et al., 1991).

The study area for this project consists of a 150 km² section of the delta foreslope offshore Sturgeon and Roberts banks (Fig. 1). Water depths in the main study area range from less than 50 m to greater than 200 m at an average gradient exceeding 3.0°. Concern over the stability of this slope and its subaerial equivalent, in response to seismic loading, has provided the impetus for this and related studies.

GEOLOGICAL SETTING

The Fraser River delta is the largest and most important delta on Canada's Pacific coast. The Fraser River drains approximately 250 000 km² of mountainous terrain with peak discharge during the snowmelt freshet in late spring and early summer (Milliman, 1980). Within the Fraser River estuary, a pronounced tidal influence, approaching 5 m at the river mouth (Kostaschuk and Luternauer, 1989), is superimposed on the fluvial regime. Tidal range within the estuary

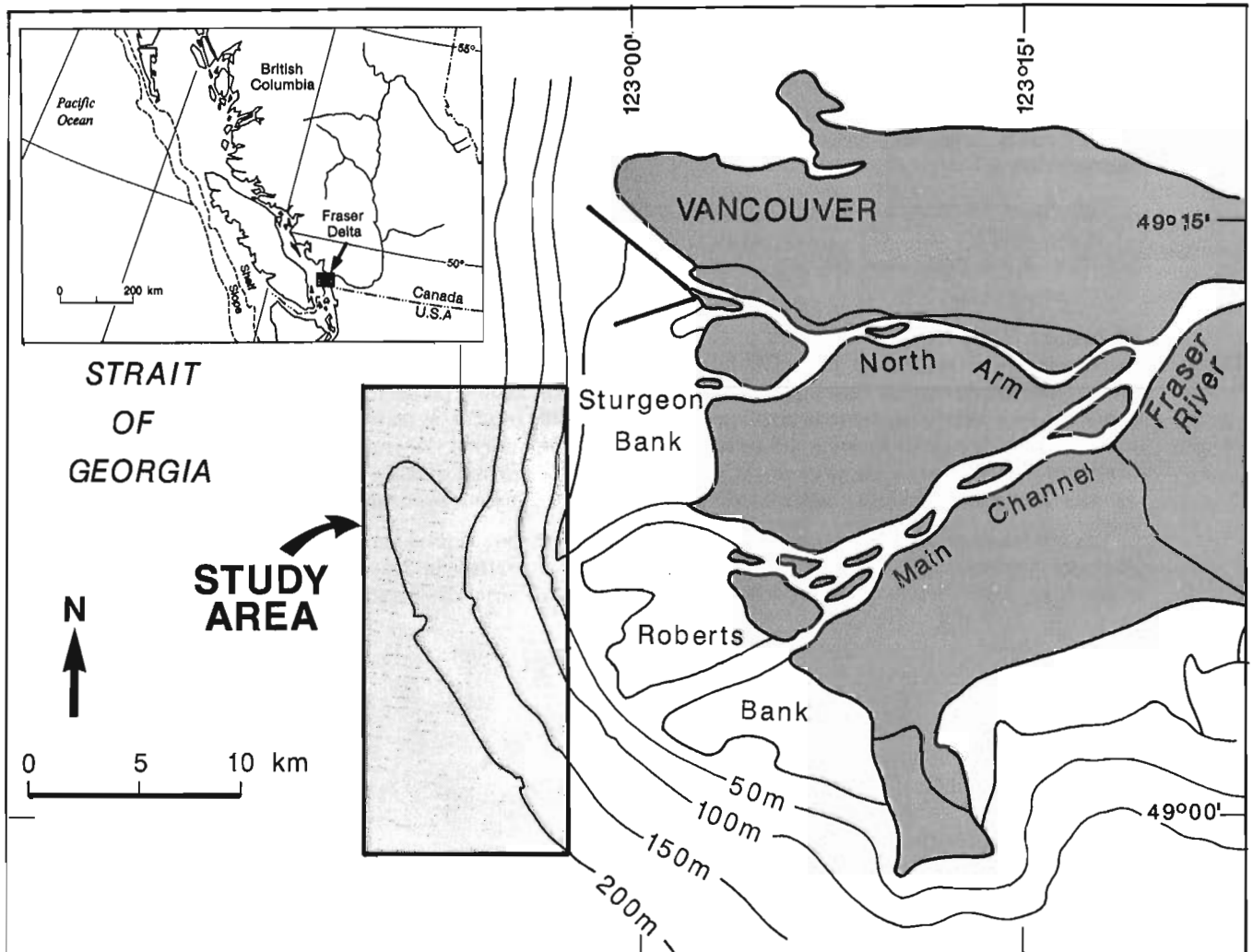


Figure 1. Study area location map. Area enclosed within rectangular box is detailed in Figure 2. (Modified from Moslow et al., 1991; Kostaschuk et al., 1992).

decreases upstream and with increasing discharge (Ages and Woolard, 1976), and in conjunction with fluvial discharge produces a pronounced salt-wedge which strongly affects local sedimentation rates and mechanics (Kostaschuk and Luternauer, 1989).

The Fraser delta shoreline along Georgia Strait is approximately 40 km in length. The seaward margin of the delta consists of a series of broad tidal flats, up to 9 km wide, with average slopes of less than 0.1° ; the foreslope extends a further 5 to 10 km seaward at an average slope of 1.5° (Clague et al., 1991).

LITHOFACIES ANALYSIS

A total of eighteen piston cores were collected from the Fraser River delta slope offshore the southern half of Sturgeon Bank and the northern half of Roberts Bank (Fig. 2). These cores were divided into lithofacies using a process sedimentologic approach to the recognition of genetically related depositional units. Five lithofacies were recognized, and one was further divided into three subfacies. Lithofacies characteristics and distributions are summarized on Table 1, and are shown schematically on Figure 3.

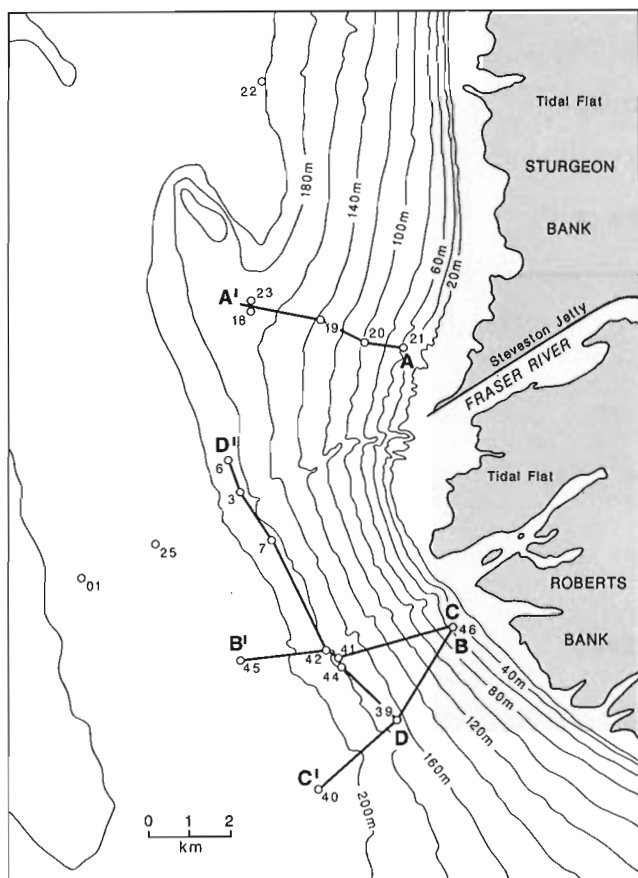


Figure 2. Detailed bathymetry and 1989 piston core locations in the study area. Cross-sections A-A' through D-D' are discussed in the text.

Facies 1

Lithofacies 1 is a silty clay with a minor organic component consisting of rafted and disseminated plant material. This unit is generally massive and internally structureless, with only rare parallel laminations.

Facies 1 is the most common facies in the study area constituting over 40% of all core recovered. It is common in the more distal portion of the delta slope, and in areas that are not subject to active processes of sedimentation, and was recovered from water depths ranging from 50 m to 280 m. Depositional mechanism is gravity settling from suspension in an area of restricted clastic input and extremely low energy.

Facies 2

Lithofacies 2 is composed of silty clays to clayey silts which are generally massive, with rare parallel silt laminations. This unit tends to be dense and compacted, and remains cohesive after dehydration. Both rafted and laminated disseminated organics are present, as are rare shell fragments and occasional burrows. The entire facies contains less than 10% silt and very fine sand laminations, but locally may consist of a visually estimated 15% to 20% of these coarser grain sizes. Silt laminae exhibit plane parallel laminations and fine sand lenses locally exhibit wavy to lenticular bedding. Individual laminae are typically 5 mm or less in thickness.

Facies 2 is the second most widely distributed facies recognized in the study area and represents approximately 27% of recovered core. Facies 2 is, in part, gradational with facies 1; the two facies combined total just under 70% of all sediment recovered in the study. Depositional mechanisms

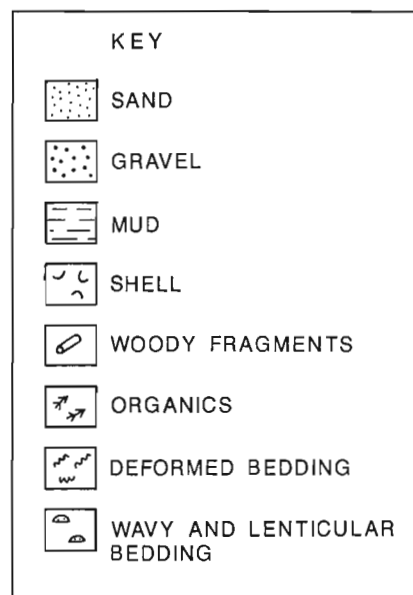


Figure 3. Sedimentological lithofacies features illustrated in Figures 4-7.

Table 1. Summary of lithofacies characteristics and distribution from the Fraser River delta foreslope

FACIES	LITHOLOGIC DESCRIPTION	CORES	INTERVAL (metres)
1	silty clay with minor disseminated organics; black when fresh, oxidizes to olive green; frequently water saturated	89A-01	
		89A-06	top
		89A-18	top to 2.3
		89A-21	top to 1.5 3.8 to base
		89A-22	
		89A-23	top to 1.55
		89A-40	0.3 to base
2	silty clay to clayey silt; <10% silt/fine sand laminations by volume; disseminated organics, rafted and laminated	89A-06	0.8 to base
		89A-07	
		89A-19	
		89A-20	top to 3.9
		89A-40	top to 0.22
		89A-41	top to 0.35
3	clayey silt with silty, very fine to medium grain sand interbeds; contacts either gradational or abrupt	89A-21	1.5 to 3.8
		89A-39	top to 0.55
		89A-46	top to 0.22
4a	silty very fine to medium sand with less than 10% silt/clay interbeds; contacts either gradational or sharp	89A-03	
		89A-18	2.3 to base
		89A-20	3.9 to base
		89A-23	1.55 to base
		89A-39	0.55 to base
		89A-41	0.35 to base
		89A-42	
		89A-44	1.65 to 2.60
4b	silty very fine to fine sand beds less than 10 cm thick; isolated	89A-06	0.66 & 0.8
		89A-20	3.25
		89A-21	2.93 to 3.0
		89A-23	1.25 to 1.3
		89A-39	0.45 m ?
4c	silty, fine to medium sand; massive; abrupt contacts	89A-25	0.10 to base
		89A-44	0.28 to 1.65
5	resedimented plant detritus, woody organics, shell fragments, mud clasts and silty very- fine to medium grained poorly sorted sand in a silty clay to clay-silt matrix	89A-40	0.22 to 0.30

for facies 2 include suspension settling combined with silt laminae deposited directly from the entrained layer of dilute, low density turbidity currents.

Facies 3

Lithofacies 3 is a clayey silt unit with silt and/or very fine sand interbeds; interbeds constitute approximately 25% to 50% of the facies by volume. Silt interbeds consist of thin plane parallel laminations. Sand lenses are silty, contain significant concentrations of both disseminated and bedded detrital organic constituents, and generally are preserved as 2 to 3 cm thick lenticular beds. Where no sand is present, this facies varies from facies 2 only in total silt content. Intrafacies contacts may be either sharp, or more commonly, gradational.

Facies 3 is a relatively minor component in cores acquired, totalling less than 10% of the recovered core. This facies is gradational with the coarser members of facies 2 and represents a similar mixture of suspension sedimentation combined with deposition from the entrained layer of unconfined turbidity currents. Background hydraulic regime is interpreted to be slightly higher energy for this facies, as reflected by the greater percentage of silt in the suspended sediment load. This is compatible with the restricted recovery of this unit from unchanneled environments in the upper to middle delta foreslope. Each of the three intervals in which this facies was noted are cut by thin turbiditic sand lenses.

Facies 4

Facies 4 includes all silty, very fine- to medium-grained sand units with less than 10% thin (<5 cm) clay or silt interbeds. This facies can be divided into three subfacies based on the presence/absence of silty-clay interbeds, and individual sand bed thicknesses and geometry.

Facies 4a includes those units with appreciable silty-clay content. Bed contacts may be either sharp or gradational in character, and locally show some evidence of loading. Bedding may be either massive, or wavy to lenticular. Internal structures include normal and inverse grading, with local plane parallel laminations marked by silty-clay and/or concentrations of rafted organics. Soft sediment deformation is present locally and includes both oversteepened laminations and rare convolute bedding. Sand beds are frequently poorly sorted, immature lithic sands with high matrix and organic content.

Well developed thickening- and coarsening-up sequences in some cores, and fining-upwards sequences in others, reflect a variety of depositional patterns including channel progradation, migration, and abandonment. Facies 4a constitutes approximately 19% of all cored lithofacies in the area, and is the predominant sand unit in the study.

Facies 4b is composed of isolated, silty, very fine to fine sand beds less than 10 cm thick. Beds are poorly sorted, generally massive, and may have either sharp or gradational contacts. Within piston cores from the study area, this facies

is volumetrically insignificant, and is usually found as thin units within facies 1 and 2. The sands in these beds are not in equilibrium with their surrounding facies, and their abrupt contacts are suggestive of a weakly erosive component to the flow. Facies 4b represents deposition from unconfined turbidity currents.

Facies 4c includes two massive, fine to medium sand beds, each greater than 1 m thick. Both occurrences exhibit sharp upper contacts, and the one example in which the bottom contact was penetrated has an abrupt basal contact marked by clay rip-up clasts.

Facies 5

Facies 5 consists of a single debris flow found near the top of a thick facies 1 interval collected in piston core VEC89A-40 from a water depth of 212 m in a prodelta/basin plain environment (Fig. 2). This unit exhibits an erosive base with an abrupt top, internally massive or chaotic bedding, and a muddy matrix with large wood fragments, shell fragments, and mud clasts (Table 1). There is no direct evidence of active channels or channellized flow in cores collected upslope from this site, however a pronounced embayment in the upslope bathymetric contours is of appropriate scale to represent a significant slump scar on the foreslope.

LITHOFACIES RELATIONSHIPS

To test for lateral patterns in lithofacies distributions across the study area, a series of three longitudinal and one transverse cross-sections were constructed (Fig. 2).

Section A-A' was constructed across the delta slope north of the Sand Heads sea valley. VEC89A-21 and VEC89A-20 represent interchannel environments on the upper foreslope in an area transected by numerous small-scale gullies. These gullies appear to be inactive based on bathymetry, and have likely been dormant since completion of Steveston Jetty. VEC89A-21 consists of a thick unit of facies 3 within facies 1, and may represent a paleo-levee (Fig. 4). VEC89A-20 consists almost entirely of facies 2 with a thin fining-up unit of facies 4a at the base and may represent an abandoned channel sequence.

VEC89A-19 represents an interchannel environment on the middle foreslope and is composed entirely of facies 2. VEC89A-18 and -23 were deposited on the lower foreslope and consist of facies 1 overlying facies 4a. Bed contacts and internal structure of facies 4a suggest sediment-gravity flow mechanisms; beds are both normally- and inversely-graded, wavy to parallel laminations are common, and bed contacts are abrupt and locally loaded.

One thin (7 cm) sandy interval with abrupt contacts and loaded base was noted at a depth of 3.0 m in VEC89A-21, and consists of poorly sorted immature sand with a muddy matrix. This bed may be correlative with other sediment gravity flow deposits immediately down slope from this location.

B-B' is a longitudinal section located immediately seaward of two abandoned tidal channels on Roberts Bank. One metre of core recovered from an interchannel environment in the upper foreslope consists of interbedded facies 3 and 4c overlying facies 4a. A single loaded contact was noted at the base of a 10 cm thick facies 4c unit;

oversteepened lamination immediately underlies this. Larger scale oversteepened laminae, marked by rafted organics, are present near the base of the interval.

VEC89A-44, -42 and -41 consist of thick channellized sequences overlain by finer grained sediment (Fig. 5). The channellized sands are silty, very fine- to medium-grained,

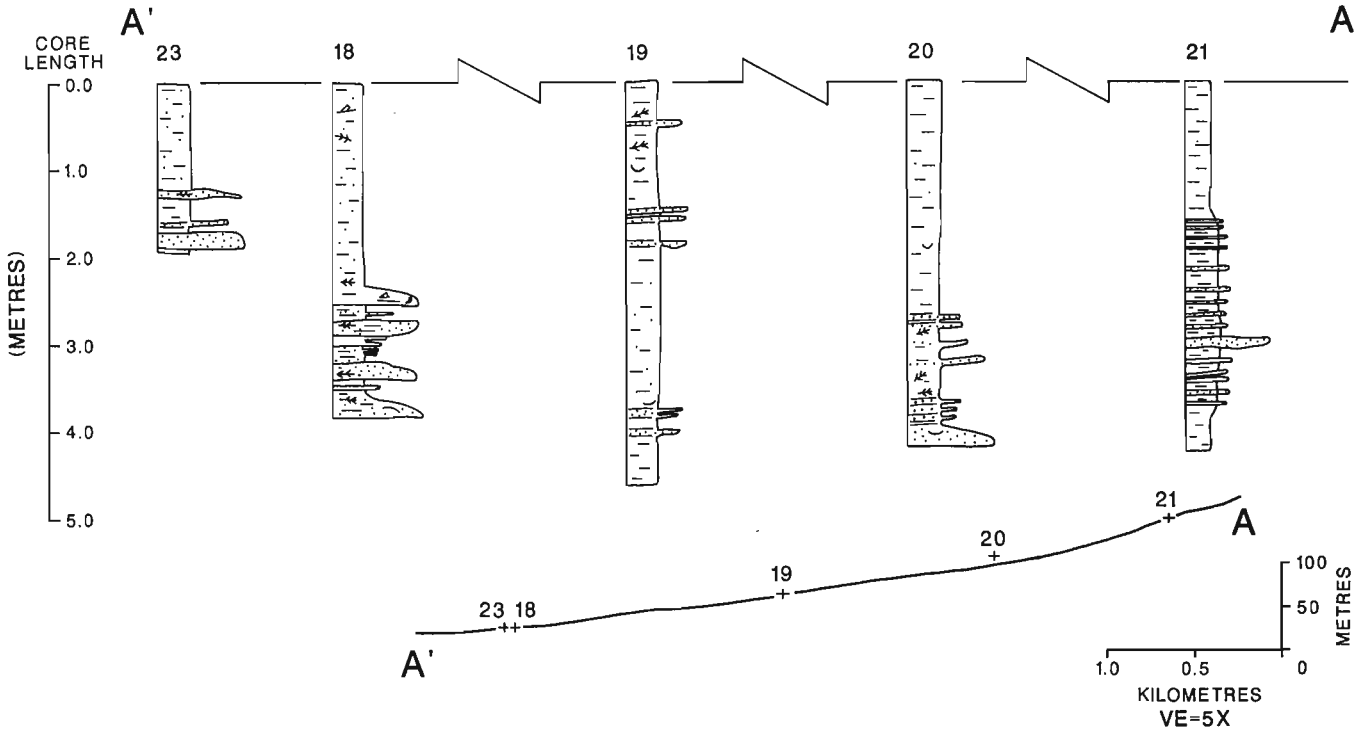


Figure 4. Cross-section A-A' and accompanying bathymetric profile; datum represents sediment-water interface. See Figure 2 for location and Figure 3 for key.

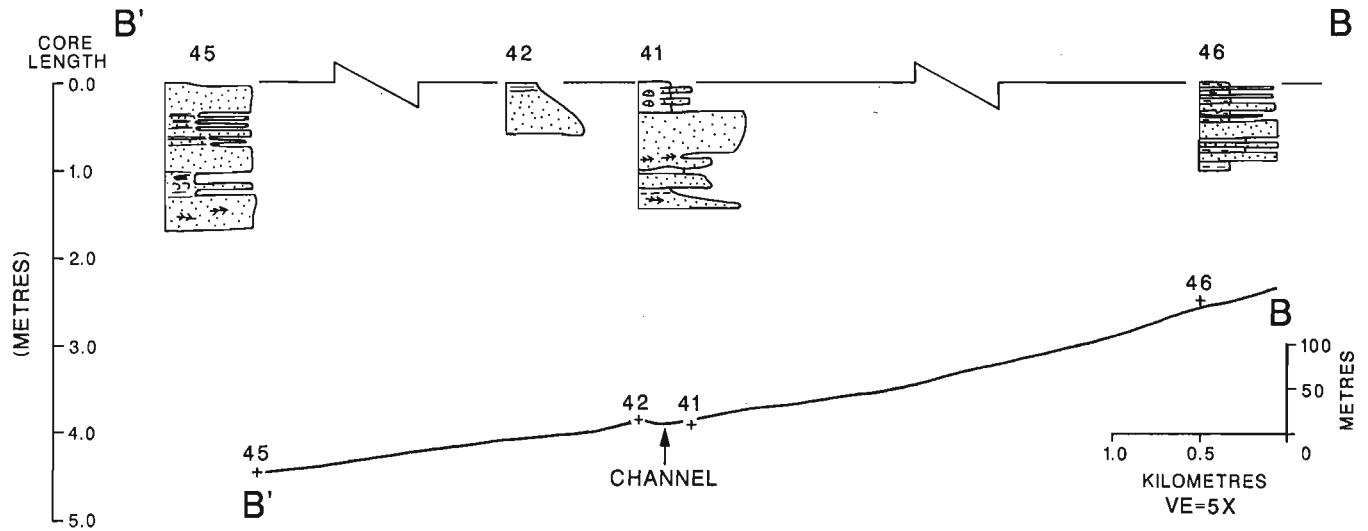


Figure 5. Cross-section B-B' and accompanying bathymetric profile; datum represents sediment-water interface. See Figure 2 for location and Figure 3 for key.

moderately sorted and clean. The units are predominantly massive, but locally exhibit well developed wavy and/or plane parallel laminations and rare clay rip-up clasts. These cores appear to reflect northward channel migration, with VEC89A-42 representing the current bathymetric expression of the channel. The channel currently appears to be inactive.

VEC89A-45 was cored in a prodelta setting along the trend of this channel system. This interval consists of greater than 80% massive, fine to medium sand, with thin beds of clayey silt and rafted organics. Internal deformation locally consists of oversteepened bedding and convolute laminations. Sedimentation at VEC89A-45 appears to be by traction mechanisms, and this site likely represents a depositional lobe associated with the above channel system.

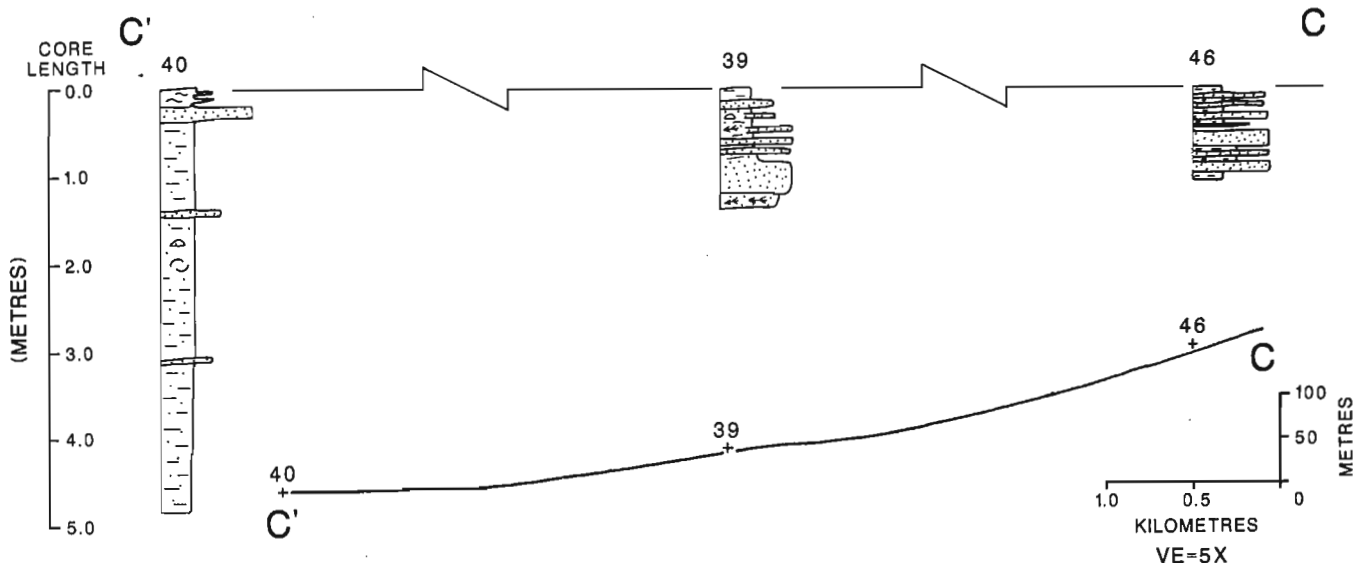


Figure 6. Cross-section C-C' and accompanying bathymetric profile; datum represents sediment-water interface. See Figure 2 for location and Figure 3 for key.

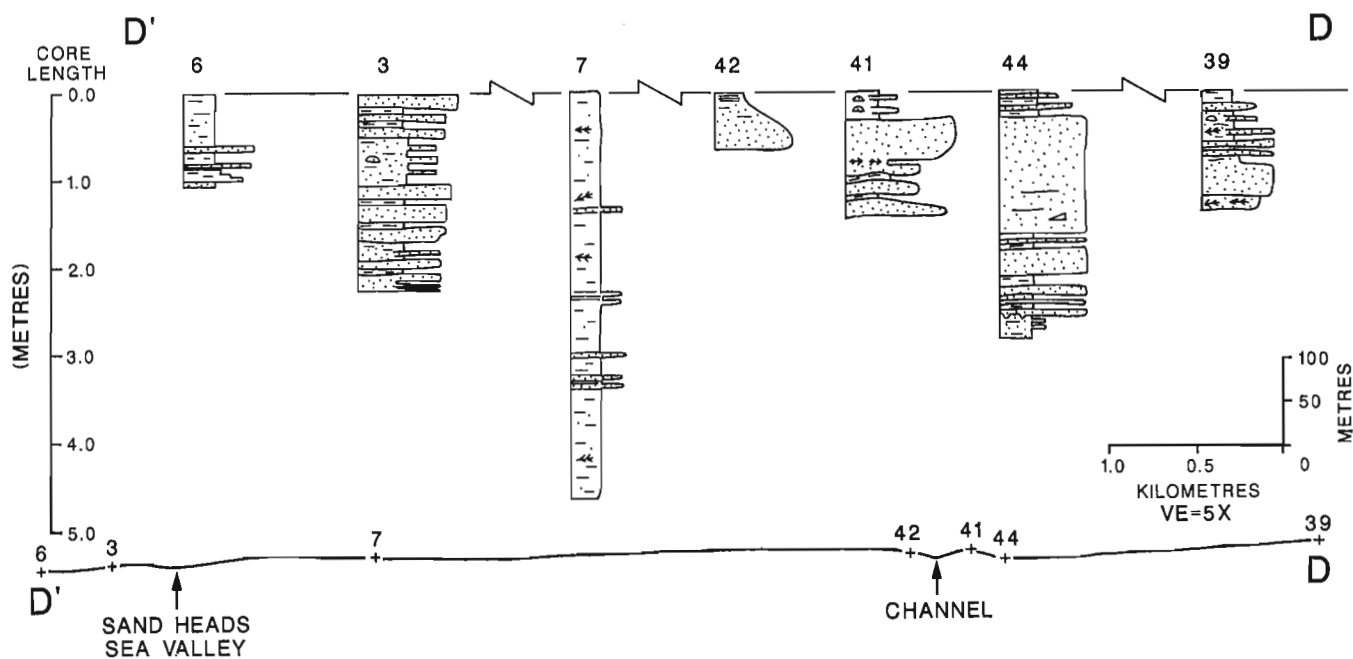


Figure 7. Cross-section D-D' and accompanying bathymetric profile; datum represents sediment-water interface. See Figure 2 for location and Figure 3 for key.

Section C-C' was constructed with a common point to section B-B' on the upper foreslope (Fig. 2). Site VEC89A-39 (lower-middle foreslope) appears to represent an abandoned channel sequence, with facies 4 overlain by facies 3 (Fig. 6). Depositional processes include channelized flow at the base, waning upsection to unconfined turbidites and suspended sediment. As there is no bathymetric evidence for a channel up slope from this site, sedimentation rates must be sufficiently high to bury the morphologic expressions of abandoned channels. Recent seismic data reveal indications of conformable sediment drapes covering channel floor locally (Hart et al., 1992, in press).

The prodelta environment cored in VEC89A-40 consists of a thick accumulation of facies 1 with a thin unit of facies 5 debris flow near the top of the interval. Although there are no active channels upslope from this site, a pronounced embayment in the bathymetric contours between VEC89A-40 and VEC89A-39 (Fig. 2) may represent a significant slump scar on the foreslope.

Section D-D' is a transverse section running the length of the delta foreslope from VEC89A-39, through the abandoned channel at site VEC89A-42, to the active channel in Sand Heads valley (Fig. 7). The interpreted channel sequence at site VEC89A-39, and the inactive channel on section B-B' have been described in detail above. Sites VEC89A-44, 41, and 42 appear to reflect northward channel migration with site 42 representing the current bathymetric expression of the channel. Depositional environments include both the inactive channel and associated levee complex.

VEC89A-07 represents interchannel sedimentation on the lower foreslope. Deposition is primarily from suspension with minor deposition from the entrained layer of unconfined turbidity currents. Rare sand-filled burrows are associated with thin sand intervals between 2.8 m and 3.4 m. Rafted organics and wood fragments, both disseminated and bedded, are present in the nonburrowed intervals.

VEC89A-03, along the flank of the main channel of the Sand Heads valley, is composed entirely of facies 4 and represents a well developed, stacked channel sequence with normally graded beds and pronounced coarsening- and thickening-up bed sets. Deposition is from traction and channelized turbidity currents. VEC89A-06 was drilled adjacent to VEC89A-03 on the inferred levee of the Sand

Heads valley (Fig. 2). The cored interval constitutes a weakly defined fining upwards sequence with facies 1 overlying facies 2 and minor amounts of facies 4b. Interpreted depositional processes include channel-overbank or inter-channel flow by dilute, unconfined turbidity currents, with concurrent background deposition of silty clay from suspension.

ACKNOWLEDGMENTS

Numerous comments and suggestions by Pat Monahan and L.E. Jackson have helped to improve and clarify this manuscript, and are gratefully acknowledged. Funding was provided by EMR and NSERC grants to TFM (Research Agreement No. 034 4 92).

REFERENCES

- Ages, A. and Woolard, A.**
1976: The tides in the Fraser Estuary; Pacific Marine Science Report 76-5, Institute of Ocean Sciences, Sidney, British Columbia, 100 p.
- Clague, J.J., Luternauer, J.L., Pullan, S.E., and Hunter, J.A.**
1991: Postglacial deltaic sediments, southern Fraser River delta, British Columbia; Canadian Journal of Earth Sciences, v. 28, p. 1386-1393.
- Hart, B.S., Prior, D.B., Barrie, J.V., Currie, R.G., and Luternauer, J.L.**
in press: A river mouth submarine channel and failure complex, Fraser Delta, Canada; *Sedimentary Geology*.
- Hart, B.S., Prior, D.B., Hamilton, T.S., Barrie, J.V., and Currie, R.G.**
1992: Patterns and styles of sedimentation, erosion and failure, Fraser Delta slope, British Columbia; in *Geotechnique and Natural Hazards: Proceedings of First Canadian Symposium on Geotechnique and Natural Hazards*; Canadian Geotechnical Society, p. 365-372.
- Kostaschuk, R.A. and Luternauer, J.L.**
1989: The role of the salt-wedge in sediment resuspension: Fraser Estuary, Canada; *Journal of Coastal Research*, v. 5, p. 93-101.
- Kostaschuk, R.A., Luternauer, J.L., McKenna, G.T., and Moslow, T.F.**
1992: Sediment transport in a submarine channel system: Fraser River Delta, Canada; *Journal of Sedimentary Petrology*, v. 62, p. 273-282.
- Milliman, L.O.**
1980: Sedimentation in the Fraser River and its estuary, British Columbia; *Estuarine and Coastal Marine Science*, v. 10, p. 609-633.
- Moslow, T.F., Luternauer, J.L., and Kostaschuk, R.A.**
1991: Patterns and rates of sedimentation on the Fraser River delta slope, British Columbia; in *Current Research, Part E*; Geological Survey of Canada, Paper 91-1E, p. 141-145.

Implications of viscosity on pluton emplacement

J.A. Roddick

Cordilleran Division, Vancouver

Roddick, J.A., 1993: Implications of viscosity on pluton emplacement; in Current Research, Part A; Geological Survey of Canada, Paper 93-1A, p. 281-286.

Abstract: The viscosity of magmatic material is too low for it to penetrate kilometres of crust in the sizes and shapes of common plutons. The viscosity of salt in diapirs is about $10^{16}\rho$. The very viscous dacite extruded at Usu, Japan, was comparatively much more fluid with a viscosity of $10^{10}\rho$, a difference of about six orders of magnitude. If the viscosity of dacite can be extrapolated to tonalite magma, roughly circular tonalitic plutons should be smaller than salt domes, if they could form at all. Magmatic plutonic material should form only dykes and small pipes comparable in size to feeders of volcanic flows. The existence of plutons requires a crustal process capable of reducing the viscosity of parts of the lower crust ($>10^{22}\rho$) to the range between it and salt. The process begins with the breakdown of some hydrous minerals in the lower crust, and creates a 'zone of plutonism'.

Résumé : La viscosité des matériaux magmatiques est trop faible pour qu'ils puissent traverser des kilomètres de la croûte terrestre sous forme de plutons habituels. La viscosité du sel dans les diapirs est d'environ $10^{16}\rho$. Les laves dacitiques très visqueuses qui se sont épanchées à Usu au Japon étaient relativement plus fluides, avec une viscosité de $10^{10}\rho$, soit une différence d'environ six ordres de grandeur. Si les valeurs de la viscosité de la dacite se laissent extrapoler au magma tonalitique, les plutons tonalitiques, qui sont approximativement circulaires, devraient être plus petits que les dômes de sel s'ils étaient effectivement en mesure de se former. Les matériaux magmatiques des plutons ne devraient constituer que des dykes et de petites cheminées de dimensions comparables à celles des cheminées émettant des coulées volcaniques. L'existence des plutons implique l'action d'un processus crustal susceptible de réduire la viscosité de portions de la croûte inférieure ($>10^{22}\rho$) à un point se situant entre cette valeur et celle du sel. Le processus commence par la décomposition de certains minéraux hydratés dans la croûte inférieure, et crée une «zone de plutonisme».

INTRODUCTION

The mechanism by which magma is brought up through many kilometres of crust in the shape and size of common plutons is not intuitive. In fact, it may not be possible. Many factors bear on the shape and size of intrusive bodies but their major dimensions are closely related to the difference in viscosity between the mobilized material and that of the confining envelope. If the difference is large, structures within the envelope will profoundly affect the structure of the intrusive body. Fractures will be filled with dyke-like bodies and variations in the competency of the envelope material will be exploited. A difference in viscosity alone, however, will not ensure that intrusion takes place. Mobilization will result only if the stress field is great enough to exploit the viscosity difference; the greater the difference, the less stress required. In plutonic environments stress can be enormous and must be to exploit the relatively small difference between pluton viscosity and that of the crust.

PLUTONS AND SALT DIAPIRS

An intrusive body, by its size and shape conveys some sense of what its viscosity must have been during emplacement. Plutons are commonly much larger than salt diapirs. Even the largest salt diapirs, like those of the Great Kavir ("salt desert")

of northern Iran (Jackson et al., 1990), are only a fraction of the size of major plutons in the Coast Plutonic Complex and elsewhere (Fig. 1). It is difficult not to conclude that during emplacement, plutonic material is more viscous than salt. This conclusion, however, raises other problems.

The viscosity of salt in salt diapirs is known to be about $10^{16}\rho$, (Weinberg, 1927; Jackson et al., 1990), which is considerably more viscous than ice in glaciers (about $10^{14}\rho$). In contrast the very viscous dacite extruded at Usu, Japan, was much more fluid with a viscosity of $10^{10}\rho$. In Figure 2, which shows the viscosity of some relevant materials, only that of plutons and upper mantle cannot be measured directly. The latter is derived from the rate of isostatic rebound following deglaciation. It falls in the range of $10^{20}\rho$ to $10^{22}\rho$ although it is not certain at what level compensation takes place (lower crust, mantle, or asthenosphere). The size and shape of common plutons indicates a viscosity during emplacement greater than that of salt (probably by at least an order of magnitude) and less than that of crust and/or mantle. A value near $10^{18}\rho$ seems probable, yet is impossibly high for any magma.

If the viscosity of the Usu dacite could be extrapolated to tonalitic magma, such plutons should be considerably smaller than salt diapirs, if they could form at all. Having a viscosity many orders of magnitude less than salt, magmatic material,

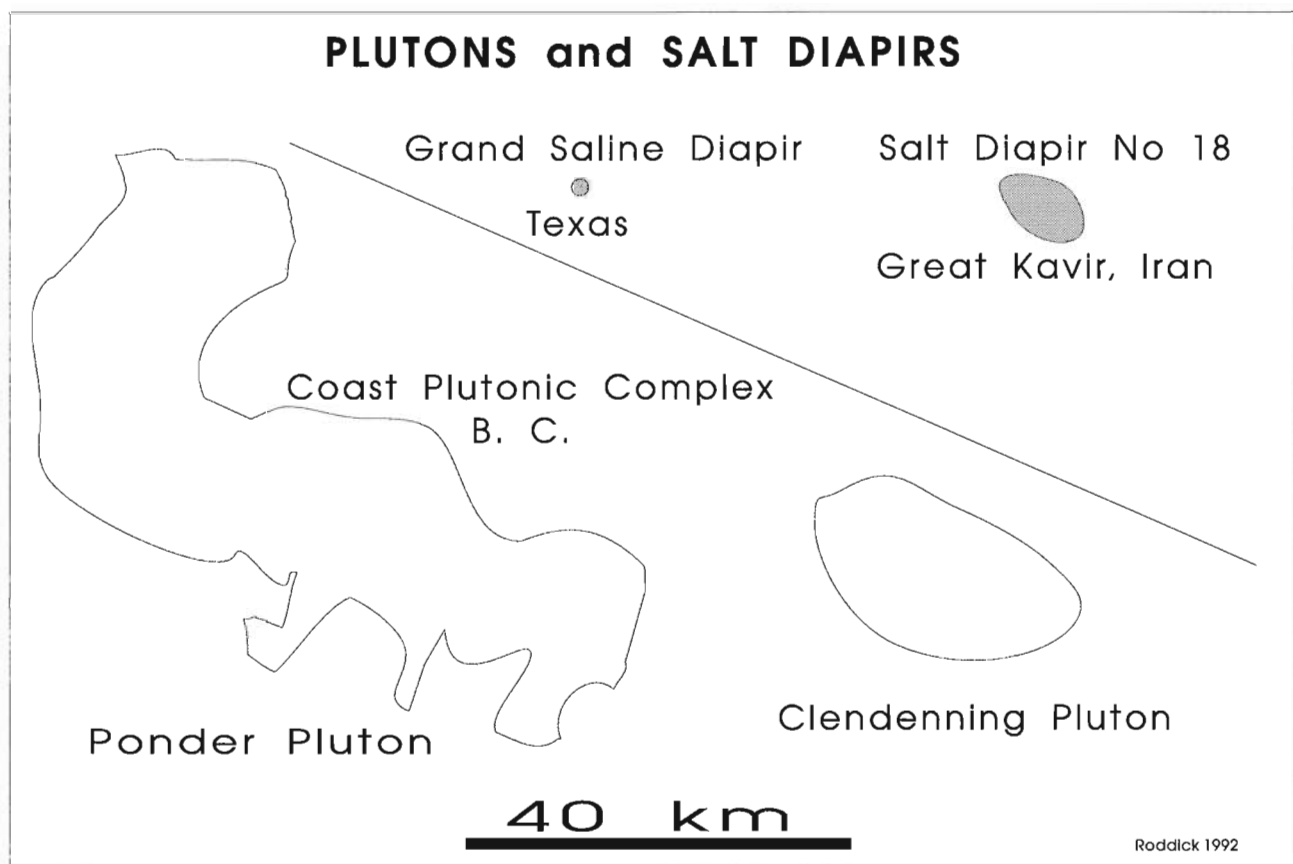


Figure 1. Samples of plan views of plutons and salt diapirs, illustrating their relative sizes.

whether destined for a volcano or a pluton, should penetrate the crust through fractures, only as dykes and small pipes, comparable in size to feeders of volcanic flows.

There are, of course, complications. Some plutons have dykes emanating from them that are comparable in dimensions to volcanic dykes, although granitoid in texture.

This implies that apophyses during emplacement have much lower viscosities than their parent plutons. In this regard, the coal intrusion at Corbin, British Columbia (Fig. 3), is instructive, not only as an example of the diverse materials which may be induced to intrude crustal strata, but also in shedding light on the mechanism involved. This intrusion is remarkable in that a thin (about 15 cm) dyke emanates from it. Coal usually does not form intrusive bodies, indicating either a normal viscosity comparable to other upper crustal strata, or, if the viscosity is slightly less, that the stress field is rarely great enough to exploit the difference and initiate intrusion. It is possible that the viscosity of the main body of the coal 'pluton' was reduced a little by the introduction of a small amount of water. The viscosity of the coal dyke, however, was reduced much more. It was almost certainly very wet. This would be a natural result of greater water penetration of the margin of the intrusion, aided possibly by fracturing during intrusion.

A similar mechanism may account for apophyses emanating from granitoid intrusions. In the hypothetical case, shown in Figure 4, a water-rich margin to the pluton is postulated to have formed during intrusion though water-bearing strata. The high water content of the margin may reduce its viscosity to common volcanic values (about 10^5-10^6 p), but not affect the very high viscosity of the main

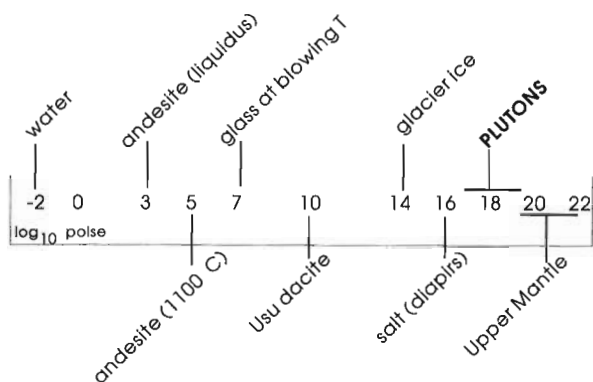


Figure 2. Approximate viscosities of some relevant materials.

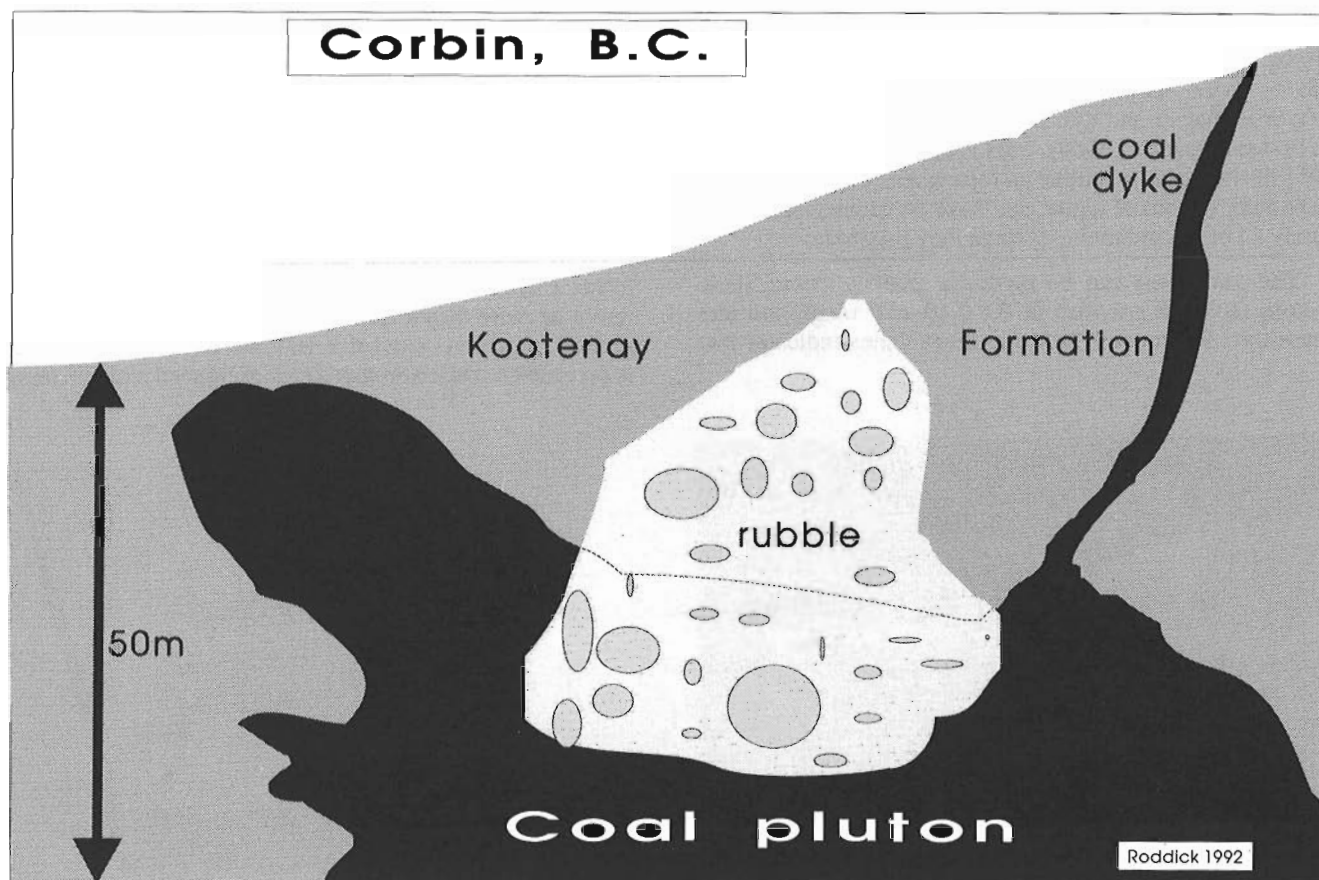


Figure 3. Cross-section of a coal intrusion at Corbin, B.C. Drawn from a photograph taken in 1980.

body of the pluton. This picture, however, is probably too simplistic. Although water will unquestionably reduce mass viscosity, can realistic amounts cause reductions of eight or more orders of magnitude? Probably not, even in the more water-rich margins. But the increase in water there may induce minor grain-boundary fusion. This additional factor could bring the viscosity down to required levels. Incidentally, it follows from this scenario that the sudden loss of the hydrous fluid, through country rock fractures would result in miarolitic cavities.

DENSITY BALLOONING

One of the more common depictions of granite emplacement is by density balloons. The central Andean transect shows 81 of these 'solutions' (Omarini and Gotze, 1991). Density ballooning was once almost synonymous with halokinesis, but has been convincingly questioned as the principal driving force of salt diapirs (Gould and de Mille, 1968). The problem is that the density difference between salt and its customary enclosing sedimentary strata is not great enough to overcome the strength of the latter. The hydraulic pumping mechanism for emplacing salt diapirs was illustrated by Balk (1949) from his studies of the Great Saline salt dome in Texas. He showed the sedimentary salt moving radially into the diapir, then pushing upwards through the enclosing strata (Fig. 5). Should the head of a salt diapir lose its connection to source beds either by their exhaustion or by faulting, upward movement ceases. Strong evidence that density difference is not the main driving force behind diapirism is provided, also, by the anhydrite diapirs and dykes found on Axel Heiberg Island (Gould and de Mille, 1968), Ellef Ringnes Island (Heywood, 1957) in the Canadian Arctic and elsewhere. These bodies are essentially devoid of halite, and have densities greater than nearly all of the sedimentary strata they penetrate.

The same case can be made for plutons. Most silicic plutons (specific gravities in the 2.60-2.70 range) are less dense than the country rock, but no evidence indicates that

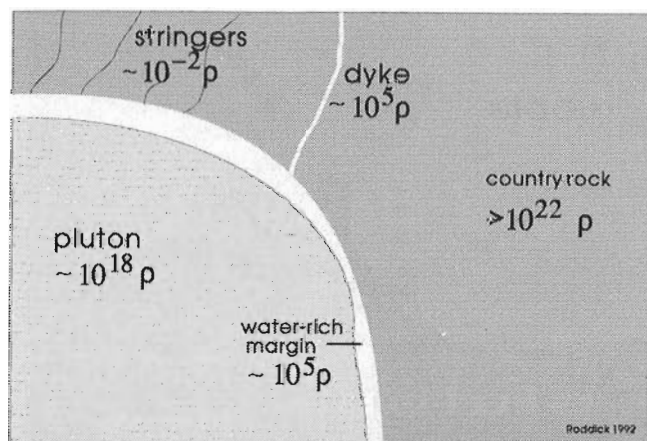


Figure 4. Diagrammatic shoulder of a pluton showing assumed viscosities of pluton core, water-rich margin, dyke,

the related forces are great enough to overcome crustal strength. In any event, many high density, mafic plutons with densities greater than their wall rocks exist.

Like salt diapirs, plutons appear to be driven upward by hydraulic pumping, in sizes and shapes consistent with their viscosity during emplacement. One magmatic scenario postulates that magma penetrates most of the crustal thickness as dykes, and swells to balloon shapes at high levels. This requires that lateral confining forces become less than the vertical, and fracture-widening supplants fracture-propagation. Also puzzling for balloon-shaped plutons is the rarity of inward-dipping (converging) pluton contacts which should result wherever erosional levels intersect plutons below the level of their maximum width.

Hutton (1992) has proposed that plutons could be built up by the injection of multiple dykes. Except for sheeted complexes, however, there is little evidence to support the mechanism. The problem of developing granitoid textures and differentiation patterns in dyke magma is a major detraction. Even for sheeted complexes, it seems much simpler to develop the plutonic texture and sheeted structure at depth before emplacement, probably by thrusting.

The low viscosity of magmas seems to exclude them from a serious role in pluton emplacement. An alternative hypothesis, however, can be constructed, and this leads to the concept of the zone of plutonism.

ZONE OF PLUTONISM

Although developed during work on the Coast Plutonic Complex of British Columbia, the following concept is not a locale-specific scenario. As generalized in Figure 6, amphibolitic-grade rocks extend down to where some hydrous minerals become unstable, and their disintegration forms a hydrous phase that commonly finds no exit. It can rarely be more than a lacy network, easily disrupted, but its pervasiveness over extensive volumes of lower crust seems unpreventable and has profound effects. Mineral reorganization

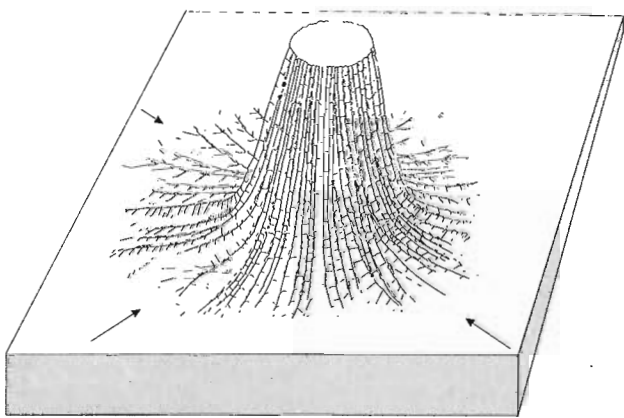


Figure 5. Idealized typical salt diapir; based on the Grand Saline salt diapir of Texas, but similar to many others (after

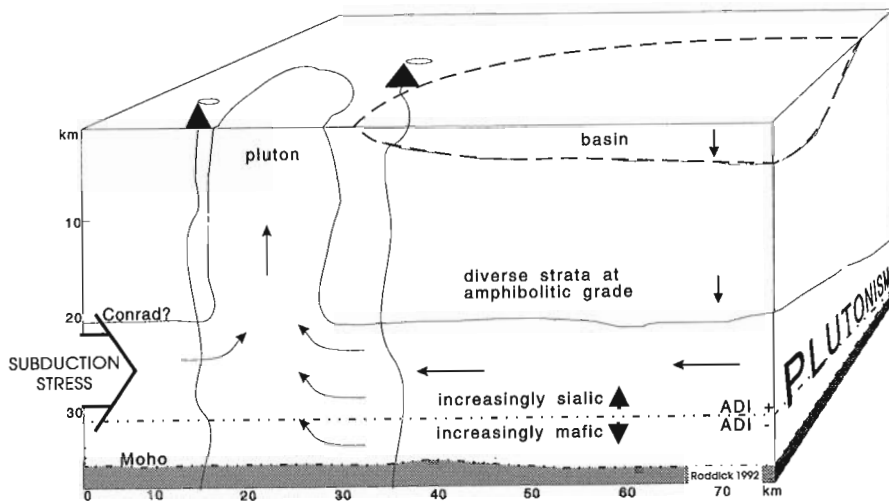


Figure 6.

Hypothetical connection between plutons and the zone of plutonism, analogous in principle to that between salt diapirs and their source beds. The ADI line marks a schematic division of plutonic rocks with average densities less than 2.89 (hypothetical amphibolite) above from those more dense below. (ADI = amphibolite departure index = $100 \times (2.89 - \text{specific gravity of rock})$)

by pressure dissolution, diffusion, and precipitation (i.e., metasomatism) is inevitable wherever the rock is 'wet'. It is not dependent on flow of the hydrous fluid, only on its presence. This is the zone of plutonism (Pzone, hereafter). In it diffusion rearranges the mineralogy (and thereby the chemical distribution within the Pzone) so as to conform to the existing temperature-pressure pattern. Minerals are destroyed by metasomatism and more stable minerals formed, and the overall grain size increased. By becoming coarser, the rock takes on a plutonic appearance. Within the limits of the hydrous network the hotter parts (normally deeper), become more basic and denser, and the cooler regions, more sialic and lighter, simply because of the difference in stability between mafic (also calcic) and sialic minerals, respectively. The division is marked symbolically in Figure 6 by the amphibolite departure line (ADI = 0). The ADI of a plutonic rock is simply its specific gravity subtracted from that of a hypothetical amphibolite, 2.89 (and multiplied by 100 to clear the decimals). The ADI is a simple way of measuring the amount of evolution of plutonic material from a common protolith, which is almost certainly amphibolite judging from its overwhelming dominance as the lithology of xenoliths in plutonic terranes.

Besides chemical effects, intergranular hydrous fluid has mechanical effects. It greatly facilitates creep and shearing (i.e., decreases viscosity), and seems to lead to the development of semihorizontal structures. The shears, enhanced by fluid, make the Pzone seismically more reflective and electrically more conductive. Only a few tenths of a per cent of water can increase the conductivity of crystalline crustal rocks by several orders of magnitude (Connerney et al., 1980). Speculatively, in cratonal crust the zone of plutonism may be defined by the Conrad discontinuity at the top and the Moho at the bottom.

Although the effect of intergranular hydrous fluid is the reduction of mass viscosity, the reduction is probably not great except in local areas where hydrous fluid may be more abundant. For mobilization of substantial rock volumes it need not be, providing that the differential stress field is

sufficiently great, and, in fact, **must not be** if large plutons are to form. Subduction may be required to generate and transmit forces great enough to cause intrusion. As envisioned in Figure 6, the mechanism of pluton emplacement is a larger scale version of salt diapirism. Creep of lower crustal material towards the base of a plutons is subhorizontal. As noted by Nelson (1992), "Moho beneath the internides of these belts [old collisional orogens] is typically sharply reflective, flat, and, from a structural point of view, 'late' in that it either crosscuts dipping reflectors in the overlying crust (e.g., Klemperer and Matthews, 1987) or acts as a decollement for overlying dipping reflectors (e.g., Cook et al., 1992)." The inflow-creep prevents the Moho from bowing up beneath plutons, and ensures a compensating sinking of surrounding regions as well as an upper crustal tensional environment. Curiously, the long term result of pluton intrusion is crustal thinning.

It follows, however, that in the zone of plutonism much larger volumes of the crust will become granitoid than will be mobilized to form plutons. Much of that material never reaches the surface, but some is brought to the surface tectonically, rather than by intrusion of plutons. In the Coast Plutonic Complex, that material forms the heterogeneous 'matrix granitoids' into which well defined plutons are emplaced.

REFERENCES

- Balk, R.
1949: Structure of the Grand Saline salt dome, Van Zandt County, Texas; American Association of Petroleum Geologists Bulletin, v. 33, p. 1791-1829.
- Connerney, J.E.P., Nekut, A., and Kuckes, A.F.
1980: Deep crustal electrical conductivity in the Adirondacks; Journal of Geophysical Research, v. 85, p. 2603-2614.
- Cook, F.A., Varsek, J.L., Clowes, R.M., Kanasewich, E.R., Spencer, C.S., Parrish, R.R., Brown, R.L., Carr, S.D., Johnson, B.J., and Price, R.A.
1992: Lithoprobe crustal reflection cross-section of the southern Canadian Cordillera I: Foreland thrust and fold belt to Fraser River Fault; Tectonics, v. 11, p. 12-36.

Gould, D.B. and de Mille, G.

1968: Piercement structures in Canadian Arctic Islands; in Diapirism and Diapirs: a Symposium; (ed.) J. Braunstein and G.D. O'Brien; American Association of Petroleum Geologists, Memoir 8, p. 183-214.

Heywood, W.W.

1957: Isachsen area, Ellef Ringnes Island, District of Franklin, Northwest Territories; Geological Survey of Canada, Paper 56-8, 36 p.

Hutton, D.H.W.

1992: Granite sheeted complexes: evidence for the dyking ascent mechanism; Transactions of the Royal Society of Edinburgh, Earth Sciences, v. 83A.

Jackson, M.P.A., Cornelius, R.R., Craig, C.H., Gansser, A.,

Stocklin, J., and Talbot, C.J.

1990: Salt diapirs of the Great Kavir, central Iran; Geological Society of America, Memoir 177, 139 p.

Klemperer, S. and Matthews, D.

1987: Iapetus suture located beneath the North Sea by BIRPS seismic reflection profiling; Geology, v. 15, p. 195-198.

Nelson, K.D.

1992: Are crustal thickness variations in old mountain belts like the Appalachians a consequence of lithospheric delamination?; Geology, v. 20, p. 498-902.

Omarini, R.H. and Gotze, H.-J.

1991: Central Andean transect, Nazca Plate to Chaco Plains, Southwestern Pacific Ocean, Northern Chile and Northern Argentina: Global Geoscience Transect 6; American Geophysical Union, Publication No. 192 of the International Lithosphere Program, 30 p. and map.

Weinberg, B.

1927: Some results of experimental study of substances having considerable internal friction; Indian Journal of Physics, v. 1, p. 279-310.

Geological Survey of Canada Project 630016

AUTHOR INDEX

Anderson, R.G.	75	Leclair, A.D.	207
Archibald, D.A.	207	Leitch, C.H.B.	97, 109
Barrie, J.V.	119, 263	Lewis, P.D.	75
Bond, L.	87	Luternauer, J.L.	245, 255, 263, 273
Broster, B.E.	167	Mahoney, J.B.	173, 235
Brown, R.L.	199	Mathewes, R.W.	119
Colpron, M.	191	Monahan, P.A.	263
Conway, K.W.	119	Monger, J.W.H.	149
Crossley, R.	69	Moslow, T.F.	255, 273
Currie, L.D.	21	Nadaraju, G.	75
Dawson, K.M.	87	Parrish, R.R.	207
Erdmer, P.	11	Patterson, R.T.	119, 245
Evenchick, C.A.	47	Porter, J.S.	47
Evoy, R.W.	255, 273	Price, R.A.	191
Fritz, W.H.	183	Read, P.B.	159
Gamba, C.A.	139	Ricketts, B.D.	69
Godwin, C.I.	87	Roddick, J.A.	281
Grasby, S.E.	199	Roots, C.F.	21
Gunning, M.H.	27	Ross, K.V.	87
Hickson, C.J.	63	Shaw, D.R.	97, 109
Higman, S.	63	Simardl, G.J.	183
Hodgson, C.J.	97, 109	Souther, J.G.	57, 129
Huntley, D.H.	167	Stevens, R.A.	11
Jackson, Jr., L.E.	1	Thompson, J.F.H.	75
Jakobs, G.	43	Turner, R.J.W.	97, 109
Johannson, G.G.	37, 75	Weiland, I.	57
Josenhans, H.W.	119	Woodsworth, G.J.	119
Journey, J.M.	221, 235		

NOTE TO CONTRIBUTORS

Submissions to the Discussion section of Current Research are welcome from both the staff of the Geological Survey of Canada and from the public. Discussions are limited to 6 double-spaced typewritten pages (about 1500 words) and are subject to review by the Chief Scientific Editor. Discussions are restricted to the scientific content of Geological Survey reports. General discussions concerning sector or government policy will not be accepted. All manuscripts must be computer word-processed on an IBM compatible system and must be submitted with a diskette using WordPerfect 5.0 or 5.1. Illustrations will be accepted only if, in the opinion of the editor, they are considered essential. In any case no redrafting will be undertaken and reproducible copy must accompany the original submissions. Discussion is limited to recent reports (not more than 2 years old) and may be in either English or French. Every effort is made to include both Discussion and Reply in the same issue. Current Research is published in January and July. Submissions should be sent to the Chief Scientific Editor, Geological Survey of Canada, 601 Booth Street, Ottawa, Canada, K1A 0E8.

AVIS AUX AUTEURS D'ARTICLES

Nous encourageons tant le personnel de la Commission géologique que le grand public à nous faire parvenir des articles destinés à la section discussion de la publication Recherches en cours. Le texte doit comprendre au plus six pages dactylographiées à double interligne (environ 1500 mots), texte qui peut faire l'objet d'un réexamen par le rédacteur scientifique en chef. Les discussions doivent se limiter au contenu scientifique des rapports de la Commission géologique. Les discussions générales sur le Secteur ou les politiques gouvernementales ne seront pas acceptées. Le texte doit être soumis à un traitement de texte informatisé par un système IBM compatible et enregistré sur disquette WordPerfect 5.0 ou 5.1. Les illustrations ne seront acceptées que dans la mesure où, selon l'opinion du rédacteur, elles seront considérées comme essentielles. Aucune retouche ne sera faite au texte et dans tous les cas, une copie qui puisse être reproduite doit accompagner le texte original. Les discussions en français ou en anglais doivent se limiter aux rapports récents (au plus de 2 ans). On s'efforcera de faire coïncider les articles destinés aux rubriques discussions et réponses dans le même numéro. La publication Recherches en cours paraît en janvier et en juillet. Les articles doivent être envoyés au rédacteur en chef scientifique, Commission géologique du Canada, 601, rue Booth, Ottawa, Canada, K1A 0E8.

Geological Survey of Canada Current Research, is now released twice a year, in January and in July. The four parts published in January 1993 (Paper 93-1, parts A to D) are listed below and can be purchased separately.

Recherches en cours, une publication de la Commission géologique du Canada, est publiée maintenant deux fois par année, en janvier et en juillet. Les quatre parties publiées en janvier 1993 (Étude 93-1, parties A à D) sont énumérées ci-dessous et vendues séparément.

Part A: Cordillera and Pacific Margin
Partie A : Cordillère et marge du Pacifique

Part B: Interior Plains and Arctic Canada
Partie B : Plaines intérieures et région arctique du Canada

Part C: Canadian Shield
Partie C : Bouclier canadien

Part D: Eastern Canada and national and general programs
Partie D : Est du Canada et programmes nationaux et généraux